TEMPORAL LOBE DYSFUNCTION IN NEUROPSYCHIATRIC DISORDER

EDITED BY: Qinji Su, Fengyu Zhang, Yujun Gao and Liang Liang
COORDINATED BY: Haohao Yan
PUBLISHED IN: Frontiers in Psychiatry

frontiers Research Topics

frontiers

ISSN 1664-8714
ISBN 978-2-83250-832-9
DOI 10.3389/978-2-83250-832-9

About Frontiers

Frontiers is more than just an open-access publisher of scholarly articles: it is a pioneering approach to the world of academia, radically improving the way scholarly research is managed. The grand vision of Frontiers is a world where all people have an equal opportunity to seek, share and generate knowledge. Frontiers provides immediate and permanent online open access to all its publications, but this alone is not enough to realize our grand goals.

Frontiers Journal Series

The Frontiers Journal Series is a multi-tier and interdisciplinary set of open-access, online journals, promising a paradigm shift from the current review, selection and dissemination processes in academic publishing. All Frontiers journals are driven by researchers for researchers; therefore, they constitute a service to the scholarly community. At the same time, the Frontiers Journal Series operates on a revolutionary invention, the tiered publishing system, initially addressing specific communities of scholars, and gradually climbing up to broader public understanding, thus serving the interests of the lay society, too.

Dedication to Quality

Each Frontiers article is a landmark of the highest quality, thanks to genuinely collaborative interactions between authors and review editors, who include some of the world's best academicians. Research must be certified by peers before entering a stream of knowledge that may eventually reach the public - and shape society; therefore, Frontiers only applies the most rigorous and unbiased reviews.
Frontiers revolutionizes research publishing by freely delivering the most outstanding research, evaluated with no bias from both the academic and social point of view. By applying the most advanced information technologies, Frontiers is catapulting scholarly publishing into a new generation.

What are Frontiers Research Topics?

Frontiers Research Topics are very popular trademarks of the Frontiers Journals Series: they are collections of at least ten articles, all centered on a particular subject. With their unique mix of varied contributions from Original Research to Review Articles, Frontiers Research Topics unify the most influential researchers, the latest key findings and historical advances in a hot research area! Find out more on how to host your own Frontiers Research Topic or contribute to one as an author by contacting the Frontiers Editorial Office: frontiersin.org/about/contact

TEMPORAL LOBE DYSFUNCTION IN NEUROPSYCHIATRIC DISORDER

Topic Editors:
Qinji Su, Guangxi Medical University, China
Fengyu Zhang, Global Clinical and Translational Research Institute, United States
Yujun Gao, Wuhan University, China
Liang Liang, Xinjiang Medical University, China

Coordinator Editor:
Haohao Yan, Central South University, China

Citation: Su, Q., Zhang, F., Gao, Y., Liang, L., Yan, H., eds. (2022). Temporal Lobe Dysfunction in Neuropsychiatric Disorder. Lausanne: Frontiers Media SA.
doi: 10.3389/978-2-83250-832-9

Table of Contents

frontiers | Frontiers in Psychiatry

TYPE Editorial
PUBLISHED 07 November 2022
DOI 10.3389/fpsyt.2022.1077398

OPEN ACCESS

EDITED AND REVIEWED BY
Stefan Borgwardt,
University of Lübeck, Germany

*CORRESPONDENCE
Fengyu Zhang
zhangfy@gcatresearch.org

SPECIALTY SECTION
This article was submitted to Neuroimaging, a section of the journal Frontiers in Psychiatry

RECEIVED 22 October 2022
ACCEPTED 27 October 2022
PUBLISHED 07 November 2022

CITATION
Gao Y, Su Q, Liang L, Yan H and Zhang F (2022) Editorial: Temporal lobe dysfunction in neuropsychiatric disorder. *Front. Psychiatry* 13:1077398. doi: 10.3389/fpsyt.2022.1077398

Editorial: Temporal lobe dysfunction in neuropsychiatric disorder

Yujun Gao[1], Qinji Su[2], Liang Liang[3], Haohao Yan[4] and Fengyu Zhang[5]*

[1]Department of Psychiatry, Renmin Hospital, Wuhan University, Wuhan, China, [2]Department of Psychiatry, The Second Affiliated Hospital, Guangxi Medical University, Nanning, China, [3]Department of Psychology, The Fourth Affiliated Hospital, Xinjiang Medical University, Urumqi, China, [4]Department of Psychiatry, The Second Xiangya Hospital, Central South University, Changsha, China, [5]Global Clinical and Translational Research Institute, Bethesda, MD, United States

KEYWORDS

temporal lobe dysfunction, neuropsychiatric disorder, functional connectivity, temporal lobe epilepsy (TLE), major depressive disorder, schizophrenia, temporal lobe (TL), resting-state functional MRI

Editorial on the Research Topic
Temporal lobe dysfunction in neuropsychiatric disorder

The temporal lobe is a significant part of the human brain forming the cerebral cortex with other lobes. It spans several cortical regions paralleling five temporal gyri, including the superior temporal gyrus (STG), the middle temporal gyrus (MTG), and inferior temporal gyrus (ITG), the fusiform gyrus, and the parahippocampal gyrus/entorhinal gyrus (1). The temporal lobe directly interacts with the limbic system, which plays essential roles in cognitive systems, emotional regulation, autonomic nervous systems, and information relay. Limbic circuits are involved in multiple neuropsychiatric disorders (2). However, the underlying neural mechanisms remain to be elucidated.

This Research Topic published 21 articles that include 20 original research using resting-state fMRI (rs-fMRI) in patients with neuropsychiatric and related disorders relative to healthy controls (HCs). Seven studies focused on temporal lobe epilepsy (TLE); Five on major depressive disorder (MDD), two of which patients underwent antidepressant treatment; Two studies about schizophrenia (SCZ); Others focused on monocular blindness (MCB), congenital blindness (CB), primary nocturnal enuresis (PNE), acoustic neuroma, sudden sensorineural hearing loss (SSHL), premenstrual syndrome (PMS), and premenstrual dysphoric disorder (PMDD).

Temporal lobe epilepsy

Two studies provided consistent evidence that patients with TLE had decreased FC in the bilateral MTG. Based on the voxel-mirrored homotopic connectivity (VMHC) (3), Wu et al. found that patients with lTLE exhibited a decreased VMHC in the bilateral

MTG and middle cingulum gyrus (CG). With a similar study design, Chu et al. found that patients with the right TLE (rTLE) had a decreased VMHC in the bilateral superior temporal pole (STP), middle temporal pole (MTP), MTG, ITG, and inferior frontal gyrus (IFG). In contrast, they exhibited an increase of VMHC in the bilateral precentral gyrus (PreCG), the postcentral gyrus (PoCG), and the supplemental motor area (SMA).

Patients with TLE may have altered network connectivity. Li et al. studied network homogeneity (NH) of the ventral somatomotor network (VSN) in patients of lTLE and rLTE and found reduced NH in the bilateral Rolandic operculum and STG, but increased in PoCG. Huang et al. showed rTLE patients had a decreased NH of default mode network (DMN) in the R-ITG and L-MTG, but an increase in the bilateral PCu and R-inferior parietal lobe. Based on the degree of centrality (DC) (4), Guo et al. showed that patients with rTLE had a reduced DC in the R-caudate, but increased network connectivity in the L-MTG, superior parietal gyrus (SPG), inferior parietal gyrus (IPG), superior frontal gyrus (SFG), medial SFG, IFG, and R-precuneus (PCu).

The basal forebrain (BF) is a cluster of subcortical structures providing axonal projection to the entire cerebral cortex and comprises four nuclei of the medial septal (MS, Ch1), the vertical limb of the diagonal band of Broca (vDbB, Ch2), the horizontal limb of the diagonal band of Broca (hDbB, Ch3), and the nucleus basalis of Meynert (nBM, Ch4) (5). Fan et al. studied TLE patients with and without focal to bilateral tonic-clonic seizure (FBTCS), using four basal forebrain subregions to examine the resting-state FC (rsFC). Regardless of FBTCS status, the TLE patients had reduced rsFC of BF subregions with the cerebellum, striatum, DMN, frontal and occipital lobes. Decreased rsFC of Ch1-3 with bilateral striatum and left cerebellum posterior lobe and Ch4 with bilateral amygdala was associated with FBTCS.

Major depressive disorder

MD is highly heterogeneous and associated with multi-faceted risk factors (6, 7). While neuroimaging studies have shown that patients with MDD tend to have altered brain structure and FC (8, 9), there is significant inconsistency. Five studies focused on brain activity and functional connectivity in MDD using various neuroimaging techniques (Supplementary Box).

Two studies examined brain activities in patients with MDD relative to HCs and after antidepressant treatment. Wang et al. studied drug-naïve first episode of adolescent MDD who also had 2-week electroconvulsive therapy (ECT). Whole brain voxel analysis showed increased activity in the R-orbital IFG, inferior occipital gyrus (IOG), and L-middle frontal gyrus (MFG) in patients with MDD. Meanwhile, patients treated with ECT significantly increased brain activity in the R-medial SFG, anterior cingulate gyrus (ACG), paracingulate gyrus (paraCG), medial CG and PCG, dorsolateral SFG, and L-MFG. Also, the increased brain activity in the frontal gyri seemed to be significantly associated with reducing clinical severity. Xiong et al. detected a high activity in the bilateral MFG, CG, and MTG in MDD; patients treated with vortioxetine for 2 weeks had decreased brain activity in the R-ITG, but increased activity in the L-low cerebellum, R-CG, and central posterior gyrus.

Three studies focused on regional homogeneity and network connectivity. Song et al. found that patients with drug-naïve first-episode MDD had an increase of ReHo in the L-anterior cingulate cortex (ACC) but decreased ReHo in the L-PreCG. However, none of these were significantly associated with the HAMD score. Luo et al. studied treatment-naïve first-episode MDD and HCs matched by gender, age, and education. They found a decreased NH in the R-PCu and abnormal executive control reaction time relative to HCs; the decreased NH was not significantly correlated to the clinical severity. In addition, Lin et al. conducted a larger-size study of 198 cases with MDD and 234 HCs using network centrality measure. Patients with MDD exhibited an elevated level of DC in the L-anterior cerebellar lobe, vermis, L-hippocampus, L-caudate, but a reduced DC in the L-posterior cerebellar lobe, L-insula, and R-caudate.

Han et al. conducted a clinical study of patients with MDD. They found that the frequency of negative evaluation and emotional words were significantly associated with the severity of MDD measured by HAMD-17.

Schizophrenia

Activation of auditory-related brain regions is one of the neuropathological mechanisms in SCZ. Disruption of functional connectivity in the L-temporal lobe, particularly L-STG has been indicated in AVH (10). Xue et al. studied voxel-wised dynamic FC (dFC) of the primary auditory cortex—Heschl's gyrus (HES) and auditory association cortex (AAC) in drug-naïve first episode SCZ with and without AVH. They found SCZ patients with AVH had an increased dFC of L-AAC with R-MTG and middle occipital gyrus (MOG) but a decreased dFC of L-HES gyrus with L-superior CG, L-cuneus, and L-PCu gyri, and R-HES gyrus with posterior CG.

Inter-hemispheric disconnection has been a notable pathological finding in SCZ (11, 12). Chen et al. studied inter-hemispheric connectivity, focusing on the STG cluster (extending into Heschl's gyrus, insula, and Rolandic operculum) and fusiform cluster (growing into the para-hippocampus). SCZ with AVH showed a reduced VMHC in the fusiform

TABLE 1 rs-fMRI study of temporal lobe dysfunctions in temporal lobe epilepsy, major depression, schizophrenia and other disorders.

Study	Disease	Sample	Measure	Region of brain activity or connectivity	
		Cases vs. HCs		Decreased	Increased
Major depressive disorder					
Wu et al.	L-TLE	59 vs. 60	VMHC	B-MTG, MCG.	
Chu et al.	R-TLE	58 vs. 60	VMHC	B-MTG, ITG, B-sup TP, B-middle TP, ITG, orbital IFG.	B-PreCG, PoCG, SMA
Li et al.	R-TLE	53 vs. 68	NH	B-Rolandic operculum, R- STG.	B-PoCG
	L-TLE	83 vs. 68	NH	R-Rolandic operculum.	L-PoCG
Huang et al.	R-TLE	42 vs. 43	NH	Left MTG, R-ITG.	B-PCu, R-inf parietal lobe.
Guo et al.	R-TLE	68 vs. 73	DC	R-caudate.	L-MTG, sup PreCG, SFG, IFG, IPG, med SFG, R-PCu.
Fan et al.	TLE and FBTCS vs. HCs	50 vs. 25	rsFC	BF with striatum, cerebellum, DMN, occipital lobe.	
	FBTCS vs. TLE	25 vs. 25	rsFC	BF with B-striatum, L-cerebellum poste lobe, B- amygdala.	
Temporal lobe epilepsy					
Wang et al.	Adolescent MDD	30 vs. 30	fALFF		R-orbital IFG, inf OG, L-MFG.
	ECT		fALFF		R-med SFG, dorsol SFG, R-MFG, ante CG, med CG, ParaCG.
Xiong et al.	MDD	25 vs. 25	ALFF		B-MFG, CG, and MTG
	Vortioxetine	25	ALFF	R-ITG	L-low cereb, R-CG, central poste gyrus.
Song et al.	MDD	52 vs. 45	ReHo	L-PreCG	L-ACC
Luo et al.	MDD	73 vs. 70	NH	R-PCu	
Lin et al.	MDD	198 vs. 234	NH	L-poste cerebellar lobe, L-insula, R- caudate.	L-anterior cerebellar lobe, Vermis, L-hipp, L-caudate.
Schizophrenia					
Xue et al.	SCZ AVH vs. NAVH+HC	107 vs. 85+104	dFC		L-AAC with R-MTG, middle OC.
			dFC	L-HES with L-SCG, L-cuneus gyrus, L-PCu gyrus.	
			dFC	R-HES with Poste CG.	
Chen et al.	SCZ AVH vs. NAVH	42 vs. 26	VMHC	Fusiform cluster (into paraHipp gyrus).	
	AVH<NAVH<HC	42, 26, 82	VMHC	STG cluster (into Heschl's gyrus, insula, Rolandic operculum).	
Other disorders					
Deng et al.	Acoustic neuroma	64 vs. 67	ReHo	Frontal lobe	
Liu et al.	SSHL	27 vs. 27	ReHo	L-cerebellum, B-ITG, L-sup TL, R-paraHipp, L-poste CC, R-SFG.	
Hu et al.	Congenital blindness	23 vs. 23	ReHo	R-orbital MFG, B-middle OG, R-dorsol SFG.	L-paracentral lobule, R-insula, and B-thalamus
Hu et al.	Monocular blindness	29 vs. 29	PerAF	L-middle OL, R-middle OL, L-middle CL.	L-sup FL, L-inf orbital FL, L-inf TL, L-inf frontal operculum

(Continued)

TABLE 1 (Continued)

Study	Disease	Sample	Measure	Region of brain activity or connectivity	
		Cases vs. HCs		Decreased	Increased
Xu et al.	MGD in severe obese	12 vs. 12	fALFF	R-cereb, L-fusifom G, R-med orbito-FG, L-triangle IFG, L-IPG	R-globus pallidus, R-ante CC and para-CG, L-Middle OL.
Zhong et al.	Nocturnal euresis	30 vs. 29	rsFC	L-rHipp with R-FFG, G, R-Rolandic operculum, L-inf parietal lobe, R-PreCG; L-cHipp with R-fusiform G, R-SMA.	

(1) AVH, auditory verbal hallucination; ECT, electroconvulsive therapy; FBTCS, focal to bilateral tonic-clonic seizure; HC, Healthy control; L-TLE, left temporal lobe epilepsy; MDD, major depressive disorder; MGB, Meibomian gland dysfunction; R-TLE, right temporal lobe epilepsy; SSHL, sudden sensorineural hearing loss.
(2) DC, degree of centrality; fALFF, fractional amplitude of low-frequency fluctuations; NH, network homogeneity; perAF, percentage of amplitude of fluctuations; ReHo, regional homogeneity; rsFC, resting-state functional connectivity; VMHC, Voxel-mirrored homotopic connectivity.
(3) ACC, anterior cingulate cortex; BF, basal forebrain; CC, cingulate cortex; CG cingulate gyrus; CL, cingulate lobe; DMN, the default mode network; FFG, fusiform gyrus; FG, frontal gyrus; FL, frontal lobe; IFG, inferior frontal gyrus, ITG, inferior temporal gyrus; IPG, inferior parietal gyrus; MFG, middle frontal gyrus; MTG, middle temporal gyrus; OG, occipital gyrus; OL, occipital lobe; ParaCG, paracingulate gyrus; PCu, precuneus; PoCG, post-central gyrus; PreCG, precentral gyrus; SFG, superior frontal gyrus; SMA, supplementary motor area; STG, superior temporal gyrus; TG, temporal gyrus; TL, temporal lobe; TP, temporal lobe.
(4) Ante, anterior; B, bilateral; cereb, cerebellum; cHipp, caudal hippocampus; dorsol, dorsolateral; Inf, inferior; L, left; Med, medial; Poste, posterior; rHipp, rostral hippocampus; R, right. Sup, superior.

cluster; A decreased VMHC in the STG cluster was observed in both SCZ with and without AVH compared to HCs.

Acoustic neuromas and sudden sensorineural hearing loss

Acoustic neuroma (AN) is a type of tumor that develops from the sheath of Schwann cells and grows in the ear and can affect hearing and body balance function. While often described as transient, the psychiatric symptoms in patients with ANs may include mood change, memory loss, hallucination, and delusion (13). Deng et al. performed a clinical neuropsychological study of patients with ANs, and then an rs-fMRI investigation. Patients with ANs exhibited a cognitive decline, reduced ReHo, and decreased connectivity in the frontal lobe. Liu et al. found a reduced ReHo in the L-cerebellum, B-ITG, L-STP, R-para-hippocampal gyrus, L-PCC, and R-SFG in patients with SSHLcompared to HCs.

Congenital and monocular blindness

Lack of visual experience may affect the development of brain structure and functions development. Hu J-J. et al. found that patients with CB decreased ReHo in the R-orbital MFG, bilateral MOG, and R-dorsolateral SFG, but an increase in the L-paracentral lobule, R-insula, and bilateral thalamus. Using the percentage of amplitude fluctuations (perAL), Hu Q. et al. found that patients with MCB had decreased brain activity in the middle OL and the L-middle cingulate lobe but increased activity in the frontal and temporal lobes.

Meibomian gland dysfunction in severely obese population

Meibomian gland dysfunction is a chronic and diffuse abnormality of meibomian glands characterized by terminal duct obstruction. Xu et al. found that Meibomian gland dysfunction (MGD) in severely obese people exhibited decreased brain activity in the R-cerebellum, L-fusiform gyrus, R-medial orbitofrontal gyrus, L-triangle IFG, and L-IPG, but increased activity in the left lingual gyrus, R-globus pallidus, right ACG and para-CG, and L-MOG. The increased brain activity in R-cerebellum and left triangle IFG seemed to be associated with a high anxiety and depression score. Notably, this analysis was based on a tiny sample ($n = 12$).

Primary nocturnal enuresis

The development of chidrlem with PNE may involve a brain-bladder control network. Zhong et al. performed a seed-based rsFC of PNE and HCs with the first attempt to focus on four regions of the left and right rostral hippocampus (rHipp) and caudal hippocampus (cHipp) as of interest (ROI). Children with PNE exhibited a decreased rsFC in L-rHipp with R-fusiform gyrus, R-Rolandic operculum, L-inferior parietal lobe (IPL), and R-PreCG, but a reduced rsFC in L-cHipp with R-fusiform gyrus and R-SMA. The reduced FC of L-rHipp with R-Rolandic operculum and left cHipp with fusiform was also associated with the disease duration. The altered functional

connectivity in these brain regions may involve multiple brain networks, including the limbic system, sensorimotor, DMN, and frontoparietal network. In addition to the brain-bladder control network, these brain regions are important in cognitive function and emotion.

Premenstrual syndrome and premenstrual dysphoric disorder

Premenstrual syndrome (PMS) is a group of clinically significant somatic and psychological symptoms or distress that women develop during the luteal phase of the menstrual cycle (about a week or two before the period) (14). Its severe form, premenstrual dysphoric disorder (PMDD), is classified as a subcategory of depression. Long et al. contributed a mini-review of neuroimaging studies of PMS and PMDD. Neuroimaging studies show more robust evidence of structural and functional alterations in the amygdala and the hippocampus's medial temporal lobe (MTL). Also, an fMRI study indicated abnormal fusiform gyrus activity in patients with PMS and PMDD.

Summary

The studies indicated temporal lobe dysfunction in neuropsychiatric and related disorders. In TLE, decreased FC in the MTG, ITG, and Rolandic operculum were identified, and reduced FCs of BF subregions with the striatum and cerebellum were associated with both TLE and FBTCS. However, increased connectivity in the PreCG and PoCG was associated with TLE (Table 1). These findings consistently appear in at least one independent studies or samples within the same study. The reduced FC between the left rHipp and the right Rolandic operculum was associated with PNE. Moreover, AVH in SCZ might be related to increased dsFC in L-AAC, decreased connectivity in the HES gyrus, and reduced inter-hemispheric connectivity in the fusiform cluster.

By contrast, findings from five studies of MDD seemed lacking consistency. Two studies with drug-naïve first episode MDD treated with antidepressant therapy did not find that antidepressant treatment significantly impacted the baseline brain activity associated with MDD. The inconsistent findings between disease association and response to treatment may pose a challenging question for interpretation. Part of the causes might be that patient heterogeneity had reduced the power to cause false-positive discovery.

The fMRI techniques have made it feasible to study the entire connectome at a large scale in humans. However, studies should move beyond the exploratory analysis of FC. Therefore, it calls for the rigor of study and advanced analytic techniques to maximize the critical tools of fMRI for neuroscience research. Furthermore, it might be more promising when fMRI combines with radionuclide scans such as positron emission tomography (PET) and structure MRI (sMRI), which can reveal the brain structure and functions at a circuit level. Multimodal neuroimaging may have a greater demand and challenge in visual data inspection, integration, and fusion for analysis (15).

Author contributions

FZ reviewed all articles, summarized individual studies' findings, and drafted the manuscript. All other editors participated in editing articles and reviewed and had access to the manuscript and related Supplementary materials. All authors contributed to the article and approved the submitted version.

Acknowledgments

We thank all authors who contributed to this Research Topic; HY provided coordination for launching this Research Topic.

Conflict of interest

The authors declare that the research was conducted in the absence of any commercial or financial relationships that could be construed as a potential conflict of interest.

Publisher's note

Supplementary material

The Supplementary Material for this article can be found online at: https://www.frontiersin.org/articles/10.3389/fpsyt.2022.1077398/full#supplementary-material

References

1. Baker CM, Burks JD, Briggs RG, Milton CK, Conner AK, Glenn CA, et al. A Connectomic Atlas of the human cerebrum-chapter 6: the temporal lobe. *Oper Neurosurg.* (2018) 15:S245–94. doi: 10.1093/ons/opy260

2. Byrum CE, Thompson JE, Heinz ER, Krishnan KR, Tien RD. Limbic circuits and neuropsychiatric disorders. Functional anatomy and neuroimaging findings. *Neuroimaging Clin N Am.* (1997) 7:79–99.

3. Zuo XN, Kelly C, Di Martino A, Mennes M, Margulies DS, Bangaru S, et al. Growing together and growing apart: regional and sex differences in the lifespan developmental trajectories of functional homotopy. *J Neurosci.* (2010) 30:15034–43. doi: 10.1523/JNEUROSCI.2612-10.2010

4. Zuo X-N, Ehmke R, Mennes M, Imperati D, Castellanos FX, Sporns O, et al. Network centrality in the human functional connectome. *Cereb Cortex.* (2012) 22 8:1862–75. doi: 10.1093/cercor/bhr269

5. Hedreen JC, Struble RG, Whitehouse PJ, Price DL. Topography of the Magnocellular basal forebrain system in human brain. *J Neuropathol Exp Neurol.* (1984) 43:1–21. doi: 10.1097/00005072-198401000-00001

6. Li Y, Lu J. Childhood adversity and depression among older adults: results from a longitudinal survey in China. *Glob Clin Transl Res.* (2019) 1:53–7. doi: 10.36316/gcatr.01.0007

7. Chen Y-Y, Yu S, Hu Y-H, Li C-Y, Artaud F, Carcaillon-Bentata L, et al. Risk of suicide among patients with Parkinson disease. *JAMA Psychiatry.* (2021) 78:293–301. doi: 10.1001/jamapsychiatry.2020.4001

8. Wise T, Radua J, Via E, Cardoner N, Abe O, Adams TM, et al. Common and distinct patterns of grey-matter volume alteration in major depression and bipolar disorder: evidence from voxel-based meta-analysis. *Mol Psychiatry.* (2017) 22:1455–63. doi: 10.1038/mp.2016.72

9. Demirtas M, Tornador C, Falcon C, Lopez-Sola M, Hernandez-Ribas R, Pujol J, et al. Dynamic functional connectivity reveals altered variability in functional connectivity among patients with major depressive disorder. *Hum Brain Mapp.* (2016) 37:2918–30. doi: 10.1002/hbm.23215

10. Alderson-Day B, McCarthy-Jones S, Fernyhough C. Hearing voices in the resting brain: a review of intrinsic functional connectivity research on auditory verbal hallucinations. *Neurosci Biobehav Rev.* (2015) 55:78–87. doi: 10.1016/j.neubiorev.2015.04.016

11. Lang X, Wang L, Zhuo CJ, Jia F, Wang LN, Wang CL. Reduction of interhemispheric functional connectivity in sensorimotor and visual information processing pathways in schizophrenia. *Chin Med J.* (2016) 129:2422–6. doi: 10.4103/0366-6999.191758

12. Friston KJ, Frith CD. Schizophrenia: a disconnection syndrome. *Clin Neurosci.* (1995) 3:89–97.

13. Kalayam B, Young RC, Tsuboyama GK. Mood disorders associated with acoustic neuromas. *Int J Psychiatry Med.* (1994) 24:31–43. doi: 10.2190/50PT-T9YD-ACKJ-1GUX

14. Yesildere Saglam H, Orsal O. Effect of exercise on premenstrual symptoms: a systematic review. *Complement Ther Med.* (2020) 48:102272. doi: 10.1016/j.ctim.2019.102272

15. Tulay EE, Metin B, Tarhan N, Arikan MK. Multimodal neuroimaging: basic concepts and classification of neuropsychiatric diseases. *Clin EEG Neurosci.* (2018) 50:20–33. doi: 10.1177/1550059418782093

frontiers | Frontiers in Psychiatry

ORIGINAL RESEARCH
published: 03 May 2022
doi: 10.3389/fpsyt.2022.902873

Correlation Between Word Frequency and 17 Items of Hamilton Scale in Major Depressive Disorder

*Jiali Han, Yuan Feng, Nanxi Li, Lei Feng, Le Xiao, Xuequan Zhu and Gang Wang**

The National Clinical Research Center for Mental Disorders and Beijing Key Laboratory of Mental Disorders, Beijing Anding Hospital and the Advanced Innovation Center for Human Brain Protection, Capital Medical University, Beijing, China

Objective: To explore the correlation between word frequency and 17 items of the Hamilton Depression Scale (HAMD-17) in assessing the severity of depression in clinical interviews.

Methods: This study included 70 patients with major depressive disorder (MDD) who were hospitalized in the Beijing Anding Hospital. Clinicians interviewed eligible patients, collected general information, disease symptoms, duration, and scored patients with HAMD-17. The words used by the patients during the interview were classified and extracted according to the HowNet sentiment dictionary, including positive evaluation words, positive emotional words, negative evaluation words, negative emotional words. Symptom severity was grouped according to the HAMD-17 score: mild depressive symptoms is 8–17 points, moderate depressive symptoms is 18–24 points and severe depressive symptoms is >24 points. Analysis of Variance (ANOVA) was used to analyze the four categories of words among the groups, and partial correlation analysis was used to analyze the correlation between the four categories of word frequencies based on HowNet sentiment dictionary and the HAMD-17 scale to evaluate the total score. Receiver operating characteristic (ROC) curves were used to determine meaningful cut-off values.

Results: There was a significant difference in negative evaluation words between groups ($p = 0.032$). After controlling for gender, age and years of education, the HAMD-17 total score was correlated with negative evaluation words ($p = 0.009$, $r = 0.319$) and negative emotional words ($p = 0.027$, $r = 0.272$), as the severity of depressive symptoms increased, the number of negative evaluation and negative emotional words in clinical interviews increased. Negative evaluation words distinguished patients with mild and moderate-severe depression. The area under the curve is 0.693 ($p = 0.006$) when the cut-off value is 8.48, the Youden index was 0.41, the sensitivity was 55.2%, and the specificity was 85.4%.

Conclusion: In the clinical interview with MDD patients, the number of word frequencies based on HowNet sentiment dictionary may be beneficial in evaluating the severity of depressive symptoms.

Keywords: major depressive disorder, symptom severity, word frequency, temporal lobe, HowNet sentiment dictionary

OPEN ACCESS

Edited by:
Yujun Gao,
Wuhan University of Science and Technology, China

Reviewed by:
Lin Liu,
Peking University, China
Jie Gong,
Xidian University, China

****Correspondence:***
Gang Wang
gangwangdoc@ccmu.edu.cn

Specialty section:
This article was submitted to Neuroimaging and Stimulation, a section of the journal Frontiers in Psychiatry

Received: *23 March 2022*
Accepted: *14 April 2022*
Published: *03 May 2022*

Citation:
Han J, Feng Y, Li N, Feng L, Xiao L, Zhu X and Wang G (2022) Correlation Between Word Frequency and 17 Items of Hamilton Scale in Major Depressive Disorder. Front. Psychiatry 13:902873. doi: 10.3389/fpsyt.2022.902873

INTRODUCTION

Major depressive disorder (MDD) is a significant public health problem. Studies in recent years have shown that it has a high incidence rate with a lifetime prevalence rate in China at about 3.4% (1), and the global prevalence rate is about 4.4% (2). Likewise, depression has a high disability rate, with 50 million people worldwide affected by depression, accounting for 7.5% of the total global disability rates (2). Depression also has a high disease burden (3), which seriously affects patients' physical health, social functions, and daily living. The current diagnosis process of depression primarily relies on the experience of clinical psychiatrists, professional scale assessments, and subjective descriptions of patients. While these functions are extensively utilized throughout the clinic, these evaluations that rely on subjective analyses and clinical experience may lead to poor consistency between assessments and differences in diagnosis and treatment (4). To thoroughly evaluate the patient, it is integral to determine the severity of depression in patients as part of the clinical diagnosis, especially as these diagnoses are of great significance to patients' treatment plans and assist in identifying life-threatening risks. Therefore, it is urgent to find objective indicators that are easy to collect and apply to assess the symptom severity of depression.

Language is an important way for human beings to transmit information. It is the principal method to transmit ideas and express emotional fluctuations and changes (5, 6). It has a high emotion recognition rate and has the characteristics of easy access, non-invasiveness, and objectivity. It can also reflect people's emotions and cognitive functions. Semantic processing, language, and conceptual categorization depends on temporal lobe. Research showed MDD patients had abnormal results in temporal lobe (7, 8). Temporal lobe injury, especially the amygdala, affects language processing in patients with MDD and lead to negative bias (9). Specifically, patients with depression pay more attention to negative stimuli and less attention to positive ones. Likewise, they are prone to negative interpretations of emotionally ambiguous events or stimuli and often suppress their positive emotional responses (10, 11). Studies have shown that compared with healthy individuals, depressed individuals use more words associated with negative emotions and less associated with positive emotions (12). At present, studies have focused on distinguishing depressive patients from healthy individuals (13, 14) or suicide monitoring (15). Given the lack of studies investigating the recognition of the severity of depressive symptoms using word frequency of depression-related words, this study aimed to evaluate whether the severity of depression symptoms could be measured by word frequency based on the HowNet sentiment dictionary.

MATERIALS AND METHODS

Participants

Subjects recruited for this study were patients with depression hospitalized in the Beijing Anding Hospital from Sep. 2020 to Mar. 2021. The inclusion criteria for this study, in which all 4 items must be met, include (1) patients 18–65 years old with diagnostic criteria of MDD or relapse without psychotic symptoms according to the International Classification of Diseases (ICD-10), (2) 17 items of Hamilton scale (HAMD-17) score >7 points, (3) an education level of primary school or above, and able to understand the content of the scale, and (4) patients that signed the informed consent. The Exclusion criteria were as follows: (1) Patients who met the diagnosis of other mental disorders in ICD-10, (2) Alcohol or drug abuse or dependence within 1 year, (3) currently suffering from oral and throat diseases and other severe physical illness, and (4) mental symptoms were too severe to cooperate with the completion of the research content. This study protocol was approved by the Ethics Committee of the Beijing Anding Hospital. All patients participated in the study and signed informed consent. Finally, 70 patients with MDD were included in this study.

Measures

We collected general information, including the patient's age, gender, educational level, age at the first onset, frequency of onset, and current course of the disease. HAMD-17 (16) to assess the severity of depressive symptoms in subjects. This scale has good reliability and validity and is widely used to assess the severity of depressive symptoms. The severity of depression was classified according to the total score of HAMD-17: no depressive symptoms are designated as 0–7 points, mild depressive symptoms is 8–17 points, moderate depressive symptoms is 18–24 points and severe depressive symptoms is >24 points. HowNet Sentiment Dictionary (17) is a sentiment dictionary based on the HowNet knowledge database, a robust knowledge database that enables natural language processing systems. This system is a known dictionary for sentiment analysis of Chinese words and is widely used. The dictionary divides vocabulary into four types: 4,534 words of positive evaluation (such as indispensable, sinking fish and geese, beautiful), 1,516 words of positive emotion (such as love, happiness, lingering dreams), and 3,745 words of negative evaluation (such as ugly, excessive, flashy), 1,959 words of negative emotional (such as sad, dubious, dissatisfied).

Procedure

Clinicians conducted interviews with eligible participants, collected general information, disease symptoms, duration, and participant dialog was recorded using honor 9X mobile. There was no restriction on the time of the interview. Then clinicians who passed the HAMD-17 consistency assessment to judge patients' severity. The audio information was transcribed and manually proofread, and finally, the words used by the patients during the interview were classified into four categories according to the HowNet sentiment dictionary. Finally, divide the four types of words by the interview time to get words per minute.

Statistical Analysis

SPSS 24.0 software was used for data management and statistical analysis. The normally distributed measurement data were expressed as the mean and standard deviation (mean ± SD), and the non-normally distributed measurement data were expressed

as the median and quartile [M (P25, P75)]. Analysis of Variance (ANOVA) was used to analyze the four categories of words between each group, and partial correlation analysis was used to analyze the correlation between word frequencies and HAMD-17 scale total scores. According to the scores with significant differences, the results were divided into Receiver operating characteristic (ROC) curves and were used to determine meaningful cut-off values. p values <0.05 were considered to be significant.

RESULTS

A total of 70 patients participated in this study, including 30 males (42.9%) and 40 females (57.1%), an average of 45.1 (±13.1) years, 7 completed primary school (10.0%), 17 completed junior high school (24.3%), and 45 (64.3%) completed high school and/or above, with 1 case (1.4%) having missing information, 30 cases (42.9%) were designated as first-episode while 40 patients (57.1%) had recurring episodes. The HAMD-17 scale score average was 19.1 (±5.4), of which 29 cases (41.4%) were mild, 27 cases (38.6%) were moderate, and 14 cases (20.0%) were severe. And the average time of the interview is 11.6 (±3.2), the maximum time is 20.2 and the minimal time is 5.1. General information had no differences between groups, as shown in **Table 1**.

Shapiro-Wilk test found that the four types of word frequencies were in line with normal distribution in each group, and the results of ANOVA showed a significant difference in negative evaluation words between groups ($p = 0.032$). Multi-comparison analysis with Least-SignificantDifference (LSD) found a significant difference in negative evaluation words between mild-moderate patients ($p = 0.022$) and mild-severe patients ($p = 0.036$).

It was found that there was a correlation between gender, age, education and word frequency. After controlling them, the HAMD-17 total score was correlated with negative evaluation words ($p = 0.009$, $r = 0.319$, **Figure 1**) and negative emotional words ($p = 0.027$, $r = 0.272$, **Figure 2**), as shown in **Table 2**. As the severity of depressive symptoms increased, the number of negative evaluation words and negative emotional words in clinical interviews increased.

Based on the predictive value of HowNet sentiment dictionary for the severity of depression, the ROC curve analysis results showed that the area under the curve of negative evaluation words could effectively distinguish patients with mild and moderate-severe was 0.693 ($p = 0.006$). When the cut-off value was 8.48, the Youden index was 0.41, the sensitivity was 55.2%, and the specificity was 85.4% (**Figure 3**). Therefore, negative evaluation words can effectively distinguish patients with moderate-severe depression.

DISCUSSION

In this study, we analyzed the word frequency of 70 patients with MDD, and the results of ANOVA showed that the difference in negative evaluation words was significant between groups ($p = 0.032$). Likewise, it was significantly different in patients with mild-moderate patients ($p = 0.022$) and mild-severe ($p = 0.036$) MDD. These findings show that the word frequency feature can distinguish moderate and severe MDD from mild disorders. Notably, the negative evaluation words ($p = 0.009$, $r = 0.319$) and negative emotional words ($p = 0.027$, $r = 0.272$) are positively correlated with the score of HAMD-17. This

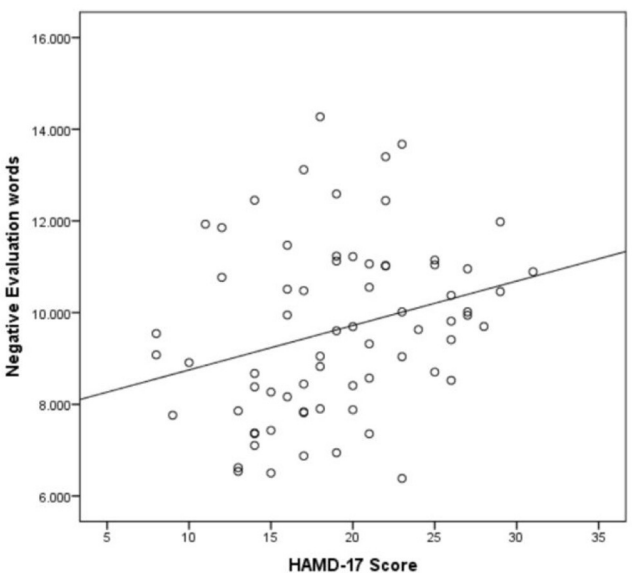

FIGURE 1 | Scatter plot of the association between negative evaluation words per minute and HAMD-17 score ($n = 70$).

TABLE 1 | General information in each group ($n = 70$).

Item	Mild ($n = 29$)	Moderate ($n = 27$)	Severe ($n = 14$)	F/χ^2	p
Gender (M/ F)	14/15	12/15	4/10	0.76	0.47
Age	44.5 ± 13.7	46.7 ± 13.6	43.4 ± 11.4	0.33	0.71
Education (years)	12.1 ± 2.8	13.0 ± 3.8	11.2 ± 3.8	1.36	0.26
Age of onset	37.4 ± 13.5	36.3 ± 12.9	39.9 ± 10.4	0.38	0.69
Course (weeks)	16.0 (4.3, 49.5)	26.0 (8, 50)	14.0 (5.8, 22)	1.57	0.47
Number of attacks	2.2 ± 1.5	2.7 ± 2.0	2.1 ± 1.5	0.67	0.52
Interview time (min)	11.8 ± 3.2	11.7 ± 2.9	11.1 ± 3.9	0.21	0.81

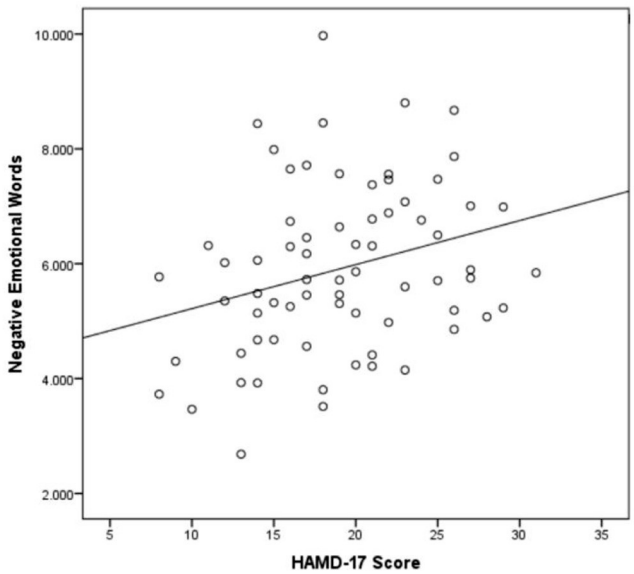

FIGURE 2 | Scatter plot of the association between negative emotional words per minute and HAMD-17 score ($n = 70$).

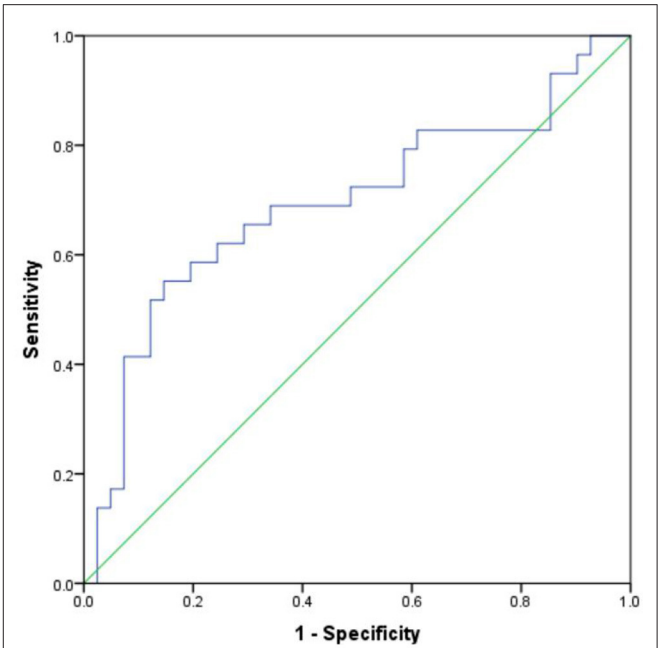

FIGURE 3 | ROC curve analysis of negative evaluation words for differentiating severity of HAMD-17 score.

TABLE 2 | Partial correlation analysis of four types of words.

Feature	Partial correlation	
	r	*p*
Positive evaluation	0.058	0.645
Positive emotion	0.042	0.735
Negative evaluation	0.319**	0.009
Negative emotional	0.272*	0.027

*$p < 0.05$, **$p < 0.01$.

means that as the severity of depressive symptoms increased, the number of negative evaluation and negative emotional words in clinical interviews increased. Extracting the expressions of negative evaluation words and negative emotion words in patients with MDD has added value in judging the severity of depressive symptoms. It provide some clues to find objective evidence of clinical diagnosis and treatment for other studies in the future. Although patients with MDD have negative emotional expressions, patients often use evaluative words to express their feelings and experiences in clinical interviews. Here, we have identified that the results of negative evaluative words are more significant than negative emotional words.

The results of ROC in this study showed that in the clinical diagnosis and treatment evaluation, the number of negative evaluation words has a significant degree of discrimination for patients with moderate-severe depression. The cut-off value was 8.48, the sensitivity was 55.2%, and the specificity was 85.4%. Since moderate-severe depressive patients need effective treatment and clinical attention, it is beneficial that the high specificity can effectively identify moderate-severe severity from mild.

Previous studies have found that patients with depressive tendencies use more negative emotion words and less (or similar) positive emotion words than others (5, 13, 18–20). But in this study, negative evaluative words were more significant than negative emotional words. This may be due to patients often using evaluative words to express their feelings and experiences in clinical interviews.

Research showed first-episode, drug-naive major depressive disorder and remitted major depressive disorder had differences in temporal gyrus activity. The temporal gyrus may play a critical role in depressive symptomatology (21). This can support that the negative bias of patients with depression is a state index (22). Therefore, it is meaningful to follow patients' word frequency. Past research did not subdivide their depressive symptom severity to explore differences in word usage among depression of different severities. Previous studies have primarily conducted word frequency extraction on people with a tendency to have depression on Weibo or Twitter, and define these subjects as a "patient." However, physicians have not systematically evaluated the "patients" of those evaluations. Therefore, the lack of necessary clinical details may affect the outcomes of their measures. Yet, in these studies, they are classified as patients with depression only according to words such as "depression" in their text. Therefore, there are some problems in its classification in those studies. To better assess these outcomes in the clinical setting, this study utilized psychiatrists who passed the HAMD-17 consistency assessment to judge patients' severity, allowing for a more reliable diagnosis of disease and severity.

We recognize several limitations of this study. Previous studies conducted data analysis by searching for textual

information of patients or non-patients on the Internet. They have a large sample size and cover a wide range of people, while this study was a small sample size for clinical interviews. Therefore, only indicators can be provided, and a machine learning model cannot be established for judging the severity of depression. The proportion of patients with MDD enrolled in this study is 20.0%, which is relatively low, so this may lead to a non-difference between the groups of moderate and severe patients. Although the HowNet sentiment dictionary has been used in a large number of studies, we didn't find literature that measures the reliability and validity of it. This may have an impact on our study. This study only counted the number of the designated four classifications of words. The association between individual word polarity and depressive symptom severity was not assessed. If the polarity of each word and the number of words are analyzed comprehensively, better results may be obtained. Patients who underwent modified electroconvulsive therapy (MECT) within 2 weeks were not excluded. MECT may affect the cognitive level of patients in a short period, affecting the expression and number of their vocabulary, thereby influencing the results of the study. This study is a cross-sectional study with no follow-up survey on patients. To further confirm that the word frequency feature can be used as a variable reflecting the severity of symptoms in patients with MDD, the patients should be followed up to explore whether the number of word frequencies changes when the patients' symptom severity is reduced.

Above all, the problems should be improved in future research to further explore the application value of language information in the symptom assessment of MDD.

CONCLUSIONS

In summary, as the severity of depressive symptoms increased, the number of negative evaluation words and negative emotional words in clinical interviews with MDD patients increased. And the word frequency based on HowNet sentiment dictionary may be beneficial in evaluating the severity of depressive symptoms.

DATA AVAILABILITY STATEMENT

The original contributions presented in the study are included in the article/supplementary material, further inquiries can be directed to the corresponding author/s.

ETHICS STATEMENT

The studies involving human participants were reviewed and approved by Ethics Committee of Beijing Anding Hospital Affiliated to Capital Medical University. The patients/participants provided their written informed consent to participate in this study.

AUTHOR CONTRIBUTIONS

JH, YF, NL, and LF developed the initial idea for the manuscript. JH wrote the main body of the paper and including citations. YF and LX contributed to revision and editing of the manuscript. XZ analyzed the data. GW revised the manuscript. All authors contributed to and have approved the final manuscript.

FUNDING

This study was supported by the Beijing Demonstrative Research Ward (Grant No. BCRW202009).

ACKNOWLEDGMENTS

The authors would like to thank all the participants and staff involved in this study.

REFERENCES

1. Huang Y, Wang Y, Wang H, Liu Z, Yu X, Yan J, et al. Prevalence of mental disorders in china: a cross-sectional epidemiological study. *Lancet Psychiatry.* (2019) 6:211–24. doi: 10.1016/S2215-0366(18)30511-X
2. World Health Organization. Depression and other common mental disorders (2018). Available online at: https://www.who.int/publications/i/item/depression-global-health-estimates (accessed: March 3, 2022).
3. Zhang H, Ji J. Prevalence of mental disorders in China. *Lancet Psychiatry.* (2019) 6:188–89. doi: 10.1016/S2215-0366(19)30034-3
4. Valenstein M, Vijan S, Zeber JE, Boehm K, Buttar A. The cost-utility of screening for depression in primary care. *Ann Intern Med.* (2001) 134:345–60. doi: 10.7326/0003-4819-134-5-200103060-00007
5. Leis A, Ronzano F, Mayer MA, Furlong LI, Sanz, F. Detecting signs of depression in tweets in Spanish: behavioral and linguistic analysis. *J Med Internet Res.* (2019) 21:e14199. doi: 10.2196/14199
6. Pulverman CS, Lorenz TA, Meston CM. Linguistic changes in expressive writing predict psychological outcomes in women with history of childhood sexual abuse and adult sexual dysfunction. *Psychol Trauma.* (2015) 7:50–7. doi: 10.1037/a0036462
7. Wang L, Li K, Zhang Q, Zeng Y, Dai W, Su Y, et al. Short-term effects of escitalopram on regional brain function in first-episode drug-naive patients with major depressive disorder assessed by resting-state functional magnetic resonance imaging. *Psychol Med.* (2014) 44:1417–26. doi: 10.1017/S0033291713002031
8. Song XH, Qiao YJ, Xie Q, Lin GZ, Shi YJ, Jin HY. Spatial pattern of brain activation during a Verbal Fluency Test in first-episode depressive disorder patients: a functional near-infrared spectroscopy study. *Chin J Contemp Neurol Neurosurg.* (2021) 21:1073–77. doi: 10.3969/j.issn.1672-6731.2021.12.008
9. Zhu Y, Mao W, Wang R. The neural mechanism of negative bias. *Adv Psychol Sci.* (2014) 22:1393–403. doi: 10.3724/SP.J.1042.2014.01393
10. Suslow T, Wildenauer K, Gunther V. Ruminative response style is associated with a negative bias in the perception of emotional facial expressions in healthy women without a history of clinical depression. *J Behav Ther Exp Psychiatry.* (2019) 62:125–32. doi: 10.1016/j.jbtep.2018.10.004
11. Vanderlind WM, Millgram Y, Baskin-Sommers AR, Clark MS, Joormann J. Understanding positive emotion deficits in depression: from emotion preferences to emotion regulation. *Clin Psychol Rev.* (2020) 76:101826. doi: 10.1016/j.cpr.2020.101826
12. Schoch-Ruppen J, Ehlert U, Uggowitzer F, Weymerskirch N, La Marca-Ghaemmaghami P. Women's word use in pregnancy: associations with maternal characteristics, prenatal stress, and neonatal birth outcome. *Front Psychol.* (2018) 9:1234. doi: 10.3389/fpsyg.2018.01234

13. Hussain J, Satti FA, Afzal M, Khan WA, Bilal HSM, Ansaar MZ, et al. Exploring the dominant features of social media for depression detection. *J Inf Sci.* (2019) 46:739–59. doi: 10.1177/0165551519860469
14. Yang C, Lai X, Hu Z, Liu Y, Shen P. Depression tendency screening use text based emotional analysis technique. *J Phys Conf Ser.* (2019) 1237:032035. doi: 10.1088/1742-6596/1237/3/032035
15. Huang ZS, Hu Q, Gu JG, Yang J, Feng Y, Wang G. Web-based intelligent agents for suicide monitoring and early warning. *China Digit Med.* (2019) 14:3–6. doi: 10.3969/j.issn.1673-7571.2019.03.001
16. Jia FZ, Chen CC. Emotional characteristics and time series analysis of Internet public opinion participants based on emotional feature words. *Int J Adv Robot Syst.* (2020) 17:1–11. doi: 10.1177/1729881420904213
17. Coppersmith G, Dredze M, Harman C, Hollingshead K. From ADHD to SAD: Analyzing the Language of Mental Health on Twitter through Self-Reported Diagnoses. In: *Proceedings of the 2nd Workshop on Computational Linguistics and Clinical Psychology: From Linguistic Signal to Clinical Reality* (Denver, CO). (2015). doi: 10.3115/v1/W15-1201
18. Hamilton M. A rating scale for depression. *J Neurol Neurosurg Psychiatry.* (1960) 23:56–62. doi: 10.1136/jnnp.23.1.56
19. Schwartz AH, Eichstaedt JC, Kern ML, Park G, Ungar LH. Towards Assessing Changes in Degree of Depression through Facebook. In: *Conference of the Association for Computational Linguistics* (Baltimore, MD). (2014). doi: 10.3115/v1/W14-3214
20. Preoiuc-Pietro D, Eichstaedt J, Park G, Sap M, Smith L, Tobolsky V, et al. The role of personality, age, and gender in tweeting about mental illness. In: *Workshop on Computational Linguistics and Clinical Psychology: FromLinguistic Signal to Clinical Reality* (Denver, CO). (2015). doi: 10.3115/v1/W15-1203
21. Yang C, Zhang A, Jia A, Ma JX, Sun N, Wang Y, et al. Identify abnormalities in resting-state brain function between first-episode, drug-naive major depressive disorder and remitted individuals: a 3-year retrospective study. *Neuroreport.* (2018) 29:907–16. doi: 10.1097/WNR.0000000000001054
22. Atchley RA, Stringer R, Mathias E, IIardi SS, Minatrea AD. The right hemisphere's contribution to emotional word processing in currently depressed, remitted depressed, and never-depressed individuals. *J Neurolinguistics.* (2007) 20:145–60. doi: 10.1016/j.jneuroling.2006.06.004

Conflict of Interest: The authors declare that the research was conducted in the absence of any commercial or financial relationships that could be construed as a potential conflict of interest.

frontiers | Frontiers in Psychiatry

ORIGINAL RESEARCH
published: 11 May 2022
doi: 10.3389/fpsyt.2022.914039

Altered Spontaneous Brain Activity Patterns of Meibomian Gland Dysfunction in Severely Obese Population Measured Using the Fractional Amplitude of Low-Frequency Fluctuations

*Yu-Ling Xu[1], Xiao-Yu Wang[1], Jun Chen[1], Min Kang[1], Yi-Xin Wang[2], Li-Juan Zhang[1], Hui-Ye Shu[1], Xu-Lin Liao[3], Jie Zou[1], Hong Wei[1], Qian Ling[1] and Yi Shao[1]**

[1] Department of Ophthalmology, The First Affiliated Hospital of Nanchang University, Nanchang, China, [2] Department of Ophthalmology and Visual Sciences, Cardiff University, Cardiff, United Kingdom, [3] Department of Ophthalmology and Visual Sciences, The Chinese University of Hong Kong, Shatin, Hong Kong SAR, China

OPEN ACCESS

Edited by:
Yujun Gao,
Wuhan University of Science and Technology, China

Reviewed by:
He Wang,
Xuzhou Medical University, China
Guigang Li,
Huazhong University of Science and Technology, China

***Correspondence:**
Yi Shao
freebee99@163.com

Specialty section:
This article was submitted to Neuroimaging and Stimulation, a section of the journal Frontiers in Psychiatry

Received: 06 April 2022
Accepted: 14 April 2022
Published: 11 May 2022

Citation:
Xu Y-L, Wang X-Y, Chen J, Kang M, Wang Y-X, Zhang L-J, Shu H-Y, Liao X-L, Zou J, Wei H, Ling Q and Shao Y (2022) Altered Spontaneous Brain Activity Patterns of Meibomian Gland Dysfunction in Severely Obese Population Measured Using the Fractional Amplitude of Low-Frequency Fluctuations. Front. Psychiatry 13:914039. doi: 10.3389/fpsyt.2022.914039

Objective: Utilizing the fractional amplitude of low-frequency fluctuations (fALFF) technique, this study sought to correlate spontaneous cerebral abnormalities with the clinical manifestations of meibomian gland dysfunction (MGD) in severely obese (SO) population.

Subjects and Methods: Twelve MGD patients in SO population (PATs) (4 males and 8 females) and twelve healthy controls (HCs) (6 males and 6 females) matched by gender and age were enrolled. Every participant underwent resting-state functional magnetic resonance imaging (rs-MRI) scanning. Spontaneous cerebral activity alterations were examined using the fALFF method. Receiver operating characteristic (ROC) curves were utilized to classify the medial fALFF values of the PATs and HCs. PATs were also asked to complete anxiety and depression score forms, permitting a correlation analysis.

Results: In contrast with HCs, PATs had prominently increased fALFF values in the left lingual gyrus, the right globus pallidus, the right anterior cingulate and paracingulate gyri and the left middle occipital lobe ($P < 0.05$), and decreased fALFF values in the right cerebellum, the left fusiform gyrus, the right medial orbitofrontal gyrus, the left triangle inferior frontal gyrus and the left inferior parietal gyrus ($P < 0.05$). The results of the ROC curve indicated that changes in regional fALFF values might help diagnose MGD in SO population. Moreover, fALFF values in the right cerebellum of PATs were positively correlated with hospital anxiety and depression scores (HADS) ($r = 0.723$, $P = 0.008$). The fALFF values in the left triangle inferior frontal gyrus of PAT were negatively correlated with HADS ($r = -0.651$, $P = 0.022$).

Conclusions: Aberrant spontaneous activity was observed in multiple regions of the cerebrum, offering helpful information about the pathology of MGD in SO population. Aberrant fALFF values in these regions likely relates to the latent pathologic mechanisms of anomalous cerebral activities in PATs.

Keywords: severe obesity, meibomian gland dysfunction, fALFF, RS-fMRI, spontaneous brain activity

INTRODUCTION

Obesity is an epidemic that affects 2 billion adults and 42 million children worldwide. Complications of obesity, such as hypertension and type 2 diabetes, are increasing (1). Obesity increases the risk of chronic organ failure, metabolic disease, and cancer. Further, it also increases the incidence of complications from acute illness (2). BMI (in kg/m^2) is the basic unit for most of the epidemiologic data about obesity, using the range of 18.5–24.9 to define normality, 25.0–29.9 for rank I obesity, 30.0–34.9 for rank II obesity, 35.0–39.9 for rank III obesity and $\geq$ 40.0 for rank IV or morbid obesity (3).

Obesity is usually accompanied by dyslipidemia, a major contributor to metabolic disease (4). Dyslipidemia is also considered to be a risk factor for MGD, which is the main cause of dry eye (5). The meibomian gland (MG) is a modified sebaceous gland in the eyelid. It produces meibomian, which is the lipid component of the tear film (6). MGD is the main cause of evaporative dry eye and is also one of the most common diseases encountered by ophthalmic nurses. MGD is characterized by obstruction of the duct at the end of the MG and/or changes in gland secretion, leading to changes in tear film stability, inflammation and irritation (7). The MG produces lipids that make up the meibomian, which have something in common with the blood. Some anecdotal reports have shown that dyslipidemia in obese patients can lead to MGD and change the composition of the meibomian lipid. Destruction of the meibomian lipid components can also increase the possibility of inflammation, an underlying cause of blepharitis, which affects the secretory function of the MG (6). This may result in decreased tear film quality and stability, and eventually leads to ocular surface inflammation in patients with MGD and dry eye (5). We observed that many SO people also had MGD. Due to the particularity of its anatomy, routine examination and diagnosis of MGD mainly relies on a corneal confocal microscope and fundus anatomy (**Figure 1**).

We use (fMRI) to detect brain changes (8, 9). fMRI is the mainstay of neuroimaging in cognitive neuroscience. Further development of image acquisition protocols, scanner technology, experimental design and analysis methods is expected to promote the capability of fMRI from simple mapping to actual research on brain tissues (10). fMRI can also be used to monitor the spontaneous activity of the human brain and offer a fresh explanation for the pathogeny of some diseases (11). Since it does not need any radioactive tracer, fMRI is appropriate for central mechanism studies. It can also detect and precisely position the spontaneous activity of the cerebrum via integrating functional and structural imaging (12). fALFF is an r-fMRI indicator that represents an improvement from ALFF and can more sensitively and specifically reflect regional spontaneous cerebral activity depending on blood oxygen level-dependent (BOLD) signal (13). Electrophysiologic research (14) has already indicated that low-frequency concussions are probably caused by spontaneous nerve actions, which is of great physiological importance. Further, the informational interactions between involved cerebral regions are reflected in the rhythmic activities of brain regions. fALFF enables us to identify brain areas

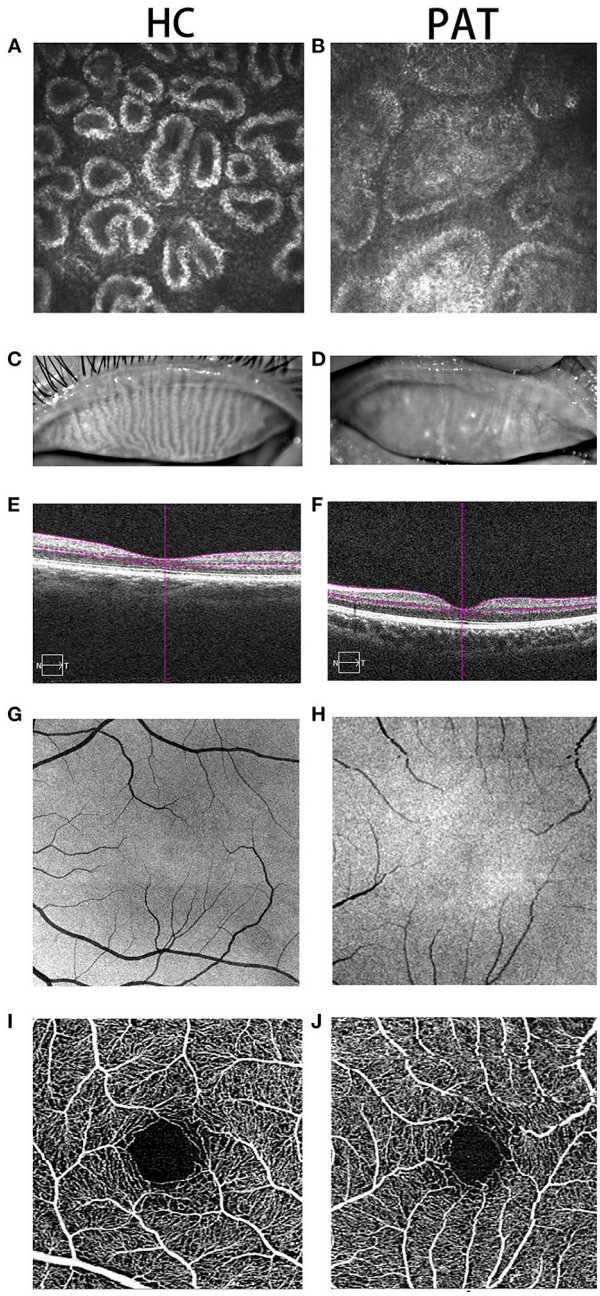

FIGURE 1 | Typical pictures of HC and PAT groups. Two groups of MGs were photographed by corneal confocal microscope. As can be seen from **(A,B)**, compared with the HC group, the MG in the PAT group was significantly blocked, and gland blockage was widened at the same time. What's more, we photographed the changes of the MGs under the naked eye in the HC group and the PAT group. From **(C,D)**, we can clearly observe that the MG in the HC group is clearer than that in the PAT group. Therefore, we can speculate that obesity may lead to tarsal gland blockage and degeneration. **(E,F)** According to the cross-sectional images of retinal thickness obtained, we can observe that the choroidal thickness in the PAT group is significantly thinner than that in the HC group. We also observed that the capillaries in the HC group **(G,I)** were more developed than those in the PAT group **(H,J)** according to the fundus vascular images we obtained, which showed that obesity may reduce the thickness of choroid and fundus blood supply, and may further cause fundus lesions. HC, healthy control; PAT, MGD patient in SO population; MG, meibomian gland.

with abnormal local functioning, thereby offering us a possible pathogenesis of MGD in SO population.

The purpose of this study was to explore the changes in spontaneous cerebral activity in MGD patients in SO population, and to explore its relationship with clinical features using fALFF.

PARTICIPANTS AND METHODS

Participants

A total of 12 MGD patients in SO population (8 men and 4 women, PATs) were enrolled from the Ophthalmology Department of the First Affiliated Hospital of Nanchang University. Inclusion criteria were: (1) BMI $\geq$ 30; (2) male' waistline $\geq$ 90 cm; female' waistline $\geq$ 85 cm; (3) diagnosed with MGD; and (4) capable of undergoing MRI scanning (no contraindications of magnetic resonance imaging such as cardiac pacemaker or implanted metal devices).

Exclusion criteria: (1) a history of a serious craniocerebral injury; (2) severe mental dysfunction; (3) history of excessive drinking; (4) history of drug abuse; (5) pregnancy; and (6) diseases that may cause changes in fMRI (systemic diseases, degenerative diseases, demyelinating diseases, and autoimmune diseases).

Twelve healthy controls (6 men and 6 women, HCs) were enlisted in this study, all of whom were age and gender matched with the PAT group. All HCs met the following criterion: (1) 24 $\geq$ BMI $\geq$ 20; (2) can undergo an MRI scan; (3) head MRI shows normal brain parenchyma; (4) no mental illness; and (5) no diseases that may cause changes in fMRI (systemic diseases, degenerative diseases, demyelinating diseases, and autoimmune diseases).

MRI Parameters

A Trio 3-Tesla MR scanner (Siemens, Munich, Germany) was utilized for conducting the process. Each participant was asked to stay sober, make sure their eyes closed, and breathe mildly during the scanning. After that, the datum were gathered by 3D damage gradient echo sequence with the subsequent augments: for 176 configurable image scans, we used a repetition time = 1900 ms, collection matrix = 256 × 256, visual field = 250 × 250 mm, echo time = 2.26 ms, thickness = 1.0 mm, interval = 0.5 mm, rollover angle = 9°. For 240 functional image scans, we utilized a repetition time = 2000 ms, acquisition matrix = 64 × 64, field of view = 220 × 220 mm, thickness = 4.0 mm, interval = 1.2 mm, echo time = 30 ms, rollover angle = 90°, and 29 axials. Every scan continued for 15 min or so.

FMRI Data Analysis

All functional datum was handled by a software percolator (www.MRIcro.com), and statistical parameter graphing was operated with SPM8 (The MathWorks, Inc., Natick, MA, USA) and rs-fMRI DPARSFA (http://rfmri.org/DPARSF) software data conducting coadjutants. The primary procedures of pretreatment included slice timing, head motion rectification, exerting Friston six-head movement parameters to eliminate head movement influences, dimensional standardization with normal echo complanate picture stencils to achieve Neurology Montreal Institute (MNI) standards, and smoothening with a Gaussian kernel of 6 × 6 × 6 mm^3 full-width at half-maximum (FW-HM). After correcting the head movement, we applied the standard echo plane image stencil to standardize the functional image for meeting the spatial standard of the Montreal Institute of Neurology. The overall impacts of changeability were diminished by distinguishing the fALFF values of every voxel by the overall average values of every participant.

Brain-Behavior Correlation Analysis

We utilized the resting-state fMRI datum analysis tool cabinet software; the cerebrum areas with disparate fALFF results between the two groups were divided into diverse portions. Definitively, correlative analysis was utilized to calculate the correlation between the medial fALFF values and behavior performance in every region of the PAT group ($P < 0.05$ significant differences).

Statistical Analysis

For fMRI data, a two-sample t-test was performed using the REST toolbox to examine the voxel-wise difference between the PATs and thr HCs; State Key Laboratory of Cognitive Neuroscience and Learning, Beijing Normal University, Beijing, China (The statistical threshold was set at the voxel level with $P < 0.05$, alphasim, and cluster size > 100 voxels for multiple comparison). These voxels were considered as regions of interest with prominent differences between the two groups.

RESULTS

Demographics and Behavioral Results

Age ($P = 0.365$) and gender ($P = 0.430$) were equivalent between the PATs and HCs. However, differences between the two groups were observed in their visual acuity, daily life score and mini-mental state examination ($P < 0.05$; **Table 1**).

TABLE 1 | Basic Information of participants in the study.

Condition	PAT	HC	t	*P*-value*
Male/female	4/8	6/6	N/A	0.430
Age (years)	34.25 ± 7.07	31.67 ± 5.98	0.925	0.365
Weight (kg)	111.92 ± 13.33	66.08 ± 10.41	8.986	<0.01#
Handedness	12R	12R	N/A	>0.99
Initial visual acuity-left eye (log Mar)	0.80 ± 0.16	0.58 ± 0.09	3.742	<0.01#
Initial visual acuity-right eye (log Mar)	0.83 ± 0.22	0.62 ± 0.13	2.813	<0.05*
Daily life score	90.92 ± 6.53	100.00 ± 0.00	4.617	<0.01#
MMSE	21.42 ± 4.37	27.83 ± 2.41	4.266	<0.01#

**P,0.05; #P,0.01; independent t-test, P-values between PATs and HCs. Data presented as mean ± standard deviation. HCs, healthy controls; PATs, MGD patients in SO population; MMSE, mini-mental state examination.*

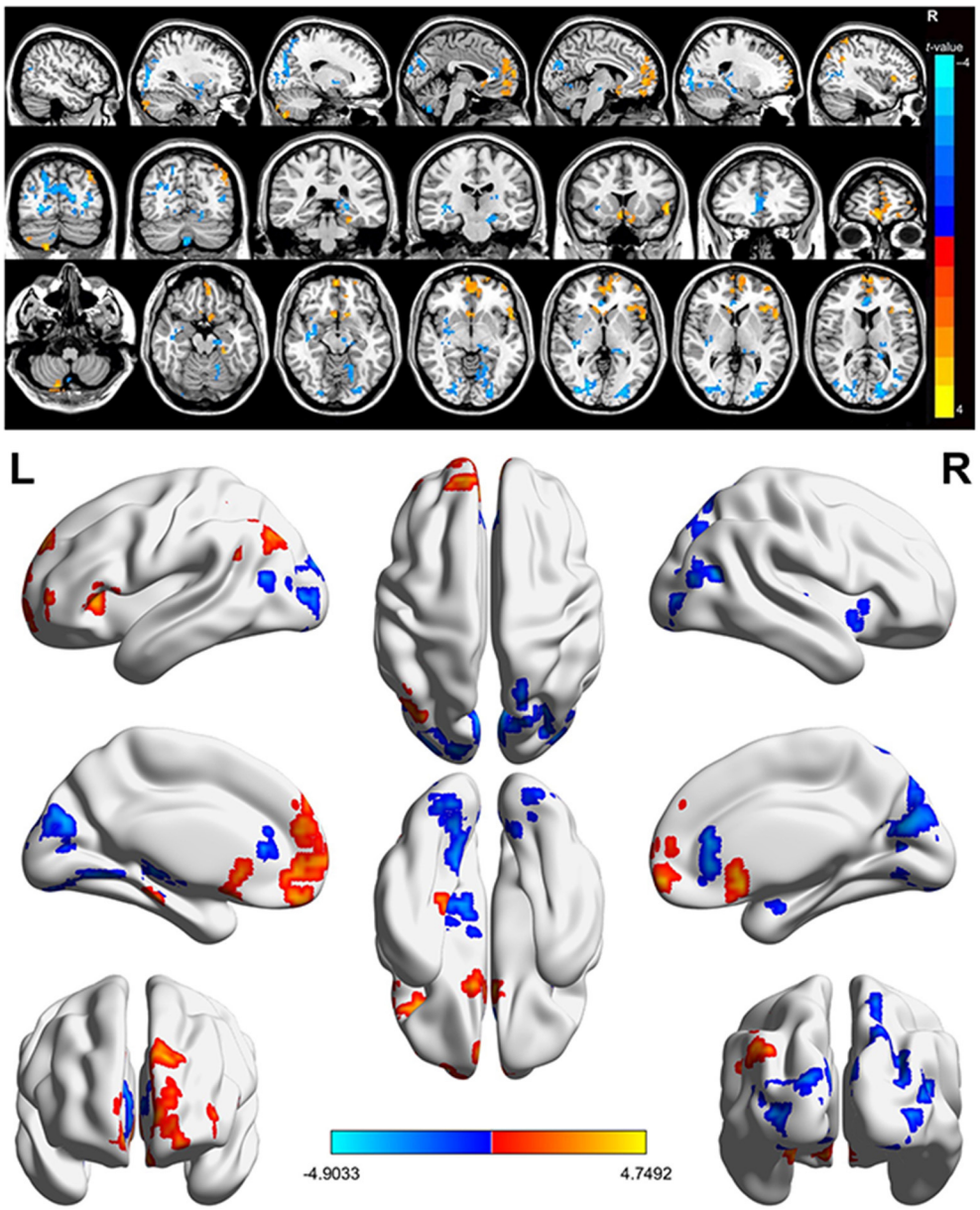

FIGURE 2 | Spontaneous brain activity in MGD patients in SO population. Red regions (left lingual gyrus, right lenticular globus pallidus, right anterior cingulate and paracingulate gyrus, left middle occipital gyrus) indicate higher fALFF values, while blue regions (right cerebellum, left fusiform gyrus, right medial orbitofrontal gyrus, left triangle inferior frontal gyrus, left inferior parietal gyrus) represent lower fALFF values ($P < 0.05$; AlphaSim-corrected; cluster size, >40). SO, severe obesity; MGD, meibomian gland dysfunction; fALFF, fractional amplitude of low-frequency fluctuations.

FALFF Differences Between PATs and HCs

In contrast with HCs, PATs had significantly decreased fALFF values in the right cerebellum, the left fusiform gyrus, the right medial orbitofrontal gyrus, the left triangle inferior frontal gyrus and the left inferior parietal gyrus, which means the activity of those brain regions are reduced, indicating dysfunctional brain activity in those lobes. Further, PATs had increased fALFF values in the left lingual gyrus, the right globus pallidus, the right anterior cingulate and paracingulate gyri and the left middle occipital gyrus, which means these brain regions are more active than the normal, indicating that there might be compensatory processes for some impaired function in other brain regions (**Figures 2–4** and **Table 2**).

Receiver Operating Characteristic Curve

There were significant differences in the fALFF values between PATs and HCs. We therefore decided that fALFF values could be used to differentiate PATs from HC. We then drew a ROC

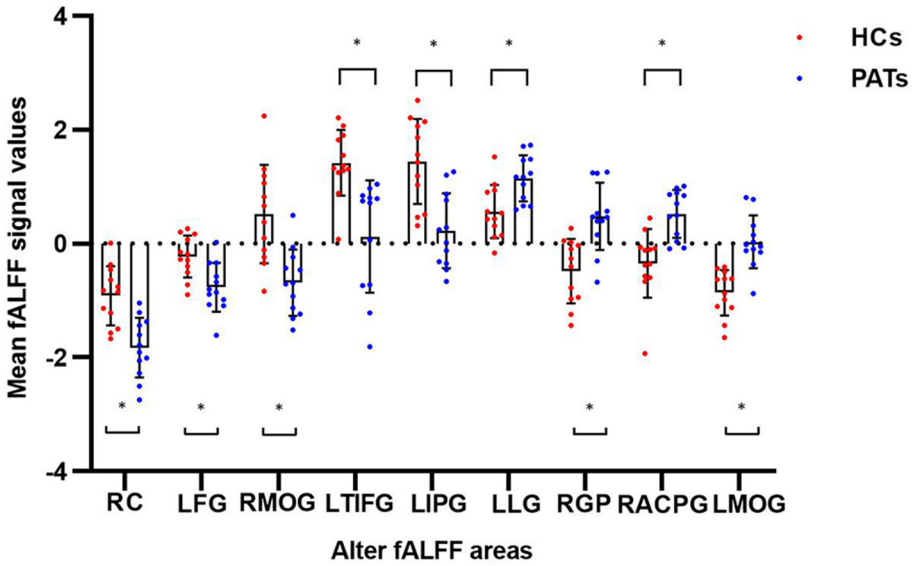

FIGURE 3 | The mean fALFF values between the PATs group and HCs. Means of altered spontaneous brain activity between the PATs group and HCs group (each $n = 12$). Compared with HCs, asterisk means the statistical significance $p < 0.05$. RC, right cerebellum; LFG, left fusiform gyrus; RMOG, right medial orbitofrontal gyrus; LTIFG, left triangle inferior frontal gyrus; LIPG, left inferior parietal gyrus; LLG, left lingual gyrus; RGP, right globus pallidum; RACPG, right anterior cingulate and paracingulate gyri; LMOG, left middle occipital gyrus; fALFF, fractional amplitude of low-frequency fluctuations; HCs, healthy controls; PATs, MGD patients in SO population.

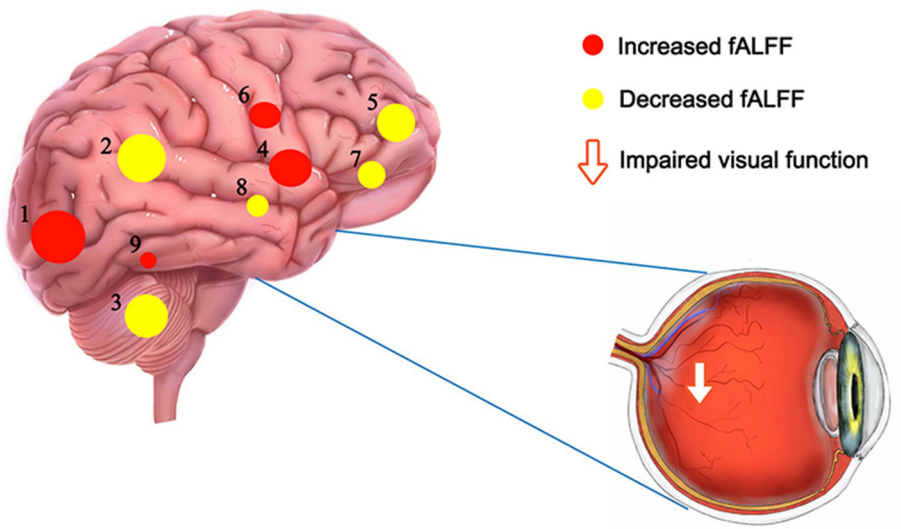

FIGURE 4 | The fALFF results of brain activity in the PAT group. Compared with the HCs, the fALFF of the following regions were increased to various extents: 1-left middle occipital gyrus (t = 4.9), 4-right globus pallidum (t = 4.36), 6-right anterior cingulate and paracingulate gyri (t = 4.24), 9-left lingual gyrus (t = 3.54), and decreased fALFF values in the 2-left inferior parietal gyrus (t = – 4.75), 3-right cerebellum (t = – 4.69), 5-right medial orbitofrontal gyrus (t = – 4.35), 7- left triangle inferior frontal gyrus (t = – 4.05) and 8-left fusiform gyrus (t = – 3.688). The sizes of the spots denote the degree of quantitative changes. HCs, healthy controls; fALFF, fractional amplitude of low-frequency fluctuations; PAT, MGD patient in SO population.

curve to analyze the medial fALFF values of disparate cerebral areas. The area under the curve (AUC) denoted the diagnosis rate. A value of 0.5 to 0.7 signified low accuracy, 0.7 to 0.9 signified medium accuracy, and >0.9 signified high accuracy. The AUCs were 0.8889 ($p < 0.005$; 95% CI: 0.7620–1.000) for the right cerebellum (RC), 0.8403 ($p < 0.005$; 95% CI: 0.6802–1.000) for the left fusiform gyrus (LFG), 0.8889 ($p < 0.005$; 95% CI: 0.7580–1.000) for the right medial orbitofrontal gyrus (RMOG), 0.9375 ($p < 0.001$; 95% CI: 0.8351–1.000) for the left triangle inferior frontal gyrus (LTIFG) and 0.8889 ($p < 0.005$; 95% CI:

0.7606–1.000) for the left inferior parietal gyrus (LIPG) [HCs > PATs]. The AUCs were 0.8472 ($p < 0.005$; 95% CI: 0.6836–1.000) for the left lingual gyrus (LLG), 0.9028 ($p < 0.001$; 95% CI: 0.7744–0.992) for the right globus pallidum (RGP), 0.9236 ($p < 0.001$; 95% CI: 0.8219–1.000) for the right anterior cingulate and paracingulate gyri (RACPG), and 0.9514 ($p < 0.001$; 95% CI: 0.8547–1.000) for the left middle occipital gyrus (LMOG) [HCs < PATs]. In summary, these results indicate that the fALFF values of different areas of the cerebral areas might help in the diagnosis of MGD in SO patients. In addition, the ROC curves showed that the fALFF values of LTIFG, RACPG, LMOG, RC, RMOG, LIPG and RGP were more clinically relevant than LFG and LLG (**Figure 5**).

TABLE 2 | Brain regions with significant differences in fALFF between the HC and PAT groups.

fALFF	Brain areas	MNI coordinates			BA	Peak voxels	*T*-value
		X	Y	Z			
HC > PAT							
1	RC	21	−81	−57		152	4.69
2	LFG	−27	−33	−18	36	103	3.688
3	RMOG	3	60	−12	10	440	4.35
4	LTIFG	−54	15	−6	45	100	4.05
5	LIPG	−48	−63	51	40	116	4.75
HC < PAT							
6	LLG	−18	−69	−12	19	106	−3.54
7	RGP	39	−21	0	13	115	−4.36
8	RACPG	6	33	12	24	138	−4.24
9	LMOG	−30	−78	3	18	782	−4.9

For fALFF data, two-sample t-test was performed to examine the voxel-wise difference between the PAT and HC groups using the REST toolbox. The statistical threshold was set at the voxel level with P<0.05, FDR corrected, and cluster size>100 voxels for multiple comparison. These voxels were regarded as the regions of interest showing significant difference between the two groups.fALFF, fractional amplitude of low-frequency fluctuations; HC, healthy control; PAT, MGD patient in SO population; RC, right cerebellum; LFG, left fusiform gyrus; RMOG, right medial orbitofrontal gyrus; LTIFG, left triangle inferior frontal gyrus; LIPG, left inferior parietal gyrus; LLG, left lingual gyrus; RGP, right globus pallidum; RACPG, right anterior cingulate and paracingulate gyri; LMOG, left middle occipital gyrus.

Rs-FMRI-FALFF Value of PATs' Brain Regions and HADS Scores

The fALFF values of the right cerebellum of PATs had a significantly positive correlation with HADS ($r = 0.723$, $P = 0.008$), and the fALFF values of the left triangle inferior frontal gyrus of PATs were significantly negatively correlated with HADS ($r = -0.651$, $P = 0.022$) (**Figure 6**).

DISCUSSION

Obesity is related to severe health risks (15). Severe obesity further increases the risk of obesity-correlative complications such as coronary heart disease, end-stage kidney disease and MGD. This study was designed to investigate the connection between MGD patients in SO population and functional cerebral changes using the fALFF technique. In contrast with HCs, PATs had significantly decreased fALFF values in their right cerebellum, left fusiform gyrus, right medial orbitofrontal gyrus, left triangle inferior frontal gyrus and left inferior parietal gyrus.

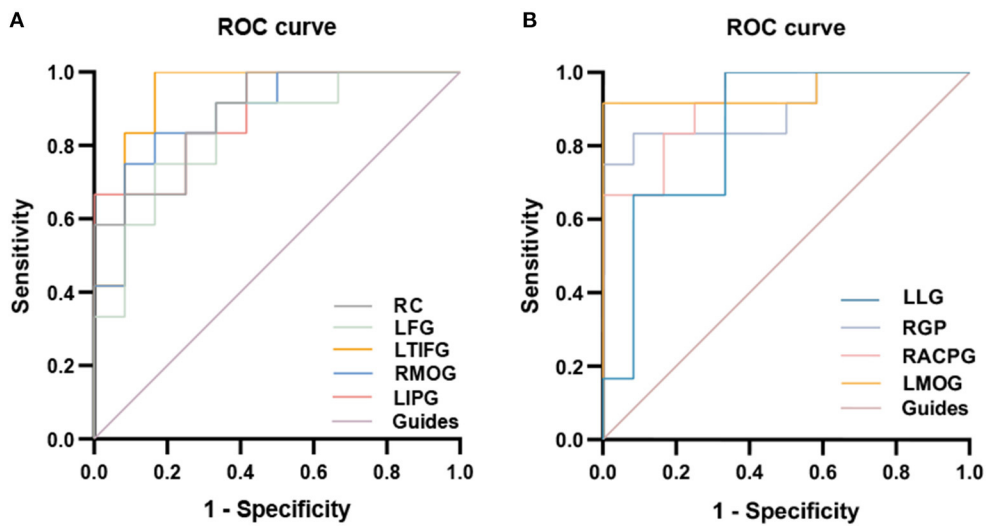

FIGURE 5 | ROC curve analysis of the mean fALFF values for altered brain regions. **(A)** The area under the ROC curve were 0.8889 ($p < 0.005$; 95% CI 0.7620–1.000) for RC, LFG 0.8403 ($p < 0.005$; 95% CI 0.6802–1.000), RMOG 0.8889 ($p < 0.005$; 95% CI 0.7580–1.000), LTIFG 0.9375 ($p < 0.001$; 95% CI 0.8351–1.000), LIPG 0.8889 ($p < 0.005$; 95% CI 0.7606–1.000) [HCs > PATs]. **(B)** The area under the ROC curve were 0.8472 ($p < 0.005$; 95% CI 0.6836–1.000) for LLG, RGP 0.9028 ($p < 0.001$; 95% CI 0.7744–0.992), RACPG 0.9236 ($p < 0.001$; 95% CI 0.8219–1.000), LMOG 0.9514 ($p < 0.001$; 95% CI 0.8547–1.000) [HCs < PATs]. fALFF, fractional amplitude of low-frequency fluctuations; ROC, receiver operating characteristic; RC, right cerebellum; LFG, left fusiform gyrus; RMOG, right medial orbitofrontal gyrus; LTIFG, left triangle inferior frontal gyrus; LIPG, left inferior parietal gyrus; LLG, left lingual gyrus; RGP, right globus pallidum; RACPG, right anterior cingulate and paracingulate gyri; LMOG, left middle occipital gyrus; HCs, healthy controls; PATs, MGD patients in SO population.

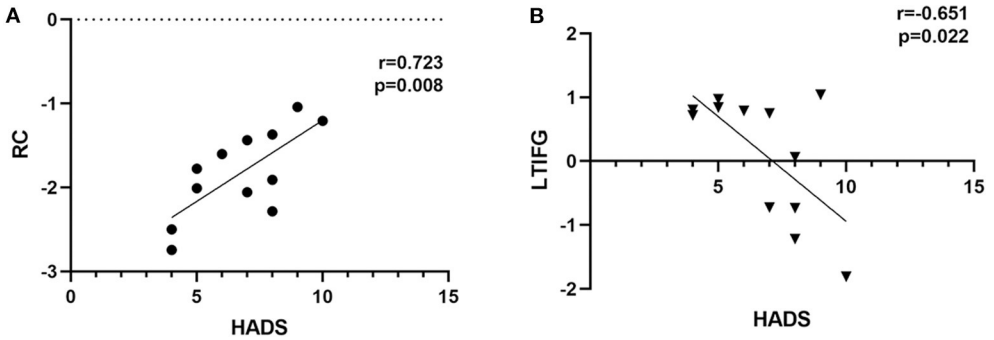

FIGURE 6 | Correlation analysis result. **(A)** The fALFF values in the right cerebellum of PAT presented significantly positive correlation with HADS ($r = 0.723$, $P = 0.008$). **(B)** The fALFF values in the left triangle inferior frontal gyrus of PAT presented significantly negative correlation with HADS ($r = -0.651$, $P = 0.022$). fALFF, fractional amplitude of low-frequency fluctuations; HADS, hospital anxiety and depression scores; PAT, MGD patient in SO population.

TABLE 3 | fALFF method applied in systemic, neurogenic and mental diseases.

	Author	Year	Disease
Systemic diseases	Zhang et al. (16)	2021	Subclinical Hypothyroidism
	Quan et al. (17)	2022	Acute Basal Ganglia Ischemic Stroke
	Zhang et al. (18)	2021	neovascular glaucoma
	Bak et al. (19)	2018	AIDS
	Zhang et al. (20)	2019	Diabetes
Neurogenic diseases	Rong et al. (21)	2021	Parkinson's Disease
	Luo et al. (22)	2020	Hemifacial Spasm
	Fulong et al. (23)	2018	Narcolepsy with Cataplexy
	Kim et al. (24)	2021	Migraine
Mental diseases	Qiu et al. (25)	2019	Major depressive disorder
	Egorova et al. (26)	2017	Post-stroke depression
	Xu et al. (27)	2015	Schizophrenia
	Qiu et al. (28)	2021	Bipolar disorder
	Liu et al. (29)	2021	Cognitive Impairment

fALFF, fractional amplitude of low-frequency fluctuations.

In contrast, increased fALFF values were seen in PATs in the left lingual gyrus, the right globus pallidus, the right anterior cingulate and paracingulate gyri and the left middle occipital lobe. fALFF has been used in a variety of diseases with success and its clinical use is likely to expand (**Table 3**). We did some research on brain regions alternations and its potential impact to better understand the brain changes in the PATs (**Table 4**).

From the results, we can see that the PATs have significantly decreased fALFF values in the right cerebellum. The right cerebellum plays a critical role in the collaboration between reflex and autonomic motion. An increasing amount of evidence has shown that the right cerebellum also plays a role in cognition and emotion (30). In late-onset depression patients, excessive cerebellar functional connectivity (FC) with the medial prefrontal lobe was significantly associated with depression symptoms (31). Su et al. (32) studied the cerebral metabolism of patients with depression using PET, suggesting that changes in cerebellar metabolism likely play an important role in depression pathophysiology. Several metabolic-related studies have found that the metabolic activity of the right posterior cerebellar lobe in patients with major depression is enhanced (33). Previous studies have also reported reduced cerebral blood flow in the cerebellums of depression patients (34). Furthermore there's research suggested that the functional decline in cerebellar gray matter is related to Alzheimer's disease (AD) (35). Other studies have shown that interruption of the connection between the cerebellum and the right dorsolateral prefrontal cortex is related to the severity of negative symptoms, leading to schizophrenia (36). These studies show a potential relation of the PATs with cognition and emotion diseases such as depression, AD and schizophrenia. This goes in line with our findings that the fALFF values of the right cerebellum of PATs had a significantly positive correlation with HADS.

The fusiform gyrus (FG), also called the lateral occipitotemporal gyrus, is a portion of the temporal lobe and occipital lobe in Brodmann area 37. Although the function of the FG is not completely clear, it has been connected with a large number of neural pathways associated with recognition. Moreover, the FG has been connected with a variety of neurological diseases such as dyslexia, prosopagnosia and alexia. The visual form area of the left FG is usually in a low activation state in dyslexia patients (37, 38). There is increasing evidence that the FG is involved in face and word processing. Selective damage to the FG can lead to serious defects in facial recognition, but printed character recognition remains relatively intact (39). There are different facial and word selection areas in the FG (40). It is conceivable that lesions that only destroy the areas of the FG that are selective to the face will lead to relatively simple facial agnosia, while lesions in the areas of the FG that are selective to words will lead to relatively simple alexia. In the present study, we found that the PATs showed reduced fALFF values in the left FG, and this might be reflective of dysfunction in that region, which means the PATs may have potential relations with the neurological diseases mentioned above.

The right medial orbitofrontal cortex (mOFC) is a critical area that records various high-order motor control processes (41).

TABLE 4 | Brain regions alternations and its potential impact.

Brain regions	Experimental result	Brain function	Anticipated results
Right cerebellum	HCs > PATs	Language and executive functions, physical balance, motor coordination,	AD,depression, Schizophrenia
Left fusiform gyrus	HCs > PATs	Visual word formation, faces and words processing	Dyslexia, prosopagnosia, alexia
Right medial orbitofrontal gyrus	HCs > PATs	Social evaluation, decision making, affective representation	anxiety, PTSD, Catatonia, Schizophrenia
Left triangle inferior frontal gyrus	HCs > PATs	Searching space extension, concepts selection, information evaluation, association inhibition	Depression, anorexia nervosa, dyslexia, conversion disorder
Left lingual gyrus	HCs < PATs	dreaming, facial expressions, terrain, face and visual word recognition	CUQ, hyperactivity with "visual snow"
Right globus pallidum	HCs < PATs	Learning and adjustment, development and control of habitual behaviors	Low self-efficacy, Huntington's disease
Right anterior cingulate and paracingulate gyri	HCs < PATs	Emotional regulation, cognitive processes, and specific motor functions.	AD,TAO,BVFD
Left middle occipital gyrus	HCs < PATs	Language, concept, number, analysis, logical reasoning, visual processing, perception	Major depression, high myopia

HCs, healthy controls; PATs, MGD patients in SO population; AD, Alzheimer's disease; PTSD, post-traumatic stress disorder; TAO, thyroid-associated ophthalmopathy; BVFD, behavioral variant frontotemporal dementia; CUQ, contralateral upper quadrantanopsias.

Changes in the mOFC may lead to a variety of neuropsychiatric disorders and their clinical symptoms (42). Function of the frontal limbic areas, especially the mOFC, is related to social evaluation, decision-making and emotional representation (43), and its impairment may directly affect the social driving force and emotion of patients with negative symptoms. de Leeuw et al. (44) observed that abnormal reward-related activation in the striatum was associated with negative symptoms in patients with schizophrenia compared with their unaffected siblings. Shukla et al. (45) also reported a decrease in the functional connectedness of the frontal striatum of patients with schizophrenia, and suggested that there is a connection between the striatum and the right mOFC in the development of negative symptoms. Hirjak et al. (46) confirmed that schizophrenic spectrum disorder (SSD) patients with catatonia mainly showed a reduction in the surface area of the mOFC compared with non-catatonic patients. mOFC anomalies have also been detected in a variety of anxiety disorders (47). Structural MRI studies suggested that reduced mOFC volume was related to anxiety disorder. Previous study found that cancer survivors with post-traumatic stress disorder (PTSD) had reduced OFC volume compared with cancer survivors and healthy groups without PTSD (48). In the present study, we found that the PATs exhibited lower fALFF values in the right medial orbitofrontal gyrus, indicating the dysfunction of them, which may be the reason for emotional disorders in the PATs.

The left triangle inferior frontal gyrus is a section of the inferior frontal gyrus (IFG) that is situated between the ascendant branch and the anterior branch. It is the central part of Broca's athletic language region and is involved in sensory and emotional information evaluation (49). Becker et al. (50) summarized that the IFG, which is already active during search and solution in verbal creative problem solving, is likely to take part in the extension of the search space that leads to the right solution. In addition, the IFG pars triangularis likely participates in the inhibition of solution irrelevant associations. The IFG pars triangularis is also associated with concept selection by means of solving competitions between active representations (51). Cheng et al. (52) reported that there is some connection between the IFG pars triangularis and Parkinson's syndrome. Qi et al. (53) pointed out that children's language performance is related to the asymmetric changes of cortical thickness in the IFG pars triangularis. In addition, Yang et al. (54) further found that the faster execution control response time was related to the smaller gFCD value in the trigonum of the IFG. In the this study, we found that the PATs exhibited lower fALFF values in the left triangle inferior frontal gyrus, indicating dysfunctional brain activity in those lobes, which may lead to emotional disorders in the PATs.

The lingual gyrus (LG) adjoins the continuous parahippocampal gyrus in the front, connecting to the talar sulcus on the medial side and the accessory sulcus separated from the medial inferior fusiform gyrus on the lateral side. It is related to terrain recognition, face recognition and dreaming. Bilateral LG activation is related to facial expression. The LG is also related to the visual recognition of characters. Lesions in the LG are related to contralateral upper quadrant insomnia and hyperactivity with "visual snow" (55). Meadows et al. (56) stated that a LG lesion was involved in prosopagnosia. Areas of abnormal brain color vision were also found in the occipitotemporal lobe (57), more precisely in the LG and the fusiform gyrus (58, 59). Bilateral lesions of the lingual and fusiform gyri can lead to achromatopsia, while unilateral right- or left-sided lesions may result in hemiachromatopsia (60). We found that the PATs have significantly higher fALFF values in the left LG, which may indicate the functional improvement to compensate for impaired visual acuity.

The globus pallidum (GP) is the main striatal outflow target and a central structure of the basal ganglia. It is a triangular cell mass located inside the putamen (61). Neuroimaging studies

(62–64) have shown that patients with Huntington's disease (HD) have severe atrophy of the GP. A brain structure study on factors related to general self-efficacy in young people reported that the degree of motivation is related to an above average diffusion rate of the right putamen, GP and caudate nucleus, and the degree of physical activity is related to the right putamen (65). Nakagawa et al. (66) reported that self-efficacy scores on the General Self-Efficacy Scale were related to lower mean diffusivity values in the lenticular nucleus (putamen and GP). GP also seems to be related to learning and adaptation. The dorsolateral posterior putamen/GP area likely plays a crucial role in the development and management of human habitual manifestation (learning) (67). Furthermore, the inner part of the GP projects to the thalamus and brainstem nucleus, which control motor behavior (regulation) (68). Insufficient function of the lenticular nucleus may therefore lead to decreased self-efficacy. Volume reduction in the indirect pathway involving the dorsolateral side of the right GP is related to the reduced understanding of the causal effects of goal-directed behavior in young patients with depression (66). In the present study, we found that the PATs exhibited significantly higher fALFF values in the right GP, which may be a compensatory process of emotional disorders.

A large number of neuroimaging studies have suggested that the anterior cingulate cortex is related to cognitive processes, emotional regulation and specific motor functions (69). Silkiss et al. (70) found that the gray matter layer of the right anterior cingulate gyrus became thinner and linked this to the emotional manifestations of thyroid-associated ophthalmopathy. Feng et al. (71) discovered that patients with Alzheimer's Disease had FC destruction in certain brain areas of the left hippocampal functional network, which includes the right anterior cingulate gyrus and the paracingulate gyrus. Moreover, the FC was reduced in certain brain areas of the right hippocampal functional network, including the bilateral anterior cingulate gyrus (71). Prior imaging (72) and pathologic case series (73) have focused on the regional relevance of the anterior cingulate, orbitofrontal and anterior insular cortices. The right hemisphere tends to contribute to behavioral variant frontotemporal dementia. In the present study, we found that the PATs have significantly higher fALFF values in the right anterior cingulate and paracingulate gyrus, which may reflects a compensatory process of emotional disorders.

The left middle occipital gyrus (L-MOG), which lies in the left hemisphere, takes part in a variety of functions such as analysis, language, notion, digit and logic. The occipital gyrus is associated with visual processing, especially early visual processing (74). MOG is also involved in the perception of softness (75), and its response to texture is more sensitive than proprioception (76). The occipital lobe, which includes the bulk of the optical cortex, is involved in communication with the cerebral cortex and the process of visual information. It also participates in the perception of facial emotion. Teng et al. (77) discovered that the fALFF of the left middle occipital gyrus was observably lower in patients with major depression than in healthy controls. An additional study characterized the role of the MOG in the regulation of unconscious face/tool processing by category-selective attention, and found that the activation of the MOG decreased under facial selective attention in the course of unconscious face processing (78). In accordance with these studies, fALFF of the L-MOG likely offers a neural basis for the interruption of visual processing in female patients with major depression. Further, high myopia patients exhibited reduced cortical surface thickness in the L-MOG compared with HCs. Wu et al. (79) believed that the multi-layer cortical thickness of

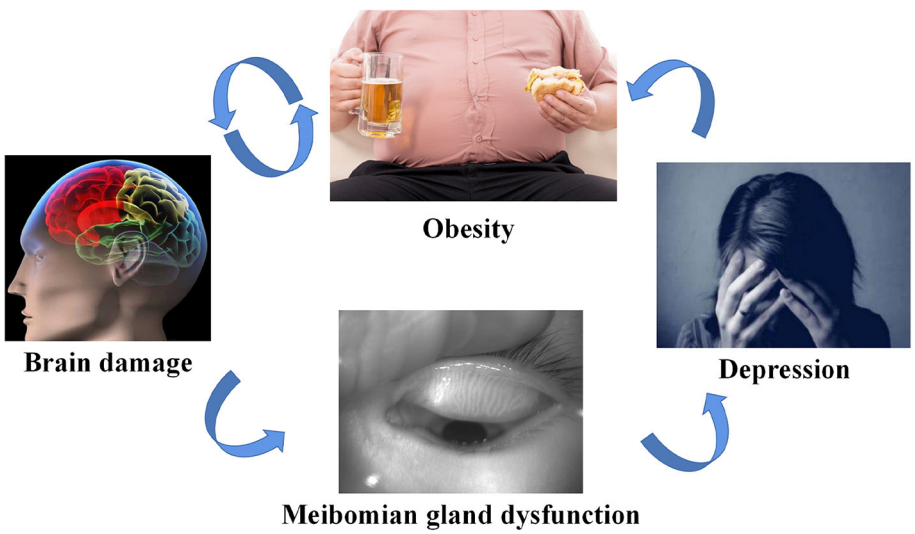

FIGURE 7 | Schematic diagram of the relationship between SO, brain dmage, MGD and depression. Compared with the HCs, fALFF values of the right cerebellum were significantly decreased in the PATs, which were more likely to suffer from anxiety and depression. (Anxiety and depression are not critical symptoms of MGD in SO population). SO, severe obesity; MGD, meibomian gland dysfunction; fALFF, fractional amplitude of low-frequency fluctuations; HCs, healthy controls; PATs, MGD patients in SO population.

patients with high myopia (HM) changed, suggesting that HM may lead to structural changes in relevant brain areas, in fragile areas that result in graver deterioration of myopia or both (79). We found that the PATs showed higher fALFF values in the L-MOG, which may be a compensatory process of impaired visual acuity and emotional disorders.

Our outcomes indicated that the anxiety and depression scores of the PAT group were higher than those of the HC group. It is likely that altered spontaneous brain activity is related to changes in the emotional processing of MGD patients in SO population (**Figure 7**).

There was limitation in our study. Our sample size is relatively small. In the follow-up in-depth study, we will expand the sample size to exclude the influence of regional and other environmental factors on the experimental results, to obtain more accurate data. But this study can still suggest some clinical significance.

CONCLUSION

Our outcomes indicate that spontaneous activity alternations were detected in many areas of the cerebrum in MGD patients in SO population compared to the healthy. Abnormal fALFF values of these cerebral regions may indicate the early stage of MGD in SO population and can be used to predict and prevent the development of the disease. This research provides brand-new insights into the cerebral abnormalities of MGD in SO population from the standpoint of dynamic regional cerebral activity, emphasizing the importance of fALFF variations in clarifying the neuropathological mechanisms of MGD in SO population and may provide a method for diagnosing this disease.

DATA AVAILABILITY STATEMENT

The original contributions presented in the study are included in the article/supplementary files, further inquiries can be directed to the corresponding authors.

ETHICS STATEMENT

The studies involving human participants were reviewed and approved by the Medical Ethics Committee of the First Affiliated Hospital of Nanchang University (Nanchang, China). The patients/participants provided their written informed consent to participate in this study.

AUTHOR CONTRIBUTIONS

All authors listed have made a substantial, direct, and intellectual contribution to the work and approved it for publication.

FUNDING

National Natural Science Foundation (No. 82160195); Central Government Guides Local Science and Technology Development Foundation (No. 20211ZDG02003); Key Research Foundation of Jiangxi Province (Nos. 20181BBG70004 and 20203BBG73059); Excellent Talents Development Project of Jiangxi Province (No. 20192BCBL23020); Natural Science Foundation of Jiangxi Province (No. 20181BAB205034).

REFERENCES

1. Stein CJ, Colditz GA. The epidemic of obesity. *J Clin Endocrinol Metab.* (2004) 89:2522–5. doi: 10.1210/jc.2004-0288
2. Barazzoni R, Bischoff S, Boirie Y, Busetto L, Cederholm T, Dicker D, et al. Sarcopenic obesity: time to meet the challenge. *Obes Facts.* (2018) 11:294–305. doi: 10.1159/000490361
3. Hales CM, Carroll MD, Fryar CD, Ogden CL. Prevalence of obesity and severe obesity among adults: united states, 2017–2018. *NCHS Data Brief.* (2020) 360:1–8.
4. Borlaug BA, Reddy YN. Getting at the heart of central obesity and the metabolic syndrome. *Circ Cardiovasc Imaging.* (2016) 9:e005110. doi: 10.1161/CIRCIMAGING.116.005110
5. Kuriakose RK, Braich P. Dyslipidemia and its association with meibomian gland dysfunction: a systematic review. *Int Ophthalmol.* (2018) 38:1809–16. doi: 10.1007/s10792-017-0633-0
6. Knop E, Knop N, Millar T, Obata H, Sullivan DA. The international workshop on meibomian gland dysfunction: report of the subcommittee on anatomy, physiology, and pathophysiology of the meibomian gland. *Invest Ophthalmol Vis Sci.* (2011) 52:1938–78. doi: 10.1167/iovs.10-6997c
7. Sabeti S, Kheirkhah A, Yin J, Dana R. Management of meibomian gland dysfunction: a review. *Surv Ophthalmol.* (2020) 65:205–17. doi: 10.1016/j.survophthal.2019.08.007
8. Bekiesińska–Figatowska M, Helwich E, Rutkowska M, Stankiewicz J, Terczyńska I. Magnetic resonance imaging of neonates in the magnetic resonance compatible incubator. *Arch Med Sci.* (2016) 12:1064–70. doi: 10.5114/aoms.2016.61913
9. Liu H, Wang X. Correlation of iron deposition and change of gliocyte metabolism in the basal ganglia region evaluated using magnetic resonance imaging techniques: an in vivo study. *Arch Med Sci.* (2016) 12:163–71. doi: 10.5114/aoms.2016.57593
10. Logothetis NK. What we can do and what we cannot do with fMRI. *Nature.* (2008) 453:869–78. doi: 10.1038/nature06976
11. Dai XJ, Liu CL, Zhou RL, Gong HH, Wu B, Gao L, et al. Long–term total sleep deprivation decreases the default spontaneous activity and connectivity pattern in healthy male subjects: a resting-state fMRI study. *Neuropsychiatr Dis Treat.* (2015) 11:761–72. doi: 10.2147/NDT.S78335
12. Biswal BB. Resting state fMRI: a personal history. *Neuroimage.* (2012) 62:938–44. doi: 10.1016/j.neuroimage.2012.01.090
13. Zou QH, Zhu CZ, Yang Y, Zuo XN, Long XY, Cao QJ, et al. An improved approach to detection of amplitude of low-frequency fluctuations (ALFF) for resting-state fMRI: fractional aLFF. *J Neurosci Methods.* (2008) 172:137–41. doi: 10.1016/j.jneumeth.2008.04.012
14. Cordes D, Haughton VM, Arfanakis K, Carew JD, Turski PA, Moritz CH, et al. Frequencies contributing to functional connectivity in the cerebral cortex in "resting–state" data. *AJNR Am J Neuroradiol.* (2001) 22:1326–33.
15. Guidelines (2013) for managing overweight and obesity in adults. preface to the expert panel report (comprehensive version which includes systematic evidence review, evidence statements, and recommendations). *Obesity (Silver Spring).* (2014) 22(Suppl. 2):S40. doi: 10.1002/oby.20822
16. Zhang Y, Yang Y, Tao B, Lv Q, Lui S, He L. Gray matter and regional brain activity abnormalities in subclinical hypothyroidism. *Front Endocrinol (Lausanne).* (2021) 12:582519. doi: 10.3389/fendo.2021.582519
17. Quan X, Hu S, Meng C, Cheng L, Lu Y, Xia Y, et al. Frequency–Specific changes of amplitude of low–frequency fluctuations in patients

with acute basal ganglia ischemic stroke. *Neural Plast.* (2022) 2022:4106131. doi: 10.1155/2022/4106131
18. Zhang YQ, Peng MY, Wu SN Yu CY, Chen SY, Tan SW, et al. Fractional amplitude of low–frequency fluctuation in patients with neovascular glaucoma: a resting–state functional magnetic resonance imaging study. *Quant Imaging Med Surg.* (2021) 11:2138–50. doi: 10.21037/qims-20-855
19. Bak Y, Jun S, Choi JY, Lee Y, Lee SK, Han S, et al. Altered intrinsic local activity and cognitive dysfunction in hIV patients: a resting–state fMRI study. *PLoS ONE.* (2018) 13:e0207146. doi: 10.1371/journal.pone.0207146
20. Zhang Q, Zhang P, Yan R, Xu X, Mao C, Liu X, et al. A single–Blinded trial using resting–State functional magnetic resonance imaging of brain activity in patients with type 2 diabetes and painful neuropathy. *Diabetes Ther.* (2019) 10:135–47. doi: 10.1007/s13300-018-0534-x
21. Rong S, Zhang P, He C, Li Y, Li X, Li R, et al. Abnormal neural activity in different frequency bands in parkinson's disease with mild cognitive impairment. *Front Aging Neurosci.* (2021) 13:709998. doi: 10.3389/fnagi.2021.709998
22. Luo FF, Xu H, Zhang M, Wang Y. Abnormal regional spontaneous brain activity and its indirect effect on spasm ratings in patients with hemifacial spasm. *Front Neurosci.* (2020) 14:601088. doi: 10.3389/fnins.2020.601088
23. Fulong X, Chao L, Dianjiang Z, Qihong Z, Wei Z, Jun Z, et al. Recursive partitioning analysis of fractional low–frequency fluctuations in narcolepsy with cataplexy. *Front Neurol.* (2018) 9:936. doi: 10.3389/fneur.2018.00936
24. Kim YE, Kim MK, Suh SI, Kim JH. Altered trigeminothalamic spontaneous low–frequency oscillations in migraine without aura: a resting–state fMRI study. *BMC Neurol.* (2021) 21:342. doi: 10.1186/s12883-021-02374-7
25. Qiu H, Li X, Luo Q, Li Y, Zhou X, Cao H. et al. Alterations in patients with major depressive disorder before and after electroconvulsive therapy measured by fractional amplitude of low–frequency fluctuations (fALFF). *J Affect Disord.* (2019) 244:92–9. doi: 10.1016/j.jad.2018.10.099
26. Egorova N, Veldsman M, Cumming T, Brodtmann A. Fractional amplitude of low–frequency fluctuations (fALFF) in post–stroke depression. *Neuroimage Clin.* (2017) 16:116–24. doi: 10.1016/j.nicl.2017.07.014
27. Xu Y, Zhuo C, Qin W, Zhu J, Yu C. Altered spontaneous brain activity in schizophrenia: a Meta–Analysis and a large–Sample study. *Biomed Res Int.* (2015) 2015:204628. doi: 10.1155/2015/204628
28. Qiu Y, Yang M, Li S, Teng Z, Jin K, Wu C, et al. Altered fractional amplitude of low–Frequency fluctuation in major depressive disorder and bipolar disorder. *Front Psychiatry.* (2021) 12:739210. doi: 10.3389/fpsyt.2021.739210
29. Liu W, Liu L, Cheng X, Ge H, Hu G, Xue C, et al. Functional integrity of executive control network contributed to retained executive abilities in mild cognitive impairment. *Front Aging Neurosci.* (2021) 13:710172. doi: 10.3389/fnagi.2021.710172
30. Ashida R, Cerminara NL, Edwards RJ, Apps R, Brooks JCW. Sensorimotor, language, and working memory representation within the human cerebellum. *Hum Brain Mapp.* (2019) 40:4732–47. doi: 10.1002/hbm.24733
31. Yin Y, Hou Z, Wang X, Sui Y, Yuan Y. Association between altered resting-state cortico-cerebellar functional connectivity networks and mood/cognition dysfunction in late-onset depression. *J Neural Transm (Vienna).* (2015) 122:887–96. doi: 10.1007/s00702-014-1347-3
32. Su L, Cai Y, Xu Y, Dutt A, Shi S, Bramon E. Cerebral metabolism in major depressive disorder: a voxel–based meta–analysis of positron emission tomography studies. *BMC Psychiatry.* (2014) 14:321. doi: 10.1186/s12888-014-0321-9
33. Hwang JP, Lee TW, Tsai SJ, Chen TJ, Yang CH, Lirng JF, et al. and subcortical abnormalities in late-onset depression with history of suicide attempts investigated with MRI and voxel–based morphometry. *J Geriatr Psychiatry Neurol.* (2010) 23:171–84. doi: 10.1177/0891988710363713
34. Liao W, Wang Z, Zhang X, Shu H, Wang Z, Liu D, et al. Cerebral blood flow changes in remitted early- and late-onset depression patients. *Oncotarget.* (2017) 8:76214–22. doi: 10.18632/oncotarget.19185
35. Gellersen HM, Guell X, Sami S. Differential vulnerability of the cerebellum in healthy ageing and alzheimer's disease. *Neuroimage Clin.* (2021) 30:102605. doi: 10.1016/j.nicl.2021.102605
36. Brady RO Jr Gonsalvez I, Lee I, Öngür D, Seidman LJ, Schmahmann JD, Eack SM, et al. Cerebellar–Prefrontal network connectivity and negative symptoms in schizophrenia. *Am J Psychiatry.* (2019) 176:512–20. doi: 10.1176/appi.ajp.2018.18040429
37. Centanni TM, Norton ES. Ozernov-Palchik O, Park A, Beach SD, Halverson K, et al. Disrupted left fusiform response to print in beginning kindergartners is associated with subsequent reading. *Neuroimage Clin.* (2019) 22:101715. doi: 10.1016/j.nicl.2019.101715
38. Centanni TM, Norton ES, Park A, Beach SD, Halverson K. Ozernov–Palchik O, et al. Early development of letter specialization in left fusiform is associated with better word reading and smaller fusiform face area. *Dev Sci.* (2018) 21:e12658. doi: 10.1111/desc.12658
39. Harris RJ, Rice GE, Young AW, Andrews TJ. Distinct but overlapping patterns of response to words and faces in the fusiform gyrus. *Cereb Cortex.* (2016) 26:3161–8. doi: 10.1093/cercor/bhv147
40. Susilo T, Duchaine B. Dissociations between faces and words: comment on behrmann and plaut. *Trends Cogn Sci.* (2013) 17:545. doi: 10.1016/j.tics.2013.09.005
41. Whelan R, Conrod PJ, Poline JB, Lourdusamy A, Banaschewski T, Barker GJ, et al. IMAGEN consortium. adolescent impulsivity phenotypes characterized by distinct brain networks. *Nat Neurosci.* (2012) 15:920–5. doi: 10.1038/nn.3092
42. Hirjak D. Meyer–Lindenberg A, Fritze S, Sambataro F, Kubera KM, Wolf RC. Motor dysfunction as research domain across bipolar, obsessive–compulsive and neurodevelopmental disorders. *Neurosci Biobehav Rev.* (2018) 95:315–35. doi: 10.1016/j.neubiorev.2018.09.009
43. Noonan MP, Sallet J, Rudebeck PH, Buckley MJ, Rushworth MF. Does the medial orbitofrontal cortex have a role in social valuation? *Eur J Neurosci.* (2010) 31:2341–51. doi: 10.1111/j.1460-9568.2010.07271.x
44. de Leeuw M, Kahn RS, Vink M. Fronto–striatal dysfunction during reward processing in unaffected siblings of schizophrenia patients. *Schizophr Bull.* (2015) 41:94–103. doi: 10.1093/schbul/sbu153
45. Shukla DK, Chiappelli JJ, Sampath H, Kochunov P, Hare SM, Wisner K, et al. Aberrant frontostriatal connectivity in negative symptoms of schizophrenia. *Schizophr Bull.* (2019) 45:1051–9. doi: 10.1093/schbul/sby165
46. Hirjak D, Kubera KM, Northoff G, Fritze S, Bertolino AL, Topor CE, et al. Cortical contributions to distinct symptom dimensions of catatonia. *Schizophr Bull.* (2019) 45:1184–94. doi: 10.1093/schbul/sby192
47. Xue SW, Lee TW, Guo YH. Spontaneous activity in medial orbitofrontal cortex correlates with trait anxiety in healthy male adults. *J Zhejiang Univ Sci B.* (2018) 19:643–653. doi: 10.1631/jzus.B1700481
48. Hakamata Y, Matsuoka Y, Inagaki M, Nagamine M, Hara E, Imoto S, et al. Structure of orbitofrontal cortex and its longitudinal course in cancer–related post–traumatic stress disorder. *Neurosci Res.* (2007) 59:383–9. doi: 10.1016/j.neures.2007.08.012
49. Briggs RG, Chakraborty AR, Anderson CD, Abraham CJ, Palejwala AH, Conner AK, et al. and white matter connections of the inferior frontal gyrus. *Clin Anat.* (2019) 32:546–56. doi: 10.1002/ca.23349
50. Becker M, Sommer T, Kühn S. Inferior frontal gyrus involvement during search and solution in verbal creative problem solving: a parametric fMRI study. *Neuroimage.* (2020) 206:116294. doi: 10.1016/j.neuroimage.2019.116294
51. Badre D, Wagner AD. Left ventrolateral prefrontal cortex and the cognitive control of memory. *Neuropsychologia.* (2007) 45:2883–901. doi: 10.1016/j.neuropsychologia.2007.06.015
52. Cheng L, Wu X, Guo R, Wang Y, Wang W, He P, et al. Discriminative pattern of reduced cerebral blood flow in parkinson's disease and parkinsonism–Plus syndrome: an aSL–MRI study. *BMC Med Imaging.* (2020) 20:78. doi: 10.1186/s12880-020-00479-y
53. Qi T, Schaadt G, Friederici AD. Cortical thickness lateralization and its relation to language abilities in children. *Dev Cogn Neurosci.* (2019) 39:100704. doi: 10.1016/j.dcn.2019.100704
54. Yang C, Luo N, Liang M, Zhou S, Yu Q, Zhang J, et al. Altered brain functional connectivity density in fast-ball sports athletes with early stage of motor training. *Front Psychol.* (2020) 11:530122. doi: 10.3389/fpsyg.2020.530122
55. Kesserwani H, Kesserwani A. Apperceptive prosopagnosia secondary to an ischemic infarct of the lingual gyrus: a case report and an update on the neuroanatomy, neurophysiology, and phenomenology of prosopagnosia. *Cureus.* (2020) 12:e11272. doi: 10.7759/cureus.11272
56. Meadows JC. The anatomical basis of prosopagnosia. *J Neurol Neurosurg Psychiatry.* (1974) 37:489–501. doi: 10.1136/jnnp.37.5.489

57. Bouvier SE, Engel SA. Behavioral deficits and cortical damage loci in cerebral achromatopsia. *Cereb Cortex.* (2006) 16:183–91. doi: 10.1093/cercor/bhi096
58. Bartels A, Zeki S. The architecture of the colour centre in the human visual brain: new results and a review. *Eur J Neurosci.* (2000) 12:172–93. doi: 10.1046/j.1460-9568.2000.00905.x
59. Beauchamp MS, Haxby JV, Jennings JE, DeYoe EA. An fMRI version of the farnsworth–Munsell 100–Hue test reveals multiple color–selective areas in human ventral occipitotemporal cortex. *Cereb Cortex.* (1999) 9:257–63. doi: 10.1093/cercor/9.3.257
60. Mase Y, Matsui Y, Uchiyama E, Matsubara H, Sugimoto M, Kubo A, et al. Cerebral trauma–induced dyschromatopsia in the left hemifield: case presentation. *BMC Ophthalmol.* (2021) 21:63. doi: 10.1186/s12886-020-01800-7
61. Singh–Bains MK, Waldvogel HJ, Faull RL. The role of the human globus pallidus in huntington's disease. *Brain Pathol.* (2016) 26:741–51. doi: 10.1111/bpa.12429
62. Aylward EH Li Q, Stine OC, Ranen N, Sherr M, Barta PE, et al. Longitudinal change in basal ganglia volume in patients with huntington's disease. *Neurology.* (1997) 48:394–9. doi: 10.1212/WNL.48.2.394
63. Douaud G, Gaura V, Ribeiro MJ, Lethimonnier F, Maroy R, Verny C, et al. Distribution of grey matter atrophy in huntington's disease patients: a combined rOI–based and voxel–based morphometric study. *Neuroimage.* (2006) 32:1562–75. doi: 10.1016/j.neuroimage.2006.05.057
64. Fennema–Notestine C, Archibald SL, Jacobson MW, Corey–Bloom J, Paulsen JS, Peavy GM, et al. In vivo evidence of cerebellar atrophy and cerebral white matter loss in huntington disease. *Neurology.* (2004) 63:989–95. doi: 10.1212/01.WNL.0000138434.68093.67
65. Nakagawa S, Takeuchi H, Taki Y, Nouchi R, Kotozaki Y, Shinada T, et al. Basal ganglia correlates of fatigue in young adults. *Sci Rep.* (2016) 6:21386. doi: 10.1038/srep21386
66. Nakagawa S, Takeuchi H, Taki Y, Nouchi R, Kotozaki Y, Shinada T, et al. Lenticular nucleus correlates of general self–efficacy in young adults. *Brain Struct Funct.* (2017) 222:3309–18. doi: 10.1007/s00429-017-1406-2
67. Tricomi E, Balleine BW, O'Doherty JP, A. specific role for posterior dorsolateral striatum in human habit learning. *Eur J Neurosci.* (2009) 29:2225–32. doi: 10.1111/j.1460-9568.2009.06796.x
68. Hong S, Hikosaka O. The globus pallidus sends reward–related signals to the lateral habenula. *Neuron.* (2008) 60:720–9. doi: 10.1016/j.neuron.2008.09.035
69. Lan DY, Zhu PW, He Y, Xu QH, Su T, Li B, et al. Gray matter volume changes in patients with acute eye pain: a voxel–Based morphometry study. *Transl Vis Sci Technol.* (2019) 8:1. doi: 10.1167/tvst.8.1.1
70. Silkiss RZ, Wade AR. Neuroanatomic variations in graves' dysthyroid ophthalmopathy as studied with mRI. *Trans Am Ophthalmol Soc.* (2016) 114:T9.
71. Deng Q, Wang M, Song Q, Wu Z, Jiang H, Pang P, et al. Correlation between hippocampus mRI radiomic features and resting–state intrahippocampal functional connectivity in alzheimer's disease. *Front Neurosci.* (2019) 13:435. doi: 10.3389/fnins.2019.00435
72. Gordon E, Rohrer JD, Fox NC. Advances in neuroimaging in frontotemporal dementia. *J Neurochem.* (2016) 138(Suppl. 1):193–210. doi: 10.1111/jnc.13656
73. Irwin DJ, McMillan CT, Xie SX, Rascovsky K, Van Deerlin VM, Coslett HB, et al. Asymmetry of post-mortem neuropathology in behavioural-variant frontotemporal dementia. *Brain.* (2018) 141:288–301. doi: 10.1093/brain/awx319
74. Chen Y, Wang X, Yu Y, Liu Y. Dissociable electroencephalograph correlates of visual awareness and feature-based attention. *Front Neurosci.* (2017) 11:633. doi: 10.3389/fnins.2017.00633
75. Kitada R, Doizaki R, Kwon J, Tanigawa T, Nakagawa E, Kochiyama T, et al. Brain networks underlying tactile softness perception: a functional magnetic resonance imaging study. *Neuroimage.* (2019) 197:156–66. doi: 10.1016/j.neuroimage.2019.04.044
76. Sathian K, Lacey S, Stilla R, Gibson GO, Deshpande G, Hu X, et al. Dual pathways for haptic and visual perception of spatial and texture information. *Neuroimage.* (2011) 57:462–75. doi: 10.1016/j.neuroimage.2011.05.001
77. Teng C, Zhou J, Ma H, Tan Y, Wu X, Guan C, et al. Abnormal resting state activity of left middle occipital gyrus and its functional connectivity in female patients with major depressive disorder. *BMC Psychiatry.* (2018) 18:370. doi: 10.1186/s12888-018-1955-9
78. Tu S, Qiu J, Martens U, Zhang Q. Category–selective attention modulates unconscious processes in the middle occipital gyrus. *Conscious Cogn.* (2013) 22:479–85. doi: 10.1016/j.concog.2013.02.007
79. Wu YJ, Wu N, Huang X, Rao J, Yan L, Shi L, et al. Evidence of cortical thickness reduction and disconnection in high myopia. *Sci Rep.* (2020) 10:16239. doi: 10.1038/s41598-020-73415-3

Conflict of Interest: The authors declare that the research was conducted in the absence of any commercial or financial relationships that could be construed as a potential conflict of interest.

frontiers | Frontiers in Psychiatry

ORIGINAL RESEARCH
published: 27 May 2022
doi: 10.3389/fpsyt.2022.925253

Decreased Connectivity in Precuneus of the Ventral Attentional Network in First-Episode, Treatment-Naïve Patients With Major Depressive Disorder: A Network Homogeneity and Independent Component Analysis

Liqiong Luo[1], Xijun Lei[1], Canmin Zhu[2], Jun Wu[3], Hongwei Ren[4], Jing Zhan[1] and Yongzhang Qin[5]*

[1] Department of Oncology, Tianyou Hospital Affiliated to Wuhan University of Science and Technology, Wuhan, China, [2] Department of Neurology, The First People's Hospital of Jiangxia District, Wuhan, China, [3] Department of Neurosurgery, Wuhan Central Hospital Affiliated to Tongji Medical College, Huazhong University of Science and Technology, Wuhan, China, [4] Department of Medical Imaging, Tianyou Hospital Affiliated to Wuhan University of Science and Technology, Wuhan, China, [5] Department of Endocrinology, First Affiliated Hospital of Gannan Medical University, Ganzhou, China

OPEN ACCESS

Edited by:
Liang Liang,
Wuhan University, China

Reviewed by:
Xiaobing Jiang,
Huazhong University of Science and Technology, China
Shubao Wei,
Jiangbin Hospital of Guangxi Zhuang Autonomous Region, China

***Correspondence:**
Canmin Zhu
zcmin07@yeah.net
Yongzhang Qin
sdiemd2008@126.com

Specialty section:
This article was submitted to Neuroimaging and Stimulation, a section of the journal Frontiers in Psychiatry

Received: 21 April 2022
Accepted: 28 April 2022
Published: 27 May 2022

Citation:
Luo L, Lei X, Zhu C, Wu J, Ren H, Zhan J and Qin Y (2022) Decreased Connectivity in Precuneus of the Ventral Attentional Network in First-Episode, Treatment-Naïve Patients With Major Depressive Disorder: A Network Homogeneity and Independent Component Analysis. Front. Psychiatry 13:925253. doi: 10.3389/fpsyt.2022.925253

Background and Objective: The ventral attentional network (VAN) can provide quantitative information on cognitive problems in patients with major depressive disorder (MDD). Nevertheless, little is known about network homogeneity (NH) changes in the VAN of these patients. The aim of this study was to examine the NH values in the VAN by independent component analysis (ICA) and compare the NH values between MDD patients and the normal controls (NCs).

Methods: Attentional network test and resting-state functional magnetic resonance imaging (rs-fMRI) data were collected from 73 patients, and 70 NCs matched by gender, age, and education years. ICA and NH were employed to evaluate the data. Moreover, the NH values were compared, and Spearman's rank correlation analysis was used to assess the correlations with the executive control reaction time (ECRT).

Results: Our results showed that the first-episode, treatment-naive MDD patients had decreased NH in the right precuneus (PCu) and abnormal ECRT compared with NCs. However, no significant correlation was found between the NH values and measured clinical variables.

Conclusion: Our results highlight the potential importance of VAN in the pathophysiology of cognitive problems in MDD, thus offering new directions for future research on MDD.

Keywords: major depressive disorder, ventral attentional network, rest-state fMRI, network homogeneity, attentional network test

INTRODUCTION

Major depressive disorder (MDD) is a heterogeneous psychiatric disorder and one of the leading causes of disability and morbidity worldwide. MDD causes various symptoms such as persistent depression, loss of interest, a pervasive loss of pleasure, reduced energy, and cognitive function disturbance. A central cognitive impairment in MDD patients is the inability to allocate attention to appropriate emotional cues (1, 2). Compared with non-depression patients, depressed adult patients pay more attention to negative stimuli (3). In addition, although depressed adults tend to process sad stimuli similarly as non-depressed individuals, they have a habit of focusing on them a few seconds longer (1). The same attention bias can also be observed in adolescent depression (4). Neuropsychological studies have shown that attention function had been also impaired in patients with remitting MDD (5, 6). However, the neurobiological mechanism underlying the symptoms of MDD has not been fully understood.

Recent evidence has indicated that MDD may affect neural networks that are critical for the brain's development (7, 8). It has even been suggested that MDD itself is a brain network disease. For example, the default mode network, attention network, etc (8, 9). The ventral attention network (VAN) is associated with the orientation toward new, and unexpected stimuli. Its key brain regions are the inferior parietal lobule, anterior insula, temporal-parietal junction, inferior frontal gyrus, and middle frontal gyrus (10). By applying resting-state functional magnetic resonance imaging (rs-fMRI), studies have shown that depression was associated with abnormal VAN function. Furthermore, a meta-analysis of resting-state functional connectivity of MDD suggested that MDD was associated with hypoconnectivity between VAN and precuneus, and extended to occipital lobe and posterior cingulate cortex (11). Another rs-fMRI meta-analysis showed that the temporal, parietal junction activation was lower in patients with depression but higher in the ventro-lateral prefrontal cortex (VLPFC) than in healthy controls (12). In addition, many studies have shown that antidepressants and course of disease have a certain effect on the brain function and structure of MDD patients (13, 14). Therefore, investigating VAN's neurobiology in the early stage of disease and untreatment may be crucial for understanding the etiology of depression. However, the specific damage to the functions of brain regions within the VAN remains poorly understood.

Resting-state fMRI (rs-fMRI) is a widely applied approach for examining the functional alterations in neuropsychiatric disorders (9, 15). It is an advanced and non-invasive neuroimaging technique, which can quickly generate functional maps of the whole brain in the absence of task-related processing. Rs-fMRI has been extensively used in basic and clinical neuroscience research (16–21). At present, rs-fMRI is often used to investigate spontaneous neural activities and functional connectivity networks in the pathogenesis of MDD. This kind of research has been focused on group-level differences between study and control populations.

Independent component analysis (ICA) is a widely used data-driven approach for processing fMRI data. It enables the optimized capture of each matrix factor to make them as independent as possible. It has been successfully applied to fMRI data analysis and other types of biomedical data (22). Data-driven investigation of brain networks has received great attention in fMRI studies. It can help capture the spontaneous fluctuations in the interesting structures representing brain activities. ICA can be applied to investigate the specific damage to brain regions' functions. On this basis, analysis of network homogeneity (NH) can be used to further explore the changes in the functions of different brain regions of the patients. NH, which estimates the homogeneity of brain networks, uses biased forum assessment of MDD. It has been acknowledged that as a mental disorder, depression involves multiple brain regions and systems (23, 24). This simple, easy, and unbiased method reveals brain networks related to clinical applications that are worthy of research.

To the best of our knowledge, no previous studies have used ICA-based approaches to explore NH value differences in VAN for MDD. In this study, we applied rs-fMRI to explore the NH value differences of the VAN in the human brain. We tested the following hypotheses: (1) whether rs-fMRI can be used to identify the VAN in MDD; does VAN has different NH values in the first-episode, treatment-naive patients with MDD; (2) whether VAN has different NH values in certain specific brain regions; (3) whether different NH values in MDD are associated with certain functional changes.

TABLE 1 | Characteristics of the participants.

Demographic data	Patients ($n = 73$)	NCs ($n = 70$)	T (or x^2)	*P*-value
Gender (male/female)	73 (43/30)	70 (40/30)	0.12	0.29[a]
Age (years)	26.32 ± 6.88	29.41 ± 5.31	1.74	0.84[b]
Years of education (years)	9.52 ± 0.93	9.52 ± 0.93	−1.33	0.62[b]
HRSD (score)	25.49 ± 7.10			
ECRT (ms)	91.60 ± 54.85	67.81 ± 48.02	2.13	0.04[b]

[a] *The p-value for gender distribution was obtained by chi-square test.*
[b] *The p-value were obtained by two sample t-tests.*
NCs, normal controls; HRSD, Hamilton Rating Scale for Depression; ECRT, executive control reaction time.

MATERIALS AND METHODS

Subjects

The study involved 73 patients with first-episode, treatment-naive depression without comorbid anxiety disorders, and 70 control participants without brain injuries or neurological diseases. All participants were from the Department of Psychiatry and Neurology, Tianyou Hospital Affiliated to Wuhan University of Science and Technology. **Table 1** displays the demographic and clinical characteristics of the samples. The patients' diagnosis was conducted according to the Diagnostic and Statistical Manual of Mental Disorders (the 4th edition, DSM-IV) independently by two trained clinical psychiatrists (25). The depression severity of the patients was evaluated following the 17-item Hamilton Rating Scale for Depression (HRSD-17). All patients had a total score >17 in the HRSD-17 at MRI evaluation. Patients' exclusion criteria were the following: family history of

neurological disorders, severe physical illnesses, substance abuse, left-handedness, children and adolescent, pregnancy, abnormal cerebral structures by initial MRI scanning, and the presence of other psychiatric disorders such as personality disorders or schizophrenia. For control participants, the exclusion standards were the same as those for MDD patients. Finally, 73 subjects with MDD and 70 healthy controls (matched for gender, age, education years) were included in the study.

All participants signed completely informed consent and/or assent before participation in this study. This experimental design was approved by the ethics committee of Tianyou Hospital Affiliated to Wuhan University of Science and Technology and in accordance with the Declaration of Helsinki.

Behavioral Paradigm

The attentional network test (ANT) designed by Fan et al. was performed using the Eprime and E-Studio software (Psychological Software Tools, Pittsburgh, PA, USA) (26). Image preprocessing and analyses mentioned below were performed according to a previously described approach (8). The standard procedures for ANT included three separate steps: (1) a "+" sign was placed in the central testing screen, which was considered as the fixation point. (2) A stimulus signal in the form of a target → or a foil* was generated above or below the central screen. Four scenarios were set for the foils: no foil, one foil in the central part (one above the central screen and another below it, and one either above or below the central screen). (3) Arrows could be found in the following scenarios: one single arrow and five arrows in either one direction or different directions. The subjects were required to perform correct and quick target orientation. Then, ECRT was calculated by subtracting RT's consistent arrow direction from the inconsistent arrow direction RT. A higher ECRT value represented a lower efficiency of the executive control network.

The rs-fMRI images were obtained by using an Achieva 3T-MRI scanner (Philips, Ingenia). The scan lasted for 10 min. Patients were asked to lie down and close their eyes; they remained awake all the time. A prototype quadrature birdcage head coil filled with foam was utilized to minimize their head movement. The following parameters were used for functional imaging: slice thickness (5 mm), pitch (1 mm), flip angle (90?), a field of view (240 × 240 mm), and the ratio of repetition time to echo time (TR/TE) (2,000/30 ms). Meanwhile, the important settings were used for the structural scan (T1-weighted): repetition time (TR) = 20 ms, echo time (TE) = 3.5 ms, slice thickness = 1 mm, spin-echo sequence, and field of view (FOV) (= 24 × cm).

Data Preprocessing

The data processing assistant for resting-state fMRI (DPARSF) software (27) in Matlab was used to precondition of the rs-fMRI imaging data. With the omission of the first 10 time points, slice time and head motion were rectified to adjust the time series of the images in order to ensure that the brain is in the same position for every image. No more than 2 mm of maximal displacement in the x, y, or z-axis and 2? of maximal rotation were allowed for all participants. The structure of each patient was recorded to its functional image and partitioned, and a template was created in order to normalize the structures of the patients after they were defined following the Montreal Neurological Institute (MNI) standard template, the standardization process of the spatial deformation of the modulation and the structure of the voxel size using $1 \times 1 \times 1$ mm^3. Moreover, the use of the structure of each patient to the function of the conversion matrix was also standardized to the MNI space. In the functional image normalization, white matter signal, head motion parameters, and cerebrospinal fluid signal were taken as the removal covariates (Nuisance regression). The voxel size of $3 \times 3 \times 3$ mm^3 was utilized to resample. Subsequently, an 8 mm full width at half-maximum Gaussian kernel was used to smoother the obtained images. The images were bandpass filtered (0.01–0.1 Hz), followed by linear detrending to reduce the effect of low-frequency drifts and physiologic high-frequency noise. Several spurious covariates, including a signal from a region centered in the white matter, a signal from a ventricular ROI, and 6 head motion parameters obtained by rigid body correction, were excluded. The global signal removal might inevitably bring artifacts into the data and affect the resting-state connectivity patterns; besides, the global signal's regression might significantly influence the results when studying clinical cases (28). Therefore, the global signal was preserved to some extent.

Ventral Attentional Network Identification

ICA was performed using the Group ICA utility to extract VAN components in templates from the GIFT fMRI toolbox (http://mialab.mrn.org/software/# gica) (29). The ICA analysis consisted of three steps from the GIFT toolbox: separation of independent components, data reduction, and back rebuilding. First, the optimal number of independent components (ICs) was estimated by the minimum description length criteria, which was 73 for MDD patients and 70 NCs. The data obtained from each participant were decomposed into spatially separated ICs using an algorithm, resulting in 73 independent spatial maps for MDD patients and 26 NCs. At last, the corresponding components for each participant were calculated. For each component, a statistical map and a threshold were set with the voxel-wise one-sample *t*-test. According to the Gaussian random field (GRF) theory, $p < 0.01$ was defined to represent a significant statistical modification of multiple comparisons, and voxel significance and cluster significance were defined at values of $p < 0.01$.Finally, the masks created for the parts in the VAN by combination were used for NH analysis.

Network Homogeneity Analysis

The NH analysis results were calculated by an in-house script in Matlab. The VAN masks presented the correlation coefficients between the provided voxel and all others. The average correlation coefficient was defined as the homogeneity of a given voxel. Then, the average correlation coefficients were transformed into z values by z-transformation, which could significantly enhance the normal distribution. The obtained values were used to generate the NH map, which was finally subjected to z-transformation for group comparison.

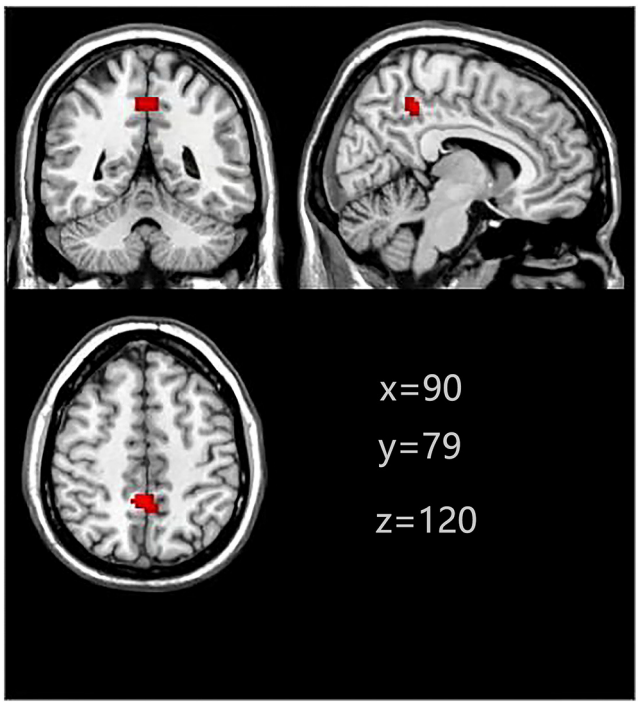

FIGURE 1 | Ventral attentional network (based on group-ICA with a threshold at z≥5).

Statistical Analysis

The demographic information (age, gender, education years) and image data of the subjects were computed. A two-sample *t*-test was used to compare the continuous variables, and a Chi-square test to compare the classified data with the IBM SPSS Statistics 22.0 software. In order to measure the discrepancy in the NH regional group, a two-sample *t*-test was used to assist the individual-level NH map to the group-level voxel *t*-test analysis. Then, in the VAN mask, a two-sample *t*-test was used to analyze the NH maps through voxel-wise cross-subject statistics. GRF theory was employed to correct the significance levels for multiple comparisons. (GRF corrected, voxel significance: $P < 0.001$; cluster significance: $P < 0.01$).

NH values were extracted from the abnormal values in brain regions. Using the IBM SPSS Statistics 22.0 software, Pearson correlations analysis was performed after evaluating the data normality. A $p < 0.05$ was considered as statistically significant.

RESULTS

Demographics and Clinical Features of the Subjects

The demographic information of the participants is shown in **Table 1**. No significant differences were found between the two groups in terms of gender, age, and years of education. Yet, the patient group had higher values of ECRT.

TABLE 2 | Signification differences in NH values between the groups.

Cluster location	Peak X	(MNI) Y	Z	Number of voxels	T value
Patients < controls Right Pcu	3	−45	48	48	−3.57

NH, network homogeneity; MNI, Montreal Neurological Institute; PCu, Precuneus.

VAN Maps Ascertained by Group ICA

Two masks from MDD patients and NCs, respectively. Finally, the two masks were combined to generate a VAN mask. The parts involved in the VAN included the right PCu, right supper frontal gyrus, right inferior frontal gyrus, right supramarginal gyrus, left middle temporal gyrus, left inferior parietal gyrus, and left Cerebelum (**Figure 1**).

Group Differences in VAN Regarding NH

The two-sample *t*-test showed significant differences in NH values between the patient and control group within the VAN masks. Compared with NCs, the MDD patients had lower NH values in right PCu (**Table 2** and **Figure 2**).

Correlation of NH With Clinical Variables

Significant group discrepancies were found in the right PCu, from which the NH values were obtained. In the patient group, Pearson linear correlation analysis was performed to investigate the correlations between NH, ECRT, and illness severity. The results showed no significant correlation between NH and those clinical variables.

DISCUSSION

A number of studies have found that under the condition of selective attention, the neural function of normal aging will change (30, 31). Furthermore, many articles have reported alteration in the cerebral hemisphere's functional network due to other factors (32). However, little is known about the changes related to MDD in the ventral attention network (VAN), which is the basis of selective attention. This study examined MDD-related changes within the VAN, focusing on abnormality between its regions. We examined 73 patients and 70 control participants based on NH values of network signals from rs-fMRI as well as ERCT of their test performance. We identified the VAN independently for both groups using spatial independent component analysis. Three main findings emerged: first, rs-fMRI could be used to identify the VAN, and MDD patients had lower NH values than control participants. Second, MDD patients had similar connectivity among posterior regions compared to control participants but lower NH values among the right precuneus (PCu). Finally, MDD patients had a shorter ECRT compared to controls. Thus, this study suggests that neuro-functional changes in MDD affect VAN values. Our results

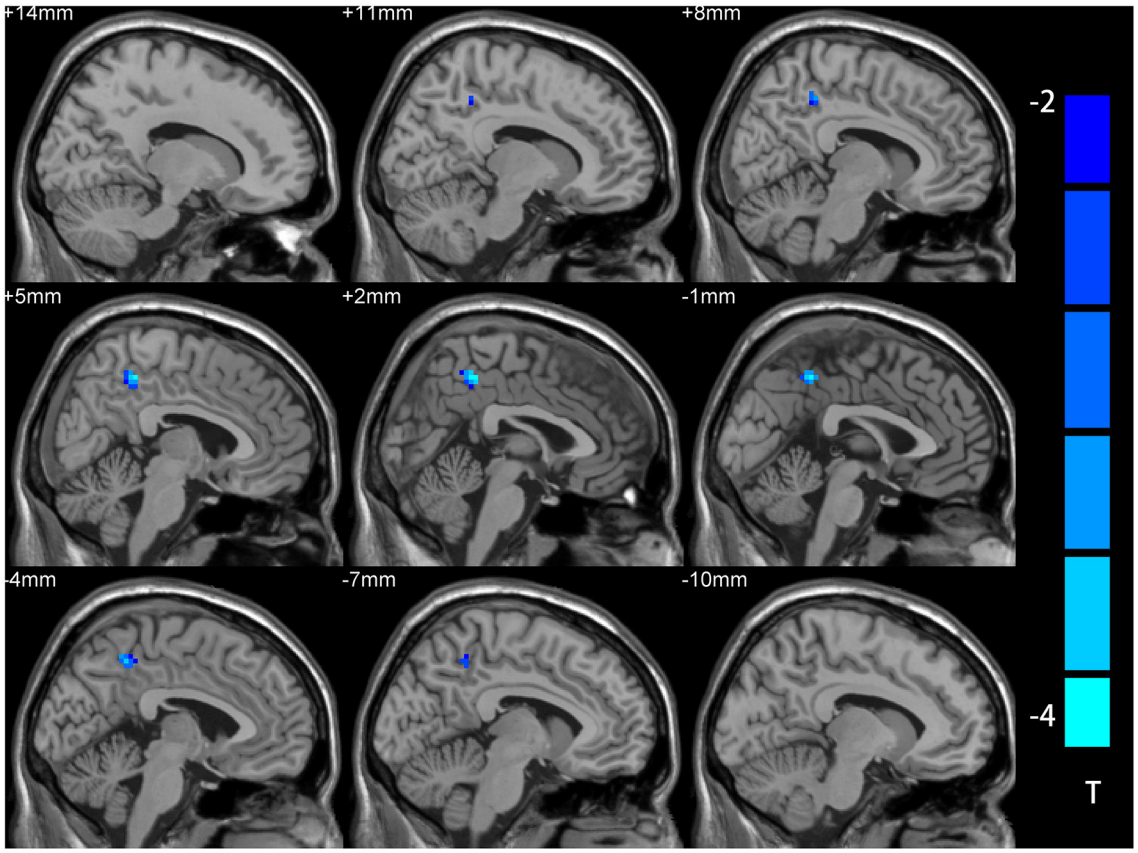

FIGURE 2 | NH differences between the MDD patient and NCs in statistical maps. NH is lower in the right precuneus (PCu) of the MDD patients. Blue represents lower NH; color bars correspond to the T values obtained from the two-sample *t*-test. NH, network homogeneity; MDD, major depressive disorder; NC, normal controls; PCu, precuneus.

revealed that anterior regions were of greater importance for MDD patients; especially the right PCu had enhanced centrality.

Currently, rs-fMRI research on MDD patients has identified a broad range of brain network abnormalities, but the underlying mechanism remains unclear (33, 34). Some studies have attributed the pathophysiological mechanism of depression to abnormal DMN connectivity (35, 36). However, these studies have only focused on the changes in DMN and have ignored the changes in other brain regions. VAN is an important mediator of stimulus-driven attention and a task-positive network that is activated during attentional orientation or reorientation. Multiple cortical areas, such as the middle and inferior frontal gyri, inferior parietal lobule, anterior insula, and temporal-parietal junction, have participate in this process (35, 37). Some previous studies have demonstrated that VAN is a key brain network for stimulus-driven attention. Still, it remains unclear how depression is related to effective connectivity within the VAN.

Recent rs-fMRI studies have shown that the PCu, orbitofrontal gyrus, and amygdala are the main cortical or brain junction areas. The PCu is an area of the brain involved in various complex cognitive functions, including self-processing, operations spatial imagery, and episodic memory retrieval. In MDD, spatial affect learning disorder is related to the PCu activation (38). Dysregulation as a neural substrate of depression, the PCu is involved in the formation of self-consciousness, which may be related to the low self-esteem of depression (39–41). The PCu is also associated with autobiographical memory dysfunction, which is another significant feature of MDD (42). The results suggest that PCu has a vital role in functional connectivity in mediating cognitive and affective functions. Herein, we utilized the rs-fMRI method and ICA analysis to explore the NH value of the PCu in the brain VAN of the patients with first-episode, treatment-naive depression. The right PCu showed statistically significant differences in NH between the MDD patients and the controls. To be more specific, the patients with first-episode, treatment-naive depression showed decreased NH values compared with the control participants. Previous studies have also confirmed the importance of VAN in the pathophysiology of psychiatric disorders (24, 43). Characterization of the network connectivity in the brain can help to further elucidate the specific functions of the PCu and shed new light on how PCu dysfunctions contribute to the clinical manifestation of MDD.

Reaction time (RT) is associated with increased amplitude response in cognitive control regions. Some research has suggested that RT-related activity can represent the amount of time taken to perform a decision process, which is relatively brief on fast RT trials and relatively long on slow RT trials. Executive control reaction time (ECRT) is a specific RT form, mainly focusing on executive control, which still needs to be evaluated in more detail. Here, we hypothesized that MDD patients have abnormal VAN homogeneity related to certain clinical variables such as ERCT. Therefore, based on previous work, we further explored whether there was a close correlation between a distinct decrease in the NH of VAN and abnormal ERCT. As a result, no significant correlation was found between NH and ERCT. In previous studies on the brain networks, there were either decreases or increases in the NH values in mental disorder patients (42, 44–46). However, in this study, the NH values exclusively showed decreases. This discrepancy may be attributed to the subjects in the present study who were first-episode, treatment-naïve depression patients without the establishment of a compensatory mechanism due to the absence of treatment.

Two neural systems for goal-directed and stimulus-driven attention, the dorsal attention network (DAN) and the VAN, have been described in the human brain. There are asymmetries in functional connection patterns related to these key nodes of the attention network. This asymmetric development pattern of the attention network may be a neural feature, i.e., with the development of attention mechanism, from the bottom-up over-representation to the greater top-down attention ability (47). Little is known about the relative uniqueness of these attention networks in the brain. Another brain system, known as the saliency network, has also been linked to functions that overlap with VAN functions, including responding to behavior-related stimuli. At the same time, some researchers suggested that the functional and anatomical overlap of the VAN and salience networks make part of the same system (48). Though there is an abundance of literature on human brain networks, little research focused on these networks' typical development and special function. This study selected the normal control participants and first-episode, treatment-naive MDD patients as the research subjects. We explored whether VAN has different NH values that were potentially more predominant in the first-episode, treatment-naive MMD patients.

This has a few limitations. First, this study was only focused on variations in the VAN and might have ignored some significant changes in other brain regions. The DAN, VAN, and the salence network are important intracranial neural networks, which cannot be completely separated from each other in organizational structure but are relatively independent or complementary to each other in function. Second, the current study was the deletion of the age factor, largely due to the unknown effects of puberty on developing the brain's attention networks. The third limitation was the influence of the recurrent factors, largely due to the unknown effects of the recurrent attacks on the brain's attention networks' cross-development. Forth, this study has a small sample size. However, our results elucidate the importance of VAN in the pathophysiology of MDD by exploring the abnormal NH values in the VAN of MDD patients.

At present, cognitive-behavioral therapy can improve network-level abnormalities with better treatment effects. At the same time, existing descriptions of the VAN lack detail and offer limited insight into the underlying structural connections of the network. This study explores the possible regulation model of PCu in the VAN and establishes a more effective treatment mode for MDD.

DATA AVAILABILITY STATEMENT

The original contributions presented in the study are included in the article/supplementary material, further inquiries can be directed to the corresponding authors.

ETHICS STATEMENT

The studies involving human participants were reviewed and approved by the Ethics Committee of Tianyou Hospital Affiliated to Wuhan University of Science and Technology. The patients/participants provided their written informed consent to participate in this study.

AUTHOR CONTRIBUTIONS

LL conceived the structure of the manuscript and wrote the manuscript. XL, JW, HR, and JZ collected and analyzed the data. CZ and YQ conceived and critically reviewed the manuscript. All authors have read and approved the final manuscript.

FUNDING

This research was supported by Health Commission of Hubei Province Scientific Research Project (Grant No. WJ2021M007), General Project of Science and Technology Department of Hubei Province (Grant No. 2020CFB512), the Science and Technology Plan of Health Commission of Jiangxi Province (Grant No. 202130648), and the Science and Technology Research Project of Department of Education of Jiangxi Province (Grant No. GJJ201522).

ACKNOWLEDGMENTS

The authors thank all individuals who served as study subjects, as well as reviewers for their proposals and criticisms.

REFERENCES

1. Peckham AD, McHugh RK, Otto MW. A meta-analysis of the magnitude of biased attention in depression. *Depress Anxiety*. (2010) 27:1135–42. doi: 10.1002/da.20755
2. Abdoli N, Salari N, Darvishi N, Jafarpour S, Solaymani M, Mohammadi M. The global prevalence of major depressive disorder (MDD) among the elderly: a systematic review and meta-analysis. *Neurosci Biobehav Rev*. (2022) 132:1067–73. doi: 10.1016/j.neubiorev.2021.10.041
3. Eizenman M, Yu LH, Grupp L, Eizenman E, Ellenbogen M, Gemar M, et al. A naturalistic visual scanning approach to assess selective attention in major depressive disorder. *Psychiatry Res*. (2003) 118:117–28. doi: 10.1016/S0165-1781(03)00068-4
4. Sylvester CM, Hudziak JJ, Gaffrey MS, Barch DM, Luby JL. Stimulus-driven attention, threat bias, and sad bias in youth with a history of an anxiety disorder or depression. *J Abnorm Child Psychol*. (2016) 44:219–31. doi: 10.1007/s10802-015-9988-8
5. Saloner R, Morgan EE, Hussain MA, Moore DJ, Heaton RK, Cherner M. Relationship of the balloon analog risk task to neurocognitive impairment differs by HIV serostatus and history of major depressive disorder. *J Neurovirol*. (2022) 1–17. doi: 10.1007/s13365-021-01046-z
6. Ronold EH, Schmid MT, Oedegaard KJ, Hammar Å. A longitudinal 5-year follow-up study of cognitive function after first episode major depressive disorder: exploring state, scar and trait effects. *Front Psychiatry*. (2020) 11:575867. doi: 10.3389/fpsyt.2020.575867
7. Gao Y, Wang X, Xiong Z, Ren H, Liu R, Wei Y, et al. Abnormal fractional amplitude of low-frequency fluctuation as a potential imaging biomarker for first-episode major depressive disorder: a resting-state fMRI study and support vector machine analysis. *Front Neurol*. (2021). 12:751400. doi: 10.3389/fneur.2021.751400
8. Gao Y, Wang M, Yu R, Li Y, Yang Y, Cui X. Abnormal default mode network homogeneity in treatment-naive patients with first-episode depression. *Front Psychiatry*. (2018) 9:697. doi: 10.3389/fpsyt.2018.00697
9. Guo W, Cui X, Liu F, Chen J, Xie G, Wu R. Increased anterior default-mode network homogeneity in first-episode, drug-naive major depressive disorder: a replication study. *J Affect Disord*. (2018) 225:767–72. doi: 10.1016/j.jad.2017.08.089
10. Liu J, Xu P, Zhang J, Jiang N, Li X, Luo Y. Ventral attention-network effective connectivity predicts individual differences in adolescent depression. *J Affect Disord*. (2019) 252:55–9. doi: 10.1016/j.jad.2019.04.033
11. Baker JT, Dillon DG, Patrick LM, Roffman JL, Brady RO Jr, Pizzagalli DA, et al. Functional connectomics of affective and psychotic pathology. *Proc Natl Acad Sci U S A*. (2019) 116:9050–9. doi: 10.1073/pnas.1820780116
12. Ding Y-D, Yang R, Yan C-G, Chen X, Bai T-J, Bo Q-J. Disrupted hemispheric connectivity specialization in patients with major depressive disorder: evidence from the REST-meta-MDD Project. *J Affect Disord*. (2021) 284:217–28. doi: 10.1016/j.jad.2021.02.030
13. Pascual-Antón R, Blasco-Serra A, Muñoz-Moreno E, Pilar-Cuéllar F, Garro-Martínez E, Florensa-Zanuy E. Structural connectivity and subcellular changes after antidepressant doses of ketamine and Ro 25-6981 in the rat: an MRI and immuno-labeling study. *Brain Struct Funct*. (2021) 226:2603–16. doi: 10.1007/s00429-021-02354-0
14. Korczak DJ, Goldstein BI. Childhood onset major depressive disorder: course of illness and psychiatric comorbidity in a community sample. *J Pediatr*. (2009) 155:118–23. doi: 10.1016/j.jpeds.2009.01.061
15. Shan X, Cui X, Liu F, Li H, Huang R, Tang Y. Shared and distinct homotopic connectivity changes in melancholic and non-melancholic depression. *J Affect Disord*. (2021) 287:268–75. doi: 10.1016/j.jad.2021.03.038
16. Zhou S, Xiong P, Ren H, Tan W, Yan Y, Gao Y. Aberrant dorsal attention network homogeneity in patients with right temporal lobe epilepsy. *Epilepsy Behav*. (2020) 111:107278. doi: 10.1016/j.yebeh.2020.107278
17. Li D, Liu R, Wang X, Xiong P-A, Ren H, Wei Y-F. Abnormal ventral attention network homogeneity in patients with right temporal lobe epilepsy. *Eur Rev Med Pharmacol Sci*. (2021) 25:2031–8. doi: 10.26355/eurrev_202102_25107
18. Gao Y, Wang X, Xiong P-G, Ren H, Zhou S-Y, Yan Y-G, et al. Abnormalities of the default-mode network homogeneity and executive dysfunction in people with first-episode, treatment-naive left temporal lobe epilepsy. *Eur Rev Med Pharmacol Sci*. (2021) 25:2039–49. doi: 10.26355/eurrev_202102_25108
19. Gao Y, Zheng J, Li Y, Guo D, Wang M, Cui X. Abnormal default-mode network homogeneity in patients with temporal lobe epilepsy. *Medicine*. (2018) 97:e11239. doi: 10.1097/MD.0000000000011239
20. Gao Y, Zheng J, Li Y, Guo D, Wang M, Cui X. Decreased functional connectivity and structural deficit in alertness network with right-sided temporal lobe epilepsy. *Medicine*. (2018) 97:e0134. doi: 10.1097/MD.0000000000010134
21. Gao Y, Xiong Z, Wang X, Ren H, Liu R, Bai B. Abnormal degree centrality as a potential imaging biomarker for right temporal lobe epilepsy: a resting-state functional magnetic resonance imaging study and support vector machine analysis. *Neuroscience*. (2022) 487:198–206. doi: 10.1016/j.neuroscience.2022.02.004
22. Hu G, Waters AB, Aslan S, Frederick B, Cong F, Nickerson LD. Snowball ICA: a model order free independent component analysis strategy for functional magnetic resonance imaging Data. *Front Neurosci*. (2020) 14:569657. doi: 10.3389/fnins.2020.569657
23. Hsu T-Y, Lee H-C, Lane TJ, Missal M. Temporal preparation, impulsivity and short-term memory in depression. *Front Behav Neurosci*. (2019) 13:258. doi: 10.3389/fnbeh.2019.00258
24. Hwang S, White SF, Nolan ZT, Williams WC, Sinclair S, Blair RJR. Executive attention control and emotional responding in attention-deficit/hyperactivity disorder–a functional MRI study. *Neuroimage Clin*. (2015) 9:545–54. doi: 10.1016/j.nicl.2015.10.005
25. Association AP. *Diagnostic and Statistical Manual of Mental Disorders (DSM-IV-TR). American Psychiatric Association*. Washington, DC: American Psychiatric Association (2000).
26. Fan J, McCandliss BD, Sommer T, Raz A, Posner MI. Testing the efficiency and independence of attentional networks. *J Cogn Neurosci*. (2002) 14:340–7. doi: 10.1162/089892902317361886
27. Chao-Gan Y, Yu-Feng Z. DPARSF: A MATLAB toolbox for "pipeline" data analysis of resting-state fMRI. *Front Syst Neurosci*. (2010) 4:13. doi: 10.3389/fnsys.2010.00013
28. Hahamy A, Calhoun V, Pearlson G, Harel M, Stern N, Attar F. Save the global: global signal connectivity as a tool for studying clinical populations with functional magnetic resonance imaging. *Brain Connect*. (2014) 4:395–403. doi: 10.1089/brain.2014.0244
29. Egolf AE, Kiehl KA, Calhoun VD. Group ICA of fMRI toolbox GIFT. *NeuroImage*. (2004) 22:14–7.
30. Madden DJ, Parks EL, Davis SW, Diaz MT, Potter GG, Chou Y-H. Age mediation of frontoparietal activation during visual feature search. *Neuroimage*. (2014) 102:262–74. doi: 10.1016/j.neuroimage.2014.07.053
31. Betzel RF, Byrge L, He Y, Goñi J, Zuo X-N, Sporns O. Changes in structural and functional connectivity among resting-state networks across the human lifespan. *Neuroimage*. (2014) 102:345–57. doi: 10.1016/j.neuroimage.2014.07.067
32. Geerligs L, Saliasi E, Maurits NM, Renken RJ, Lorist MM. Brain mechanisms underlying the effects of aging on different aspects of selective attention. *Neuroimage*. (2014) 91:52–62. doi: 10.1016/j.neuroimage.2014.01.029
33. Zhang J, Wang J, Wu Q, Kuang W, Huang X, He Y. Disrupted brain connectivity networks in drug-naive, first-episode major depressive disorder. *Biol Psychiatry*. (2011) 70:334–42. doi: 10.1016/j.biopsych.2011.05.018
34. Boeken Jonas O. Functional connectivity of the dorsal and ventral frontoparietal attentional systems. In: *MEi: CogSci Conference 2015*. Ljubljana (2015).
35. Domakonda MJ, He X, Lee S, Cyr M, Marsh R. Increased functional connectivity between ventral attention and default mode networks in adolescents with bulimia nervosa. *J Am Acad Child Adolesc Psychiatry*. (2019) 58:232–41. doi: 10.1016/j.jaac.2018.09.433
36. Schmidt SA, Carpenter-Thompson J, Husain FT. Connectivity of precuneus to the default mode and dorsal attention networks: a possible invariant marker of long-term tinnitus. *Neuroimage Clin*. (2017) 16:196–204. doi: 10.1016/j.nicl.2017.07.015
37. Jimenez AM, Lee J, Wynn JK, Cohen MS, Engel SA, Glahn DC. Abnormal ventral and dorsal attention network activity during single

and dual target detection in schizophrenia. *Front Psychol.* (2016) 7:323. doi: 10.3389/fpsyg.2016.00323
38. Gollan JK, Norris CJ, Hoxha D, Irick JS, Hawkley LC, Cacioppo JT. Spatial affect learning restricted in major depression relative to anxiety disorders and healthy controls. *Cogn Emot.* (2014) 28:36–45. doi: 10.1080/02699931.2013.794772
39. Burrows K, Stewart JL, Kuplicki R, Figueroa-Hall L, Spechler PA, Zheng H. Elevated peripheral inflammation is associated with attenuated striatal reward anticipation in major depressive disorder. *Brain Behav Immun.* (2021) 93:214–25. doi: 10.1016/j.bbi.2021.01.016
40. Luo Z, Chen G, Jia Y, Zhong S, Gong J, Chen F. Shared and specific dynamics of brain segregation and integration in bipolar disorder and major depressive disorder: a resting-state functional magnetic resonance imaging study. *J Affect Disord*. (2021). 280:279–86. doi: 10.1016/j.jad.2020.11.012
41. Gong J, Wang J, Qiu S, Chen P, Luo Z, Wang J. Common and distinct patterns of intrinsic brain activity alterations in major depression and bipolar disorder: voxel-based meta-analysis. *Transl Psychiatry.* (2020) 10:353. doi: 10.1038/s41398-020-01036-5
42. Yan M, Cui X, Liu F, Li H, Huang R, Tang Y. Abnormal default-mode network homogeneity in melancholic and nonmelancholic major depressive disorder at rest. *Neural Plast*. (2021) 2021:6653309. doi: 10.1155/2021/6653309
43. Kane MJ, Meier ME, Smeekens BA, Gross GM, Chun CA, Silvia PJ, et al. Individual differences in the executive control of attention, memory, and thought, and their associations with schizotypy. *J Exp Psychol Gen*. (2016) 145:1017. doi: 10.1037/xge0000184
44. Cao Y, Yang H, Zhou Z, Cheng Z, Zhao X. Abnormal default-mode network homogeneity in patients with mild cognitive impairment in Chinese communities. *Front Neurol*. (2021) 11:569806. doi: 10.3389/fneur.2020.569806
45. Respino M, Hoptman MJ, Victoria LW, Alexopoulos GS, Solomonov N, Stein AT. Cognitive control network homogeneity and executive functions in late-life depression. *Biol Psychiatry Cogn Neurosci Neuroimaging.* (2020) 5:213–21. doi: 10.1016/j.bpsc.2019.10.013
46. Xue S, Wang X, Wang W, Liu J, Qiu J. Frequency-dependent alterations in regional homogeneity in major depression. *Behav Brain Res.* (2016) 306:13–9. doi: 10.1016/j.bbr.2016.03.012
47. Farrant K, Uddin LQ. Asymmetric development of dorsal and ventral attention networks in the human brain. *Dev Cogn Neurosci.* (2015) 12:165–74. doi: 10.1016/j.dcn.2015.02.001
48. Kucyi A, Hodaie M, Davis KD. Lateralization in intrinsic functional connectivity of the temporoparietal junction with salience- and attention-related brain networks. *J Neurophysiol*. (2012) 108:3382–92. doi: 10.1152/jn.00674.2012

Conflict of Interest: The authors declare that the research was conducted in the absence of any commercial or financial relationships that could be construed as a potential conflict of interest.

Publisher's Note: All claims expressed in this article are solely those of the authors and do not necessarily represent those of their affiliated organizations, or those of the publisher, the editors and the reviewers. Any product that may be evaluated in this article, or claim that may be made by its manufacturer, is not guaranteed or endorsed by the publisher.

frontiers | Frontiers in Psychiatry

ORIGINAL RESEARCH
published: 01 June 2022
doi: 10.3389/fpsyt.2022.924431

Abnormal Reginal Homogeneity in Left Anterior Cingulum Cortex and Precentral Gyrus as a Potential Neuroimaging Biomarker for First-Episode Major Depressive Disorder

Yan Song[1†], *Chunyan Huang*[2†], *Yi Zhong*[3], *Xi Wang*[4*] *and Guangyuan Tao*[1*]

[1] Nanning Fifth People's Hospital, Nanning, China, [2] Department of Cardiology, Tongren Hospital of Wuhan University (Wuhan Third Hospital), Wuhan, China, [3] Peking University Sixth Hospital, Peking University Institute of Mental Health, NHC Key Laboratory of Mental Health (Peking University), Beijing, China, [4] Department of Mental Health, Taihe Hospital, Hubei University of Medicine, Shiyan, China

OPEN ACCESS

Edited by:
Liang Liang,
Xinjiang Medical University, China

Reviewed by:
Hetao Bian,
Wuhan University, China
Jin Liu,
Central South University, China

***Correspondence:**
Xi Wang
422718058@qq.com
Guangyuan Tao
164110402@qq.coms

[†]These authors have contributed equally to this work

Specialty section:
This article was submitted to Neuroimaging and Stimulation, a section of the journal Frontiers in Psychiatry

Received: 20 April 2022
Accepted: 06 May 2022
Published: 01 June 2022

Citation:
Song Y, Huang C, Zhong Y, Wang X and Tao G (2022) Abnormal Reginal Homogeneity in Left Anterior Cingulum Cortex and Precentral Gyrus as a Potential Neuroimaging Biomarker for First-Episode Major Depressive Disorder. Front. Psychiatry 13:924431. doi: 10.3389/fpsyt.2022.924431

Objective: There is no objective method to diagnose major depressive disorder (MDD). This study explored the neuroimaging biomarkers using the support vector machine (SVM) method for the diagnosis of MDD.

Methods: 52 MDD patients and 45 healthy controls (HCs) were involved in resting-state functional magnetic resonance imaging (rs-fMRI) scanning. Imaging data were analyzed with the regional homogeneity (ReHo) and SVM methods.

Results: Compared with HCs, MDD patients showed increased ReHo in the left anterior cingulum cortex (ACC) and decreased ReHo in the left precentral gyrus (PG). No correlations were detected between the ReHo values and the Hamilton Rating Scale for Depression (HRSD) scores. The SVM results showed a diagnostic accuracy of 98.96% (96/97). Increased ReHo in the left ACC, and decreased ReHo in the left PG were illustrated, along with a sensitivity of 98.07%(51/52) and a specificity of100% (45/45).

Conclusion: Our results suggest that abnormal regional neural activity in the left ACC and PG may play a key role in the pathophysiological process of first-episode MDD. Moreover, the combination of ReHo values in the left ACC and precentral gyrusmay serve as a neuroimaging biomarker for first-episode MDD.

Keywords: regional homogeneity, major depressive disorder, rs-fMRI, support vector machine, biomarker

INTRODUCTION

Major depressive disorder (MDD) is a very prevalent psychiatric disorder that significantly impacts patients' quality of life and physical health. According to the World Health Organization, more than 300 million people in the world suffered from depression. The suffering caused by self-mutilation, suicide, and other behaviors of depression patients to patients and their families and the loss to society cannot be ignored (1). In the past few decades, researchers have sought breakthroughs in the diagnosis of depression, from relying solely on symptomatic diagnosis to the birth of

various markers, such as blood biomarkers and molecular genetics biomarkers: BDNF Val66Met, 5-HTTLPR risk gene biomarkers, and gut microbiota (2–4). However, a simple and objectively effective diagnostic marker has not been found.

Functional Magnetic Resonance Imaging (fMRI) is a feasible non-invasive medical imaging to examine the structure and connectivity of the brain (5). fMRI can be utilized to explore the working mechanism and regularity of the brain in the resting state, which mainly reflects the functional connection characteristics of the neural network of the brain (6). The principle of fMRI is to capture the hemodynamic changes under neural activity. Given that the brain's neural activity requires the local blood flow with sufficient oxygen supply, increasing the local blood oxygen supply results in the change in blood oxygen concentration, leading to the change of the magnetic resonance signal in the local brain area. This latter change can be detected by The Blood Oxygenation Level Dependent (BOLD) signal of each voxel point of the brain and recorded as the magnetic resonance imaging signal (7). Therefore, fMRI can decipher the differences of BOLD signals in various regions in the brain of depressed patients from healthy populations, facilitating the diagnosis of MDD.

A large number of studies have found that patients with depression have abnormal signals in various brain regions on fMRI (8–11). The most prominent regions are the medial prefrontal cortex, the limbic system, and the default network (12–15). Adolescent patients with MDD have been associated with heightened connectivity within default mode network (DMN) regions and diminished connectivity within FPN regions (16). A study of MDD patients with somatic symptoms showed that both ReHo and ALFF values in the bilateral precentral gyrus, postcentral gyrus, and left paracentral gyrus were lower than those in the control group (17). First-episode, treatment-naive patients with MDD showed decreased activity in the left dorsolateral prefrontal cortex and bilateral medial orbitofrontal cortex (18), and reduced ALFF was found in bilateral orbital frontal cortex (OFC), while increased ALFF in the bilateral temporal lobe extending to theinsular and left fusiform cortices in MDD patients compared to healthy controls (19). A meta-analysis of whole-brain rs-fMRI studies found that MDD patients displayed decreased ALFF in the bilateral cerebellum and bilateral precuneus cortex (20). The inconsistency of these results may be related to the interference of different disease courses, medications, and other factors. Therefore, selecting patients with first-episode drug-naïve depression as study subjects can reduce the interference of these confounding factors.

The support vector machine (SVM) has solved clinical problems since the mid-nineties. Several studies have used SVM combined with neuroimaging data to explore the diagnosis and treatment response prediction of depression at the individual level to improve the diagnostic accuracy of depression (21–27). By using SVM analysis, the possibility of distinguishing MDD from healthy controls by using the extracted abnormal ReHo values in brain regions can be examined in our study. We aimed to explore specific or distinctive alterations in first-episode MDD and whether the alterations could be used to separate first-episode MDD from healthy controls. We hypothesized that first-episode untreated depression patients have multiple abnormal ReHo brain regions, and these abnormal brain regions singly/combined as a biomarker to assist in diagnosing depression patients.

METHODS

Participants

Fifty-two first-episode MDD patients and 45 age-, gender-, education-matched, health controls were recruited from the First Affiliated Hospital of Guangxi Medical University, China. All participants were right-handed. The patient's final diagnoses were independently confirmed by two experienced psychiatrists using the Structured Clinical Interview of the DSM-IV (SCID) (28) and assessed by the 17-item Hamilton Rating Scale for Depression (HRSD-17). The inclusion criteria for MDD patients were as follows: first major depressive episode; 17-item Hamilton Rating Scale for Depression (HRSD-17) total scores $\geq$17. Exclusion criteria were as follows for the patients: any history of head injury or lost consciousness, serious physical or neurological illness, other mental disorders meeting DSM-IV diagnostic criteria, such as a cute physical illness, substance abuse or dependence, schizophrenia, bipolar disorder. None of the healthy controls had a severe physical illness, history of mental disorders, or family history of mental disorders.

Each participant has submitted a written informed consent before enrollment. The study was approved by the Medical Research Ethics Committee of the First Affiliated Hospital of Guangxi Medical University, China, and performed in accordance with the Declaration of Helsinki.

Image Acquisition

The resting-state MRI data were obtained by using an Achieva 3.0T scanner (Philips, Amsterdam, the Netherlands) at the First Affiliated Hospital of Guangxi Medical University in the first day after enrollment. All the participants were instructed to lie still, close their eyes, and remain awake during the scan. The resting-state functional images were employed, using an echo-planar imaging sequence with the following parameters: repetition time/echo time (TR/TE) 2000/30ms, 31 slices, 90° flip angles, 22 cm× 22 cmFOV, 5 mm slice thickness, and 1 mm gap.

Data Preprocessing

DPARSF software in MATLAB was used to preprocess imaging data (29). Due to initial signal instability and participants' adaption time, the first five-time points were deleted in order to minimize the influence of participants' adaption time and the instability of the initial signal. Slice time and head motion were corrected.

All imaging data were with a maximum displacement in the x-, y-, or z-axis no more than 2 mm and maximum angular rotation no more than 2°. The corrected imaging data were spatially normalized to the standard Montreal Neurological Institute space and resampled to 1 mm × 1 mm × 1 mm. The obtained fMRI data were temporally band-pass filtered (0.01–0.08 Hz) and linearly detrended. Several spurious covariates were removed from the imaging data, such as the signal from the ventricular

TABLE 1 | Clinical information of the participants.

Characteristics	Patients ($n = 52$)	Healthy controls ($n = 45$)	t(or $\chi 2$)	p-value
Gender (male/female)	52 (15/37)	45 (12/33)	0.057	0.811[A]
Age (years)	25.77 ± 5.41	24.85 ± 4.17	0.923	0.358[B]
Years of education(years)	12.46 ± 2.63	12.40 ± 3.40	0.100	0.920[B]
Illness duration(months)	1.62 ± 1.07			
HRSD scores	22.37 ± 3.98			

HRSD, Hamilton Rating Scale for Depression; [A]The p-value was obtained by a Chi-square test; [B]The p-value was obtained by two-sample t-tests.

TABLE 2 | Brain regions with abnormal ReHo in MDD.

Cluster location	Peak(MNI)			Number of voxels	t-value	p-value
	X	Y	Z			
Patients>controls						
Left ACC	0	18	18	142	2.62	
Patients< controls						
Left PG	−30	−18	60	187	−3.45	

ReHo, regional homogeneity; MDD, major depressive disorder; MNI, Montreal Neurological Institute; ACC, anterior cingulum cortex; PG, precentral gyrus.

seed-based region of interest, the six-head motion parameters obtained by rigid body correction, and the white matter-centered region. The global signal was regressed out during the processing of the resting-state functional connectivity data.

ReHo analysis was performed using REST software. The formula used to calculate ReHo according to the previous study (30).

Classification Analysis

Distributions of age, years of education, and voxel-based comparisons of whole-brain ReHo maps were compared by using two-sample t-tests. The gender ratio was compared by using Chi-square test. The resulting statistical maps were set at a threshold ($p < 0.01$) for multiple comparisons (GRF corrected, voxel significance: $P < 0.01$; clustering significance: $p < 0.01$). Furthermore, linear correlations were calculated between abnormal ReHo values and psychological performances. The significance threshold was set at $p < 0.05$.

SVM analysis was applied to examine the possibility of distinguishing MDD from healthy controls by using the extracted abnormal ReHo values in brain regions. The method of SVM was operated using the LIBSVM software package in MATLAB. The best parameters including C (penalty coefficient) and gamma value were selected. Through the LIBSVM tool, the grid of parameters were evaluated and all the parameter settings' accuracies were acquired. The highest cross-validation accuracy of the parameter was determined.

RESULTS

Demographics Characteristics and Clinical Information

A total of 52 MDD patients and 45 healthy controls were involved in the study. No significant differences in age, gender, and year of education were observed between the two groups. Demographic information and clinical characteristics were shown in **Table 1**.

ReHo: Patients vs. Controls

Compared with healthy controls, patients with MDD exhibited a significantly increased ReHo in the left anterior cingulum cortex (ACC) and decreased ReHo in the left precentral gyrus (PG) (**Table 2**; **Figure 1**).

The Correlations Between the ReHo Values and Other Factors

There was no correlations detected between the ReHo values and the Hamilton Rating Scale for Depression (HRSD) scores. There were no other factors such as gender and years of education in MDD patients were detected be related to the abnormal ReHo values.

SVM Results

A combination of the increased ReHo values in the left ACC and decreased ReHo in the left PG was used as a potential biomarker to diagnose MDD patients by the SVM method. The classification accuracies were as follows: diagnostic accuracy of 98.96% (96/97), a sensitivity of 98.07%(51/52), and a specificity of 100% (45/45) (**Figure 2**).

DISCUSSION

The objective, effective and rapid diagnosis of MDD has always been a hot spot in clinical research. However, there are no effective diagnostic methods for MDD, and its diagnosis still depends on depressive syndromes. Rs-fMRI research is increasingly used to assist clinical diagnosis. This study explored the utility of altered ReHo values in the left ACC and PG as a potential neuroimaging biomarker for the first-episode MDD by the SVM method.

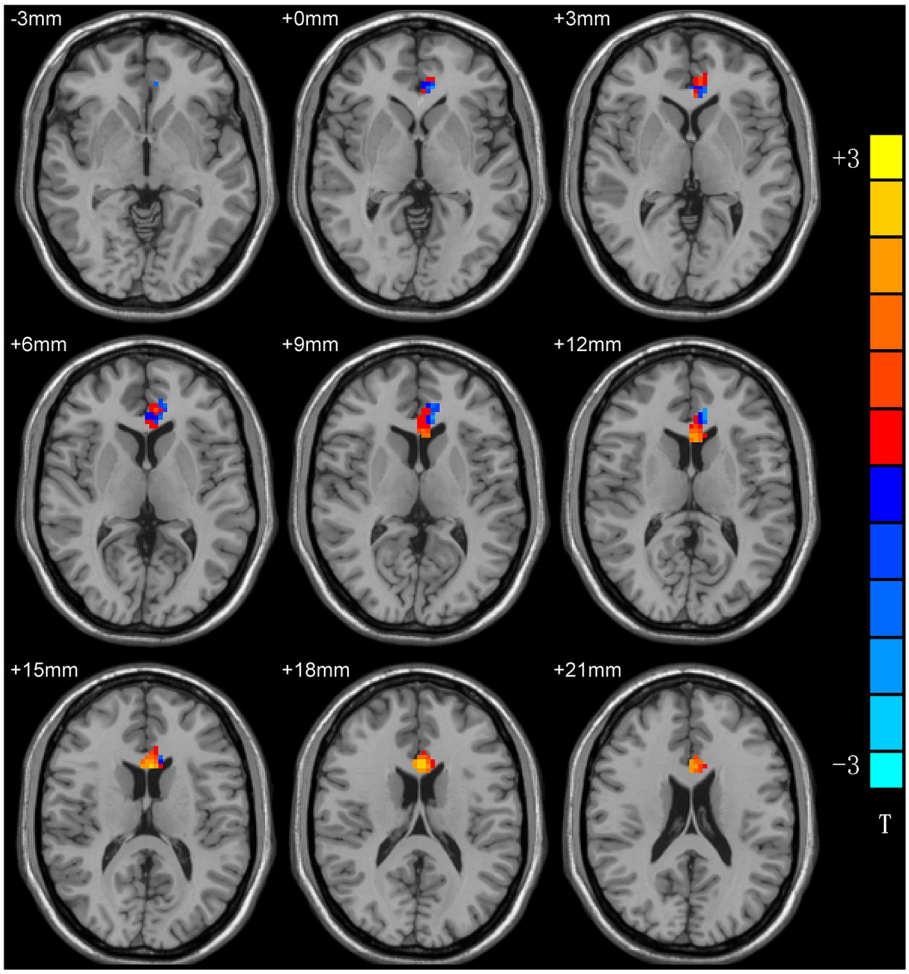

FIGURE 1 | ReHo differences between patients with MDD and HCs. Red and blue denote higher and lower ReHo, respectivsely, and the color bars represent the *T*-values from the two-sample *t*-test of the group analysis. ReHo, regional homogeneity; MDD, major depressive disorder; HCs, healthy controls.

The cingulum is a key component of the limbic lobe, and it also plays a key role in the DMN. The cingulum is the major interconnecting apparatus of all cerebral lobes (31). It has been described as the "seat of dynamic vigilance by which environmental experiences are endowed with an emotional awareness" by Papez (32). Based on the characteristics and anatomy of the cingulum gyrus, the cingulum gyrus is divided into four subregions such as the ACC, middle cingulum cortex, posterior cingulum cortex, and retrosplenial cortex (33). Anterior cerebrum The ACC is the first half of the cingulum gyrus, which is closely related to human cognitive execution, emotional processing, and other brain functions (34). When ACC is damaged, it will produce many clinical symptoms, including inattention, dysfunction of autonomic function regulation, emotional instability (35, 36). Studies have found that the ACC is prone to damage in depression (37, 38). Structural magnetic resonance study found that the anterior cingulum white matter fibrosis of the ACC recovered after 8 weeks of antidepressant treatment (39, 40). In the present study, similar results were noticed. Increased ReHo values of the left ACC and decreased PG were found in the patients with MDD, and thus we speculated that abnormal ReHo in the left ACC and PG has a critical role in the physiological processes of MDD. Another finding of this study was left-sided affected brain regions in MDD patients. As the ACC is considered to have a key role in the pathophysiology of the disorder, lack of normal symmetries in ACC has been long observed. In task-related fMRI, decreased functional connectivity between the left amygdala and the left ACC during negative stimuli in participants with MDD was found (41), while the increased depression duration was correlated with decreased perfusion of the right ACC (42). Consistent with the previous findings, our results suggest that lack of normal symmetries may be a characteristic for patients with MDD.

Prefrontal lobe dysfunction is associated with a variety of depressive symptoms, such as attention deficit, psychomotor retardation, executive dysfunction, etc., and is related to the treatment of depression (43). The prefrontal-striatal neural circuit underlies behavioral disinhibition (32). Previous studies

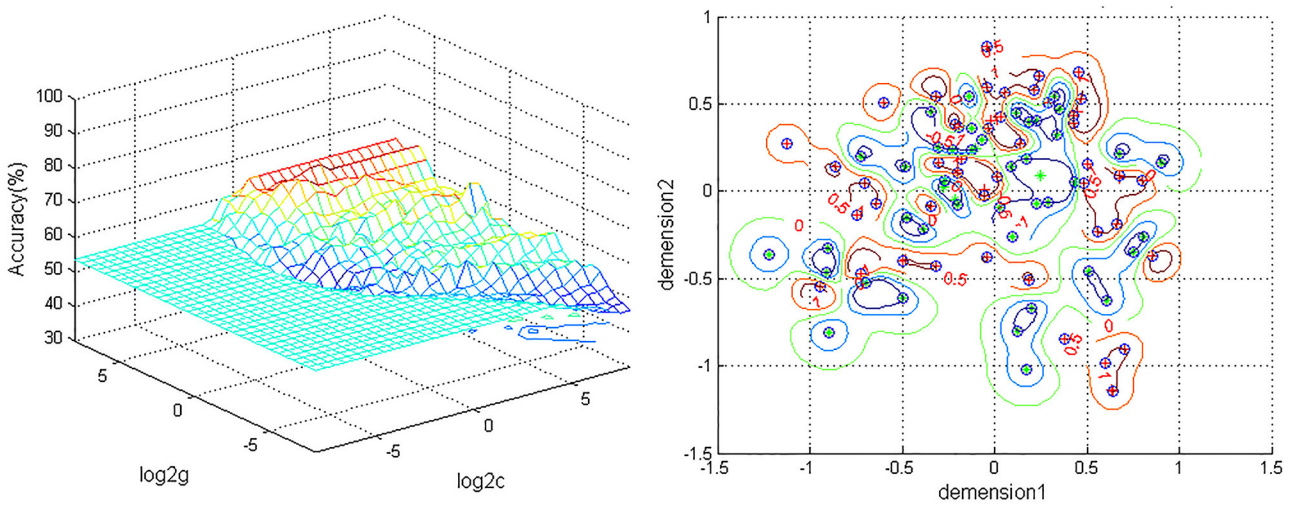

FIGURE 2 | Depiction of classifications based on the SVM using a combination of ReHo values in the left ACC and PG to differentiate MDD patients from HCs. Left: SVM parameters result of 3D view. g, means gamma; c, penalty coefficient; Right, dimension 1 and dimension 2 represent the ReHo values in the left ACC and PG. Green crosses represent MDD patients, and the red crosses represent HCs. SVM, support vector machine; ReHo, regional homogeneity; ACC, anterior cingulum cortex; PG, precentral gyrus; MDD, major depressive disorder; HCs,s healthy controls.

have found that dorsal medial prefrontal gyrus lesions are associated with susceptibility to depression (44). In MDD patients, behavioral disinhibition is associated with increased suicidal behavior, mental agitation, impulsivity loss, and substance use disorders. related to (44, 45). Furthermore, Structural magnetic resonance studies found that the precentral gyrus volume was reduced in patients with depression compared with normal people (46). Carlson et al. also found that in patients with MDD, increased depression was associated with a decrease in PFC volume (47). A recent study also found that compared with MDD patients who did not attempt suicide, suicide attempters had a greater surface area in the left retrocentral gyrus and lateral occipital gyrus but a smaller surface area in the left superior frontal gyrus (48). These studies suggest that the damage to the precentral cortex in patients with depression is involved in the pathological mechanism of depression.

Antidepressants may have an effect on brain structure and function (49–51). Therefore, it is essential to select drug-naive patients as a starting point to minimize the potentialeffects of medication. Long illness duration may have a neurotoxic effect on brain structure (52). Guo and his companies found that the combination of abnormal ReHo in the right fusiform gyrus/cerebellar and right superior/middle occipital gyrus showed an accuracy of 83.05%, the sensitivity of 90.32%, and specificity was 75.00%, which was used to distinguish depressive MDD patients from non-depressed MDD patients, and the combination of abnormal ReHo in right fusiform gyrus/cerebellar and left precentral gyrus showed the accuracy of 98.41%, sensitivity of 96.77%, and specificity of 100.00%, used to distinguish depressive MDD patients from healthy controls (21). In the present study, our study found abnormal ReHo values in ACC and PG within patients with first-episode MDD. Furthermore, an SVM was used to combine the ReHo signals of these two abnormal brain regions as a biomarker for diagnosing MDD with an accuracy of 98.96%, a sensitivity of 98.07%,and a specificity of 100%. A slightly larger sample size, unmedicated, and shorter disease duration may explain our results may have better clinical value.

Some limitations exist in the study. First, the age of the patients is concentrated in the young and the mean illness duration is <2 months. Further study is needed to justify these results in order to enhance the possibility of generalizing the results of this study to MDD patients with various clinical characteristics. Second, we did not know whether changes in the left anterior Cingulum cortex and Precentral gyrus occurred before or as a result of MDD. A long-term follow-up observation may help us to understand the cause and effect.

CONCLUSION

In conclusion, the altered ReHo in the left ACC and PG may be state-related changes of MDD. Also, the combination of increased ReHo in the left ACC and left PG may be a potential neuroimaging biomarker for the first-episode MDD.

DATA AVAILABILITY STATEMENT

The original contributions presented in the study are included in the article/supplementary material, further inquiries can be directed to the corresponding author/s.

ETHICS STATEMENT

The studies involving human participants were reviewed and approved by the Medical Research Ethics Committee of the First Affiliated Hospital of Guangxi Medical University, China. The patients/participants provided their written informed consent to participate in this study.

AUTHOR CONTRIBUTIONS

XW and GT contributed to the conception and design of the study. CH and YZ supervised the progress of the study. YS performed the data analysis and wrote the manuscript. All authors contributed to manuscript revision, and approved it for publication.

ACKNOWLEDGMENTS

The investigation was supported by grants from the Natural Science Foundation of Guangxi Province for Distinguished Young Scientists (Grant No. 2014GXNSFGA118010) and the Health Commission of Guangxi Province Self-Funded Research Project (Grant No. Z20201097). We thank all the individuals who served as the research participants.

REFERENCES

1. Chen M, Ketenci M, Lee JS, Srinivasan A, Wang YM, Rosoklija G, et al. Proteomics profiling of MDD, suicide and SSRI treatment in the human hippocampus. *Biol Psychiatry.* (2020) 87:S213. doi: 10.1016/j.biopsych.2020.02.553
2. Bai SJ, Bai HL Li DT, Zhong Q, Xie J, Chen JJ. Gut Microbiota-related inflammation factors as a potential biomarker for diagnosing major depressive disorder. *Front Cell Infect Microbiol.* (2022) 12:831186. doi: 10.3389/fcimb.2022.831186
3. Zhang GY, Xu SX, Zhang ZQ, Zhang Y, Wu YK, An J, et al. Identification of key genes and the pathophysiology associated with major depressive disorder patients based on integrated bioinformatics analysis. *Front Psychiatry.* (2020) 11:192. doi: 10.3389/fpsyt.2020.00192
4. Whittlesey, R. *Identification of Potential Biomarkers in PDAC*. Chapel Hill, NC: University of North Carolina at Chapel Hill Graduate School (2014).
5. Fox MD, Raichle ME. Spontaneous fluctuations in brain activity observed with functional magnetic resonance imaging. *Nat Rev Neurosci.* (2007) 8:700–11. doi: 10.1038/nrn2201
6. Forman SD, Cohen JD, Fitzgerald M, Eddy WF, Mintun MA, Noll DC. Improved assessment of significant activation in functional magnetic resonance imaging (fMRI): use of a cluster-size threshold. *Magn Reson Med.* (1995) 33:636–47. doi: 10.1002/mrm.1910330508
7. Fransson P. Spontaneous low-frequency BOLD signal fluctuations: an fMRI investigation of the resting-state default mode of brain function hypothesis. *Hum Brain Mapp.* (2005) 26:15–29. doi: 10.1002/hbm.20113
8. Marchitelli R, Paillère-Martinot ML, Bourvis N, Guerin-Langlois C, Kipman A, Trichard C, et al. Dynamic functional connectivity in adolescence-onset major depression: relationships with severity and symptom dimensions. *Biol Psychiatry Cogn Neurosci Neuroimaging.* (2022) 7:385–96. doi: 10.1016/j.bpsc.2021.05.003
9. Han SQ, Cui Q, Wang X, Li L, Li D, He ZL, et al. Resting state functional network switching rate is differently altered in bipolar disorder and major depressive disorder. *Hum Brain Mapp*. (2020) 41:3295–304. doi: 10.1002/hbm.25017
10. Burrows K, Stewart JL, Kuplicki R, Figueroa-Hall L, Spechler PA, Zheng H, et al. Elevated peripheral inflammation is associated with attenuated striatal reward anticipation in major depressive disorder. *Brain Behav Immun.* (2021) 93:214–25. doi: 10.1016/j.bbi.2021.01.016
11. Van Tol MJ, Van der Wee NJA, Veltman DJ. Fifteen years of NESDA neuroimaging: an overview of results related to clinical profile and bio-social risk factors of major depressive disorder and common anxiety disorders. *J Affect Disord.* (2021) 289:31–45. doi: 10.1016/j.jad.2021.04.009
12. Hou ZH, Kong YY, Yin YY, Zhang YQ, Yuan YG. Identification of first-episode unmedicated major depressive disorder using pretreatment features of dominant coactivation patterns. *Prog Neuropsychopharmacol Biol Psychiatry.* (2021) 104:110038. doi: 10.1016/j.pnpbp.2020.110038
13. Liang SG, Deng W, Li XJ, Greenshaw AJ, Wang Q, Li ML, et al. Biotypes of major depressive disorder: neuroimaging evidence from resting-state default mode network patterns. *Neuroimage Clin.* (2020) 28:102514. doi: 10.1016/j.nicl.2020.102514
14. Provenzano J, Fossati P, Dejonckheere E, Verduyn P, Kuppens P. Inflexibly sustained negative affect and rumination independently link default mode network efficiency to subclinical depressive symptoms. *J Affect Disord.* (2021) 293:347–54. doi: 10.1016/j.jad.2021.06.051
15. Pan YZ, Liu ZN, Xue ZM, Sheng YY, Cai Y, Cheng YX, et al. Abnormal network properties and fiber connections of DMN across major mental disorders: a probability tracing and graph theory study. *Cereb Cortex*. (2021). doi: 10.1093/cercor/bhab405. [Epub ahead of print].
16. Qu YY, Rappaport BI, Luby JL, Barch DM. No associations in preregistered study of youth depression and functional connectivity of fronto-parietal and default mode networks. *Neuroimage.* (2021) 3:100036. doi: 10.1016/j.ynirp.2021.100036
17. Liu PH, Tu HW, Zhang AX, Yang CX, Liu ZF, Lei L, et al. Brain functional alterations in MDD patients with somatic symptoms: a resting-state fMRI study. *J Affect Disord*. (2021) 295:788–96. doi: 10.1016/j.jad.2021.08.143
18. Wang L, Dai WJ, Su YN, Wang G, Tan YL, Jin Z, et al. Amplitude of low-frequency oscillations in first-episode, treatment-naive patients with major depressive disorder: a resting-state functional MRI study. *PLoS One*. (2012) 7: e48658. doi: 10.1371/journal.pone.0048658
19. Zhang XC, Zhu XL, Wang X, Zhu XZ, Zhong MT Yi JY, et al. First-episode medication-naive major depressive disorder is associated with altered resting brain function in the affective network. *PLoS ONE.* (2014) 9:e85241. doi: 10.1371/journal.pone.0085241
20. Gong JY, Wang JJ, Qiu SJ, Chen P, Luo ZY, Wang JR, et al. Common and distinct patterns of intrinsic brain activity alterations in major depression and bipolar disorder: voxel-based meta-analysis. *Transl Psychiatry.* (2020) 10:353. doi: 10.1038/s41398-020-01036-5
21. Yan MQ, He YQ, Cui XL, Liu F, Li HB, Huang RZ, et al. Disrupted regional homogeneity in melancholic and non-melancholic major depressive disorder at rest. *Front Psychiatry.* (2021) 12:618805. doi: 10.3389/fpsyt.2021.618805
22. Sen B, Cullen KR, Parhi KK. Classification of adolescent major depressive disorder via static and dynamic connectivity. *IEEE J Biomed Health Inform.* (2021) 25:2604–14. doi: 10.1109/JBHI.2020.3043427
23. Shan XX, Cui XL, Liu F, Li HB, Huang RZ, Tang YQ, et al. Shared and distinct homotopic connectivity changes in melancholic and non-melancholic depression. *J Affect Disord.* (2021) 287:268–75. doi: 10.1016/j.jad.2021.03.038
24. Gao YJ, Wang X, Xiong ZY, Ren HW, Liu RS, Wei YF, et al. Abnormal fractional amplitude of low-frequency fluctuation as a potential imaging biomarker for first-episode major depressive disorder: a resting-state fmri study and support vector machine analysis. *Front Neurol.* (2021) 12:751400. doi: 10.3389/fneur.2021.751400
25. Gao YJ, Xiong ZY, Wang X, Ren HW, Liu RS, Bai B, et al. Abnormal degree centrality as a potential imaging biomarker for right temporal lobe epilepsy: a resting-state functional magnetic resonance imaging study and support vector machine analysis. *Neuroscience.* (2022) 487:198–206. doi: 10.1016/j.neuroscience.2022.02.004

26. Gao YJ, Wang X, Xiong PG, Ren HW, Zhou SY, Yan YG, et al. Abnormalities of the default-mode network homogeneity and executive dysfunction in people with first-episode, treatment-naive left temporal lobe epilepsy. *Eur Rev Med Pharmacol Sci.* (2021) 25:2039–49.
27. Li DB, Liu RS, Wang X, Xiong PA, Ren HW, Wei YF, et al. Abnormal ventral attention network homogeneity in patients with right temporal lobe epilepsy. *Eur Rev Med Pharmacol Sci.* (2021) 25:2031–8.
28. Lobbestael J, Leurgans M, Arntz A. Inter-rater reliability of the Structured Clinical Interview for DSM-IV Axis I Disorders (SCID I) and Axis II Disorders (SCID II). *Clin Psychol Psychother*. (2011)18:75–9. doi: 10.1002/cpp.693
29. Yan CG, Zang YF, DPARSF. A MATLAB Toolbox for "Pipeline" Data Analysis of Resting-State fMRI. *Front Syst Neurosci.* (2010) 4:13. doi: 10.3389/fnsys.2010.00013
30. Song Y, Su QJ, Jiang ML, Liu F, Yao DP Dai Y, et al. Abnormal regional homogeneity and its correlations with personality in first-episode, treatment-naive somatization disorder. *Int J Psychophysiol.* (2015) 97:108–12. doi: 10.1016/j.ijpsycho.2015.05.012
31. Wade-Kane R, Ba E, Camara M, Thiam M. Contribution of the neuroanatomy of the cingulate Gyrus to the neuroscientific approach to depression. *O J Psychs*. (2022) 12:37–48. doi: 10.4236/ojpsych.2022.121004
32. Petrides M, Pandya DN. Efferent association pathways from the rostral prefrontal cortex in the macaque monkey. *J Neurosci.* (2007) 27:11573–86. doi: 10.1523/JNEUROSCI.2419-07.2007
33. Papez JW. A proposed mechanism of emotion, 1937. *J Neuropsychiatry Clin Neurosci*. (1995) 7:103–12. doi: 10.1176/jnp.7.1.103
34. Devinsky O, Morrell MJ, Vogt BA, Review article. Contributions of anterior cingulate cortex to behaviour. *Brain.* (1995) 118:279–306. doi: 10.1093/brain/118.1.279
35. Asayesh V, Nikjeh MT, Asayesh A. Investigation the differences of Anterior Cingulate Cortex (ACC) and frontal lobe activity between MDD and control group with EEG. *7th Iranian Human Brain Mapping Congress*. (2021). Available online at: https://civilica.com/doc/1257490
36. Wei YC, Qi KM, Yu Y, Lu W, Xu W, Yang CZ, et al. Analysis of Differentially Expressed Genes in the Dentate Gyrus and Anterior Cingulate Cortex in a Mouse Model of Depression. *Biomed Res Int.* (2021) 2021:5013565. doi: 10.1155/2021/5013565
37. Zavorotnyy M, Zöllner R, Rekate H, Dietsche P, Bopp M, Sommer J, et al. Intermittent theta-burst stimulation moderates interaction between increment of N-Acetyl-Aspartate in anterior cingulate and improvement of unipolar depression. *Brain Stimul.* (2020) 13:943–52. doi: 10.1016/j.brs.2020.03.015
38. Seewoo BJ, Rodger J, Demitrack MA, Heart KL, Port JD, Strawn JR, et al. Neurostructural differences in adolescents with treatment resistant depression and treatment effects of transcranial magnetic stimulation. *Int J Neuropsychopharmacol.* (2022). doi: 10.1093/ijnp/pyac007. [Epub ahead of print].
39. Han KM, Han MR, Kim A, Kang W, Kang Y, Kang J, et al. A study combining whole-exome sequencing and structural neuroimaging analysis for major depressive disorder. *J Affect Disord.* (2020) 262:31–9. doi: 10.1016/j.jad.2019.10.039
40. Chen LP Dai HY, Dai ZZ, Xu CT, Wu RH. Anterior cingulate cortex and cerebellar hemisphere neurometabolite changes in depression treatment: A 1H magnetic resonance spectroscopy study. *Psychiatry Clin Neurosci.* (2014) 68:357–64. doi: 10.1111/pcn.12138
41. Robert G, Bannier E, Comte M, Domain L, Corouge I, Dondaine T, et al. Multimodal brain imaging connectivity analyses of emotional and motivational deficits in depression among women. *J Psychiatry Neurosci.* (2021) 46:E303–12. doi: 10.1503/jpn.200074
42. Tastevin M, Boyer L, Korchia T, Fond G, Lançon C, Richieri R, et al. Brain SPECT perfusion and PET metabolism as discordant biomarkers in major depressive disorder. *EJNMMI Res.* (2020) 10:121. doi: 10.1186/s13550-020-00713-2
43. Hamon M, Blier P. Monoamine neurocircuitry in depression and strategies for new treatments. *Prog Neuro-psychopharmacol Biol Psychiatry.* (2013) 45:54–63. doi: 10.1016/j.pnpbp.2013.04.009
44. Koenigs M, Huey ED, Calamia M, Raymont V, Tranel D, Grafman J. Distinct regions of prefrontal cortex mediate resistance and vulnerability to depression. *J Neurosci.* (2008) 28:12341–8. doi: 10.1523/JNEUROSCI.2324-08.2008
45. Kittnar O. Selected sex related differences in pathophysiology of cardiovascular system. *Physiol Res.* (2020) 69:21–31. doi: 10.33549/physiolres.934068
46. Taki Y, Kinomura S, Awata S, Inoue K, Sato K, Ito H, et al. Male elderly subthreshold depression patients have smaller volume of medial part of prefrontal cortex and precentral gyrus compared with age-matched normal subjects: a voxel-based morphometry. *J Affect Disord.* (2005) 88:313–20. doi: 10.1016/j.jad.2005.08.003
47. Carlson JM, Depetro E, Maxwell J, Harmon-Jones E, Hajcak G. Gender moderates the association between dorsal medial prefrontal cortex volume and depressive symptoms in a subclinical sample. *Psychiatry Res.* (2015) 233:285–8. doi: 10.1016/j.pscychresns.2015.06.005
48. Chang CH, Chen MC, Qiu MH, Lu J. Ventromedial prefrontal cortex regulates depressive-like behavior and rapid eye movement sleep in the rat. *Neuropharmacology.* (2014) 86:125–32. doi: 10.1016/j.neuropharm.2014.07.005
49. Jaworska N, Salle S D L, Ibrahim MH, Blier P, Knott V. Leveraging machine learning approaches for predicting antidepressant treatment response using Electroencephalography (EEG) and clinical data. *Front Psychiatry.* (2019) 9:768. doi: 10.3389/fpsyt.2018.00768
50. Vinne NVD, Vollebregt MA, Rush AJ, Eebes M, Putten MJAM, Arns M, et al. biomarker informed prescription of antidepressants in MDD: a feasibility trial. *Eur Neuropsychopharmacol.* (2021) 44:14–22. doi: 10.1016/j.euroneuro.2020.12.005
51. Wu CK, Tseng PT, Wu MK Li DJ, Chen TY, Kuo FC, et al. Antidepressants during and after menopausal transition: a systematic review and meta-analysis. *Sci Rep.* (2020) 10:8026. doi: 10.1038/s41598-020-64910-8
52. Sheng W, Cui Q, Jiang KX, Chen YY, Tang Q, Wang C, et al. Individual variation in brain network topology is linked to course of illness in major depressive disorder. *Cereb Cortex*. (2022). doi: 10.1093/cercor/bhac01. [Epub ahead of print].

Conflict of Interest: The authors declare that the research was conducted in the absence of any commercial or financial relationships that could be construed as a potential conflict of interest.

frontiers | Frontiers in Psychiatry

ORIGINAL RESEARCH
published: 02 June 2022
doi: 10.3389/fpsyt.2022.888150

Correlation Between the Functional Connectivity of Basal Forebrain Subregions and Vigilance Dysfunction in Temporal Lobe Epilepsy With and Without Focal to Bilateral Tonic-Clonic Seizure

Binglin Fan[1†], Linlin Pang[1†], Siyi Li[2†], Xia Zhou[1], Zongxia Lv[1], Zexiang Chen[1] and Jinou Zheng[1]*

[1] Department of Neurology, The First Affiliated Hospital of Guangxi Medical University, Nanning, China, [2] Department of Neurology, The People's Hospital of Guangxi Zhuang Autonomous Region, Nanning, China

OPEN ACCESS

Edited by:
Liang Liang,
Xinjiang Medical University, China

Reviewed by:
Qiang Xu,
Nanjing University, China
Tianhua Yang,
Sichuan University, China
Zhiyun Lian,
Chongqing Hospital of Traditional Chinese Medicine, China

***Correspondence:**
Jinou Zheng
jinouzheng@163.com

[†]These authors have contributed equally to this work

Specialty section:
This article was submitted to Neuroimaging and Stimulation, a section of the journal Frontiers in Psychiatry

Received: 02 March 2022
Accepted: 12 May 2022
Published: 02 June 2022

Citation:
Fan B, Pang L, Li S, Zhou X, Lv Z, Chen Z and Zheng J (2022) Correlation Between the Functional Connectivity of Basal Forebrain Subregions and Vigilance Dysfunction in Temporal Lobe Epilepsy With and Without Focal to Bilateral Tonic-Clonic Seizure. Front. Psychiatry 13:888150. doi: 10.3389/fpsyt.2022.888150

Purpose: Previous research has shown that subcortical brain regions are related to vigilance in temporal lobe epilepsy (TLE). However, it is unknown whether alterations in the function and structure of basal forebrain (BF) subregions are associated with vigilance impairment in distinct kinds of TLE. We aimed to investigate changes in the structure and function BF subregions in TLE patients with and without focal to bilateral tonic-clonic seizures (FBTCS) and associated clinical features.

Methods: A total of 50 TLE patients (25 without and 25 with FBTCS) and 25 healthy controls (HCs) were enrolled in this study. The structural and functional alterations of BF subregions in TLE were investigated using voxel-based morphometry (VBM) and resting-state functional connectivity (rsFC) analysis. Correlation analyses were utilized to investigate correlations between substantially altered imaging characteristics and clinical data from patients.

Results: FBTCS patients had a lower rsFC between Ch1-3 and the bilateral striatum as well as the left cerebellum posterior lobe than non-FBTCS patients. In comparison to non-FBTCS patients, the rsFC between Ch4 and the bilateral amygdala was also lower in FBTCS patients. Compared to HCs, the TLE patients had reduced rsFC between the BF subregions and the cerebellum, striatum, default mode network, frontal lobe, and occipital lobes. In the FBTCS group, the rsFC between the left Ch1-3 and striatum was positive correlated with the vigilance measures. In the non-FBTCS group, the rsFC between the left Ch4 and striatum was significantly negative correlated with the alertness measure.

Conclusion: These results extend current understanding of the pathophysiology of impaired vigilance in TLE and imply that the BF subregions may serve as critical nodes for developing and categorizing TLE biomarkers.

Keywords: temporal lobe epilepsy, focal to bilateral tonic-clonic seizure, basal forebrain subregions, functional connectivity, vigilance function

INTRODUCTION

Temporal lobe epilepsy (TLE), the most frequent form of focal epilepsy in humans, is characterized by sclerosis of the medial temporal lobe and recurring seizures that mainly occur in the hippocampus and amygdala (1). In general, TLE can be classified into three categories: focal awareness seizures (FAS), focal impaired awareness seizures (FIAS), and focal to bilateral tonic-clonic seizures (FBTCS) (2). Over one-third of patients with TLE suffer from FBTCS, which can result in injury or death as a result of accidents or falls, as well as seizure-related brain damage and, in severe or prolonged cases, sudden death (3, 4).

Patients with TLE frequently experience a variety of cognitive, mental, and behavioral impairments, most notably affecting memory, executive function, language, and attention, making it difficult to perform routine tasks, work, and maintain personal relationships, all of which have a negative effect on their quality of life (5, 6). While many factors can contribute to or exacerbate cognitive impairment, the type of seizure has a substantial impact on TLE patients' cognitive prognosis (7). Numerous FBTCS patients suffer from severe cognitive impairments, the most common of which are difficulties with attention and memory (8). Attention is the cornerstone of all cognitive function, and alertness is the most crucial component of attention (9). FBTCS is the most severe form of TLE and is associated with significantly more cognitive impairment than other forms of TLE. Thus, it is critical to shed light on impaired alertness in FBTCS patients.

Cognitive deficits in TLE patients and animal models of limbic seizures have been linked to anomalies in subcortical brain areas that regulate vigilance (10, 11). Subcortical structures regulate vigilance by modifying sleep-wake rhythms and consciousness, and their impairment may result in sleep-wake abnormalities, impaired vigilance, and even consciousness disturbance (12). The main subcortical structures are the ascending reticular activating system (ARAS) nuclei in the brainstem, basal forebrain (BF), intralaminar thalamic nuclei, pulvinar, and posterior hypothalamus (13). The locus coeruleus (LC), a component of the ARAS nuclei, and the thalamus are two subcortical brain areas that are involved in alertness and attention (8, 14). Converging evidence indicates that anatomical and functional anomalies in the basal forebrain can result in insomnia or parasomnias (15–17). Furthermore, according to Adaptive Resonance Theory, Stephen Grossberg proposed that acetylcholine (ACh) release by cells in the basal forebrain can modulate vigilance (18). However, whether the basal forebrain influences alertness in TLE patients is unclear.

The BF, which consists of four subcellular groups (Ch1–4), is critical for the generation and distribution of ACh to the neocortex, amygdala, and hippocampus (19, 20), as well as for modulating neuron excitability and numerous cognitive functions (21). Recent studies have proven that significant BF neuron degeneration and loss of cortical cholinergic innervation promote cognitive decline in Alzheimer's disease, Parkinson's disease, Wilson's disease, and multiple sclerosis (22–25). Hern'an et al. observed aberrant functional connectivity and community between the nucleus basalis of Meynert (NBM) and cerebral hemisphere, related to cognitive impairments in TLE(1).

We postulate that BF neurons deteriorate in patients with different kinds of TLE, disrupting their innervated functional networks and resulting in alert impairment. To verify this hypothesis, we examined the gray volume of the BF in TLE patients with and without FBTCS as well as healthy controls (HCs), followed by functional connectivity analysis to identify aberrant connectivity between the BF subregions (Ch1-4) and the cerebral hemisphere. Linear regression was used to determine whether abnormalities in the structure and functional connectivity in patients with TLE were linked to their clinical data.

METHODS

Participants

Patients with unilateral TLE were enrolled from the Department of Neurology at the First Affiliated Hospital of Guangxi Medical University between January 2017 and September 2021. According to the classification standard guidelines of 1981, 1989 and 2017 formulated by ILAE (26), the secondary generalization diagnosis of complex partial seizures and partial seizures was performed. Inclusion criteria were as follows: (1) all patients had unilateral (left and right) TLE, which was confirmed by MRI structural image, video electroencephalography (EEG) assessment and clinical manifestation analysis. (2) All patients took antiepileptic drugs (AEDs) regularly; (3) All patients were right-handed. Exclusion criteria were as follows: (1) comorbidities affecting cognitive function, including traumatic brain injury, intracranial tumor, stroke, infection, multiple sclerosis, and Alzheimer's disease; (2) Patients with a score <24 on MMSE; (3) patients who take or are taking topiramate and barbiturates; (4) MRI structural images showing abnormalities except hippocampal sclerosis.

Every patient had FIAS and/or FAS, with some also having FBTCS. Patients were divided into two groups for this study based on their medical history at the time of scanning. The "non-FBTCS" group included 25 patients who had never experienced FBTCS, the "FBTCS" group included 25 patients with recurrent FBTCS in the year before scanning, and 25 healthy control subjects with matching demographic features were recruited as a neuroimaging reference group. As confirmed by health screening techniques, the control group had no psychological or neurological issues. All procedures were approved by the Ethics Committee of Guangxi Medical University's First Affiliated Hospital. All individuals provided written informed consent for the study.

Neuropsychological Assessment

The Montreal Cognitive Assessment (MoCA) was used to evaluate cognitive impairment.

The ANT was used to assess each subject's vigilance, as previously stated (27). Participants were instructed to keep their eyes on a fixation cross in the screen's center and determine the direction of the target arrow throughout the trials. Participants were told to press a button to provide an answer as accurately and quickly as they could. The formal test included three blocks of 96 trials, plus the practice block. The entire test took approximately 25 min. In the test, participants had to decide whether the middle

arrow would point left or right next. They were given three types of hints: (1) a center cue, characterized by the presence of an asterisk at the central fixation point; (2) double cues, characterized by an asterisk positioned above and below the fixation cross; or (3) no cue, characterized by a pair of arrows pointing in the opposite direction as the target arrow, or a pair of dashes, flanking the fixation point. Each test contained unique clues, targets, and surrounding interference data, and they were presented in a random order. The device automatically detected and recorded participants' reaction time (RT). the no-cue condition indicated tonic alertness and represented a state of general wakefulness, similar to sustained attention. The double-cue condition indicated phasic alertness and represented the ability of the participant to be response ready for a short period of time subsequent to the presentation of external cues or stimuli. Alertness was reflected by the RT in the two different warning conditions. Alertness was determined by subtracting the median of the double cue condition from the median of the no cue condition. The larger the alertness value was, the greater the degree of alertness.

Imaging Acquisition

The images of the participants were acquired at the First Affiliated Hospital of Guangxi Medical University utilizing a 3.0 Tesla MRI scanner (Philips, The Netherlands) equipped with a standard eight-channel head coil. Throughout the scan, all individuals were instructed to close their eyes and relax but not to sleep. Foam cushions and noise-canceling earplugs were used to reduce noise and head movements. A T1-3D BRAVO sequence was used to acquire high-resolution sagittal T1WI images with the following acquisition parameters: repetition time (TR) = 7.8 ms, echo time (TE) = 3.4 ms, flip angle = 9°, field of view (FOV) = 256 × 256 mm, matrix = 256 × 256 mm, slice thickness = 1 mm without slice gap, voxel size = 0.89 × 0.89 × 1 mm, and 176 sagittal slices. Resting-state functional MRI images were collected by using gradient-echo single-shot echo-planar imaging sequences with a TR = 2,000 ms, TE = 30 ms, FOV = 220 × 220 mm, FA = 90°, matrix = 64 × 64, slice thickness = 3.5 mm, slice gap = 0.5 mm, voxel size = 3.44 × 3.44 × 4 mm, 41 slices, and 225 volumes. For data quality control, the scan was evaluated by two professional neuroradiologists who were blinded to the clinical information.

MRI Analysis

Resting-State fMRI Data Pre-processing

All resting-state functional MRI images were preprocessed using the data processing and analysis for brain imaging (DPABI) software (http://rfmri.org/dpabi), which is based on SPM12 and runs on MATLAB R2018b. First, the first ten volumes of each participant were discarded, and slice timing correction was used to account for the temporal delay between slices. By realigning all functional images to the center image, we excluded subjects who moved their heads more than 2 mm or 2°. Then, the motion-corrected functional volumes were coregistered with the high-resolution anatomical images and standardized to the MNI space. Space smoothing was performed using a 6-mm full-width at half maximum (FWHM) Gaussian kernel. Low-frequency drift and high-frequency noise were reduced by detrending the data. Finally, the covariance of head movement, mean white matter signal and cerebrospinal fluid were regressed, and the residual signals were filtered at 0.08–0.1 Hz.

Structural MRI Data Pre-processing

We used the cat12 toolbox (http://www.neuro.unijena.de/cat/), which is based on the SPM12 package (http://www.fil.ion.ucl.ac.uk/spm/software/spm12/), to process structural images. First, we used an adaptive maximum a posteriori technique to segment individual structural images into gray matter, white matter, and CSF. Next, the generated gray matter maps were normalized to MNI space using a high-dimensional "DARTEL" technique and then adjusted for spatial normalization effects. Finally, the gray matter maps were smoothed spatially using an 8-mm FWHM Gaussian kernel.

Definition of BF Subregions

Subregions of the BF were defined utilizing stereotaxic probabilistic maps of the BF's cytoarchitectonic boundaries generated by the SPM Anatomy Toolbox (13). Ch1-4 were defined using the Anatomy toolkit's BF probability maps. Following a 50% probability threshold, the ROIs were resampled and warped to the MNI space.

Gray Matter Volume of BF Subregions

The mean gray matter volume (GMV) of each subject was computed across all voxels, and each BF subregion was subsequently evaluated. The volume of the BF was determined using CAT12, which is based on SPM12. They were then non-linearly registered to the MNI152 standard space after segmentation. Each study's GM template was created by averaging and flipping the normalized images. To account for the non-linear component of the transformation, all native GM images were divided by the warp field's Jacobian. Finally, an isotropic 3-mm Gaussian kernel was used to smooth the modulated GM images. A BF mask was used to extract each participant's BF volume. The collected BF volumes were also analyzed statistically.

Functional Connectivity Analysis

Seed-Based Resting-State Functional Connectivity of BF Subregions

The mean time series for each BF subregion was acquired first and then correlated with the time series for each voxel throughout the entire brain (Pearson correlation). As a result, each subject's whole-brain resting-state functional connectivity (rsFC) was provided in four maps. To normalize the rsFC maps, Fisher's r-to-z transformation was used on each of the generated maps.

Statistical Analysis

SPSS 20.0 (SPSS Inc., Chicago, IL, USA) was used to perform statistical analyses. To compare normally distributed data among the three groups ($P < 0.05$), one-way analysis of variance (ANOVA) was employed, and chi-square tests were utilized to analyze categorical variables. To compare clinical factors between the two groups of patients, Student's *t*-tests for normally

TABLE 1 | The demographic and clinical characteristics of the two TLE groups and HCs.

	FBTCS group (25)	Non-FBTCS group (25)	HCs (25)	*P*-value
Age (M ± SD)	31.28 ± 8.44	32.72 ± 11.99	27.16 ± 5.88	0.091[b]
Sex (M/F)	9/16	5/20	10/15	0.276[a]
Handedness, R/L/A	24/1/0	23/1/1	22/2/1	0.982[*]
Seizure focus, LT/RT	12/13	11/14	NA	0.78[a]
Age of seizure onset, years (M ± SD)	24.28 ± 7.14	23.86 ± 8.93	NA	0.427[e]
Duration of disease, years, median (range)	7.2 (2.5–35.3)	7.6 (3.0–21.0)	NA	0.319[d]
Frequency of seizure, n/month, median (range)	2.0 (0–12.0)	2.0 (0–10.0)	NA	0.99[d]
Seizure type				
FAS	0	5		
FIAS	0	17		
FAS + FIAS		3		
FAS + FBTCS	5	0		
FIAS + FBTCS	20	0		
Mean FD, mm (mean ± SD)	0.057 ± 0.030	0.070 ± 0.053	0.049 ± 0.021	0.143[c]
Current antiepileptic drugs by category				
VGNC	18	16		
GABAa agonist	4	2		
SV2a receptor-mediated	12	8		
CRMP2 receptor-mediated	3	1		
Multiaction	7	5		
MoCA (mean ± SD)	26.92 ± 2.86	26.32 ± 3.28	28.80 ± 1.58	0.005[b*]
RT_{no-cue} (ms)	694.32 ± 140.58	716.12 ± 97.92	601.10 ± 68.36	0.001[bΔ]
$RT_{double-cue}$ (ms)	650.05 ± 145.30	650.06 ± 100.01	554.35 ± 60.24	0.003[b†]
Alertness (ms)	0.082 ± 0.040	0.081 ± 0.046	0.084 ± 0.033	0.188[b]

*[a]P was calculated using the chi-square test; [b]P was calculated using an ANOVA; [c]P was calculated using the Kruskal–Wallis test; [d]P was calculated using the Mann–Whitney test; [e]P was calculated using two independent sample t-tests; Fisher's exact test was performed instead, as 20% of cells had an expected count <5. *, post-hoc comparison showed a significant difference between FBTCS and non-FBTCS patients and HCs, no difference between FBTCS and non-FBTCS patients; Δ, post-hoc comparison showed a significant difference between FBTCS and non-FBTCS patients and HCs, no difference between FBTCS and non-FBTCS patients; †post-hoc comparison showed a significant difference between FBTCS and non-FBTCS patients and HCs, no difference between FBTCS and non-FBTCS patients; HCs, healthy controls; M, male; F, female; M ± SD, mean ± standard deviation; FAS, focal aware seizures; FIAS, focal impaired awareness seizures; FBTCS, focal to bilateral tonic–clonic seizures; FD, framewise displacement; AEDs, antiepileptic drugs; VGNC, voltage-gated Na^+ channel blockers, e.g., oxcarbazepine, lamotrigine (plus T Type $Ca2^+$ channel blockers); SV2a receptor mediated, e.g., levetiracetam; Multiaction, e.g., Na^+ valproate (VGNC + GABAa agonist), topiramate (VGNC + GABAa agonist + AMPA/kainate receptor blocker + carbonic anhydrase inhibitor). Multiple antiepileptic drugs in the same category taken by one patient were only counted once. ANOVA, one-way analysis of variance; χ^2, chi-square tests; NA, not available; MoCA, Montreal Cognitive Assessment; RT, response time; FBTCS, focal to bilateral tonic-clonic seizures; and non-FBTCS, no focal to bilateral tonic-clonic seizures.*

distributed variables and Mann–Whitney tests for non-normally distributed data were used. $P<0.05$ was chosen as the level of statistical significance.

We used DPABI's statistical analysis toolkits to compare FC and GMV maps for each ROI among the three groups. ANOVA was used to compare the imaging variables among the groups, with age, sex, and head motion as covariates ($P<0.05$). Multiple comparisons were corrected using a false discovery rate (FDR) correction for clusters with more than 30 voxels. Then, pairwise comparisons of regions with significant group differences in FC were undertaken. We used two-tailed paired comparison *t*-tests and a false discovery rate (FDR) correction at $P < 0.05$. Correlation analyses between imaging characteristics and clinical factors for patients were conducted in SPSS 20.0, revealing substantial group differences. Multiple comparisons were adjusted using the Bonferroni method. Parametric comparisons were performed with Pearson's correlation analysis, and non-parametric comparisons were performed with Spearman's correlation analysis.

Multiclass Discriminant Analysis

To ascertain the ability of seed-based rsFC to discriminate among the three groups, multiclass discriminant analysis was performed using PRoNTo v2.0 software in MATLAB 2018b (28). Specifically, the multiclass classification was transformed into three binary classifiers using a one-vs.-one coding method. To reduce the dimensionality of initial features, starting features were selected from voxels with significant group effects ($P < 0.05$, uncorrected). After that, the outputs of all binary classifiers were combined using an error-correcting output code technique. A 10-fold cross-validation approach was used to assure generalization during this process. Finally, we calculated the total and group-specific accuracies.

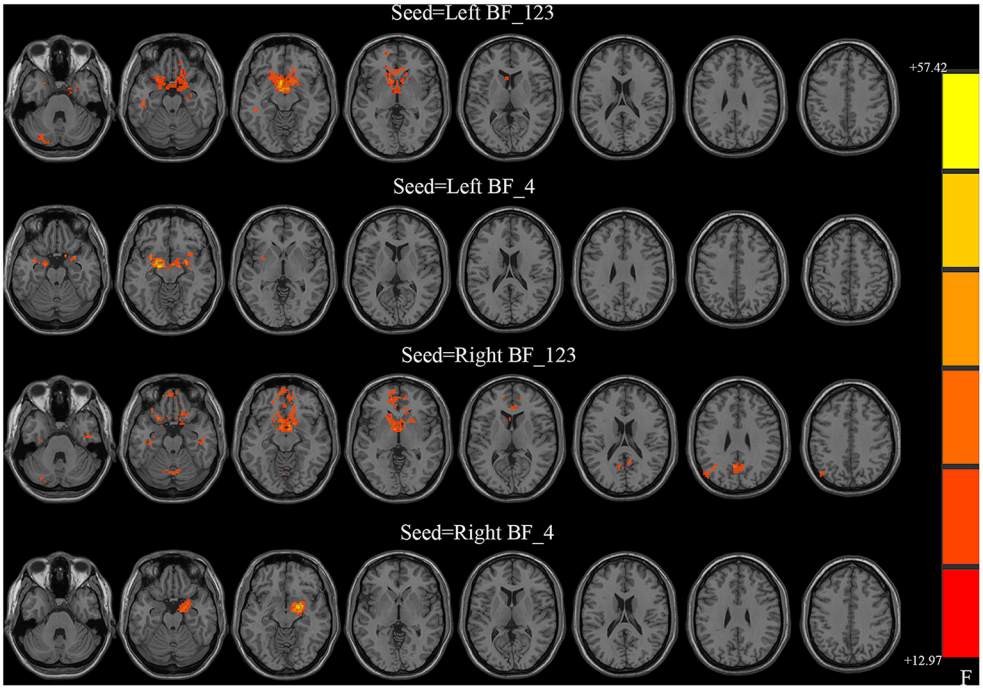

FIGURE 1 | Between-group differences in the resting-state functional connectivity (RSFC) with all four basal forebrain subregions in groups with temporal lobe epilepsy (TLE). The colored bars indicate the *P* values. SPM software was used to map the data onto the brain's surface.

RESULTS

Clinical and Demographic Characteristics

The demographic and clinical data of all participants are summarized in **Table 1**. No differences in age, sex, handedness, seizure focus, age of seizure onset, disease duration, or seizure frequency were discovered among the three groups ($P > 0.05$). However, the RTs on the no cue and double cue conditions were significantly different among these three groups. A *post-hoc* test revealed no significant differences between FBTCS and non-FBTCS patients but significant differences between FBTCS or non-FBTCS patients and HCs. In addition, the RTs of the TLE group were longer than those of the HC group.

Intact GMV in the Patients

There was no significant difference in GMV among the three groups for the BF subregions ($P > 0.05$ [FDR corrected]).

rsFC Values Differed Between Groups

All four seeds exhibited significant group effects (**Figure 1** and **Table 2**). Specifically, significant alterations in rsFC were detected in four clusters in the left Ch1-3, including rsFC with the right cerebellar posterior lobe, bilateral striatum, left superior frontal gyrus, and right middle temporal gyrus. Significant alterations in rsFC were found in four clusters of the right Ch1-3, primarily rsFC with the right cerebellar posterior lobe, bilateral striatum, right precuneus, and left middle occipital gyrus. The bilateral amygdala had significant anomalies in rsFC with the left Ch4, and the left amygdala had significant anomalies in rsFC with the right Ch4.

With the left Ch1-3 as a seed, the FBTCS and non-FBTCS patients showed considerably lower FC than HCs with the right cerebellum posterior lobe, bilateral striatum, left superior frontal gyrus, and right middle temporal gyrus, respectively, and the FBTCS group demonstrated decreased FC compared to HCs with the right cerebellum posterior lobe, bilateral striatum, and left superior frontal gyrus, respectively (**Figure 2A**). Using the right Ch1-3 as a seed, the FBTCS and non-FBTCS groups showed significantly decreased FC compared to HCs with the right cerebellar posterior lobe, bilateral striatum, right precuneus, and left middle occipital gyrus, respectively, and the FBTCS group showed lower FC than the non-FBTCS group with the bilateral striatum (**Figure 2B**). When the left Ch4 was used as a seed, the FBTCS group showed significantly lower FC than the non-FBTCS and HC groups with the bilateral amygdala (**Figure 2C**). Using the right Ch4 as a seed, the FBTCS group showed significantly decreased FC with the right amygdala compared with the non-FBTCS and HC groups (**Figure 2D**).

To further explore whether there were differences in the brain regions between left and right mTLE in the different TLE groups, an ANOVA was performed. We found that there was no significant difference ($P > 0.05$) between the two TLE groups. Details are shown in **Supplementary Material 1**.

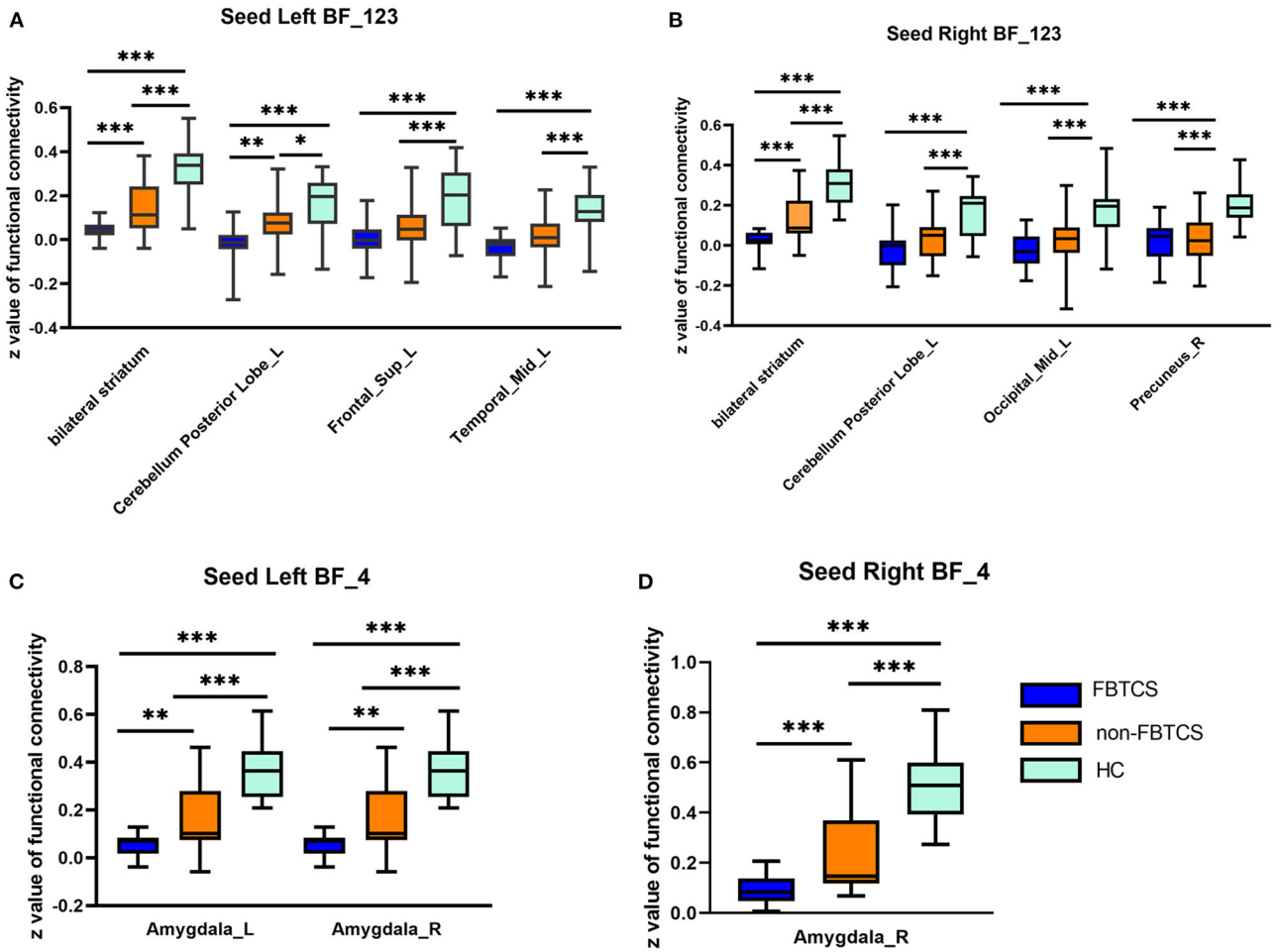

FIGURE 2 | (A–D) Altered resting-state functional connectivity (RSFC) of the basal forebrain (BF) subregions in patients with temporal lobe epilepsy (TLE). HCs, healthy controls. ***$P < 0.001$; **$P < 0.01$; *$P < 0.05$.

Correlations Between Altered rsFC With the BF Subregions and Clinical Characteristics

The rsFC between the left Ch1-3 and striatum had a significant positive correlation with performance in the double cue ($r = 0.48$, $P = 0.015$) and no cue conditions ($r = 0.495$, $p = 0.012$) in the FBTCS group. In the non-FBTCS group, the rsFC between the left Ch4 and striatum had a moderate negative correlation with performance in the double cue ($r = -0.458$, $P = 0.021$) and no cue conditions ($r = -0.507$, $p = 0.0097$); additionally, the rsFC between the right Ch1-3 and striatum had a moderate negative correlation with performance in the no cue condition ($r = -0.44$, $p = 0.028$) (**Figure 3**).

Multiclass Classification

Table 3 summarizes the overall and group-level accuracy. In general, among fourth basal forebrain subregions to voxel functional connectivity in differentiating subjects from each other, the right Ch1-3 and left Ch4 subregions performed better than the left Ch1-3 and right Ch4 subregions in identifying the three groups (accuracy 85.33 and 81.00% vs. 78.67 and 78.67%).

DISCUSSION

In this study, we investigated the structural and functional changes in BF subregions in patients with different kinds of TLE as well as HCs by analyzing VBM and functional connectivity. Our primary findings were as follows: (i) the rsFC between Ch1-3 and the bilateral striatum as well as the left cerebellar posterior lobe was considerably lower in FBTCS patients than in non-FBTCS patients. Additionally, patients with FBTCS had reduced rsFC between Ch4 and the bilateral amygdala. In comparison to HCs, the two TLE groups showed significantly lower rsFC between the basal forebrain subregions and bilateral hemisphere, most notably in the FC between the BF subregions and the cerebellum, striatum, default mode network, frontal lobe, and occipital lobe. (ii) Significant positive or negative correlations were observed between abnormal rsFC with the striatum and alertness metrics. Overall, our findings suggest that disrupted

TABLE 2 | Group differences in FC.

ROI	Cluster	Brain regions/AAL	Peak MNI coordinates			Cluster size	Peak F value
			X	Y	Z		
LBF_123	Cluster 1	Cerebellum Posterior Lobe_L	−27	−84	−36	44	13.3895
	Cluster 2	Striatum_L/Striatum_R	−6	9	−12	1066	47.6569
	Cluster 3	Superior Frontal Gyrus_L	−21	66	−6	35	12.9727
	Cluster 4	Temporal_Mid_L	−45	−33	−15	30	13.7519
LBF_4	Cluster 1	Amygdala_R	27	−3	−12	39	19.2485
	Cluster 2	Amygdala_L	−18	−9	−12	272	38.1336
RBF_123	Cluster 1	Cerebellum Posterior Lobe_L	−21	−87	−36	39	13.4447
	Cluster 2	Striatum_L/Striatum_R	6	0	−9	808	41.9343
	Cluster 3	Precuneus_R	3	−57	24	124	14.2744
	Cluster 4	Occipital_Mid_L	−48	−78	33	54	15.4561
RBF_4	Cluster 1	Amygdala_R	21	−3	−12	235	57.4224

The results were corrected by FDR. ROI, regions of interest; AAL, automated anatomical labeling atlas; MNI, Montreal Neurological Institute.

cholinergic activity may contribute to decreased vigilance in many types of TLE, providing a more complete explanation of the cognitive mechanism underlying pathological damage.

Changes in the BF Structure

The BF is located in the front of the forebrain, beneath the striatum. The BF has many cholinergic projections to the neocortex, which is involved in the neuromodulation of cognitive performance. In this study, there was no difference in the volume of the BF subregions among the three groups. Memory loss has been linked to Ch4 neuron deterioration in neurodegenerative disorders such as Alzheimer's disease, mild cognitive impairment, Parkinson's disease with moderate cognitive impairment, and Wilson disease (29, 30). However, Ma et al. found no difference in the volume of BF subregions in a previous study on short-term and chronic insomnia (17). There has been no research on the volume of the basal forebrain in TLE until now. We found no differences in BF volume among the three groups. This could be because TLE originates mostly in the hippocampus and amygdala and has less direct influence on the BF or because differences in volume take a longer time to manifest. The small sample size of this study is another possible explanation for our findings. More information about changes in basal forebrain volume could be achieved from further studies with larger sample sizes and longitudinal designs.

Changes in Functional Connectivity With the BF

The BF nuclei, which contain four distinct cell groups (Ch1–4), are the primary sources of cholinergic projections to the neocortex, amygdala, and hippocampus (31). In comparison to the non-FBTCS group, we discovered that FC was reduced between Ch1-3 and the bilateral striatum as well as the left posterior cerebellar lobe (PCL) in FBTCS patients; additionally, FC was reduced between Ch4 and the amygdala. The striatum is crucial for a number of complex functions, ranging from motor control to action selection and attention (32). Electron microscopy demonstrated that the ventral and dorsal striatum provide synaptic input to cholinergic BF neurons (33). A neuropathological analysis established a direct anatomical relationship between the striatum and basal forebrain, providing behavioral and structural evidence (34). Striatal structure and function are altered in attention-deficit/hyperactivity disorder (35) and a variety of epileptic conditions, including focal to bilateral tonic-clonic seizures (36) and pediatric epilepsy (37). Additionally, we found a significant correlation between the rsFC of Ch1-3 and the striatum and vigilance measurements. We postulate that recurrent seizures have a detrimental effect on the striatum, reducing ACh levels in the basal forebrain and impairing vigilance. Numerous studies have demonstrated that the cerebellum is essential for normal cognitive function. A lesion in the PCL can result in cerebellar cognitive-affective syndrome, characterized by issues with executive function, visual-spatial processing, linguistic abilities, and emotional regulation. In TLE with or without FBTCS as well as right TLE, we previously described aberrant FC between deep cerebellar nuclei and the cerebral cortex (38, 39). In the current study, we found decreased rsFC between Ch1-3 and the left posterior cerebellar lobe in FBTCS patients, which is consistent with earlier findings. Our findings imply that disruption of the rsFC between the basal forebrain and cerebellum may contribute to cognitive impairment in TLE. Prior research has established that the amygdala regulates the prefrontal cortex (PFC) and hippocampus directly via cholinergic projections from the basal forebrain and subsequent acetylcholine release (40). According to Adam et al. (40), cholinergic projections from the basal forebrain moderate activity in the greater amygdala during the processing of physiologically relevant stimuli in humans. The Ch4 subregion has cholinergic projections to the neocortex and amygdala. In our investigation, we found that the rsFC between Ch 4 and the amygdala was considerably lower in the FBTCS group than in the non-FBTCS group. We postulate that repeated FBTCS seizures disturb the basal forebrain-amygdala circuit by reducing the amount of ACh projected from the basal forebrain to the

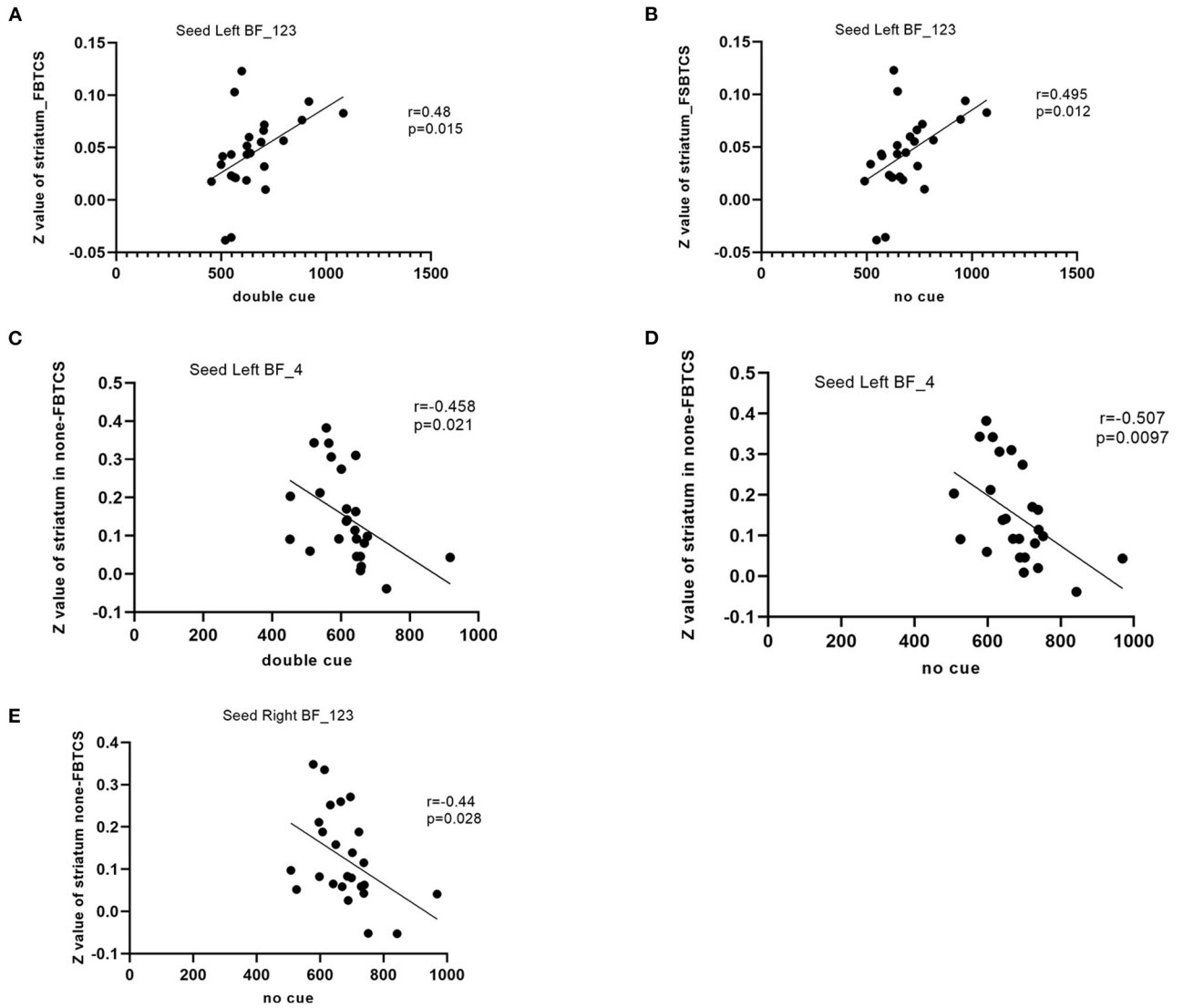

FIGURE 3 | (A–E) Scatter plots depicting the correlations between the altered resting-state functional connectivity (RSFC) in the BF subregions and the clinical variables in patients.

amygdala. Together, aberrant rsFC between basal subregions and the striatum, cerebellum posterior lobe, and amygdala influence alertness and may be a critical neuroimaging biomarker for differentiating FBTCS and non-FBTCS patients.

The DMN is involved in working memory, emotions, cognitive performance, and epileptic activity. Mounting data suggest that disrupting the DMN may cause epileptic activity, cognitive dysfunction, and mental dysfunction in TLE patients (41). The precuneus and middle temporal gyrus (MTG) are key components of the DMN, as they participate in processes related to consciousness, self-reflection, visuospatial function, and cognition (42–44). Nair et al. (45) demonstrated that gamma oscillations were restricted to the BF and that BF gamma-band activity had a direct effect on a DMN hub in rats, implying that the BF may be an important target for DMN regulation. In our study, both groups of patients displayed significantly lower rsFC between the right Ch1-3 and right precuneus as well as left MTG in comparison to HCs, indicating decreased synchronous neuronal activity between the DMN and basal forebrain. We speculate that the DMN might be a target for epilepsy and cognitive control in the basal forebrain. Both the DMN and the basal forebrain subregions influence cognitive function, suggesting that disrupted rsFC from the basal forebrain to the DMN could impact cognition in TLE patients.

In addition, compared to HCs, both patient groups had lower rsFC between Ch1-3 and cortical regions, such as the left superior frontal gyrus (SFG) and left occipital middle gyrus, indicating reduced cholinergic innervation in these cortical regions. Damage to the SFG, which is a crucial

TABLE 3 | Results of multiclass classification.

Seed	Actual class	Predicted class			Accuracy (%)	
		HC	Non-FBTCS	FBTCS	Group	Total
Left Ch1-3	HCs	19	4	2	76.00	78.67
	Non-FBTCS	5	18	2	72.00	
	FBTCS	3	0	22	88.00	
Right Ch1-3	HCs	22	2	1	88.00	85.33
	Non-FBTCS	3	20	2	80.00	
	FBTCS	0	2	22	88.00	
Left Ch4	HCs	20	5	0	80.00	81.00
	Non-FBTCS	3	21	1	84.00	
	FBTCS	0	5	20	80.00	
Right Ch4	HCs	21	2	2	84.00	78.67
	Non-FBTCS	4	20	1	80.00	
	FBTCS	5	2	18	72.00	

HCs, healthy controls; FBTCS, focal to bilateral tonic-clonic seizure.

component of the frontoparietal network, might cause vigilance deficits. The FC between Ch1-3 and the left SFG was considerably lower in the patient groups than in the HCs, implying that diminished ACh in the frontal cortex may contribute to cognitive impairment in TLE. The findings were in line with earlier research that showed disturbed rsFC in the frontal cortices, linking it to deficits in alertness (46) and executive function (47) in TLE. fMRI studies have demonstrated that the visual cortex is engaged and cerebral blood flow is elevated during attention-related tasks (48, 49). In rTLE patients, the functional activity of the superior occipital gyrus in the alertness-related network was higher than that in HCs (46). Julia Schumacher et al. also identified aberrant functional connectivity between the basal forebrain and occipital cortex in Lewy body dementia and Alzheimer's disease, which they believe may indicate a cholinergic system imbalance and a shift in the cholinergic input to the occipital cortex (22). Additionally, gray matter volume reduction and hypometabolism were detected in the visual cortex of patients with TLE (50, 51). Therefore, our findings support the concept that in TLE the basal forebrain improperly modulates the frontoparietal and sensory networks, resulting in cognitive dysfunction.

Limitations

This investigation has some limitations. First, the sample size is relatively small. As a result, our findings need to be confirmed in a broader patient group. Second, this was a cross-sectional study. Therefore, a longitudinal assessment of resting-state fMRI in temporal lobe epilepsy will be required to confirm these findings. Third, we did not take into account the effect of antiepileptic medicines on FC and VBM. Fourth, we cannot rule out the effect of interictal discharges on patient alertness because a synchronous electroencephalogram was not performed during the acquisition of imaging data. Finally, we defined BF subregions using a probabilistic map extracted from the SPM Anatomy Toolbox, which has been extensively used in previous research (1, 17). However, the BF subregions are segregated in additional ways (52). In the future, it is vital to employ different parcellation methods to acquire a thorough understanding of BF alterations in TLE.

CONCLUSION

To the best of our knowledge, this is the first study to use BF subregions as seeds for performing FC analysis on patients with and without FBTCS. Patients with FBTCS showed disrupted rsFC between BF subregions and many brain regions compared to individuals without FBTCS or HCs. There was a substantial correlation between abnormal rsFC from the BF to the striatum and alertness metrics. Our findings reveal a link between altered basal forebrain-cerebral connections and reduced alertness in patients with FBTCS and suggest that cholinergic BF degradation may be a critical physiopathological mechanism underlying impaired alertness in TLE. Our results suggest that the BF subregions could serve as critical nodes for identifying TLE subtype-specific diagnostic and classification biomarkers, as well as more effective treatment alternatives.

DATA AVAILABILITY STATEMENT

The original contributions presented in the study are included in the article/**Supplementary Material**, further inquiries can be directed to the corresponding author/s.

ETHICS STATEMENT

The studies involving human participants were reviewed and approved by Ethics Committee of The First Affiliated Hospital of Guangxi Medical University. The patients/participants

provided their written informed consent to participate in this study.

AUTHOR CONTRIBUTIONS

BF and LP designed the study. BF conducted the study and data analyses. BF and SL wrote the manuscript. XZ handled the data curation and methodology. ZL and ZC oversaw data curation and investigation. JZ handled the funding acquisition and project administration. All authors finally agreed to publish this manuscript.

FUNDING

This research was funded by the National Natural Science Foundation of China (Grant No. 81560223) and Natural Science Foundation of Guangxi Province (2016GXNSFAA380182).

SUPPLEMENTARY MATERIAL

The Supplementary Material for this article can be found online at: https://www.frontiersin.org/articles/10.3389/fpsyt.2022.888150/full#supplementary-material

REFERENCES

1. González HF, Narasimhan S, Johnson GW, Wills KE, Haas KF, Konrad PE, et al. Role of the nucleus basalis as a key network node in temporal lobe epilepsy. *Neurology*. (2021) 96:e1334–46. doi: 10.1212/wnl.0000000000011523
2. Fisher RS, Cross JH, French JA, Higurashi N, Hirsch E, Jansen FE, et al. Operational classification of seizure types by the international league against epilepsy: position paper of the ILAE commission for classification and terminology. *Epilepsia*. (2017) 58:522–30. doi: 10.1111/epi.13670
3. Caciagli L, Allen LA, He X, Trimmel K, Vos SB, Centeno M, et al. Thalamus and focal to bilateral seizures: a multiscale cognitive imaging study. *Neurology*. (2020) 95:e2427–41. doi: 10.1212/WNL.0000000000010645
4. Sinha N, Peternell N, Schroeder GM, de Tisi J, Vos SB, Winston GP, et al. Focal to bilateral tonic-clonic seizures are associated with widespread network abnormality in temporal lobe epilepsy. *Epilepsia*. (2021) 62:729–41. doi: 10.1111/epi.16819
5. Allone C, Buono VL, Corallo F, Pisani LR, Pollicino P, Bramanti P, et al. Neuroimaging and cognitive functions in temporal lobe epilepsy: a review of the literature. *J Neurol Sci*. (2017) 381:7–15. doi: 10.1016/j.jns.2017.08.007
6. Ives-Deliperi V, Butler JT. Mechanisms of cognitive impairment in temporal lobe epilepsy: a systematic review of resting-state functional connectivity studies. *Epilepsy Behav*. (2021) 115:107686. doi: 10.1016/j.yebeh.2020.107686
7. Prevey ML, Delaney RC, Cramer JA, Mattson RH, Study VE. Complex partial and secondarily generalized seizure patients: cognitive functioning prior to treatment with antiepileptic medication. VA epilepsy cooperative study 264 group. *Epilepsy Res*. (1998) 30:1–9. doi: 10.1016/s0920-1211(97)00091-0
8. Liu J, Zhang Z, Zhou X, Pang X, Liang X, Huang H, et al. Disrupted alertness and related functional connectivity in patients with focal impaired awareness seizures in temporal lobe epilepsy. *Epilepsy Behav*. (2020) 112:107369. doi: 10.1016/j.yebeh.2020.107369
9. Posner MI. Measuring alertness. *Ann NY Acad Sci*. (2008) 1129:193–9. doi: 10.1196/annals.1417.011
10. Englot DJ, D'Haese PF, Konrad PE, Jacobs ML, Gore JC, Abou-Khalil BW, et al. Functional connectivity disturbances of the ascending reticular activating system in temporal lobe epilepsy. *J Neurol Neurosurg Psych*. (2017) 88:925–32. doi: 10.1136/jnnp-2017-315732
11. Englot DJ, Modi B, Mishra AM, DeSalvo M, Hyder F, Blumenfeld H. Cortical deactivation induced by subcortical network dysfunction in limbic seizures. *J Neurosci*. (2009) 29:13006–18. doi: 10.1523/jneurosci.3846-09.2009
12. Blumenfeld H. Impaired consciousness in epilepsy. *Lancet Neurol*. (2012) 11:814–26. doi: 10.1016/s1474-4422(12)70188-6
13. Zaborszky L, Hoemke L, Mohlberg H, Schleicher A, Amunts K, Zilles K. Stereotaxic probabilistic maps of the magnocellular cell groups in human basal forebrain. *Neuroimage*. (2008) 42:1127–41. doi: 10.1016/j.neuroimage.2008.05.055
14. Chen XM, Huang DH, Chen ZR, Ye W, Lv ZX, Zheng JO. Temporal lobe epilepsy: decreased thalamic resting-state functional connectivity and their relationships with alertness performance. *Epilepsy Behav*. (2015) 44:47–54. doi: 10.1016/j.yebeh.2014.12.013
15. Gersel Stokholm M, Iranzo A, Østergaard K, Serradell M, Otto M, Bacher Svendsen K, et al. Cholinergic denervation in patients with idiopathic rapid eye movement sleep behaviour disorder. *Eur J Neurol*. (2020) 27:644–52. doi: 10.1111/ene.14127
16. Kato S, Watanabe H, Senda J, Hirayama M, Ito M, Atsuta N, et al. Widespread cortical and subcortical brain atrophy in Parkinson's disease with excessive daytime sleepiness. *J Neurol*. (2012) 259:318–26. doi: 10.1007/s00415-011-6187-6
17. Ma X, Fu S, Yin Y, Wu Y, Wang T, Xu G, et al. Aberrant functional connectivity of basal forebrain subregions with cholinergic system in short-term and chronic insomnia disorder. *J Affect Disord*. (2021) 278:481–7. doi: 10.1016/j.jad.2020.09.103
18. Grossberg S. Acetylcholine neuromodulation in normal and abnormal learning and memory: vigilance control in waking, sleep, autism, amnesia and alzheimer's disease. *Front Neural Circuits*. (2017) 11:82. doi: 10.3389/fncir.2017.00082
19. Mesulam MM, Geula C. Nucleus basalis (Ch4) and cortical cholinergic innervation in the human brain: observations based on the distribution of acetylcholinesterase and choline acetyltransferase. *J Comp Neurol*. (1988) 275:216–40. doi: 10.1002/cne.902750205
20. Mesulam MM, Mufson EJ, Levey AI, Wainer BH. Cholinergic innervation of cortex by the basal forebrain: cytochemistry and cortical connections of the septal area, diagonal band nuclei, nucleus basalis (substantia innominata), and hypothalamus in the rhesus monkey. *J Comp Neurol*. (1983) 214:170–97. doi: 10.1002/cne.902140206
21. Ballinger EC, Ananth M, Talmage DA, Role LW. Basal forebrain cholinergic circuits and signaling in cognition and cognitive decline. *Neuron*. (2016) 91:1199–218. doi: 10.1016/j.neuron.2016.09.006
22. Schumacher J, Thomas AJ, Peraza LR, Firbank M, O'Brien JT, Taylor JP. Functional connectivity of the nucleus basalis of Meynert in Lewy body dementia and Alzheimer's disease. *Int Psychoger IF 2.4*. (2021) 33:89–94. doi: 10.1017/s1041610220003944
23. Wilson H, de Natale ER, Politis M. Nucleus basalis of Meynert degeneration predicts cognitive impairment in Parkinson's disease. *Handb Clin Neurol*. (2021) 179:189–205. doi: 10.1016/b978-0-12-819975-6.00010-8
24. Wu Y, Hu S, Wang Y, Dong T, Wu H, Zhang Y, et al. The degeneration changes of basal forebrain are associated with prospective memory impairment in patients with Wilson's disease. *Brain Behav*. (2021) 11:e2239. doi: 10.1002/brb3.2239
25. Hildesheim FE, Benedict RH, Zivadinov R, Dwyer MG, Fuchs T, Jakimovski D, et al. Weinstock-Guttman, and N. Bergsland. Nucleus basalis of meynert damage and cognition in patients with multiple sclerosis. *J Neurol*. (2021) 268:4796–808. doi: 10.1007/s00415-021-10594-7
26. Scheffer IE, Berkovic S, Capovilla G, Connolly MB, French J, Guilhoto L, et al. ILAE classification of the epilepsies: position paper of the ILAE commission for classification and terminology. *Epilepsia*. (2017) 58:512–21. doi: 10.1111/epi.13709
27. Fan J, Gu X, Guise KG, Liu X, Fossella J, Wang H, et al. Testing the behavioral interaction and integration of attentional networks. *Brain Cogn*. (2009) 70:209–20. doi: 10.1016/j.bandc.2009.02.002

28. Schrouff J, Rosa MJ, Rondina JM, Marquand AF, Chu C, Ashburner J, et al. PRoNTo: pattern recognition for neuroimaging toolbox. *Neuroinformatics*. (2013) 11:319–37. doi: 10.1007/s12021-013-9178-1
29. Schumacher J, Taylor JP, Hamilton CA, Firbank M, Cromarty RA, Donaghy PC, et al. *In vivo* nucleus basalis of Meynert degeneration in mild cognitive impairment with Lewy bodies. *Neuroimage Clin*. (2021) 30:102604. doi: 10.1016/j.nicl.2021.102604
30. Wilkins KB, Parker JE, Bronte-Stewart HM. Gait variability is linked to the atrophy of the nucleus basalis of Meynert and is resistant to STN DBS in Parkinson's disease. *Neurobiol Dis*. (2020) 146:105134. doi: 10.1016/j.nbd.2020.105134
31. Woolf NJ. Cholinergic systems in mammalian brain and spinal cord. *Prog Neurobiol*. (1991) 37:475–524. doi: 10.1016/0301-0082(91)90006-m
32. Valjent E, Gangarossa G. The Tail of the striatum: from anatomy to connectivity and function. *Trends Neurosci*. (2021) 44:203–14. doi: 10.1016/j.tins.2020.10.016
33. Záborszky L, Gombkoto P, Varsanyi P, Gielow MR, Poe G, Role LW, et al. Specific basal forebrain–cortical cholinergic circuits coordinate cognitive operations. *J Neurosci: Off J Soc Neurosci*. (2018) 38:9446–58. doi: 10.1523/JNEUROSCI.1676-18.2018
34. Shu SY, Jiang G, Zheng Z, Ma L, Wang B, Zeng Q, et al. A new neural pathway from the ventral striatum to the nucleus basalis of meynert with functional implication to learning and memory. *Mol Neurobiol*. (2019) 56:7222–33. doi: 10.1007/s12035-019-1588-0
35. Greven CU, Bralten J, Mennes M, O'Dwyer L, van Hulzen KJ, Rommelse N, et al. Developmentally stable whole-brain volume reductions and developmentally sensitive caudate and putamen volume alterations in those with attention-deficit/hyperactivity disorder and their unaffected siblings. *JAMA Psychiatry*. (2015) 72:490–9. doi: 10.1001/jamapsychiatry.2014.3162
36. Xu Q, Zhang Q, Yang F, Weng Y, Xie X, Hao J, et al. Stufflebeam,. Cortico-striato-thalamo-cerebellar networks of structural covariance underlying different epilepsy syndromes associated with generalized tonic-clonic seizures. *Hum Brain Mapp*. (2021) 42:1102–15. doi: 10.1002/hbm.25279
37. MacEachern SJ, Santoro JD, Hahn KJ, Medress ZA, Stecher X, Li MD, et al. Children with epilepsy demonstrate macro- and microstructural changes in the thalamus, putamen, and amygdala. *Neuroradiology*. (2020) 62:389–97. doi: 10.1007/s00234-019-02332-8
38. Nie L, Jiang Y, Lv Z, Pang X, Liang X, Chang W, et al. Deep cerebellar nuclei functional connectivity with cerebral cortex in temporal lobe epilepsy with and without focal to bilateral tonic-clonic seizures: a resting-state fMRI study. *Cerebellum*. (2022) 21:253–63. doi: 10.1007/s12311-021-01266-3
39. Zhou X, Zhang Z, Liu J, Qin L, Pang X, Zheng J. Disruption and lateralization of cerebellar-cerebral functional networks in right temporal lobe epilepsy: a resting-state fMRI study. *Epilepsy Behav*. (2019) 96:80–6. doi: 10.1016/j.yebeh.2019.03.020
40. Gorka AX, Knodt AR, Hariri AR. Basal forebrain moderates the magnitude of task-dependent amygdala functional connectivity. *Soc Cogn Affect Neurosci*. (2015) 10:501–7. doi: 10.1093/scan/nsu080
41. Gonen OM, Kwan P, O'Brien TJ, Lui E. Resting-state functional MRI of the default mode network in epilepsy. *Epilepsy Behav*. (2020) 111:107308. doi: 10.1016/j.yebeh.2020.107308
42. Cunningham SI, Tomasi D, Volkow ND. Structural and functional connectivity of the precuneus and thalamus to the default mode network. *Hum Brain Mapp*. (2017) 38:938–56. doi: 10.1002/hbm.23429
43. Cavanna AE. The precuneus and consciousness. *CNS Spectr*. (2007) 12:545–52. doi: 10.1017/s1092852900021295
44. Mahayana IT, Tcheang L, Chen CY, Juan CH, Muggleton NG. The precuneus and visuospatial attention in near and far space: a transcranial magnetic stimulation study. *Brain Stimul*. (2014) 7:673–9. doi: 10.1016/j.brs.2014.06.012
45. Nair J, Klaassen AL, Arato J, Vyssotski AL, Harvey M, Rainer G. Basal forebrain contributes to default mode network regulation. *Proc Natl Acad Sci USA*. (2018) 115:1352–7. doi: 10.1073/pnas.1712431115
46. Li J, Chen X, Ye W, Jiang W, Liu H, Zheng J. Alteration of the alertness-related network in patients with right temporal lobe epilepsy: a resting state fMRI study. *Epilepsy Res*. (2016) 127:252–9. doi: 10.1016/j.eplepsyres.2016.09.013
47. Zhou X, Zhang Z, Liu J, Qin L, Zheng J.. Aberrant topological organization of the default mode network in temporal lobe epilepsy revealed by graph-theoretical analysis. *Neurosci Lett*. (2019) 708:134351. doi: 10.1016/j.neulet.2019.134351
48. Kim J, Whyte J, Wang J, Rao H, Tang KZ, Detre JA, et al. Continuous ASL perfusion fMRI investigation of higher cognition: quantification of tonic CBF changes during sustained attention and working memory tasks. *Neuroimage*. (2006) 31:376–85. doi: 10.1016/j.neuroimage.2005.11.035
49. Prado J, Weissman DH. Weissman. Spatial attention influences trial-by-trial relationships between response time and functional connectivity in the visual cortex. *Neuroimage*. (2011) 54:465–73. doi: 10.1016/j.neuroimage.2010.08.038
50. Akman CI, Ichise M, Olsavsky A, Tikofsky RS, Van Heertum RL, Gilliam F. Epilepsy duration impacts on brain glucose metabolism in temporal lobe epilepsy: results of voxel-based mapping. *Epilepsy Behav*. (2010) 17:373–80. doi: 10.1016/j.yebeh.2009.12.007
51. Kim JS, Koo DL, Joo EY, Kim ST, Seo DW, Hong SB. Asymmetric gray matter volume changes associated with epilepsy duration and seizure frequency in temporal-lobe-epilepsy patients with favorable surgical outcome. *J Clin Neurol*. (2016) 12:323–31. doi: 10.3988/jcn.2016.12.3.323
52. Herdick M, Dyrba M, Fritz HC, Altenstein S, Ballarini T, Brosseron F, et al. Multimodal MRI analysis of basal forebrain structure and function across the Alzheimer's disease spectrum. *Neuroimage Clin*. (2020) 28:102495. doi: 10.1016/j.nicl.2020.102495

Conflict of Interest: The authors declare that the research was conducted in the absence of any commercial or financial relationships that could be construed as a potential conflict of interest.

frontiers | Frontiers in Psychiatry

CLINICAL TRIAL
published: 15 June 2022
doi: 10.3389/fpsyt.2022.923583

The Bilateral Precuneus as a Potential Neuroimaging Biomarker for Right Temporal Lobe Epilepsy: A Support Vector Machine Analysis

Chunyan Huang[1†], Yang Zhou[2,3†], Yi Zhong[4], Xi Wang[5] and Yunhua Zhang[6,7,8*]*

[1] Wuhan Third Hospital, Tongren Hospital of Wuhan University, Wuhan, China, [2] Wuhan Mental Health Center, Wuhan, China, [3] Wuhan Hospital for Psychotherapy, Wuhan, China, [4] NHC Key Laboratory of Mental Health (Peking University), Peking University Institute of Mental Health, Peking University Sixth Hospital, Beijing, China, [5] Department of Sleep and Psychosomatic Medicine Center, Taihe Hospital, Affiliated Hospital of Hubei University of Medicine, Shiyan, China, [6] Hubei Provincial Hospital of Traditional Chinese Medicine, Wuhan, China, [7] Clinical Medical College of Hubei University of Chinese Medicine, Wuhan, China, [8] Hubei Province Academy of Traditional Chinese Medicine, Wuhan, China

OPEN ACCESS

Edited by:
Liang Liang,
Xinjiang Medical University, China

Reviewed by:
Dongbin Li,
Harbin Medical University, China
Xiaobing Jiang,
Huazhong University of Science and Technology, China
Lin Liu,
Peking University, China

***Correspondence:**
Xi Wang
422718058@qq.com
Yunhua Zhang
316577527@qq.com

[†] These authors have contributed equally to this work and share first authorship

Specialty section:
This article was submitted to Neuroimaging and Stimulation, a section of the journal Frontiers in Psychiatry

Received: 19 April 2022
Accepted: 29 April 2022
Published: 15 June 2022

Citation:
Huang C, Zhou Y, Zhong Y, Wang X and Zhang Y (2022) The Bilateral Precuneus as a Potential Neuroimaging Biomarker for Right Temporal Lobe Epilepsy: A Support Vector Machine Analysis. Front. Psychiatry 13:923583. doi: 10.3389/fpsyt.2022.923583

Background and Objective: While evidence has demonstrated that the default-mode network (DMN) plays a key role in the broad-scale cognitive problems that occur in right temporal lobe epilepsy (rTLE), little is known about alterations in the network homogeneity (NH) of the DMN in TLE. In this study, we used the NH method to investigate the NH of the DMN in TLE at rest, and an support vector machine (SVM) method for the diagnosis of rTLE.

Methods: A total of 43 rTLE cases and 42 healthy controls (HCs) underwent resting-state functional magnetic resonance imaging (rs-fMRI). Imaging data were analyzed with the NH and SVM methods.

Results: rTLE patients have a decreased NH in the right inferior temporal gyrus (ITG) and left middle temporal gyrus (MTG), but increased NH in the bilateral precuneus (PCu) and right inferior parietal lobe (IPL), compared with HCs. We found that rTLE had a longer performance reaction time (RT). No significant correlation was found between abnormal NH values and clinical variables of the patients. The SVM results showed that increased NH in the bilateral PCu as a diagnostic biomarker distinguished rTLE from HCs with an accuracy of 74.12% (63/85), a sensitivity 72.01% (31/43), and a specificity 72.81% (31/42).

Conclusion: These findings suggest that abnormal NH of the DMN exists in rTLE, and highlights the significance of the DMN in the pathophysiology of cognitive problems occurring in rTLE, and the bilateral PCu as a neuroimaging diagnostic biomarker for rTLE.

Keywords: right temporal lobe epilepsy, resting-state functional magnetic resonance, default mode network, network homogeneity, biomarker

INTRODUCTION

Temporal lobe epilepsy (TLE), the most common form of adult epilepsy, is a common nervous system disease (1, 2). It is characterized by complex partial seizures, and secondary generalizations resulting from abnormal electrical activity in the temporal lobe, presenting as epileptic foci (3, 4). The recurring seizures in most people with TLE, result in cognitive dysfunction in areas such as learning, language, memory, emotion, perception, attention, consciousness, and behavior, which has a serious impact on their cognitive abilities and their lives (5–7). Existing studies have shown that the pathogenesis of epilepsy can be further understood through the study of the brain network properties, and interactions between different brain regions. However, the exact mechanism of the onset of this disorder is still not clear.

Advances in neuroimaging techniques have enabled increasingly detailed observation of alterations in the brain that are involved in the pathophysiology of TLE. Such observations have shown that topological patterns of brain structural networks were aberrant in patients with TLE (8). Abnormalities of the uncinate fasciculus correlate with executive dysfunction in patients with left TLE (9). Resting-state functional magnetic resonance imaging (fMRI), has a potential to detect abnormal neural activity, and is therefore extensively used in neuroscience. Up to the present, there are a large number of studies using fMRI to study TLE, investigating diverse abnormalities in different brain regions (10–15). However, according to the findings of these studies, the pathophysiology of TLE is still unclear.

In recent, the growing body of functional neuroimaging, at-rest data has opened up new avenues for surveys of the previously neglected field of intrinsic network organization. TLE is increasingly thought to be a disorder involving abnormal epileptogenic networks, rather than a single focal epileptogenic source (16–18). Accumulating evidence has shown that TLE exists in several networks disturbances, including alertness network (19), attention network (20) and default mode network (DMN) (13, 21, 22). However, there are only a few reports concerning the DMN and its function in patients with TLE.

Interestingly, the DMN has received increasing attention because it plays important roles in many medical or neurological illnesses. This network is characterized by showing higher activity at rest, deactivating during task-related cognitive processes (23, 24). Recently, the DMN was thought to include several special brain regions, such as medial prefrontal cortex (MPFC), lateral posterior cortices, posterior cingulate cortex / precuneus (PCC / PCu) (25), lateral temporal gyrus (26), cerebellar Crus 1 and Crus 2 (27). Researchers have demonstrated that the DMN is closely correlated with episodic memory processing, negative ruminations, complex self-referential stimuli (28) and in some special mind-states, such as anesthesia and sleep (29). Furthermore, the DMN is associated with cognitive functioning, especially executive function (30).

In addition, increasing evidence has shown a connectivity of abnormal resting state within the DMN in patients with epilepsy, but the results are mixed. For instance, many findings showed that there are increased PCC, and decreased medial prefrontal cortex (MPFC) functional connectivities in TLE (31, 32). However, other studies found decreased DMN connectivities in PCC, anterior frontal, and parietal regions (33, 34). Moreover, antiepileptic drugs and duration of illness could also contribute to the abnormality of DMN (35). These findings consistently show that the DMN plays a crucial role in TLE. However, the homogeneity of this network has not been fully explored.

Recently, the SVM is widely used in neuropsychiatric diseases due to its scientificity and effectivity (10, 11, 15, 36–38). An optimal separating hyperplane of the high-dimensional space can be confirmed by the SVM. In the fMRI analysis, a discrimination map can be generated by superimposing the SVM weights back to the original brain space, and the most significant weights can be visually traced back to the most discriminative parts of the brain. The SVM method has great potential to provide clinically useful criteria for decision-making from such high-dimensional neuroimaging data. In this study, we investigated NH of DMN in rTLE patients, and hypothesized NH values in altered brain regions could be used as potential neuroimaging biomarkers to diagnose rTLE through the SVM method. In this work, we used a method called network homogeneity (NH) (39) to analyze resting state data in TLE. This informative approach studies a given network without specifying the location of network abnormalities. It assesses the correlation of a voxel with all other voxels within a specific network of interest. Homogeneity is defined to be the average correlation of the time series of any given voxel with the time series of all other voxels within the network. The NH method has been used for depression, somatization, attention-deficit/hyperactivity disorder, schizophrenia and their unaffected siblings (39–46). Epilepsy encompasses different epileptic types with differing discharge places, which illustrates the differences in structure and functional impairment are possible (31). Even in identical brain regions, the left and right sides show differences (47). Thus, studies on unilateral TLE may have the advantage when assessing brain function, because it lessens the confounding effects of differences in discharging places. Using the NH method, we studied the NH of the DMN in people with rTLE, and examined the characteristics of the DMN and possible mechanism that causes rTLE in patients with rTLE. Furthermore, we try to find a potential biomarker to diagnosis rTLE from healthy controls (HCs).

MATERIALS AND METHODS

Subjects

A total of 43 patients with rTLE were recruited from the Epilepsy Clinic at the Department of Neurology, Sleep and Psychosomatic Medicine Center, Taihe Hospital, Hubei University of Medicine. The diagnosis of rTLE was made according to the diagnostic criteria of the International League Against Epilepsy (48). Patients with epilepsy who met any two of the following symptoms were classified as patients with rTLE: (1) the clinical onset of symptoms suggested the location of epileptogenic focus in the temporal lobe; (2) interictal electroencephalographic (EEG) traces illustrated lesions in the right temporal lobe; and (3) an MRI showed sclerosis or atrophy in the right temporal

lobe. Exclusion criteria were as follows: left-handed; pregnant or breastfeeding, history of tobacco, alcoholic, drug abuse, and history of serious medical diseases; mental disorders or other neurological illnesses; a score <24 in a mini-mental state examination (MMSE), and contraindications for MRI.

A total of 42 age-, gender-, and years of education- matched healthy controls were recruited from the community. Exclusion criteria for the healthy controls were: (1) history of brain operations; (2) history of severe neuropsychiatric diseases; (3) serious medical illness; and (4) pregnant or breastfeeding; history of tobacco, alcoholic, drug abuse. Participants who had any contraindications for MRI were excluded. Patients and healthy controls were subjected to an MMSE to evaluate cognitive function. The reaction time (RT) measurements obtained from the Attentional Network Test (49) were used to assess executive function. All participants provided a written informed consent before entering the study. The ethics committee of the Taihe Hospital, Hubei University of Medicine approved the study.

Scan Acquisition

Scanning was conducted using an Achieva 3T MRI scanner (Philips, Netherlands). Participants were asked to lie down with their eyes closed and to remain awake. We used a prototype quadrature birdcage head coil fitted with foam padding to minimize head movement. The scanning parameters were as follows: (1) structural scan (T1-weighted): spin-echo sequence, repetition time (TR) = 20 ms, echo - time (TE) = 3.5 ms, slice thickness = 1 mm, and field of view (FOV) = 24*24 cm, scan time about 7 min. (2) rs - fMRI scan: gradient echo - echo planar imaging sequence (echo - planar imaging T2* weighted), TR/TE = 2,000/30 ms, slice thickness = 5 mm, pitch = 1 mm, FOV = 220 × 220 mm^2, and flip angle = 90°, scan time was about 9 min.

Data Preprocessing

DPARSF software (50) was used in MATLAB for preprocessing rs-fMRI imaging data. First, the first 5 time points were discarded. Then, slice-time and head-motion correction were performed. At this point, participants who had more than 2 mm of maximal displacement on the x, y, or z axis, and more than 2° of maximal rotation were excluded. Subsequently, normalization and resampling were performed to generate the dimensions of 3 × 3 × 3 mm. During the process of functional image normalization, head motion parameters, white matter signal and cerebrospinal fluid signal were used as removal covariates, and a voxel size of 3 x 3 x 3 mm was used as a functional covariate. After that, an 8 mm, full-width at half-maximum Gaussian kernel was used to smooth the acquired images. Temporal bandpass filtering (0.01–0.08 Hz) and linear detrending were used to reduce the influence of low-frequency drifts, and physiological high-frequency noise. During preprocessing, the signal from a region centered in the white matter, six head motion parameters obtained by rigid body correction, and signal from a ventricular region of interest were removed. However, the global signal was preserved, given that removal may introduce artifacts into the data and distort resting-state connectivity patterns, and the regression of the global signal may significantly distort results when studying clinical populations (51, 52).

DMN Identification

The group independent component analysis (ICA) method was used to pick out DMN components according to the templates provided by GIFT (53). Briefly, the ICA analysis included three main steps using the GIFT toolbox (52): data reduction; independent component separation; and back reconstruction. The generated DMN was used as a mask for further NH analyses.

NH Analysis

NH analysis was performed using an in-house script in Matlab. For each subject, the correlation coefficient of each voxel was computed against all other voxels within the DMN mask. Then, the mean correlation coefficient was averaged and subsequently changed into a z-value by using a z-transformation. The resultant values generated the NH maps. Finally, the NH maps were z-transformed for group comparison.

Statistical Analyses

Demographic information, including age, gender, years of educational, and imaging data were compared between the rTLE and the HCs. Chi-square test and the two-sample *t*-test were, respectively used to compare the categorical data and continuous variables. The NH maps of patients and HCs were analyzed with a two-sample *t*-test via voxel-wise cross-subject statistics within the DMN mask. The significance level was set to be $p < 0.01$, and corrected for multiple comparisons using Gaussian Random Field (GRF) theory (GRF corrected, voxel significance: $p < 0.001$, cluster significance: $p < 0.01$).

Classification Analyses

LIBSVM (a Library for Support Vector Machines) software package was applied to examine whether abnormal NH in the DMN could be used as potential biomarkers for diagnosis of rTLE.

RESULTS

Demographics and Clinical Characteristics of the Subjects

No patients or controls were excluded due to excessive head movement. No significant differences were found between the two groups in terms of gender, age, years of education and MMSE. The rTLE group had longer RTs, but no significant differences in RT were found between the rTLE group and the HCs. The demographic data for the recruited subjects are given in **Table 1**.

The DMN Maps Determined by Group ICA

The DMN mask was constructed from the control group using the ICA method. The DMN included the following brain regions: bilateral MPFC; PCC/PCu; ventral anterior cingulate cortex; lateral temporal cortex; medial, lateral, inferior parietal lobes; and cerebellum Crus 1 and Crus 2. The generated DMN mask was used in the subsequent NH analysis.

TABLE 1 | Characteristics of the participants.

Demographic data	Patients ($n = 43$)	NC ($n = 42$)	T (or x^2)	*P*-value
Gender (male/female)	43 (23/20)	42(22/20)	0.12	0.29[a]
Age (years)	27.91 ± 6.48	26.96 ± 5.31	0.74	0.46[b]
Years of education (years)	13.01 ± 2.67	13.67 ± 1.88	−1.33	0.19[b]
Illness duration (years)	8.49 ± 7.1	67.81 ± 48.02	2.13	0.04[b]
ECRT	91.60 ± 54.85			

[a] *The p-value for gender distribution was obtained by chi-square test.*
[b] *The p-value were obtained by two sample t-tests.*
NC, normal control; ECRT, executive control reaction time.

TABLE 2 | Signification differences in NH values between the groups.

Cluster location	Peak X	(MNI) Y	Z	Number of voxels	T value
Patients<controls					
Right ITG	51	6	−36	135	−4.80
Left MTG	−48	−3	30	70	−4.64
Patients >controls					
Right PCu	12	−60	30	45	4.59
Left PCu	0	−78	33	50	3.59
Right IPL	51	−57	48	47	4.16

MNI, Montreal Neurological Institute; ITG, inferior temporal gyrus; MTG, middle temporal lobe; PCu, Precuneus; IPL, inferior parietal lobe.

NH: Group Differences in the DMN

With the two-sample *t*-tests *via* voxel-wise, cross-subject comparisons, significant differences were observed within the DMN, between the NH values for the patient and control groups. Compared to HCs, the rTLE patients had decreased NH in the right inferior temporal gyrus (ITG) and left middle temporal lobe (MTG), but increased NH in the bilateral precuneus (PCu) and right inferior parietal lobe (IPL) (**Table 2**, **Figure 1**).

Correlations Between NH and Clinical Variables

The mean NH values were extracted in the four regions (right ITG, left MTG, bilateral PCu, and right IPL), with significant group differences. Pearson's linear correlation analyses were performed between NH and these clinical variables in the patient group: RT; illness duration; and age at seizure onset. Results showed no significant correlation between NH and these clinical variables.

SVM Results

The increased NH in the bilateral PCu in the rTLE patients were analyzed by the SVM method with a classification accuracy of 74.12%, a sensitivity of 72.01%, and a specificity of 72.81% (**Figure 2**).

DISCUSSION

NH is a new approach for detecting specific loci of compromised connectivity, and for studying within-network coherence. It has been used to study several diseases, such as attention deficit/hyperactivity disorder (39), major depressive disorder (54, 55), schizophrenia (42) and mild cognitive impairment (56). We applied this method to estimate the DMN homogeneity in TLE at rest. The results showed that rTLE patients have a decreased NH in the right ITG and left MTG, but increased NH in the bilateral PCu and right IPL when compared with HCs.

In TLE, it is widely considered that the temporal lobe plays an important part in the regulation and propagation of epileptic discharges, because of the presentation of epileptic foci. Hence, the temporal lobe has proven to be a common target for both structural and functional study of TLE. One study showed altered intrinsic functional connectivity in the temporal regions during both the latent and chronic periods of TLE (4). Among the numerous studies, aberrant regional activation of ITG and/or MTG were repeatedly found from neuroimaging. The ITG, with the localization of lateral and inferior surface of the temporal neocortex, is thought to be the central region for language formulation, and a tertiary visual association cortex region (57), which related to cognitive functions such as memory, language, and visual perception (58, 59). Consistent results from neuroimaging studies of major depressive disorder have demonstrated that this region is involved in emotional processing and social cognition (46, 60). Moreover, the ITG is a key node in a widespread network of frontal, temporal, parietal, occipital, and sub-cortical structures. Thus, abnormal activation of this region could significantly impair the function of the temporal lobe. The MTG plays a critical role in semantic memory and language processing (61). As a result, abnormal activation in the MTG could also consequently affect the function of the temporal lobe. In this study, we demonstrated decreased NH in the right ITG and the MTG. Accordingly, these abnormalities could impair memory and language functions, and result in dysfunction in rTLE patients.

The PCu, a key region of the DMN, is selectively connected with the intraparietal sulcus, the inferior and superior parietal lobules, and the caudal parietal operculum. Acting in concert, these structures are involved in the processing of visuo-spatial information (62–64). It is a significant and integrative structure which exhibits widespread connectivity with some cortical and sub-cortical regions (65). The PCu is responsible for various, essential, cognitive and behavioral functions, including episodic memory retrieval, visuospatial imagery, self-processing operations, and consciousness (65, 66). The right IPL is crucial in the DMN and the frontal parietal network, participating in sustaining attention, alertness, and task switching. Studies in rTLE using resting state fMRI, found that the right IPL had lower functional connectivity (FC) in TLE when compared with the control group (14, 67), which might result in alertness impairment in patients. Because the parietal lobe is connected to the temporal lobe, epileptic discharges from the epileptogenic zone (right temporal lobe) can spread to distant brain regions through the superior longitudinal fasciculus. However, we did not find the same activation pattern in our study. The discrepancy in findings might be attributed to there different epileptic focal positions in patients recruited in previous studies. A smaller sample size, or the application of different methods might also have influenced the results. Here, the inconsistent result

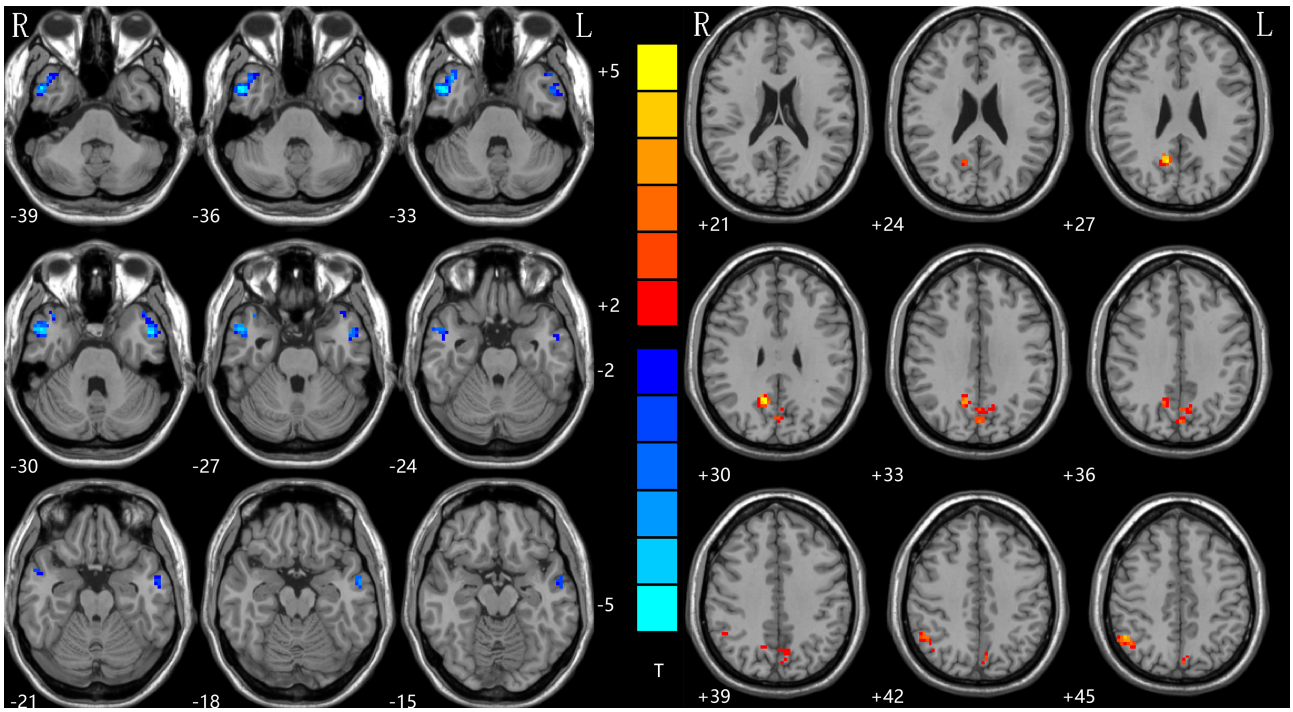

FIGURE 1 | NH differences between patients with rTLE and HCs. Red and blue denote higher and lower NH, respectively, and the color bars represent the T values from the two-sample *t*-test of the group analysis. NH, network homogeneity; rTLE, right temporal lobe epilepsy; HCs, healthy controls.

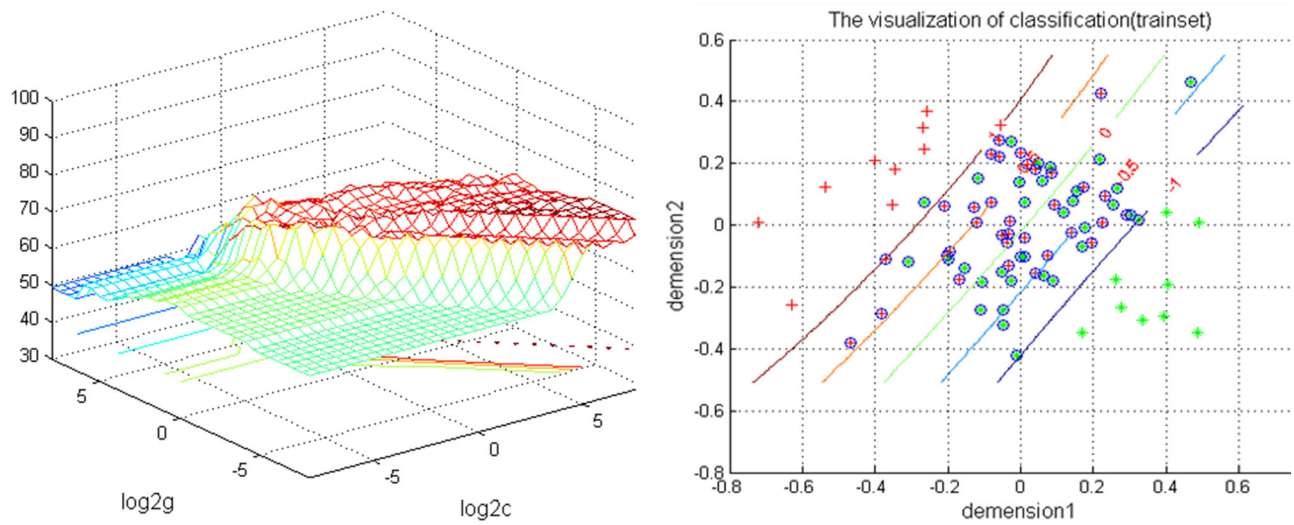

FIGURE 2 | Depiction of classifications based on the SVM using a combination of NH values in the bilateral PCu to differentiate rTLE patients from HCs. Left: SVM parameters result of 3D view. g means gamma, c means penalty coefficient. Right: dimension 1 and dimension 2 represent the NH values in the bilateral PCu. Green crosses represent rTLE patients, and the red crosses represent HCs. SVM, support vector machine; NH, network homogeneity; PCu, precuneus; rTLE, right temporal lobe epilepsy; HCs, healthy controls.

may relate to the different analysis methods. Another probable explanation is as follows: according the roles of IPL and PCu in the cognition process, the increased NH in the bilateral PCu and right IPL might be a compensatory function for the damage to the temporal lobe, and this function becomes stronger depending on the severity of the temporal lobe damage. In addition, by measuring the abnormal NH values of lTLE, our previous study suggested that NH could be utilized as a neuroimaging biomarker

for monitoring lTLE progression (unpublished). In this study, SVM analysis showed that increased NH values in the bilateral PCu could be used to distinguish rTLE patients from HCs with an accuracy of 74.12% (63/85), a sensitivity 72.01% (31/43), and a specificity 72.81% (31/42).

In the network mode of the human brain, DMN is characterized with a group of brain regions that are functionally consistent, that is, high activity while in a resting state, but decreased activity during non-specific task execution such as paying attention. It is closely related to the mental activities of other advanced cognitive functions, such as introspection, scene memory, environmental monitoring and awareness levels (68–72). A previous study confirmed that the DMN changed, which may be relevant to altered cognition and memory in TLE (13, 14, 73). Consistent with the studies referred to above, we thought that the DMN is dysfunctional in TLE, thereby negatively influencing memory and cognition in TLE patients. Furthermore, our study showed a dissociation pattern of activity in DMN, with hypoactivity in anterior regions of the DMN (right ITL and left MTL), but hyperactivity in posterior regions of the DMN (bilateral PCu and right IPL). Other studies of TLE have found significant differences in activity in the resting-state of the DMN, which may explain the symptoms of patients with TLE, such as loss of consciousness, impairments to learning and memory, emotions; and motor, sensory, or psychiatric symptoms (74, 75). The consistent results indicated that the DMN was disturbed, and this aberrance plays an important role in the pathophysiology of TLE.

It is worth noting that patients with rTLE had longer RTs, but no significant correlations between abnormal NH values and RT were found. As studies have demonstrated, TLE patients usually exhibit executive functional impairment. Since it is universally acknowledged that the DMN plays a crucial role in executive functions, we speculate that the regions showing abnormal NH in this study indirectly participate in executive functions. No significant correlations were found between abnormal NH values and RT, nor age of seizure onset or illness duration. These observations might imply that the abnormal NH values for the DMN, might be a trait change in rTLE patients.

There are several limitations to this study. First, the patients were not drug naïve, which might influence the results. Second, we could not thoroughly remove the physiological noise at rest, such as cardiac and respiratory rhythms using a 2-s repetition time, and that may bias the results. Third, this study focused on the DMN. Understanding the neurophysiological abnormalities of the DMN in rTLE would be helpful. For the same reason, some meaningful findings from other brain regions besides this network may have been excluded. Lastly, previous studies have shown that there are some morphological differences between the Chinese population and the others (76). For this reason, the use of the Chinese brain atlas for the data processing in this study may also partly limit the results.

In conclusion, the altered NH in the right ITG, left MTG, left MTG and bilateral PCu may be state-related changes of rTLE. And, the increased NH in the bilateral PCu may be a potential neuroimaging biomarker for rTLE.

DATA AVAILABILITY STATEMENT

The original contributions presented in the study are included in the article/supplementary material, further inquiries can be directed to the corresponding authors.

ETHICS STATEMENT

The studies involving human participants were reviewed and approved by the Ethics Committee of the Taihe Hospital, Hubei University of Medicine. The patients/participants provided their written informed consent to participate in this study.

AUTHOR CONTRIBUTIONS

All authors listed have made a substantial, direct, and intellectual contribution to the work and approved it for publication.

FUNDING

This work was funded by Health Commission of Hubei Province Scientific Research Project: (Grant Nos. WJ2019H232 and WJ2019H233).

REFERENCES

1. Verriello L, Pauletto G, Nilo A, Lonigro I, Betto E, Valente M, et al. Epilepsy and episodic ataxia type 2: family study and review of the literature. *J Neurol.* (2021) 268:4296–302. doi: 10.1007/s00415-021-10555-0
2. Wu YC, Liao YS, Yeh WH, Liang SF, Shaw FZ. Directions of deep brain stimulation for epilepsy and Parkinson's disease. *Front Neurosci.* (2021) 15:680938. doi: 10.3389/fnins.2021.680938
3. French JA, Williamson PD, Thadani VM, Darcey TM, Mattson RH, Spencer SS, et al. Characteristics of medial temporal lobe epilepsy: I. results of history and physical examination. *Ann Neurol.* (1993) 34:774–80. doi: 10.1002/ana.410340604
4. Lee H, Jung S, Lee P, Jeong Y. Altered intrinsic functional connectivity in the latent period of epileptogenesis in a temporal lobe epilepsy model. *Exp Neurol.* (2017) 296:89–98. doi: 10.1016/j.expneurol.2017.07.007
5. Banjac S, Roger E, Pichat C, Cousin E, Mosca C, Lamalle L, et al. Reconfiguration dynamics of a language-and-memory network in healthy participants and patients with temporal lobe epilepsy. *NeuroImage Clin.* (2021) 31:102702. doi: 10.1016/j.nicl.2021.102702
6. Tombini M, Assenza G, Quintiliani L, Ricci L, Lanzone J, Ulivi M, et al. Depressive symptoms and difficulties in emotion regulation in adult patients with epilepsy: association with quality of life and stigma. *Epilepsy Behav.* (2020) 107:107073. doi: 10.1016/j.yebeh.2020.107073
7. Redinbaugh MJ, Afrasiabi M, Phillips JM, Kambi NA, Mohanta S, Saalmann YB. Thalamic deep brain stimulation as a paradigm to reduce consciousness: implications for cortico-striatal dynamics, absence epilepsy and consciousness studies. *bioRxiv [Preprint].* (2021) doi: 10.1101/2021.07.27.453855
8. Yasuda CL, Chen Z, Beltramini GC, Coan AC, Morita ME, Kubota B, et al. Aberrant topological patterns of brain structural network in temporal lobe epilepsy. *Epilepsia.* (2015) 56:1992–2002. doi: 10.1111/epi.13225

9. Diao L, Yu H, Zheng J, Chen Z, Huang, D, Yu L. Abnormalities of the uncinate fasciculus correlate with executive dysfunction in patients with left temporal lobe epilepsy. *Magn Reson Imaging.* (2015) 33:544–50. doi: 10.1016/j.mri.2015.02.011
10. Zhou S, Xiong P, Ren H, Tan W, Yan Y, Gao Y. Aberrant dorsal attention network homogeneity in patients with right temporal lobe epilepsy. *Epilepsy Behav*. (2020) 111:107278. doi: 10.1016/j.yebeh.2020.107278
11. Li DB, Liu RS, Wang X, Xiong PA, Ren HW, Wei YF, et al. Abnormal ventral attention network homogeneity in patients with right temporal lobe epilepsy. *Eur Rev Med Pharmacol Sci.* (2021) 25:2031–8. doi: 10.26355/eurrev_202102_25107
12. Gao YJ, Wang X, Xiong PG, Ren HW, Zhou SY, Yan YG, et al. Abnormalities of the default-mode network homogeneity and executive dysfunction in people with first-episode, treatment-naive left temporal lobe epilepsy. *Eur Rev Med Pharmacol Sci.* (2021) 25:2039–49. doi: 10.26355/eurrev_202102_25108
13. Gao Y, Zheng J, Li Y, Guo D, Wang M, Cui X, et al. Abnormal default-mode network homogeneity in patients with temporal lobe epilepsy. *Medicine.* (2018) 97:e11239. doi: 10.1097/MD.0000000000011239
14. Gao Y, Zheng J, Li Y, Guo D, Wang M, Cui X, et al. Decreased functional connectivity and structural deficit in alertness network with right-sided temporal lobe epilepsy. *Medicine.* (2018) 97:e0134. doi: 10.1097/MD.0000000000010134
15. Gao Y, Xiong Z, Wang X, Ren H, Liu R, Bai B, et al. Abnormal degree centrality as a potential imaging biomarker for right temporal lobe epilepsy: a resting-state functional magnetic resonance imaging study and support vector machine analysis. *Neuroscience.* (2022) 487:198–206. doi: 10.1016/j.neuroscience.2022.02.004
16. Hosseini MP, Tran TX, Pompili D, Elisevich K, Soltanian-Zadeh H. Multimodal data analysis of epileptic EEG and rs-fMRI *via* deep learning and edge computing. *Artif Intell Med.* (2020) 104:101813. doi: 10.1016/j.artmed.2020.101813
17. Dumlu SN, Ademoglu A, Sun W. Investigation of functional variability and connectivity in temporal lobe epilepsy: a resting state fMRI study - sciencedirect. *Neurosci Lett*. (2020). 733:135076. doi: 10.1016/j.neulet.2020.135076
18. Milton CK, O'Neal CM, Conner AK. Functional connectivity of hippocampus in temporal lobe epilepsy depends on hippocampal dominance: a systematic review of the literature. *J Neurol.* (2022) 269:221–32. doi: 10.1007/s00415-020-10391-8
19. Liu J, Zhang Z, Zhou X, Pang X, Liang X, Huang H, et al. Disrupted alertness and related functional connectivity in patients with focal impaired awareness seizures in temporal lobe epilepsy. *Epilepsy Behav.* (2020) 112:107369. doi: 10.1016/j.yebeh.2020.107369
20. Qin Y, Tong X, Li W, Zhang L, Zhang Y, Li X, et al. Divergent anatomical correlates and functional network connectivity patterns in temporal lobe epilepsy with and without depression. *Brain Topogr.* (2021) 34:525–36. doi: 10.1007/s10548-021-00848-y
21. Shuhada JM, Husbani MAR, Hamid IA, Muhammad. The default mode network in patient with temporal lobe epilepsy (TLE): a resting state fMRI study. *Asian J Med Biomedicine.* (2020). 4:23–30. doi: 10.37231/ajmb.2020.4.1.326
22. Nenning KH, Fösleitner O, Schwartz E, Schwarz M, Schmidbauer V, Geisl G, et al. The impact of hippocampal impairment on task-positive and task-negative language networks in temporal lobe epilepsy. *Clin Neurophysiol.* (2021) 132:404–11. doi: 10.1016/j.clinph.2020.10.031
23. Gusnard DA, Akbudak, E, Shulman GL, Raichle ME. Medial prefrontal cortex and self-referential mental activity: relation to a default mode of brain function. *Proc Natl Acad Sci U S A.* (2001) 98:4259–64. doi: 10.1073/pnas.071043098
24. Mazoyer B, Zago L, Mellet E, Bricogne S, Etard O, Houdé O, et al. Cortical networks for working memory and executive functions sustain the conscious resting state in man. *Brain Res Bull.* (2001) 54:287–98. doi: 10.1016/S0361-9230(00)00437-8
25. Liang S, Deng W, Li X, Greenshaw AJ, Wang Q, Li M, et al. Biotypes of major depressive disorder: neuroimaging evidence from resting-state default mode network patterns. *NeuroImage Clin.* (2020) 28:102514. doi: 10.1016/j.nicl.2020.102514
26. Park H, Cha J, Kim H, Joo E. 0724 Altered brain network organization in patients with obstructive sleep apnea. *Sleep.* (2020) 43:A275–6. doi: 10.1093/sleep/zsaa056.720
27. Habas C, Kamdar N, Nguyen D, Prater K, Beckmann CF, Menon V, et al. Distinct cerebellar contributions to intrinsic connectivity networks. *Neuroimage.* (2009) 29:8586–94. doi: 10.1016/S1053-8119(09)71566-6
28. Davey CG, Pujol J, Harrison BJ. Mapping the self in the brain's default mode network. *Neuroimage.* (2016) 132:390–7. doi: 10.1016/j.neuroimage.2016.02.022
29. Horovitz SG, Fukunaga M, de Zwart JA, van Gelderen P, Fulton SC, Balkin TJ, et al. Low frequency BOLD fluctuations during resting wakefulness and light sleep: a simultaneous EEG-fMRI study. *Hum Brain Mapp.* (2008) 29:671–82. doi: 10.1002/hbm.20428
30. Zhang L, Zuo XN, Ng KK, Chong JSX, Shim HY, Ong MQW, et al. Distinct BOLD variability changes in the default mode and salience networks in Alzheimer's disease spectrum and associations with cognitive decline. *Sci Rep.* (2020) 10:6457. doi: 10.1038/s41598-020-63540-4
31. Song M, Du H, Wu N, Hou B, Wu G, Wang J, et al. Impaired resting-state functional integrations within default mode network of generalized tonic-clonic seizures epilepsy. *PLoS ONE.* (2012) 6:e17294. doi: 10.1371/journal.pone.0017294
32. Wang Z, Lu G, Zhang Z, Zhong Y, Jiao Q, Zhang Z, et al. Altered resting state networks in epileptic patients with generalized tonic-clonic seizures. *Brain Res.* (2011) 1374:134. doi: 10.1016/j.brainres.2010.12.034
33. Gotman J, Grova C, Bagshaw A, Kobayashi E, Aghakhani Y, Dubeau F. Generalized epileptic discharges show thalamocortical activation and suspension of the default state of the brain. *Proc Natl Acad Sci.* (2005) 102:15236–40. doi: 10.1073/pnas.0504935102
34. Benuzzi F, Ballotta D, Mirandola L, Ruggieri A, Vaudano AE, Zucchelli M, et al. An EEG-fMRI study on the termination of generalized spike-and-wave discharges in absence epilepsy. *PLoS ONE.* (2015) 10:e0130943. doi: 10.1371/journal.pone.0130943
35. Minzenberg MJ, Yoon J, Carter CS. Modafinil modulation of the default mode network. *Psychopharmacology.* (2011) 215:23–31. doi: 10.1007/s00213-010-2111-5
36. He H, Liu X, Hao Y. A progressive deep wavelet cascade classification model for epilepsy detection. *Artif Intell Med.* (2021) 118:102117. doi: 10.1016/j.artmed.2021.102117
37. Yan M, He Y, Cui X, Liu F, Li H, Huang R, et al. Disrupted regional homogeneity in melancholic and non-melancholic major depressive disorder at rest. *Front Psychiatry.* (2021) 12:618805. doi: 10.3389/fpsyt.2021.618805
38. Gao Y, Wang X, Xiong Z, Ren H, Liu R, Wei Y, et al. Abnormal fractional amplitude of low-frequency fluctuation as a potential imaging biomarker for first-episode major depressive disorder: a resting-state fMRI study and support vector machine analysis. *Front Neurol.* (2021) 12:751400. doi: 10.3389/fneur.2021.751400
39. Uddin LQ, Kelly AM, Biswal BB, Margulies DS, Shehzad Z, Shaw D, et al. Network homogeneity reveals decreased integrity of default-mode network in ADHD. *J Neurosci Methods.* (2008) 169:249–54. doi: 10.1016/j.jneumeth.2007.11.031
40. Guo W, Liu F, Yao D, Jiang J, Su Q, Zhang Z, et al. Decreased default-mode network homogeneity in unaffected siblings of schizophrenia patients at rest. *Psychiatry Res.* (2014) 224:218–24. doi: 10.1016/j.pscychresns.2014.08.014
41. Guo W, Liu F, Chen J, Wu R, Li L, Zhang Z, et al. Olanzapine modulates the default-mode network homogeneity in recurrent drug-free schizophrenia at rest. *Aust N Z J Psychiatry*. (2017) 51:1000–9. doi: 10.1177/0004867417714952
42. Guo W, Yao D, Jiang J, Su Q, Zhang Z, Zhang J, et al. Abnormal default-mode network homogeneity in first-episode, drug-naive schizophrenia at rest. *Prog Neuropsychopharmacol Biol Psychiatry.* (2014) 49:16–20. doi: 10.1016/j.pnpbp.2013.10.021
43. Wei S, Su Q, Jiang M, Liu F, Yao D, Dai Y, et al. Abnormal default-mode network homogeneity and its correlations with personality in drug-naive somatization disorder at rest. *J Affect Disord.* (2016) 193:81–8. doi: 10.1016/j.jad.2015.12.052
44. Guo W, Liu F, Yu M, Zhang J, Zhang Z, Liu J, et al. Decreased regional activity and network homogeneity of the fronto-limbic network at rest in drug-naive major depressive disorder. *Aust N Z J Psychiatry.* (2015) 49:550–6. doi: 10.1177/0004867415577978

45. Cui X, Guo W, Wang Y, Yang TX, Yang XH, Wang Y, et al. Aberrant default mode network homogeneity in patients with first-episode treatment-naive melancholic depression. *Int J Psychophysiol.* (2017) 112:46–51. doi: 10.1016/j.ijpsycho.2016.12.005
46. Guo W, Liu F, Zhang J, Zhang Z, Yu L, Liu J, et al. Abnormal default-mode network homogeneity in first-episode, drug-naive major depressive disorder. *PLoS ONE.* (2014) 9:e91102. doi: 10.1371/journal.pone.0091102
47. Seidenberg M, Kelly KG, Parrish J, Geary E, Dow C, Rutecki P, et al. Ipsilateral and contralateral MRI volumetric abnormalities in chronic unilateral temporal lobe epilepsy and their clinical correlates. *Epilepsia.* (2005) 46:420–30. doi: 10.1111/j.0013-9580.2005.27004.x
48. Manford M, Fish DR, Shorvon SD. An analysis of clinical seizure patterns and their localizing value in frontal and temporal lobe epilepsies. *Brain.* (1996) 119:17–40. doi: 10.1093/brain/119.1.17
49. Fan J, McCandliss BD, Sommer T, Raz A, Posner MI. Testing the efficiency and independence of attentional networks. *J Cogn Neurosci.* (2002) 14:340–7. doi: 10.1162/089892902317361886
50. Chao-Gan Y, Yu-Feng Z. DPARSF A MATLAB toolbox for "pipeline" data analysis of resting-state fMRI. *Front Syst Neurosci.* (2010) 4:13. doi: 10.3389/fnsys.2010.00013
51. Saad ZS, Gotts SJ, Murphy K, Chen G, Jo HJ, Martin A, et al. Trouble at rest: how correlation patterns and group differences become distorted after global signal regression. *Brain Connect.* (2012) 2:25–32. doi: 10.1089/brain.2012.0080
52. Hahamy A, Calhoun V, Pearlson G, Harel M, Stern N, Attar F, et al. Save the global: global signal connectivity as a tool for studying clinical populations with functional magnetic resonance imaging. *Brain Connect.* (2014) 4:395–403. doi: 10.1089/brain.2014.0244
53. Sheline YI, Barch DM, Price JL, Rundle MM, Vaishnavi SN, Snyder AZ, et al. The default mode network and self-referential processes in depression. *Proc Natl Acad Sci U S A.* (2009) 106:1942–7. doi: 10.1073/pnas.0812686106
54. Gao Y, Wang M, Yu R, Li Y, Yang Y, Cui X, et al. Abnormal default mode network homogeneity in treatment-naive patients with first-episode depression. *Front Psychiatry.* (2018) 9:697. doi: 10.3389/fpsyt.2018.00697
55. Yan M, Cui X, Liu F, Li H, Huang R, Tang Y, et al. Abnormal default-mode network homogeneity in melancholic and nonmelancholic major depressive disorder at rest. *Neural Plast.* (2021) 2021:1–12. doi: 10.1155/2021/6653309
56. Cao Y, Yang H, Zhou Z, Cheng Z, Zhao X. Abnormal default-mode network homogeneity in patients with mild cognitive impairment in Chinese communities. *Front Neurol.* (2021) 11:569806. doi: 10.3389/fneur.2020.569806
57. Dien J, Brian ES, Molfese DL, Gold BT. Combined ERP/fMRI evidence for early word recognition effects in the posterior inferior temporal gyrus. *Cortex.* (2013) 49:2307–21. doi: 10.1016/j.cortex.2013.03.008
58. Ojemann GA, Schoenfield-McNeill J, Corina DP. Anatomic subdivisions in human temporal cortical neuronal activity related to recent verbal memory. *Nat Neurosci.* (2002) 5:64–71. doi: 10.1038/nn785
59. Noppeney U, Price CJ. Retrieval of visual, auditory, abstract semantics. *Neuroimage.* (2002) 15:917–26. doi: 10.1006/nimg.2001.1016
60. Gallagher HL, Frith CD. Functional imaging of 'theory of mind'. *Trends Cogn Sci.* (2003) 7:77–83. doi: 10.1016/S1364-6613(02)00025-6
61. Kiehl KA, Smith AM, Mendrek A, Forster BB, Hare RD, Liddle PF. Temporal lobe abnormalities in semantic processing by criminal psychopaths as revealed by functional magnetic resonance imaging. *Psychiatry Res.* (2004) 130:297–312. doi: 10.1016/j.pscychresns.2004.02.002
62. Selemon LD, Goldman-Rakic PS. Common cortical and subcortical targets of the dorsolateral prefrontal and posterior parietal cortices in the rhesus monkey: evidence for a distributed neural network subserving spatially guided behavior. *J Neurosci.* (1988) 8:4049–68. doi: 10.1523/JNEUROSCI.08-11-04049.1988
63. Cavada C, Goldman-Rakic PS. Posterior parietal cortex in rhesus monkey: II. Evidence for segregated corticocortical networks linking sensory and limbic areas with the frontal lobe. *J Comp Neurol.* (1989) 287:422–45. doi: 10.1002/cne.902870403
64. Leichnetz GR. Connections of the medial posterior parietal cortex (area 7m) in the monkey. *Anat Rec.* (2001) 263:215–36. doi: 10.1002/ar.1082
65. Cavanna AE, Trimble MR. The precuneus: a review of its functional anatomy and behavioural correlates. *Brain.* (2006) 129(Pt 3):564–83. doi: 10.1093/brain/awl004
66. Ogiso T, Kobayashi K, Sugishita M. The precuneus in motor imagery: a magnetoencephalographic study. *Neuroreport.* (2000) 11:1345–9. doi: 10.1097/00001756-200004270-00039
67. Li J, Chen X, Ye W, Jiang W, Liu H, Zheng J. Alteration of the alertness-related network in patients with right temporal lobe epilepsy: a resting state fMRI study. *Epilepsy Res.* (2016) 127:252–9. doi: 10.1016/j.eplepsyres.2016.09.013
68. Greicius MD, Krasnow B, Reiss LA, Menon V. Functional connectivity in the resting brain: a network analysis of the default mode hypothesis. *Proc Natl Acad Sci U S A.* (2003) 100:253–8. doi: 10.1073/pnas.0135058100
69. Raichle ME, MacLeod AM, Snyder AZ, Powers WJ, Gusnard DA, Shulman GL, et al. default mode of brain function. *Proc Natl Acad Sci U S A.* (2001) 98:676–82. doi: 10.1073/pnas.98.2.676
70. Raichle ME, Gusnard DA. Intrinsic brain activity sets the stage for expression of motivated behavior. *J Comp Neurol.* (2005) 493:167–76. doi: 10.1002/cne.20752
71. Raichle ME, Snyder AZ. A default mode of brain function: a brief history of an evolving idea. *Neuroimage.* (2007) 37:1083–90; discussion 1097–9. doi: 10.1016/j.neuroimage.2007.02.041
72. Fox MD, Raichle ME. Spontaneous fluctuations in brain activity observed with functional magnetic resonance imaging. *Nat Rev Neurosci.* (2007) 8:700–11. doi: 10.1038/nrn2201
73. Haneef Z, Lenartowicz A, Yeh HJ, Engel J Jr, Stern JM. Effect of lateralized temporal lobe epilepsy on the default mode network. *Epilepsy Behav.* (2012) 25:350–7. doi: 10.1016/j.yebeh.2012.07.019
74. Maccotta L, He BJ, Snyder AZ, Eisenman LN, Benzinger TL, Ances BM, et al. Impaired and facilitated functional networks in temporal lobe epilepsy. *Neuroimage Clin.* (2013) 2:862–72. doi: 10.1016/j.nicl.2013.06.011
75. Kandratavicius L, Lopes-Aguiar C, Bueno-Júnior LS, Romcy-Pereira RN, Hallak JE, Leite JP. Psychiatric comorbidities in temporal lobe epilepsy: possible relationships between psychotic disorders and involvement of limbic circuits. *Rev Bras Psiquiatr.* (2012) 34:454–66. doi: 10.1016/j.rbp.2012.04.007
76. Liang P, Shi L, Chen N, Luo Y, Wang X, Liu K, et al. Construction of brain atlases based on a multi-center MRI dataset of (2020). *Chinese Adults Sci Rep.* (2015) 5:18216. doi: 10.1038/srep18216

Conflict of Interest: The authors declare that the research was conducted in the absence of any commercial or financial relationships that could be construed as a potential conflict of interest.

The reviewer LL declared a shared affiliation with the author YiZ at the time of review.

frontiers | Frontiers in Psychiatry

ORIGINAL RESEARCH
published: 17 June 2022
doi: 10.3389/fpsyt.2022.877956

Abnormal Ventral Somatomotor Network Homogeneity in Patients With Temporal Lobe Epilepsy

Dongbin Li[1,2], Ruoshi Liu[3], Lili Meng[4,5], Pingan Xiong[6], Hongwei Ren[7], Liming Zhang[1] and Yujun Gao[8]**

[1] Department of Neurology, The First Affiliated Hospital of Harbin Medical University, Harbin, China, [2] First Department of Neurology and Neuroscience Center, Heilongjiang Provincial Hospital, Harbin, China, [3] Department of Neurology, The Fourth Affiliated Hospital of Harbin Medical University, Harbin, China, [4] Department of Psychiatry, Wuhan Mental Health Center, Wuhan, China, [5] Department of Sleep, Wuhan Hospital for Psychotherapy, Wuhan, China, [6] Department of Taihe Hospital Reproductive Medicine Center Affiliated To Hubei University of Medicine, Shiyan, China, [7] Department of Medical Imaging, Tianyou Hospital Affiliated To Wuhan University of Science and Technology, Wuhan, China, [8] Department of Psychiatry, Renmin Hospital of Wuhan University, Wuhan, China

Background: Abnormalities of functional connectivity in the somatomotor network have been thought to play an essential role in the pathophysiology of epilepsy. However, there has been no network homogeneity (NH) study about the ventral somatomotor network (VSN) in patients with temporal lobe epilepsy (TLE). Therefore, we explored the NH of the VSN in TLE patients in this study.

Methods: The sample included 52 patients with left temporal lobe epilepsy, 83 patients with right temporal lobe epilepsy, and 68 healthy controls. The NH method was utilized to analyze the resting-state functional magnetic resonance imaging data.

Results: Compared to the controls, rTLE patients had significantly higher NH in the bilateral postcentral gyrus, and significantly lower NH in the bilateral Rolandic operculum and the right superior temporal gyrus (STG). The NH values of the left postcentral gyrus were significantly higher in lTLE patients than in the healthy controls, and lTLE patients had lower NH in the right Rolandic operculum. The altered NH in the postcentral gyrus was negatively correlated with the illness duration, and the decreased NH in the left Rolandic operculum was negatively correlated with the executive control reaction time (ECRT).

Conclusion: Our findings suggest that altered NH of the postcentral gyrus, Rolandic operculum and STG might be associated with the pathophysiology of TLE, and thus, highlight the contribution of the VSN to the pathophysiology of TLE.

Keywords: temporal lobe epilepsy, ventral somatomotor network, network homogeneity, resting-state functional magnetic resonance imaging, executive function

OPEN ACCESS

Edited by:
Linda J. Larson-Prior, University of Arkansas for Medical Sciences, United States

Reviewed by:
Jinping Liu, Guilin Medical University, China
Jinou Zheng, Guangxi Medical University, China

****Correspondence:***
Liming Zhang
zfx001@yahoo.com
Yujun Gao
gaoyujun19820214@163.com

Specialty section:
This article was submitted to Neuroimaging and Stimulation, a section of the journal Frontiers in Psychiatry

Received: *17 February 2022*
Accepted: *16 May 2022*
Published: *17 June 2022*

Citation:
Li D, Liu R, Meng L, Xiong P, Ren H, Zhang L and Gao Y (2022) Abnormal Ventral Somatomotor Network Homogeneity in Patients With Temporal Lobe Epilepsy. Front. Psychiatry 13:877956. doi: 10.3389/fpsyt.2022.877956

INTRODUCTION

Epilepsy is one of the most common neurological disorders, affecting over 70 million people worldwide and putting a considerable strain on health-care infrastructure and the economy (1). Temporal lobe epilepsy (TLE) is the most common type of partial epilepsy referred for surgery, accounting for more than 40% of surgical cases, because of the failure of antiepileptic drug

therapy (2). TLE is characterized by cognitive dysfunction, which includes memory, executive functioning, and general intellectual functioning disorders, thus contributing to a poor quality of life (3). Although temporal lobectomy results in seizure-free status in 70% of TLE patients (4), surgical resection is still invasive and has undesirable side effects. Recent work has linked TLE with network-level disruption (5), and resting-state functional magnetic resonance imaging (rs-fMRI) studies have revealed its neural connections. MRI is thought to be the most direct method for demonstrating functional connectivity among separated regions of the brain at rest and is the primary method used for studying brain networks.

The somatomotor network is a resting-state network composed of bilateral pre- and postcentral gyri. Based on large amounts of resting-state fMRI data and a data-driven clustering approach (6), Biswal et al. (7) found that the somatomotor network belongs to the conventional group of seven cortical neuronal networks. Several studies have confirmed that the somatomotor network has strong positive connectivity with various brain areas, including the ventral attention networks, frontoparietal networks, and default mode networks (8). In addition, the somatomotor network is closely correlated with the occurrence and progression of diseases such as autism spectrum disorder, schizophrenia, and major depressive disorder (8–10). However, there have been a few reports on the somatomotor network in patients with epilepsy. Furthermore, the symptoms of epilepsy, such as myotonia, myoclonia, and atonic seizures, are closely related to the motor system. In this study, we focused our work on the potential functional mechanism of the ventral somatomotor network (VSN), which is a subdivision of the somatomotor network, in patients with TLE.

With the development of imaging technology in recent years, many brain structural and functional differences have been reported in patients with TLE and healthy controls. For example, Gao et al. (11) found a decrease in functional connectivity and structural deficits in the alerting network of patients with right-sided TLE (rTLE) by using the seed-based functional connectivity method. Mankinen et al. (12) found that interictal epileptiform activity may lead to the reorganization of resting-state brain networks by using independent component analysis (ICA). The seed-based region-of-interest (ROI) functional connectivity method and ICA are two approaches that are often used to assess brain networks. However, these analytical methods have several disadvantages. For example, ROI seed-based methods are critical for selecting an *a priori* ROI within a network. Unlike the ROI seed-based method, ICA does not require an *a priori* definition of seed regions; however, the results are highly dependent on the number of components the algorithm is asked to produce (13). To address these issues, an unbiased method for assessing imaging data is critical.

Network homogeneity (NH) (14) is a survey method that has been widely used in investigating many diseases, such as attention-deficit/hyperactivity disorder and depression, and has also been used to assess connectivity among brain networks (14, 15). The NH method is a novel method that combines the advantages of ICA and ROI seed-based functional connectivity. Thus, it provides an unbiased, hypothesis-driven measure for evaluating a specific brain network associated with a pathophysiologic process or a disorder. The NH method investigates a given network without requiring prior knowledge of the location of network abnormalities. As a voxel-wise survey, NH can be utilized to assess the connectivity of a voxel with the other brain voxels in a predefined network. Homogeneity is defined as the average connectivity of a given voxel. However, VSN homogeneity in patients with TLE has not been reported. In the present study, we analyzed rs-fMRI data from patients with TLE to investigate abnormalities in the NH of the VSN and explore the potential mechanism of impaired somatomotor function in TLE.

MATERIALS AND APPROACHES

Subjects

Fifty-two patients with left temporal lobe epilepsy (lTLE) and 83 patients with right temporal lobe epilepsy (rTLE) were recruited from the Department of Neurology, Tianyou Hospital Affiliated to Wuhan University of Science and Technology. Sixty-eight healthy people were recruited from those who underwent a standard physical examination at the medical examination center of the Tianyou Hospital Affiliated to Wuhan University of Science and Technology. Patients were diagnosed with TLE based on the diagnostic manual from the International League Against Epilepsy (16). The inclusion criteria for TLE were as follows (epilepsy patients who met any two of the following symptoms): (1) the clinical onset of symptoms suggested epileptic foci in the temporal lobe, such as psychiatric symptoms, abnormal emotional experiences, automatisms, epigastric rising, or dystonic posturing of the limb; (2) the imaging results showed atrophy or sclerosis in the right/left temporal lobe; and (3) the interictal electroencephalographic traces suggested an abnormality in the right/left temporal lobe. The exclusion criteria for all subjects were as follows: (1) left-handed; (2) any lifetime psychiatric disorder; (3) history of serious medical diseases or other neurological illness; and (4) Mini-Mental State Examination scores (MMSE) < 24. All subjects gave written, informed consent before participating in the study. All participants were right-handed, and the groups were matched by age, education level, and sex ratio. Our study was performed according to the Declaration of Helsinki and approved by the Medical Ethics Committee of the Tianyou Hospital Affiliated to Wuhan University of Science and Technology.

Behavioral Paradigm

The executive function was assessed by the attentional network test (ANT) (17). The stimulus signals of ANT visually appear on a screen, and the subjects were required to correctly and quickly identify the orientation in which a central target arrow pointed. The reaction time (RT) of all the subjects were recorded, and the executive control reaction time (ECRT) was calculated by subtracting the consistent arrow direction RT from the inconsistent arrow direction RT (17). A longer ECRT indicated inferior executive control performance.

Scan Acquisition

Images were acquired with an Achieva 3T MRI scanner (Philips, Amsterdam, the Netherlands) for resting-state functional magnetic resonance imaging (rsfMRI). "Participants were instructed to lie down with their eyes closed and remain awake. A prototype quadrature birdcage head coil filled with foam padding was used to limit the head motion. The scanning parameters were as follows: ratio of repetition time to echo time (TR/TE) (2,000/30 ms), slice thickness (5 mm), pitch (1 mm), field of view (240 × 240 mm), and flip angle (90°). On the structural scan (T1-weighted), the following settings were used: spin-echo sequence, repetition time (TR) = 20 ms, echo time (TE) = 3.5 ms, slice thickness = 1 mm, and field of view (FOV) = 24 × 24 cm." [excerpted from our previous study (15)].

Data Preprocessing

Imaging data of rs-fMRI were preprocessed using the DPARSF software (18) in MATLAB (Mathworks). "After signal stabilization, head motion and slice-timing correction were conducted (19, 20). The subjects had a maximal translation ≤ 2 mm in the x, y, or z direction and an angular rotation $\leq 2^{\circ}$ on each axis. The functional images were normalized to the standard template in Montreal Neurological Institute (MNI) template and spatially resampled to a voxel size of 3 mm × 3 mm × 3 mm. The head motion parameters obtained by rigid body correction, the white matter signal, and the cerebrospinal fluid signal were removed from the images by linear regression. The signal was bandpass filtered (0.01–0.1 Hz) and linearly detrended to reduce high-frequency physiological noise and low-frequency drift. The global signal removal may introduce artifacts into the data and distort resting-state connectivity patterns. Furthermore, the regression of the global signal may significantly distort results when studying clinical populations. Therefore, the global signal was preserved (21, 22)" [excerpted from our previous study (15)].

Ventral Somatomotor Network Identification

The toolbox GIFT[1] was used to pick out VSN as a mask from all participants through the group ICA method. "Three steps from the GIFT toolbox were used as following: data reduction, separation of independent components, and back rebuilding. On the consideration of every component, the voxel-wise one-sample *t*-test set a statistical map and a threshold. Based on Gaussian random field (GRF) theory, $p < 0.01$ represents a significant statistical modification of multiple comparisons. Voxel significance: $p < 0.01$, and cluster significance: $p < 0.01$). Masks were created for the VSN components. Finally, the masks were combined to generate a VSN mask utilized in the following NH analysis." [excerpted from our previous study (15)].

Network Homogeneity Analysis

MATLAB was used for NH analysis (14). "For each patient, the correlation coefficients were obtained in a given voxel with all other voxels within the VSN mask. The mean correlation coefficient was defined as the homogeneity of the given voxel, and subsequently changed into *z*-value by using z-transformation to improve the normal distribution as described. The resultant values generated the NH map that finally underwent z-transformation for group comparison" [excerpted from our previous study (15)].

[1]http://mialab.mrn.org/software/#gica

TABLE 1 | Characteristics of the participants.

Characteristics	NC (*n* = 68)	rTLE (*n* = 83)	lTLE (*n* = 52)
Gender (male/female)	68 (36/32)	83 (43/40)	52 (33/19)
Age, years	26.55 ± 4.90	28.64 ± 8.52	27.74 ± 7.89
Years of education, years	12.32 ± 2.40	11.89 ± 2.68	11.73 ± 2.01
Illness duration, years	–	8.63 ± 7.04	7.98 ± 6.70
ECRT	72.88 ± 36.03	129.22 ± 42.95*	124.07 ± 31.96*
Head motion	0.11 ± 0.03	0.10 ± 0.04	0.09 ± 0.03

*A non-parametric statistics (Kruskal-Wallis test) was used for continuous data, and the X^2 test for categorical data. Compared with normal controls, *P < 0.01. NC, normal controls; RT, reaction time.*

Statistical Analyses

Demographic information, including sex, age, education degree, and imaging data, were calculated between the patient and control groups. Non-parametric Kruskal-Wallis test was used to compare the distributions between multiple groups because not all samples were in compliance with normal distribution. Categorical data were analyzed with a chi-square test using the IBMSPSS Statistics 22.0 software. Analyses of covariance were executed to compare differences across the three groups on voxel-based VSN maps. Then, *post-hoc t*-tests were executed to compare VSN differences between every two groups. Sex, age, years of education, and head motion were applied as covariates in group comparisons to limit the possible effects of these components. The significance level was set at the corrected $p < 0.01$ for multiple comparisons using the Gaussian Random Field (GRF) theory (GRF-corrected, voxel significance: $p < 0.001$, cluster significance: $p < 0.01$). Correlations between clinical variables were analyzed using partial correlations with head motion as a covariate. Bonferroni correction for multiple comparisons was used in the correlation analysis.

RESULTS

Demographics and Clinical Characteristics of Subjects

In this study, 135 TLE patients (52 lTLE patients and 83 rTLE patients) and 68 age- and sex-matched healthy controls were recruited for the study. The demographic and clinical characteristics of the study subjects are provided in **Table 1**. No significant differences were observed among the three groups regarding age, sex, and years of education. The patient group showed a longer executive control reaction time.

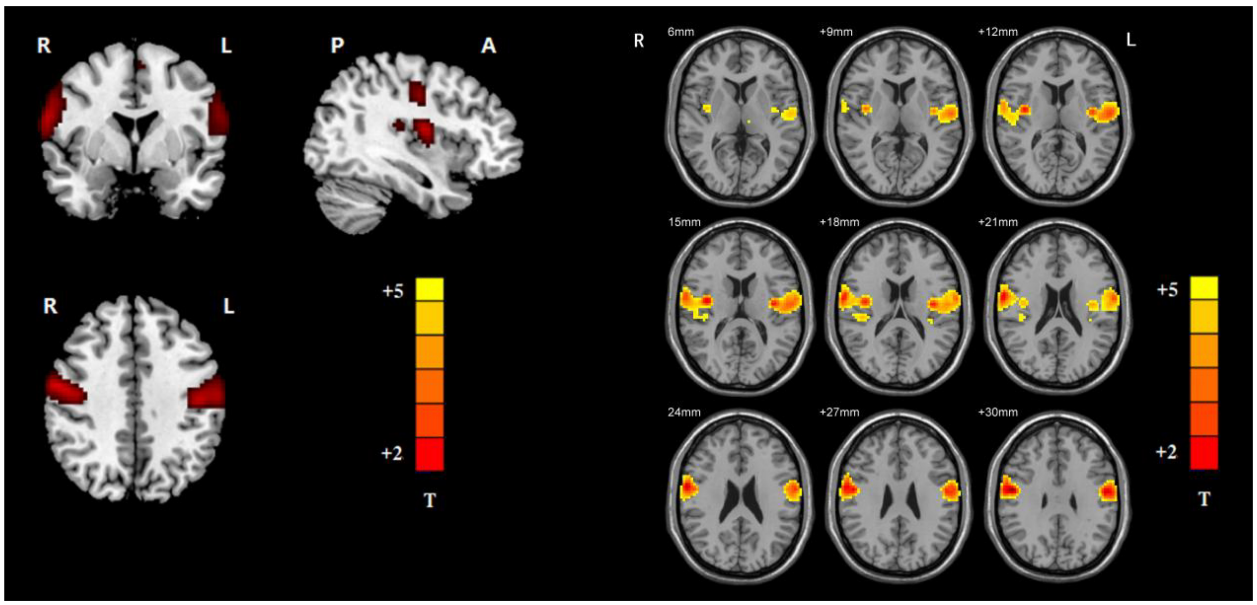

FIGURE 1 | Ventral somatomotor network (left: axial, coronal, and sagittal images of VSN; right: the detailed axial images of VSN. Based on group ICA with a threshold at $z \geq 5$).

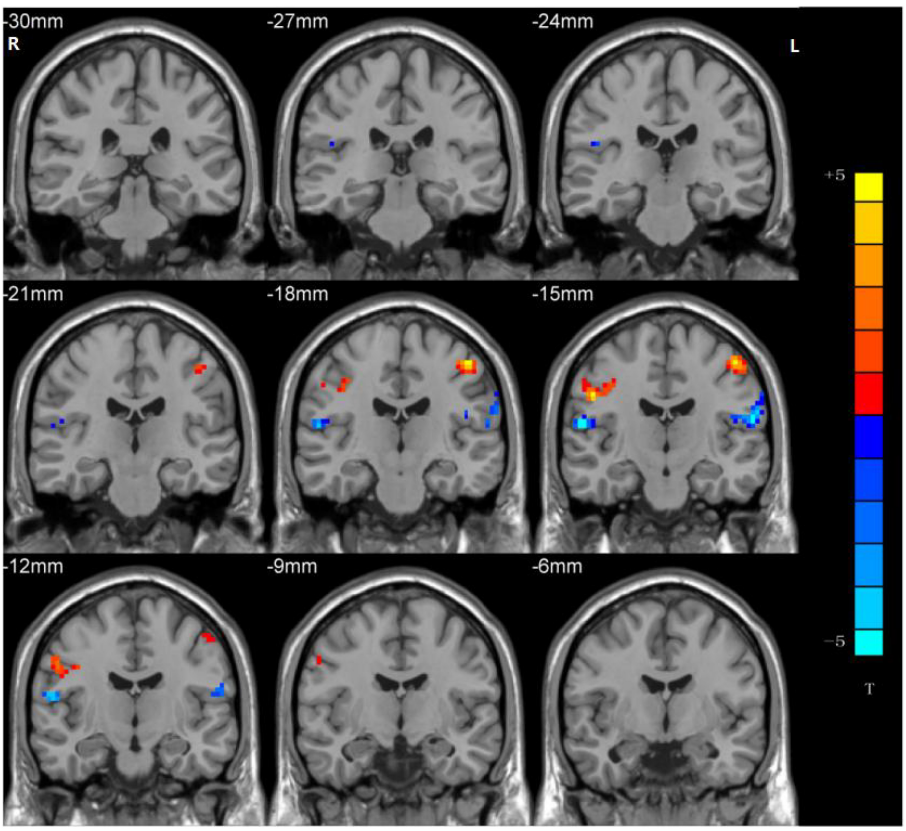

FIGURE 2 | Statistical maps showing NH differences in the bilateral postcentral gyrus, the bilateral Rolandic operculum and the right STG between the rTLE group and control group. (Blue indicates lower NH and the color bar indicates the *t*-values from the two-sample *t*-test).

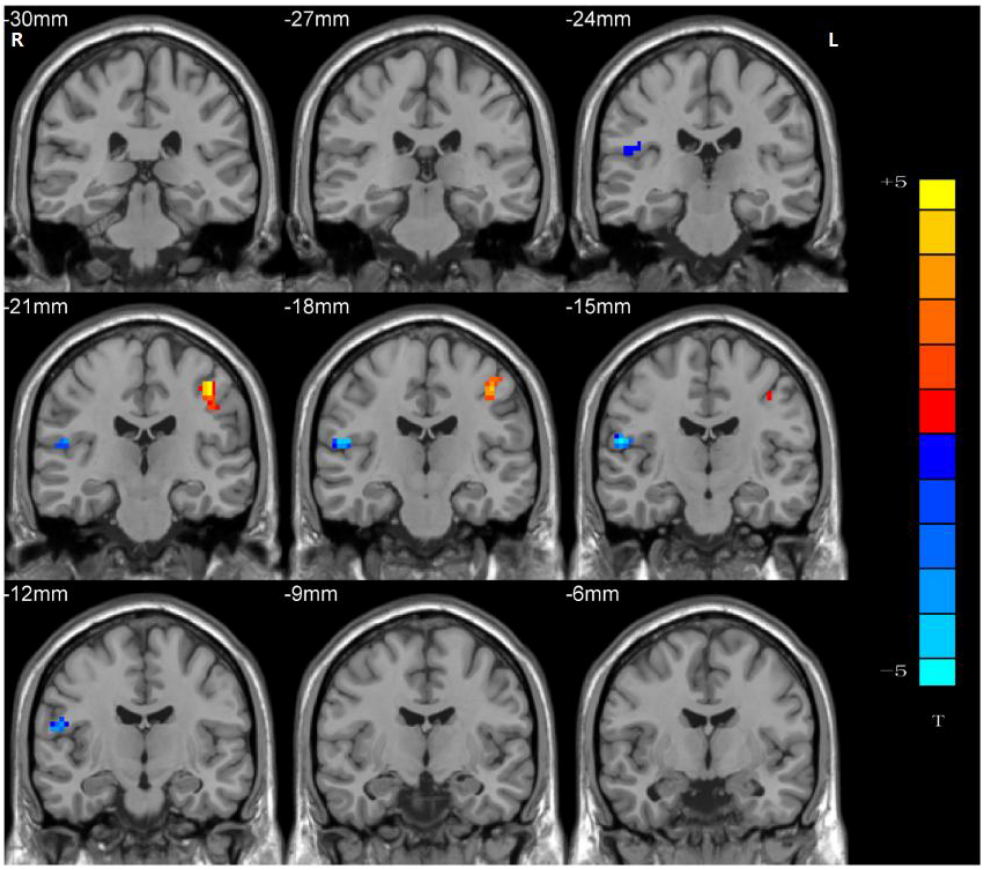

FIGURE 3 | Statistical maps showing NH differences in the left postcentral gyrus and the right Rolandic operculum between the lTLE group and the control group. (Blue indicates lower NH and the color bar indicates the *t*-values from the two-sample *t*-test).

Ventral Somatomotor Network Maps Determined by Group Independent Component Analysis

By employing ICA, the VSN masks were chosen from the control group. The parts involved in the VSN were the bilateral postcentral and Rolandic operculum (**Figure 1**). The VSN was used as a mask in the following NH analysis.

Group Differences in Ventral Somatomotor Network Regarding Network Homogeneity

Significant group differences in NH values between the patients (rTLE/lTLE) and the controls within the VSN mask were observed *via* two-sample *t*-tests. Compared to the controls, rTLE patients had significantly higher NH in the bilateral postcentral gyrus, and significantly lower NH in the bilateral Rolandic operculum and right superior temporal gyrus (STG) (**Figure 2**). The NH values of the left postcentral gyrus were significantly higher in lTLE patients than in the healthy controls, and lTLE patients had lower NH in the right Rolandic operculum (**Figure 3**). The NH values of the right Rolandic operculum and left postcentral gyrus were significantly higher in rTLE patients than in the lTLE patients (**Figure 4**).

Correlation of Network Homogeneity With Clinical Variables

The correlations between abnormal NH and clinical variables in the patients were examined. The increased NH of the left postcentral gyrus was negatively correlated with the illness duration in the lTLE group ($r = -0.393$, $p = 0.004$) (**Figure 5A**). The increased NH of the right postcentral gyrus was negatively correlated with the illness duration in the rTLE group ($r = -0.345$, $p = 0.001$) (**Figure 5C**). And the decreased NH in the left Rolandic operculum was negatively correlated with the ECRT in the rTLE group ($r = -0.326$, $p = 0.003$) (**Figure 5B**). No other correlations were observed in the participants.

DISCUSSION

Temporal lobe epilepsy is the most common drug-resistant form of epilepsy in adults (23) and is the most common indication for surgical intervention. However, surgical treatment is invasive and has several undesirable and serious side effects, and not

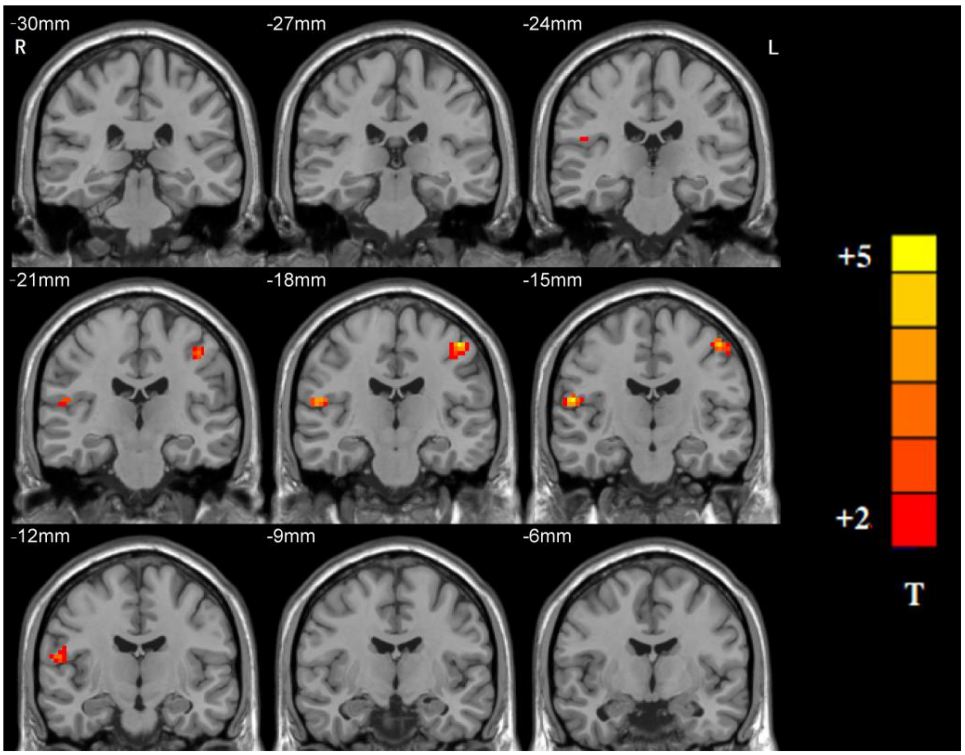

FIGURE 4 | Statistical maps showing NH differences in the right Rolandic operculum and the left postcentral gyrus between the rTLE group and the lTLE group. (Blue indicates lower NH and the color bar indicates the *t*-values from the two-sample *t*-test).

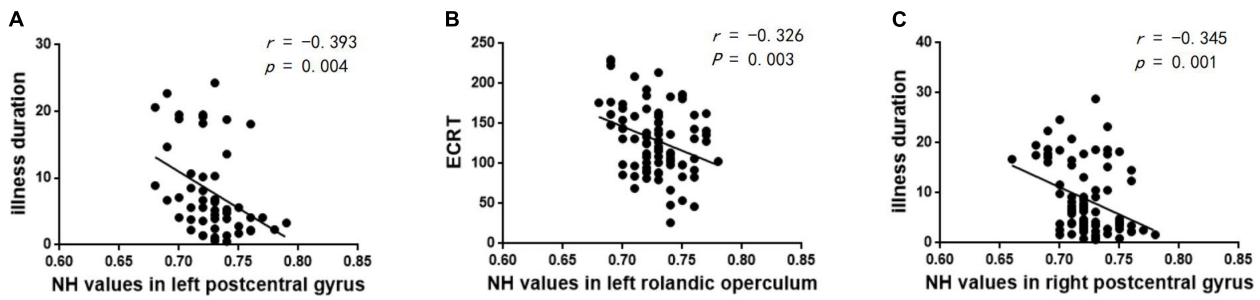

FIGURE 5 | Correlations between abnormal NH and clinical variables. **(A)** Negative correlation between the NH values in the left postcentral gyrus and illness duration in the lTLE group. **(B)** Negative correlation between the NH values in the left Rolandic operculum and ECRT in the rTLE group. **(C)** Negative correlation between the NH values in the right postcentral gyrus and illness duration in the rTLE group.

every patient is a candidate for surgical intervention. Given the limited treatment options available for those with drug-resistant TLE, it is crucial to understand the pathophysiologic mechanism of TLE. Because TLE patients usually have motor and sensory impairment (24), we aimed to investigate the abnormal ventral somatomotor network in patients with rTLE/lTLE. In this study, we used an NH method to investigate the VSN region, which is associated with motor and somatosensory function, in patients with TLE (rTLE/lTLE). Compared to healthy controls, rTLE patients had significantly higher NH in the bilateral postcentral gyrus and significantly lower NH in the bilateral Rolandic operculum. Compared to healthy controls, lTLE patients had significantly higher NH in the left postcentral gyrus and lower NH in the right Rolandic operculum. These patients had a longer ECRT. In addition, the altered NH in the postcentral gyrus was negatively correlated with the illness duration, and the decreased NH in the left Rolandic operculum was negatively correlated with the ECRT. We speculated that abnormal NH in the postcentral gyrus and Rolandic operculum play a critical role in the pathophysiology of TLE.

The postcentral gyrus, which is located on the lateral surface of the parietal lobe between the central sulcus and postcentral sulcus and caudal to the central sulcus, corresponds to Brodmann areas 3b, 1, and 2 (25), which contain the primary somatosensory

network and are thereby crucial for proprioception and motor control (26). Furthermore, the postcentral gyrus also includes the secondary somatosensory network, which is involved in integrating memories with somatosensory stimuli (27). Because of its unique characteristics, the postcentral gyrus is often affected in psychiatric illness. Li et al. (28) and Kilts et al. (29) found that increased activity of the postcentral gyrus is associated with decreased social anxiety symptoms. Zhuo et al. (30) reported decreased density in the resting-state global functional connectivity of the postcentral gyrus in patients with major depressive disorder. Larabi et al. (31) observed lowered activation of the postcentral gyrus during suppression, which resulted in poorer self-reflectiveness in schizophrenia patients. Jalbrzikowski et al. (32) confirmed that increased postcentral surface area is associated with less severe negative symptoms and better executive cognition in bipolar disorder. With a whole-brain voxel-based unbiased resting-state functional connectivity method, Cheng et al. (33) demonstrated reduced connectivity in the bilateral postcentral gyrus of patients with autism. Song et al. (34) demonstrated that destructive lesions in the postcentral gyrus, as well as changes in its outflow pathways to neighboring motor areas, could lead to epileptic negative myoclonus. These findings could be attributed to the location, structure and function of the postcentral gyrus. As reported by DiGuiseppi et al. (35), axons from the ventral posterolateral nucleus travel from the thalamus through the posterior limb of the internal capsule and terminate in the appropriate region of the postcentral gyrus. The postcentral gyrus has numerous connections with other brain areas, including the insula (36), amygdala (37), limbic system (38), cerebellum (39), and parietal lobe (40). Because of these numerous connections, the postcentral gyrus is able to perform a variety of functions, including those involved in somatic perceptual processes. The postcentral gyrus can also integrate sensory-motor connections associated with poor attentional set shifting and participate in suppression and cognitive insight because emotion-specific representations convey emotions and emotion processing. Our results showed significantly higher NH in the bilateral postcentral gyrus in patients with rTLE and higher NH in the left postcentral gyrus in patients with lTLE, which is consistent with previous studies (41–43). Furthermore, the altered NH values of the left postcentral gyrus were negatively correlated with the duration of the illness in the lTLE group. And similar finding was observed in the rTLE group that altered NH values of the right postcentral gyrus were negatively correlated with the illness duration. We speculate that as rTLE/lTLE progressed, the correlation of the postcentral region with all other regions in the VSN decreased, resulting in functional loss in the postcentral region. We hypothesize that altered NH values in the postcentral gyrus may be responsible for cognitive dysfunctions in TLE patients, including executive cognition (32), attention alertness (44), emotion processing (29), and primary information processing.

The Rolandic operculum is defined as the confluence of the most caudal parts of the pre- and postcentral gyri, is contiguous to the oropharyngeal muscle control area of M1S1 and adjacent to the insula, and corresponds to Brodmann areas 6, 4, and 43 (45, 46). The most well-known function of the Rolandic operculum is its contribution to articulation and tongue movement during speech production, as it includes the ventral portion of the somatotopic tongue and lip representations (47). Furthermore, many other functions of the Rolandic operculum have been discovered in recent years. Fink et al. (48) found that an activated Rolandic operculum supports multimodal input processing from various motor, sensory, and perceptual sources. Ventre-Dominey (49) reported that the Rolandic operculum overlaps with a cortical network that is thought to be associated with self-referential processes that involve self-location in space. Blefari et al. (50) confirmed that the Rolandic operculum is crucial for interoceptive awareness and bodily self-consciousness by processing integrated exteroceptive-interoceptive signals. The findings of Wu et al. (51) suggest that functional impairments of the left Rolandic operculum in patients with schizophrenia are related to delusional thoughts, and patients with schizophrenia have been found to have increased mean connectivity in the left Rolandic operculum (52). Shan et al. (53) discovered that an activated Rolandic operculum is associated with cognitive disabilities in Alzheimer's disease and mild cognitive impairment. Wang et al. (54) reported that the Rolandic operculum is associated with the neural mechanisms of tic generation. Decades ago, it was discovered that critical electrical discharges in temporal lobe epilepsy always affect extratemporal structures, such as the Rolandic operculum (55). In the present study, lower NH was found in the bilateral Rolandic operculum of patients with rTLE and in the right Rolandic operculum of patients with lTLE. Furthermore, we found that decreased NH in the left Rolandic operculum was negatively correlated with the ECRT between the control group and rTLE group. A longer ECRT indicates inferior executive control performance, and thus, we speculated that abnormal NH in the left Rolandic operculum played a critical role in the executive function of patients with rTLE.

In the present study, we observed that rTLE and lTLE patients had altered NH values in the postcentral gyrus and Rolandic operculum. Because the postcentral gyrus and Rolandic operculum in play critical roles in cognitive function, we speculate that network homogeneity abnormalities caused by temporal lobe epilepsy may account for cognitive dysfunctions in TLE patients. Additionally, this may be the cause of abnormal electrical discharge in patients with TLE. However, our results are consistent with those of some previous studies (56, 57). Li et al. (56) found that increased functional connectivity of the Rolandic operculum was lateralized in patients with rTLE, and Zhou et al. (57) reported that decreased functional connectivity of the postcentral gyrus was lateralized in patients with rTLE. However, we found that the altered NH of the Rolandic operculum and postcentral gyrus were bilateral in patients with rTLE. We speculate that the following factors may account for this phenomenon. (1) There might be a compensatory mechanism that occurs in patients with lTLE/rTLE at rest. As part of the VSN, the postcentral gyrus and the Rolandic operculum share many similarities and overlaps in function; for example, they are both closely related to depression, schizophrenia, epilepsy, and emotion and sensation processing. Bettus et al. (58) reported decreased basal functional connectivity within epileptogenic

networks with concurrent contralaterally increased connectivity, which confirmed our suspicions. Campo et al. (59) discovered decreased effective connectivity in the medial temporal lobe of the lesional hemisphere and increased effective connectivity in the medial temporal lobe/inferior frontal cortex of the contralesional hemisphere. Similar to these findings regarding functional connectivity in patients with epilepsy, our results demonstrated increased NH values in the ipsilesional postcentral gyrus and decreased NH values in the contralesional Rolandic operculum. (2) Because TLE is a chronic disorder, epileptic discharges propagating into the contralateral gyrus and recurrent epileptic activities might be responsible for the contralateral structural and functional decline as TLE progressed. Jokeit et al. (60) confirmed the TLE patients had altered glucose metabolism in the contralateral hippocampus, which was related to seizure frequency. Additionally, the duration of TLE may have a greater impact on the contralateral measure of hippocampal metabolism than the ipsilateral measure. Following a multiple regression analysis, there was a subsequent decrease in the hippocampal volume contralateral to the primary temporal seizure focus (61, 62). We believe that similar processing occurs in the postcentral gyrus and Rolandic operculum, which is strongly supported by the results of our study.

The STG plays a key role in language function (63), and study showed that the activity of STG was strongly associated with the listeners' subjective experience (64). A fMRI study enrolled 43 TLE patients with language-impaired and 42 TLE patients with non-language-impaired confirmed that activations within the STG was the most predictive of language impairment (65). A Chinese tasks based fMRI study showed that the main effect region of auditory naming and picture naming tasks was in right STG, and the main effect region of semantic fluency task was in left STG (66). Meanwhile, to protect the language function in the postoperative patients, the task-state fMRI and intraoperative electroencephalography were suggested to be used to develop a personalized surgical plan for epilepsy treatment (66). Moreover, the dysfunction in the STG was related to the cognitive dysfunction in epilepsy patients. A rs-fMRI study found that decreased functional connectivity of the left precentral gyrus with the bilateral STG has a significant effect on intelligence in children and adolescents with focal epilepsy (67). The right STG was found blunted neural response to emotional faces in pediatric epilepsy, which was regarded as a marker of risk for social cognitive deficits (68). In our study, lower NH in the right STG was found in the rTLE, and no significant correlation was found between the NH and clinical variables including the ECRT. Based on these prior studies, we speculate that the decreased NH was associated with the language function in TLE, though relevant language task hadn't perform in our study.

There were several limitations in the study: (1) Physiological noise cannot be completely removed. (2) We focused only on abnormalities of the VSN in patients with TLE, and although illuminating the pathophysiological contribution of the VSN is critical, other significant brain networks might have been neglected. (3) Antiepileptic drugs may also have effects on functional networks in epilepsy, and we did not account for this confounding factor.

CONCLUSION

In conclusion, we used the NH method to analyze resting-state fMRI data in patients with TLE, and abnormal NH values in the VSN were confirmed. The importance of NH alterations in the VSN implies the importance of the postcentral gyrus, STG and Rolandic operculum in the progression of TLE and provides new insights into the pathophysiological mechanism of TLE.

DATA AVAILABILITY STATEMENT

The raw data supporting the conclusions of this article will be made available by the authors, without undue reservation.

ETHICS STATEMENT

The studies involving human participants were reviewed and approved by the Medical Ethics Committee of the Tianyou Hospital Affiliated to Wuhan University of Science and Technology. The patients/participants provided their written informed consent to participate in this study. Written informed consent was obtained from the individual(s) for the publication of any potentially identifiable images or data included in this article.

AUTHOR CONTRIBUTIONS

DL and LM: writing the article. PX, HR, and RL: collection and assembly of data. LZ and YG: research concept and design, data analysis, and interpretation. All authors contributed to the article and approved the submitted version.

FUNDING

The investigation was supported by the grant from the Health Commission of Hubei Province Scientific Research Project (Grant No. 2020CFB512) and the Epilepsy Research Fund of China Association Against Epilepsy (CW-2022-003).

REFERENCES

1. Thijs RD, Surges R, O'Brien TJ, Sander JW. Epilepsy in adults. *Lancet.* (2019) 393:689–701. doi: 10.1016/S0140-6736(18)32596-0
2. Sheilabi MA, Takeshita LY, Sims EJ, Falciani F, Princivalle AP. The sodium channel B4-subunits are dysregulated in temporal lobe epilepsy drug-resistant patients. *Int J Mol Sci.* (2020) 21:2955. doi: 10.3390/ijms2108 2955
3. Chen YY, Huang S, Wu WY, Liu CR, Yang XY, Zhao HT, et al. Associated and predictive factors of quality of life in patients with temporal lobe epilepsy. *Epilepsy Behav.* (2018) 86:85–90. doi: 10.1016/j.yebeh.2018.0 6.025

4. McIntosh AM, Wilson SJ, Berkovic SF. Seizure outcome after temporal lobectomy: current research practice and findings. *Epilepsia.* (2001) 42:1288–307. doi: 10.1046/j.1528-1157.2001.02001.x
5. Bernhardt BC, Bonilha L, Gross DW. Network analysis for a network disorder: the emerging role of graph theory in the study of epilepsy. *Epilepsy Behav.* (2015) 50:162–70. doi: 10.1016/j.yebeh.2015.06.005
6. Yeo BT, Krienen FM, Sepulcre J, Sabuncu MR, Lashkari D, Hollinshead M, et al. The organization of the human cerebral cortex estimated by intrinsic functional connectivity. *J Neurophysiol.* (2011) 106:1125–65. doi: 10.1152/jn.00338.2011
7. Biswal B, Yetkin FZ, Haughton VM, Hyde JS. Functional connectivity in the motor cortex of resting human brain using echo-planar MRI. *Magn Reson Med.* (1995) 34:537–41. doi: 10.1002/mrm.1910340409
8. Korgaonkar MS, Goldstein-Piekarski AN, Fornito A, Williams LM. Intrinsic connectomes are a predictive biomarker of remission in major depressive disorder. *Mol Psychiatry.* (2020) 25:1537–49. doi: 10.1038/s41380-019-0574-2
9. Lee M, Sehatpour P, Hoptman MJ, Lakatos P, Dias EC, Kantrowitz JT, et al. Neural mechanisms of mismatch negativity dysfunction in schizophrenia. *Mol Psychiatry.* (2017) 22:1585–93. doi: 10.1038/mp.2017.3
10. Stoodley CJ. Distinct regions of the cerebellum show gray matter decreases in autism. ADHD, and developmental dyslexia. *Front Syst Neurosci.* (2014) 8:92. doi: 10.3389/fnsys.2014.00092
11. Gao Y, Zheng J, Li Y, Guo D, Wang M, Cui X, et al. Decreased functional connectivity and structural deficit in alertness network with right-sided temporal lobe epilepsy. *Medicine (Baltimore).* (2018) 97:e0134. doi: 10.1097/MD.0000000000010134
12. Mankinen K, Jalovaara P, Paakki JJ, Harila M, Rytky S, Tervonen O, et al. Connectivity disruptions in resting-state functional brain networks in children with temporal lobe epilepsy. *Epilepsy Res.* (2012) 100:168–78. doi: 10.1016/j.eplepsyres.2012.02.010
13. Fox MD, Raichle ME. Spontaneous fluctuations in brain activity observed with functional magnetic resonance imaging. *Nat Rev Neurosci.* (2007) 8:700–11. doi: 10.1038/nrn2201
14. Uddin LQ, Kelly AM, Biswal BB, Margulies DS, Shehzad Z, Shaw D, et al. Network homogeneity reveals decreased integrity of default-mode network in ADHD. *J Neurosci Methods.* (2008) 169:249–54. doi: 10.1016/j.jneumeth.2007.11.031
15. Gao Y, Wang M, Yu R, Li Y, Yang Y, Cui X, et al. Abnormal default mode network homogeneity in treatment-naive patients with first-episode depression. *Front Psychiatry.* (2018) 9:697. doi: 10.3389/fpsyt.2018.00697
16. Manford M, Fish DR, Shorvon SD. An analysis of clinical seizure patterns and their localizing value in frontal and temporal lobe epilepsies. *Brain.* (1996) 119:17–40. doi: 10.1093/brain/119.1.17
17. Fan J, McCandliss BD, Sommer T, Raz A, Posner MI. Testing the efficiency and independence of attentional networks. *J Cogn Neurosci.* (2002) 14:340–7. doi: 10.1162/089892902317361886
18. Yan CG, Zang YF. DPARSF: a MATLAB toolbox for "Pipeline" data analysis of resting-state fMRI. *Front Syst Neurosci.* (2010) 4:13. doi: 10.3389/fnsys.2010.00013
19. Nichols TE, Das S, Eickhoff SB, Evans AC, Glatard T, Hanke M, et al. Best practices in data analysis and sharing in neuroimaging using MRI. *Nat Neurosci.* (2017) 20:299–303. doi: 10.1038/nn.4500
20. Winkler AM, Ridgway GR, Douaud G, Nichols TE, Smith SM. Faster permutation inference in brain imaging. *Neuroimage.* (2016) 141:502–16. doi: 10.1016/j.neuroimage.2016.05.068
21. Saad ZS, Gotts SJ, Murphy K, Chen G, Jo HJ, Martin A, et al. Trouble at rest: how correlation patterns and group differences become distorted after global signal regression. *Brain Connect.* (2012) 2:25–32. doi: 10.1089/brain.2012.0080
22. Hahamy A, Calhoun V, Pearlson G, Harel M, Stern N, Attar F, et al. Save the global: global signal connectivity as a tool for studying clinical populations with functional magnetic resonance imaging. *Brain Connect.* (2014) 4:395–403. doi: 10.1089/brain.2014.0244
23. Blümcke I, Thom M, Aronica E, Armstrong DD, Bartolomei F, Bernasconi A, et al. International consensus classification of hippocampal sclerosis in temporal lobe epilepsy: a task force report from the ILAE commission on diagnostic methods. *Epilepsia.* (2013) 54:1315–29. doi: 10.1111/epi.12220
24. McLachlan RS. A brief review of the anatomy and physiology of the limbic system. *Can J Neurol Sci.* (2009) 36:S84–7.
25. Akselrod M, Martuzzi R, Serino A, van der Zwaag W, Gassert R, Blanke O. Anatomical and functional properties of the foot and leg representation in areas 3b, 1 and 2 of primary somatosensory cortex in humans: a 7T fMRI study. *Neuroimage.* (2017) 159:473–87. doi: 10.1016/j.neuroimage.2017.06.021
26. Borich MR, Brodie SM, Gray WA, Ionta S, Boyd LA. Understanding the role of the primary somatosensory cortex: opportunities for rehabilitation. *Neuropsychologia.* (2015) 79:246–55. doi: 10.1016/j.neuropsychologia.2015.07.007
27. Chen TL, Babiloni C, Ferretti A, Perrucci MG, Romani GL, Rossini PM, et al. Human secondary somatosensory cortex is involved in the processing of somatosensory rare stimuli: an fMRI study. *Neuroimage.* (2008) 40:1765–71. doi: 10.1016/j.neuroimage.2008.01.020
28. Li Y, Meng Y, Yuan M, Zhang Y, Ren Z, Zhang Y, et al. Therapy for adult social anxiety disorder: a meta-analysis of functional neuroimaging studies. *J Clin Psychiatry.* (2016) 77:e1429–38. doi: 10.4088/JCP.15r10226
29. Kilts CD, Kelsey JE, Knight B, Ely TD, Bowman FD, Gross RE, et al. The neural correlates of social anxiety disorder and response to pharmacotherapy. *Neuropsychopharmacology.* (2006) 31:2243–53. doi: 10.1038/sj.npp.1301053
30. Zhuo C, Zhu J, Wang C, Qu H, Ma X, Qin W. Different spatial patterns of brain atrophy and global functional connectivity impairments in major depressive disorder. *Brain Imaging Behav.* (2017) 11:1678–89. doi: 10.1007/s11682-016-9645-z
31. Larabi DI, van der Meer L, Pijnenborg GHM, Ćurčić-Blake B, Aleman A. Insight and emotion regulation in schizophrenia: a brain activation and functional connectivity study. *Neuroimage Clin.* (2018) 20:762–71. doi: 10.1016/j.nicl.2018.09.009
32. Jalbrzikowski M, Freedman D, Hegarty CE, Mennigen E, Karlsgodt KH, Olde Loohuis LM, et al. Structural brain alterations in youth with psychosis and bipolar spectrum symptoms. *J Am Acad Child Adolesc Psychiatry.* (2019) 58:1079–91. doi: 10.1016/j.jaac.2018.11.012
33. Cheng W, Rolls ET, Gu H, Zhang J, Feng J. Autism: reduced connectivity between cortical areas involved in face expression, theory of mind, and the sense of self. *Brain.* (2015) 138:1382–93. doi: 10.1093/brain/awv051
34. Song IU, Lee DG, Kim JS, An JY, Lee SB, Kim YI, et al. Unilateral epileptic negative myoclonus following focal lesion of the postcentral cerebral cortex due to acute middle cerebral infarction. *J Clin Neurol.* (2006) 2:272–5. doi: 10.3988/jcn.2006.2.4.272
35. DiGuiseppi J, Tadi P. Neuroanatomy, postcentral gyrus. *StatPearls*. (Treasure Island, FL: StatPearls Publishing) (2021).
36. Addicott MA, Luber B, Nguyen D, Palmer H, Lisanby SH, Appelbaum LG. Low– and high-frequency repetitive transcranial magnetic stimulation effects on resting-state functional connectivity between the postcentral gyrus and the insula. *Brain Connect.* (2019) 9:322–8. doi: 10.1089/brain.2018.0652
37. Höistad M, Barbas H. Sequence of information processing for emotions through pathways linking temporal and insular cortices with the amygdala. *Neuroimage.* (2008) 40:1016–33. doi: 10.1016/j.neuroimage.2007.12.043
38. Purves D, Augustine GJ, Fitzpatrick D, Hall WC, LaMantia AS, White LE. *Neuroscience*. 5th ed. Sunderland: Sinauer Associates (2012).
39. Ramos TC, Balardin JB, Sato JR, Fujita A. Abnormal cortico-cerebellar functional connectivity in autism spectrum disorder. *Front Syst Neurosci.* (2019) 12:74. doi: 10.3389/fnsys.2018.00074
40. Zhang L, Qiu F, Zhu H, Xiang M, Zhou L. Neural efficiency and acquired motor skills: an fmri study of expert athletes. *Front Psychol.* (2019) 10:2752. doi: 10.3389/fpsyg.2019.02752
41. Jiang Y, Song L, Li X, Zhang Y, Chen Y, Jiang S, et al. Dysfunctional white-matter networks in medicated and unmedicated benign epilepsy with centrotemporal spikes. *Hum Brain Mapp.* (2019) 40:3113–24. doi: 10.1002/hbm.24584
42. Guo L, Bai G, Zhang H, Lu D, Zheng J, Xu G. Cognitive functioning in temporal lobe epilepsy: a BOLD-fMRI study. *Mol Neurobiol.* (2017) 54:8361–9. doi: 10.1007/s12035-016-0298-0
43. Zhu H, Zhu J, Bao FS, Liu H, Zhu X, Wu T, et al. Statistical parametric mapping for analyzing interictal magnetoencephalography in patients with left frontal lobe epilepsy. *Seizure.* (2016) 34:38–43. doi: 10.1016/j.seizure.2015.11.003
44. Liu J, Zhou X, Zhang Z, Qin L, Ye W, Zheng J. Disrupted functional network in patients with temporal lobe epilepsy with impaired alertness. *Epilepsy Behav.* (2019) 101:106573. doi: 10.1016/j.yebeh.2019.106573

45. Tzourio-Mazoyer N, Landeau B, Papathanassiou D, Crivello F, Etard O, Delcroix N, et al. Automated anatomical labeling of activations in SPM using a macroscopic anatomical parcellation of the MNI MRI single-subject brain. *Neuroimage.* (2002) 15:273–89. doi: 10.1006/nimg.2001.0978
46. Brown S, Ngan E, Liotti M. A larynx area in the human motor cortex. *Cereb Cortex.* (2008) 18:837–45. doi: 10.1093/cercor/bhm131
47. Brown S, Laird AR, Pfordresher PQ, Thelen SM, Turkeltaub P, Liotti M. The somatotopy of speech: phonation and articulation in the human motor cortex. *Brain Cogn.* (2009) 70:31–41. doi: 10.1016/j.bandc.2008.12.006
48. Fink A, Bay JU, Koschutnig K, Prettenthaler K, Rominger C, Benedek M, et al. Brain and soccer: functional patterns of brain activity during the generation of creative moves in real soccer decision-making situations. *Hum Brain Mapp.* (2019) 40:755–64. doi: 10.1002/hbm.24408
49. Ventre-Dominey J. Vestibular function in the temporal and parietal cortex: distinct velocity and inertial processing pathways. *Front Integr Neurosci.* (2014) 8:53. doi: 10.3389/fnint.2014.00053
50. Blefari ML, Martuzzi R, Salomon R, Bello-Ruiz J, Herbelin B, Serino A, et al. Bilateral rolandic operculum processing underlying heartbeat awareness reflects changes in bodily self-consciousness. *Eur J Neurosci.* (2017) 45:1300–12. doi: 10.1111/ejn.13567
51. Wu C, Zheng Y, Li J, She S, Peng H, Li L. Cortical gray matter loss, augmented vulnerability to speech-on-speech masking, and delusion in people with schizophrenia. *Front Psychiatry.* (2018) 9:287. doi: 10.3389/fpsyt.2018.00287
52. Andreou C, Nolte G, Leicht G, Polomac N, Hanganu-Opatz IL, Lambert M, et al. Increased resting-state gamma-band connectivity in first-episode schizophrenia. *Schizophr Bull.* (2015) 41:930–9. doi: 10.1093/schbul/sbu121
53. Shan Y, Wang JJ, Wang ZQ, Zhao ZL, Zhang M, Xu JY, et al. Neuronal specificity of acupuncture in Alzheimer's disease and mild cognitive impairment patients: a functional MRI study. *Evid Based Complement Alternat Med.* (2018) 2018:7619197. doi: 10.1155/2018/7619197
54. Wang Z, Maia TV, Marsh R, Colibazzi T, Gerber A, Peterson BS. The neural circuits that generate tics in Tourette's syndrome. *Am J Psychiatry.* (2011) 168:1326–37. doi: 10.1176/appi.ajp.2011.09111692
55. Bossi L, Munari C, Stoffels C, Bonis A, Bacia T, Talairach J, et al. Manifestations motrices et posturales dans les crises d'épilepsie d'origine temporale [Motor and postural manifestations of temporal lobe epilepsy seizure]. *Rev Electroencephalogr Neurophysiol Clin.* (1982) 12:101–6. doi: 10.1016/s0370-4475(82)80032-4
56. Li J, Chen X, Ye W, Jiang W, Liu H, Zheng J. Alteration of the alertness-related network in patients with right temporal lobe epilepsy: a resting state fMRI study. *Epilepsy Res.* (2016) 127:252–9. doi: 10.1016/j.eplepsyres.2016.09.013
57. Zhou X, Zhang Z, Liu J, Qin L, Pang X, Zheng J. Disruption and lateralization of cerebellar-cerebral functional networks in right temporal lobe epilepsy: a resting-state fMRI study. *Epilepsy Behav.* (2019) 96:80–6. doi: 10.1016/j.yebeh.2019.03.020
58. Bettus G, Guedj E, Joyeux F, Confort-Gouny S, Soulier E, Laguitton V, et al. Decreased basal fMRI functional connectivity in epileptogenic networks and contralateral compensatory mechanisms. *Hum Brain Mapp.* (2009) 30:1580–91. doi: 10.1002/hbm.20625
59. Campo P, Garrido MI, Moran RJ, García-Morales I, Poch C, Toledano R, et al. Network reconfiguration and working memory impairment in mesial temporal lobe epilepsy. *Neuroimage.* (2013) 72:48–54. doi: 10.1016/j.neuroimage.2013.01.036
60. Jokeit H, Ebner A, Arnold S, Schüller M, Antke C, Huang Y, et al. Bilateral reductions of hippocampal volume, glucose metabolism, and wada hemispheric memory performance are related to the duration of mesial temporal lobe epilepsy. *J Neurol.* (1999) 246:926–33. doi: 10.1007/s004150050484
61. Barr WB, Ashtari M, Schaul N. Bilateral reductions in hippocampal volume in adults with epilepsy and a history of febrile seizures. *J Neurol Neurosurg Psychiatry.* (1997) 63:461–7. doi: 10.1136/jnnp.63.4.461
62. Salmenperä T, Kälviäinen R, Partanen K, Pitkänen A. Hippocampal damage caused by seizures in temporal lobe epilepsy. *Lancet.* (1998) 351:35. doi: 10.1016/S0140-6736(05)78092-2
63. Bigler ED, Mortensen S, Neeley ES, Ozonoff S, Krasny L, Johnson M, et al. Superior temporal gyrus, language function, and autism. *Dev Neuropsychol.* (2007) 31:217–38. doi: 10.1080/87565640701190841
64. Yi HG, Leonard MK, Chang EF. The encoding of speech sounds in the superior temporal gyrus. *Neuron.* (2019) 102:1096–110. doi: 10.1016/j.neuron.2019.04.023
65. Kaestner E, Reyes A, Macari AC, Chang YH, Paul BM, Hermann BP, et al. Identifying the neural basis of a language-impaired phenotype of temporal lobe epilepsy. *Epilepsia.* (2019) 60:1627–38. doi: 10.1111/epi.16283
66. Wang P, Du F, Li J, Yu H, Tang C, Jiang R. Functional magnetic resonance imaging based on Chinese tasks to protect language function in epileptics. *Brain Behav.* (2021) 11:e01979. doi: 10.1002/brb3.1979
67. Songjiang L, Tijiang Z, Heng L, Wenjing Z, Bo T, Ganjun S, et al. Impact of brain functional network properties on intelligence in children and adolescents with focal epilepsy: a resting-state MRI study. *Acad Radiol.* (2021) 28:225–32. doi: 10.1016/j.acra.2020.01.004
68. Morningstar M, Hung A, Grannis C, French RC, Mattson WI, Ostendorf AP, et al. Blunted neural response to emotional faces in the fusiform and superior temporal gyrus may be marker of emotion recognition deficits in pediatric epilepsy. *Epilepsy Behav.* (2020) 112:107432. doi: 10.1016/j.yebeh.2020.107432

Conflict of Interest: The authors declare that the research was conducted in the absence of any commercial or financial relationships that could be construed as a potential conflict of interest.

frontiers | Frontiers in Psychiatry

ORIGINAL RESEARCH
published: 22 June 2022
doi: 10.3389/fpsyt.2022.925412

Altered Regional Homogeneity in Patients With Congenital Blindness: A Resting-State Functional Magnetic Resonance Imaging Study

*Jiong-Jiong Hu[1], Nan Jiang[2], Jun Chen[3], Ping Ying[4], Ming Kang[4], San-Hua Xu[4], Jie Zou[4], Hong Wei[4], Qian Ling[4] and Yi Shao[4]**

[1] Department of Ophthalmology, Zhongshan Hospital Fudan University, Shanghai, China, [2] Molecular Neuropharmacology Laboratory, School of Optometry and Ophthalmology and Eye Hospital, Wenzhou Medical University, Wenzhou, China, [3] Jiangxi University of Traditional Chinese Medicine, Nanchang, China, [4] Department of Ophthalmology, The First Affiliated Hospital of Nanchang University, Nanchang, China

OPEN ACCESS

Edited by:
Yujun Gao,
Wuhan University of Science and Technology, China

Reviewed by:
Wensi Tao,
University of Miami Health System, United States
Guanghui Liu,
Fujian Provincial People's Hospital, China

***Correspondence:**
Yi Shao
freebee99@163.com

Specialty section:
This article was submitted to Neuroimaging and Stimulation, a section of the journal Frontiers in Psychiatry

Received: 21 April 2022
Accepted: 09 May 2022
Published: 22 June 2022

Citation:
Hu J-J, Jiang N, Chen J, Ying P, Kang M, Xu S-H, Zou J, Wei H, Ling Q and Shao Y (2022) Altered Regional Homogeneity in Patients With Congenital Blindness: A Resting-State Functional Magnetic Resonance Imaging Study. Front. Psychiatry 13:925412. doi: 10.3389/fpsyt.2022.925412

In patients with congenital blindness (CB), the lack of any visual experience may affect brain development resulting in functional, structural, or even psychological changes. Few studies to date have addressed or focused on the synchronicity of regional brain activity in patients with CB. Our study aimed to investigate regional brain activity in patients with CB in a resting state and try to explain the possible causes and effects of any anomalies. Twenty-three CB patients and 23 healthy control (HC) volunteers agreed to undergo resting state functional magnetic resonance imaging (fMRI) scans. After the fMRI data were preprocessed, regional homogeneity (ReHo) analysis was conducted to assess the differences in brain activity synchronicity between the two groups. Receiver operating characteristic (ROC) curve analysis was used to explore whether the brain areas with statistically significant ReHo differences have diagnostic and identification values for CB. All CB patients were also required to complete the Hospital Anxiety and Depression Scale (HADS) to evaluate their anxiety and depression levels. The results showed that in CB patients mean ReHo values were significantly lower than in HCs in the right orbital part of the middle frontal gyrus (MFGorb), bilateral middle occipital gyrus (MOG), and the right dorsolateral superior frontal gyrus (SFGdl), but significantly higher in the left paracentral lobule (PCL), right insula and bilateral thalamus. The ReHo value of MFGorb showed a negative linear correlation with both the anxiety score and the depression score of the HADS. ROC curve analysis revealed that the mean ReHo values which differed significantly between the groups have excellent diagnostic accuracy for CB (especially in the left PCL and right SFGdl regions). Patients with CB show abnormalities of ReHo values in several specific brain regions, suggesting potential regional structural changes, functional reorganization, or even psychological effects in these patients. FMRI ReHo analysis may find use as an objective method to confirm CB for medical or legal purposes.

Keywords: congenital blindness, regional homogeneity, resting-state fMRI, anxiety, depression

INTRODUCTION

Congenital blindness (CB) refers to a group of diseases or conditions occurring in the neonatal period or infancy that result in permanent blindness later in life if left untreated (1). In China, the incidence of blindness in children under the age of 5 is <0.10% or about 70000 children in this age range (2). The three most common causes of blindness in Chinese children are cataract, retinal dystrophy, and optic nerve hypoplasia (3). The development of vision is a complicated neural process. Visual stimulation begins at photoreceptors and then travels to the brain's visual centers *via* a series of pathways and connections (4). Normal visual function requires the optics of the eye and the retinal/brain neural networks to function well. Studies have found that visual deprivation before the critical period is likely to cause functional reorganization of the brain (5) with the visual cortex or visual-related area becoming more involved in non-visual information processing such as auditory, tactile, or cognitive tasks (6). In individuals with CB, the visual cortex may process non-visual information through cross-modal plasticity (7, 8). In addition, many studies have reported brain anatomical changes in patients with CB (9). For instance, CB patients may have a thicker occipital cortex than sighted individuals (10) and significantly reduced lateral geniculate nucleus (LGN) volume (11). Therefore, CB may be closely associated with these brain dysfunctions or anatomical abnormalities.

Static functional magnetic resonance imaging (fMRI) is a reliable and informative method to study brain activity in a resting state and has been widely applied in CB patients. The regional homogeneity (ReHo) method has proven a reliable and sensitive resting-state fMRI data analysis method since it was introduced in 2004 (12). Each voxel's Kendall coefficient of concordance is obtained by analyzing the consistency between its blood oxygen level-dependent signals and that of 26 adjacent voxels in a given time period. Higher ReHo value indicates greater consistency. We have applied the ReHo method to evaluate the regional consistency of brain activity in patients with eye disease or conditions including acute eye pain (13), corneal ulcer (14), diabetic optic neuropathy (15), diabetic retinopathy (16), dry eye (17), dysthyroid optic neuropathy (18), late monocular blindness (19), optic neuritis (20), post-ophthalmectomy (21), retinal detachment (22), retinal vein occlusion (23), and strabismus (24, 25). In the present research, we use fMRI and ReHo analysis intending to determine whether spontaneous brain activity is normal in CB, and thus to better understand these patients.

SUBJECTS AND METHODS

Subjects

Twenty-three CB patients (15 males and 8 females, mean age 14.80 ± 2.03 years) were enrolled in the CB group. They were all recruited from the Ophthalmology Department of the First Affiliated Hospital of Nanchang University. Since birth, they had minimal or no visual experience and had no history or objective signs of light perception (response to light or objects). In most of the patients, CB was due to retinopathy of prematurity, but in some cases, the cause was congenital glaucoma, ocular tumor, or unknown. Demographic information and the causes of CB are summarized in **Table 1**.

Twenty-three (15 male and 8 female) age-, gender-, and handedness-matched subjects were also enrolled in the healthy control (HC) group with best corrected visual acuity better than 0.8 (decimal notation) with no severe ocular disease history. Subjects from both groups met the following criteria: (i) no systemic disease history and no abnormalities found on brain MRI; (ii) no history of mental illness; (iii) no contraindications to MRI scans.

Our research followed the Declaration of Helsinki and was approved by the Medical Ethics Committee of the First Affiliated Hospital of Nanchang University. Every subject voluntarily participated in this research after understanding the objective of this research and the possible risks.

MRI Parameters

The magnetic resonance imaging was completed by MAGNETOM Trio 3T (Siemens AG, Munich, Germany). All subjects were required to close their eyes, keep their heads still, stay awake and relax during the scanning. Conventional T1 weighted image (T1WI), conventional T2 weighted image (T2WI), three-dimensional T1-weighted gradient-echo (3D

TABLE 1 | Demographic data of congenital blind individuals.

ID	Sex	Age	Dx month	Residual vision	Handness	Etiology
CB01	M	14	3	NLP	Right	Retinopathy of pre-maturity
CB02	M	16	2	NLP	Right	Retinopathy of pre-maturity
CB03	M	17	8	NLP	Right	Retinopathy of pre-maturity
CB04	M	11	2	NLP	Right	Retinopathy of pre-maturity
CB05	F	14	1	NLP	Right	Retinopathy of pre-maturity
CB06	M	17	Birth	NLP	Right	Unknown
CB07	M	15	Birth	NLP	Right	Unknown
CB08	F	12	3	NLP	Right	Retinopathy of pre-maturity
CB09	F	16	3–5	NLP	Right	Retinopathy of pre-maturity
CB10	M	17	Birth	NLP	Right	Congenital glaucoma
CB11	F	17	Birth	NLP	Right	Retinopathy of pre-maturity
CB12	M	15	Birth	NLP	Right	Retinopathy of pre-maturity
CB13	M	18	Birth	NLP	Right	Retinopathy of pre-maturity
CB14	M	16	Birth	NLP	Right	Unknown
CB15	M	17	3–5	NLP	Right	Unknown
CB16	F	15	2	NLP	Right	Retinopathy of pre-maturity
CB17	F	15	1	NLP	Right	Retinopathy of pre-maturity
CB18	M	15	4	NLP	Right	Retinopathy of pre-maturity
CB19	M	15	Birth	NLP	Right	Unknown
CB20	F	11	3–4	NLP	Right	Ocular tumors
CB21	M	13	Birth	NLP	Right	Unknown
CB22	F	14	3–5	NLP	Right	Retinopathy of pre-maturity
CB23	M	11	Birth	NLP	Right	Unknown

Dx months, the age of months of subjects first found as congenital blindness; NLP, no light perception.

T1W GRE) imaging, and resting-state fMRI data were all collected. The 3D T1W GRE scan parameters were set as repetition time(TR) 1,900 ms, echo time (TE) 2.26 ms, the field of view 250 × 250 mm, flip angle 90°, acquisition matrix 256 × 256, thickness 1.0 mm, gap 0.5 mm, voxel size = 1 × 1 × 1mm^3. Two hundred and forty functional images were also obtained. The echo-planar imaging (EPI) scan parameters were set as TR 2,000 ms, TE 30 ms, field of view 220 × 220 mm, flip angle 90°, acquisition matrix 64 × 64, thickness 4.0 mm, gap 1.2 mm. The scanning time was 5 and 10 min for each.

fMRI Data Processing

Raw image data were first filtered by MRIcro software (https://people.cas.sc.edu /rorden/mricro/mricro.html) and then preprocessed by using Statistical Parametric Mapping software (http://www.fil.ion.ucl.ac.uk/spm/) and Data Processing Assistant for Resting-State fMRI v4.0 software (http://rfmri.org/DPARSF). To reduce the influence of the initial magnetic field instability of magnetic resonance, the first 10 scans were removed from the analysis. Slice time correction is used to eliminate scan errors at different timing. And the head motion was corrected to make the scanning results more reliable. Then co-registration and spatial normalization (Montreal Neurological Institute Brain Atlas, resampling voxels = 3 × 3 × 3 mm^3) were executed to allow the fMRI scanning results for group analysis. To remove the impact of physiological noise and low-frequency drift, band-pass temporal filtering and linear detrending were performed. After ReHo analysis, we applied spatial smoothing by using the Gaussian kernel (full width at half maximum, FWHM = 6 mm) to improve the signal-to-noise ratio.

Statistical Analysis

Resting State fMRI Data Analysis Toolkit software (REST, http://www.restfmri.net /forum/) was run for getting the ReHo value of every voxel by calculating the Kendall coefficient of concordance (KCC) of adjacent 26 voxels. KCC's calculation is shown as follow:

$$W = 12\frac{\sum_{i=1}^{n}(R_i - \overline{R})^2}{K^2(n^3 - n)}$$

where W represents the KCC among given voxels; K represents the number of neighbors, which is 27 in this study; n represents the number of total time points; R_i represents the sum of the rank of signals of a certain voxel and its neighbors at time point i; $\bar{R}$ represents the average of R_1 to R_n, which means the overall mean rank of all voxels in the cluster throughout the total time series. And ReHo value= standardized ReHo (Z-score) = (KCC of this voxel–average KCC of total voxels)/standard deviation of KCC of total voxels (26). The ReHo value represents the consistency of the BOLD signal between a certain voxel and the surrounding voxels within a period of time and reflects the consistency of the brain activities in the specific area. The higher the ReHo value, the stronger consistency of the local brain activities have. An independent samples *t*-test was carried out by REST Software to detect the significant ReHo differences between the two groups. The statistical threshold was set at the voxel level with $P < 0.05$ and multiple comparison was conducted with false discovery rate (FDR) corrected and cluster size > 50 voxels. ROC curves were used to identify the CB patients by certain brain region ReHo values. The area under the ROC curve (AUC) was computed to evaluate the diagnostic ability. In addition, all the CB patients were provided with vocal version of the Hospital Anxiety and Depression Scale (HADS) (27), and the results were collected. We then use the anxiety score and depression score obtained in the HADS to assess the CB patient's anxiety and depression level (Normal: 0 ∼ 7, Borderline: 8 ∼ 10, Abnormal: 11 ∼ 21). The onset and the duration of blindness in the CB group were also recorded. Pearson correlation analysis was performed by GraphPad Prism 9 software (https://www.graphpad.com/scientific-software/prism/) to evaluate whether there is a linear correlation between the ReHo value in right MFGorb and the anxiety score/depression score and whether there is a linear relationship between duration of blindness and ReHo values of significantly different brain regions.

RESULT

Demographic Information

Basic information about the two groups is shown in **Table 2**. There is no difference between the sex ratio, age, and handedness.

Regional Homogeneity Differences

Figures 1A,B show the brain regions in which ReHo differences were significantly different between the two groups. For CB patients, the mean ReHo values (Z-score) were significantly lower than controls in the right orbital part of the middle frontal gyrus (RMFGorb), bilateral middle occipital gyrus (MOG), and right dorsolateral superior frontal gyrus (RSFGdl), but higher than controls in the left paracentral lobule (LPCL), right insula and bilateral thalamus (**Figures 1A,B**, **Table 3**). The mean standardized ReHo values in these regions are shown in **Figure 2**.

ROC Curve Analysis

We hypothesized that the mean ReHo values of certain brain areas may be an effective marker for CB. To test this hypothesis, we generated receiver operating characteristic (ROC) curves to analyze the responses in specific brain areas with significant ReHo differences between groups. The regions with lower area under the curve (AUC) for CB than for HC are as follows: RMFGorb, AUC 0.905 [$p < 0.0001$; 95% CI (0.810–1.000)]; RightMOG, 0.902 [$p < 0.0001$; 95% CI (0.812–0.992)]; LeftMOG, 0.896 [$p < 0.0001$; 95% CI (0.806–0.986)]; and RSFGdl, 0.977 [*p*

TABLE 2 | Clinical characteristics of participants in this study.

Condition	CB (mean ± SD)	HCs (mean ± SD)	*T*-value	*P*-value
Male/female	15/8	15/8	N/A	>0.99
Age (years)	14.8 ± 2.03	14.70 ± 1.97	0.87	0.88
Handedness	23R	23R	N/A	>0.99
Duration of CB (years)	14.62 ± 2.10	N/A	N/A	N/A

CB, Congenital blindness; HCs, Healthy controls; SD standard deviation; N/A, not applicable.

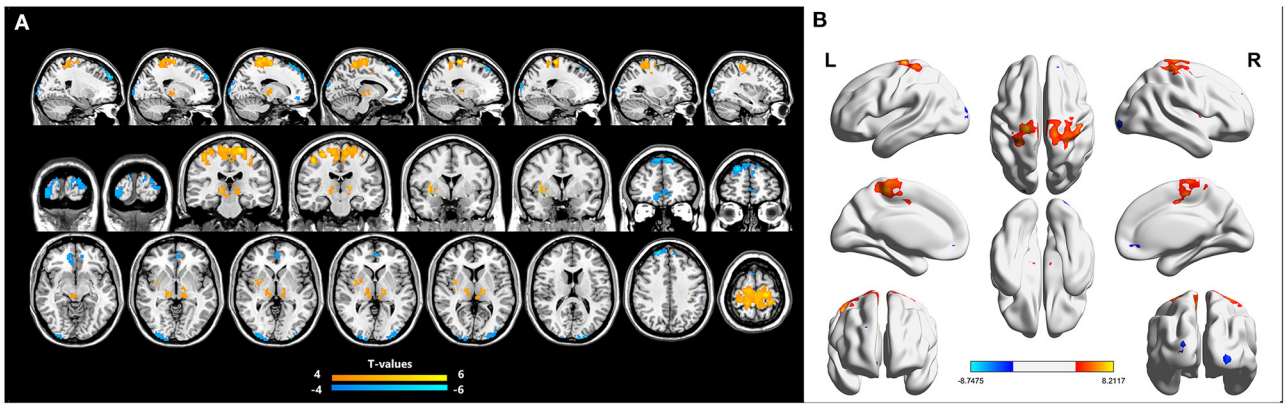

FIGURE 1 | Significantly different ReHo brain areas in patients with congenital blindness. Blue regions (RMFGorb, bilateral MOG, RSFGdl) indicate lower ReHo values, while red regions (the bilateral thalamus, the right insula, and the LPCL) represent higher ReHo values (single voxel $P < 0.05$, AlphaSim corrected; cluster size > 50). The map of the brain regions with statistical differences between two groups **(A)** and three-dimensional distributions **(B)**. ReHo, regional homogeneity; RMFGorb, the right orbital part of middle frontal gyrus; MOG, the middle occipital gyrus; RSFGdl, the right dorsolateral superior frontal gyrus; LPCL, the left paracentral lobule.

TABLE 3 | Brain areas with significantly different ReHo values between groups.

ReHo difference	Side	Brain areas	Peak voxels	*T*-value	MNI coordinates		
					X	Y	Z
CB < HC	Right	Orbital part of MFG	104	−5.62	12	45	−9
	Right	Middle occipital gyrus	112	−5.96	30	−96	0
	Left	Middle occipital gyrus	81	−5.94	−21	−99	15
	Right	Dorsolateral SFG	352	−8.75	21	54	39
CB > HC	Right	Thalamus	80	5.98	12	−24	−3
	Left	Thalamus	68	6.03	−15	−18	6
	Right	Insula	54	6.2	36	0	0
	Left	Paracentral lobule	1,547	8.21	−18	−24	69

The correction level was set voxel-wisely P < 0.05 FDR corrected, and cluster size > 50 voxels for multiple comparison. ReHo, regional homogeneity; CB, congenital blindness; HC, healthy control; BA, Brodmann area; MNI, Montreal neurological institute; MFG, middle frontal gyrus; SFG, superior frontal gyrus.

< 0.0001; 95% CI (0.944–1.000); **Figure 3A**]. Regions in which AUC was higher in CB than in HC were: LPCL, 0.955 [$p < 0.0001$; 95% CI (0.902–1.000)]; Right Thalamus, 0.909 [$p < 0.0001$; 95% CI (0.821–1.000)]; Left Thalamus, 0.898 [$p < 0.0001$; 95% CI (0.807–0.989)]; and Right Insula 0.907 [$p < 0.0001$; 95% CI (0.825–0.990); **Figure 3B**].

Correlation Analysis

Pearson's correlation was used to analyze the relationship between the ReHo value of RMFGorb and the anxiety and depression scores obtained from the HADS, and between the altered brain regions and the duration of CB. It is worth noting that among the 23 patients with CB, only 9 had normal HADS scores; one patient was in a state of depression and anxiety, one was in a state of depression and borderline anxiety, nine were in a state of borderline depression and borderline anxiety, two had borderline anxiety only, and one had borderline depression only. The ReHo value of RMFGorb was significantly negatively correlated with both the HADS anxiety score (**Figure 4A**) and depression score (**Figure 4B**), but no linear relationship was found between the duration of blindness and the mean ReHo values in the altered brain areas (**Table 4**).

DISCUSSION

Functional MRI may be used to measure cerebral activity and simultaneously determine the active location. This provides an effective and reliable means by which to understand the brain activity anomalies in cognition-related disorders or diseases. Resting-state fMRI does not require patients to perform specific tasks during scans, so it can reduce the influence of motor neural activity which occurs in a task-based fMRI scan. In addition, ReHo analysis has been used to reveal abnormal brain activity in ophthalmology (**Table 5**).

In contrast to the HCs, patients in the CB group showed significantly decreased mean ReHo values in the RMFGorb, bilateral MOG, and right posterior dorsolateral part of superior frontal gyrus (RSFGdl_p) (**Figure 5**).

The middle frontal gyrus (MFG) is located in the middle of the frontal lobe. The dorsolateral prefrontal cortex lies in the MFG which may be related to depression (31). The cortical regions associated with visual fixation of peripheral targets are known as the frontal eye fields (FEF) and lie in a region around the junction of the MFG and the precentral gyrus. The FEF is thought to be associated with the control of eye movements and visual attention since unilateral FEF impairment is associated with both eyes deviating to the ipsilateral side. CB patients are not able to consciously move their eyes and lack the vestibulo-ocular reflex while eye movement is practically normal in those with acquired blindness (32, 33). Since visual input is absent from birth in CB patients, their voluntary eye movements may be compromised. The MFG has also been found

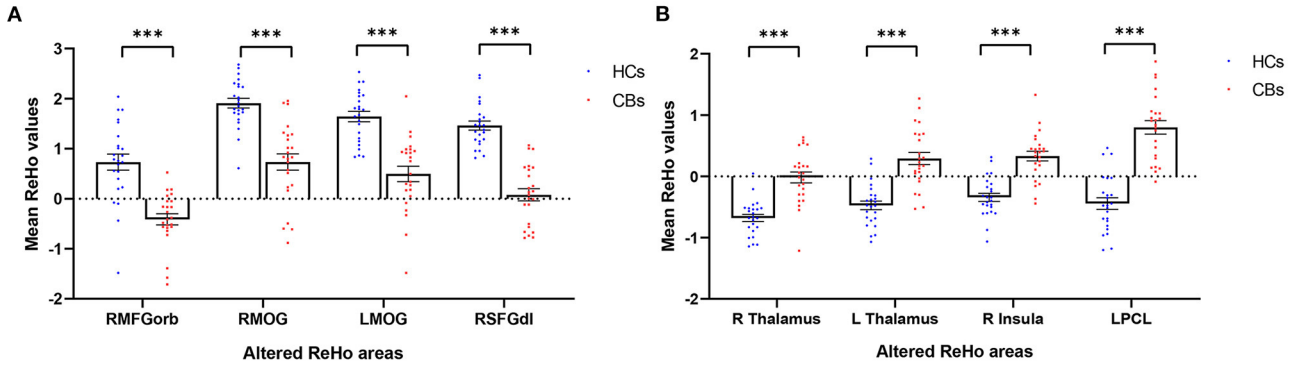

FIGURE 2 | Mean ReHo values (Z-score) of significantly altered brain areas between the CB and HC groups. **(A)** Compared to HCs, The mean ReHo values of the following regions were decreased in CB patients: RMFGorb ($t = -5.62$), the RMOG ($t = -5.96$), LMOG ($t = -5.94$), and the RSFGdl ($t = -8.75$). **(B)** Compared to HCs, the mean ReHo values of the following regions were increased in CB patients: the R Thalamus ($t = 5.98$), the L Thalamus ($t = 6.23$), the R insula ($t = 6.2$), the LPCL ($t = 8.21$).ReHo, regional homogeneity; CB, congenital blindness; HC, healthy control; R, right; L, left; RMFGorb, right orbital part of middle frontal gyrus; RMOG, right middle occipital gyrus; LMOG, left middle occipital gyrus; RSFGdl, right dorsolateral superior frontal gyrus; LPCL, left paracentral lobule. ***Represents the significant differences in ReHo value between the two groups ($p < 0.001$).

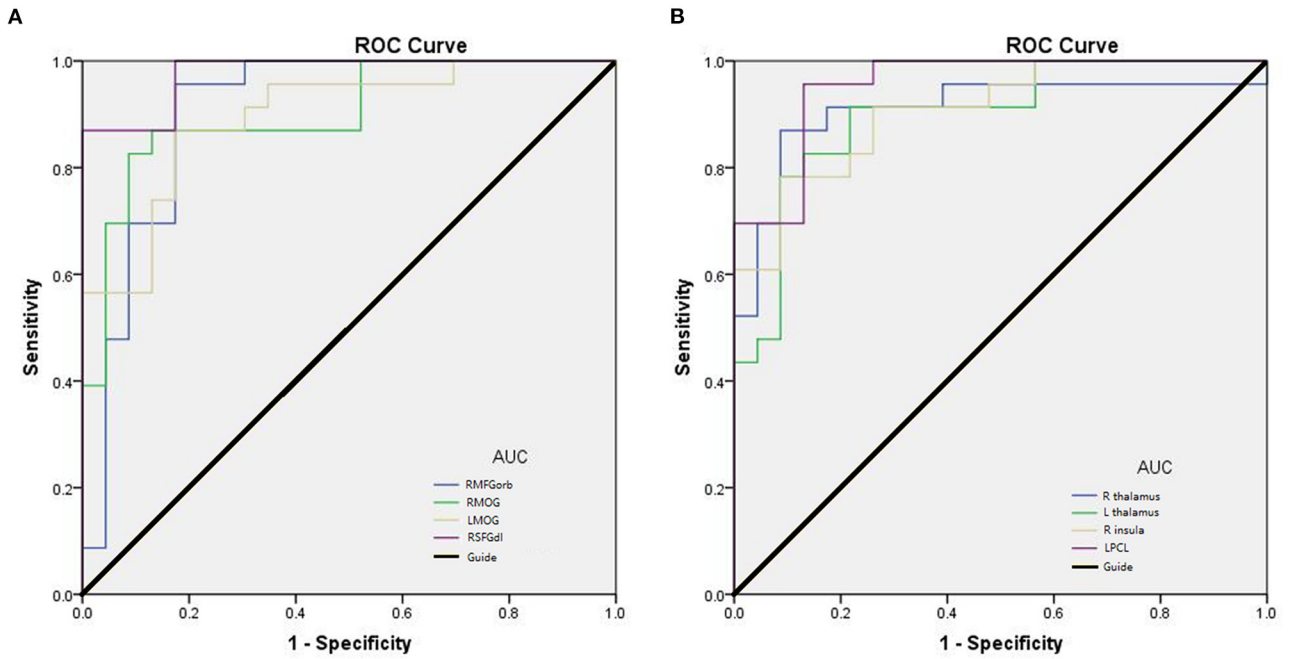

FIGURE 3 | Receiver operating characteristic (ROC) curve analysis of mean ReHo in corresponding brain regions. **(A)** The AUC were 0.905 [$p < 0.0001$; 95% CI (0.810–1.000)] for the RMFGorb; RMOG 0.902, [$p < 0.0001$; 95% CI (0.812–0.992)]; LMOG 0.896, [$p < 0.0001$; 95% CI (0.806–0.986)]; RSFGdl 0.977, [$p < 0.0001$; 95% CI (0.944–1.000)]. **(B)** The AUC were 0.909 [$p < 0.0001$; 95% CI (0.821–1.000)] for R thalamus; L thalamus 0.898, [$p < 0.0001$; 95% CI (0.807–0.989)]; R insula 0.907, [$p < 0.0001$; 95% CI (0.825–0.990)]; LPCL 0.955, [$p < 0.0001$; 95% CI (0.902–1.000)]. AUC area under the curve; CI confidence interval; R, right; L, left; RMFGorb, right orbital part of middle frontal gyrus; RMOG, right middle occipital gyrus; LMOG, left middle occipital gyrus; RSFGdl, right dorsolateral superior frontal gyrus; LPCL, left paracentral lobule.

to be involved in cognitive function and emotion processing. Previous studies indicate that the right MFG may play a part in contingency awareness (34) and reorienting attention (35), that right MFG gray matter volume is reduced in late-life depression and remitting depression patients (31, 36), and that activity of the right orbital part of MFG is reduced in patients with depression and anxiety (37). It is known that visual impairment and difficult living conditions will have a notable psychological impact on CB patients. Anomalies may occur in the brain regions associated with emotional processing, and the fact that 14 of 23 CB patients in our study showed borderline or abnormal states of anxiety or depression is consistent with this possibility. The abnormal

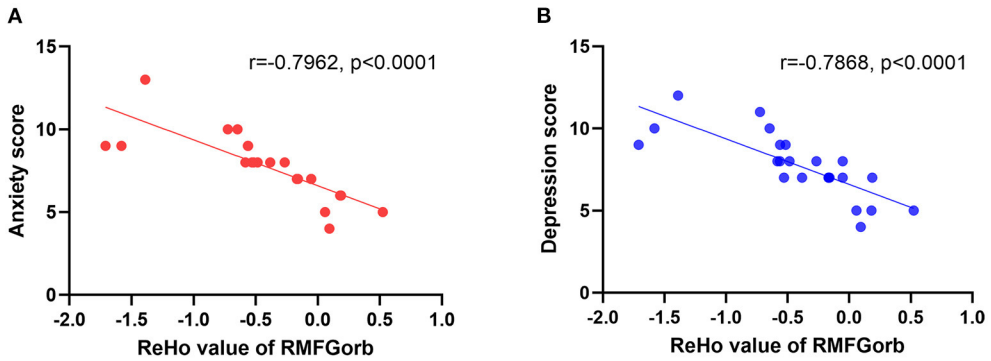

FIGURE 4 | The linear relationship between the ReHo value of the RMGForb and the anxiety score/depression score. **(A)** The anxiety score obtained from the HADS was negatively correlated with the ReHo value of RMFGorb, $r = -0.7962$, $p < 0.0001$; **(B)** The depression score obtained from the HADS was also negatively correlated with the ReHo value of RMFGorb, $r = -0.7868$, $p < 0.0001$. ReHo, regional homogeneity; RMFGorb, right orbit part of middle frontal gyrus; HADS, Hospital Anxiety and Depression Scale.

TABLE 4 | Pearson correlation analysis between the ReHo values in the altered brain areas and the duration of blindness.

Brain regions	ReHo value (mean ± SD)	Duration (years) (mean ± SD)	*R*-value	*P*-value
RMFGorb	−0.413 ± 0.543	14.623 ± 2.098	0.05043	0.8192
RMOG	0.732 ± 0.798		0.06588	0.7652
LMOG	0.495 ± 0.747		−0.1096	0.6185
RSFGdl	0.078 ± 0.595		0.06702	0.7613
R thalamus	−0.018 ± 0.433		−0.1687	0.4416
L thalamus	0.291 ± 0.485		−0.2172	0.3194
R insula	0.330 ± 0.393		−0.1279	0.5608
LPCL	0.799 ± 0.539		0.1392	0.5265

ReHo, regional homogeneity; SD, standard deviation.

TABLE 5 | Application of ReHo in ophthalmological diseases.

Diseases	Author	Year	References
Glaucoma	Song et al.	2014	(28)
Diabetic retinopathy	Cui et al.	2014	(29)
Optic neuritis	Shao et al.	2015	(20)
Open-globe injury	Huang et al.	2016	(30)
Late monocular blindness	Huang et al.	2017	(19)
Retinal detachment	Huang et al.	2017	(22)
Acute eye pain	Tang et al.	2018	(13)
Strabismus and amblyopia	Shao et al.	2019	(25)
Corneal ulcer	Xu et al.	2019	(14)
Retinal vein occlusion	Wen et al.	2019	(23)
Dysthyroid optic neuropathy	Jiang et al.	2021	(18)
Dry eye	Yu et al.	2021	(17)

changes at RMFGorb may help us to detect anxiety or depression in CB patients earlier. Other studies have also found that CB patients are indeed prone to suffer from depression and anxiety (38–40). We found a significantly decreased mean ReHo value at the RMFGorb in CB patients compared with HCs and the ReHo value of RMFGorb in CB patients was negatively correlated with their anxiety and depression scores. These findings may be related to the impaired voluntary eye movements in CB patients due to their visual deprivation and may be associated with the psychiatric changes such as depression and anxiety that occur in CB patients (**Figure 6**).

The occipital lobe is located at the posterior part of the cerebrum and is known as the vision and visual processing center (41). The primary visual cortex (also known as the striate cortex, V1) is at the medial and posterior part of the occipital lobe within the calcarine sulcus in each hemisphere. Goodale and Milner first established the classic hypothesis of two visual pathways (42). They believed the primary visual cortex projects information to two pathways, namely the dorsal/localization or "where" stream, mainly processing motion or stereoscopic depth visual information, and the ventral/identification pathway or "what" stream, mainly dealing with colors, shapes and other detailed visual information. However, some researchers have found that the two pathways may not be so clearly distinguished (43, 44). Congenitally blind patients lack visual experience, which suggests that their visual pathway does not develop normally. Previous studies have found that people with early-onset blindness may have brain anatomical changes such as decreased white matter volume in part of the visual pathway and decreased gray matter volume in the visual cortex (45). Despite the anatomical changes, less functional connectivity within the occipital lobe has also been found in early-onset blindness (46). Three gyri (the superior, the middle, and the inferior occipital gyrus) are located along the lateral portion of the occipital lobe (47). Studies have shown that the occipital cortex of people with CB is engaged in other forms of sensory processing, since the occipital cortices, the lingual-gyrus (Brodmann area 18), parts of the cuneus, and the MOG were activated more in early blindness than in sighted control subjects undertaking auditory and tactile tasks (48, 49). The right MOG is part of the dorsal/localization stream and shows

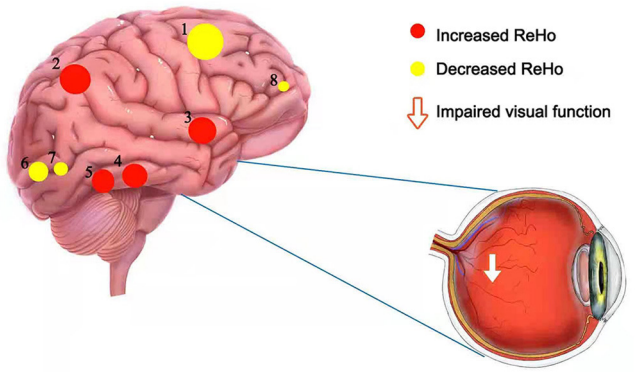

FIGURE 5 | The schematic brain region map of CB patients with significant ReHo differences compared to HC. The ReHo values of CB patients were reduced to varying degrees compared with HCs in the following regions: 8-the right orbital part of the middle frontal gyrus (BA 32, $t = -5.62$), 6-the right middle occipital gyrus (BA 18, $t = -5.96$), 7-the left middle occipital gyrus (BA 18, $t = -5.94$), 1-the right dorsolateral superior frontal gyrus (BA 8, $t = -8.75$). Instead, the ReHo values of CB patients in the following regions were increased compared with HCs: 5-the right thalamus ($t = 5.98$), 4-the left thalamus ($t = 6.23$), 3-the right insula ($t = 6.2$), 2-the left paracentral lobule (BA 3, $t = 8.21$). CB, congenital blindness; HC, healthy control; ReHo, regional homogeneity; BA, Brodmann's area.

increased activity during spatial tactile and auditory tasks in people with early-onset blindness. However, the bilateral MOG showed significantly decreased ReHo values in CB compared to HCs in our resting-state fMRI test, implying that spatial tactile and auditory task-related areas may be inhibited in the resting state.

The superior frontal gyrus (SFG), also known as the marginal gyrus, is located in the superior part of the prefrontal cortex (50) and is involved in higher cognitive functions such as working memory (51). The audio-spatial working memory of CB patients is compromised since visual experience supports spatial memory (52). Significantly reduced ReHo values have been demonstrated in the right dorsolateral part of Brodmann area 8, located at the posterior dorsolateral part of SFG (SFGdl_p), in CB patients (53). This area includes the FEF, known to be related to voluntary eye movements, visual search, and attention control (54, 55). The right and left FEF have slightly different functions, the right FEF playing a role in signal integration (56). The SFGdl_p also has a connection with brain regions that are associated with cognitive control, such as the posterior parietal cortex and dorsolateral prefrontal cortex (57). While FEF may be related to stronger endogenous orienting of non-visual attention (such as verbal cues) in CB patients (58), ReHo is decreased in the right SFGdl_p of CB patients compared with HCs.

However, the mean ReHo values of the CB group in the left paracentral lobule (PCL), right insula, and bilateral thalamus were significantly higher compared with those in HCs (**Figure 5**).

The PCL is on the medial side of each cerebral hemisphere and is responsible for controlling motor innervations and processing sensory information of the contralateral lower limbs. The left side upper postcentral gyrus (Brodmann area 3) is the precise area with increased ReHo value. The postcentral gyrus is located at the lateral parietal lobe and is also known as the primary somatosensory cortex (59). All of the CB patients and HCs in the present study were right-handed. Increased ReHo of the postcentral gyrus contralateral to the dominant hand in CB patients indicates that they may have more sensitive tactile perception than controls. Several behavioral studies also support the concept of superior tactile abilities in early-blind persons (60, 61). One previous study also found increased activity in the postcentral gyrus in CB subjects compared with sighted individuals on a tactile task (62), consistent with our suggestion.

The insular cortex folds deep within the lateral sulcus in each hemisphere of the brain. The insulae are generally thought to be involved in multimodal sensory processing, taste, self-awareness, motor control, homeostasis, auditory perception, salience, emotions, and other functions. People with CB are thought to be highly sensitive to salient non-visual stimuli. Enhanced intra- and inter-network connectivity such as salience network and frontoparietal network in CB may optimize their abilities to use non-visual stimuli and their attention control, which may help them to adapt to their environment (63). The anterior insula (AI) is believed to be part of the salience network that detects and facilitates higher cognitive processing of the most relevant stimuli in a multitude of forms of sensory information. The functional connectivity between the dorsal AI and the dorsal/localization (where) stream and between the ventral AI and the ventral/identification (what) stream is enhanced in CB (64). This may support our finding that the bilateral insulae are more activated in CB in the resting state. The AI cortex is also believed to be engaged in emotional cognition (empathy), interoceptive awareness (hunger, thirst) and may play a role in conveying this information to consciousness (65). fMRI results show that the AI is correlated with the ability to feel one's own heartbeat and emotion elicitation (66). Increased activity and gray matter volume of the right AI in normal subjects are correlated with higher accuracy of interoceptive sense (measuring own heartbeat). In addition, more negative feelings (higher scores on the questionnaire of the Hamilton Anxiety Scale) are correlated with their interoceptive task accuracy (67). Whether these abilities in CB people are superior remains to be studied in the future. In our study, the increased ReHo at the right insula in CB patients may indicate that they have better interoceptive awareness during the resting state compared to sighted individuals.

The thalamus comprises a pair of large oval gray matter nuclei located in the dorsal part of the diencephalon, just beside the third ventricle. The left and right thalami are connected by a gray matter mass. The thalamus plays roles ranging from sensation relay, regulation of memory and emotion, consciousness, and others (68). The nuclei in the thalamus are separated by a Y-shaped white matter plate into anterior, lateral, and medial groups. Various sensory pathways (except olfactory) replace neurons at the thalamus and then project to the cerebral cortex. For instance, the LGN (part of the thalamus) is the most important relay station in the visual pathway. The retinal ganglion cell gathers visual information from the retina and projects it to the LGN which then projects fibers

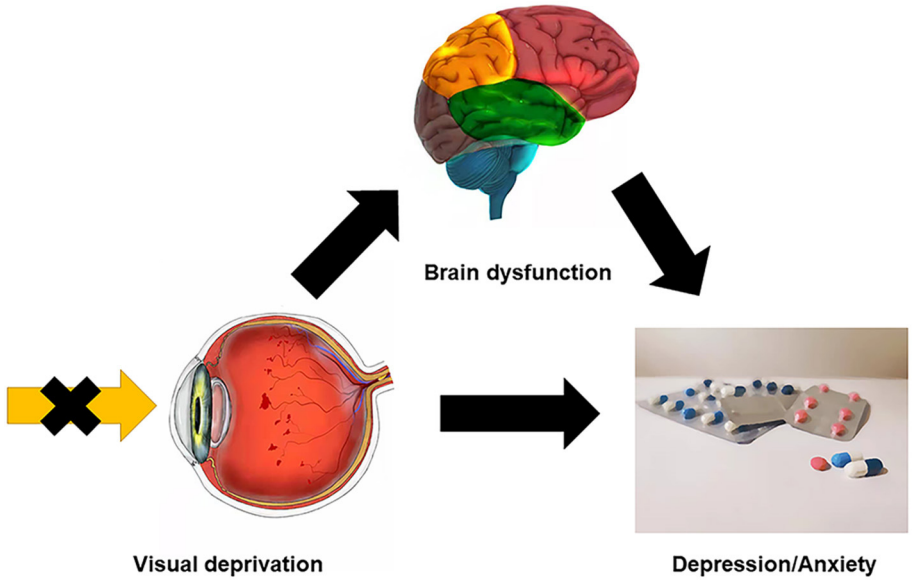

FIGURE 6 | Relationship between clinical manifestation, brain dysfunction, and psychological conditions of CB patients. CB patients could get certain brain region dysfunction because of visual deprivation, for example, the ReHo values were significantly decreased at MFG in CB patients, which could be relevant to anxiety and depression. And the visual disability itself may bring physiological or psychosocial problems, which make CB patients more susceptible to psychological disorders. CB, congenital blindness; MFG, middle frontal gyrus; ReHo, regional homogeneity.

to the primary visual cortex (area V1). Notably, the LGN not only receives neural projections from the retina, but also has extensive interconnections with the thalamus, brainstem, and visual cortex. Brain functional and structural changes occur after early visual deprivation. One study found that the mean volumes of structures along the visual pathway (including LGN) were reduced by 50% in CB patients (69). Although the LGN may have impaired function and reduced size in CB, volumes of other relay nuclei such as the medial geniculate nucleus (MGN), ventrolateral nucleus (VL), and ventral posterior nucleus (VP) were not affected (70). In addition, studies have found that tactile stimulation in people with CB can stimulate occipital cortical activities. This phenomenon is most likely accomplished by the thalamocortical pathway (71). In animal studies, the deprivation of hamsters' visual systems at birth can lead to retinal projections to the auditory thalamus (72) and the primary visual cortices of enucleated opossums receive projections from nuclei other than LGN, including MGN (auditory), VP (sensation), VL (motor), and anterior nuclear groups (alertness, learning) (73). Human studies have shown that in CB patients the occipital cortex is responsive to auditory stimuli and the superior colliculus is recruited by the auditory system (74). The increased ReHo values of the bilateral thalamus in CB patients probably reflect the structural and functional variations due to early visual deprivation.

Pearson correlation analysis demonstrated no linear correlation between the duration of CB and the mean ReHo values in the significantly altered brain regions.

ROC analysis in our study demonstrates the potential diagnostic value of mean ReHo values (Z-score) of the brain regions found to differ between CB patients and HCs (**Figure 3**).

TABLE 6 | Altered brain regions and their potential impact.

Brain regions (ReHo difference)	Brain function	Possible impact
RMFGorb (CBs < HCs)	Eye movements, cognitive functions, emotional processing, attention	Impaired voluntary eye movements, depression/anxiety, cognitive activity disorder
Bilateral MOG (CBs < HCs)	Visual related, spacial tactile, & auditory task	Impaired visual function, object recognition
RSGFdl (CBs < HCs)	Visuospatial attention, eye movements, awareness	Impaired voluntary eye movements, awareness
LPCL (CBs > HCs)	Motor & sensory innervations	Superior tactile skills
Right insula (CBs > HCs)	Multimodal sensory processing, cognitive-emotional process, salience, taste, self-awareness	Better interoceptive awareness
Bilateral thalamus (CBs > HCs)	Relaying sensory/motor signals, regulations of consciousness and alertness arousal, attention, motivation	Reorganization of the sensory and motor systems

RMFGorb, the right orbital part of middle frontal gyrus; MOG, middle occipital gyrus; RSFGdl, the right dorsolateral superior frontal gyrus; LPCL, the left paracentral lobule.

The AUC of each of these regions was >0.85, indicating effective accuracy in the identification of CB. The AUC of RSFGdl and LPCL was as high as 0.977 and 0.955, respectively. However, these CB patients had been blind for some years (mean age 14.80 ± 2.03

years, with minimum 10.8 years old and maximum 17.8 years old), and it remains unclear whether these positive results hold in newborn blind patients. But ReHo analysis do have the potential to be used for legal or medical proof of CB grown-ups since it is an objective examination.

Patients with CB in our study can only be prevented from the cause at early stages. For these patients who have been CB for years, there is currently no good way to restore sight. Future treatments for patients with CB, such as the use of artificial prosthesis (75), may reverse the abnormalities in these altered brain regions. And the ReHo analysis could help in tracking the treatment effect and assess the function restoration.

CONCLUSION

Our experimental results found that patients with CB can have regional abnormal brain activities at a resting state. These abnormal neural activities are likely to be associated with the potential regional structural changes, functional reorganization, and even psychological impact on CB patients (**Table 6**). These abnormal brain regions suggest the possible location of primary or secondary brain damage in CB, which may help to study the pathogenesis and development of CB in the future. ReHo analysis can record changes of regional brain activities non-invasively. It is of great significance use for clinical follow-up and research, and has great application value in the clinic to discover abnormalities related to brain function. Moreover, our ROC result shows ReHo analysis has the potential to be a safe and effective approach to identify CB for medical or legal purpose. It can also be used in diagnosing of patients with CB with complex causes or for whom vision examination is not available. However, our study does have some limitations. Firstly, the sample size of our study was relatively small. Individual differences may have an impact on our result, so a larger population study is needed to prove our findings. In addition, the 15-min scanning time may result in small unavoidable movements which may undermine the accuracy of our analysis. Also, because some of the CB patients didn't have intact medical records, their histories are based on the subjective description of their parents which might be not accurate. In the future, we will minimize the possible influencing factors to obtain more reliable results.

DATA AVAILABILITY STATEMENT

The datasets used and/or analyzed during the current study are available from the corresponding author on reasonable request.

ETHICS STATEMENT

The studies involving human participants were reviewed and approved by Medical Ethics Committee of the First Affiliated Hospital of Nanchang University. The patients/participants provided their written informed consent to participate in this study.

AUTHOR CONTRIBUTIONS

J-JH and NJ were major contributors, both conceived and designed the experiments, analyzed the data, wrote, and revised the manuscript. JC, PY, MK, and S-HX recruited the patients and healthy controls for the study, performed the MRI experiments, and helped finish the questionnaires. JZ, HW, and QL collected and treated the data. YS designed the study and offered financial support. All authors read and approved the final manuscript.

ACKNOWLEDGMENTS

We thank reviewers for their excellent criticism of the article.

REFERENCES

1. Khandekar R. Visual disabilities in children including childhood blindness. *Middle East Afr J Ophthalmol.* (2008) 15:129. doi: 10.4103/0974-9233.51988
2. Xu T, Wang B, Liu H, Wang H, Yin P, Dong W, et al. Prevalence and causes of vision loss in China from 1990 to 2019: findings from the global burden of disease study 2019. *Lancet Public Health.* (2020) 5:e682–91. doi: 10.1016/S2468-2667(20)30254-1
3. Shi Y, Xu Z. [An investigation on causes of blindness of children in seven blind schools in East China]. *Zhonghua Yan Ke Za Zhi.* (2002) 38:747–9.
4. Yue L, Weiland JD, Roska B, Humayun MS. Retinal stimulation strategies to restore vision: fundamentals and systems. *Prog Retin Eye Res.* (2016) 53:21–47. doi: 10.1016/j.preteyeres.2016.05.002
5. Qin W, Xuan Y, Liu Y, Jiang T, Yu C. Functional connectivity density in congenitally and late blind subjects. *Cereb Cortex.* (2015) 25:2507–16. doi: 10.1093/cercor/bhu051
6. Fine I, Park JM. Blindness and human brain plasticity. *Annu Rev Vis Sci.* (2018) 4:337–56. doi: 10.1146/annurev-vision-102016-061241
7. Leo A, Bernardi G, Handjaras G, Bonino D, Ricciardi E, Pietrini P. Increased BOLD variability in the parietal cortex and enhanced parieto-occipital connectivity during tactile perception in congenitally blind individuals. *Neural Plast.* (2012) 2012:720278. doi: 10.1155/2012/720278
8. Castaldi E, Lunghi C, Morrone MC. Neuroplasticity in adult human visual cortex. *Neurosci Biobehav Rev.* (2020) 112:542–52. doi: 10.1016/j.neubiorev.2020.02.028
9. Aguirre GK, Datta R, Benson NC, Prasad S, Jacobson SG, Cideciyan AV, et al. Patterns of individual variation in visual pathway structure and function in the sighted and blind. *PLoS ONE.* (2016) 11:e164677. doi: 10.1101/065441
10. Voss P, Zatorre RJ. Early visual deprivation changes cortical anatomical covariance in dorsal-stream structures. *Neuroimage.* (2015) 108:194–202. doi: 10.1016/j.neuroimage.2014.12.063
11. Bridge H, Cowey A, Ragge N, Watkins K. Imaging studies in congenital anophthalmia reveal preservation of brain architecture in 'visual' cortex. *Brain.* (2009) 132 (Pt. 12):3467–80. doi: 10.1093/brain/awp279
12. Zang Y, Jiang T, Lu Y, He Y, Tian L. Regional homogeneity approach to fMRI data analysis. *Neuroimage.* (2004) 22:394–400. doi: 10.1016/j.neuroimage.2003.12.030
13. Tang LY, Li HJ, Huang X, Bao J, Sethi Z, Ye L, et al. Assessment of synchronous neural activities revealed by regional homogeneity in individuals with acute eye pain: a resting-state functional magnetic resonance imaging study. *J Pain Res.* (2018) 11:843–50. doi: 10.2147/JPR.S156634

14. Xu MW, Liu HM, Tan G, Su T, Xiang CQ, Wu W, et al. Altered regional homogeneity in patients with corneal ulcer: a resting-state functional MRI Study. *Front Neurosci.* (2019) 13:743. doi: 10.3389/fnins.2019.00743
15. Guo GY, Zhang LJ, Li B, Liang RB, Ge QM, Shu HY, et al. Altered spontaneous brain activity in patients with diabetic optic neuropathy: a resting-state functional magnetic resonance imaging study using regional homogeneity. *World J Diabetes.* (2021) 12:278–91. doi: 10.4239/wjd.v12.i3.278
16. Liao XL, Yuan Q, Shi WQ, Li B, Su T, Lin Q, et al. Altered brain activity in patients with diabetic retinopathy using regional homogeneity: a resting-state fMRI study. *Endocr Pract.* (2019) 25:320–7. doi: 10.4158/EP-2018-0517
17. Yu K, Guo Y, Ge QM, Su T, Shi WQ, Zhang LJ, et al. Altered spontaneous activity in the frontal gyrus in dry eye: a resting-state functional MRI study. *Sci Rep.* (2021) 11:12943. doi: 10.1038/s41598-021-97182-x
18. Jiang YP, Yang YC, Tang LY, Ge QM, Shi WQ, Su T, et al. Altered spontaneous brain activity patterns in dysthyroid optic neuropathy: a resting-state fMRI study. *J Integr Neurosci.* (2021) 20:375–83. doi: 10.31083/j.jin2002037
19. Huang X, Ye CL, Zhong YL, Ye L, Yang QC, Li HJ, et al. Altered regional homogeneity in patients with late monocular blindness: a resting-state functional MRI study. *Neuroreport.* (2017) 28:1085–91. doi: 10.1097/WNR.0000000000000855
20. Shao Y, Cai FQ, Zhong YL, Huang X, Zhang Y, Hu PH, et al. Altered intrinsic regional spontaneous brain activity in patients with optic neuritis: a resting-state functional magnetic resonance imaging study. *Neuropsychiatr Dis Treat.* (2015) 11:3065–73. doi: 10.2147/NDT.S92968
21. Zhang B, Li B, Liu RQ, Shu YQ, Min YL, Yuan Q, et al. Altered spontaneous brain activity pattern in patients with ophthalmectomy: an resting-state fMRI study. *Int J Ophthalmol.* (2020) 13:263–70. doi: 10.18240/ijo.2020.02.10
22. Huang X, Li D, Li HJ, Zhong YL, Freeberg S, Bao J, et al. Abnormal regional spontaneous neural activity in visual pathway in retinal detachment patients: a resting-state functional MRI study. *Neuropsychiatr Dis Treat.* (2017) 13:2849–54. doi: 10.2147/NDT.S147645
23. Wen SM, Min YL, Yuan Q, Li B, Lin Q, Zhu PW, et al. Altered spontaneous brain activity in retinal vein occlusion as determined by regional homogeneity: a resting-state fMRI study. *Acta Radiol.* (2019) 60:1695–702. doi: 10.1177/0284185119845089
24. Huang X, Li SH, Zhou FQ, Zhang Y, Zhong YL, Cai FQ, et al. Altered intrinsic regional brain spontaneous activity in patients with comitant strabismus: a resting-state functional MRI study. *Neuropsychiatr Dis Treat.* (2016) 12:1303–8. doi: 10.2147/NDT.S105478
25. Shao Y, Li QH, Li B, Lin Q, Su T, Shi WQ, et al. Altered brain activity in patients with strabismus and amblyopia detected by analysis of regional homogeneity: a restingstate functional magnetic resonance imaging study. *Mol Med Rep.* (2019) 19:4832–40. doi: 10.3892/mmr.2019.10147
26. Zuo XN, Xu T, Jiang L, Yang Z, Cao XY, He Y, et al. Toward reliable characterization of functional homogeneity in the human brain: preprocessing, scan duration, imaging resolution and computational space. *Neuroimage.* (2013) 65:374–86. doi: 10.1016/j.neuroimage.2012.10.017
27. Zigmond AS, Snaith RP. The hospital anxiety and depression scale. *Acta Psychiatr Scand.* (1983) 67:361–70. doi: 10.1111/j.1600-0447.1983.tb09716.x
28. Song Y, Mu K, Wang J, Lin F, Chen Z, Yan X, et al. Altered spontaneous brain activity in primary open angle glaucoma: a resting-state functional magnetic resonance imaging study. *PLoS ONE.* (2014) 9:e89493. doi: 10.1371/journal.pone.0089493
29. Cui Y, Jiao Y, Chen YC, Wang K, Gao B, Wen S, et al. Altered spontaneous brain activity in type 2 diabetes: a resting-state functional MRI study. *Diabetes.* (2014) 63:749–60. doi: 10.2337/db13-0519
30. Huang X, Li HJ, Ye L, Zhang Y, Wei R, Zhong YL, et al. Altered regional homogeneity in patients with unilateral acute open-globe injury: a resting-state functional MRI study. *Neuropsychiatr Dis Treat.* (2016) 12:1901–6. doi: 10.2147/NDT.S110541
31. Chang CC, Yu SC, McQuoid DR, Messer DF, Taylor WD, Singh K, et al. Reduction of dorsolateral prefrontal cortex gray matter in late-life depression. *Psychiatry Res.* (2011) 193:1–6. doi: 10.1016/j.pscychresns.2011.01.003
32. Kompf D, Piper HF. Eye movements and vestibulo-ocular reflex in the blind. *J Neurol.* (1987) 234:337–41. doi: 10.1007/BF00314291
33. Schneider RM, Thurtell MJ, Eisele S, Lincoff N, Bala E, Leigh RJ. Neurological basis for eye movements of the blind. *PLoS ONE.* (2013) 8:e56556. doi: 10.1371/journal.pone.0056556
34. Carter RM, O'Doherty JP, Seymour B, Koch C, Dolan RJ. Contingency awareness in human aversive conditioning involves the middle frontal gyrus. *Neuroimage.* (2006) 29:1007–12. doi: 10.1016/j.neuroimage.2005.09.011
35. Japee S, Holiday K, Satyshur MD, Mukai I, Ungerleider LG. A role of right middle frontal gyrus in reorienting of attention: a case study. *Front Syst Neurosci.* (2015) 9:23. doi: 10.3389/fnsys.2015.00023
36. Quinn ME, Stange JP, Jenkins LM, Corwin S, DelDonno SR, Bessette KL, et al. Cognitive control and network disruption in remitted depression: a correlate of childhood adversity. *Soc Cogn Affect Neurosci.* (2018) 13:1081–90. doi: 10.1093/scan/nsy077
37. Zhao P, Yan R, Wang X, Geng J, Chattun MR, Wang Q, et al. Reduced resting state neural activity in the right orbital part of middle frontal gyrus in anxious depression. *Front Psychiatry.* (2019) 10:994. doi: 10.3389/fpsyt.2019.00994
38. Osaba M, Doro J, Liberal M, Lagunas J, Kuo IC, Reviglio VE. Relationship between legal blindness and depression. *Med Hypothesis Discov Innov Ophthalmol.* (2019) 8:306–11. PubMed PMID: 31788493.
39. Meer EA, Lee YH, Repka MX, Borlik MF, Velez FG, Perez C, et al. Association of mood disorders, substance abuse, and anxiety disorders in children and teens with serious structural eye diseases. *Am J Ophthalmol.* (2022) 240:135–42. doi: 10.1016/j.ajo.2022.03.016
40. Rasendran C, Imran Y, Talcott KE. Incremental economic burden of depression in ophthalmic patients. *Am J Ophthalmol.* (2021) 229:184–93. doi: 10.1016/j.ajo.2021.03.062
41. Clark D., Boutros N, Mendez M. Occipital and parietal lobes. In: *The Brain and Behavior: An Introduction to Behavioral Neuroanatomy*. Cambridge: Cambridge University Press (2018). p. 33–55. doi: 10.1017/9781108164320.005
42. Goodale MA, Milner AD. Separate visual pathways for perception and action. *Trends Neurosci.* (1992) 15:20–5. doi: 10.1016/0166-2236(92)90344-8
43. McIntosh RD, Schenk T. Two visual streams for perception and action: current trends. *Neuropsychologia.* (2009) 47:1391–6. doi: 10.1016/j.neuropsychologia.2009.02.009
44. Franz VH, Gegenfurtner KR, Bulthoff HH, Fahle M. Grasping visual illusions: no evidence for a dissociation between perception and action. *Psychol Sci.* (2000) 11:20–5. doi: 10.1111/1467-9280.00209
45. Pan WJ, Wu G, Li CX, Lin F, Sun J, Lei H. Progressive atrophy in the optic pathway and visual cortex of early blind Chinese adults: a voxel-based morphometry magnetic resonance imaging study. *Neuroimage.* (2007) 37:212–20. doi: 10.1016/j.neuroimage.2007.05.014
46. Liu Y, Yu C, Liang M, Li J, Tian L, Zhou Y, et al. Whole brain functional connectivity in the early blind. *Brain.* (2007) 130 (Pt. 8):2085–96. doi: 10.1093/brain/awm121
47. Albohn DN, Adams RB. Chapter 8 - social vision: at the intersection of vision and person perception. In: Absher JR, Cloutier J, editors. *Neuroimaging Personality, Social Cognition, and Character*. San Diego, CA: Academic Press (2016). p. 159–86. doi: 10.1016/B978-0-12-800935-2.00008-7
48. Renier LA, Anurova I, De Volder AG, Carlson S, VanMeter J, Rauschecker JP. Preserved functional specialization for spatial processing in the middle occipital gyrus of the early blind. *Neuron.* (2010) 68:138–48. doi: 10.1016/j.neuron.2010.09.021
49. Collignon O, Vandewalle G, Voss P, Albouy G, Charbonneau G, Lassonde M, et al. Functional specialization for auditory-spatial processing in the occipital cortex of congenitally blind humans. *Proc Natl Acad Sci USA.* (2011) 108:4435–40. doi: 10.1073/pnas.1013928108
50. Petrides M, Pandya DN. Comparative cytoarchitectonic analysis of the human and the macaque ventrolateral prefrontal cortex and corticocortical connection patterns in the monkey. *Eur J Neurosci.* (2002) 16:291–310. doi: 10.1046/j.1460-9568.2001.02090.x
51. du Boisgueheneuc F, Levy R, Volle E, Seassau M, Duffau H, Kinkingnehun S, et al. Functions of the left superior frontal gyrus in humans: a lesion study. *Brain.* (2006) 129 (Pt. 12):3315–28. doi: 10.1093/brain/awl244
52. Setti W, Cuturi LF, Engel I, Picinali L, Gori M. The influence of early visual deprivation on audio-spatial working memory. *Neuropsychology.* (2022) 36:55–63. doi: 10.1037/neu0000776
53. Li W, Qin W, Liu H, Fan L, Wang J, Jiang T, et al. Subregions of the human superior frontal gyrus and their connections. *Neuroimage.* (2013) 78:46–58. doi: 10.1016/j.neuroimage.2013.04.011

54. Watanabe M. [Brodmann areas 8 and 9 including the frontal eye field]. *Brain Nerve.* (2017) 69:347–54. doi: 10.11477/mf.1416200751
55. Lane AR, Ball K, Smith DT, Schenk T, Ellison A. Near and far space: understanding the neural mechanisms of spatial attention. *Hum Brain Mapp.* (2013) 34:356–66. doi: 10.1002/hbm.21433
56. Lane AR, Smith DT, Schenk T, Ellison A. The involvement of posterior parietal cortex and frontal eye fields in spatially primed visual search. *Brain Stimul.* (2012) 5:11–7. doi: 10.1016/j.brs.2011.01.005
57. Vincent JL, Kahn I, Snyder AZ, Raichle ME, Buckner RL. Evidence for a frontoparietal control system revealed by intrinsic functional connectivity. *J Neurophysiol.* (2008) 100:3328–42. doi: 10.1152/jn.90355.2008
58. Garg A, Schwartz D, Stevens AA. Orienting auditory spatial attention engages frontal eye fields and medial occipital cortex in congenitally blind humans. *Neuropsychologia.* (2007) 45:2307–21. doi: 10.1016/j.neuropsychologia.2007.02.015
59. Viaene AN, Petrof I, Sherman SM. Synaptic properties of thalamic input to layers 2/3 and 4 of primary somatosensory and auditory cortices. *J Neurophysiol.* (2011) 105:279–92. doi: 10.1152/jn.00747.2010
60. D'Angiulli A, Waraich P. Enhanced tactile encoding and memory recognition in congenital blindness. *Int J Rehabil Res.* (2002) 25:143–5. doi: 10.1097/00004356-200206000-00008
61. Norman JF, Bartholomew AN. Blindness enhances tactile acuity and haptic 3-D shape discrimination. *Atten Percept Psychophys.* (2011) 73:2323–31. doi: 10.3758/s13414-011-0160-4
62. Sadato N, Okada T, Honda M, Yonekura Y. Critical period for cross-modal plasticity in blind humans: a functional MRI study. *Neuroimage.* (2002) 16:389–400. doi: 10.1006/nimg.2002.1111
63. Wang D, Qin W, Liu Y, Zhang Y, Jiang T, Yu C. Altered resting-state network connectivity in congenital blind. *Hum Brain Mapp.* (2014) 35:2573–81. doi: 10.1002/hbm.22350
64. Liu L, Yuan C, Ding H, Xu Y, Long M, Li Y, et al. Visual deprivation selectively reshapes the intrinsic functional architecture of the anterior insula subregions. *Sci Rep.* (2017) 7:45675. doi: 10.1038/srep45675
65. Mayer EA. Gut feelings: the emerging biology of gut-brain communication. *Nat Rev Neurosci.* (2011) 12:453–66. doi: 10.1038/nrn3071
66. Zaki J, Davis JI, Ochsner KN. Overlapping activity in anterior insula during interoception and emotional experience. *Neuroimage.* (2012) 62:493–9. doi: 10.1016/j.neuroimage.2012.05.012
67. Critchley HD, Wiens S, Rotshtein P, Ohman A, Dolan RJ. Neural systems supporting interoceptive awareness. *Nat Neurosci.* (2004) 7:189–95. doi: 10.1038/nn1176
68. Jones EG. *The Thalamus*. New York, NY: Springer Science & Business Media (2012). Available online at: https://link.springer.com/book/10.1007/978-1-4615-1749-8
69. Ptito M, Pare S, Dricot L, Cavaliere C, Tomaiuolo F, Kupers R. A quantitative analysis of the retinofugal projections in congenital and late-onset blindness. *Neuroimage Clin.* (2021) 32:102809. doi: 10.1016/j.nicl.2021.102809
70. Cecchetti L, Ricciardi E, Handjaras G, Kupers R, Ptito M, Pietrini P. Congenital blindness affects diencephalic but not mesencephalic structures in the human brain. *Brain Struct Funct.* (2016) 221:1465–80. doi: 10.1007/s00429-014-0984-5
71. Muller F, Niso G, Samiee S, Ptito M, Baillet S, Kupers R. A thalamocortical pathway for fast rerouting of tactile information to occipital cortex in congenital blindness. *Nat Commun.* (2019) 10:5154. doi: 10.1038/s41467-019-13173-7
72. Ptito M, Kupers R. Cross-modal plasticity in early blindness. *J Integr Neurosci.* (2005) 4:479–88. doi: 10.1142/S0219635205000951
73. Karlen SJ, Kahn DM, Krubitzer L. Early blindness results in abnormal corticocortical and thalamocortical connections. *Neuroscience.* (2006) 142:843–58. doi: 10.1016/j.neuroscience.2006.06.055
74. Coullon GS, Jiang F, Fine I, Watkins KE, Bridge H. Subcortical functional reorganization due to early blindness. *J Neurophysiol.* (2015) 113:2889–99. doi: 10.1152/jn.01031.2014
75. Stiles N, Patel VR, Weiland JD. Multisensory perception in argus II retinal prosthesis patients: leveraging auditory-visual mappings to enhance prosthesis outcomes. *Vision Res.* (2021) 182:58–68. doi: 10.1016/j.visres.2021.01.008

Conflict of Interest: The authors declare that the research was conducted in the absence of any commercial or financial relationships that could be construed as a potential conflict of interest.

frontiers | Frontiers in Psychiatry

MINI REVIEW
published: 28 June 2022
doi: 10.3389/fpsyt.2022.954211

The Prominent Role of the Temporal Lobe in Premenstrual Syndrome and Premenstrual Dysphoric Disorder: Evidence From Multimodal Neuroimaging

Jingyi Long[1,2,3†], *Yuejie Wang*[1,2†], *Lianzhong Liu*[1,2,3*] *and Juan Zhang*[1,2,3*]

[1] Wuhan Mental Health Center, Wuhan, China, [2] Affiliated Wuhan Mental Health Center, Tongji Medical College of Huazhong University of Science and Technology, Wuhan, China, [3] Research Center for Psychological and Health Sciences, China University of Geosciences, Wuhan, China

OPEN ACCESS

Edited by:
Qinji Su,
Guangxi Medical University, China

Reviewed by:
Hongxian Shen,
Central South University, China
Xuyi Wang,
Central South University, China

***Correspondence:**
Lianzhong Liu
184923047@qq.com
Juan Zhang
1365716662@qq.com

†These authors have contributed equally to this work and share first authorship

Specialty section:
This article was submitted to Neuroimaging and Stimulation, a section of the journal Frontiers in Psychiatry

Received: 27 May 2022
Accepted: 08 June 2022
Published: 28 June 2022

Citation:
Long JY, Wang YJ, Liu LZ and Zhang J (2022) The Prominent Role of the Temporal Lobe in Premenstrual Syndrome and Premenstrual Dysphoric Disorder: Evidence From Multimodal Neuroimaging. Front. Psychiatry 13:954211. doi: 10.3389/fpsyt.2022.954211

Premenstrual syndrome (PMS) is a group of psychological, physical, and behavioral symptoms that recur with the menstrual cycle, usually occurring a few days before menstruation and ceasing with the onset of menstruation. Premenstrual dysphoric disorder (PMDD) is a severe form of PMS that has been included in a subcategory of depression in the Diagnostic and Statistical Manual of Mental Disorders (DSM-V) according to the latest diagnostic criteria. Patients usually present with mild to moderate emotional and physical symptoms that affect their routine work, social activities, and family lives. The pathogenesis of PMDD remains unclear, and some researchers believe that it is related to fluctuations in ovarian hormone levels. However, the details of the interrelationships and regulating effects between ovarian hormones, symptoms, and the brain need to be more comprehensively determined. Recent studies have revealed some novel findings on PMS and PMDD based on brain morphology, function, and metabolism. Additionally, multiple studies have suggested that PMS and PMDD are closely related to brain structural and functional variations in certain core temporal lobe regions, such as the amygdala and hippocampus. We summarized neuroimaging studies of PMS and PMDD related to the temporal lobe by retrospectively reviewing relevant literature over the past decade. This review contributes to further clarifying the significant role of the temporal lobe in PMS and PMDD and understanding the neurochemical links between hormones, symptoms, and the brain.

Keywords: premenstrual syndrome, premenstrual dysphoric disorder, temporal lobe, magnetic resonance imaging, multimodal neuroimaging

INTRODUCTION

Estrogen and progesterone have far-reaching effects on females throughout their lifespan (1). Many female psychiatric disorders are related to reproductive events, such as pubertal depression, premenstrual dysphoric disorder (PMDD), and postpartum depression (2, 3). Approximately 85% of females have experienced mild premenstrual symptoms at least once (4), and 57% of women

of childbearing age experienced mild "anger/irritability" or "tearfulness/mood swings" during the premenstrual period (5). About 30–40% of women suffer from premenstrual syndrome (PMS) (6, 7), and 3–8% of females suffer from PMDD (8). PMS incidence is approximately 21.1% in China, and the incidence of PMDD is 2.1% (9). The symptoms range across mental, physical, and behavioral dimensions (10), and difficulty in regulating emotion is the clinical manifestation (4, 6, 11, 12). Remarkably, PMDD is a relatively stable and disabling disease that usually impacts patients' occupational activities, interpersonal relationships, social life, and family life (6, 13) and is responsible for 14.5 million disability-adjusted life years in the United States (8). As a disorder with familial risk, it displays 44 to 56% heritability (14, 15), and the global incidence and associated suicide rate have been continuously increasing (16, 17). In 2013, the American Psychiatric Association classified PMDD as a subcategory of depressive disorders in the Diagnostic and Statistical Manual of Mental Disorders (DSM-V) (4, 18). Currently, diagnosis mainly depends on self-rating scales such as the Daily Record of Severity of Problems. Nevertheless, this diagnostic model is also prone to misdiagnosis of patients (11). Therapeutic modalities include pharmacological, non-pharmacological, and surgical approaches. Usually, selective serotonin reuptake inhibitors are the first-line treatment for PMDD, and ovariectomy is the recommended plan following failure of conservative treatments (6, 10).

In the past three decades, the application of modern science and technology to investigate PMS and PMDD has lagged significantly behind that of other diseases. Today, while neuroimaging research is starting to be applied to these disorders, the neuropathological mechanisms are unclear (11). Even so, mounting evidence has confirmed that certain temporal lobe regions, such as the amygdala and hippocampus, are the most vulnerable regions in PMS and PMDD. This indicates that the temporal lobes have a prominent role in the pathogenesis of PMS and PMDD (19). Furthermore, relevant findings are being continuously updated. Hence, it is indispensable to conduct retrospective analyses and collate results from the most up-to-date literature. Aiming to provide the latest reference for a more comprehensive and in-depth understanding of PMS and PMDD, the present mini-review summarized relevant studies from recent years. These findings are summarized in **Table 1**.

TABLE 1 | Summary of findings of the neuroimaging studies in the menstrual cycle, PMS, or PMDD associated with the temporal lobe.

Subjects	Mode	Findings/results	References/year
Healthy women	fMRI	Eigenvector centrality in the hippocampus heightened during the LP.	(20) 2020
	fMRI	Irrespective of the task, estradiol boosted hippocampal activation during the pre-ovulatory cycle phase.	(21) 2019
	fMRI	The amygdala and salience network connectivity increased with higher endogenous and synthetic hormone levels.	(22) 2018
	DTI	FA values in the bilateral hippocampus had a significant positive correlation with estrogen.	(23) 2016
	fMRI & sMRI	FC enhanced between the hippocampi and the bilateral superior parietal lobe in the late FP; the bilateral hippocampal volume increased in late FP than in early FP.	(24) 2015
	fMRI	The amygdala response activity increased in the mid-LP; the right anterior hippocampus activity increased in early PF than LP.	(25) 2014
	sMRI	Gray matter volume of the left amygdala increased during the premenstrual phase than in late FP.	(26) 2013
Women with PMS	fMRI & sMRI	The volume of the bilateral amygdalae increased; FC increased between the amygdala and the right temporal pole and decreased between the bilateral amygdalae and the right hippocampus.	(27) 2018
	sMRI	PMS patients exhibited increased subcortical volumes of the amygdala.	(28) 2018
	fMRI	The fALFF value of the left hippocampus and left inferior temporal cortex increased at LP.	(29) 2017
	fMRI	FC between the left medial/superior temporal gyri and precentral gyrus within the DMN was enhanced; FC between the middle frontal and parahippocampal gyrus decreased.	(30) 2015
Women with PMDD	DTI	FA value increased in the left uncinate fasciculus; volume in the right uncinate fasciculus increased.	(31) 2022
	fMRI	PMDD women had elevated ReHo in the temporal lobe (BA42).	(32) 2021
	fMRI	FC of the anterior temporal lobe decreased across menstrual phases.	(33) 2020
	fMRI	FC of the left middle temporal gyrus and left ECN were significantly enhanced; FC of the left amygdala and cingulate cortex heightened during the FP vs. LP.	(34) 2019
	fMRI & sMRI	FC increased between the left hippocampus and right frontal cortex and decreased between the right hippocampus and right premotor cortex in BDPMDD vs. BD; cortical thickness of the right middle temporal decreased and increased in the left superior temporal gyri BDPMDD vs. BD.	(35) 2018
	fMRI	The amygdala reactivity increased to social stimuli in the LP; altered amygdala reactivity correlated positively with changes in progesterone levels.	(36) 2014
	DTI	Gray matter density significantly increased in the hippocampal cortex and decreased in the parahippocampal gyrus.	(37) 2012
	fMRI	The bilateral amygdala reactivities increased in FP and positively correlated with progesterone serum concentrations; the right amygdala reactivity positively correlated with depression scores in the LP.	(38) 2012

ARTICLE TYPES

Mini-Review.

MANUSCRIPT FORMATTING

Critical Regions of the Temporal Lobe in PMS and PMDD

Amygdala

It is well-known that the medial temporal lobe (MTL) includes the amygdala, hippocampal region, and entorhinal cortex and is responsible for memory and emotion processing (39). Extensive research has shown that the amygdala exhibits variation in structural and functional tendencies during the menstrual cycle in healthy women (22, 26, 40, 41). In other words, ovarian hormones can trigger the remodeling of the amygdala. For example, structural magnetic resonance imaging (sMRI) analyses demonstrated an increase in gray matter volume of the amygdala from the late luteal phase (LP) to the late follicular phase (FP) in healthy subjects (26). In addition, menstrual cycle-related variations in gray matter volume in the amygdala were associated with the severity of negative affect (19). Furthermore, functional magnetic resonance imaging (fMRI) research showed that progesterone selectively increased amygdala reactivity and regulated the functional coupling of the amygdala with some distant brain regions (22, 40, 41). These alterations may involve regulatory feedback mechanisms related to the menstrual cycle. In contrast, morphological measurements in PMS patients, compared with healthy individuals, indicated significantly enlarged subcortical volumes in the bilateral amygdala (27, 28). Moreover, several studies have verified that enhanced functional activity of the amygdala correlated with emotion dysregulation such as degree of anxiety and depression in LP (12, 38). In terms of functional connectivity (FC), FC between the right amygdala and left anterior cingulate cortex and between the right precentral gyrus and left medial prefrontal cortex exhibited positive correlations with the severity of premenstrual symptoms in PMS females (27). In PMDD women, FC between the left amygdala and cingulate cortex and between the right amygdala and the middle frontal gyrus was markedly strengthened in the FP compared with the LP (34).

The amygdala is located deep in the MTL and plays an essential role in the limbic system and central emotional circuitry (27). Its function involves memory, arousal, alertness, and attention, especially in emotion processing and pain (42–44). Previous findings have shown that anxiety (45), depression (46), and acute and chronic pain (44, 47) could induce abnormalities in the amygdala. Furthermore, the structural and functional alterations of the amygdala in PMS and PMDD are closely associated with emotional regulation (33). Sufficient research evidence suggests that fluctuations in sex hormones, especially progesterone, may be a pivotal factor in brain structural remodeling (2, 38). Given that emotional instability is a core symptom of PMS and PMDD and the amygdala plays a vital role in emotional processing, it is not difficult to explain why neuroimaging abnormalities of the amygdala are so prevalent in patients. The critical question is, how exactly do sex hormones affect the brain? Currently, researchers generally agree that damage to the amygdala leads to aberrations in top-down inhibition processes in the limbic system, which is the core pathological mechanism of PMDD (12, 19, 38, 48). Heightened amygdala responsiveness to social (36) and negative emotional (49) stimuli in PMDD patients confirms the breakdown of another aspect of this inhibitory regulation. Concurrent research on hormones, symptoms, and function surprisingly found that concentrations of sex hormones significantly influence the severity of symptoms and brain activity (36, 38, 48). These findings collectively support the notion that this disruption in top-down inhibition may be the key link in the pathogenesis of PMDD. Although this is the most mainstream academic view on PMDD, there is still some controversy. For instance, Pessoa proposed that the key to emotion regulation is not the limbic system but interactions spanning the entire neuroaxis of a network model of the emotional brain. This network mainly constitutes a functional integration system and emphasizes that abnormal interactions among multiple brain regions lead to PMDD rather than giving the amygdala dominant status in the limbic system (43).

Hippocampus and Parahippocampal Gyrus

More recent evidence has shown that the hippocampus is a rich-club hub and the most sensitive region to menstrual cycle changes (50). In healthy females, the hippocampus displayed more intense reactivity during cognitive and affective processes during FP (21, 24), and the responses of the hippocampus were strengthened in the late FP and mid-LP compared with the early FP and late LP during an affective task (25, 51). At the structural level, gray matter volume in the bilateral hippocampi increased in the late FP compared with the early FP (24), and an enlarged volume from LP to FP was positively related to improvements in verbal memory performance (52). Moreover, serum concentrations of estradiol positively correlated with the volume size and fractional anisotropy (FA) values in the hippocampus (23). Overall, it can clearly be seen that the level of estradiol is positively correlated with functional activity (21, 51), volume (24), and white matter integrity (23) of the hippocampus. In contrast, patients with PMDD presented more significantly increases in gray matter density in the hippocampus and decreases in gray matter density in the parahippocampal gyrus than healthy women (37). During the LP, functional activities of the left hippocampus and left inferior temporal cortex were clearly enhanced in PMS (29). Additionally, FC between the right parahippocampal gyrus and middle frontal gyrus in PMS females was weakened (30). It is worth noting that patients with bipolar disorder comorbid with PMDD (BDPMDD) also exhibited diverse abnormalities in FC, such as an enhancement between the left hippocampus and left inferior temporal cortex and a decrease between the right hippocampus and right premotor cortex (35). To date, numerous human and animal studies have confirmed that estrogen has the potential to modify the structure, metabolism, and function of the hippocampus.

How do sex hormones act on the hippocampus? These actions are mainly due to the neurotrophic influence of estradiol (53) and the synaptic remodeling and energy homeostasis

effects of progesterone (54). Both estrogen-dependent synaptic remodeling (50) and progesterone-dependent enhancements in synaptic density (54) have been observed in the hippocampus. Indeed, ovarian gonadal hormones can pass through the blood-brain barrier and subsequently affect mood and behavioral patterns by regulating neural activity (2). Notably, sex hormones can profoundly affect the hypothalamus-pituitary-adrenal (HPA) axis and neurotransmitters such as serotonin, dopaminergic, and γ-aminobutyric acid (GABA) (55). These substances are all involved in affective and cognitive processes and in the pathogenesis of depressive disorders (55–57). A rat model of premenstrual depression found that GABA and allopregnanolone expression levels decreased in the hippocampus and that depressive-like symptoms disappeared after ovariectomy and relapsed after hormone priming therapy (58). These findings are in alignment with the theory that neuronal activity in patients with depressive symptoms is being influenced by GABA-mediated inhibition.

Another key question is why the amygdala and hippocampal region are the most susceptible regions in PMS and PMDD. In brief, the amygdala and hippocampus are potential targets of sex hormone effects (50). There is an extensive distribution of estradiol and progesterone receptors in the limbic system, and these receptors are the most densely concentrated in the neurons and glial cells of the amygdala and hippocampus (50, 59). Therefore, ovarian hormones and neurotransmitters and their receptors are crucial factors in inducing structural and functional abnormalities in the amygdala and hippocampal region and subsequently triggering symptoms of PMS and PMDD. As the most vulnerable nodes, the amygdala and hippocampus are expected to be specific neuroimaging targets to assist in diagnosing and treating PMS and PMDD. For instance, it may be that women who do not respond to conservative therapy and refuse hysterectomy and oophorectomy may respond to transcranial magnetic stimulation of these regions, which may alleviate or eradicate symptoms.

Other Regions of the Temporal Lobe

In addition to the MTL, other temporal lobe regions are also relevant in PMS and PMDD. Fractional amplitude of low-frequency fluctuation (fALFF) values in the left inferior temporal cortex and left hippocampus were higher in PMS females than in healthy individuals (29). Regional homogeneity (ReHo) in the left inferior temporal cortex was more intense during the LP in PMS females than in healthy women (60). With exposure to emotional stimuli, functional activity in the temporal lobe in PMDD patients was activated to a greater degree than in controls (32). Notably, increased connectivity between the left medial temporal gyrus (MTG) and precentral gyrus negatively correlated with the severity of depression in PMS (30). Furthermore, PMDD patients exhibited hyperconnectivity between the middle temporal gyrus and right amygdala in the FP compared with level of connectivity in the LP (34). Nonetheless, another study observed different manifestations: reduced cortical connectivity across the whole brain, especially within the temporal lobe, and mediation analysis further indicated that 57% of those connections were related to emotional and behavioral symptoms in PMDD (33). The above findings unanimously indicated that the abnormal connectome of the temporal gyrus might mediate deficits in emotion regulation in PMS and PMDD.

Additionally, other evidence suggests that the fusiform gyrus also changes with the menstrual cycle in healthy women. An fMRI study reported abnormal functional activity in the amygdala, fusiform gyrus, inferior temporal gyrus, and middle temporal gyrus (61). Progesterone has been shown to trigger decreases in neural activity in the amygdala and fusiform gyrus, whereas it increases the hippocampal response (62). Moreover, in an emotional recognition task, hypoconnectivity between the fusiform gyrus and amygdala was directly linked to progesterone in healthy subjects (41). However, the existing studies on PMS and PMDD rarely include the fusiform gyrus, and thus, specific neuroimaging characterizations are lacking.

Temporal Lobe-Related Neural Circuitry in PMS and PMDD

Regions with different properties and locations in the brain form neural circuits through various forms of complex connections. When a particular node is abnormal, other brain regions within the circuit are likely to be disrupted, thereby affecting the overall function of the circuit. In fact, the amygdala and hippocampus occupy core positions in several pivotal neural circuits, such as the hippocampus-amygdala, hippocampus-entorhinal cortex, hippocampus-prefrontal circuit, amygdala-prefrontal cortex, and amygdala-thalamus circuits (63).

Of note, significant variations in several circuits assessed with neuroimaging have also been found in PMS and PMDD. Taking the hippocampus-amygdala circuit as an example, functional activity in this circuit basically coincides with fluctuating levels of ovarian gonadal hormones across menstrual cycle phases in healthy females (61). Namely, the hippocampus-amygdala circuit was positively associated with estradiol levels. As previously described, progesterone and its derivatives regulate emotion and memory processing by modulating the activity of the amygdala, which in turn affects the hippocampus and fusiform gyrus, which are also related to this neural circuit (62). PMS females exhibited weakened FC between the amygdala and right hippocampus and increased FC between the amygdala and right temporal lobe compared with healthy women (27). The above statement is affiliated with the functioning of the hippocampus-amygdala circuit. Particularly, in addition to the amygdala-hippocampus circuit, previous results in PMS and PMDD have focused on the amygdala-prefrontal cortex circuit. Under physiological conditions, the prefrontal lobe maintains bottom-up inhibitory effects on the amygdala and keeps the amygdala in a highly inhibited state, which is vital for maintaining normal emotional behavior. When exposed to estrogen and progestin, inhibitory effects of the prefrontal cortex on the amygdala are weakened, leading to overactivation of the amygdala, which can lead to premenstrual symptoms (12, 19, 38, 48). It is noteworthy that a brain structure study found that the central circuitry of emotion, which includes the amygdala, lateral prefrontal cortex, and orbitofrontal cortex, participated in the pathogenesis of PMS (28). By its nature, abnormal activation of the endocrine system

in women and its effects on cognitive and affective circuits may underlie the pathogenesis of PMS and PMDD (33). Admittedly, existing research on neural circuits of PMS and PMDD is insufficient, and a more meticulous analysis of the relevant neural circuits is urgently needed.

Temporal Lobe-Related Brain Networks in PMS and PMDD

Besides neural circuits, brain regions also constitute neural networks—the execution and maintenance of normal function in bodies rely on homeostasis within and coordination between these networks (64, 65). Previous neuroimaging studies have investigated features of several brain networks in healthy women during the menstrual cycle, but few have focused on PMS and PMDD (33). Earlier findings demonstrated that estrogen and progesterone could mediate sensitivity of mood, cognition, and impairments in brain networks (20). Recently, a refined study gathered MRI data from a woman for 30 consecutive days and repeated it a year later: the recombination and rhythm of the human brain network involved in the menstrual cycle were discovered, and it was confirmed that estradiol plays a crucial role in the brain network (66). Regarding the default mode network (DMN), multiple FC abnormalities, including connections with the parahippocampal gyrus, medial superior temporal gyrus, and MTG, were found in women with PMS (30). In executive control networks (ECN), the connectivity between the left ECN and left middle temporal gyrus was significantly enhanced and closely correlated with emotion regulation in patients with PMDD (34). This finding indicated that the intrinsic network dynamics in the left ECN differ between PMDD patients and healthy subjects. Similarly, a network dynamics study found that fluctuations in ovarian hormone levels during the menstrual cycle affect core brain regions, which may profoundly impact the dynamics of the whole brain network (67). More importantly, a comprehensive topological rearrangement took place in brain networks in healthy women under the influence of sex hormones (31). Topological changes were also present in PMS. Comparing topological parameters in patients from mid-FP to late-LP and healthy subjects demonstrated reduced segregation and enhanced integration among functional brain networks (33). In particular, the specific network for emotional regulation consisting of the amygdala, hippocampus, thalamus, and ventral striatum was closely related to the evaluation and expression of emotion (68). This discovery provided further clues that revealed interactive effects between emotions, brain networks, and sex hormone fluctuations. Moreover, structural research has verified that the fiber tracts responsible for connecting the temporal lobe showed significant microstructural changes, and the FA value in the superior longitudinal fasciculus positively correlated with

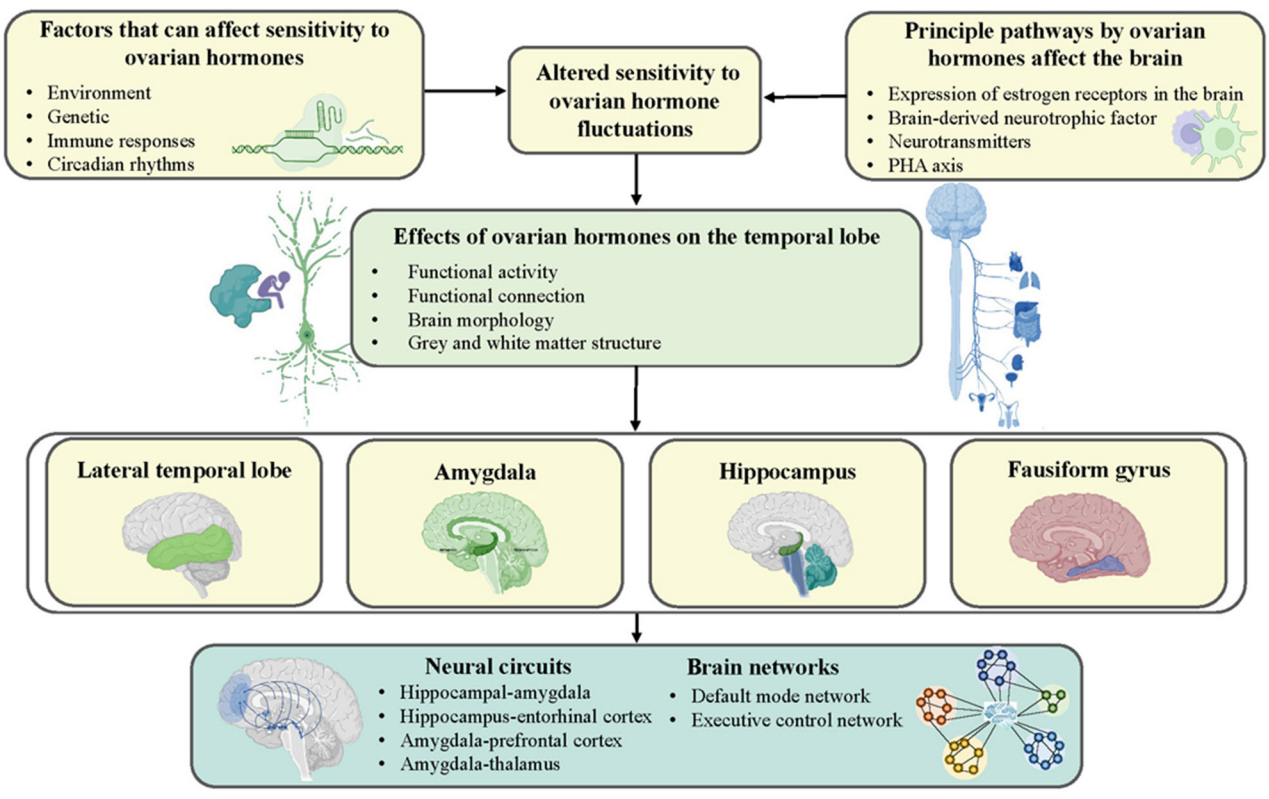

FIGURE 1 | Schematic representation of possible mechanisms by which ovarian hormones contribute to the development of PMS and PMDD. Genetics, environment, immune response, and circadian rhythms increase women's sensitivity to ovarian hormones and shape the temporal lobe by affecting neurotransmitters and hormonal systems.

the severity of premenstrual symptoms in those with PMDD (69). Conversely, unlike other psychiatric disorders, PMDD patients had higher structural integrity of the white matter. This opposite performance could be explained by the neuroprotection of sex hormones positively shaping brain structure in hormone-dependent diseases (69).

Overall, insight into the susceptibility and plasticity of network dynamics and topology is necessary to comprehensively explore the neuropathological mechanisms underlying PMS and PMDD (50, 66). However, existing studies of brain network dynamics seriously lack convincing evidence, especially regarding the structural aspects. On the bright side, existing findings evaluating brain networks have mainly converged on temporal lobe-related regions such as the amygdala and hippocampus, which coincided with research on independent brain regions. All these mechanisms are illustrated in **Figure 1**.

CONCLUSION

In general, harmonious covariations between the metabolism, structure, and function of the brain and ovarian gonadal hormone levels during the menstrual cycle exist in healthy females. In contrast, the diverse array of inappropriate manifestations and remodeling of metabolism, structure, and function have occurred in multiple regions in PMS and PMDD women. However, there was a high level of heterogeneity in the current results due to differences in MRI scanning equipment and sequence parameters, analysis methods, and the menstrual phase in which women were scanned. Nevertheless, the existing neuroimaging findings showed high consistency regarding the involvement of temporal lobe regions, such as the amygdala and hippocampus, which confirms the prominent role of the temporal lobe in PMS and PMDD. Furthermore, genetics and environmental factors, abnormal immune responses, and changes in circadian rhythms trigger increased sensitivity to sex hormones, which in turn affect other neurotransmitters and hormonal systems (e.g., brain-derived neurotrophic factor), thereby influencing the temporal lobe and further affecting mental health and behavior (70–72). Therefore, in near future, it is essential to perform research at multiple time points using multimodal neuroimaging techniques, and more attention is warranted on biomarkers, specific neural circuits, structural-functional coupling, vulnerability and controllability of network dynamics, and comorbidity with other psychiatric diseases. Similarly, specific distinctions of menstrual cycle stages and more detailed analyses of brain subregions are needed. If these types of studies can be performed, they will provide a valid foundation of evidence to guide the individualized identification, classification, and treatment of PMS and PMDD.

AUTHOR CONTRIBUTIONS

All authors contributed to the article and approved the submitted version.

FUNDING

This work was supported by the Health Commission of Wuhan scientific research project (WX19D62 to LL).

ACKNOWLEDGMENTS

The authors thank all females affected by PMS or PMDD who make our research meaningful.

REFERENCES

1. Bakker J. The sexual differentiation of the human brain: role of sex hormones vs. sex chromosomes. *Curr Top Behav Neurosci.* (2019) 43:45–67. doi: 10.1007/7854_2018_70
2. Stickel S, Wagels L, Wudarczyk O, Jaffee S, Habel U, Schneider F, et al. Neural correlates of depression in women across the reproductive lifespan—an fmri review. *J Affect Disord.* (2019) 246:556–70. doi: 10.1016/j.jad.2018.12.133
3. Slyepchenko A, Minuzzi L, Frey BN. Comorbid premenstrual dysphoric disorder and bipolar disorder: a review. *Front Psychiatry.* (2021) 12:719241. doi: 10.3389/fpsyt.2021.719241
4. *Diagnostic and Statistical Manual of Mental Disorders.* 5th Ed. Arlington, VA: American Psychiatric Association (2013).
5. Tschudin S, Bertea PC, Zemp E. Prevalence and predictors of premenstrual syndrome and premenstrual dysphoric disorder in a population-based sample. *Arch Womens Ment Health.* (2010) 13:485–94. doi: 10.1007/s00737-010-0165-3
6. Ryu A, Kim TH. Premenstrual syndrome: a mini review. *Maturitas.* (2015) 82:436–40. doi: 10.1016/j.maturitas.2015.08.010
7. Tolossa FW, Bekele ML. Prevalence, impacts and medical managements of premenstrual syndrome among female students: cross-sectional study in college of health sciences, Mekelle university, Mekelle, Northern Ethiopia. *BMC Womens Health.* (2014) 14:52. doi: 10.1186/1472-6874-14-52
8. Halbreich U, Borenstein J, Pearlstein T, Kahn LS. The prevalence, impairment, impact, and burden of Premenstrual dysphoric disorder (Pms/Pmdd). *Psychoneuroendocrinology.* (2003) 28:1–23. doi: 10.1016/S0306-4530(03)00098-2
9. Qiao M, Zhang H, Liu H, Luo S, Wang T, Zhang J, et al. Prevalence of premenstrual syndrome and premenstrual dysphoric disorder in a population-based sample in China. *Eur J Obstet Gynecol Reprod Biol.* (2012) 162:83–6. doi: 10.1016/j.ejogrb.2012.01.017
10. Lanza di Scalea T, Pearlstein T. Premenstrual dysphoric disorder. *Med Clin North Am.* (2019) 103:613–28. doi: 10.1016/j.mcna.2019.02.007
11. Epperson CN, Steiner M, Hartlage SA, Eriksson E, Schmidt PJ, Jones I, et al. Premenstrual dysphoric disorder: evidence for a new category for Dsm-5. *Am J Psychiatry.* (2012) 169:465–75. doi: 10.1176/appi.ajp.2012.11081302
12. Petersen N, Ghahremani DG, Rapkin AJ, Berman SM, Liang L, London ED. Brain activation during emotion regulation in women with premenstrual dysphoric disorder. *Psychol Med.* (2018) 48:1795–802. doi: 10.1017/S0033291717003270
13. Hylan TR, Sundell K, Judge R. The impact of premenstrual symptomatology on functioning and treatment-seeking behavior: experience from the United States, United Kingdom, and France. *J Women's Health Gend-Based Med.* (1999) 8:1043–52. doi: 10.1089/jwh.1.1999.8.1043
14. Kendler KS, Karkowski LM, Corey LA, Neale MC. Longitudinal population-based twin study of retrospectively reported premenstrual symptoms and lifetime major depression. *Am J Psychiatry.* (1998) 155:1234–40. doi: 10.1176/ajp.155.9.1234
15. Treloar SA, Heath AC, Martin NG. Genetic and environmental influences on premenstrual symptoms in an Australian twin sample. *Psychol Med.* (2002) 32:25–38. doi: 10.1017/S0033291701004901

16. Gao M, Gao D, Sun H, Cheng X, An L, Qiao M. Trends in research related to premenstrual syndrome and premenstrual dysphoric disorder from 1945 to 2018: a bibliometric analysis. *Front Public Health.* (2021) 9:596128. doi: 10.3389/fpubh.2021.596128
17. Wittchen HU, Becker E, Lieb R, Krause P. Prevalence, incidence and stability of premenstrual dysphoric disorder in the community. *Psychol Med.* (2002) 32:119–32. doi: 10.1017/S0033291701004925
18. Francesmonneris A, Pincus H, First M. *Diagnostic and Statistical Manual of Mental Disorders: Dsm-V*. American Psychiatric Association (2013).
19. Dubol M, Epperson CN, Sacher J, Pletzer B, Derntl B, Lanzenberger R, et al. Neuroimaging the menstrual cycle: a multimodal systematic review. *Front Neuroendocrinol.* (2021) 60:100878. doi: 10.1016/j.yfrne.2020.100878
20. Toffoletto S, Lanzenberger R, Gingnell M, Sundström-Poromaa I, Comasco E. Emotional and cognitive functional imaging of estrogen and progesterone effects in the female human brain: a systematic review. *Psychoneuroendocrinology.* (2014) 50:28–52. doi: 10.1016/j.psyneuen.2014.07.025
21. Pletzer B, Harris TA, Scheuringer A, Hidalgo-Lopez E. The cycling brain: menstrual cycle related fluctuations in hippocampal and fronto-striatal activation and connectivity during cognitive tasks. *Neuropsychopharmacology.* (2019) 44:1867–75. doi: 10.1038/s41386-019-0435-3
22. Engman J, Sundström Poromaa I, Moby L, Wikström J, Fredrikson M, Gingnell M. Hormonal cycle and contraceptive effects on amygdala and salience resting-state networks in women with previous affective side effects on the pill. *Neuropsychopharmacology.* (2018) 43:555–63. doi: 10.1038/npp.2017.157
23. Barth C, Steele CJ, Mueller K, Rekkas VP, Arélin K, Pampel A, et al. *In-Vivo* dynamics of the human hippocampus across the menstrual cycle. *Sci Rep.* (2016) 6:32833. doi: 10.1038/srep32833
24. Lisofsky N, Mårtensson J, Eckert A, Lindenberger U, Gallinat J, Kühn S. Hippocampal volume and functional connectivity changes during the female menstrual cycle. *Neuroimage.* (2015) 118:154–62. doi: 10.1016/j.neuroimage.2015.06.012
25. Bayer J, Schultz H, Gamer M, Sommer T. Menstrual-cycle dependent fluctuations in ovarian hormones affect emotional memory. *Neurobiol Learn Mem.* (2014) 110:55–63. doi: 10.1016/j.nlm.2014.01.017
26. Ossewaarde L, van Wingen GA, Rijpkema M, Bäckström T, Hermans EJ, Fernández G. Menstrual cycle-related changes in amygdala morphology are associated with changes in stress sensitivity. *Hum Brain Mapp.* (2013) 34:1187–93. doi: 10.1002/hbm.21502
27. Deng D, Pang Y, Duan G, Liu H, Liao H, Liu P, et al. Larger volume and different functional connectivity of the amygdala in women with premenstrual syndrome. *Eur Radiol.* (2018) 28:1900–8. doi: 10.1007/s00330-017-5206-0
28. Liu P, Wei Y, Fan Y, Liao H, Wang G, Li R, et al. Cortical and subcortical changes in patients with premenstrual syndrome. *J Affect Disord.* (2018) 235:191–7. doi: 10.1016/j.jad.2018.04.046
29. Liao H, Duan G, Liu P, Liu Y, Pang Y, Liu H, et al. Altered fractional amplitude of low frequency fluctuation in premenstrual syndrome: a resting state fmri study. *J Affect Disord.* (2017) 218:41–8. doi: 10.1016/j.jad.2017.04.045
30. Liu Q, Li R, Zhou R, Li J, Gu Q. Abnormal resting-state connectivity at functional mri in women with premenstrual syndrome. *PLoS ONE.* (2015) 10:e0136029. doi: 10.1371/journal.pone.0136029
31. Arélin K, Mueller K, Barth C, Rekkas PV, Kratzsch J, Burmann I, et al. Progesterone mediates brain functional connectivity changes during the menstrual cycle-a pilot resting state mri study. *Front Neurosci.* (2015) 9:44. doi: 10.3389/fnins.2015.00044
32. Gao M, Qiao M, An L, Wang G, Wang J, Song C, et al. Brain reactivity to emotional stimuli in women with premenstrual dysphoric disorder and related personality characteristics. *Aging.* (2021) 13:19529–41. doi: 10.18632/aging.203363
33. Dan R, Reuveni I, Canetti L, Weinstock M, Segman R, Goelman G, et al. Trait-related changes in brain network topology in premenstrual dysphoric disorder. *Horm Behav.* (2020) 124:104782. doi: 10.1016/j.yhbeh.2020.104782
34. Petersen N, Ghahremani DG, Rapkin AJ, Berman SM, Wijker N, Liang L, et al. Resting-state functional connectivity in women with Pmdd. *Transl Psychiatry.* (2019) 9:339. doi: 10.1038/s41398-019-0670-8
35. Syan SK, Minuzzi L, Smith M, Costescu D, Allega OR, Hall GBC, et al. Brain structure and function in women with comorbid bipolar and premenstrual dysphoric disorder. *Front Psychiatry.* (2017) 8:301. doi: 10.3389/fpsyt.2017.00301
36. Gingnell M, Ahlstedt V, Bannbers E, Wikström J, Sundström-Poromaa I, Fredrikson M. Social stimulation and corticolimbic reactivity in premenstrual dysphoric disorder: a preliminary study. *Biol Mood Anxiety Disord.* (2014) 4:3. doi: 10.1186/2045-5380-4-3
37. Jeong HG, Ham BJ, Yeo HB, Jung IK, Joe SH. Gray matter abnormalities in patients with premenstrual dysphoric disorder: an optimized voxel-based morphometry. *J Affect Disord.* (2012) 140:260–7. doi: 10.1016/j.jad.2012.02.010
38. Gingnell M, Morell A, Bannbers E, Wikström J, Sundström Poromaa I. Menstrual cycle effects on amygdala reactivity to emotional stimulation in premenstrual dysphoric disorder. *Horm Behav.* (2012) 62:400–6. doi: 10.1016/j.yhbeh.2012.07.005
39. Squire LR, Stark CE, Clark RE. The medial temporal lobe. *Annu Rev Neurosci.* (2004) 27:279–306. doi: 10.1146/annurev.neuro.27.070203.144130
40. Dan R, Canetti L, Keadan T, Segman R, Weinstock M, Bonne O, et al. Sex differences during emotion processing are dependent on the menstrual cycle phase. *Psychoneuroendocrinology.* (2019) 100:85–95. doi: 10.1016/j.psyneuen.2018.09.032
41. van Wingen GA, van Broekhoven F, Verkes RJ, Petersson KM, Bäckström T, Buitelaar JK, et al. Progesterone selectively increases amygdala reactivity in women. *Mol Psychiatry.* (2008) 13:325–33. doi: 10.1038/sj.mp.4002030
42. Tye KM, Prakash R, Kim SY, Fenno LE, Grosenick L, Zarabi H, et al. Amygdala circuitry mediating reversible and bidirectional control of anxiety. *Nature.* (2011) 471:358–62. doi: 10.1038/nature09820
43. Pessoa L. A network model of the emotional brain. *Trends Cogn Sci.* (2017) 21:357–71. doi: 10.1016/j.tics.2017.03.002
44. Simons LE, Moulton EA, Linnman C, Carpino E, Becerra L, Borsook D. The human amygdala and pain: evidence from neuroimaging. *Hum Brain Mapp.* (2014) 35:527–38. doi: 10.1002/hbm.22199
45. Etkin A, Wager TD. Functional neuroimaging of anxiety: a meta-analysis of emotional processing in ptsd, social anxiety disorder, and specific phobia. *Am J Psychiatry.* (2007) 164:1476–88. doi: 10.1176/appi.ajp.2007.07030504
46. Murray EA, Wise SP, Drevets WC. Localization of dysfunction in major depressive disorder: prefrontal cortex and amygdala. *Biol Psychiatry.* (2011) 69:e43–54. doi: 10.1016/j.biopsych.2010.09.041
47. Bornhövd K, Quante M, Glauche V, Bromm B, Weiller C, Büchel C. Painful stimuli evoke different stimulus-response functions in the amygdala, prefrontal, insula and somatosensory cortex: a single-trial fmri study. *Brain.* (2002) 125:1326–36. doi: 10.1093/brain/awf137
48. Comasco E, Sundström-Poromaa I. Neuroimaging the menstrual cycle and premenstrual dysphoric disorder. *Curr Psychiatry Rep.* (2015) 17:77. doi: 10.1007/s11920-015-0619-4
49. Protopopescu X, Tuescher O, Pan H, Epstein J, Root J, Chang L, et al. Toward a functional neuroanatomy of premenstrual dysphoric disorder. *J Affect Disord.* (2008) 108:87–94. doi: 10.1016/j.jad.2007.09.015
50. McEwen BS, Milner TA. Understanding the broad influence of sex hormones and sex differences in the brain. *J Neurosci Res.* (2017) 95:24–39. doi: 10.1002/jnr.23809
51. Albert K, Pruessner J, Newhouse P. Estradiol levels modulate brain activity and negative responses to psychosocial stress across the menstrual cycle. *Psychoneuroendocrinology.* (2015) 59:14–24. doi: 10.1016/j.psyneuen.2015.04.022
52. Protopopescu X, Butler T, Pan H, Root J, Altemus M, Polanecsky M, et al. Hippocampal structural changes across the menstrual cycle. *Hippocampus.* (2008) 18:985–8. doi: 10.1002/hipo.20468
53. Eberling JL, Wu C, Tong-Turnbeaugh R, Jagust WJ. Estrogen- and tamoxifen-associated effects on brain structure and function. *Neuroimage.* (2004) 21:364–71. doi: 10.1016/j.neuroimage.2003.08.037
54. Acharya KD, Nettles SA, Sellers KJ, Im DD, Harling M, Pattanayak C, et al. The progestin receptor interactome in the female mouse hypothalamus: interactions with synaptic proteins are isoform specific and ligand dependent. *eNeuro.* (2017) 4: ENEURO.0272–17.2017. doi: 10.1523/ENEURO.0272-17.2017
55. Zsido RG, Villringer A, Sacher J. Using positron emission tomography to investigate hormone-mediated neurochemical changes across the female

lifespan: implications for depression. *Int Rev Psychiatry.* (2017) 29:580–96. doi: 10.1080/09540261.2017.1397607
56. Almey A, Milner TA, Brake WG. Estrogen receptors in the central nervous system and their implication for dopamine-dependent cognition in females. *Horm Behav.* (2015) 74:125–38. doi: 10.1016/j.yhbeh.2015.06.010
57. Borrow AP, Cameron NM. Estrogenic mediation of serotonergic and neurotrophic systems: implications for female mood disorders. *Prog Neuropsychopharmacol Biol Psychiatry.* (2014) 54:13–25. doi: 10.1016/j.pnpbp.2014.05.009
58. Wei S, Geng X, Li Z, Xu K, Hu M, Wu H, et al. A forced swim-based rat model of premenstrual depression: effects of hormonal changes and drug intervention. *Aging.* (2020) 12:24357–70. doi: 10.18632/aging.202249
59. Brinton RD, Thompson RF, Foy MR, Baudry M, Wang J, Finch CE, et al. Progesterone receptors: form and function in brain. *Front Neuroendocrinol.* (2008) 29:313–39. doi: 10.1016/j.yfrne.2008.02.001
60. Liao H, Pang Y, Liu P, Liu H, Duan G, Liu Y, et al. Abnormal spontaneous brain activity in women with premenstrual syndrome revealed by regional homogeneity. *Front Hum Neurosci.* (2017) 11:62. doi: 10.3389/fnhum.2017.00062
61. Dreher JC, Schmidt PJ, Kohn P, Furman D, Rubinow D, Berman KF. Menstrual cycle phase modulates reward-related neural function in women. *Proc Natl Acad Sci U S A.* (2007) 104:2465–70. doi: 10.1073/pnas.0605569104
62. van Wingen G, van Broekhoven F, Verkes RJ, Petersson KM, Bäckström T, Buitelaar J, et al. How progesterone impairs memory for biologically salient stimuli in healthy young women. *J Neurosci.* (2007) 27:11416–23. doi: 10.1523/JNEUROSCI.1715-07.2007
63. Cossart R, Khazipov R. How development sculpts hippocampal circuits and function. *Physiol Rev.* (2022) 102:343–78. doi: 10.1152/physrev.00044.2020
64. Gao Y, Wang M, Yu R, Li Y, Yang Y, Cui X, et al. Abnormal default mode network homogeneity in treatment-naive patients with first-episode depression. *Front Psychiatry.* (2018) 9:697. doi: 10.3389/fpsyt.2018.00697
65. Gao Y, Wang X, Xiong Z, Ren H, Liu R, Wei Y, et al. Abnormal fractional amplitude of low-frequency fluctuation as a potential imaging biomarker for first-episode major depressive disorder: a resting-state fmri study and support vector machine analysis. *Front Neurol.* (2021) 12:751400. doi: 10.3389/fneur.2021.751400
66. Pritschet L, Santander T, Taylor CM, Layher E, Yu S, Miller MB, et al. Functional reorganization of brain networks across the human menstrual cycle. *Neuroimage.* (2020) 220:117091. doi: 10.1016/j.neuroimage.2020.117091
67. Hidalgo-Lopez E, Mueller K, Harris T, Aichhorn M, Sacher J, Pletzer B. Human menstrual cycle variation in subcortical functional brain connectivity: a multimodal analysis approach. *Brain Struct Funct.* (2020) 225:591–605. doi: 10.1007/s00429-019-02019-z
68. Davey CG, Whittle S, Harrison BJ, Simmons JG, Byrne ML, Schwartz OS, et al. Functional brain-imaging correlates of negative affectivity and the onset of first-episode depression. *Psychol Med.* (2015) 45:1001–9. doi: 10.1017/S0033291714002001
69. Gu X, Dubol M, Stiernman L, Wikström J, Hahn A, Lanzenberger R, et al. White matter microstructure and volume correlates of premenstrual dysphoric disorder. *J Psychiatry Neurosci.* (2022) 47:E67–76. doi: 10.1503/jpn.210143
70. Comasco E, Hahn A, Ganger S, Gingnell M, Bannbers E, Oreland L, et al. Emotional fronto-cingulate cortex activation and brain derived neurotrophic factor polymorphism in premenstrual dysphoric disorder. *Hum Brain Mapp.* (2014) 35:4450–8. doi: 10.1002/hbm.22486
71. Hantsoo L, Epperson CN. Premenstrual dysphoric disorder: epidemiology and treatment. *Curr Psychiatry Rep.* (2015) 17:87. doi: 10.1007/s11920-015-0628-3
72. Rehbein E, Hornung J, Sundström Poromaa I, Derntl B. Shaping of the female human brain by sex hormones: a review. *Neuroendocrinology.* (2021) 111:183–206. doi: 10.1159/000507083

Conflict of Interest: The authors declare that the research was conducted in the absence of any commercial or financial relationships that could be construed as a potential conflict of interest.

frontiers | Frontiers in Psychiatry

ORIGINAL RESEARCH
published: 29 June 2022
doi: 10.3389/fpsyt.2022.950885

Vortioxetine Modulates the Regional Signal in First-Episode Drug-Free Major Depressive Disorder at Rest

Shihong Xiong[1†], Wei Li[2†], Yang Zhou[3], Hongwei Ren[4], Guorong Lin[3], Sheng Zhang[5*] and Xi Xiang[6*]*

[1] Department of Nephrology, Tianyou Hospital Affiliated to Wuhan University of Science and Technology, Wuhan, China, [2] Department of Otolaryngology-Head and Neck Surgery, Wuhan Asia General Hospital, Wuhan, China, [3] Wuhan Mental Health Center, Wuhan, China, [4] Department of Medical Imaging, Tianyou Hospital Affiliated to Wuhan University of Science and Technology, Wuhan, China, [5] Liyuan Hospital of Tongji Medical College, Huazhong University of Science and Technology, Wuhan, China, [6] Department of Spine and Orthopedics, Tianyou Hospital Affiliated to Wuhan University of Science and Technology, Wuhan, China

OPEN ACCESS

Edited by:
Qinji Su,
Guangxi Medical University, China

Reviewed by:
Xiaobing Jiang,
Huazhong University of Science and Technology, China
Jian Xu,
Hubei Minzu University, China

***Correspondence:**
Guorong Lin
424268936@qq.com
Sheng Zhang
42701213@qq.com
Xi Xiang
594074990@qq.com

[†] These authors have contributed equally to this work and share first authorship

Specialty section:
This article was submitted to Neuroimaging and Stimulation, a section of the journal Frontiers in Psychiatry

Received: 23 May 2022
Accepted: 08 June 2022
Published: 29 June 2022

Citation:
Xiong S, Li W, Zhou Y, Ren H, Lin G, Zhang S and Xiang X (2022) Vortioxetine Modulates the Regional Signal in First-Episode Drug-Free Major Depressive Disorder at Rest. Front. Psychiatry 13:950885. doi: 10.3389/fpsyt.2022.950885

Background: Previous studies on brain functional alterations associated with antidepressants for major depressive disorder (MDD) have produced conflicting results because they involved short treatment periods and a variety of compounds.

Methods: Resting-state functional magnetic resonance imaging scans were obtained from 25 first-episode drug-free patients with MDD and 25 healthy controls. The patients, who were treated with vortioxetine for 8 weeks, were scanned at two-time points (baseline and week 8 of treatment). The amplitude of low-frequency fluctuation (ALFF) in the imaging data was used to analyze local brain signal alterations associated with antidepressant treatment.

Results: Compared with the controls, the patients at baseline showed decreased ALFF values in the right inferior temporal gyrus and increased ALFF values in the left inferior cerebellum, right cingulate gyrus and postcentral gyrus. After 8 weeks of vortioxetine treatment, patients showed increased ALFF values in the bilateral cingulate gyrus, middle temporal gyrus, medial superior frontal gyrus, and inferior cerebellum.

Conclusion: This study provided evidence that vortioxetine modulates brain signals in MDD sufferers. These findings contribute to the understanding of how antidepressants effect brain function.

Keywords: major depressive disorder, MRI, amplitude of low-frequency fluctuation, vortioxetine, temporal lobe

INTRODUCTION

Major depressive disorder (MDD) is a global psychiatric disorder characterized by low mood, decreased interest, and loss of pleasure accompanied by marked cognitive decline (1–4). According to statistics from the World Health Organization, as of 2015, there were about 322 million people afflicted with depression in the world, accounting for 4.4% of the total population. There are more than 54 million MDD patients in China, and the lifetime prevalence rate is 6.9%. MDD was the third leading cause of disability globally in 2017 and is projected to be the predominant disease

burden by 2030 (5). MDD leads to obvious impairments in cognitive functions, such as executive function, memory, and learning (6, 7). Cognitive functions refer to processes that occur when acquiring, encoding, manipulating, extracting, and using sensory input during the cognition of objective things and includes perception, memory, thinking, and attention (8). Impaired cognitive function seriously affects the MDD patients' ability to learn, live, and work. Therefore, it is vital that we improve the treatment of cognitive function in patients with depression.

At present, antidepressant drugs have no known direct effect on cognitive function. Vortioxetine is a new type of antidepressant drug that (9), in 2013, was approved for marketing by the US FDA, and in November 2017, it was approved for marketing in China by the State Drug Administration for the treatment of adult depression. Clinical studies have shown that vortioxetine can simultaneously improve the symptoms and cognitive function of patients with depression and promote the recovery of their ability to carry out social roles (10, 11). The drug can increase the levels of norepinephrine (NE) and acetylcholine by antagonizing the 5-HT3 receptor, but this only leads to an indirect improvement in cognitive symptoms through the modification of depressive symptoms (12). However, the mechanism through which vortioxetine regulates the neural circuits of cognitive networks in the brain is unclear.

A large number of multimodal magnetic resonance studies have shown that the structures, functions, and neural circuits related to cognitive function are impaired in the brains of patients with depression (13, 14). For example, structural magnetic resonance studies have found that the integrity of white matter fibers in brain regions, such as the insula, temporal lobe, and posterior cingulate gyrus, is damaged and cortical thickness is thinned in patients with depression (15–17). In recent years, fMRI technology has also been rapidly applied in clinical research into depression (18–21). Resting-state functional magnetic resonance imaging is no less important than structural magnetic resonance imaging in diagnosing brain function diseases (22). A resting-state fMRI study found abnormal amplitude of low-frequency fluctuations (ALFF) signals in the left orbitofrontal-insula circuit in patients with MDD, and abnormal ALFF values were correlated with cognitive scores in patients with depression (23). Some studies have also found that abnormal ALFF values are related to the expression of the NET-Rs28386840 gene (24, 25). The findings of these imaging studies have also revealed many new perspectives on the neuroimaging mechanisms of depression.

In terms of depression research, the following issues remain unresolved. First, studies have used different designs and focused on various aspects of brain function and therefore produced different results. For this reason, a standard format is urgently needed. Resting-state fMRI has the potential to be a standard technique for fMRI studies on clinical populations, as it is relatively easy to perform and to prevent performance-confounding factors in clinical studies. Second, the brain function of patients with MDD is often affected by antidepressants and other treatments (26–28). Therefore, in this study, we selected first-episode untreated depression patients as research subjects to eliminate these confounding factors to a large extent.

The ALFF in the BOLD signal on rs-fMRI can characterize spontaneous brain functional activity and, therefore, is often used to evaluate brain diseases such as schizophrenia and depression (29–31). In recent years, the ALFF value has proven to be a potential predictive value for evaluating the treatment outcomes in MDD patients (31). We examined ALFF alterations at two-time points (baseline and week 8 of treatment) in first-episode drug-free MDD patients at rest. Based on previous studies that reported the modulating effect of vortioxetine on cognitive function and local brain signal (32), we hypothesized that vortioxetine modulates ALFF in MDD patients. Given that previous studies reported significant correlations between alterations in brain function and symptomatic improvement, correlations between changes in ALFF values, and reductions in all the symptom scores, as rated *via* the Perceived Deficits Questionnaire for Depression (PQD-D), were expected.

MATERIALS AND METHODS

Clinical Data

The treatment group comprised 25 patients with first-time onset and untreated MDD registered at the Wuhan Mental Health Center outpatient clinic from January 2019 to October 2020. MDD was diagnosed by a physician using the Diagnostic and Statistical Manual of Mental Disorders-Fourth Edition (DSM-IV) criteria (33). The inclusion criteria of MDD were (1) patients diagnosed with MDD for the first time less than 1 week prior to enrollment; (2) those aged between 20 and 60; (3) those with no contraindications to oral vortioxetine hydrobromide; and (4) those with no history of depressive episodes, family history of other mental illnesses, no significant physical diseases, no history of alcohol or drug abuse, and right handedness. Exclusion criteria for patients with depression and healthy controls were as follows: those with (1) organic brain disease; (2) physical severe disease; (3) family history of mental or neurological diseases; and (4) contraindications to magnetic resonance; and (5) other mental diseases or substance addictions. Twenty-five healthy controls matched by age, gender, and years of education who volunteered to participate in this study during the same period were selected. The medical ethics committee of the hospital approved this study, and all patients or their families signed informed consent.

Scale Assessment

The 17-item version of the Hamilton Depression Scale (HAMD) and the Perceived Deficits Questionnaire for Depression (PQD-D) were used to assess the severity of illness and cognitive impairment in all patients (34).

Treatment Methods

The treatment group was given oral vortioxetine hydrobromide tablets (trade name: Xindayue, Lundbeck, Beijing; Pharmaceutical Information Consulting Co., Ltd., approval number: H20170382). The initial and maintenance doses were 10–20 mg/d. During the study period, other antidepressants,

TABLE 1 | Demographic information.

Characteristics	Pre-treatment patient (n = 25)	Post-treatment patient (n = 25)	Controls (n = 25)	F or $\times 2$ or T	P-value
Gender (male/female)	25 (6/19)	25 (6/19)	25 (7/18)	18.25	> 0.05
Age (years)	28.80 ± 7.54	28.80 ± 7.54	27.24 ± 8.17	0.34	> 0.05
Education (years)	11.24 ± 2.58	11.24 ± 2.58	12.80 ± 2.46	3.13	> 0.05
HAMD scores	26.40 ± 5.29	11.20 ± 1.25		4.21	0.03
PQD-D scores	52.15 ± 11.24	38.85 ± 11.14		4.35	0.04

HAMD, Hamilton Rating Scale for Depression; PQD-D, Perceived Deficits Questionnaire for Depression.

TABLE 2 | Alterations of ALFF among patients (at baseline, after treatment) and controls.

Cluster location	Peak (MNI)			Number of voxels	T-value
	X	Y	Z		
Bilateral MFG	36	−15	−51	33	7.64
Bilateral CG	9	−6	−6	28	2.18
Bilateral MTG	−30	12	18	−27	8.62

ALFF, amplitude of low-frequency fluctuation MFG, middle frontal gyrus; CG, cingulate gyrus; MTG, middle temporal gyrus.

antipsychotics, sedative-hypnotics, and other psychiatric drugs were prohibited.

Data Collection

Rs-fMRI scans were performed with a Philips 3.0 MRI machine. The subjects were instructed to relax, breathe calmly, close their eyes, and keep their minds awake during the scan. All subjects underwent rs-fMRI scans with a scanning sequence as follows: (1) structural image adoption of 3D spoiler gradient echo, TR = 8.4 ms, TE = 3.2 ms, flip angle = 12°, slice thickness = 1 mm, FOV = 24 cm × 24 cm, matrix = 256 × 256, and a scanning time of about 15 min; (2) rs-fMRI imaging parameters were echo plane imaging sequence, TR = 2,000 ms, TE = 40 ms, FOV = 24 cm × 24 cm, matrix = 60 × 60, flip angle = 90°, slice thickness = 4 mm, layer spacing = 0 mm, number of layers = 33, and a scanning time of about 11 min.

Data Processing

The data were processed using the DPABI2.2 and SPM12 toolkits on the Matlab platform (35). The processing steps were as follows: first, DICOM map was converted to NIFTI format; the 10 time points were removed at the beginning of the scan to obtain the stability of the image acquisition; then the functional image was resampled and registered to the structural image of each subject. This was followed by Gaussian smoothing of 6 mm × 6 mm × 6 mm. Full-width and half-height de-linear drift and filtering were performed to extract signals in the frequency range of 0.01–0.08 Hz. Finally, the ALFF value of each voxel in the whole brain was calculated and divided by the average ALFF value of the entire brain to obtain the standard ALFF value.

Statistical Analysis

SPSS22.0 was used for statistical analysis of general demographic data and symptom scores. Statistical analysis software with REST was employed to perform statistical analysis on ALFF images. Firstly, an analysis of the results for the three groups of subjects was carried out. Then, two independent-sample t-tests were carried out on the healthy group results before and after treatment. The Rest Slice Viewer was used for multiple comparison corrections and the obtained images. Differences in brain regions with $P < 0.01$ were defined as statistically significant. The correlation between significant changes in the ALFF value and HAMD score or disease course were analyzed.

RESULTS

There were no statistically significant differences in gender, age, or years of education between the depression patient group (25 patients before and after treatment) and the standard control group. There were statistically significant decreased scores in HAMD and PQD-D after treatment (**Table 1**).

The analysis of variance between the ALFF values of the depression group and the control group before and after treatment showed that the ALFF values of the bilateral middle frontal gyrus (MFG), cingulate gyrus (CG), and middle temporal gyrus (MTG) increased significantly in the depression group, as shown in **Table 2** and **Figure 1**.

The t-test results comparing two independent samples from the depression group before treatment and the standard control group showed that ALFF values in the right inferior temporal gyrus (ITG) decreased significantly, while those in the left low cerebellum, right CG, and central posterior gyrus (CPG) increased dramatically and significantly in the patient group, as shown in **Table 3** and **Figure 2**.

After treatment, the t-test results of two independent samples from the depression group and control group showed that ALFF values increased in the bilateral CG, bilateral MTG, bilateral medial superior frontal gyrus (MSFG), and bilateral inferior cerebellum in patients in the depression group, as shown in **Table 4** and **Figure 3**.

DISCUSSION

In this study, the ALFF analysis method proposed by Yan et al. (36) was used to study brain functional changes in patients with depression before and after treatment with vortioxetine. The brain regions with increased ALFF values included the left inferior cerebellum, right cingulate gyrus (CG), and posterior

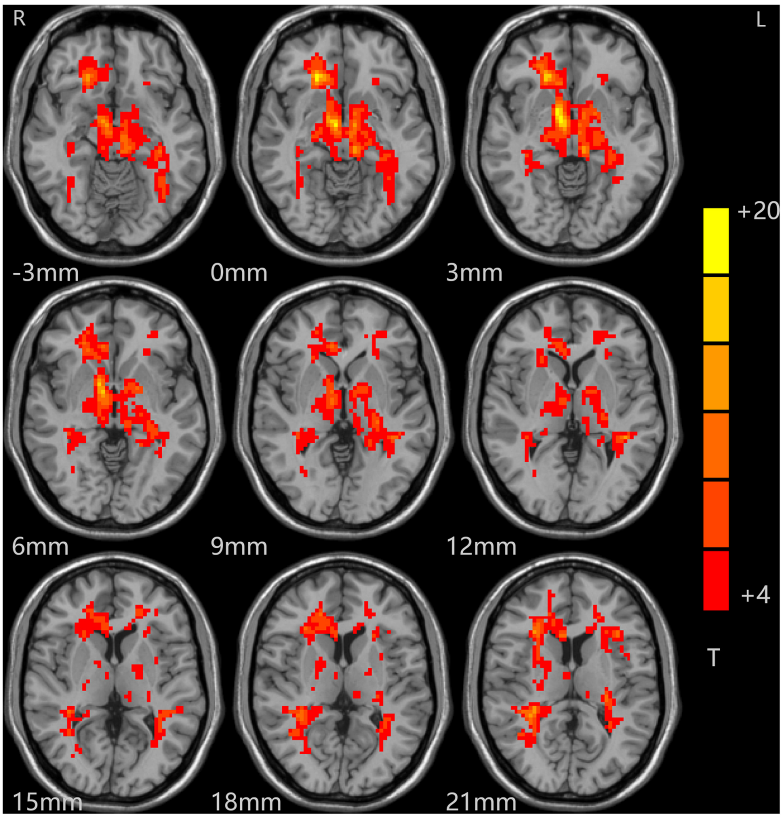

FIGURE 1 | Alterations in ALFF among patients (at baseline, after treatment) and controls. Red indicates the brain area where ALFF values were significantly increased, and the color depth indicates the differences between the three groups.

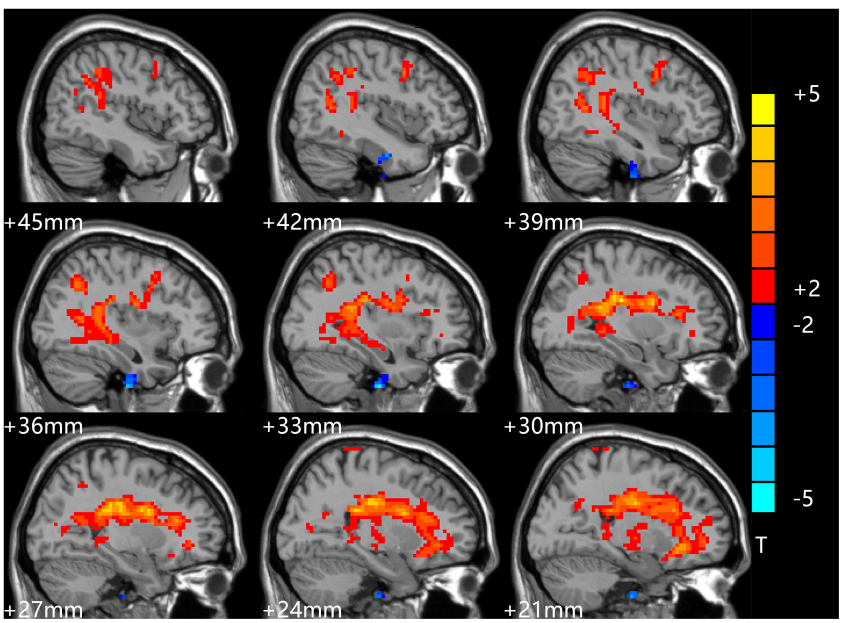

FIGURE 2 | Comparison of patients and controls at baseline. Blue indicates the brain area where ALFF values were significantly reduced. Red indicates the brain area where ALFF values were significantly increased, and the color depth indicates the difference between the two groups.

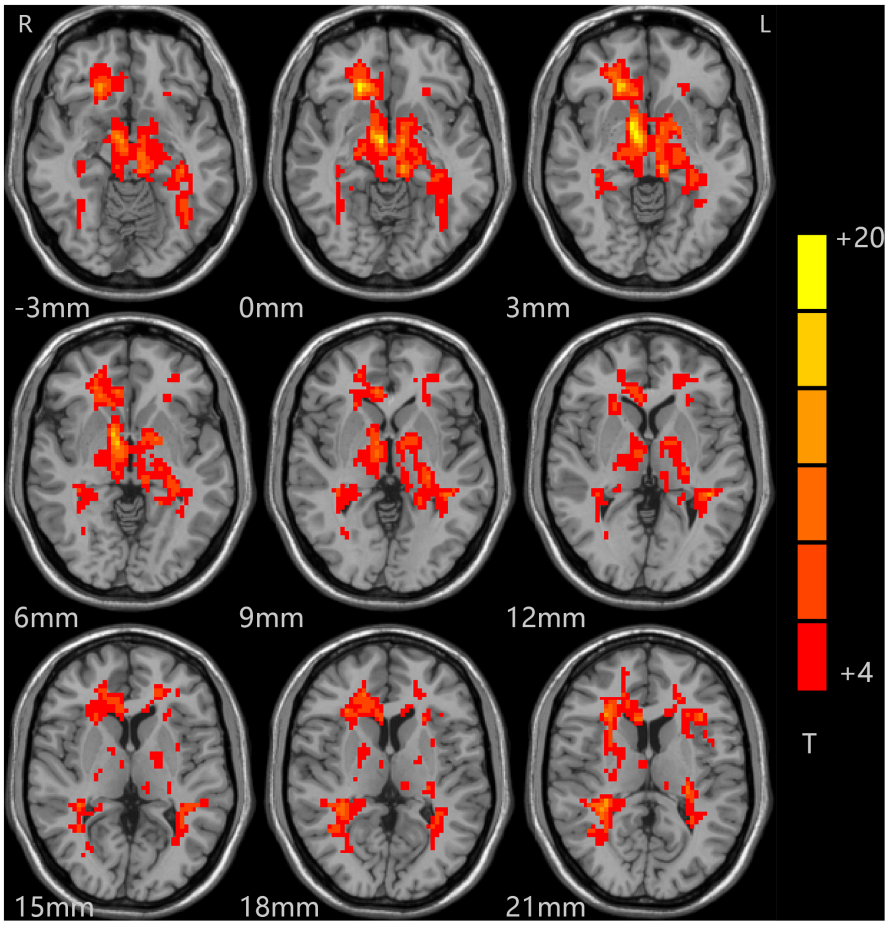

FIGURE 3 | Comparison of patients and controls after treatment. Red indicates the brain area where ALFF values were significantly increased, and the color depth indicates the difference between the two groups.

central gyrus (PCG). In this study, data from a study of first-episode patients with depression without antidepressant drugs and various treatments were collected (37–39). After 8 weeks of standard vortioxetine antidepressant therapy, brain areas with significantly decreased spontaneous activity in patients with depression were corrected. The brain areas with considerably increased ALFF values were mainly distributed in the bilateral CG, medial superior frontal gyrus (MSFG), middle temporal gyrus (MTG), cerebellum, and right inferior temporal gyrus (ITG), middle frontal gyrus (MFG). Our findings showed that vortioxetine can effectively control depressive symptoms and improve cognitive function in patients with MDD.

In this study, the areas of brain functional changes in patients with depression were mainly concentrated in the frontal lobe, temporal lobe, CG, and ITG. A large number of studies have shown that the frontal lobe has key roles in attention, emotional processing, reward and cognitive punishment functions, and is involved in the inhibition of various behaviors (40). A near-infrared imaging study found changes in functional signals in the MFG in patients with major depression, and a momentary mood found correlations between rumination responses during induced stress and everyday stress rumination (41). Depressed mood and delayed thinking in patients with depression may be related to the development of frontal lobe dysfunction, resulting in poor prognosis and co-morbid psychiatric disorders. The temporal lobe and CG are important components of the default and limbic networks (42), which are involved in the human brain's emotional processing and self-control functions, and they indirectly connect important areas affecting the frontal lobe through the Papez circuit, mainly the corticostriatal-pallidus-thalamic neuroanatomical circuit (43). A multicenter study found differences in resting functional connectivity in the emotional circuit of the marginal structure frontal lobe striatum thalamus between unipolar and bipolar depressive disorder brains (44). Another meta-analysis found distinct patterns of intrinsic brain activity alterations in the local brains of patients with monophasic and bipolar depression (45). Therefore, there are certain abnormalities in the brain function networks of patients with depression, mainly concentrated in the temporal lobe and CG. In addition to functional changes, there are also corresponding structural changes in these brain regions. Structural magnetic resonance imaging showed that patients with

TABLE 3 | Alterations of ALFF between patients at baseline and controls.

Cluster location	Peak (MNI)			Number of voxels	*T*-value
	X	Y	Z		
Right ITG	33	−15	−51	67	−3.60
Left cerebellum	−27	−30	−33	28	3.868
Right CG	12	3	−3	49	6.23
Right CPG	15	−51	78	32	4.11

ALFF, amplitude of low-frequency fluctuation; ITG, inferior temporal gyrus; CG, cingulate gyrus; CPG, central posterior gyrus.

TABLE 4 | Alterations of ALFF between patients after treatment and controls.

Cluster location	Peak (MNI)			Number of voxels	*T*-value
	X	Y	Z		
Bilateral CG	18	30	51	36	3.29
Bilateral MTG	21	30	−27	30	3.50
Bilateral MSFG	6	63	33	63	3.45
Bilateral cerebellum	39	−30	−9	65	6.56

ALFF, amplitude of low-frequency fluctuation; CG, cingulate gyrus; MTG, middle temporal gyrus; MSFG, medial superior frontal gyrus.

depression had stronger deep white matter signals and decreased gray matter volume in the cortex and anterior cerebellar lobe (46). These studies suggested that marginal networks are directly involved in the pathogenesis of depression.

The CG has been an important role subject of focus in previous pathological studies of depression, and the signs seen during the pathogenesis of depression are different between the anterior CG and posterior CG. The anterior CG is mainly related to self-control and emotional control, while the posterior CG is primarily related to early awakening, introspection, memory, and thought flexibility (47). Differences in the signs of depression between the two may be related to the core brain regions of the posterior CG involved in the default network. The default network forms connections between brain areas that are active when the patient is in a quiescent state and there are no tasks or other forms of stimulation. It is believed to be related to human emotional regulation as well as attention and sleep circadian rhythm disorders. There are various research reports on the role of the CG in depression, but there are also opposing views. For example, Fan and his colleagues found decreased VMHC in the bilateral posterior cingulate cortex (PCC) extending to the precuneus in patients with MDD compared with healthy controls (48). Relative to healthy controls, melancholic patients also displayed decreased VMHC in the PCC (49). However, a recent meta-analysis MDD of the PCC showed higher FC in the bilateral MTG (47). The inconsistencies in these research results may have been caused by the different sample sizes, analysis methods, and software used, and the lack of a guarantee of complete homogeneity in the subjects selected. For example, the course of pathogenesis in some patients is inconsistent with what is typical with depression, and some signs are caused by interference from drug treatment, psychotherapy, or physical therapy (50–54). The right ITG in the human brain is related to depression and decreased pleasure, but it is also directly involved in memory, appetite, and other functions, as well as being indirectly involved in cognitive functions such as attention and vigilance.

Based on the results of this study, we inferred that the decrease in ALFF values in the right ITG may be related to depression. The new antidepressant vortioxetine has multiple modes of action that can comprehensively improve the depressive symptoms of patients. Clinical observations provide support for the drug's significant curative effects, including its ability to reduce the frequency of depression recurrence and improve patients' social and cognitive function (32). Our study found that the ALFF values of the right ITG of patients returned to normal after vortioxetine antidepressant treatment, which may be related to the concurrent improvements in depressive symptoms. This provides a biological mechanism for the effect of vortioxetine as an antidepressant drug that can effectively improve cognitive function from the perspective of neuroimaging.

Over recent years, scholars have found that the cerebellum plays a specific role in the default network. Guo Wenbin's team found enhanced signals of cerebellar functional connection in patients with depression, and this compensatory mechanism is used to resist the early clinical symptoms of patients with depression (55). Our study also found spontaneous signal enhancement in the cerebellum after treatment. Therefore, we speculated that the changes in cerebellar spontaneous activity in patients with depression may be related to their symptoms of negative thinking and depression.

There were some limitations to this study. First, the sample size was too small for satisfactory statistical power. Second, we did not exclude patients with bipolar disorder, who may only show depression in the early stages of the condition. These factors may have affected the stability of the research results. Lastly, this report only discusses differences in spontaneous signals occurring in the whole brain of patients with depression from the perspective of low-frequency amplitude functional magnetic resonance and speculates on the pathophysiological mechanisms of depression and the possible antidepressant and cognitive function mechanisms of votioxetine. In the future, it will be beneficial to further explore the specific diagnosis and treatment of depression from multiple perspectives.

CONCLUSION

This study used resting magnetic resonance imaging technology and the ALFF analysis method to explore brain functional changes in first-episode drug-free patients with MDD before and after vortioxetine treatment to provide an objective basis for the diagnosis and treatment of patients with MDD.

DATA AVAILABILITY STATEMENT

The original contributions presented in this study are included in the article/supplementary material, further inquiries can be directed to the corresponding author/s.

ETHICS STATEMENT

The studies involving human participants were reviewed and approved by the Medical Ethics Committee of the Hospital approved this study, and all patients or their families signed informed consent. The patients/participants provided their written informed consent to participate in this study.

AUTHOR CONTRIBUTIONS

All authors listed have made a substantial, direct, and intellectual contribution to the work, and approved it for publication.

FUNDING

This study was supported by the Health Commission of Hubei Province Scientific research project (grant no. 2020CFB512).

ACKNOWLEDGMENTS

We would like to thank all the reviewers who participated in the review and MJEditor (www.mjeditor.com) for its linguistic assistance during the preparation of this manuscript.

REFERENCES

1. First MB, Williams Janet BW, Spitzer RL, Gibbon M, et al. *Structured Clinical Interview for DSM-IV Axis I Disorders-Patient Edition (SCID-I/P).* (1997). Oxford: Oxford University Press.
2. Xu LL, Liu GY, Zhang L, Cao L, Zhang J, Ma LY. Resting-state functional magnetic resonance imaging study in first-episode depression and subjects at high risk for depression. *J Clin Psychiatry.* (2018) 28:93–7.
3. Conradi HJ, Bos EH, Kamphuis JH, de Jonge P. The ten-year course of depression in primary care and long-term effects of psychoeducation, psychiatric consultation and cognitive behavioral therapy. *J Affect Disord.* (2017) 217:174–82. doi: 10.1016/j.jad.2017.03.064
4. Ten Have M, de Graaf R, van Dorsselaer S, Tuithof M, Kleinjan M, Penninx B. Recurrence and chronicity of major depressive disorder and their risk indicators in a population cohort. *Acta Psychiatr Scand.* (2018) 137:503–15. doi: 10.1111/acps.12874
5. Lu J, Xu X, Huang Y, Li T, Ma C, Xu G, et al. Prevalence of depressive disorders and treatment in China: a cross-sectional epidemiological study. *Lancet Psychiatry.* (2021) 8:981–90. doi: 10.1016/S2215-0366(21)00251-0
6. Thalamuthu A, Mills NT, Berger K, Minnerup H, Grotegerd D, Dannlowski U, et al. Genome-wide interaction study with major depression identifies novel variants associated with cognitive function. *Mol Psychiatry.* (2022) 27:1111–9. doi: 10.1038/s41380-021-01379-5
7. Sumiyoshi T, Hoshino T, Mishiro I, Hammer-Helmich L, Ge H, Moriguchi Y, et al. Prediction of residual cognitive disturbances by early response of depressive symptoms to antidepressant treatments in patients with major depressive disorder. *J Affect Disord.* (2022) 296:95–102. doi: 10.1016/j.jad.2021.09.025
8. Lan T, Cao Z, Zhao F, Perham N. The Association Between Effectiveness of Tinnitus Intervention and Cognitive Function-A Systematic Review. *Front Psychol.* (2020) 11:553449. doi: 10.3389/fpsyg.2020.553449
9. Australas Psychiatry. Vortioxetine. *Australas Psychiatry.* (2015) 23:306, 15. doi: 10.1177/1039856215584241
10. du Jardin KG, Jensen JB, Sanchez C, Pehrson AL. Vortioxetine dose-dependently reverses 5-HT depletion-induced deficits in spatial working and object recognition memory: a potential role for 5-HT1A receptor agonism and 5-HT3 receptor antagonism. *Eur Neuropsychopharmacol.* (2014) 24:160–71. doi: 10.1016/j.euroneuro.2013.07.001
11. Chakroborty S, Geisbush TR, Dale E, Pehrson AL, Sanchez C, West AR. Impact of vortioxetine on synaptic integration in prefrontal-subcortical circuits: comparisons with escitalopram. *Front Pharmacol.* (2017) 8:764. doi: 10.3389/fphar.2017.00764
12. Guilloux JP, Mendez-David I, Pehrson A, Guiard BP, Reperant C, Orvoen S, et al. Antidepressant and anxiolytic potential of the multimodal antidepressant vortioxetine (Lu AA21004) assessed by behavioural and neurogenesis outcomes in mice. *Neuropharmacology.* (2013) 73:147–59. doi: 10.1016/j.neuropharm.2013.05.014
13. Koutsouleris N, Dwyer DB, Degenhardt F, Maj C, Urquijo-Castro MF, Sanfelici R, et al. Multimodal Machine Learning Workflows for Prediction of Psychosis in Patients With Clinical High-Risk Syndromes and Recent-Onset Depression. *JAMA Psychiatry.* (2021) 78:195–209. doi: 10.1001/jamapsychiatry.2020.3604
14. Zhang Y, Wu W, Toll RT, Naparstek S, Maron-Katz A, Watts M, et al. Identification of psychiatric disorder subtypes from functional connectivity patterns in resting-state electroencephalography. *Nat Biomed Eng.* (2021) 5:309–23. doi: 10.1038/s41551-020-00614-8
15. Schmaal L, Hibar DP, Samann PG, Hall GB, Baune BT, Jahanshad N, et al. Cortical abnormalities in adults and adolescents with major depression based on brain scans from 20 cohorts worldwide in the ENIGMA Major Depressive Disorder Working Group. *Mol Psychiatry.* (2017) 22:900–9. doi: 10.1038/mp.2016.60
16. Radonjic NV, Hess JL, Rovira P, Andreassen O, Buitelaar JK, Ching CRK, et al. Structural brain imaging studies offer clues about the effects of the shared genetic etiology among neuropsychiatric disorders. *Mol Psychiatry.* (2021) 26:2101–10. doi: 10.1038/s41380-020-01002-z
17. van Velzen LS, Kelly S, Isaev D, Aleman A, Aftanas LI, Bauer J, et al. White matter disturbances in major depressive disorder: a coordinated analysis across 20 international cohorts in the ENIGMA MDD working group. *Mol Psychiatry.* (2020) 25:1511–25. doi: 10.1038/s41380-019-0477-2
18. Guo W, Liu F, Liu J, Yu L, Zhang J, Zhang Z, et al. Abnormal causal connectivity by structural deficits in first-episode, drug-naive schizophrenia at rest. *Schizophr Bull.* (2015) 41:57–65. doi: 10.1093/schbul/sbu126
19. Guo W, Liu F, Zhang Z, Liu G, Liu J, Yu L, et al. Increased Cerebellar Functional Connectivity With the Default-Mode Network in Unaffected Siblings of Schizophrenia Patients at Rest. *Schizophr Bull.* (2015) 41:1317–25. doi: 10.1093/schbul/sbv062
20. Zhu F, Liu F, Guo W, Chen J, Su Q, Zhang Z, et al. Disrupted asymmetry of inter- and intra-hemispheric functional connectivity in patients with drug-naive, first-episode schizophrenia and their unaffected siblings. *EBioMedicine.* (2018) 36:429–35. doi: 10.1016/j.ebiom.2018.09.012
21. Li H, Guo W, Liu F, Chen J, Su Q, Zhang Z, et al. Enhanced baseline activity in the left ventromedial putamen predicts individual treatment response in drug-naive, first-episode schizophrenia: results from two independent study samples. *EBioMedicine.* (2019) 46:248–55. doi: 10.1016/j.ebiom.2019.07.022
22. Kambeitz J, Cabral C, Sacchet MD, Gotlib IH, Zahn R, Serpa MH, et al. Detecting Neuroimaging Biomarkers for Depression: a Meta-analysis of Multivariate Pattern Recognition Studies. *Biol Psychiatry.* (2017) 82:330–8. doi: 10.1016/j.biopsych.2016.10.028
23. Zhang X, Di X, Lei H, Yang J, Xiao J, Wang X, et al. Imbalanced spontaneous brain activity in orbitofrontal-insular circuits in individuals with cognitive vulnerability to depression. *J Affect Disord.* (2016) 198:56–63. doi: 10.1016/j.jad.2016.03.001
24. Logothetis NK, Pauls J, Augath M, Trinath T, Oeltermann A. Neurophysiological investigation of the basis of the fMRI signal. *Nature.* (2001) 412:150–7. doi: 10.1038/35084005
25. Tomasi D, Wang GJ, Volkow ND. Energetic cost of brain functional connectivity. *Proc Natl Acad Sci USA.* (2013) 110:13642–7. doi: 10.1073/pnas.1303346110
26. Wiebking C, Northoff G. Neural activity during interoceptive awareness and its associations with alexithymia-An fMRI study in major depressive disorder

and non-psychiatric controls. *Front Psychol.* (2015) 6:589. doi: 10.3389/fpsyg.2015.00589
27. Carvalho S, Goncalves OF, Brunoni AR, Fernandes-Goncalves A, Fregni F, Leite J. Transcranial direct current stimulation as an add-on treatment to cognitive-behavior therapy in first episode drug-naive major depression patients: the ESAP study protocol. *Front Psychiatry.* (2020) 11:563058. doi: 10.3389/fpsyt.2020.563058
28. Crowther A, Smoski MJ, Minkel J, Moore T, Gibbs D, Petty C, et al. Resting-state connectivity predictors of response to psychotherapy in major depressive disorder. *Neuropsychopharmacology.* (2015) 40:1659–73. doi: 10.1038/npp.2015.12
29. Liu X, Li L, Li M, Ren Z, Ma P. Characterizing the subtype of anhedonia in major depressive disorder: a symptom-specific multimodal MRI study. *Psychiatry Res Neuroimaging.* (2021) 308:111239. doi: 10.1016/j.pscychresns.2020.111239
30. Guo W, Liu F, Chen J, Wu R, Li L, Zhang Z, et al. Olanzapine modulates the default-mode network homogeneity in recurrent drug-free schizophrenia at rest. *Aust N Z J Psychiatry.* (2017) 51:1000–9. doi: 10.1177/0004867417714952
31. Gao Y, Wang X, Xiong Z, Ren H, Liu R, Wei Y, et al. Abnormal fractional amplitude of low-frequency fluctuation as a potential imaging biomarker for first-episode major depressive disorder: a resting-state fMRI study and support vector machine analysis. *Front Neurol.* (2021) 12:751400. doi: 10.3389/fneur.2021.751400
32. McIntyre RS, Harrison J, Loft H, Jacobson W, Olsen CK. The effects of vortioxetine on cognitive function in patients with major depressive disorder: a meta-analysis of three randomized controlled trials. *Int J Neuropsychopharmacol.* (2016) 19:yw055. doi: 10.1093/ijnp/pyw055
33. Lobbestael J, Leurgans M, Arntz A. Inter-rater reliability of the Structured Clinical Interview for DSM-IV Axis I Disorders (SCID I) and Axis II Disorders (SCID II). *Clin Psychol Psychother.* (2011) 18:75–9. doi: 10.1002/cpp.693
34. Shi C, Wang G, Tian F, Han X, Sha S, Xing X, et al. Reliability and validity of Chinese version of perceived deficits questionnaire for depression in patients with MDD. *Psychiatry Res.* (2017) 252:319–24. doi: 10.1016/j.psychres.2017.03.021
35. Chao-Gan Y, Yu-Feng Z. DPARSF: a MATLAB toolbox for "pipeline" data analysis of resting-state fMRI. *Front Syst Neurosci.* (2010) 4:13. doi: 10.3389/fnsys.2010.00013
36. Yan C, Liu D, He Y, Zou Q, Zhu C, Zuo X, et al. Spontaneous brain activity in the default mode network is sensitive to different resting-state conditions with limited cognitive load. *PLoS One.* (2009) 4:e5743. doi: 10.1371/journal.pone.0005743
37. Bulubas L, Padberg F, Mezger E, Suen P, Bueno PV, Duran F, et al. Prefrontal resting-state connectivity and antidepressant response: no associations in the ELECT-TDCS trial. *Eur Arch Psychiatry Clin Neurosci.* (2021) 271:123–34. doi: 10.1007/s00406-020-01187-y
38. Kempton MJ, Salvador Z, Munafo MR, Geddes JR, Simmons A, Frangou S, et al. Structural neuroimaging studies in major depressive disorder. Meta-analysis and comparison with bipolar disorder. *Arch Gen Psychiatry.* (2011) 68:675–90. doi: 10.1001/archgenpsychiatry.2011.60
39. Ge R, Gregory E, Wang J, Ainsworth N, Jian W, Yang C, et al. Magnetic seizure therapy is associated with functional and structural brain changes in MDD: therapeutic versus side effect correlates. *J Affect Disord.* (2021) 286:40–8. doi: 10.1016/j.jad.2021.02.051
40. Anton M, Alen F, Gomez de Heras R, Serrano A, Pavon FJ, Leza JC, et al. Oleoylethanolamide prevents neuroimmune HMGB1/TLR4/NF-kB danger signaling in rat frontal cortex and depressive-like behavior induced by ethanol binge administration. *Addict Biol.* (2017) 22:724–41. doi: 10.1111/adb.12365
41. Rosenbaum D, Int-Veen I, Laicher H, Torka F, Kroczek A, Rubel J, et al. Insights from a laboratory and naturalistic investigation on stress, rumination and frontal brain functioning in MDD: an fNIRS study. *Neurobiol Stress.* (2021) 15:100344. doi: 10.1016/j.ynstr.2021.100344
42. Guo W, Cui X, Liu F, Chen J, Xie G, Wu R, et al. Increased anterior default-mode network homogeneity in first-episode, drug-naive major depressive disorder: a replication study. *J Affect Disord.* (2018) 225:767–72. doi: 10.1016/j.jad.2017.08.089
43. Fang P, Zeng LL, Shen H, Wang L, Li B, Liu L, et al. Increased cortical-limbic anatomical network connectivity in major depression revealed by diffusion tensor imaging. *PLoS One.* (2012) 7:e45972. doi: 10.1371/journal.pone.0045972
44. Corponi F, Anmella G, Verdolini N, Pacchiarotti I, Samalin L, Popovic D, et al. Symptom networks in acute depression across bipolar and major depressive disorders: a network analysis on a large, international, observational study. *Eur Neuropsychopharmacol.* (2020) 35:49–60. doi: 10.1016/j.euroneuro.2020.03.017
45. Gong J, Wang J, Qiu S, Chen P, Luo Z, Wang J, et al. Common and distinct patterns of intrinsic brain activity alterations in major depression and bipolar disorder: voxel-based meta-analysis. *Transl Psychiatry.* (2020) 10:353. doi: 10.1038/s41398-020-01036-5
46. Guo W, Liu F, Yu M, Zhang J, Zhang Z, Liu J, et al. Functional and anatomical brain deficits in drug-naive major depressive disorder. *Prog Neuropsychopharmacol Biol Psychiatry.* (2014) 54:1–6. doi: 10.1016/j.pnpbp.2014.05.008
47. Zhu Z, Wang Y, Lau WKW, Wei X, Liu Y, Huang R, et al. Hyperconnectivity between the posterior cingulate and middle frontal and temporal gyrus in depression: based on functional connectivity meta-analyses. *Brain Imaging Behav.* (2022). 1–14. doi: 10.1007/s11682-022-00628-7
48. Fan H, Yang X, Zhang J, Chen Y, Li T, Ma X. Analysis of voxel-mirrored homotopic connectivity in medication-free, current major depressive disorder. *J Affect Disord.* (2018) 240:171–6. doi: 10.1016/j.jad.2018.07.037
49. Shan X, Cui X, Liu F, Li H, Huang R, Tang Y, et al. Shared and distinct homotopic connectivity changes in melancholic and non-melancholic depression. *J Affect Disord.* (2021) 287:268–75. doi: 10.1016/j.jad.2021.03.038
50. Shao D, Zhao ZN, Zhang YQ, Zhou XY, Zhao LB, Dong M, et al. Efficacy of repetitive transcranial magnetic stimulation for post-stroke depression: a systematic review and meta-analysis of randomized clinical trials. *Braz J Med Biol Res.* (2021) 54:e10010. doi: 10.1590/1414-431X202010010
51. Dai L, Wang P, Zhang P, Guo Q, Du H, Li F, et al. The therapeutic effect of repetitive transcranial magnetic stimulation in elderly depression patients. *Medicine (Baltimore).* (2020) 99:e21493. doi: 10.1097/MD.0000000000021493
52. Guo WB, Liu F, Xue ZM, Yu Y, Ma CQ, Tan CL, et al. Abnormal neural activities in first-episode, treatment-naive, short-illness-duration, and treatment-response patients with major depressive disorder: a resting-state fMRI study. *J Affect Disord.* (2011) 135:326–31. doi: 10.1016/j.jad.2011.06.048
53. Liu F, Hu M, Wang S, Guo W, Zhao J, Li J, et al. Abnormal regional spontaneous neural activity in first-episode, treatment-naive patients with late-life depression: a resting-state fMRI study. *Prog Neuropsychopharmacol Biol Psychiatry.* (2012) 39:326–31. doi: 10.1016/j.pnpbp.2012.07.004
54. Liu F, Guo W, Liu L, Long Z, Ma C, Xue Z, et al. Abnormal amplitude low-frequency oscillations in medication-naive, first-episode patients with major depressive disorder: a resting-state fMRI study. *J Affect Disord.* (2013) 146:401–6. doi: 10.1016/j.jad.2012.10.001
55. Guo W, Liu F, Liu J, Yu L, Zhang Z, Zhang J, et al. Is there a cerebellar compensatory effort in first-episode, treatment-naive major depressive disorder at rest? *Prog Neuropsychopharmacol Biol Psychiatry.* (2013) 46:13–8. doi: 10.1016/j.pnpbp.2013.06.009

Conflict of Interest: The authors declare that the research was conducted in the absence of any commercial or financial relationships that could be construed as a potential conflict of interest.

The reviewer XJ declared a shared affiliation with the author SZ at the time of review.

Publisher's Note: All claims expressed in this article are solely those of the authors and do not necessarily represent those of their affiliated organizations, or those of the publisher, the editors and the reviewers. Any product that may be evaluated in this article, or claim that may be made by its manufacturer, is not guaranteed or endorsed by the publisher.

frontiers | Frontiers in Psychiatry

TYPE Original Research
PUBLISHED 22 July 2022
DOI 10.3389/fpsyt.2022.967391

OPEN ACCESS

EDITED BY
Qinji Su,
Guangxi Medical University, China

REVIEWED BY
Qingguo Chen,
Huazhong University of Science and Technology, China
Yi Shao,
Nanchang University, China

*CORRESPONDENCE
Miao Tong
cake-ll@163.com
Qian Li
1535379485@qq.com

SPECIALTY SECTION
This article was submitted to Neuroimaging and Stimulation, a section of the journal Frontiers in Psychiatry

RECEIVED 12 June 2022
ACCEPTED 30 June 2022
PUBLISHED 22 July 2022

CITATION
Liu L, Fan J, Zhan H, Huang J, Cao R, Xiang X, Tian S, Ren H, Tong M and Li Q (2022) Abnormal regional signal in the left cerebellum as a potential neuroimaging biomarker of sudden sensorineural hearing loss. *Front. Psychiatry* 13:967391. doi: 10.3389/fpsyt.2022.967391

Abnormal regional signal in the left cerebellum as a potential neuroimaging biomarker of sudden sensorineural hearing loss

Lei Liu[1], Jun Fan[1], Hui Zhan[1], Junli Huang[2], Rui Cao[1], Xiaoran Xiang[1], Shuai Tian[1], Hongwei Ren[2], Miao Tong[3]* and Qian Li[1]*

[1]Department of Otorhinolaryngology, Tianyou Hospital, Affiliated to Wuhan University of Science and Technology, Wuhan, China, [2]Department of Medical Imaging, Tianyou Hospital, Affiliated to Wuhan University of Science and Technology, Wuhan, China, [3]Department of Stomatology, Tianyou Hospital, Affiliated to Wuhan University of Science and Technology, Wuhan, China

Objective: While prior reports have characterized visible changes in neuroimaging findings in individuals suffering from sudden sensorineural hearing loss (SSNHL), the utility of regional homogeneity (ReHo) as a means of diagnosing SSNHL has yet to be established. The present study was thus conducted to assess ReHo abnormalities in SSNHL patients and to establish whether these abnormalities offer value as a diagnostic neuroimaging biomarker of SSNHL through a support vector machine (SVM) analysis approach.

Methods: Resting-state functional magnetic resonance imaging (rs-fMRI) analyses of 27 SSNHL patients and 27 normal controls were conducted, with the resultant imaging data then being analyzed based on a combination of ReHo and SVM approaches.

Results: Relative to normal control individuals, patients diagnosed with SSNHL exhibited significant reductions in ReHo values in the left cerebellum, bilateral inferior temporal gyrus (ITG), left superior temporal pole (STP), right parahippocampal gyrus (PHG), left posterior cingulum cortex (PCC), and right superior frontal gyrus (SFG). SVM analyses suggested that reduced ReHo values in the left cerebellum were associated with high levels of diagnostic accuracy (96.30%, 52/54), sensitivity (92.59%, 25/27), and specificity (100.00%, 27/27) when distinguishing between SSNHL patients and control individuals.

Conclusion: These data suggest that SSNHL patients exhibit abnormal resting-state neurological activity, with changes in the ReHo of the left cerebellum offering value as a diagnostic neuroimaging biomarker associated with this condition.

KEYWORDS

sudden sensorineural hearing loss, regional homogeneity, resting-state fMRI, support vector machine, neuroimaging biomarker

Introduction

Sudden sensorineural hearing loss (SSNHL) is a medical emergency wherein affected individuals present with sensorineural hearing loss (≥30 dB over ≥3 consecutive frequencies) of unknown origin within 3 days. SSNHL is often accompanied by symptoms including tinnitus, vertigo, and aural fullness (1). SSNHL is estimated to affect 5–27 per 100,000 persons, and its annual incidence continues to rise (2, 3). Just 5% of SSNHL cases are bilateral, with most patients exhibiting a unilateral loss of hearing without any side preference (1, 4). Although the most common suspected etiologies of SSNHL in adult patients include viral infection, vascular or hematologic disease, immune-mediated disease, tumors, trauma, and other causes, the precise etiology of SSNHL remains unclear (5). SSNHL can contribute to social difficulties and psychiatric disorders in certain cases (6), with SSNHL patients exhibiting a higher risk of depression, and depression patients similarly exhibiting increased odds of developing SSNHL (7). As such, a failure to rapidly diagnose and treat SSNHL can lead to permanent hearing loss and associated adverse effects on quality of life (8). A combination of medical history information and pure tone audiometry (PTA) is generally used to diagnose SSNHL. However, imageological approaches capable of diagnosing SSNHL are lacking.

Rapid advances in neuroimaging technologies in recent years have enabled the diagnostic evaluation of a range of neurological systems. For example, increases in the fractional amplitude of low-frequency fluctuation in the right precuneus and left superior frontal gyrus may offer value as a biomarker associated with first-episode major depressive disorder (MDD) incidence (9). Abnormal network homogeneity values of the right posterior cingulate cortex/precuneus have also been successfully used to differentiate between individuals diagnosed with obsessive-compulsive disorder and control individuals with respective sensitivity and specificity values of 67.50% and 76.32% (10). Notably, several imaging studies have reported functional and structural changes in certain brain functional networks in SSNHL patients during the acute phase (≤30 days) (6, 11–13). However, neuroimaging biomarkers that can be used to guide SSNHL patients diagnosis have not been reported to date.

Resting-state functional magnetic resonance imaging (rs-fMRI) is a sensitive, non-invasive imaging approach that can offer detailed insight regarding altered brain function and neuronal activity. Accordingly, rs-fMRI imaging is commonly used for the evaluation of tinnitus patients and individuals suffering from bilateral or unilateral sensorineural hearing loss (14–17). Regional homogeneity (ReHo) is a robust algorithmic approach that enables the quantification of the resting-state local synchronization of adjacent voxels (18, 19), thereby providing insight regarding the consistency of whole-brain neural activity patterns. Abnormal ReHo detected *via* rs-fMRI in particular brain regions may be indicative of aberrant spontaneous neural activity among and within these areas of the brain. Specifically, increased ReHo values correspond to improved neuronal synchrony, whereas reduced ReHo values indicate impaired local neuronal activity.

While the use of rs-fMRI approaches to study SSNHL is becoming increasingly common, no studies to date have utilized a combination of ReHo and support vector machine (SVM) approaches to analyze these rs-fMRI-derived data. SVM approaches rely on the use of a robust machine learning algorithm capable of analyzing data, recognizing patterns, and using the resultant insights to gauge diagnostic accuracy. By identifying the maximal margin separating a hyperplane, this SVM algorithm maintains enhanced generalizability and resists overfitting, providing optimal predictive accuracy for test data that have not yet been analyzed. By overlaying SVM-derived weight values onto the original brain space utilized for fMRI analyses, the areas of the brain that can most effectively differentiate between different groups of individuals can be identified (20). As SVM algorithms can effectively locate and differentiate patterns within a particular dataset, the interpretability of the associated model is improved (20). SVM analyses are ideally suited to high-dimensional datasets in which there are more features than there are samples, with multiple prior reports having achieved success in the use of SVM to identify brain states (20, 21), enabling the discrimination between individuals diagnosed with particular neurological disorders and healthy controls (9, 22–25). Whether ReHo abnormalities can be effectively employed to differentiate between individuals with and without SSNHL through an SVM analysis, however, remains to be assessed. As such, the present study was designed to explore ReHo in patients with SSNHL, to establish which brain regions exhibit abnormal SSNHL-related ReHo, and to employ an SVM approach to gauge the value of abnormal ReHo as a neuroimaging biomarker of SSNHL.

Methods

Subjects

Between August 2020 and December 2021, a total of 27 patients diagnosed with SSNHL and 27 normal controls from the Otolaryngology Head and Neck Surgery Department of Tianyou Hospital affiliated with Wuhan University of Science and Technology were enrolled in this study. Participants were eligible for enrollment if they exhibited: (a) ≥30 dB in ≥3 contiguous frequencies with an air-bone gap < 10 dB, as measured *via* PTA; (b) a new-onset case of SSNHL with no prior history of this condition; (c) hearing loss of unknown origin; (d) no known neurological disease; (e) MRI and CT imaging results that excluded the presence of any space-occupying lesions within the intracranial space or internal auditory canal. SSNHL patients were excluded from this study if they (a) had any history

of noise exposure, ototoxic drug use, or ear surgery; (b) were experiencing fluctuating hearing loss; (c) had a family history of neurological disease; or (d) exhibited any inflammation of the external or middle ear. All enrolled normal control subjects exhibited normal otoscopic tympanic membrane findings and their pure-tone air conduction thresholds <25 dB HL at 0.25, 0.5, 1, 2, 4, and 8 kHz. Control participants were also free of any history of neurological or otologic disease. Pure-tone thresholds at 0.25, 0.5, 1, 2, 4, and 8 kHz were recorded at the start and the end of treatment. The Institutional Review Board of Tianyou Hospital Ethics Committee approved this study, and all participants provided informed consent.

TABLE 1 Demographic and clinical characteristics.

	SSNHL	NC	*P* value
Number (*n*)	27	27	–
Sex (*n*)			
Male	19	14	0.163
Female	8	13	
Age (year)	47.96 ± 9.37	44.04 ± 8.28	0.109
Hearing loss duration (day)	4.89 ± 5.86	–	–
PTA of affected ear (dB HL)			
Pre-treatment	72.50 ± 16.73	–	–
Post-treatment	60.15 ± 25.08	–	<0.001
PTA of unaffected ear (dB HL)			
Pre-treatment	24.54 ± 9.36	–	–
Post-treatment	23.83 ± 8.98	–	0.024

Data presented as mean ± SD. n means number; SSNHL, sudden sensorineural hearing loss; NC, normal controls; PTA, pure tone audiometry. The p-value for the gender distribution was obtained by the Chi-square test. Age was compared using the two-sample t test; PTA was compared with the paired-sample Wilcoxon test. $p < 0.05$ was considered significant.

Image acquisition

An Ingenia 3.0 T MRI scanner (Philips, Amsterdam, Netherlands) was used to analyze all study subjects in the Department of Medical Imaging. Participants were positioned with their heads being placed within a foam-filled prototype quadrature birdcage head coil designed to limit motion. During fMRI scanning, participants were directed to remain still and awake with their eyes close. Scanning parameters were: TR = 2000 ms, TE = 30 ms, flip angle = 90°, FOV = 220 × 220 mm^2, matrix size = 64 × 64, slice gap = 0.7 mm, slice thickness =3.5 mm, slice number = 33, and pitch = 1 mm.

Data preprocessing

MATLAB was used for the pre-processing of rs-fMRI data with the DPARSF software (26). Initially, the first five time points for each participant were excluded from analysis to reduce initial signal instability and to ensure that participants had sufficient time to adapt to the imaging. Samples were then corrected for head motion and slice time. Participants were not included in subsequent analyses if they exhibited over 2 mm of maximal displacement in any of the *x*, *y*, or *z* directions or over 2° of maximal rotation. Corrected imaging data were then subjected to spatial normalization based upon the standard Montreal Neurological Institute space, followed by resampling at 3 × 3 × 3 mm^3. Images were then subjected to bandpass filtering (0.01–0.08 Hz) and linear detrending. Spurious covariates were then removed, including six head motion parameters derived from rigid body correction, signal from a region centered in the white matter, and signal derived from a ventricular seed-based region of interest.

ReHo analysis

ReHo analyses were conducted using the DPABI software (http://rfmri.org/dpabi). Kendall coefficients of the time series consistency between individual voxels and neighboring voxels were used to construct ReHo brain maps, with smoothing then being performed using a Gaussian kernel with a full width and half height of 4 mm to minimize the impact of noise and deformation on the standardization process, thereby improving image effects, signal-to-noise ratio values, and statistical efficiency.

Classification analysis

The MATLAB LIBSVM package was used to conduct SVM classification analyses in an effort to establish the ability of ReHo values extracted from abnormal regions of the brain to differentiate between SSNHL patients and normal control individuals. This analytical approach was performed using a leave-one-out technique.

Statistical analyses

Demographic and clinical data

Statistical analyses were performed using SPSS 22.0, with demographic data being compared between groups using chi-square tests (sex) and two-sample *t*-tests (age). Hearing levels were compared *via* the Wilcoxon test. $P < 0.05$ was the threshold of significance.

ReHo values

The DPABI software was used to perform two-sample *t*-test analyses of ReHo graphs for the patient and normal

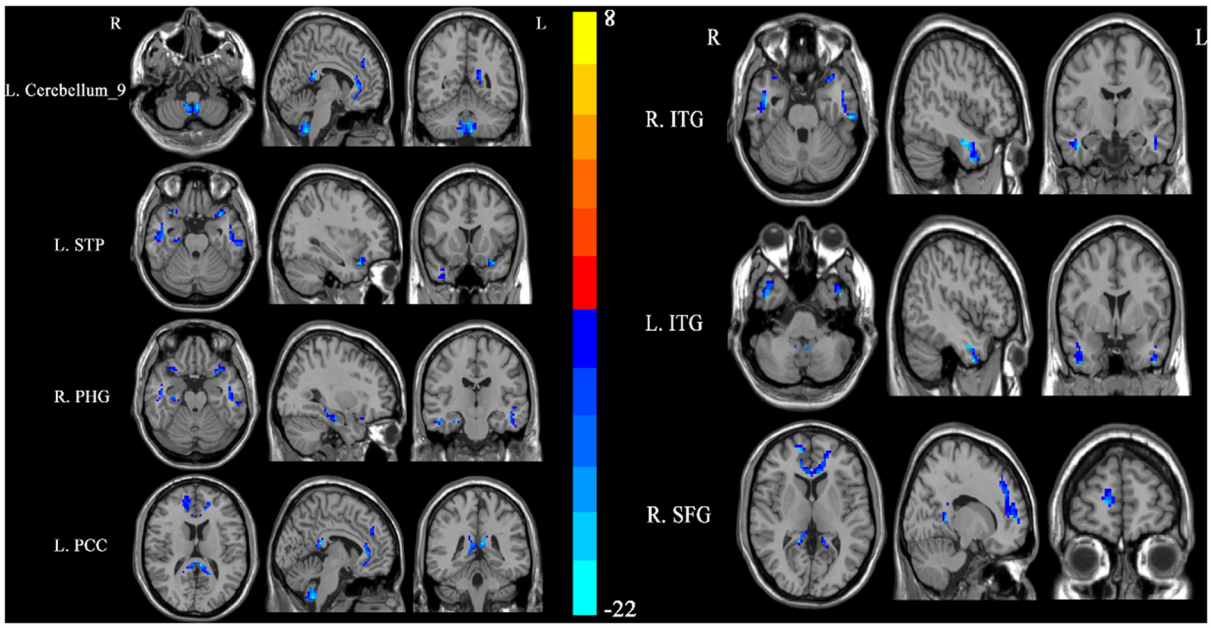

FIGURE 1
Differences in regional homogeneity (ReHo) values between SSNHL patients and normal controls. Decreased ReHo values (left cerebellum, left STP, right PHG, left PCC, right SFG, and bilateral ITG) were presented on the blue color, and the color bar indicates the T values of the group analysis. L, left; R, right; STP, superior temporal pole; PHG, parahippocampal gyrus; PCC, posterior cingulum cortex; SFG, superior frontal gyrus; ITG, inferior temporal gyrus.

control groups, with age and sex being treated as covariates. Brain templates were selected for overlay, and analyses were subjected to Gaussian Random Field (GRF) correction with a correction threshold of $P < 0.01$. Those brain regions exhibiting significant differences between these two groups were extracted as a template mask, with ReHo values for individual subjects then being extracted based on this template.

Results

Patient characteristics

In total, this study incorporated 27 patients diagnosed with unilateral SSNHL and 27 normal controls. There were no significant differences between these groups with respect to the age or sex of participants ($P > 0.05$), while there were significant differences between pre- and post-treatment hearing levels among SSNHL patients ($P < 0.05$). For further details regarding participant characteristics, see Table 1.

SSNHL-related ReHo abnormalities

SSNHL patients exhibited significant reductions in ReHo in the left cerebellum, bilateral inferior temporal gyrus (ITG), left superior temporal pole (STP), right parahippocampal gyrus (PHG), left posterior cingulum cortex (PCC), and right superior frontal gyrus (SFG) relative to normal controls (Figure 1, Table 2).

TABLE 2 Clusters with abnormal regional homogeneity in the patients with SSNHL.

Cluster location	Peak (MNI)			Number of voxels	*T*-value
	X	*Y*	*Z*		
Left cerebellum	−6	−51	−54	121	−22.4941
Right ITG	45	−9	−27	142	−22.6682
Left ITG	−45	3	−42	145	−23.2774
Left STP	−33	15	−24	36	−20.5900
Right PHG	30	−18	−21	36	−17.1846
Left PCC	−6	−39	15	128	−21.3446
Right SFG	15	57	6	410	−21.1893

SSNHL, sudden sensorineural hearing loss; MNI, Montreal Neurological Institute; ITG, inferior temporal gyrus; STP, superior temporal pole; PHG, parahippocampal gyrus; PCC, posterior cingulum cortex; SFG, superior frontal gyrus.

SVM analysis results

An SVM approach was used to separately analyze abnormal ReHo values in seven regions of the brain (left cerebellum,

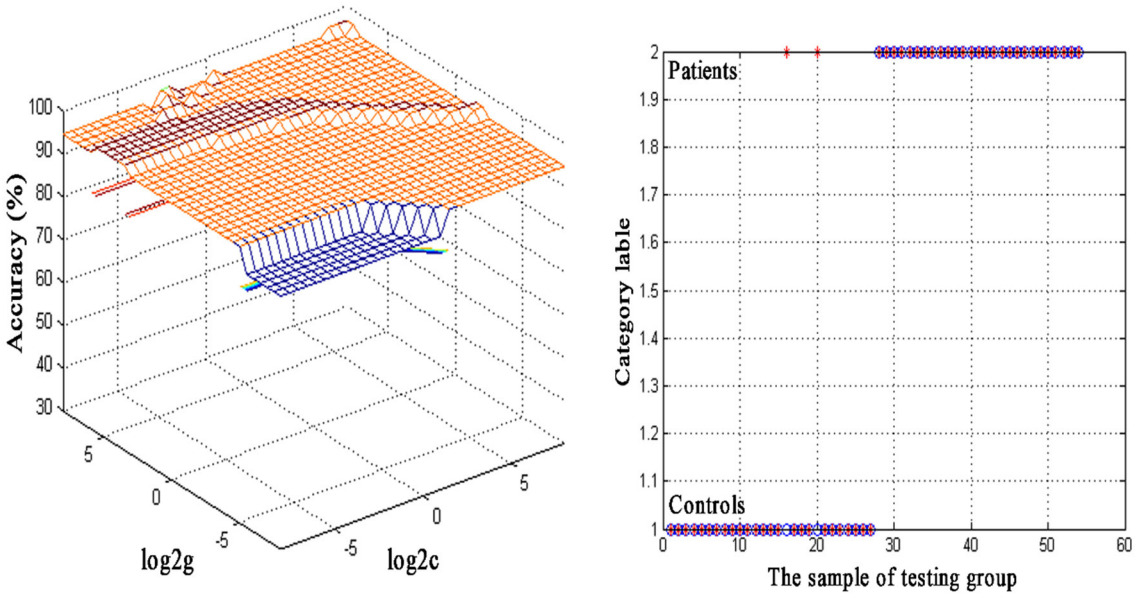

FIGURE 2
Visualization of classifications through support vector machine (SVM) using the decreased regional homogeneity (ReHo) values in the left cerebellum to discriminate SSNHL patients from normal controls. Left: SVM parameters result of 3D view. g means gamma, c means penalty coefficient. Right: Classified map of the ReHo values in the left cerebellum. Blue circle means true value and the red asterisk means predict value.

bilateral ITG, left STP, right PHG, left PCC, and right SFG), revealing decreased ReHo in the left cerebellum to exhibit the highest diagnostic accuracy (96.30%, 52/54) when differentiating between SSNHL patients and normal controls, with a sensitivity of 92.59% (25/27) and a specificity of 100.00% (27/27) (Figure 2).

Discussion

Here, whole-brain ReHo was assessed at rest in both SSNHL patients and normal control individuals. Significant reductions in ReHo values were observed in the left cerebellum, bilateral ITG, left STP, right PHG, left PCC, and right SFG of SSNHL patients during the acute hearing loss period relative to control individuals. These data suggest that these seven regions of the brain exhibit abnormal spontaneous neural activity in individuals affected by acute-phase SSNHL. SVM analyses further indicated that reductions in ReHo in the left cerebellum may offer value as a neuroimaging biomarker that can distinguish between patients with SSNHL and unaffected controls.

The reduced ReHo of seven brain regions in SSNHL may present the baseline abnormality of sensory cortices in SSNHL at rest. Recent work suggests that the cerebellum plays a central role in the coordination of emotional, sensory, and cognitive processes (27, 28). Moreover, the cerebellum mediates the processing of acoustic information derived from auditory-associated brain regions (29). Xu et al. (15) determined that patients suffering from long-term moderately severe bilateral sensorineural hearing loss exhibit atypical patterns of spontaneous neural activity within the cerebellum, in line with the results of this present study. Here, decreased ReHo of the left cerebellum may reflect abnormal brain function in sensory and cognitive information processing in SSNHL patients, and an adaptation to engage other sensory systems as a compensatory mechanism for the acute hearing impairment. Thus, we speculated that the lack of sufficient acoustic input may have impaired the function of the cerebellum as reflected by reduced ReHo values in this brain region. The SVM analysis results for this region further yielded an accuracy of 96.30% (52/54), suggesting that reductions in left cerebellar ReHo values may offer utility as a putative neuroimaging biomarker that can aid in diagnosing SSNHL.

The ITG has been found to play a role in multiple functional brain networks associated with emotional regulation, language comprehension, memory, and visual processing (30–32). Much like the ITG, the temporal pole is a component of the association complex associated with emotion, language processing, and the multimodal integration of sensory inputs (33–37), and both the STP and ITG are components of the temporal lobe. Therefore, abnormal activity of the two brain regions could influence the function of the temporal lobe. The temporal lobe is the location of the auditory center, and it is also involved in functions relating to emotion, speech, balance, memory, and visual perception. Thus, SSNHL could lead to structural and functional impairment of the temporal lobe.

The PHG is a center that is reportedly associated with higher-order cognitive functions such as visual-spatial processing and the encoding/retrieval of memories (38, 39). Lin et al. (38) conducted a tractography analysis that confirmed the existence of extensive cortico-cortical correlations between the PHG and other regions of the brain including the occipital, parietal, temporal, and frontal cortices. The temporal pole has also been regarded as a component of the parahippocampal region in humans as well as in non-human primates (39, 40). As such, the ITG, STP, and PHG are closely related to one another both functionally and structurally. Multiple reports have identified abnormal changes in the PHG and ITG in individuals suffering from hearing loss. Yang et al. (41) determined that individuals affected by long-term right-sided unilateral hearing loss exhibit significantly lower gray matter volumes in the right PHG, left superior/middle/inferior temporal gyrus, bilateral PCC, and precuneus. Chen et al. (42) also observed lower ReHo values in the precuneus, PHG, superior temporal gyrus, and inferior parietal lobe in presbycusis patients. In the present analysis, SSNHL patients exhibited resting-state ReHo abnormalities in the STP, ITG, and PHG, thus suggesting a role for these regions in the pathophysiology of this condition.

The PCC is a component of the posteromedial cortex located in the medial portion of the inferior parietal lobe (43). As a key default mode network (DMN) component, the function of the PCC has been linked to cognition, emotional regulation, and the retrieval of episodic memories. The DMN consists of the medial prefrontal cortex, precuneus, inferior parietal lobe, and PCC (44), and plays roles in negative ruminations, memory retrieval, cognitive functioning, and self-related thoughts (44–46). Reductions in ReHo values in the PCC in the present analysis are likely reflective of altered spontaneous neural activity in this region and between the PCC and connected regions. The SFG, located in the superior prefrontal cortex, has previously been separated based on diffusion tensor tractography into the anteromedial, dorsolateral, and posterior SFG subregions by Li et al. (47), revealing both the anteromedial and dorsolateral SFG to be primarily connected with the DMN when conducting resting-state analyses of functional connectivity. The SFG is also an integral component of emotional processing, cognitive control, and working memory (48–51), and several reports have documented altered ReHo values in the SFG. Patients with MDD, for example, reportedly exhibit elevated ReHo values in the left SFG, medial superior frontal gyrus, and left middle temporal gyrus (52). Relative to healthy individuals, diabetic optic neuropathy patients also exhibit significant reductions in ReHo values in the SFG, left anterior cingulate, and right middle frontal gyrus (53). Diabetic vitreous hemorrhage patients also reportedly present with significant increases in bilateral SFG, bilateral cerebellar posterior lobes, and right superior/middle occipital gyrus ReHo values (54). However, few studies to date have explored SSNHL-related changes in ReHo values in the SFG. Here, SSNHL patients were found to exhibit significantly reduced ReHo values in the right SFG as compared to normal controls, consistent with the weakening of the consistency of spontaneous neural activity in this region. The observed ReHo abnormalities in the PCC and SFG may thus be suggestive of abnormal structures in the DMN in patients affected by SSNHL.

Prior research has revealed SSNHL incidence to be correlated with higher rates of affective disorders including depression and anxiety (55, 56). The results of this analysis suggest that acute auditory deprivation may alter spontaneous neuronal activity following SSNHL incidence, contributing to changes in higher-order brain functions. Together, these results may offer new insight regarding the underlying neuropathological mechanisms of SSNHL and associated alterations in higher-order brain functions.

The advent of novel imaging technologies has spurred a growing interest in the use of neuroimaging biomarkers as tools for the diagnosis and monitoring of a range of diseases and disorders. Gao et al. (25) reported that the increased degree centrality of the right inferior parietal lobule and the left dorsolateral superior frontal gyrus could be used as a combined imaging biomarker of right temporal lobe epilepsy (rTLE) with respective sensitivity and specificity values of 100% and 98.55%. Abnormal ReHo values in particular brain regions have also shown promise as a tool for differentiating between schizophrenia patients and healthy controls (57). This study, however, is the first to have employed an SVM approach to examine the utility of ReHo abnormalities as SSNHL-related neuroimaging biomarkers. ReHo is an indicator of local brain regions activity. SVM is a mature and effective algorithm in machine learning and it has successfully been used in prior reports to guide the diagnosis of first-episode MDD (9), schizophrenia (58), obsessive-compulsive disorder (10), and rTLE (25). Here, an SVM approach was used to analyze the diagnostic utility of abnormal ReHo values in the left cerebellum, bilateral ITG, left STP, right PHG, left PCC, and right SFG, revealing that the left cerebellum exhibited respective accuracy, sensitivity, and specificity values of 96.30%, 92.59%, and 100.00% when differentiating between SSNHL patients and normal controls.

There are certain limitations to this analysis. For one, the sample size was relatively limited. Additionally, scanner-derived noise could not be fully eliminated even though participants were provided with earplugs. Lastly, no analyses of the correlations between ReHo and clinical findings were performed.

Conclusion

In conclusion, these results suggest that reduced ReHo in the left cerebellum, bilateral ITG, left STP, right PHG, left PCC, and right SFG correspond to abnormal spontaneous brain activity in

patients diagnosed with SSNHL. Moreover, decreases in ReHo within the left cerebellum may offer value as a neuroimaging biomarker that can aid in the diagnosis of SSNHL.

Data availability statement

The original contributions presented in the study are included in the article/supplementary material, further inquiries can be directed to the corresponding author.

Ethics statement

The studies involving human participants were reviewed and approved by the Institutional Review Board of Tianyou Hospital Ethics Committee. The patients/participants provided their written informed consent to participate in this study.

Author contributions

LL, JF, and HZ designed the experiment and wrote this article. JH, RC, XX, ST, and HR collected and analyzed these data. MT and QL guided the experiment and revised the article. All authors contributed to the article and approved the submitted version.

Funding

This research was supported by the grant from the Education Department of Hubei Province scientific research project (Grant No. D20201101).

Acknowledgments

We are grateful to all subjects for participating in the study.

Conflict of interest

The authors declare that the research was conducted in the absence of any commercial or financial relationships that could be construed as a potential conflict of interest.

Publisher's note

All claims expressed in this article are solely those of the authors and do not necessarily represent those of their affiliated organizations, or those of the publisher, the editors and the reviewers. Any product that may be evaluated in this article, or claim that may be made by its manufacturer, is not guaranteed or endorsed by the publisher.

References

1. Schreiber BE, Agrup C, Haskard DO, Luxon LM. Sudden sensorineural hearing loss. *Lancet.* (2010) 375:1203–11. doi: 10.1016/s0140-6736(09)62071-7

2. Kim SH, Kim SJ, Im H, Kim TH, Song JJ, Chae SW, et al. Trend in sudden sensorineural hearing loss: data from a population-based study. *Audiol Neurootol.* (2017) 22:311–6. doi: 10.1159/000485313

3. Alexander TH, Harris JP. Incidence of sudden sensorineural hearing loss. *Otol Neurotol.* (2013) 34:1586–9. doi: 10.1097/mao.0000000000000222

4. Oh JH, Park K, Lee SJ, Shin YR, Choung YH. Bilateral versus unilateral sudden sensorineural hearing loss. *Otolaryngol—Head Neck Surg.* (2007) 136:87–91. doi: 10.1016/j.otohns.2006.05.015

5. Chau JK, Lin JR, Atashband S, Irvine RA, Westerberg BD. Systematic review of the evidence for the etiology of adult sudden sensorineural hearing loss. *Laryngoscope.* (2010) 120:1011–21. doi: 10.1002/lary.20873

6. Chen J, Hu B, Qin P, Gao W, Liu C, Zi D, et al. Altered brain activity and functional connectivity in unilateral sudden sensorineural hearing loss. *Neural Plast.* (2020) 2020:9460364. doi: 10.1155/2020/9460364

7. Kim SY, Min C, Lee CH, Park B, Choi HG. Bidirectional relation between depression and sudden sensorineural hearing loss: two longitudinal follow-up studies using a national sample cohort. *Sci Rep.* (2020) 10:1482. doi: 10.1038/s41598-020-58547-w

8. Dallan I, Fortunato S, Casani AP, Bernardini E, Sellari-Franceschini S, Berrettini S, et al. Long-term follow up of sudden sensorineural hearing loss patients treated with intratympanic steroids: audiological and quality of life evaluation. *J Laryngol Otol.* (2014) 128:669–73. doi: 10.1017/s0022215114001595

9. Gao Y, Wang X, Xiong Z, Ren H, Liu R, Wei Y, et al. Abnormal fractional amplitude of low-frequency fluctuation as a potential imaging biomarker for first-episode major depressive disorder: a resting-state fmri study and support vector machine analysis. *Front Neurol.* (2021) 12:751400. doi: 10.3389/fneur.2021.751400

10. Chen Y, Ou Y, Lv D, Yang R, Li S, Jia C, et al. Altered network homogeneity of the default-mode network in drug-naive obsessive-compulsive disorder. *Prog Neuropsychopharmacol Biol Psychiatry.* (2019) 93:77–83. doi: 10.1016/j.pnpbp.2019.03.008

11. Li YT, Chen JW, Yan LF, Hu B, Chen TQ, Chen ZH, et al. Dynamic alterations of functional connectivity and amplitude of low-frequency fluctuations in patients with unilateral sudden sensorineural hearing loss. *Neurosci Lett.* (2022) 772:136470. doi: 10.1016/j.neulet.2022.136470

12. Wang Q, Chen Q, Liu P, Zhang J, Zhou L, Peng L. Functional magnetic resonance imaging reveals early connectivity changes in the auditory and vestibular cortices in idiopathic sudden sensorineural hearing loss with vertigo: a pilot study. *Front Hum Neurosci.* (2021) 15:719254. doi: 10.3389/fnhum.2021.719254

13. Fan W, Zhang W, Li J, Zhao X, Mella G, Lei P, et al. Altered contralateral auditory cortical morphology in unilateral sudden sensorineural hearing loss. *Otol Neurotol.* (2015) 36:1622–7. doi: 10.1097/mao.0000000000000892

14. Zhou GP, Shi XY, Wei HL, Qu LJ Yu YS, Zhou QQ, et al. Disrupted intraregional brain activity and functional connectivity in unilateral acute tinnitus patients with hearing loss. *Front Neurosci.* (2019) 13:1010. doi: 10.3389/fnins.2019.01010

15. Xu XM, Jiao Y, Tang TY, Zhang J, Lu CQ, Luan Y, et al. Dissociation between cerebellar and cerebral neural activities in humans with long-term bilateral sensorineural hearing loss. *Neural Plast.* (2019) 2019:8354849. doi: 10.1155/2019/8354849

16. Liu B, Feng Y, Yang M, Chen JY Li J, Huang ZC, et al. Functional connectivity in patients with sensorineural hearing loss using resting-state MRI. *Am J Audiol.* (2015) 24:145–52. doi: 10.1044/2015_aja-13-0068

17. Zhang GY, Yang M, Liu B, Huang ZC, Chen H, Zhang PP, et al. Changes in the default mode networks of individuals with long-term

unilateral sensorineural hearing loss. *Neuroscience.* (2015) 285:333–42. doi: 10.1016/j.neuroscience.2014.11.034

18. Liu Y, Wang K, Yu C, He Y, Zhou Y, Liang M, et al. Regional homogeneity, functional connectivity and imaging markers of Alzheimer's disease: a review of resting-state fMRI studies. *Neuropsychologia.* (2008) 46:1648–56. doi: 10.1016/j.neuropsychologia.2008.01.027

19. Zang Y, Jiang T, Lu Y, He Y, Tian L. Regional homogeneity approach to fMRI data analysis. *Neuroimage.* (2004) 22:394–400. doi: 10.1016/j.neuroimage.2003.12.030

20. Shah YS, Hernandez-Garcia L, Jahanian H, Peltier SJ. Support vector machine classification of arterial volume-weighted arterial spin tagging images. *Brain Behav.* (2016) 6:e00549. doi: 10.1002/brb3.549

21. LaConte S, Strother S, Cherkassky V, Anderson J, Hu X. Support vector machines for temporal classification of block design fmri data. *Neuroimage.* (2005) 26:317–29. doi: 10.1016/j.neuroimage.2005.01.048

22. Shan X, Cui X, Liu F, Li H, Huang R, Tang Y, et al. Shared and distinct homotopic connectivity changes in melancholic and non-melancholic depression. *J Affect Disord.* (2021) 287:268–75. doi: 10.1016/j.jad.2021.03.038

23. Zhang X, Wang YT, Wang Y, Jung TP, Huang M, Cheng CK, et al. Ultra-slow frequency bands reflecting potential coherence between neocortical brain regions. *Neuroscience.* (2015) 289:71–84. doi: 10.1016/j.neuroscience.2014.12.050

24. Librenza-Garcia D, Kotzian BJ, Yang J, Mwangi B, Cao B, Pereira Lima LN, et al. The impact of machine learning techniques in the study of bipolar disorder: a systematic review. *Neurosci Biobehav Rev.* (2017) 80:538–54. doi: 10.1016/j.neubiorev.2017.07.004

25. Gao Y, Xiong Z, Wang X, Ren H, Liu R, Bai B, et al. Abnormal degree centrality as a potential imaging biomarker for right temporal lobe epilepsy: a resting-state functional magnetic resonance imaging study and support vector machine analysis. *Neuroscience.* (2022) 487:198–206. doi: 10.1016/j.neuroscience.2022.02.004

26. Karpiel I, Klose U, Drzazga Z. Optimization of rs-fMRI parameters in the seed correlation analysis (SCA) in DPARSF toolbox: a preliminary study. *J Neurosci Res.* (2019) 97:433–43. doi: 10.1002/jnr.24364

27. Baumann O, Borra RJ, Bower JM, Cullen KE, Habas C, Ivry RB, et al. Consensus paper: the role of the cerebellum in perceptual processes. *Cerebellum.* (2015) 14:197–220. doi: 10.1007/s12311-014-0627-7

28. Adamaszek M, D'Agata F, Ferrucci R, Habas C, Keulen S, Kirkby KC, et al. Consensus paper: cerebellum and emotion. *Cerebellum.* (2017) 16:552–76. doi: 10.1007/s12311-016-0815-8

29. Petacchi A, Laird AR, Fox PT, Bower JM. Cerebellum and auditory function: an ALE meta-analysis of functional neuroimaging studies. *Hum Brain Mapp.* (2005) 25:118–28. doi: 10.1002/hbm.20137

30. Lin YH, Young IM, Conner AK, Glenn CA, Chakraborty AR, Nix CE, et al. Anatomy and white matter connections of the inferior temporal gyrus. *World Neurosurg.* (2020) 143:e656–e66. doi: 10.1016/j.wneu.2020.08.058

31. Buckley MJ, Gaffan D, Murray EA. Functional double dissociation between two inferior temporal cortical areas: perirhinal cortex versus middle temporal gyrus. *J Neurophysiol.* (1997) 77:587–98. doi: 10.1152/jn.1997.77.2.587

32. Gao YJ, Wang X, Xiong PG, Ren HW, Zhou SY, Yan YG, et al. Abnormalities of the default-mode network homogeneity and executive dysfunction in people with first-episode, treatment-naive left temporal lobe epilepsy. *Eur Rev Med Pharmacol Sci.* (2021) 25:2039–49. doi: 10.26355/eurrev_202102_25108

33. Olson IR, Plotzker A, Ezzyat Y. The enigmatic temporal pole: a review of findings on social and emotional processing. *Brain.* (2007) 130(Pt 7):1718–31. doi: 10.1093/brain/awm052

34. Skipper LM, Ross LA, Olson IR. Sensory and semantic category subdivisions within the anterior temporal lobes. *Neuropsychologia.* (2011) 49:3419–29. doi: 10.1016/j.neuropsychologia.2011.07.033

35. Aust S, Alkan Härtwig E, Koelsch S, Heekeren HR, Heuser I, Bajbouj M. How emotional abilities modulate the influence of early life stress on hippocampal functioning. *Soc Cogn Affect Neurosci.* (2014) 9:1038–45. doi: 10.1093/scan/nst078

36. Hickok G, Poeppel D. The cortical organization of speech processing. *Nat Rev Neurosci.* (2007) 8:393–402. doi: 10.1038/nrn2113

37. Pehrs C, Zaki J, Schlochtermeier LH, Jacobs AM, Kuchinke L, Koelsch S. The temporal pole top-down modulates the ventral visual stream during social cognition. *Cereb Cortex.* (2017) 27:777–92. doi: 10.1093/cercor/bhv226

38. Lin YH, Dhanaraj V, Mackenzie AE, Young IM, Tanglay O, Briggs RG, et al. Anatomy and white matter connections of the parahippocampal gyrus. *World Neurosurg.* (2021) 148:e218–e26. doi: 10.1016/j.wneu.2020.12.136

39. Blaizot X, Mansilla F, Insausti AM, Constans JM, Salinas-Alamán A, Pró-Sistiaga P, et al. The human parahippocampal region: I. Temporal pole cytoarchitectonic and MRI correlation. *Cereb Cortex.* (2010) 20:2198–212. doi: 10.1093/cercor/bhp289

40. Insausti R, Amaral DG, Cowan WM. The entorhinal cortex of the monkey: II. Cortical afferents. *J Compar Neurol.* (1987) 264:356–95. doi: 10.1002/cne.902640306

41. Yang M, Chen HJ, Liu B, Huang ZC, Feng Y, Li J, et al. Brain structural and functional alterations in patients with unilateral hearing loss. *Hear Res.* (2014) 316:37–43. doi: 10.1016/j.heares.2014.07.006

42. Chen YC, Chen H, Jiang L, Bo F, Xu JJ, Mao CN, et al. Presbycusis disrupts spontaneous activity revealed by resting-state functional MRI. *Front Behav Neurosci.* (2018) 12:44. doi: 10.3389/fnbeh.2018.00044

43. Parvizi J, Van Hoesen GW, Buckwalter J, Damasio A. Neural connections of the posteromedial cortex in the Macaque. *Proc Natl Acad Sci U S A.* (2006) 103:1563–8. doi: 10.1073/pnas.0507729103

44. Gao Y, Wang M, Yu R, Li Y, Yang Y, Cui X, et al. Abnormal default mode network homogeneity in treatment-naive patients with first-episode depression. *Front Psychiatry.* (2018) 9:697. doi: 10.3389/fpsyt.2018.00697

45. Greicius MD, Krasnow B, Reiss AL, Menon V. Functional connectivity in the resting brain: a network analysis of the default mode hypothesis. *Proc Natl Acad Sci U S A.* (2003) 100:253–8. doi: 10.1073/pnas.0135058100

46. Gao Y, Zheng J, Li Y, Guo D, Wang M, Cui X, et al. Abnormal default-mode network homogeneity in patients with temporal lobe epilepsy. *Medicine.* (2018) 97:e11239. doi: 10.1097/md.0000000000011239

47. Li W, Qin W, Liu H, Fan L, Wang J, Jiang T, et al. Subregions of the human superior frontal gyrus and their connections. *Neuroimage.* (2013) 78:46–58. doi: 10.1016/j.neuroimage.2013.04.011

48. Alagapan S, Lustenberger C, Hadar E, Shin HW, Fröhlich F. Low-frequency direct cortical stimulation of left superior frontal gyrus enhances working memory performance. *Neuroimage.* (2019) 184:697–706. doi: 10.1016/j.neuroimage.2018.09.064

49. du Boisgueheneuc F, Levy R, Volle E, Seassau M, Duffau H, Kinkingnehun S, et al. Functions of the left superior frontal gyrus in humans: a lesion study. *Brain.* (2006) 129(Pt 12):3315–28. doi: 10.1093/brain/awl244

50. Andrews-Hanna JR, Smallwood J, Spreng RN. The default network and self-generated thought: component processes, dynamic control, and clinical relevance. *Ann N Y Acad Sci.* (2014) 1316:29–52. doi: 10.1111/nyas.12360

51. Raichle ME. The brain's default mode network. *Annu Rev Neurosci.* (2015) 38:433–47. doi: 10.1146/annurev-neuro-071013-014030

52. Liu S, Ma R, Luo Y, Liu P, Zhao K, Guo H, et al. Facial expression recognition and reho analysis in major depressive disorder. *Front in Psychol.* (2021) 12:688376. doi: 10.3389/fpsyg.2021.688376

53. Guo GY, Zhang LJ Li B, Liang RB, Ge QM, Shu HY, et al. Altered spontaneous brain activity in patients with diabetic optic neuropathy: a resting-state functional magnetic resonance imaging study using regional homogeneity. *World J Diabetes.* (2021) 12:278–91. doi: 10.4239/wjd.v12.i3.278

54. Zhang YQ, Zhu FY, Tang LY Li B, Zhu PW, Shi WQ, et al. Altered regional homogeneity in patients with diabetic vitreous hemorrhage. *World J Diabetes.* (2020) 11:501–13. doi: 10.4239/wjd.v11.i11.501

55. Kim JY, Lee JW, Kim M, Kim MJ, Kim DK. Association of idiopathic sudden sensorineural hearing loss with affective disorders. *JAMA Otolaryngol Head Neck Surg.* (2018) 144:614–21. doi: 10.1001/jamaoto.2018.0658

56. Arslan F, Aydemir E, Kaya YS, Arslan H, Durmaz A. Anxiety and depression in patients with sudden one-sided hearing loss. *Ear Nose Throat J.* (2018) 97:E7–10. doi: 10.1177/0145561318097010-1101

57. Iwabuchi SJ, Palaniyappan L. Abnormalities in the effective connectivity of visuothalamic circuitry in schizophrenia. *Psychol Med.* (2017) 47:1300–10. doi: 10.1017/s0033291716003469

58. Steardo L Jr., Carbone EA, de Filippis R, Pisanu C, Segura-Garcia C, Squassina A, et al. Application of support vector machine on fmri data as biomarkers in schizophrenia diagnosis: a systematic review. *Front. Psychiatry.* (2020) 11:588. doi: 10.3389/fpsyt.2020.00588

frontiers | Frontiers in Psychiatry

TYPE Original Research
PUBLISHED 25 July 2022
DOI 10.3389/fpsyt.2022.972968

OPEN ACCESS

EDITED BY
Yujun Gao,
Wuhan University, China

REVIEWED BY
Fei Chen,
Yancheng Third People's Hospital, China
Mi Zhou,
Sichuan Academy of Medical Sciences and Sichuan Provincial People's Hospital, China

*CORRESPONDENCE
Zhi-Wei Zhang
zhangzhiwei@hospital.cqmu.edu.cn
Fa-Jin Lv
fajinlv@163.com
Ren-Qiang Yu
yurenqiang@hospital.cqmu.edu.cn

†These authors have contributed equally to this work

SPECIALTY SECTION
This article was submitted to Neuroimaging and Stimulation, a section of the journal Frontiers in Psychiatry

RECEIVED 19 June 2022
ACCEPTED 05 July 2022
PUBLISHED 25 July 2022

CITATION
Wang X-Y, Tan H, Li X, Dai L-Q, Zhang Z-W, Lv F-J and Yu R-Q (2022) Resting-state functional magnetic resonance imaging-based identification of altered brain the fractional amplitude of low frequency fluctuation in adolescent major depressive disorder patients undergoing electroconvulsive therapy. *Front. Psychiatry* 13:972968. doi: 10.3389/fpsyt.2022.972968

Resting-state functional magnetic resonance imaging-based identification of altered brain the fractional amplitude of low frequency fluctuation in adolescent major depressive disorder patients undergoing electroconvulsive therapy

Xing-Yu Wang[1†], Huan Tan[1†], Xiao Li[2], Lin-Qi Dai[2], Zhi-Wei Zhang[1*], Fa-Jin Lv[1*] and Ren-Qiang Yu [1*]

[1]Department of Radiology, The First Affiliated Hospital of Chongqing Medical University, Chongqing, China, [2]Department of Psychiatry, The First Affiliated Hospital of Chongqing Medical University, Chongqing, China

Purpose: While electroconvulsive therapy (ECT) has been repeatedly been shown to effectively and efficiently treat the major depressive disorder (MDD), the mechanistic basis for such therapeutic efficacy remains to be firmly established. As such, further research exploring the ECT-based treatment of MDD in an adolescent population is warranted.

Methods: This study included 30 treatment-naïve first-episode MDD patients and 30 healthy control (HC) individuals (aged 12–17 years). All participants were scanned using rs-fMRI, and the 30 MDD patients were scanned again after 2 weeks of the ECT treatment period. Intrinsic local activity in each voxel was assessed based on the fractional amplitude of low frequency fluctuation (fALFF) parameter, with all fALFF analyses being completed using the REST application. Correlations between ECT-related changes in fALFF and clinical parameters were additionally examined.

Results: Relative to HCs, MDD patients exhibited increased fALFF values in the right inferior frontal gyrus (ORBinf), inferior occipital gyrus (IOG), and the left middle frontal gyrus (MFG) at baseline. Following ECT, these patients exhibited significant increases in fALFF values in the right medial superior frontal gyrus (SFGmed), dorsolateral superior frontal gyrus (SFGdor), anterior cingulate, and paracingulate gyrus (ACG), median cingulate and paracingulate gyrus (DCG), and left MFG. MDD patient HAMD scores were negatively correlated with fALFF

values when analyzing pre-ECT vs. post-HCT ΔHAMD and fALFF values in the right SFGmed, SFGdor, and the left MFG.

Conclusion: These data suggest that ECT induced altered fALFF in some regions of the brain, suggesting that these alterations may serve as a neurobiological indicator of ECT effectiveness in MDD adolescents.

KEYWORDS

major depressive disorder (MDD), adolescent, fALFF, electroconvulsive therapy, resting-state fMRI

Introduction

Major depressive disorder (MDD) is a potentially life-threatening psychiatric condition that occurs in response to a range of genetic factors, environmental inputs, stressors, and other factor (1–3), resulting in symptoms including persistent depression, cognitive impairments, and high levels of morbidity including an elevated risk of suicide, with MDD patients exhibiting a lifetime suicide rate of 2–12% (4). In recent years, the number of individuals diagnosed with MDD has risen substantially, particularly among younger segments of the population, with adolescents in particular being highly susceptible to depression (5). Some estimates suggest suicide to be the second most common cause of death for persons 10–24 years of age (6). Owing to the marked structural changes in the brain that occur during adolescence, it is regarded as an important window of susceptibility for the onset of MDD (7, 8). Lee et al. (9) noted that the drivers of depression are highly diverse and complex, with adults and adolescents diagnosed with MDD exhibiting distinct clinical. In some cases, adolescents suffering from depression are more likely to develop difficult-to-treat conditions such bipolar disorder, comorbid borderline personality disorder, suicidal thoughts, and self-harming behaviors (10, 11).

Electroconvulsive therapy (ECT) (12, 13) is an approach wherein a brief jolt of electricity is administered to the brain in an effort to treat certain mental disorders, resulting in the simultaneous firing of cells throughout the brain, resulting in convulsions and altered neural metabolic processes that can improve MDD patient outcomes (14). Several studies have explored the drivers of abnormal brain activity and ECT-related therapeutic benefits. For example, Liu et al. (15) conducted a systematic analysis of the effects of ECT-related antidepressant activity and reported a correlation between such activity and subgenual anterior cingulate activity and connectivity in MDD. Moreover, Strober et al. (16) explored the impact of ECT on adolescents diagnosed with severe endogenous depression such that they were able to identify certain phenomenological characteristics predictive of ECT responses. Consoli et al. (17) assessed the effects of ECT on severe forms of treatment-resistant self-injurious behavior and aggression (SIB/AGG) in young individuals diagnosed with intellectual disabilities and comorbid psychiatric disorders, confirming the efficacy of ECT in this setting. As such, these results suggest a close link between the mechanism whereby ECT exerts its therapeutic activity and neurological activity in humans, although further work is essential to fully elucidate these mechanisms in adolescent MDD patients.

Resting-state functional magnetic resonance imaging (rs-fMRI) is a high-performance imaging modality that is easy to operate and resistant to interference (5, 18), leading to its widespread use in the analysis of brain function, neural network activity, and in the diagnosis of a range of conditions impacting the central nervous system (19, 20, 21). In addition, rs-fMRI can be leveraged to study the pathogenesis of MDD and treatment-related changes in brain activity. Of the parameters that can be measured in this neuroimaging context, regional cerebral blood flow (rCBF), blood oxygen level-dependent (BOLD) signal, and deoxyhemoglobin content (22) values attributable to low-frequency unconscious brain activity are used to assess resting-state amplitude of low-frequency fluctuation (ALFF) (23) values, providing an accurate and highly representative means of examining brain activity based on fMRI data (24, 25).

As an improved ALFF method (26, 27), the fractional amplitude of low frequency fluctuation (fALFF) can eliminate the impact of physiological noise on the resultant data while providing greater specificity and sensitivity for the detection of spontaneous brain activity based on the use of average signal oscillation intensity in the 0.01–0.08 Hz range and the ratio of the whole frequency band oscillations.

Here, rs-fMRI was used to explore the mechanisms underlying the efficacy of ECT in adolescent patients diagnosed with MDD. Specifically, fALFF data pertaining to these MDD patients' brain activity was compared before and after ECT treatment through an fMRI approach, enabling us to explore the processes underlying the ECT's antidepressant effects in this patient group.

Materials and methods

Participants

This study enrolled 30 MDD patients and 30 healthy control (HC) individuals 12–17 years of age. All patients with MDD in this study were recruited from inpatient clinics at the Department of Psychiatry of the First Affiliated Hospital of Chongqing Medical University, China, from October 2019 to October 2021. Patients were eligible for study inclusion if they were experiencing first-episode depression without any prior history of mania or hypomania, had no history of antidepressant treatment, were right-handed, were of Han ethnicity, exhibited a Hamilton Depression Scale (HAMD-24) score $>$ 17, were 12–17 years of age, had not taken any psychotropic drugs, and had not used sedative, anesthetic, or analgesic drugs within the past 1-month period. Patients were excluded from this study if they had any prior history of mental health disorders including bipolar disorder or schizophrenia, had been diagnosed with organic brain diseases or other serious physical illnesses, reported substance abuse or dependence, or exhibited contraindications for MRI scanning. Patients with MRI scan contraindications.

HC study participants were recruited from as volunteers from local schools, and were eligible for inclusion if they exhibited a HAMD-24 score $<$ 7, were right-handed, were of Han ethnicity, were 12–17 years of age, and weren't suffering from any severe mental or physical illness. Exclusion criteria for HCs were identical to those for MDD patients.

Adolescents and their parents or guardians gave their written informed permission to participate in the research, and the Human Research and Ethics Committee at the First Affiliated Hospital of Chongqing Medical University gave its approval (no.2017-157).

Electroconvulsive therapy

A Thymatron DGx instrument (Somatics, LLC., Venice, IL, United States) was used to perform modified bi-frontotemporal ECT for all patients at the First Affiliated Hospital of Chongqing Medical University. The initial three ECT courses were performed on consecutive days, with the remaining courses then being completed every other day. No courses were performed on weekends. After a 2-week treatment course, the ECT process was complete. The energy level used for ECT was determined based on the age of the patient being treated (energy percentage = age $\times$ 0.5%), with stimulation energy then being adjusted based on seizure time, increasing by 5% during subsequent treatments when the seizure time was $<$ 25 s. Succinylcholine (0.5–1 mg/kg) and diprivan (1.5–2 mg/kg) were used to induce anesthesia. In this study, individuals were treated with antidepressants.

Resting-state functional magnetic resonance imaging data acquisition

A 3T GE Signa HDxt scanner (GE Healthcare, Boston, IL, United States) equipped with an 8-channel head coil was used for rs-fMRI scanning of all participants. During scanning, participants were directed to remain still and awake with their eyes closed while not thinking about anything specific to the greatest extent possible. Head motion and machine noise were, respectively, mitigated using foam pads and earplugs. All echoplanar imaging pulse sequences were performed with the following parameters: repetition time (TR) = 2000 ms, echo time (TE) = 40 ms, field of view (FOV) = 240 mm $\times$ 240 mm, matrix = 64 $\times$ 64, flip angle = 90°, slice number = 33, slice thickness/gap = 4.0/0 mm; scanner time = 8 min, and 240 volumes. Three-dimensional T1-weighted MRI scans used for rs-fMRI co-registration were performed using the following settings: TR = 24 ms; TE = 9 ms; FOV = 240 mm $\times$ 240 mm, matrix = 256 $\times$ 256, flip angle = 90°, and slice thickness/gap = 1.0/0 mm.

Data preprocessing

The SPM software platform and the DPABI tool[1] (28) were used to process fMRI data. The initial 10 images for each patient were discarded to ensure sufficient time for adaptation to the scanning process, with the remaining 230 volumes then being analyzed. Data were corrected for head movement, and patients were not eligible for inclusion in subsequent analyses If they exhibited a maximum displacement of $>$ 1.5 mm along the x, y, or z axes or angular displacement $>$ 1.5°. Slice correction was performed to control for acquisition delay. All fMRI images were subjected to normalization and registered to the standard Montreal Neurological Institute (MNI) with 3 mm$\times$ 3 mm $\times$ 3 mm resampling. Images were also smoothed with an 8-mm full-width at half-maximum Gaussian kernel and were bandpass filtered (0.01–0.08Hz) to eliminate low-frequency drift and high-frequency noises including respiratory and cardiac noise.

The fractional amplitude of low frequency fluctuation calculations

The REST software was used to measure fALFF values, which served as a measure of the intrinsic local spontaneous neuronal activity in each voxel. For these analyses, individual processed rs-fMRI datasets were transformed via fast Fourier transformation to a frequency domain, followed by the

1 http://www.restfmri.net

calculation of the square root of the power spectrum. Then, fALFF values were established based on the averaged square root across the 0.01–0.1 Hz range. Then, to account for local variations, we normalized each participant's voxels levels fALFF values by their global mean fALFF value. Overall, this approach allowed fALFF to be determined as the mean power spectrum in a specific low-frequency band (0.01–0.1 Hz) by dividing the spectrum in that band by the spectrum throughout the entire frequency range (29).

Statistical analyses

Differences in patient clinical and demographic characteristics before and after treatment, continuous variables were compared using paired *t*-tests. Paired sample *t*-tests were used to examine changes in fALFF before and after ECT therapy in SPM12, and SPSS v26.0 (IBM, Chicago, NY, United States) was used for all other analyses with a false discovery rate (FDR)-corrected P value < 0.05 as the cutoff for significance. Significant variations in patient clinical symptoms, as defined by HAMD scores, were correlated with mean values for specified parameters in various brain areas using Pearson correlation analysis. Similarly, Pearson correlation analyses were used to determine whether there was a statistically significant relationship between fALFF values and the degree to which clinical symptom changes (ΔHAMD = pre-ECT HAMD – post-ECT HAMD).

Results

Table 1 lists the demographic characteristics of the participants. At baseline, no significant differences in age, sex, or level of education were found between MDD patients and HCs ($P > 0.05$). Following a 2-week ECT treatment period, MDD patients exhibited significant reductions in total HAMD scores ($P < 0.05$) (Table 2).

TABLE 1 Demographics and clinical characters of healthy controls (HCs) and MDD patients.

Demographic data	MDD ($n = 30$)	HCs ($n = 30$)	T (orx^2)	P-value
Gender (male/female)	30(9/21)	30(8/22)	0.774	0.082[a]
Age (years)	14.77 ± 1.43	15.50 ± 1.87	−1.705	0.093[b]
Years of education (years)	8.90 ± 1.729	9.83 ± 2.198	−1.828	0.073[b]
HAMD score	28.63 ± 6.01	0.10 ± 0.403	25.952	0.001

[a]The p value for gender distribution was obtained by chi-square test.
[b]The p value were obtained by two sample I-tests.
NC, normal control; HAMD, Hamilton depression scale.

TABLE 2 Comparisons of the HAMD scoress between pre- and post-ECT.

	pre-ECT	post-ECT	T-value	P-value
HAMD score	28.63 ± 6.01	13.70 ± 8.929	7.600	<0.001

Whole-brain voxel-level analyses revealed significant increases in fALFF in the right orbital inferior frontal gyrus (ORBinf), inferior occipital gyrus (IOG), and left middle frontal gyrus (MFG) in MDD patients relative to HCs (Figure 1) when using a cluster threshold of $P < 0.05$ ($P < 0.001$, Voxel size > 50). However, for these areas, we found no statistically significant associations between HAMD scores and fALFF values that exhibited significant baseline differences between individuals with MDD and controls.

Subsequently, MDD patients exhibited significant alterations in whole-brain fALFF. Specifically, fALFF was significantly elevated in the right medial superior frontal gyrus (SFGmed), anterior cingulate and paracingulate gyrus (ACG), median cingulate and paracingulate gyrus (DCG) dorsolateral superior frontal gyrus (SFGdor) and the left middle frontal gyrus (MFG) following treatment with a cluster threshold of $P < 0.05$ ($P < 0.001$, Voxel size > 50).

Correlation analyses revealed ΔHAMD to be significantly negatively correlated with fALFF in the right SFGmed, SFGdor, and left MFG when comparing pre- and post-ECT data ($R^2 = 0.2333$, $P = 0.0069$; $R^2 = 0.1853$, $P = 0.0176$; $R^2 = 0.1907$, $P = 0.0158$) (Figure 2).

Discussion

All MDD patients enrolled in the present study were treatment-naïve at the time of enrollment and exhibited HAMD-17 scores that were significantly lower following ECT treatment consistent with the improvement of depressive symptoms. Following ECT, MDD patients exhibited significant increases in fALFF in the right SFGmed, ACG, SFGdor, DCG, and left MFG. A negative correlation was observed between ECT effectiveness and fALFF changes in the right SFGmed, SFGdor, and left MFG based on correlation studies. Several studies of MDD to date have identified a direct link between the incidence of depressive symptoms and reductions in the levels of certain excitatory neurotransmitters in the prefrontal lobe with corresponding decreases in frontal lobe neuronal synapses (30–32), with this region being one of the most commonly impaired in MDD patients (32). Overall, fALFF values in the SFGmed.R, SFGdor.R and MFG.L regions were significantly increased following ECT.

Prior work has shown MDD patients to exhibit changes in ALFF/fALFF in numerous brain regions such as the right SFGmed, ACG, SFGdor, DCG, and left MFG. Individuals

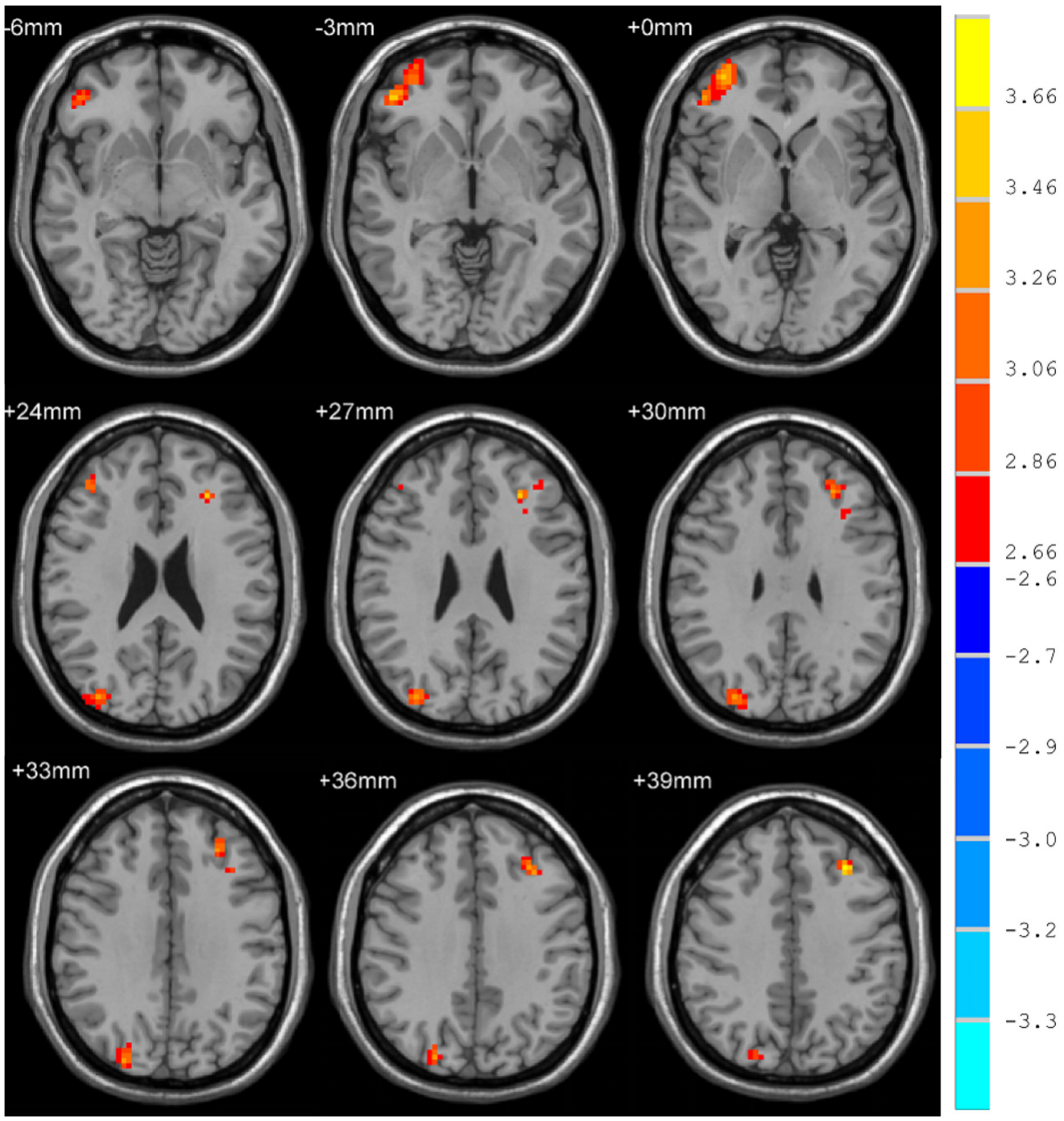

FIGURE 1
Brain regions where fALFF levels are significantly different in MDD patients to that of healthy controls.

with MDD and those at a greater risk for developing MDD have been shown to have frontal lobe abnormalities, both anatomical and functional, these results have yet to be leveraged to effectively treat or prevent this debilitating psychiatric condition. Hongqing et al. (33) employed an MRI approach to examine potential drivers of suicidal ideation among adolescents suffering from depression, ultimately determining that these MDD patients exhibited abnormal levels of autonomic neural activity in the left hippocampus and left MFG. The left MFG is a component of the left dorsolateral prefrontal cortex (DLPFC), which primarily governs executive function and cognition (34), in addition to being linked to processes including working memory (35), social perceptions and the processing of social information (36), memory retrieval (37), emotional regulation, and processing emotional stimuli (38). Li et al. (39) determined through a comparison of non-remitting and remitting patients that the former group exhibited reductions in gray matter volume in the left DLPFC, potentially suggesting that MDD patients with remittent disease may exhibit distinct morphological and cognitive features from patients with non-remittent disease. Accordingly, voxel-based structural changes in this region may be characteristic of a subset of recurrent MDD patients that fail to reliably respond to antidepressant treatment. Kong et al. additionally reported increased ALFF values in the left MFG, right MFG, and orbital regions in line with the results of the present analysis, although they also determined that elderly MDD patients exhibited reductions in ALFF values in the right SFG and MFG following

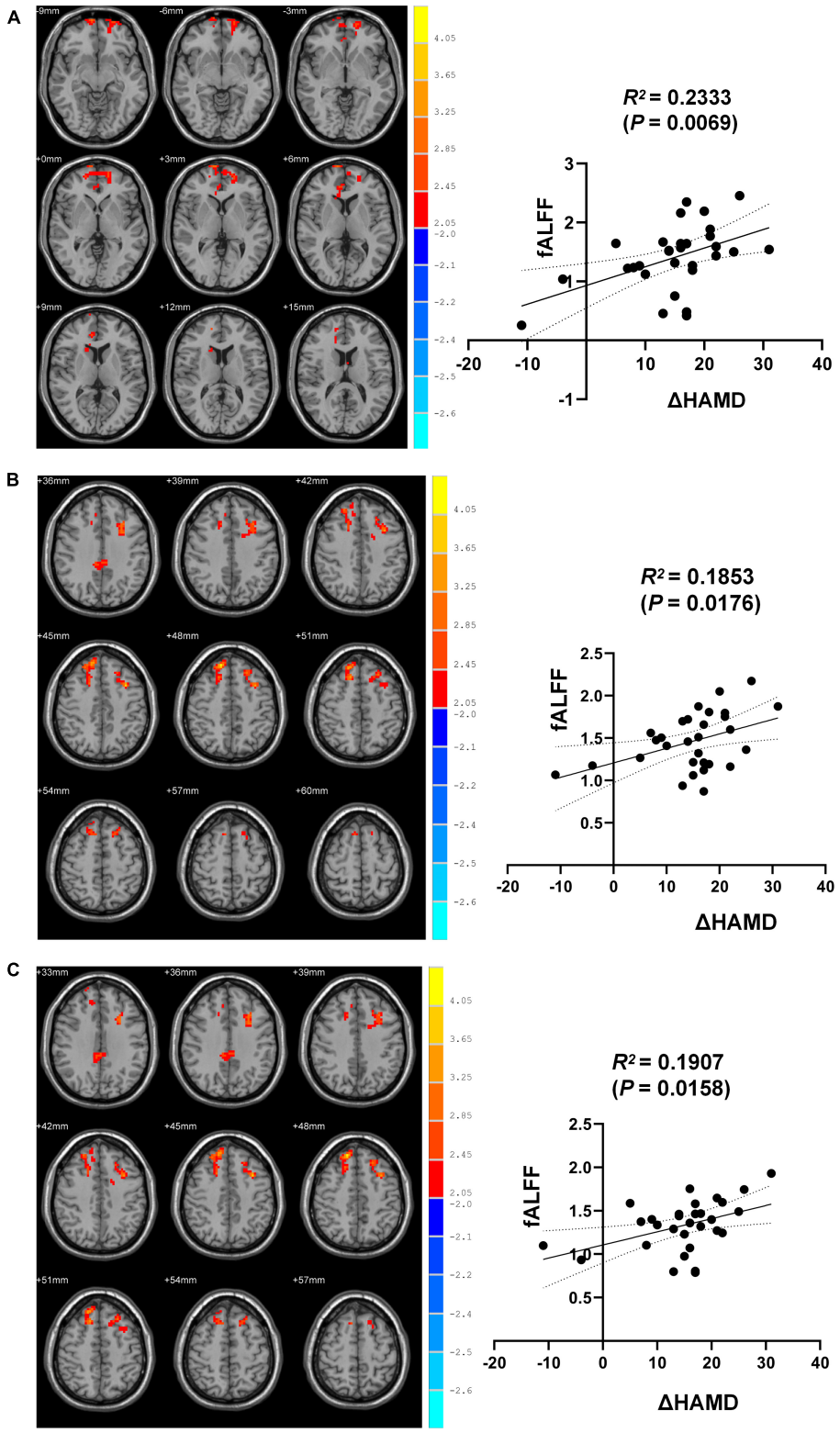

FIGURE 2
Brain regions differences between pre-and post-ECT. **(A)** Correlation analysis of fALFF in brain regions (the right SFGmed) with difference and ΔHAMD. **(B)** Correlation analysis of fALFF in brain regions (the right SFGdor) with difference and ΔHAMD. **(C)** Correlation analysis of fALFF in brain regions (the left MFG) with difference and ΔHAMD.

ECT (40), potentially suggesting the existence of marked differences between adolescent and elderly MDD patients, in line with other data from a study performed by Lee et al. (9).

To date, few analyses have specifically focused on ECT-related changes in fALFF values in the right SFG, including the right SFGmed, and SFGdor, in adolescent MDD patients. Most studies that have explored ECT-related changes in adolescent MDD patients have reported altered ALFF/fALFF values in the precentral gyrus, right fusiform gyrus, left MFG, and right middle temporal pole gyrus. Even so, studies focused on various other psychiatric conditions have demonstrated a relationship between the right SFGmed and SFGdor and treatment outcomes (41–44).

Wang et al. (45) reported gray matter volume in the right SFG to be significantly positively correlated with superiority bias, suggesting a structural basis for such bias. Li et al. (39), in contrast, found that reductions in gray matter volume in the right SFG were not sufficient to differentiate between MDD patients that did and did not achieve remission. Regional homogeneity (ReHo) values in the right SFG and superior MGF in bipolar disorder patients have previously been found to be higher than those for MDD patients, suggesting that these values can be leveraged to distinguish between patients with these two psychiatric disorders (46). Prerona et al. (47) employed an rs-fMRI approach to analyze schizophrenia patients, and found that elevated activity in the right MFG and SFG was positively correlated with elevated levels of consciousness or subliminal activity. Han et al. (48) additionally found the right SFG and MFG to be closely linked to a range of psychiatric disorders, suggesting that fALFF intensity may correspond to a neurological mechanism tied to the treatment of certain mental health conditions.

Rosalux et al. (41) established a close relationship between the right SFG and the reappraisal of the emotional impact of particular events, with this ability and associated activity being linked to long-term mental health outcomes. Li et al. (43) additionally found fALFF levels in the right precuneus and SFGdor to be significantly negatively correlated with extraverted behavior among adolescents and children, suggesting a role for the right SFGdor in the regulation of emotion. By combining imaging and genetic strategies, Yuan et al. (44) further explored biomarkers linked to the diagnosis of MDD and to the prediction of therapeutic outcomes, ultimately establishing that relative to non-responding depression, responsive depression exhibited lower right SFGdor nodes, with the ALFF values in the bilateral occipital gyrus (MOG), left lentiform nuclear, right superior temporal gyrus, and the CBF in the right calcarine gyrus, and left caudate nucleus being significantly correlated with baseline MDD severity or early efficacy. In their study, analyses of the CBF of the left caudate and the right MFG together with the ALFF of the right inferior temporal gyrus were better able to predict non-responsive depression. Cui et al. (49) further performed the rs-fMRI-based experimental evaluation of brain functional changes in idiopathic trigeminal neuralgia patients, ultimately establishing a link between increased fALFF and sensory integration or pain regulation in these patients.

The left MFG is involved in an important role in emotional regulation, executive function, cognition, working memory, and the processing of emotional stimuli. Right MFG activity levels are positively correlated with the strength of consciousness or subliminal activities (47). The right SFG is also associated with the reappraisal of the emotional impact of particular events and associated long-term mental health outcomes (41). Here, MDD patients were found to exhibit significant increases in the fALFF of the right medial SFG, the right ACG, the right SFGdor, the left MFG, and the right median DCG. Through correlation analyses, the efficacy of ECT treatment was found to be negatively correlated with changes in neuroimaging findings in the right SFGmed, SFGdor, and left MFG regions when comparing pre- and post-treatment fMRI images. This may thus support a model wherein the therapeutic effects of ECT are dependent on the synergistic treatment of these three regions of the brain. Brain networks that facilitate systemic adaptation and flexibility are responsible for small-worldness (42) which is defined as the dynamic remodeling of the small-world topology and related community structure. Functional connectivity between the right precuneus and the right SFGdor was discovered by Li et al. (43) to mitigate the mediating effects of small-worldness. Similarly, these findings are consistent with the hypothesis that the right SFGmed, SFGdor, and the left MFG all have a role in determining patient outcomes via processes analogous to small-worldness in MDD.

Overall, the results of these prior studies are only partially consistent with the results of the present analyses. These inconsistencies may be attributable to differences in the therapeutic approaches, diagnoses, disease severity, and patient assessment methods employed in these various research efforts. In addition, differentiating between unipolar and bipolar depression in adolescent individuals can be challenging, complicating these research efforts. Few studies used fMRI-based studies to determine ECT efficacy in treating MDD in adolescents. The study findings may suggest the mechanism by which ECT improves outcomes for MDD patients by pointing to changes in fALFF across many brain regions.

Conclusion

In summary, the results of this study revealed that ECT was able to effectively treat MDD in adolescents while offering direct insight into ECT-related neuroimaging changes through fMRI analyses. Specifically, following ECT, MDD patients exhibited significantly increased fALFF in the right SFGmed, ACG, SFGdor, DCG, and left MFG. Correlation analyses revealed ECT clinical efficacy (ΔHAMD) to be significantly negatively correlated with changes in fALFF in the right SFGdor, SFGmed, and in the left MFG when comparing pre- and post-ECT results.

As such, these data suggest a potential therapeutic mechanism whereby ECT can synergistically alter brain activity in the right SFGmed, SFGdor, and left MFG.

Limitations

This study is subject to certain limitations. Firstly, this study had a small sample size. Furthermore, it is not feasible to rule out the possibility that these findings were influenced by resting respiratory and cardiac rhythms. Moreover, all patients underwent antidepressant therapy during the course of ECT treatment, thus potentially impacting brain function.

Data availability statement

The original contributions presented in this study are included in the article/**supplementary material**, further inquiries can be directed to the corresponding authors.

Ethics statement

The studies involving human participants were reviewed and approved by the Human Research and Ethics Committee of The First Affiliated Hospital of Chongqing Medical University. Written informed consent to participate in this study was provided by the participants' legal guardian/next of kin. Written informed consent was obtained from the individual(s), and minor(s)' legal guardian/next of kin, for the publication of any potentially identifiable images or data included in this article.

Author contributions

X-YW and HT: writing – original draft and scanning MRI data. HT: analyzed the data. XL and L-QD: investigation. Z-WZ, F-JL, and R-QY: conceptualization, checking the data, methodology, and writing – review and editing. All authors contributed to the article and approved the submitted version.

Acknowledgments

The authors sincerely appreciate all the participants and their families for participating in our study.

Conflict of interest

The authors declare that the research was conducted in the absence of any commercial or financial relationships that could be construed as a potential conflict of interest.

Publisher's note

References

1. Papakostas GI, Fava M. Predictors, moderators, and mediators (correlates) of treatment outcome in major depressive disorder. *Dialogues Clin Neurosci.* (2022) 10:439–51.

2. Flory JD, Yehuda R. Comorbidity between post-traumatic stress disorder and major depressive disorder: alternative explanations and treatment considerations. *Dialogues Clin Neurosci.* (2022) 17:141–50. doi: 10.31887/DCNS.2015.17.2/jflory

3. Kennedy SH. Core symptoms of major depressive disorder: relevance to diagnosis and treatment. *Dialogues Clin Neurosci.* (2022) 10:271–7.

4. Borges G, Nock MK, Haro Abad JM, Hwang I, Sampson NA, Alonso J, et al. Twelve-month prevalence of and risk factors for suicide attempts in the world health organization world mental health surveys. *J Clin Psychiatry.* (2010) 71:1617–28. doi: 10.4088/JCP.08m04967blu

5. Huang C, Spuhler K, DeLorenzo C, Parsey R. 604. Association between major depressive disorder and the comt polymorphism as assessed by diffusion MRI. *Biol Psychiatry.* (2017) 81:S244–5. doi: 10.1016/j.biopsych.2017.02.474

6. Say L, Chou D, Gemmill A, Tunçalp Ö, Moller A-B, Daniels J, et al. Global causes of maternal death: a WHO systematic analysis. *Lancet Glob Health.* (2014) 2:e323–33. doi: 10.1016/s2214-109x(14)70227-x

7. Gong Q, He Y. Depression, neuroimaging and connectomics: a selective overview. *Biol Psychiatry.* (2015) 77:223–35. doi: 10.1016/j.biopsych.2014.08.009

8. Sotiras A, Toledo JB, Gur RE, Gur RC, Satterthwaite TD, Davatzikos C. Patterns of coordinated cortical remodeling during adolescence and their associations with functional specialization and evolutionary expansion. *Proc Natl Acad Sci USA.* (2017) 114:3527–32. doi: 10.1073/pnas.1620928114

9. Lee HJ, Kim SH, Lee MS. Understanding mood disorders in children. *Adv Exp Med Biol.* (2019) 1192:251–61. doi: 10.1007/978-981-32-9721-0_12

10. Horesh N, Orbach I, Gothelf D, Efrati M, Apter A. Comparison of the suicidal behavior of adolescent inpatients with borderline personality disorder and major depression. *J Nerv Ment Dis.* (2003) 191:582–8. doi: 10.1097/01.nmd.0000087184.56009.61

11. Huang Q, Xiao M, Ai M, Chen J, Wang W, Hu L, et al. Disruption of neural activity and functional connectivity in adolescents with major depressive disorder who engage in non-suicidal self-injury: a resting-state fMRI study. *Front Psychiatry.* (2021) 12:571532. doi: 10.3389/fpsyt.2021.571532

12. Porta-Casteràs D, Cano M, Camprodon JA, Loo C, Palao D, Soriano-Mas C, et al. A multimetric systematic review of fMRI findings in patients with MDD receiving ECT. *Prog Neuro-Psychopharmacol Biol Psychiatry.* (2021) 108:110178. doi: 10.1016/j.pnpbp.2020.110178

13. Bahji A, Hawken ER, Sepehry AA, Cabrera CA, Vazquez G. ECT beyond unipolar major depression: systematic review and meta-analysis of

electroconvulsive therapy in bipolar depression. *Acta Psychiatr Scand.* (2019) 139:214–26. doi: 10.1111/acps.12994

14. Sanghani SN, Petrides G, Kellner CH. Electroconvulsive therapy (ECT) in schizophrenia: a review of recent literature. *Curr Opin Psychiatry.* (2018) 31:213–22. doi: 10.1097/YCO.0000000000000418

15. Liu Y, Du L, Li Y, Liu H, Zhao W, Liu D, et al. Antidepressant effects of electroconvulsive therapy correlate with subgenual anterior cingulate activity and connectivity in depression. *Medicine (Baltimore).* (2015) 94:e2033. doi: 10.1097/MD.0000000000002033

16. Strober M, Rao U, DeAntonio M, Liston E, State M, Amaya-Jackson L, et al. Effects of electroconvulsive therapy in adolescents with severe endogenous depression resistant to pharmacotherapy. *Biol Psychiatry.* (1998) 43:335–8. doi: 10.1016/s0006-3223(97)00205-9

17. Consoli A, Cohen J, Bodeau N, Guinchat V, Wachtel L, Cohen D. Electroconvulsive therapy in adolescents with intellectual disability and severe self-injurious behavior and aggression: a retrospective study. *Eur Child Adolesc Psychiatry.* (2013) 22:55–62. doi: 10.1007/s00787-012-0320-7

18. Zhao K, Liu H, Yan R, Hua L, Chen Y, Shi J, et al. Altered patterns of association between cortical thickness and subcortical volume in patients with first episode major depressive disorder: a structural MRI study. *Psychiatry Res Neuroimaging.* (2017) 260:16–22. doi: 10.1016/j.pscychresns.2016.12.001

19. Jarnum H, Eskildsen SF, Steffensen EG, Lundbye-Christensen S, Simonsen CW, Thomsen IS, et al. Longitudinal MRI study of cortical thickness, perfusion, and metabolite levels in major depressive disorder. *Acta Psychiatr Scand.* (2011) 124:435–46. doi: 10.1111/j.1600-0447.2011.01766.x

20. Penner J, Ford KA, Taylor R, Schaefer B, Theberge J, Neufeld RW, et al. Medial prefrontal and anterior insular connectivity in early schizophrenia and major depressive disorder: a resting functional mri evaluation of large-scale brain network models. *Front Hum Neurosci.* (2016) 10:132. doi: 10.3389/fnhum.2016.00132

21. Ueda I, Kakeda S, Watanabe K, Yoshimura R, Kishi T, Abe O, et al. Relationship between G1287A of the NET gene polymorphisms and brain volume in major depressive disorder: a voxel-based MRI Study. *PLoS One* (2016) 11:e0150712. doi: 10.1371/journal.pone.0150712

22. Eker C, Gonul AS. Volumetric MRI studies of the hippocampus in major depressive disorder: meanings of inconsistency and directions for future research. *World J Biol Psychiatry.* (2010) 11:19–35. doi: 10.3109/15622970902737998

23. Wagner G, Koch K, Schachtzabel C, Schlösser RGM. Altered brain structures in patients with major depressive disorder and high-risk for suicide: a structural MRI study. *J Affect Disord.* (2010) S68. 122:doi: 10.1016/j.jad.2010.02.094

24. Iosifescu DV, Papakostas GI, Lyoo IK, Lee HK, Renshaw PF, Alpert JE, et al. Brain MRI white matter hyperintensities and one-carbon cycle metabolism in non-geriatric outpatients with major depressive disorder (Part I). *Psychiatry Res.* (2005) 140:291–9. doi: 10.1016/j.pscychresns.2005.09.003

25. Lacerda ALT, Nicoletti MA, Brambilla P, Sassi RB, Mallinger AG, Frank E, et al. Anatomical MRI study of basal ganglia in major depressive disorder. *Psychiatry Res Neuroimaging.* (2003) 124:129–40. doi: 10.1016/s0925-4927(03)00123-9

26. Zou QH, Zhu CZ, Yang Y, Zuo XN, Long XY, Cao QJ, et al. An improved approach to detection of amplitude of low-frequency fluctuation (ALFF) for resting-state fMRI: fractional ALFF. *J Neurosci Methods.* (2008) 172:137–41. doi: 10.1016/j.jneumeth.2008.04.012

27. Qiu H, Li X, Luo Q, Li Y, Zhou X, Cao H, et al. Alterations in patients with major depressive disorder before and after electroconvulsive therapy measured by fractional amplitude of low-frequency fluctuations (fALFF). *J Affect Disord.* (2019) 244:92–9. doi: 10.1016/j.jad.2018.10.099

28. Yan CG, Wang XD, Zuo XN, Zang YF. DPABI: data processing & analysis for (Resting-State) brain imaging. *Neuroinformatics.* (2016) 14:339–51. doi: 10.1007/s12021-016-9299-4

29. Zang YF, He Y, Zhu CZ, Cao QJ, Sui MQ, Liang M, et al. Altered baseline brain activity in children with ADHD revealed by resting-state functional MRI. *Brain Dev.* (2007) 29:83–91. doi: 10.1016/j.braindev.2006.07.002

30. Nitschke JB, Mackiewicz KL. Prefrontal and anterior cingulate contributions to volition in depression. *Int Rev Neurobiol.* (2005) 67:73–94. doi: 10.1016/S0074-7742(05)67003-1

31. Peng GJ, Tian JS, Gao XX, Zhou YZ, Qin XM. Research on the pathological mechanism and drug treatment mechanism of depression. *Curr Neuropharmacol.* (2015) 13:514–23. doi: 10.2174/1570159x1304150831120428

32. Pizzagalli DA, Roberts AC. Correction: prefrontal cortex and depression. *Neuropsychopharmacology.* (2022) 47:609. doi: 10.1038/s41386-021-01160-w

33. Hongqing Pan SL, Yuanli W, Peipei LV, Feiyan LI, Yao Z, Wuyang Z. Resting state functional magnetic resonance imaging of low frequency amplitude in adolescent depression with suicidal ideation. *Chinese J Behav Med Brain Sci.* (2019) 28:1091–95. doi: 10.3760/cma.j.issn.1674-6554.2019.12.007

34. Wen J, Yu T, Liu L, Hu Z, Yan J, Li Y, et al. Evaluating the roles of left middle frontal gyrus in word production using electrocorticography. *Neurocase.* (2017) 23:263–9. doi: 10.1080/13554794.2017.1387275

35. Zhang J. Frontal activations associated with accessing and evaluating information in working memory: an fMRI study. *NeuroImage.* (2003) 20:1531–9. doi: 10.1016/s1053-8119(03)00466-x

36. Gallagher HL, Happé F, Brunswick N, Fletcher PC, Frith U, Frith CD. Reading the mind in cartoons and stories: an fMRI study of "theory of mind" in verbal and nonverbal tasks. *Neuropsychologia.* (2000) 38:11–21. doi: 10.1016/s0028-3932(99)00053-6

37. Tulving E, Kapur S, Markowitsch HJ, Craik FI, Habib R, Houle S. Neuroanatomical correlates of retrieval in episodic memory: auditory sentence recognition. *Proc Natl Acad Sci USA.* (1994) 91:2012–5. doi: 10.1073/pnas.91.6.2012

38. Gross JJ. Emotion regulation in adulthood: timing is everything. *Curr Direct Psychol Sci.* (2016) 10:214–9. doi: 10.1111/1467-8721.00152

39. Li CT, Lin CP, Chou KH, Chen IY, Hsieh JC, Wu CL, et al. Structural and cognitive deficits in remitting and non-remitting recurrent depression: a voxel-based morphometric study. *NeuroImage.* (2010) 50:347–56. doi: 10.1016/j.neuroimage.2009.11.021

40. Kong XM, Xu SX, Sun Y, Wang KY, Wang C, Zhang J, et al. Electroconvulsive therapy changes the regional resting state function measured by regional homogeneity (ReHo) and amplitude of low frequency fluctuations (ALFF) in elderly major depressive disorder patients: An exploratory study. *Psychiatry Res Neuroimaging.* (2017) 264:13–21. doi: 10.1016/j.pscychresns.2017.04.001

41. Falquez R, Couto B, Ibanez A, Freitag MT, Berger M, Arens EA, et al. Detaching from the negative by reappraisal: the role of right superior frontal gyrus (BA9/32). *Front Behav Neurosci.* (2014) 8:165. doi: 10.3389/fnbeh.2014.00165

42. Jiang W, Zhao Z, Wu Q, Wang L, Zhou L, Li D, et al. Study on brain structure network of patients with delayed encephalopathy after carbon monoxide poisoning: based on diffusion tensor imaging. *Radiol Med.* (2021) 126:133–41. doi: 10.1007/s11547-020-01222-x

43. Li J, Yao G, Liu S, Li X, Zhao W, Du X, et al. Mechanisms of the effects of parental emotional warmth on extraversion in children and adolescents. *Neuroscience.* (2021) 467:134–41. doi: 10.1016/j.neuroscience.2021.05.021

44. Yong-gui Y. A Study of diagnosis and early efficacy prediction biomarkers for major depressive disorder. *Acta Neuropharmacol.* (2018) 8:42–4.

45. Yongchao Wang TB, Jiang Q. Mediating effect of right superior frontal gyrus on the relationship between superiority bias and depressive mood. In: *Proceedings of the Abstracts of the 19th National Psychological Conference*. Xi'an (2016). p. 2016.

46. Jiang X, Fu S, Yin Z, Kang J, Wang X, Zhou Y, et al. Common and distinct neural activities in frontoparietal network in first-episode bipolar disorder and major depressive disorder: preliminary findings from a follow-up resting state fMRI study. *J Affect Disord.* (2020) 260:653–9. doi: 10.1016/j.jad.2019.09.063

47. Mukherjee P, Whalley HC, McKirdy JW, Sprengelmeyer R, Young AW, McIntosh AM, et al. Altered amygdala connectivity within the social brain in schizophrenia. *Schizophr Bull.* (2014) 40:152–60. doi: 10.1093/schbul/sbt086

48. Han YY, Yin H, Zhou Y, Zhang G, Wu YH, Xing W, et al. Investigation on the changes of dependent signal on the amplitude of low frequency fluctuations at blood oxygen level in brain after acupuncture Neiguan (PC 6). *Chinese Acupunct Moxibust.* (2009) 29:647–51.

49. Yuan J, Cao S, Huang Y, Zhang Y, Xie P, Zhang Y, et al. Altered spontaneous brain activity in patients with idiopathic trigeminal neuralgia: a resting-state functional MRI study. *Clin J Pain.* (2018) 34:600–9. doi: 10.1097/AJP.0000000000000578

frontiers | Frontiers in Psychiatry

TYPE Original Research
PUBLISHED 26 July 2022
DOI 10.3389/fpsyt.2022.958294

OPEN ACCESS

EDITED BY
Qinji Su,
Guangxi Medical University, China

REVIEWED BY
Weijla Wan,
Huazhong University of Science and Technology, China
Baojun Xie,
Renmin Hospital of Wuhan University, China

*CORRESPONDENCE
Wei Li
70660053@qq.com
Sheng Zhang
42701213@qq.com
Hongwei Ren
14214949@qq.com

†These authors share first authorship

SPECIALTY SECTION
This article was submitted to Neuroimaging and Stimulation, a section of the journal Frontiers in Psychiatry

RECEIVED 31 May 2022
ACCEPTED 28 June 2022
PUBLISHED 26 July 2022

CITATION
Chu Y, Wu J, Wang D, Huang J, Li W, Zhang S and Ren H (2022) Altered voxel-mirrored homotopic connectivity in right temporal lobe epilepsy as measured using resting-state fMRI and support vector machine analyses.
Front. Psychiatry 13:958294.
doi: 10.3389/fpsyt.2022.958294

Altered voxel-mirrored homotopic connectivity in right temporal lobe epilepsy as measured using resting-state fMRI and support vector machine analyses

Yongqiang Chu[1,2†], Jun Wu[3†], Du Wang[1], Junli Huang[1], Wei Li[4*], Sheng Zhang[5*] and Hongwei Ren[1*]

[1]Department of Imaging Center, Tianyou Hospital, Affiliated to Wuhan University of Science and Technology, Wuhan, China, [2]Key Laboratory of Occupational Hazards and Identification, Wuhan University of Science and Technology, Wuhan, China, [3]Department of Neurosurgery, The Central Hospital of Wuhan, Tongji Medical College, Huazhong University of Science and Technology, Wuhan, China, [4]Department of Otolaryngology-Head and Neck Surgery, Wuhan Asia General Hospital, Wuhan, China, [5]Department of Psychiatry, Liyuan Hospital, Tongji Medical College, Huazhong University of Science and Technology, Wuhan, China

Background: Prior reports revealed abnormalities in voxel-mirrored homotopic connectivity (VMHC) when analyzing neuroimaging data from patients with various psychiatric conditions, including temporal lobe epilepsy (TLE). Whether these VHMC changes can be leveraged to aid in the diagnosis of right TLE (rTLE), however, remains to be established. This study was thus developed to examine abnormal VMHC findings associated with rTLE to determine whether these changes can be used to guide rTLE diagnosis.

Methods: The resultant imaging data of resting-state functional MRI (rs-fMRI) analyses of 59 patients with rTLE and 60 normal control individuals were analyzed using VMHC and support vector machine (SVM) approaches.

Results: Relative to normal controls, patients with rTLE were found to exhibit decreased VMHC values in the bilateral superior and the middle temporal pole (STP and MTP), the bilateral middle and inferior temporal gyri (MTG and ITG), and the bilateral orbital portion of the inferior frontal gyrus (OrbIFG). These patients further exhibited increases in VMHC values in the bilateral precentral gyrus (PreCG), the postcentral gyrus (PoCG), and the supplemental motor area (SMA). The ROC curve of MTG VMHC values showed a great diagnostic efficacy in the diagnosis of rTLE with AUCs, sensitivity, specificity, and optimum cutoff values of 0.819, 0.831, 0.717, and 0.465. These findings highlight the value of the right middle temporal gyrus (rMTG) when differentiating between rTLE and control individuals, with a corresponding SVM analysis yielding respective accuracy, sensitivity, and specificity values of 70.59% (84/119), 78.33% (47/60), and 69.49% (41/59).

Conclusion: In summary, patients with rTLE exhibit various forms of abnormal functional connectivity, and SVM analyses support the potential value of abnormal VMHC values as a neuroimaging biomarker that can aid in the diagnosis of this condition.

KEYWORDS

right temporal lobe epilepsy, network homogeneity, voxel-mirrored homotopic connectivity, resting-state functional magnetic resonance imaging, support vector machine analyses

Introduction

Right temporal lobe epilepsy (rTLE) accounts for the majority of partial epilepsy cases (1) and results from excessive abnormal synchronous neuronal firing (2, 3). In prior reports, rTLE has been linked to the deterioration of emotional, cognitive, and psychological functionality with disease progression (4–6). While EEG analyses can be used to diagnose epilepsy, certain patients with TLE experience disease relapse following surgical or medical intervention (7–9). A growing body of evidence also suggests that epileptic activity is linked to the dysfunction of brain networks rather than individual sites in the brain, with these networks contributing to the incidence of interictal brain dysfunction (10).

While many studies explored the development and progression of rTLE with a focus on both clinical symptoms and associated physiological changes (7, 8, 11), the pathogenesis of this condition remains incompletely understood. Different network organization patterns have long been known to be linked to the incidence of left TLE (lTLE) and rTLE owing to hemispheric asymmetry in the human brain (12–14), yet the functional networks associated with lTLE and rTLE differ from one another (10, 14–16). Indeed, one study reported to significantly altered functional connectivity was only evident in lTLE and not in rTLE (17), while another group reported a greater reduction in the functional connectivity of the limbic network in patients with rTLE relative to those with lTLE (18). More prominent reductions in functional connectivity in individuals with rTLE and associated lower baseline levels may suggest that this condition is more amenable to structural and functional changes such that impairment in patients with rTLE may more readily contribute to functional reorganization and lateralization (19, 20). However, data exploring these possibilities have been relatively limited to date, and changes in brain function in individuals with rTLE are not restricted to the temporal lobe, underscoring the need for additional research examining the functional changes in these patients and associated regional involvement.

Progressive advances in neuroimaging techniques have been leveraged to guide the diagnosis of many psychiatric conditions. The change of network homogeneity (NH) is used to explain the aberrant connectivity of the default mode network (DMN) in patients with depression or lTLE (21, 22) and also to explain alterations in the dorsal attachment network (DAN) and the ventral attachment network (VAN) in patients with rTLE (23, 24). Functional connectivity (FC) is often used as a neuroimaging biomarker when assessing intrahemispheric and interhemispheric salience and auditory network abnormalities in patients with somatization disorders (25). Degree centrality (DC) has also been leveraged as an imaging biomarker to aid in rTLE diagnosis (1). Given the growing interest in analyses of interhemispheric connectivity, VMHC has been used to examine functional homotopy between bilateral cerebral hemispheres as a means of comparing interhemispheric FC based on rs-fMRI data, with changes in such connectivity potentially accounting for abnormal homotopic connectivity among specific regions of the brain in patients with rTLE (26). FC has also been leveraged when comparing connectivity strength differences among patients with TLE based upon abnormal VMHC values (27), and VMHC studies revealed altered alertness networks in patients with rTLE (28). This is done by calculating the synergy of functional connections between each voxel in one hemisphere and its mirror voxel in the other hemisphere. As a result, VMHC shows that the pattern of communication between the bilateral cerebral hemispheres is critical for information integration and brain function modifications. Higher VMHC levels indicate better synchronization of functional connections between the brain hemispheres, according to the VMHC data.

The growing complexity of high-dimensional imaging datasets has led to the development of support vector machine (SVM) analyses, which consist of powerful supervised learning models and algorithms that can aid in a variety of classification problems (29). SVM approaches have been successfully used to identify patients affected by autism spectrum disorders, Alzheimer's disease, and cognitive impairment (30–32). However, the utility of VMHC-based SVM analyses as a means of differentiating between patients with rTLE and normal control individuals has yet to be reported.

The present study leveraged rs-fMRI data to compare abnormal functional homotopic connectivity in different regions of the brain in patients with rTLE with the goal of establishing a model capable of differentiating between these patients and healthy control individuals.

Experimental procedures

Participants

In total, 59 patients with rTLE diagnosed according to the International League Against Epilepsy diagnostic criteria (33) were recruited from the Tianyou Hospital Affiliated with the Wuhan University of Science and Technology. In addition, 60 age-matched and sex-matched healthy control individuals undergoing standard physical examinations were recruited. To be eligible for study participation, patients with rTLE had to meet the following criteria: (1) patients exhibited standard rTLE symptoms and were diagnosed based on clinical findings, EEG, and MRI analyses; (2) patients were right-handed; (3) patients had undergone routine antiepileptic drug therapy; (4) patients were 18–50 years of age; and (5) patients exhibited a Mini-Mental State Examination (MMSE) score $>$ 24. Patients were excluded if they did not meet any of these criteria, if they had any history of traumatic brain injury, psychiatric disorders, or other neurological conditions, or if they failed to comply with examination procedures or exhibited MRI contraindications. All patients provided written informed consent to participate in this study, which received approval from the Medical Ethics Committee of the Tianyou Hospital Affiliated with the Wuhan University of Science and Technology and was performed as per the Declaration of Helsinki.

TABLE 1 The clinical properties of patients and healthy controls.

Characteristics	Patients ($n = 59$)	HCs ($n = 60$)	P value
Gender (male/female)	59 (27/32)	60 (31/29)	0.519
Age, years	28.97 ± 7.73	26.54 ± 4.96	0.043
Years of education, years	12.37 ± 2.73	12.67 ± 2.33	0.529
Illness duration, years	8.45 ± 6.17		

HCs, healthy controls. Compared with normal controls, $^*P < 0.01$.

Image acquisition

An Ingenia 3.0 T scanner (Philips, Amsterdam, The Netherlands) was used to collect all rs-fMRI data. Scanning was conducted while patients remained awake and still with their eyes closed using the following settings: repetition time/echo time (TR/TE) 2,000/30 ms; 36 slices; 90° flip angle; 220 mm × 220 mm field of view; 3 mm slice thickness; and 1 mm pitch (34).

Data preprocessing

MATLAB DPARSF software was used to preprocess data after collection (35). To eliminate the impact of initial signal instability and participant adaptation to the imaging apparatus, the first five-time points were omitted from analyses. Data were corrected for head movement and slice time. No participants exhibited $>$ 2 mm of maximum displacement in the x, y, or z directions or maximum rotation $>$ 2°. The standard Montreal Neurological Institute space was used to normalize the corrected data, which were then resampled at 3 × 3 × 3 mm^3, subjected to bandpass filtering (0.01–0.08 Hz), and linearly detrended. Covariates of spurious importance were then eliminated, including six head motion parameters derived from rigid body correction and the signal from a region centered in the white matter and the signal from a ventricular seed-based region of interest. Global signal data were retained when analyzing these resting-state results (34).

VMHC analyses

REST (http://www.restfmri.net/) software was used to conduct all VMHC analyses. Normalized gray matter images for each study participant were averaged together to generate a normalized mean gray matter template. This template was averaged to generate group-specific symmetrical templates, with gray matter images then being registered to the produced symmetrical templates. Each subject's normalized gray matter images were averaged to create a mean nonlinear registration to this symmetrical template, with the associated transformation them being applied to the preprocessed fMRI images for each study participant. Images were then smoothed using a 6 mm full-width at half-maximum isotropic Gaussian kernel. Individual VMHC maps were produced by assessing the Fisher z-transformed Pearson's correlation between a particular voxel and the mirrored voxel in the opposite hemisphere, with the resultant correlations for these voxel pairs being used to establish the VMHC maps utilized for group-level analyses.

SVM analyses

The MATLAB LIBSVM package was used to conduct SVM analyses aimed at differentiating between patients with rTLE and healthy control individuals based upon VMHC values

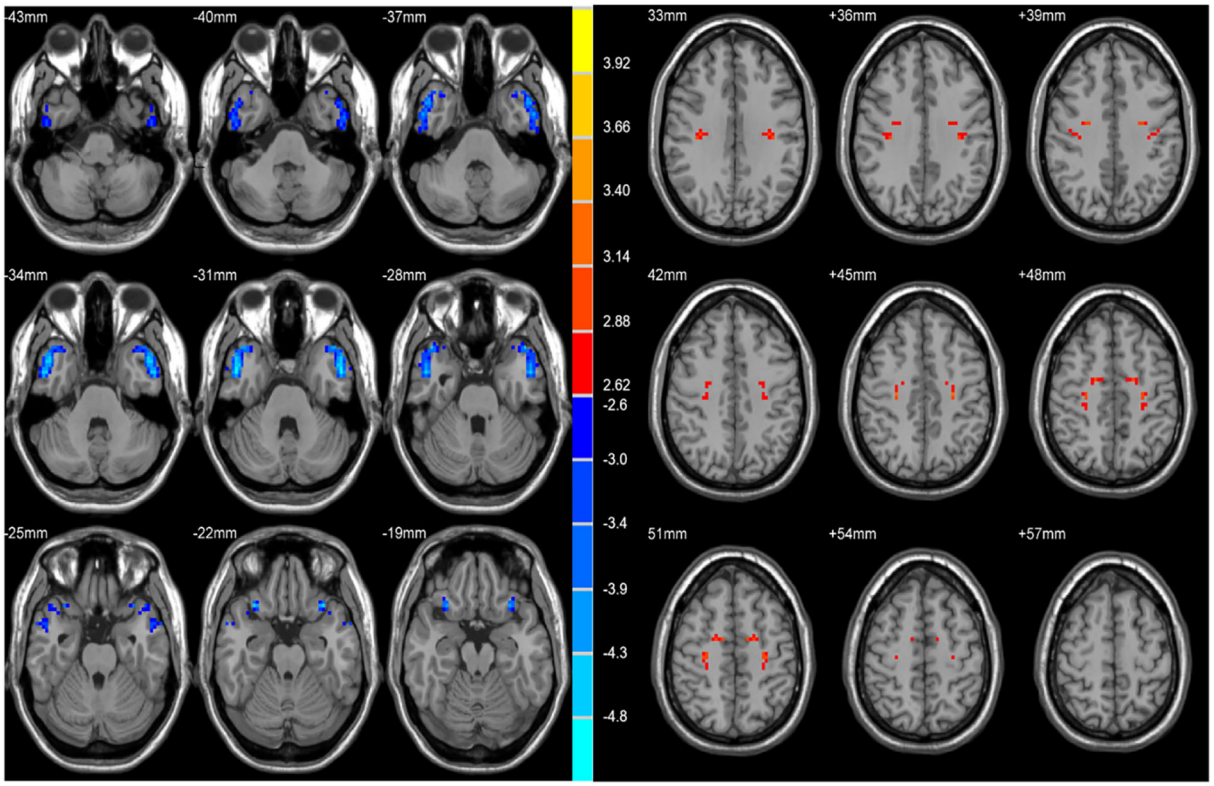

FIGURE 1
Statistical maps showing VHMC differences between the subject groups. Blue denotes lower VHMC, red denotes higher VHMC, and the color bar indicates the *T* values from 2-sample *t*-tests.

extracted from the right and left middle temporal gyri (rMTG and lMTG), with this analysis being conducted using a "leave-one-out" approach.

Statistical analyses

All data were analyzed using SPSS 22.0. Sex distributions were assessed *via* chi-square tests, while age and years of education of patients with rTLE and healthy controls were compared using two-sample *t*-tests. Group differences were identified through an analysis of covariance (ANCOVA) conducted based upon individual whole-brain VHMC maps from the two groups in a voxel-by-voxel manner, with results being GRF corrected at a p-value < 0.01.

Correlation analyses

Mean voxel-based VMHC values were extracted from regions of the brain exhibiting differences between the rTLE and healthy control patient groups, after which Pearson's correlation analyses were used to examine the relationships between these abnormal VMHC values and patient clinical characteristics.

Results

Patient characteristics

In total, this study recruited 59 patients with rTLE and 60 healthy controls. No significant differences in age, sex, years of education, or other demographic or clinical characteristics were observed between these groups (Table 1).

Differences in VMHC values among groups

Two-sample *t*-tests revealed significant differences in VMHC values in the bilateral STP, MTP, MTG, ITG, OrbIFG, PreCG, PoCG, and SMA when comparing patients with rTLE to healthy controls (Figure 1 and Table 2). Relative to healthy control individuals, patients with rTLE exhibited a marked decrease in VMHC in the bilateral STP, MTP, MTG, ITG,

TABLE 2 Signification differences in VHMC values between the groups.

Cluster location	Peak (MNI)			Number of voxels	*T* value
	X	Y	Z		
MTG	± 51	0	−30	227	−5.2444
PreCG	± 27	−18	45	65	3.1404

MNI, Montreal Neurological Institute; MTG, middle temporal gyrus; PreCG, precentral gyrus.

and OrbIFG, whereas VMHC values in these patients were significantly increased in the bilateral PreCG, PoCG, and SMA.

The ROC curve and SVM results

Using VMHC analysis, we confirmed the presence of significant abnormalities in the bilateral MTG (Figure 2). We extracted these two regions as ROIs for the subsequent SVM analysis.

Abnormal VMHC values in the bilateral MTG were separately assessed using an SVM approach, revealing that reduced VMHC values in the rMTG were associated with good diagnostic accuracy, sensitivity, and specificity values of 70.59% (84/119), 78.33% (47/60), and 69.49% (41/59), respectively, when used to differentiate between patients with rTLE and healthy control individuals (Figure 3).

Correlations between VMHC values and clinical findings

Average VMHC values in four regions of the brain that differed significantly between groups (the bilateral MTG and PreCG) were used to assess any potential correlations between these values and other clinical variables, but no significant correlative relationships were observed in patients with rTLE.

Discussion

Here, differences in VMHC values in patients with rTLE and healthy control individuals were compared based on whole-brain rs-fMRI data. This approach revealed that individuals diagnosed with rTLE exhibited reductions in VMHC values in the bilateral temporal lobe, particularly in the bilateral MTP and ITG. Moreover, these patients exhibited increased VMHC values in the bilateral PreCG, PoCG, and SMA. SVM analyses further revealed reductions in VMHC values in the rMTG to offer potential value as a neuroimaging biomarker for differentiating between patients with rTLE and healthy control individuals.

The temporal pole (TP) is a structure that has been termed Brain Area 38 by Brodmann or Temporopolar Area TG by Von Economo and that has been suggested to play an integral role in many higher-order cognitive functions (36, 37). The TP has been subdivided into various areas using assorted different methods. For example, diffusion tensor imaging (DTI) connectivity-based research revealed TP afferents from the MTG, ITG, OrbIFG, and the auditory cortex of the superior temporal gyrus in addition to being affected by the superior frontal gyrus (SFG) (38). Other EcoG studies observed TP involvement at seizure onset and posited that this may explain the failure of temporal lobectomy in some cases (7), in addition to confirming the association between the white matter network of the TP and that of other regions. In the present analysis, the TP was defined as the area of the anterior temporal lobe (ATL) beneath the lateral sulcus at the rostral tip of the temporal lobe inside the most rostral portion of the middle cranial fossa. This definition is in line with that used in prior clinical histological and connectivity analyses of the TP (38). Many studies reported the TP to exhibit distinct functions pertaining to autobiographical memory, facial recognition, language and semantic processing, socioemotional processing, and the recognition and analysis of complex objects (36). While many studies confirmed a role for the TP in psychiatric and neurological conditions, as in the case of TP atrophy being related to impaired memory and semantic deficiencies in individuals with Alzheimer's disease, few articles specifically assessed patients with rTLE (39–42). Another analysis of abnormal DMN homogeneity in patients with TLE reported a reduction in network homogeneity in individuals diagnosed with rTLE (34). In this study, patients with rTLE exhibited significantly decreased VMHC values in the bilateral MTP and STP relative to healthy controls, consistent with the existence of homotopic connectivity between the same brain regions as the contralateral side while indicating weaker functional connections with other regions of the brain. It is similar to a study exploring alterations of the alertness network in patients with rTLE, in which reduced FC values were found in STP (43). Aberrant TP brain activity in patients with rTLE and the associated abnormal homotopic connectivity of these regions may thus play an important role in the pathophysiology of rTLE. These results may further help to explain observed decreases in semantic and language processing in patients suffering from this condition.

This analysis also revealed decreased VMHC values in the bilateral ITG and MTG in patients with rTLE. In a previous study assessing alertness in unilateral patients with TLE, similar bilateral reductions in VMHC values in the MTG were reported in study subjects (28). Moreover, resting-state brain entropy analyses in patients with rTLE and the assessment of the relationship between these results, and alertness revealed synchronous alterations in the rMTG and

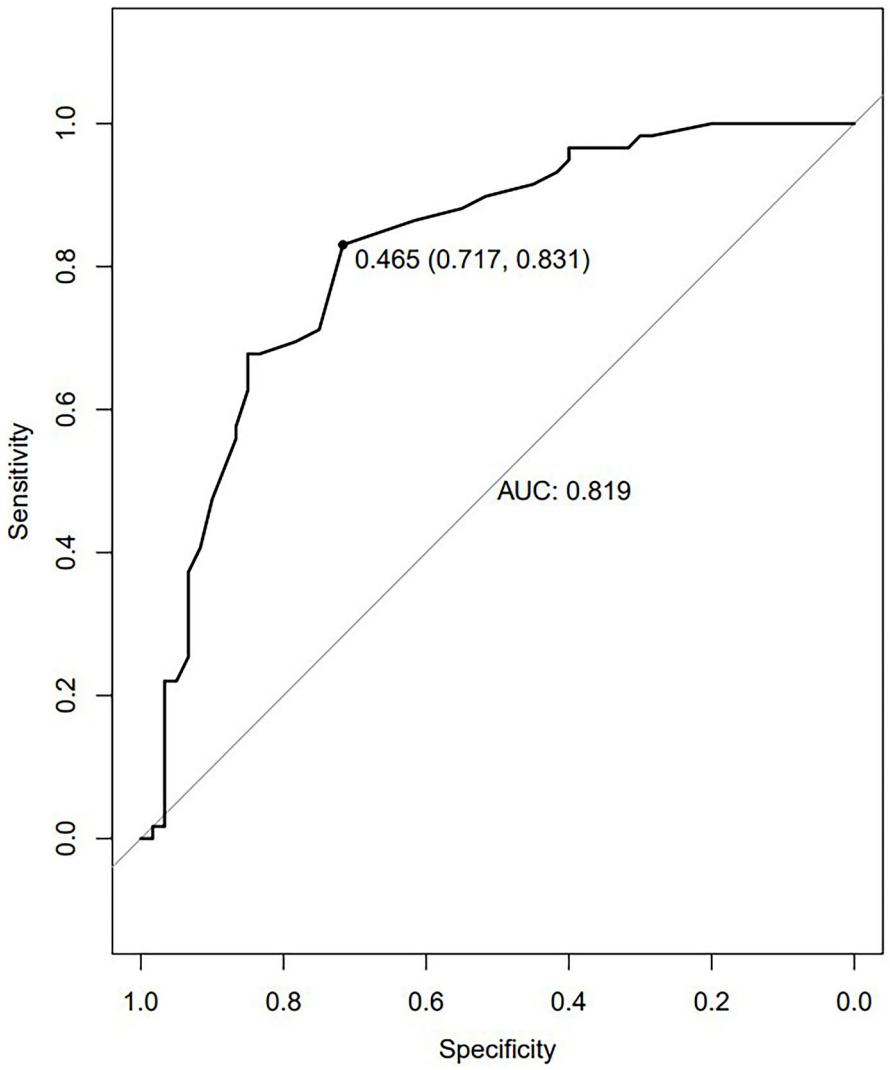

FIGURE 2
The ROC curves of the altered brain regions in the diagnosis of TLE. The ROC curve of MTG VMHC values. The AUC was 0.819. The optimum cutoff value was 0.465 (sensitivity: 0.831 and specificity: 0.717).

rITG (44). Consistently, another DTI-based study of 67 chronic left hemisphere stroke survivors revealed distinct damage in the ITG and MTG among individuals experiencing word comprehension difficulties, suggesting that these regions play an important role in the integration of auditory and conceptual processing (45). In addition to being linked anatomically by the white matter network, these regions may thus also be linked at a functional level. The results of this study suggest the existence of homotopic connectivity in patients with rTLE between the bilateral MTG and ITG, despite their distinct functions on either side of the brain.

Bilateral OrbIFG VMHC values were also found to be decreased in patients with rTLE, consistent with functional homotopic connectivity and synchronous alterations between the OrbIFG and TL. The arcuate fibers also reciprocally connect the OrbIFG and TP, and these structures make up the uncinate fasciculus (UF) (38, 46). One analysis of a blending aromatic mixture revealed that OrbIFG activation was consistent with a connection with the LP (47), supporting a role for this region in mediating configural percepts between the TP and OrbIFG associated with memory processes. Related studies also reported shifts in language dominance to homologous regions in the other hemisphere of the brain, with DTI having revealed poorer tract integrity in the right UF in patients with rTLE relative to patients with lTLE (19), potentially suggesting better recovery of language function. In our study, VMHC values were also decreased in the bilateral OrbIFG in patients with rTLE,

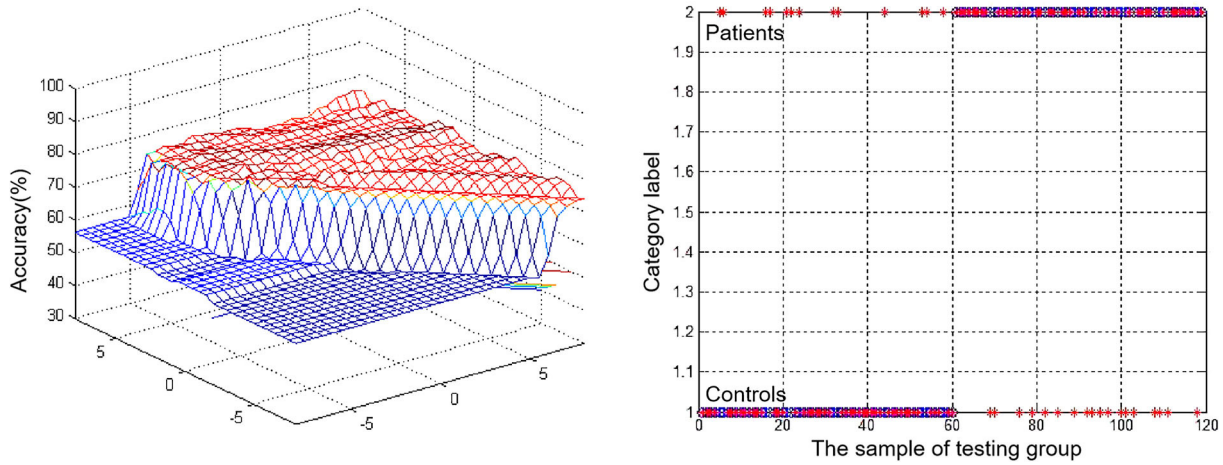

FIGURE 3
Visualization of classifications through support vector machine (SVM) using the decreased VMHC values in rMTG to discriminate patients with rTLE from healthy controls. Left: SVM parameters result of 3D view. Right: Classified map of the VMHC values in rMTG.

suggesting the existence of tight homotopic connectivity between the TP and OrbIFG. This may explain the observed positive correlations between the OrbIFG and TP in these patients and the rubs in the aspect of the default semantic network (DSN).

In other prior reports, bilateral STP were shown to be positively correlated with SMA (38, 48). There is also a dominant connection between the STP and other major default mode network (DMN) regions, potentially suggesting that the lateral temporal cortex, as a previously defined DMN subsystem, may further extend to the TP (49). DMN has been reported to be associated with the semantic memory system in the functional space (50). The results of this analysis suggest that increased VMHC values in the bilateral SMA may correspond to negative homotopic connectivity between the TP and SMA. One prior electrophysiological analysis demonstrated that SMA stimulation in patients with epilepsy resulted in the elicitation of complex contralateral movements (51). This aligns with the results of the present study indicating increased VMHC values in the left SMA, potential explaining why the abnormal activation of this region can result in certain clinical symptoms such as the promotion of inhibition of movement, thus impacting motor control (52). Given the role that the SMA plays in planning, initiating, and anticipating particular movements, its activation may explain the incidence of abnormal involuntary movements.

It is additionally important to note the increased VMHC values in the bilateral PerCG and PoCG in patients with rTLE, as these regions respectively correspond to the motor and sensory centers and serve as sensorimotor areas (53). In one study of changes in gray matter volume in patients with mTLE, a loss of PoCG volume was found to be negatively correlated with increased EGG current density (11). Another DTI-based study of PerCG and PoCG in the context of normal brain aging revealed that physical training could delay the progression of brain aging with the PerCG as the primary motion cortex (54). An analysis of hand-mouth movements as a representative ethologically relevant behavior exhibited integrated synergies in the PerCG (55). Regional homogeneity analyses in patients with TLP similarly exhibited an increase in the regional homogeneity of the PerCG and PoCG (12). These prior results are consistent with the data from the present study indicating increased VMHC values in these regions corresponding to their abnormal activation. This further suggests that TLE can lead to the abnormal activation of other functional regions of the brain, owing to abnormal connectivity among these regions in the form of a compensatory function.

The advent of increasingly advanced neuroimaging technologies has led to growing interest in the computer-aided diagnosis of neurological diseases and other pathological conditions. SVM approaches have been used with great success in the diagnosis of schizophrenia, Huntington's disease, and major depression (56–60). Here, considering the possible diagnostic role of the altered VMHC values in some different brain regions, the ROC curve was performed, and the results are shown in Figure 2. We found the better AUCs of the ROC were 0.819 for the bilateral MTG with sensitivity and specificity values of 0.831 and 0.717. What can be determined is that VMHC values can be used as a highly accurate diagnostic tool by the reduced VMHC values in bilateral MTG with a cutoff value of 0.465. An SVM analysis of decreased VMHC values in the rMTG exhibited respective accuracy, sensitivity, and specificity values of 70.59%, 78.33%,

and 69.49% when differentiating between patients with rTLE and healthy controls. When sensitivity or specificity values were below 60%, the selected biomarker may be poorly suited to use as a diagnostic biomarker (61). This study is the first to our knowledge to have examined the diagnostic utility of abnormal VMHC values in the rMTG as a neuroimaging biomarker of rTLE. In prior reports, DC values have been successfully leveraged as neuroimaging biomarkers in the evaluation of rTLE, with greater accuracy, sensitivity, and specificity being observed when assessing increased DC values in the combination of two abnormal regions of the brain (1). One advantage of this present approach is that abnormal VMHC values in just one region of the brain are necessary to yield comparable diagnostic accuracy, specificity, and sensitivity, making the associated analyses more efficient and intuitive.

There are multiple limitations to this analysis. For one, included patients with rTLE were undergoing long-term treatment with standard antiepileptic drugs, potentially impacting the resultant analyses. Second, the sample size for this study was relatively small. Lastly, further work should be conducted to similarly examine the neuroimaging features capable of specifically aiding in the diagnosis of patients with lTLE.

Conclusion

In summary, the results of this study suggest that patients with rTLE exhibit several abnormalities in VMHC values consistent with aberrant functional connectivity in the whole brain and among particular brain regions. The SVM results from this study suggest that altered VMHC within the rMTG can be leveraged as a neuroimaging biomarker to differentiate between patients with rTLE and healthy controls. Overall, these findings support the existence of altered bilateral functional coordination in patients with rTLE, offering new insight into the role of functional homotopic dysregulation in this disease and thus providing a foundation for future research aimed at clarifying the underlying pathological basis for rTLE development.

Data availability statement

The raw data supporting the conclusions of this article will be made available by the authors, without undue reservation.

Ethics statement

The studies involving human participants were reviewed and approved by the Medical Ethics Committee of the Tianyou Hospital Affiliated to Wuhan University of Science and Technology. The patients/participants provided their written informed consent to participate in this study. Written informed consent was obtained from the individual(s) for the publication of any potentially identifiable images or data included in this article.

Author contributions

DW, JH, JW, and HR: conceptualization, project planning and methodology, manuscript review, and editing. YC, SZ, and WL: data analysis and manuscript first draft. All authors contributed to the article and approved the submitted version.

Funding

The investigation was supported by a grant from the Health Commission of Hubei Province Scientific research project (Grant No. 2020CFB512), the Health Commission of Hubei Province Scientific research project (Grant No. WJ2021M007), the Education Department of Hubei Province research project (Grant No. B2021022), and the Natural Science Joint Foundation of Hubei province (Grant No. WJ2019H232 and Grant No. WJ2019H233).

Acknowledgments

We express sincere thanks to all participants. The authors would like to express their gratitude to REST (http://www.restfmri.net/) for the services provided and MJEditor (www.mjeditor.com) for its linguistic assistance during the preparation of this manuscript.

Conflict of interest

The authors declare that the research was conducted in the absence of any commercial or financial relationships that could be construed as a potential conflict of interest.

Publisher's note

References

1. Gao Y, Xiong Z, Wang X, Ren H, Liu R, Bai B, et al. Abnormal degree centrality as a potential imaging biomarker for right temporal lobe epilepsy: a resting-state functional magnetic resonance imaging study and support vector machine analysis. *Neuroscience.* (2022) 487:198–206. doi: 10.1016/j.neuroscience.2022.02.004

2. Wu Y, Wang XF, Mo XA, Sun HB Li JM, Zeng Y, et al. Expression of laminin beta1 in hippocampi of patients with intractable epilepsy. *Neurosci Lett.* (2008) 443:160–4. doi: 10.1016/j.neulet.2008.07.080

3. Walterfang M, Choi Y, O'Brien TJ, Cordy N, Yerra R, Adams S, et al. Utility and validity of a brief cognitive assessment tool in patients with epileptic and nonepileptic seizures. *Epilepsy Behav.* (2011) 21:177–83. doi: 10.1016/j.yebeh.2011.02.025

4. Johnson AL, McLeish AC, Shear PK, Privitera M. Panic and epilepsy in adults: a systematic review. *Epilepsy Behav.* (2018) 85:115–9. doi: 10.1016/j.yebeh.2018.06.001

5. Périn B, Godefroy O, Fall S, de Marco G. Alertness in young healthy subjects: an fMRI study of brain region interactivity enhanced by a warning signal. *Brain Cogn.* (2010) 72:271–81. doi: 10.1016/j.bandc.2009.09.010

6. Guo L, Bai G, Zhang H, Lu D, Zheng J, Xu G. Cognitive functioning in temporal lobe epilepsy: a BOLD-fMRI study. *Mol Neurobiol.* (2017) 54:8361–9. doi: 10.1007/s12035-016-0298-0

7. Abel TJ, Woodroffe RW, Nourski KV, Moritani T, Capizzano AA, Kirby P, et al. Role of the temporal pole in temporal lobe epilepsy seizure networks: an intracranial electrode investigation. *J Neurosurg.* (2018) 129:165–73. doi: 10.3171/2017.3.JNS162821

8. Zhao B, Yang B, Tan Z, Hu W, Sang L, Zhang C, et al. Intrinsic brain activity changes in temporal lobe epilepsy patients revealed by regional homogeneity analysis. *Seizure.* (2020) 81:117–22. doi: 10.1016/j.seizure.2020.07.030

9. Sala-Padro J, Miró J, Rodriguez-Fornells A, Rifa-Ros X, Plans G, Santurino M, et al. Mapping connectivity fingerprints for presurgical evaluation of temporal lobe epilepsy. *BMC Neurol.* (2021) 21:442. doi: 10.1186/s12883-021-02469-1

10. Coito A, Plomp G, Genetti M, Abela E, Wiest R, Seeck M, et al. Dynamic directed interictal connectivity in left and right temporal lobe epilepsy. *Epilepsia.* (2015) 56:207–17. doi: 10.1111/epi.12904

11. Fujisao EK, Alves KF, Rezende TOP, Betting LE. Analysis of interictal epileptiform discharges in mesial temporal lobe epilepsy using quantitative EEG and neuroimaging. *Front Neurol.* (2020) 11:569943. doi: 10.3389/fneur.2020.569943

12. Zhou L, Tian N, Geng ZJ, Wu BK, Dong LY, Wang MR. Diffusion tensor imaging study of brain precentral gyrus and postcentral gyrus during normal brain aging process. *Brain Behav.* (2020) 10:e01758. doi: 10.1002/brb3.1758

13. Yasuda CL, Chen Z, Beltramini GC, Coan AC, Morita ME, Kubota B, et al. Aberrant topological patterns of brain structural network in temporal lobe epilepsy. *Epilepsia.* (2015) 56:1992–2002. doi: 10.1111/epi.13225

14. Besson P, Dinkelacker V, Valabregue R, Thivard L, Leclerc X, Baulac M, et al. Structural connectivity differences in left and right temporal lobe epilepsy. *Neuroimage.* (2014) 100:135–44. doi: 10.1016/j.neuroimage.2014.04.071

15. Haneef Z, Lenartowicz A, Yeh HJ, Engel J, Stern JM. Effect of lateralized temporal lobe epilepsy on the default mode network. *Epilepsy Behav.* (2012) 25:350–7. doi: 10.1016/j.yebeh.2012.07.019

16. Pang X, Liang X, Zhao J, Wu P, Li X, Wei W, et al. Abnormal static and dynamic functional connectivity in left and right temporal lobe epilepsy. *Front Neurosci.* (2021) 15:820641. doi: 10.3389/fnins.2021.820641

17. Výtvarová E, Mareček R, Fousek J, Strýček O, Rektor I. Large-scale cortico-subcortical functional networks in focal epilepsies: The role of the basal ganglia. *Neuroimage Clin.* (2017) 14:28–36. doi: 10.1016/j.nicl.2016.12.014

18. Chiang S, Stern JM, Engel J, Levin HS, Haneef Z. Differences in graph theory functional connectivity in left and right temporal lobe epilepsy. *Epilepsy Res.* (2014) 108:1770–81. doi: 10.1016/j.eplepsyres.2014.09.023

19. Neudorf J, Kress S, Gould L, Gibb K, Mickleborough M, Borowsky R. Language lateralization differences between left and right temporal lobe epilepsy as measured by overt word reading fMRI activation and DTI structural connectivity. *Epilepsy Behav.* (2020) 112:107467. doi: 10.1016/j.yebeh.2020.107467

20. Johnson GW, Cai LY, Narasimhan S, González HFJ, Wills KE, Morgan VL, et al. Temporal lobe epilepsy lateralisation and surgical outcome prediction using diffusion imaging. *J Neurol Neurosurg Psychiatry.* (2022) 93:599–608. doi: 10.1136/jnnp-2021-328185

21. Gao Y, Wang M, Yu R, Li Y, Yang Y, Cui X, et al. Abnormal default mode network homogeneity in treatment-naive patients with first-episode depression. *Front Psychiatry.* (2018) 9:697. doi: 10.3389/fpsyt.2018.00697

22. Gao YJ, Wang X, Xiong PG, Ren HW, Zhou SY, Yan YG, et al. Abnormalities of the default-mode network homogeneity and executive dysfunction in people with first-episode, treatment-naive left temporal lobe epilepsy. *Eur Rev Med Pharmacol Sci.* (2021) 25:2039–49. doi: 10.26355/eurrev_202102_25108

23. Zhou S, Xiong P, Ren H, Tan W, Yan Y, Gao Y. Aberrant dorsal attention network homogeneity in patients with right temporal lobe epilepsy. *Epilepsy Behav.* (2020) 111:107278. doi: 10.1016/j.yebeh.2020.107278

24. Li DB, Liu RS, Wang X, Xiong PA, Ren HW, Wei YF, et al. Abnormal ventral attention network homogeneity in patients with right temporal lobe epilepsy. *Eur Rev Med Pharmacol Sci.* (2021) 25:2031–8. doi: 10.26355/eurrev_202102_25107

25. Su Q, Yu M, Liu F, Li Y, Li D, Deng M, et al. Abnormal Functional Asymmetry in the Salience and Auditory Networks in First-episode, Drug-naive Somatization Disorder. *Neuroscience.* (2020) 444:1–8. doi: 10.1016/j.neuroscience.2020.07.043

26. Mancuso L, Costa T, Nani A, Manuello J, Liloia D, Gelmini G, et al. The homotopic connectivity of the functional brain: a meta-analytic approach. *Sci Rep.* (2019) 9:3346. doi: 10.1038/s41598-019-40188-3

27. Shi K, Pang X, Wang Y, Li C, Long Q, Zheng J. Altered interhemispheric functional homotopy and connectivity in temporal lobe epilepsy based on fMRI and multivariate pattern analysis. *Neuroradiology.* (2021) 63:1873–82. doi: 10.1007/s00234-021-02706-x

28. Liu HH, Wang J, Chen XM Li JP, Ye W, Zheng J. Interhemispheric functional and structural alterations and their relationships with alertness in unilateral temporal lobe epilepsy. *Eur Rev Med Pharmacol Sci.* (2016) 20:1526–36.

29. Guo CY, Chou YC, A. novel machine learning strategy for model selections - stepwise support vector machine (StepSVM). *PLoS ONE.* (2020) 15:e0238384. doi: 10.1371/journal.pone.0238384

30. Khan T, Jacobs PG. Prediction of mild cognitive impairment using movement complexity. *IEEE J Biomed Health Inform.* (2021) 25:227–36. doi: 10.1109/JBHI.2020.2985907

31. Vaidya CJ, You X, Mostofsky S, Pereira F, Berl MM, Kenworthy L. Data-driven identification of subtypes of executive function across typical development, attention deficit hyperactivity disorder, and autism spectrum disorders. *J Child Psychol Psychiatry.* (2020) 61:51–61. doi: 10.1111/jcpp.13114

32. Huang Z, Sun M, Guo C. Automatic diagnosis of alzheimer's disease and mild cognitive impairment based on CNN + SVM networks with end-to-end training. *Comput Intell Neurosci.* (2021) 2021:9121770. doi: 10.1155/2021/9121770

33. Berg AT, Berkovic SF, Brodie MJ, Buchhalter J, Cross JH, van Emde Boas W, et al. Revised terminology and concepts for organization of seizures and epilepsies: report of the ILAE commission on classification and terminology, 2005-2009. *Epilepsia.* (2010) 51:676–85. doi: 10.1111/j.1528-1167.2010.02522.x

34. Gao Y, Zheng J, Li Y, Guo D, Wang M, Cui X, et al. Abnormal default-mode network homogeneity in patients with temporal lobe epilepsy. *Medicine (Baltimore).* (2018) 97:e11239. doi: 10.1097/MD.0000000000011239

35. Karpiel I, Klose U, Drzazga Z. Optimization of rs-fMRI parameters in the Seed Correlation Analysis (SCA) in DPARSF toolbox: a preliminary study. *J Neurosci Res.* (2019) 97:433–43. doi: 10.1002/jnr.24364

36. Herlin B, Navarro V, Dupont S. The temporal pole: From anatomy to function-A literature appraisal. *J Chem Neuroanat.* (2021) 113:101925. doi: 10.1016/j.jchemneu.2021.101925

37. Dupont S. Investigating temporal pole function by functional imaging. *Epileptic Disord.* (2002) 4 Suppl. 1:S17–22.

38. Fan L, Wang J, Zhang Y, Han W, Yu C, Jiang T. Connectivity-based parcellation of the human temporal pole using diffusion tensor imaging. *Cereb Cortex.* (2014) 24:3365–78. doi: 10.1093/cercor/bht196

39. Nag S, Yu L, Boyle PA, Leurgans SE, Bennett DA, Schneider JA. TDP-43 pathology in anterior temporal pole cortex in aging and Alzheimer's disease. *Acta Neuropathol Commun.* (2018) 6:33. doi: 10.1186/s40478-018-0531-3

40. Ramos Bernardes da. Silva Filho S, Oliveira Barbosa JH, Rondinoni C, Dos Santos AC, Garrido Salmon CE, da Costa Lima NK, et al. Neuro-degeneration profile of Alzheimer's patients: a brain morphometry study. *Neuroimage Clin.* (2017) 15:15–24. doi: 10.1016/j.nicl.2017.04.001

41. Irish M, Piguet O, Hodges JR, Hornberger M. Common and unique gray matter correlates of episodic memory dysfunction in frontotemporal dementia and Alzheimer's disease. *Hum Brain Mapp.* (2014) 35:1422–35. doi: 10.1002/hbm.22263

42. Irish M, Addis DR, Hodges JR, Piguet O. Considering the role of semantic memory in episodic future thinking: evidence from semantic dementia. *Brain.* (2012) 135:2178–91. doi: 10.1093/brain/aws119

43. Gao Y, Zheng J, Li Y, Guo D, Wang M, Cui X, et al. Decreased functional connectivity and structural deficit in alertness network with right-sided temporal lobe epilepsy. *Medicine (Baltimore).* (2018) 97:e0134. doi: 10.1097/MD.0000000000010134

44. Zhou M, Jiang W, Zhong D, Zheng J. Resting-state brain entropy in right temporal lobe epilepsy and its relationship with alertness. *Brain Behav.* (2019) 9:e01446. doi: 10.1002/brb3.1446

45. Bonilha L, Hillis AE, Hickok G, den Ouden DB, Rorden C, Fridriksson J. Temporal lobe networks supporting the comprehension of spoken words. *Brain.* (2017) 140:2370–80. doi: 10.1093/brain/awx169

46. Briggs RG, Khan AB, Chakraborty AR, Abraham CJ, Anderson CD, Karas PJ, et al. Anatomy and white matter connections of the superior frontal gyrus. *Clin Anat.* (2020) 33:823–32. doi: 10.1002/ca.23523

47. Sinding C, Hummel T, Béno N, Prescott J, Bensafi M, Coureaud G, et al. Configural memory of a blending aromatic mixture reflected in activation of the left orbital part of the inferior frontal gyrus. *Behav Brain Res.* (2021) 402:113088. doi: 10.1016/j.bbr.2020.113088

48. Abboud R, Noronha C, Diwadkar VA. Motor system dysfunction in the schizophrenia diathesis: Neural systems to neurotransmitters. *Eur Psychiatry.* (2017) 44:125–33. doi: 10.1016/j.eurpsy.2017.04.004

49. Buckner RL, Andrews-Hanna JR, Schacter DL. The brain's default network: anatomy, function, and relevance to disease. *Ann N Y Acad Sci.* (2008) 1124:1–38. doi: 10.1196/annals.1440.011

50. Binder JR, Desai RH, Graves WW, Conant LL. Where is the semantic system? A critical review and meta-analysis of 120 functional neuroimaging studies. *Cereb Cortex.* (2009) 19:2767–96. doi: 10.1093/cercor/bhp055

51. Fried I, Katz A, McCarthy G, Sass KJ, Williamson P, Spencer SS, et al. Functional organization of human supplementary motor cortex studied by electrical stimulation. *J Neurosci.* (1991) 11:3656–66. doi: 10.1523/JNEUROSCI.11-11-03656.1991

52. Sumner P, Nachev P, Morris P, Peters AM, Jackson SR, Kennard C, et al. Human medial frontal cortex mediates unconscious inhibition of voluntary action. *Neuron.* (2007) 54:697–711. doi: 10.1016/j.neuron.2007.05.016

53. Liu Y, Latremoliere A, Li X, Zhang Z, Chen M, Wang X, et al. Touch and tactile neuropathic pain sensitivity are set by corticospinal projections. *Nature.* (2018) 561:547–50. doi: 10.1038/s41586-018-0515-2

54. Wei G, Luo J, Li Y. Brain structure in diving players on MR imaging studied with voxel-based morphometry. *Prog Nat Sci.* (2009) 19:1397–402. doi: 10.1016/j.pnsc.2008.12.009

55. Desmurget M, Richard N, Harquel S, Baraduc P, Szathmari A, Mottolese C, et al. Neural representations of ethologically relevant hand/mouth synergies in the human precentral gyrus. *Proc Natl Acad Sci U S A.* (2014) 111:5718–22. doi: 10.1073/pnas.1321909111

56. Rocha NP, Mwangi B, Gutierrez Candano CA, Sampaio C, Furr Stimming E, Teixeira AL. The clinical picture of psychosis in manifest huntington's disease: a comprehensive analysis of the Enroll-HD database. *Front Neurol.* (2018) 9:930. doi: 10.3389/fneur.2018.00930

57. Steardo L, Carbone EA, de Filippis R, Pisanu C, Segura-Garcia C, Squassina A, et al. Application of support vector machine on fMRI Data as biomarkers in schizophrenia diagnosis: a systematic review. *Front Psychiatry.* (2020) 11:588. doi: 10.3389/fpsyt.2020.00588

58. Sacchet MD, Livermore EE, Iglesias JE, Glover GH, Gotlib IH. Subcortical volumes differentiate major depressive disorder, bipolar disorder, and remitted major depressive disorder. *J Psychiatr Res.* (2015) 68:91–8. doi: 10.1016/j.jpsychires.2015.06.002

59. Bendfeldt K, Taschler B, Gaetano L, Madoerin P, Kuster P, Mueller-Lenke N, et al. MRI-based prediction of conversion from clinically isolated syndrome to clinically definite multiple sclerosis using SVM and lesion geometry. *Brain Imaging Behav.* (2019) 13:1361–74. doi: 10.1007/s11682-018-9942-9

60. Gao Y, Wang X, Xiong Z, Ren H, Liu R, Wei Y, et al. Abnormal fractional amplitude of low-frequency fluctuation as a potential imaging biomarker for first-episode major depressive disorder: a resting-state fMRI study and support vector machine analysis. *Front Neurol.* (2021) 12:751400. doi: 10.3389/fneur.2021.751400

61. Gong Q, Wu Q, Scarpazza C, Lui S, Jia Z, Marquand A, et al. Prognostic prediction of therapeutic response in depression using high-field MR imaging. *Neuroimage.* (2011) 55:1497–503. doi: 10.1016/j.neuroimage.2010.11.079

frontiers | Frontiers in Psychiatry

TYPE Original Research
PUBLISHED 27 July 2022
DOI 10.3389/fpsyt.2022.981728

OPEN ACCESS

EDITED BY
Qinji Su,
Guangxi Medical University, China

REVIEWED BY
Xiaobing Jiang,
Huazhong University of Science and Technology, China
Yunhua Zhang,
Hubei Provincial Hospital of Traditional Chinese Medicine, China

*CORRESPONDENCE
Haibo Wang
hai_bo_wang@foxmail.com
Shengxi Jin
jsx2455852966@qq.com
Hongwei Ren
14214949@qq.com

SPECIALTY SECTION
This article was submitted to Neuroimaging and Stimulation, a section of the journal Frontiers in Psychiatry

RECEIVED 29 June 2022
ACCEPTED 08 July 2022
PUBLISHED 27 July 2022

CITATION
Guo R, Zhao Y, Jin H, Jian J, Wang H, Jin S and Ren H (2022) Abnormal hubs in global network as neuroimaging biomarker in right temporal lobe epilepsy at rest.
Front. Psychiatry 13:981728.
doi: 10.3389/fpsyt.2022.981728

Abnormal hubs in global network as neuroimaging biomarker in right temporal lobe epilepsy at rest

Ruimin Guo[1,2], Yunfei Zhao[3], Honghua Jin[1], Jihua Jian[1], Haibo Wang[4]*, Shengxi Jin[3]* and Hongwei Ren[1]*

[1]Department of Medical Imaging, Tianyou Hospital of Wuhan University of Science and Technology, Wuhan, China, [2]Key Laboratory of Occupational Hazards and Identification, Wuhan University of Science and Technology, Wuhan, China, [3]Department of Neurosurgery, Tianyou Hospital of Wuhan University of Science and Technology, Wuhan, China, [4]Department of Medical Imaging, Renmin Hospital of Wuhan University, Wuhan, China

While abnormal neuroimaging features have been reported in patients suffering from right temporal lobe epilepsy (rTLE), the value of altered degree centrality (DC) as a diagnostic biomarker for rTLE has yet to be established. As such, the present study was designed to examine DC abnormalities in rTLE patients in order to gauge the diagnostic utility of these neuroimaging features. In total, 68 patients with rTLE and 73 healthy controls (HCs) participated in this study. Imaging data were analyzed using DC and receiver operating characteristic (ROC) methods. Ultimately, rTLE patients were found to exhibit reduced right caudate DC and increased left middle temporal gyrus, superior parietal gyrus, superior frontal gyrus, right precuneus, frontal gyrus Inferior gyrus, middle-superior frontal gyrus, and inferior parietal gyrus DC relative to HC. ROC analyses indicated that DC values in the right caudate nucleus could be used to differentiate between rTLE patients and HCs with a high degree of sensitivity and specificity. Together, these results thus suggest that rTLE is associated with abnormal DC values in the right caudate nucleus, underscoring the relevance of further studies of the underlying pathophysiology of this debilitating condition.

KEYWORDS

temporal lobe epilepsy, degree centrality, magnetic resonance imaging, receiver operating characteristic, caudate

Introduction

Temporal lobe epilepsy (TLE) is a chronic neurological disease that can arise in response to a range of factors (1). Repeated abnormal epileptic discharges in affected patients can contribute to neuronal degeneration and necrotic death, in turn contributing to impaired cognition and altered brain tissue structural characteristics (2, 3). These structural changes in the brain of TLE patients can also disrupt normal

memory and learning activity (4). TLE accounts for over 40% of all epilepsy cases and is the most common form thereof (5). However, at present, the diagnosis of epilepsy is largely dependent on a combination of medical history and EEG results. While EEG can accurately diagnose epilepsy in some cases, the successful recording of epileptic discharges generally only occurs in half of affected patients, and some healthy individuals may also exhibit false-positive EEG readings (6). As seizures occur without warning and are transient in nature, this can further complicate diagnostic efforts. Recent advances in neuroimaging technologies have led to a growing focus on the use of computer-aided imaging as a means of automating efforts to diagnose patients and localize lesions (7–9). Multimodal neuroimaging efforts can also clarify changes in the brains of TLE patients, providing new insight into the pathogenesis of this disease while aiding in efforts to predict and diagnose affected individuals (9).

Several different non-invasive, high-resolution neuroimaging modalities have been leveraged to aid in the diagnosis of specific neurological conditions. To date, several different functional magnetic resonance imaging (fMRI) studies have reported detecting a distinct blood oxygen level-dependent (BOLD) signal in brain regions where seizure foci are located (10, 11). These fMRI techniques enable the effective localization of epileptic lesions with a combination of high temporal and spatial resolution (12). Reduced regional signal in the right posterior cingulate cortex and precuneus (PCu) regions, for example, has been identified as a biomarker characteristic of patients with epilepsy (13, 14). Moreover, altered amplitude of low-frequency fluctuation (ALFF) values in particular regions of the brain can reliably differentiate between epilepsy patients and healthy controls (HCs) with high levels of sensitivity and specificity (15, 16). Structural MRI studies have revealed that several brain regions in patients with epilepsy also exhibit structural abnormalities detectable through neuroimaging (17). However, no simple and accurate neuroimaging biomarker capable of guiding the early detection of TLE has yet been established.

Degree centrality (DC) is a whole-brain connectivity index that describes the global features of a given node through the use of graph theory models to assess the functional connectivity between that node and nodes throughout the brain (18). DC-based analytical approaches have recently been used to successfully evaluate patients diagnosed with schizophrenia, depression, and mild cognitive impairment (19–21). Moreover, the combination of DC and machine learning algorithms can predict responses to treatment in children with epilepsy undergoing antiepileptic medication treatment (22). Increases in voxel-wise DC values in specific brain regions correspond to an increased degree of global connectivity, whereas reductions in voxel-wise DC values are indicative of a reduction in the degree of global connectivity. Studies of voxel-based DC have been used to analyze altered brain functionality in patients with epilepsy at the whole-brain level, with one recent report having revealed the existence of abnormal DC findings in the medial superior frontal gyrus (MSFG), left dorsolateral superior frontal gyrus, right inferior parietal lobule, and the left postcentral region of adults with epilepsy (9). Therefore, it is necessary to combine DC and operating characteristic (ROC) methods when exploring imaging biomarkers of right temporal lobe epilepsy (rTLE).

The present study was developed with the goal of assessing whether rTLE patients exhibit abnormal DC activity, with the hypothesis that these abnormal DC values could be utilized as neuroimaging biomarkers to reliably distinguish between rTLE patients and HC individuals.

Materials and methods

Participants

In total, this study enrolled 68 patients with rTLE diagnosed as per the criteria established by the International Anti-Epilepsy League that were recruited from Tianyou Hospital Affiliated to Wuhan University of Science and Technology. In addition, 73 age- and sex-matched HC individuals were recruited from among patients at Tianyou hospital undergoing routine physical examinations. To be eligible for study inclusion, rTLE patients had to meet the following criteria: (1) patients exhibited typical TLE symptoms suggestive of the presence of epileptic foci in the right temporal lobe; (2) patients exhibited interictal EEG results consistent with the potential presence of right temporal lobe lesions; and (3) patients exhibited MRI results indicative of right hippocampal atrophy or sclerosis. Patients were excluded if they were left-handed or had any history of traumatic brain injury, psychiatric disease, or other neurological diseases. All participants provided written informed consent. The medical ethics committee of Tianyou Hospital Affiliated to Wuhan University of Science and Technology approved this study, which was consistent with the Declaration of Helsinki.

Magnetic resonance imaging acquisition and processing

A 3.0T Philips MRI instrument was used to collect all resting-state fMRI data at Tianyou Hospital. Participants were directed to remain awake with their eyes closed during imaging. All echoplanar imaging sequences were acquired with the following settings: repetition time/echo time (TR/TE) 2000/30 ms, 31 slices, 220 × 220 matrix, 90° flip angle, 24 cm field of view, 5 mm thick layers without gaps. The processing of all fMRI data was performed using the Data Processing Assistant for rs-fMRI, which functions with SPM12 implemented in MATLAB. The first 10 images for each participant were excluded

from the analysis to allow for patient adaptation and to mitigate the potential effects of initial MRI signal instability. Participants were excluded if they exhibited maximum displacement >2 mm in the *x*-, *y*-, or *z*-axis directions or >2° of maximum angular rotation after correction for head movement and slice timing. The corrected imaging data were spatially normalized to the MNI space and resampled at 3 mm × 3 mm × 3 mm, after which they were subjected to temporal bandpass filtering (0.01–0.08 Hz) and linear detrending. Certain spurious covariates were removed from these images, including signals from ventricular seed-related regions and white matter central regions, as well as 24 head motion parameters derived from rigid body correction. Global signals were preserved when processing resting-state functional connectivity data, as in prior reports (23).

Degree centrality calculation

Degree centrality measurements were made using the REST-DC toolkit from the REST package[1]. Pearson correlation coefficients were used to compute DC values, with Pearson correlation coefficients corresponding to the relationship between all voxel pairs in a time series being used to establish a graph for each study participant. In this graph, individual brain voxels are regarded as nodes, while significant correlations between nodes are regarded as edges. The n*n Pearson correlation coefficient matrix between each pair of voxels was then utilized to establish subjective whole-brain functional connectivity. To enhance the normalization of these data, they were transformed into a *Z*-score matrix by applying Fisher's *R*-to-*Z* transformation, with the sum of *Z* values between selected voxels and all other voxels being used to generate weighted voxel DC values. To eliminate any potential false connectivity, a Pearson correlation coefficient threshold of $r > 0.25$ was established by thresholding each correlation at $P < 0.01$.

Statistical analysis

Data were analyzed using SPSS 22.0 (SPSS Inc., IL, United States). Demographic differences were compared between groups using two-sample *t*-tests and chi-square tests.

Correlation analysis

Degree centrality values were extracted from brain regions that exhibited abnormalities between these two groups, after which Pearson correlation coefficients were used to detect the relationships between these abnormal DC values and clinical variables of interest.

1 http://www.restfmri.net/

Results

Demographics and clinical features

Participant demographic and clinical characteristics are shown in Table 1. There were no significant differences in age, sex, or education level between rTLE patients and HCs ($P > 0.05$).

Degree centrality differences

Significant differences in DC values in different regions of the brain were next identified by comparing data from rTLE patients and HCs. Relative to HC individuals, rTLE patients exhibited significantly reduced DC values in the right caudate gyrus, as well as significantly increased DC values in the left middle temporal gyrus (MTG), superior parietal gyrus (SPG), superior frontal gyrus (SFG) and right PCu, inferior frontal gyrus (IFG), MSFG, and inferior parietal gyrus (IPG; Figure 1 and Table 2). There were no significant correlations between any of the identified DC values and rTLE patient disease duration.

TABLE 1 Demographic information.

Characteristics	Patients ($n = 68$)	Controls ($n = 73$)	x^2 or T	P value
Gender (male/female)	68 (35/33)	73 (37/36)	0.67	0.06[a]
Age (years)	28.59 ± 6.09	28.30 ± 4.24	0.34	0.73[b]
Education (years)	12.12 ± 2.43	12.01 ± 2.70	1.77	0.19[b]
Illness duration (months)	8.35 ± 2.93			

[a]The *p* value for gender distribution was obtained by chi-square test.
[b]The *p* value were obtained by two sample *t*-tests.

TABLE 2 Alterations of DC between patients and controls.

Cluster location	Peak (MNI)			Number of voxels	*T*-value	*P*
	X	*Y*	*Z*			
Left MTG	−48	−42	−9	40	3.48	<0.01
Right PCu	6	−48	18	111	3.69	<0.01
Right IFG	51	42	6	30	3.49	<0.01
Right MSFG	9	63	24	67	3.94	<0.01
Right IPG	39	−45	45	30	3.33	<0.01
Right caudate	12	−3	27	47	−4.02	<0.01
Left SFG	−12	60	21	66	3.55	<0.01
Left SPG	−18	−42	63	70	3.57	<0.01

DC, degree centrality; MTG, middle temporal gyrus; PCu, precuneus; IFG, inferior frontal gyrus; MSFG, medial superior frontal gyrus; IPG, inferior parietal gyrus; and SFG, superior parietal gyrus.

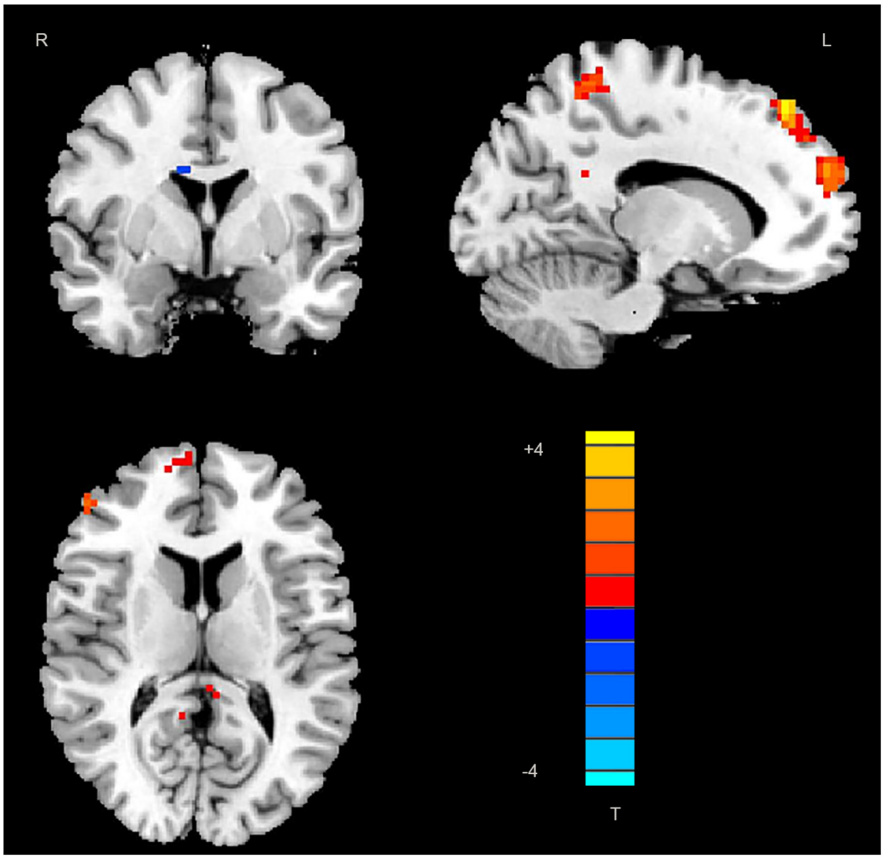

FIGURE 1
Decreased DC values in the right caudate and increased DC values in the left middle temporal gyrus, superior parietal gyrus, superior frontal gyrus, right precuneus, frontal gyrus Inferior gyrus, middle-superior frontal gyrus, and inferior parietal gyrus in patients. DC, degree centrality; MTG, middle temporal gyrus; SPG, superior parietal gyrus; SFG, superior frontal gyrus; PCu, precuneus; IFG, frontal gyrus Inferior gyrus; MSFG, middle-superior frontal gyrus; and IPG, inferior parietal gyrus.

Receiver operating characteristic results

In total, rTLE patients exhibited abnormal DC values in 8 regions of the brain (right caudate, left MTG, SFG, SPG, right PCu, IFG, MSFG, and IPG). Subsequent ROC analyses indicated that abnormal DC values in the right caudate nucleus exhibited the highest AUC value (0.8898; **Figure 2**).

Discussion

Here, DC values were used to differentiate between rTLE patients and HCs. Overall, patients diagnosed with rTLE were found to exhibit reduced DC values in the right caudate with corresponding increases in DC values in the left MTG, SPG, SFG, and right PCu, IFG, MSFG, and IPG relative to HCs. The abnormal DC values in the right caudate nucleus were able to effectively discriminate between these two participant groups with an AUC value of 0.8898.

Receiver operating characteristic analyses are commonly used for the diagnosis of neuropsychiatric disorders such as schizophrenia or major depression (24–26). To be reliable, a diagnostic indicator must exhibit an ROC value of 0.6 or higher (27). The AUC value derived from the ROC analysis of the right caudate nucleus was higher than that for any other tested regions exhibiting DC abnormalities between rTLE patients and controls. The caudate nucleus is an important mediator of cognition, and certain neurological disorders have been shown to differentially impact the dorsal and ventral caudate nuclei (28). Both functional activity and connectivity can be used to subdivide the caudate into these ventral and dorsal regions, with the dorsal caudate nucleus being closely associated with the dorsolateral prefrontal cortex and shaping executive function and working memory (29, 30). In contrast, the ventral caudate nucleus is more closely linked to the limbic system and to pain processing and other emotional functions. Many studies have evaluated the caudate nucleus in patients (31, 32). Here, right caudate nucleus DC values were significantly reduced in rTLE patients relative to HCs, with

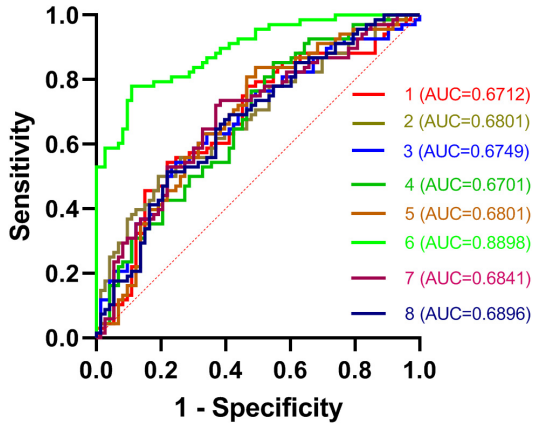

FIGURE 2
ROC curves for the differentiation between TLE patients and HCs based on DC values in abnormal brain regions. TLE, temporal lobe epilepsy; ROC, receiver operating characteristic; HCs, healthy controls; and DC, degree centrality.

the connection strength between this region and other regions of the brain thus being reduced, potentially explaining the observed declines in learning, attention, and memory that these patients experience. However, these reduced DC values were not correlated with patient symptom severity or disease duration, suggesting that they are independent of disease severity in rTLE patients. Notably, this DC reduction in the right caudate nucleus was able to readily differentiate between rTLE patients and HCs, suggesting that this change is characteristic of this form of epilepsy.

The frontal lobe is a key mediator of cognitive control, with abnormalities in the structure and function of the frontal lobe being reported in prior studies of patients with TLE (33, 34). Patients exhibiting cognitive impairments including decreased language fluency and processing speed have been reported relative to HCs, as has a case of patients with notably poor cognitive function. Here, abnormal DC values in the MFG were observed in rTLE patients, potentially partially accounting for the cognitive deficits that TLE patients experience.

Many structural and functional studies of TLE patients focus on the temporal lobe, including the amygdala, HIC, parahippocampal gyrus, and entorhinal cortex (1). The MTG is an important component of semantic memory and language processing-related activity (35, 36). Recently, one study found that TLE was associated with alterations in the intrinsic connectivity of both temporal regions (37). The temporal lobe is also closely related to social cognition and emotional processing (4). Moreover, the MTG is a key node in a broad network of frontal, parietal, occipital, and subcortical structures, with abnormal MTG activation thus potentially being an important pathophysiological component of rTLE-related brain damage (38). Abnormal MTG activity may also impact temporal lobe function given its role as a regulator of language processing and semantic memory. Observed increases in DC in the MTG in rTLE patients may thus be linked to cognitive deficits, although memory testing was not employed in the present study.

The parietal lobe is closely related to key cognitive and sensory functions including memory, attention, motor learning, spatial perception, and visuomotor integration (39, 40). Anatomical and functional characteristics are used to subdivide the parietal lobe into five regions, two of which are related to motor processes and visual orientation, whereas the remaining three are associated with reasoning, working memory, visual perception, attention, and spatial cognition (41). The SPL region has been specifically linked to interaction and locomotion in macaques. Adult TLE patients exhibt increases in SPL density detected through structural MRI and fMRI studies (42). The SPL and the associated intraparietal groove are important in the context of multi-object tracking as analyzed based on changes in BOLD signal, with both of these regions being related to sustained attention and object indexing (43). The SPL additionally interacts with the prefrontal cortex to coordinate stimulus-oriented processes and executive function, and correlates with inhibition in the left inferior parietal cortex (44). Neuroimaging analyses have demonstrated a relationship between decreased visual acuity and the bilateral SPL (43). The contralateral posterior parietal cortex, ipsilateral inferior frontal gyrus, and ipsilateral frontal areas also exhibit more robust anatomical connections to the right posterior SPL rather than the left SPL. The results of this study suggest that increases in DC values in the SPL may be linked to the pathogenesis of rTLE.

The PCu is the master node of the default mode network, and is involved in the processing of visuospatial information, metaphors, mental imagery, and episodic memory (45). Structural MRI studies have revealed that significantly altered spontaneous brain activity in the bilateral PCu is linked to the pathophysiology of epilepsy and depression (46). Functional MRI analyses have further highlighted decreased activation clusters in the precuneus and supramarginal gyrus of TLE patients as compared to HCs, with positive correlations between conceptual creativity and the gray matter volume of the PCu (47). Enhanced PCu cortical surface area is also linked to morphological variations in the adult midsagittal brain. Recent work suggests that the PCu may also coordinate correlations between vivid memories and egocentric perspectives, with an increase in PCu volume being related to an increased tendency to recall egocentric episodic autobiographical memories (48). Reduced right PCu ReHo has been reported to be related to higher levels of verbal innovation capacity linked to improved flexibility, ingenuity, and fluency (49). These characteristics are common among TLE patients. One meta-analysis found PCu to be activated in response to familiarity (50). The PCu can also promote consciousness networks that exhibit selective hypometabolism in epilepsy patients (51). Here, enhanced PCu DC values in rTLE patients may thus represent a compensatory mechanism associated with the pathogenesis of this disease.

There are multiple limitations to this study. For one, patients were treated with antiepileptic drugs, which may have influenced the brain networks in these patients. However, it was not possible to exclude antiepileptic drug use from a patient care perspective. Second, this study had a limited sample size. Third, neuropsychological scale assessments for all patients were not available owing to patient reluctance to undergo these analyses.

In summary, these data suggest that rTLE patients exhibit abnormal DC values in several regions of the brain, with altered DC in the right caudate offering potential value as neuroimaging biomarker of rTLE.

Data availability statement

The original contributions presented in the study are included in the article/supplementary material, further inquiries can be directed to the corresponding authors.

Ethics statement

The studies involving human participants were reviewed and approved by the Medical Ethics Committee of the Tianyou Hospital Affiliated to Wuhan University of Science and Technology. The patients/participants provided their written informed consent to participate in this study.

Author contributions

RG: writing the manuscript. YZ, HJ, and JJ: study conceptualization, organization, and analysis outcome verification. JJ and HW: data collection and analysis. HW, HR, and SJ: manuscript preparation. RG, HR, and SJ: collect pictures and process them. All authors contributed to the article and approved the submitted version.

Funding

The investigation was supported by the grant from the Natural Science Joint Foundation of Hubei province (Nos. WJ2019H232 and WJ2019H233) and Health of Hubei Province Scientific Resarch Project (2020CFB512).

Acknowledgments

The authors thank all individuals who served as study subjects and MJEditor (www.mjeditor.com) for its linguistic assistance during the preparation of this manuscript.

Conflict of interest

The authors declare that the research was conducted in the absence of any commercial or financial relationships that could be construed as a potential conflict of interest.

Publisher's note

References

1. Vinti V, Dell'Isola GB, Tascini G, Mencaroni E, Di Cara G, Striano P, et al. Temporal lobe epilepsy and psychiatric comorbidity. *Front Neurol.* (2021) 12:775781. doi: 10.3389/fneur.2021.775781

2. Falconer MA, Serafetinides EA, Corsellis JN. Etiology and pathogenesis of temporal lobe epilepsy. *Arch Neurol.* (1964) 10:233–48. doi: 10.1001/archneur.1964.00460150003001

3. Shah P, Bassett DS, Wisse LE, Detre JA, Stein JM, Yushkevich PA, et al. Structural and functional asymmetry of medial temporal subregions in unilateral temporal lobe epilepsy: a 7T MRI study. *Hum Brain Mapp.* (2019) 40:2390–8. doi: 10.1002/hbm.24530

4. Smolensky IV, Zubareva OE, Kalemenev SV, Lavrentyeva VV, Dyomina AV, Karepanov AA, et al. Impairments in cognitive functions and emotional and social behaviors in a rat lithium-pilocarpine model of temporal lobe epilepsy. *Behav Brain Res.* (2019) 372:112044. doi: 10.1016/j.bbr.2019.112044

5. Galovic M, van Dooren VQ, Postma TS, Vos SB, Caciagli L, Borzì G, et al. Progressive cortical thinning in patients with focal epilepsy. *JAMA Neurol.* (2019) 76:1230–9. doi: 10.1001/jamaneurol.2019.1708

6. Amin U, Benbadis SR. The role of EEG in the erroneous diagnosis of epilepsy. *J Clin Neurophysiol.* (2019) 36:294–7. doi: 10.1097/WNP.0000000000000572

7. Gao Y, Zheng J, Li Y, Guo D, Wang M, Cui X, et al. Abnormal default-mode network homogeneity in patients with temporal lobe epilepsy. *Medicine.* (2018) 97:e11239. doi: 10.1097/MD.0000000000011239

8. Gao Y, Zheng J, Li Y, Guo D, Wang M, Cui X, et al. Decreased functional connectivity and structural deficit in alertness network with right-sided temporal lobe epilepsy. *Medicine.* (2018) 97:e0134. doi: 10.1097/MD.0000000000010134

9. Gao Y, Xiong Z, Wang X, Ren H, Liu R, Bai B, et al. Abnormal degree centrality as a potential imaging biomarker for right temporal lobe epilepsy: a resting-state functional magnetic resonance imaging study and support vector machine analysis. *Neuroscience.* (2022) 487:198–206. doi: 10.1016/j.neuroscience.2022.02.004

10. Sarica C, Yamamoto K, Loh A, Elias GJ, Boutet A, Madhavan R, et al. Blood oxygen level-dependent (BOLD) response patterns with thalamic deep brain stimulation in patients with medically refractory epilepsy. *Epilepsy Behav.* (2021) 122:108153. doi: 10.1016/j.yebeh.2021.108153

11. Qin Y, Jiang S, Zhang Q, Dong L, Jia X, He H, et al. BOLD-fMRI activity informed by network variation of scalp EEG in juvenile myoclonic epilepsy. *NeuroImage Clin.* (2019) 22:101759. doi: 10.1016/j.nicl.2019.101759

12. Tang Y, Choi JY, Alexopoulos A, Murakami H, Daifu-Kobayashi M, Zhou Q, et al. Individual localization value of resting-state fMRI in epilepsy presurgical evaluation: a combined study with stereo-EEG. *Clin Neurophysiol.* (2021) 132:3197–206. doi: 10.1016/j.clinph.2021.07.028

13. Gonen OM, Moffat BA, Desmond PM, Lui E, Kwan P, O'Brien TJ. Seven-tesla quantitative magnetic resonance spectroscopy of glutamate, γ-aminobutyric acid, and glutathione in the posterior cingulate cortex/precuneus in patients with epilepsy. *Epilepsia.* (2020) 61:2785–94. doi: 10.1111/epi.16731

14. Zhou S, Xiong P, Ren H, Tan W, Yan Y, Gao Y. Aberrant dorsal attention network homogeneity in patients with right temporal lobe epilepsy. *Epilepsy Behav.* (2020) 111:107278. doi: 10.1016/j.yebeh.2020.107278

15. Zhu J, Xu C, Zhang X, Qiao L, Wang X, Zhang X, et al. Altered amplitude of low-frequency fluctuations and regional homogeneity in drug-resistant epilepsy patients with vagal nerve stimulators under different current intensity. *CNS Neurosci Ther.* (2021) 27:320–9. doi: 10.1111/cns.13449

16. Wang J, Li Y, Wang Y, Huang W. Multimodal data and machine learning for detecting specific biomarkers in pediatric epilepsy patients with generalized tonic-clonic seizures. *Front Neurol.* (2018) 9:1038. doi: 10.3389/fneur.2018.01038

17. Reddy SD, Younus I, Sridhar V, Reddy DS. Neuroimaging biomarkers of experimental epileptogenesis and refractory epilepsy. *Int J Mol Sci.* (2019) 20:220. doi: 10.3390/ijms20010220

18. Grubb J, Lopez D, Mohan B, Matta J. Network centrality for the identification of biomarkers in respondent-driven sampling datasets. *PLoS One.* (2021) 16:e0256601. doi: 10.1371/journal.pone.0256601

19. Chen C, Wang H-L, Wu S-H, Huang H, Zou J-L, Chen J, et al. Abnormal degree centrality of bilateral putamen and left superior frontal gyrus in schizophrenia with auditory hallucinations: a resting-state functional magnetic resonance imaging study. *Chine Med J.* (2015) 128:3178–84. doi: 10.4103/0366-6999.170269

20. Li S, Chen Y, Duan G, Pang Y, Liu H, Wei Y, et al. *Altered Brain Network Degree Centrality in Major Depressive Disorder via Electro-Acupuncture Stimulation at Baihui (GV20)*. Nanning: Reaearch Square. (2021). doi: 10.21203/rs.3.rs-525264/v1

21. Li H, Jia X, Li Y, Jia X, Yang Q. Aberrant amplitude of low-frequency fluctuation and degree centrality within the default mode network in patients with vascular mild cognitive impairment. *Brain Sci.* (2021) 11:1534. doi: 10.3390/brainsci11111534

22. Wang X, Hu T, Yang Q, Jiao D, Yan Y, Liu L. Graph-theory based degree centrality combined with machine learning algorithms can predict response to treatment with antiepileptic medications in children with epilepsy. *J Clin Neurosci.* (2021) 91:276–82. doi: 10.1016/j.jocn.2021.07.016

23. Hahamy A, Calhoun V, Pearlson G, Harel M, Stern N, Attar F, et al. Save the global: global signal connectivity as a tool for studying clinical populations with functional magnetic resonance imaging. *Brain Connect.* (2014) 4:395–403. doi: 10.1089/brain.2014.0244

24. Wanderley Espinola C, Gomes JC, Mônica Silva Pereira J, dos Santos WP. Detection of major depressive disorder, bipolar disorder, schizophrenia and generalized anxiety disorder using vocal acoustic analysis and machine learning: an exploratory study. *Res Biomed Eng.* (2022):1–17. doi: 10.1007/s42600-022-00222-2

25. Shor O, Glik A, Yaniv-Rosenfeld A, Valevski A, Weizman A, Khrennikov A, et al. EEG p-adic quantum potential accurately identifies depression, schizophrenia and cognitive decline. *PLoS One.* (2021) 16:e0255529. doi: 10.1371/journal.pone.0255529

26. Lin C-H, Su H, Hung C-C, Lane H-Y, Shiea J. Characterization of potential protein biomarkers for major depressive disorder using matrix-assisted laser desorption ionization/time-of-flight mass spectrometry. *Molecules.* (2021) 26:4457. doi: 10.3390/molecules26154457

27. Obuchowski NA, Bullen JA. Receiver operating characteristic (ROC) curves: review of methods with applications in diagnostic medicine. *Phys Med Biol.* (2018) 63:07TR01. doi: 10.1088/1361-6560/aab4b1

28. Doi T, Fan Y, Gold JI, Ding L. The caudate nucleus contributes causally to decisions that balance reward and uncertain visual information. *eLife.* (2020) 9:e56694. doi: 10.7554/eLife.56694

29. Bick SK, Patel SR, Katnani HA, Peled N, Widge A, Cash SS, et al. Caudate stimulation enhances learning. *Brain.* (2019) 142:2930–7. doi: 10.1093/brain/awz254

30. Driscoll ME, Bollu PC, Tadi P. Neuroanatomy, nucleus caudate. *StatPearls [Internet]*, ed. M. E. Driscoll (Treasure Island, FL: StatPearls Publishing) (2021).

31. Jiang Y, Nie L. *ML of Striatum rs-fMRI Features Predicts TLE Diagnosis*. Nanning: Reaearch Square. (2021). doi: 10.21203/rs.3.rs-638717/v1

32. Du T, Chen Y, Shi L, Liu D, Liu Y, Yuan T, et al. Deep brain stimulation of the anterior nuclei of the thalamus relieves basal ganglia dysfunction in monkeys with temporal lobe epilepsy. *CNS Neurosci Ther.* (2021) 27:341–51. doi: 10.1111/cns.13462

33. Faglioni P. The frontal lobe. In: Pizzamiglio L, Denes G editors. *Handbook of Clinical and Experimental Neuropsychology*. London: Psychology Press (2020). p. 525–70.

34. Bonet CNR, Hwang G, Hermann B, Struck AF, Cook CJ, Nair VA, et al. Neuroticism in temporal lobe epilepsy is associated with altered limbic-frontal lobe resting-state functional connectivity. *Epilepsy Behav.* (2020) 110:107172. doi: 10.1016/j.yebeh.2020.107172

35. Reyes A, Kaestner E, Ferguson L, Jones JE, Seidenberg M, Barr WB, et al. Cognitive phenotypes in temporal lobe epilepsy utilizing data-and clinically driven approaches: moving toward a new taxonomy. *Epilepsia.* (2020) 61:1211–20. doi: 10.1111/epi.16528

36. Buck S, Bastos F, Baldeweg T, Vargha-Khadem F. A functional MRI paradigm suitable for language and memory mapping in pediatric temporal lobe epilepsy. *Front Neurol.* (2020) 10:1384. doi: 10.3389/fneur.2019.01384

37. Yaranagula SD, Asranna A, Nagappa M, Nayak CS, Pratyusha P, Mundlamuri RC, et al. Sleep profile and polysomnography in patients with drug-resistant temporal lobe epilepsy (TLE) due to hippocampal sclerosis (HS) and the effect of epilepsy surgery on sleep-a prospective cohort study. *Sleep Med.* (2021) 80:176–83. doi: 10.1016/j.sleep.2020.12.016

38. Jain P, Tomlinson G, Snead C, Sander B, Widjaja E. Systematic review and network meta-analysis of resective surgery for mesial temporal lobe epilepsy. *J Neurol Neurosurg Psychiatry.* (2018) 89:1138–44. doi: 10.1136/jnnp-2017-317783

39. Buxbaum LJ, Randerath J. Limb apraxia and the left parietal lobe. *Handb Clin Neurol.* (2018) 151:349–63. doi: 10.1016/B978-0-444-63622-5.00017-6

40. Coslett HB, Schwartz MF. The parietal lobe and language. *Handb Clin Neurol.* (2018) 151:365–75. doi: 10.1016/B978-0-444-63622-5.00018-8

41. Rizzolatti G, Rozzi S. The mirror mechanism in the parietal lobe. *Handb Clin Neurol.* (2018) 151:555–73. doi: 10.1016/B978-0-444-63622-5.00028-0

42. Husbani MAR. The default mode network in patient with temporal lobe epilepsy (TLE) : a resting state fMRI study. *Asian J Med Biomed.* (2020) 4:1–8.

43. Shuhada J, Husbani M, Hamid A. The default mode network in patient with temporal lobe epilepsy (TLE) : a resting state fMRI study. *Asian J Med Biomed.* (2020) 4:23–30.

44. Howell ST, Grushina A, Holzner F, Brugger J. Thermal scanning probe lithography—a review. *Microsyst Nanoeng.* (2020) 6:1–24. doi: 10.1038/s41378-019-0124-8

45. Cavanna AE, Trimble MR. The precuneus: a review of its functional anatomy and behavioural correlates. *Brain.* (2006) 129:564–83. doi: 10.1093/brain/awl004

46. Zhu X, He Z, Luo C, Qiu X, He S, Peng A, et al. Altered spontaneous brain activity in MRI-negative refractory temporal lobe epilepsy patients with major depressive disorder: a resting-state fMRI study. *J Neurol Sci.* (2018) 386:29–35. doi: 10.1016/j.jns.2018.01.010

47. Shuhada J, Husbani M, Hamid A, Muhammad A, editors. Evaluation of default mode network in temporal lobe epilepsy patients and healthy subjects: a preliminary result. *Proceedings of the IOP Conference Series: Materials Science and Engineering*. Bristol: IOP Publishing (2020).

48. Oyegbile TO, VanMeter JW, Motamedi GK, Bell WL, Gaillard WD, Hermann BP. Default mode network deactivation in pediatric temporal lobe epilepsy: relationship to a working memory task and executive function tests. *Epilepsy Behav.* (2019) 94:124–30. doi: 10.1016/j.yebeh.2019.02.031

49. Liu W, Yue Q, Wu X, Gong Q, Zhou D. Abnormal blood oxygen level-dependent fluctuations and remote connectivity in sleep-related hypermotor epilepsy. *Acta Neurol Scand.* (2021) 143:514–20. doi: 10.1111/ane.13379

50. Dharan AL, Bowden SC, Lai A, Peterson AD, Cheung MW-L, Woldman W, et al. Resting-state functional connectivity in the idiopathic generalized epilepsies: a systematic review and meta-analysis of EEG and MEG studies. *Epilepsy Behav.* (2021) 124:108336. doi: 10.1016/j.yebeh.2021.108336

51. Tan Z, Long X, Tian F, Huang L, Xie F, Li S. Alterations in brain metabolites in patients with epilepsy with impaired consciousness: a case-control study of interictal multivoxel 1H-MRS findings. *Am J Neuroradiol.* (2019) 40:245–52. doi: 10.3174/ajnr.A5944

frontiers | Frontiers in Psychiatry

TYPE Original Research
PUBLISHED 01 August 2022
DOI 10.3389/fpsyt.2022.968859

OPEN ACCESS

EDITED BY
Yujun Gao,
Wuhan University, China

REVIEWED BY
Ke Ren,
Xiamen University, China
Huize Pang,
The First Affiliated Hospital of China Medical University, China

*CORRESPONDENCE
Lihua Liu
liudilin1990@126.com
Xuhui Hui
huixuhuiwch@126.com

†These authors have contributed equally to this work and share first authorship

SPECIALTY SECTION
This article was submitted to Neuroimaging and Stimulation, a section of the journal Frontiers in Psychiatry

RECEIVED 14 June 2022
ACCEPTED 08 July 2022
PUBLISHED 01 August 2022

CITATION
Deng X, Liu L, Zhen Z, Chen Q, Liu L and Hui X (2022) Cognitive decline in acoustic neuroma patients: An investigation based on resting-state functional magnetic resonance imaging and voxel-based morphometry.
Front. Psychiatry 13:968859.
doi: 10.3389/fpsyt.2022.968859

Cognitive decline in acoustic neuroma patients: An investigation based on resting-state functional magnetic resonance imaging and voxel-based morphometry

Xueyun Deng[1,2†], Lizhen Liu[3†], Zhiming Zhen[3†], Quan Chen[4], Lihua Liu[5*] and Xuhui Hui[2*]

[1]Department of Neurosurgery, The Affiliated Nanchong Central Hospital of North Sichuan Medical College, Nanchong, China, [2]Department of Neurosurgery, West China Hospital of Sichuan University, Chengdu, China, [3]Department of Radiology, Southwest Hospital, Third Military Medical University (Army Medical University), Chongqing, China, [4]Department of Neurology, Chenjiaqiao Hospital, Chongqing, China, [5]Department of Geriatrics, The Affiliated Nanchong Central Hospital of North Sichuan Medical College, Nanchong, China

Objective: Acoustic neuroma (AN) is a clinically common benign tumor. There are few neuropsychological investigations for AN, especially cognitive neuropsychology. Herein, the study probed into cognitive function changes in AN patients and expounded possible mechanisms through structural and functional magnetic resonance imaging (fMRI).

Materials and methods: Neuropsychological tests were performed between 64 patients with AN and 67 healthy controls. Then, using resting-state fMRI, the possible mechanisms of cognitive decline in AN patients were further explored by calculating the amplitude of low-frequency fluctuations (ALFF) and regional homogeneity (ReHo). Furthermore, using high-resolution T1-weighted images, voxel-based morphometry (VBM) was adopted to investigate the changes in gray matter volume (GMV) and white matter volume (WMV) in AN patients.

Results: AN patients had worse cognitive performance than those in the healthy controls. Relative to the healthy individuals, the mALFF value was increased in the right caudate nucleus of the patients with left-sided AN (LAN) and the right rectus region of the patients with right-sided AN (RAN). The mReHo values of the bilateral superior frontal gyrus and middle frontal gyrus were decreased in LAN patients. Compared with healthy subjects, the GMV values were elevated in the left fusiform gyrus, parahippocampal gyrus, calcarine gyrus, and cuneus in LAN patients as well as in the right fusiform gyrus and parahippocampal gyrus in RAN patients. Meanwhile, the WMV values showed elevations in the bilateral putamen, left rectal gyrus, and thalamus in LAN patients.

Conclusion: Cognitive dysfunction occurs in AN patients. Cognitive decline in AN patients activates functional activity in some brain regions, thereby compensating for cognition decline. Additionally, the ReHo values were reduced in the frontal lobe in LAN patients, and the connectivity was decreased, affecting the functional differentiation and integration of the brain, which may be associated with the decline in cognitive function. Lateralized brain reorganization induced by unilateral hearing loss was presented in AN patients. LAN caused a more significant interference effect on the brain while RAN patients showed more stable cerebral cortices. Altogether, responding to cognition decline in AN patients, structural reorganization occurs, and compensative increases in cognitive-related brain regions, which compensates for cognitive impairment.

KEYWORDS

cognition, acoustic neuroma, vestibular schwannoma, rs-fMRI, VBM

Introduction

The functions of the brain are constantly changed and remodeled to functionally adapt to changing sensory signals (1, 2). Prior studies have demonstrated that the auditory center of deaf patients can be activated by non-auditory stimuli (3), which indicates cross-modal sensory plasticity in deaf patients (4). Plasticity can be also presented in the auditory cortex, with structural changes outside the auditory area (5–7). Hearing loss can affect different aspects of cognitive function in pre- and post-lingually deaf populations, such as attention deficit (8, 9), impairment in short-term memory (10), and executive function (11–13). There are at least two forms of brain plasticity during hearing impairment: cross-modal plasticity suggests that the body can compensate for hearing loss by optimizing multiple sensory systems (4), while changes in cognitive function suggest that more cognitive resources must be utilized during auditory processing to compensate for hearing loss (10, 14).

Unlike bilateral deafness, patients with unilateral hearing loss (UHL) retain most of their ability to capture auditory signals but have more complicated auditory processing (15–18). UHL shows asymmetric auditory input, which not only affects overall auditory perception (19) but also affects the processing of higher-order auditory representations (20–22). Therefore, it is reasonable to propose that the connectivity of sensors with advanced control networks and the integration between these networks may be functionally reorganized in the UHL patients.

Studies have illustrated the plasticity of the central auditory pathway in UHL, but most of these studies are limited to the auditory cortex and auditory pathway (23, 24). Up to now, few studies have investigated the relationship between UHL and cognitive function, particularly the mechanisms of cognitive decline. Whether unilateral auditory deprivation affects the neural circuits of cognitive control networks other than the sensory cortex remains unclear. Zhang et al. (25) enrolled 11 patients with left sensorineural hearing loss and 10 patients with right sensorineural hearing loss and 11 healthy individuals, and found differences in the regional homogeneity (ReHo) values in the default mode network (DMN), which is considered to be related to cognitive impairment. However, no significant differences were detected in the neuropsychological test scores (MMSE, TMTA, TMTB, etc.) among the three groups, which may be related to the small sample size and low statistical power, and MMSE is less sensitive than MoCA. Wang et al. (26) investigated 21 patients with left and 21 patients with right-sided acoustic neuroma and 24 healthy subjects and analyzed the gray matter volume (GMV) with voxel-based morphometry (VBM). Their results uncovered volume decreases in key brain regions for cognitive processing such as bilateral anterior cingulate cortex, right superior frontal gyrus, and bilateral middle frontal gyrus. They speculated that long-term partial hearing impairment could change the auditory cortex and affect higher-level cognitive function; whereas, no difference was noted in the MMSE score of the enrolled patients, suggesting no difference concerning cognitive function among the three groups, so the changes in white matter volume were not assessed.

Resting-state functional magnetic resonance imaging (rs-fMRI) is a promising imaging technique for the non-invasive

Abbreviations: AN, acoustic neuroma; HC, healthy control; LAN, left acoustic neuroma; MoCA, Montreal cognitive assessment; PTA, pure tone average; RAN, right acoustic neuroma; RAVLT, Rey Auditory Verbal Learning Test; SDMT, symbol-digital modalities test; TMT, trail-making test; UHL, unilateral hearing loss; ALFF, amplitude of low-frequency fluctuations; ReHo, regional homogeneity; VBM, voxel-based morphometry; GMV, gray matter volume; WMV, white matter volume.

detection of whole-brain functional activity. Amplitude of low-frequency fluctuations (ALFF), which indicates the intensity of local brain activity, and ReHo, which represents the synchrony of the blood-oxygen level-dependent (BOLD) signal adjacent to voxels over time, are two robust indicators showing high test-retest reliability (27, 28). It is quite valuable for exploring the neural basis of individual differences in sensory deprivation.

We hypothesized that the cognitive decline caused by patients with acoustic neuroma could lead to changes in ALFF and ReHo in related brain regions, as well as in the cerebral cortex involved in cognitive function. Therefore, this experiment was designed to analyze and calculate relevant indicators to identify the brain regions presenting differences and analyze their correlations with cognitive function, so as to find changes in brain function and cortical structural reorganization after cognitive impairment in patients.

Materials and methods

Demographics, clinical data, and cognitive function of subjects

Sixty-four right-handed AN patients (21 males and 43 females, age range: 19–75 years) were recruited from the outpatient and ward of Neurosurgery of West China Hospital of Sichuan University, from October 2019 to July 2020. Sixty-seven right-handed hearing controls (21 males and 46 females, age range: 26–74 years) were also enrolled. The demographic information is shown in Supplementary Tables 1, 2. The experiment was approved by the Hospital Ethics Committee, and all participants signed the informed consent.

The average air conduction thresholds at four frequencies (0.5, 1, 2, and 4 kHz) were calculated as the pure tone average (PTA), representing the hearing levels of the subjects. According to the World Health Organization, hearing loss was classified as mild (PTA 26–40 dB HL), moderate (PTA 41–60 dB HL), severe (PTA 61–80 dB HL), and profound (PTA > 81 dB HL).

Patients with acoustic neuroma are often complicated with tinnitus symptoms. In this study, AN patients accompanying tinnitus were assessed using the tinnitus handicap inventory (THI) scale (29). Higher scores indicate greater severity and greater impact on daily life.

All subjects were performed MoCA, RAVLT immediate memory and delayed memory, Stroop color-word test A, B, and C (Stroop A, B, and C), symbol digit modalities test (SDMT), trail making test A and B (TMT A and B).

MRI scanning parameters

A GE 750 W 3.0 T magnetic resonance apparatus was used for 3D T1 image acquisition from all enrolled patients and healthy controls, and data were collected using a 32-channel head coil. rs-fMRI scanning parameters were set as follows: repetition time (TR) = 2,000 ms, echo time (TE) = 30 ms, field of view (FOV) = 24.0 cm × 24.0 cm, acquisition matrix = 64 × 64, flip angle = 90°, slice thickness/slice spacing = 4.0 mm/0.0 mm, voxel size = 3.75 × 3.75 × 4.0 mm^3. In total, 35-slice whole-brain images were scanned inter-slice at 240 time points, with a scanning time of about 8 min and 10 s. The T1 scan parameters were as follows: slice thickness = 1 mm, TR = 8.68 ms, TE = 3.20 ms, scan matrix = 512 × 512, voxel size = 0.5 × 0.5 × 1.0 mm^3, and the scan time is about 4 min and 37 s. The head of the patient was appropriately fixed with soft silicone on both sides to reduce the possibility of head displacement.

Image data processing process

The rs-fMRI data were preprocessed, and ALFF and ReHo values were calculated using the Restplus software package (RESTplus V1.2, http://restfmri.net/forum/RESTplusV1.2). The data preprocessing process is as follows: (1) removal of volumes at the first 10 time points; (2) followed by slice timing and realign. The translational head movement should not exceed 2 mm and increased to within 3 mm for very few subjects who are easy to agitate due to dementia, diseases, and other reasons; (3) normalization: one-step registration method; (4) detrend; (5) regression of covariates, such as white matter, cerebrospinal fluid, and head movement signals to reduce their influence on the experiment; (6) Filter; and (7) Smooth.

It should be noted that ALFF was calculated without filtering during the preprocessing process, and ReHo was not smoothed during the preprocessing but smoothed after it was calculated, to allow the data to be normalized, which would be conducive to statistical analysis and indicator standardization; the mean ALFF (mALFF) value was generated and mean ReHo (mReHo) value was obtained for later analysis.

VBM preprocessing process

Using MATLAB2013b (Math Works, Natick, MA, USA), the SPM8 software package (30) was run with the steps as follows: (1) Conversion of DICOM format images to 3D NIFTI format files; (2) origin-corrected anatomical image (3) Image tissue segmentation and spatial normalization. (4) Calculation of final volume after image segmentation. (5) Smoothing: within the range of the full width at half maximum (FWHM) of the Gaussian smoothing kernel of 6–10, 8 mm was selected in this study.

Statistical analysis

Statistical analysis was performed using SPSS 23.0 (IBM). Continuous variables that met the normal distribution and homogeneity of variance were presented as the mean ± standard deviation, otherwise, the median (interquartile range) was used. Categorical variables were expressed as numerical values (percentages). Independent data between two groups were compared by the *t*-test if the data met the normal distribution and homogeneity of variance, otherwise, the non-parametric Mann-Whitney U test was used. The comparisons between the two acoustic neuroma subgroups and three groups (including healthy controls) were performed by one-way ANOVA if the data conformed to the normal distribution and homogeneity of variance, otherwise, by the Kruskal-Wallis H test. Qualitative data were compared using the χ^2 test. Spearman correlation analysis was conducted to explore the correlations of clinical indicators with cognitive function, depression, and anxiety. A *p*-value <0.05 was considered statistically significant.

The SPM12.0 software package was employed to perform an independent-sample *t*-test for the inter-group comparisons of left-sided and right-sided acoustic neuroma patients and healthy subjects. The analysis of covariance (ANCOVA) was adopted for intra-group comparisons of differences between the groups by limiting the scope of analysis, based on controlling age, gender, and years of education. The differential brain regions were made into a mask, followed by a *post-hoc* comparison within the range limited by this mask. An adjusted cluster-level test was conducted for statistical analysis of gray matter and white matter, and significance was defined as $p < 0.001$ at the voxel level, and family-wise error (FWE)-corrected *p*-value < 0.05 at the cluster level. The GMV and WMV values of differential brain regions were extracted and their correlations with cognitive function scale scores and clinical indicators were assessed by Spearman correlation analysis. $p < 0.05$ was considered to be a significant statistical difference.

Results

Results of demographics and clinical data comparisons among groups

The demographics and clinical characteristics of the subjects are presented in Table 1. In total, 131 subjects were enrolled in this study, including 64 patients with acoustic neuroma (left: right = 40: 24) and 67 healthy controls. We observed no significant difference in age, gender, and education level between the acoustic neuroma patients and healthy controls ($p > 0.05$). The results of the cognitive function scale and mental health scale of acoustic neuroma patients and healthy controls are outlined in Supplementary Tables 1, 2.

The cognitive function and mental statuses were compared among patients with left-sided and right-sided acoustic neuroma and healthy controls. There were no noticeable differences concerning gender, age, and years of education among the three groups ($p > 0.05$). As depicted in Table 1, no significant difference was noted in the course of disease and THI score between the left-sided and right-sided acoustic neuroma patients ($p > 0.05$). As compared to healthy controls, patients with left-sided acoustic neuroma showed significantly poorer performance in MoCA score, RAVLT immediate memory and delayed memory, Stroop B, Stroop C, SDMT, TMT A, and TMT B ($p < 0.05$), while patients with right-sided acoustic neuroma displayed notably poorer performance in MoCA score, RAVLT immediate memory and delayed memory, Stroop A, Stroop B, Stroop C, SDMT, TMT A, and TMT B ($p < 0.05$). The results are summarized in Tables 1, 2.

Patients with acoustic neuroma are often complicated with tinnitus symptoms. Correlation analysis showed that there was no significant correlation between THI and cognitive scale, or THI and anxiety, depression scale.

Comparisons of ALFF and ReHo values of rs-fMRI among groups

Relative to healthy controls, the mALFF values in the right caudate nucleus and right thalamus were increased in patients with left-sided acoustic neuroma and the right rectal gyrus in patients with right-sided acoustic neuroma; reversely, the mReHo values in bilateral superior frontal gyrus and middle frontal gyrus were detected in patients with left-sided acoustic neuroma, while no obvious change was found in the patients with right-sided acoustic neuroma (Figures 1–3, Supplementary Figure 1).

Comparisons of GMV and WMV values of VBM

The patients with left-sided acoustic neuroma showed increases in the GMV values of the left fusiform gyrus, parahippocampal gyrus, calcarine gyrus, and cuneus while the patients with right-sided acoustic neuroma exhibited elevations in the GMV values of the right fusiform gyrus and parahippocampal gyrus when compared with those in healthy controls. Additionally, the WMV values of the bilateral putamen, left rectal gyrus, and thalamus were all increased in the patients with left-sided acoustic neuroma vs. those of healthy controls, yet no significant changes were found in the patients with right-sided acoustic neuroma. Furthermore, the GMV

TABLE 1 Comparison of clinical data and cognitive function among LAN, RAN, and HC groups.

	LAN ($n = 40$)	RAN ($n = 24$)	HC ($n = 67$)	F/H/T values	p-value	*Post-hoc*
Gender (male)	16 (40.0%)	5 (20.8%)	21 (31.3%)	2.562	0.278[a]	N/A
Age (yrs)	49.00 ± 14.32	50.50 ± 12.27	46.64 ± 10.06	1.105	0.334[b]	N/A
Years of education (yrs)	10.00 (7.80)	8.50 (8.30)	9.00 (7.00)	4.825	0.090[c]	N/A
Course of disease (yrs)	2.00 (5.23)	2.75 (5.25)	N/A	1.487	0.223[d]	N/A
THI	14.00 (6.00)	10.00 (6.00)	N/A	0.221	0.639[d]	N/A
Left PTA (dB HL)	55.73 ± 26.14	22.15 ± 10.67	N/A	6.304	<0.001[e*]	N/A
Right PTA (dB HL)	17.50 (10.00)	66.74 ± 34.06	N/A	−6.031	<0.001[d*]	N/A
MoCA scores	21.00 (6.00)	19.00 (9.00)	26.00 (5.00)	37.407	<0.001[c*]	RAN<HC LAN<HC
RAVLT immediate recall	34.00 (16.00)	31.00 (15.00)	47.00 (19.00)	31.927	<0.001[c*]	RAN<HC LAN<HC
RAVLT delay recall	6.28 ± 3.52	5.29 ± 2.97	9.06 ± 3.32	15.404	<0.001[b*]	RAN<HC LAN<HC
Stroop A (s)	32.50 (27.50)	36.00 (17.50)	27.00 (12.50)	10.053	0.007[c*]	RAN>HC
Stroop B (s)	48.50 (33.00)	54.00 (32.00)	37.00 (19.00)	16.996	<0.001[c*]	RAN>HC LAN>HC
Stroop C (s)	125.50 (85.00)	131.00 (64.00)	86.00 (52.00)	22.064	<0.001[c*]	RAN>HC LAN>HC
SDMT	35.36 ± 15.66	31.38 ± 17.06	45.16 ± 16.84	8.574	0.004[b*]	RAN<HC LAN<HC
TMT A (s)	52.00 (68.00)	73.50 (62.00)	38.00 (31.00)	19.890	<0.001[c*]	RAN>HC LAN>HC
TMT B (s)	180.50 (190.00)	231.00 (191.00)	104.00 (111.00)	16.473	<0.001[c*]	RAN>HC LAN>HC
HAMD	8.00 (8.00)	10.00 (5.00)	2.00 (3.00)	65.865	<0.001[c*]	RAN>HC LAN>HC
HAMA	6.00 (6.00)	7.00 (6.00)	2.00 (2.00)	61.010	<0.001[c*]	RAN>HC LAN>HC

[a]p and [b]p-values were obtained by the R × C chi-square test and ANOVA test, respectively. [c]p and [d]p-values were obtained by Kruskal-Wallis and Mann-Whitney (non-parametric test), respectively. [e]p-values obtained by t-test. F values, H values, and T values were obtained by ANOVA, Kruskal-Wallis, and t-test, respectively. All data were expressed as mean ± SD, median (interquartile range), or number (percentage). The significance level was set at $p < 0.05$. [*]$p < 0.05$. LAN, left acoustic neuroma; RAN, right acoustic neuroma; HC, healthy controls; PTA, pure tone average; THI, tinnitus handicap inventory; N/A, not available.

values of the left fusiform gyrus and parahippocampal gyrus and WMV values of the left rectal gyrus and precentral gyrus were higher in patients with left-sided acoustic neuroma than the patients with right-sided acoustic neuroma. No reductions were observed in the GMV and WMV values of the brain regions among all acoustic neuroma patients (Figures 4–7).

Correlations of ALFF and ReHo values with cognitive function

As shown in Tables 3, 4, increased mALFF values could be observed in the right caudate nucleus of the patients with left-sided acoustic neuroma and the right rectal gyrus of the patients with right-sided acoustic neuroma, which were negatively correlated with cognitive function. On the contrary, the mReHo values of bilateral superior frontal gyrus and middle frontal gyrus were decreased, sharing positive correlations with cognitive function.

Correlations of GMV and WMV values with cognitive function

We assessed the relevance of GMV and WMV values in the differential brain regions to the cognitive

TABLE 2 Comparison of MoCA among LAN, RAN, and HC groups.

	LAN ($n = 40$)	RAN ($n = 24$)	HC ($n = 67$)	H values	*p*-value	*Post-hoc*
Visuospatial executive	3.00 (2.00)	2.00 (2.00)	4.00 (2.00)	44.844	<0.001*	RAN<HC LAN<HC
Naming	3.00 (1.00)	2.00 (2.00)	3.00 (1.00)	10.569	0.005*	RAN<HC RAN<LAN
Attention	5.00 (1.00)	5.00 (1.00)	6.00 (0.00)	27.776	<0.001*	RAN<HC LAN<HC
Language	1.50 (1.00)	1.00 (2.00)	2.00 (2.00)	18.815	<0.001*	RAN<HC LAN<HC
Language: sentence repetition	1.00 (1.00)	0.00 (1.00)	1.00 (1.00)	15.045	0.001*	RAN<HC LAN<HC
Language: fluency task	1.00 (0.00)	1.00 (1.00)	1.00 (0.00)	14.677	0.001*	RAN<HC LAN<HC
Abstract thinking	1.00 (2.00)	1.00 (2.00)	2.00 (1.00)	9.391	0.009*	RAN<HC
Delayed recall	2.00 (2.00)	2.00 (2.00)	3.00 (3.00)	13.884	0.001*	RAN<HC LAN<HC
Orientation	6.00 (1.00)	6.00 (1.00)	6.00 (0.00)	12.543	0.002*	RAN<HC LAN<HC
MoCA scores	21.00 (6.00)	19.00 (9.00)	26.00 (5.00)	37.407	<0.001*	RAN<HC LAN<HC

p- and H values were obtained by Kruskal-Wallis H (non-parametric test). Data were expressed as median (interquartile range). * $p < 0.05$. LAN, left acoustic neuroma; RAN, right acoustic neuroma; HC, healthy controls; MoCA, Montreal cognitive assessment.

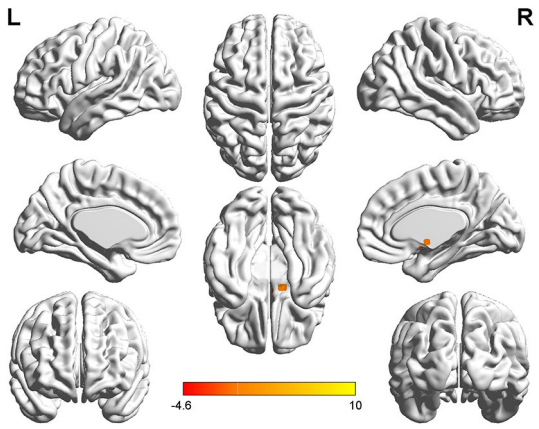

FIGURE 1
T-value map of differential results of mALFF between left auditory neuroma and healthy controls. Compared with healthy controls, the value of mALFF in the right caudate nucleus of patients with left acoustic neuroma was increased, and there was no significant decrease in the brain regions. The statistical threshold was voxel-wise $p < 0.001$ with cluster-wise FWE corrected $p < 0.05$ (122 voxels).

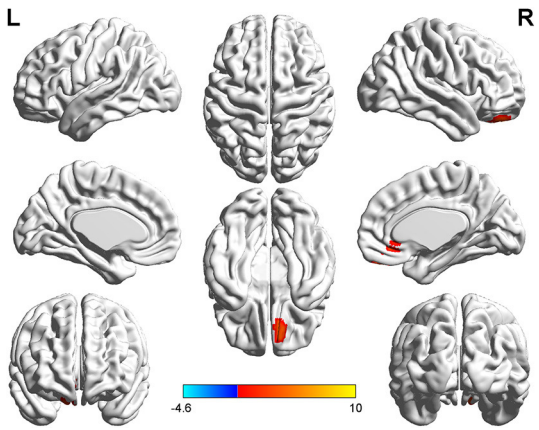

FIGURE 2
T-value map of differential results of mALFF between right auditory neuroma and healthy controls. Compared with healthy controls, the value of mALFF in the right rectus gyrus of patients with right acoustic neuroma was increased, and there was no significant decrease in the brain regions. The statistical threshold was voxel-wise $p < 0.001$ with cluster-wise FWE corrected $p < 0.05$ (122 voxels).

function scale and found that cognitive function was negatively correlated with the GMV and WMV values in the differential brain regions (Figures 8–10, Table 5).

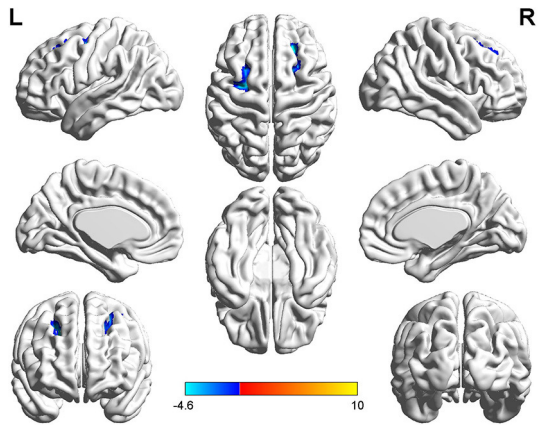

FIGURE 3
T-value map of differential results of mReHo between left auditory neuroma and healthy controls. Compared with healthy controls, the brain regions with decreased mReHo in the patients with left acoustic neuroma were: the bilateral superior and middle frontal gyrus, with no significant decrease in the brain regions. The statistical threshold was voxel-wise $p < 0.001$ with cluster-wise FWE corrected $p < 0.05$ (122 voxels).

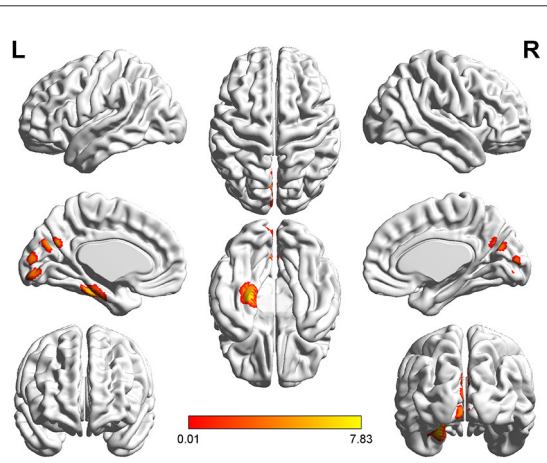

FIGURE 4
T-value map of increased gray matter volume in the patients with left acoustic neuroma compared with healthy controls. Compared with healthy controls, the brain regions with increased gray matter volume in the patients with left acoustic neuroma were: the left parahippocampal gyrus, the fusiform, the calcarine, and the cuneus. The statistical threshold was voxel-wise $p < 0.001$ with cluster-wise FWE corrected $p < 0.05$ (487 voxels).

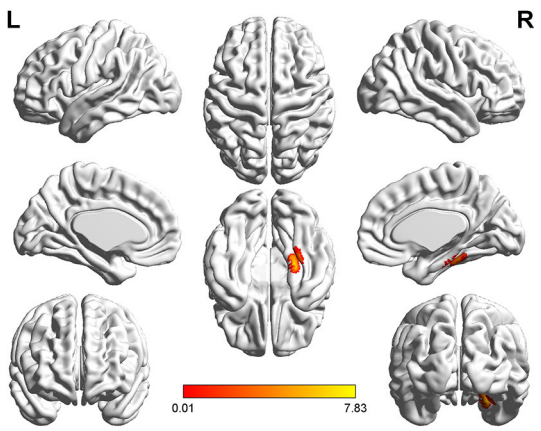

FIGURE 5
T-value map of increased gray matter volume in the patients with right acoustic neuroma compared with healthy controls. Compared with healthy controls, the brain regions with increased gray matter volume in the patients with right acoustic neuroma were: the right fusiform and parahippocampal gyrus. The statistical threshold was voxel-wise $p < 0.001$ with cluster-wise FWE corrected $p < 0.05$ (513 voxels).

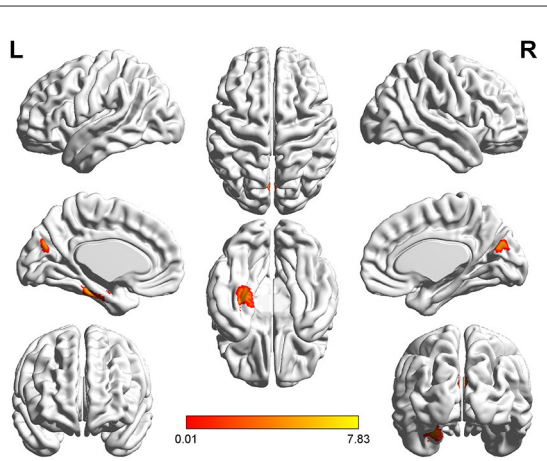

FIGURE 6
T-value map of increased gray matter volume in the patients with left acoustic neuroma compared with right acoustic neuroma. Compared with the patients with right acoustic neuroma, the brain regions with increased gray matter volume in the patients with left acoustic neuroma were: the left parahippocampal gyrus and fusiform. The statistical threshold was voxel-wise $p < 0.001$ with cluster-wise FWE corrected $p < 0.05$ (319 voxels).

Discussion

Cognitive function of acoustic neuroma patients

In comparison with the healthy subjects, patients with left-sided acoustic neuroma and right-sided acoustic neuroma had unfavorable outcomes in the MoCA score, RAVLT memory, Stroop, SDMT, and TMT, showing a statistically significant difference. It is, therefore, illustrated that the cognitive function is declined in the patients with either left-sided or right-sided acoustic neuroma, and their memory, attention, executive function,

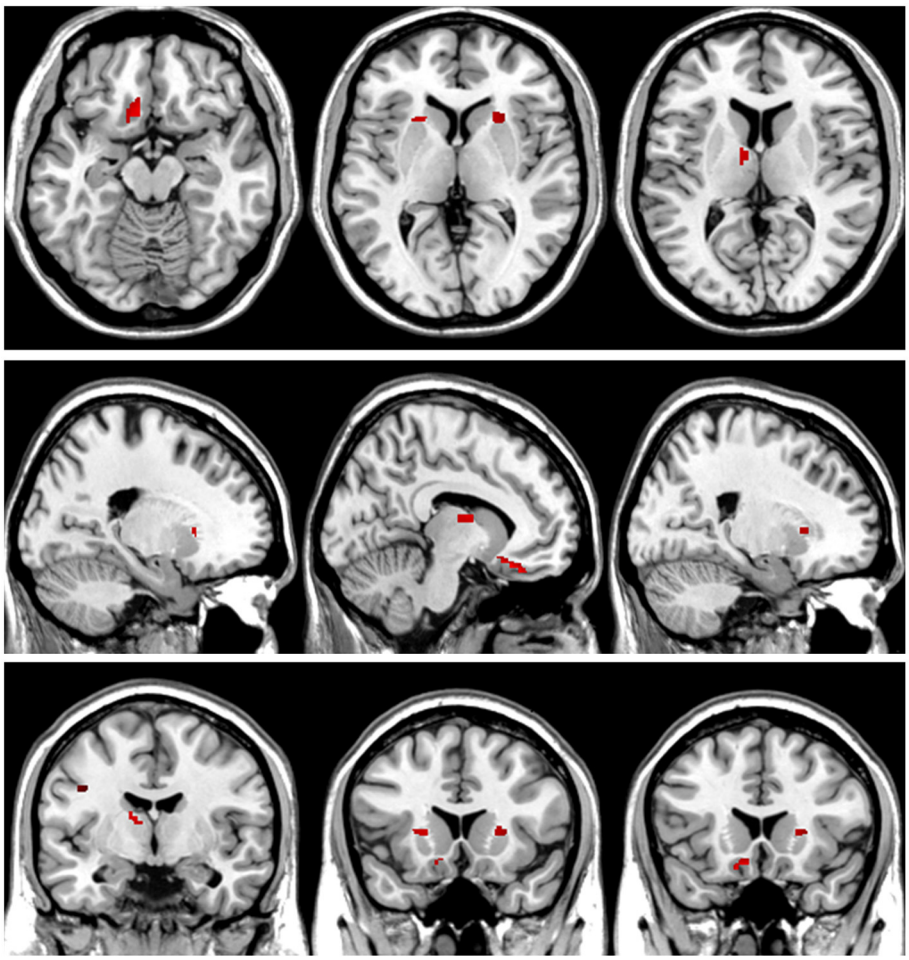

FIGURE 7
T-value map of increased white matter volume in the patients with left acoustic neuroma compared with healthy controls. Compared with the healthy controls, the brain regions with increased white matter volume in the patients with left acoustic neuroma were: the bilateral putamen, left rectus, and left thalamus. The statistical threshold was voxel-wise $p < 0.001$ with cluster-wise FWE corrected $p < 0.05$ (28 voxels).

motor speed, and information processing speed are greatly affected.

Previous studies have shown that children with UHL have worse language developmental outcomes and cognitive function than healthy children, corresponding to manifestations such as delayed language development and inattention (31), and the proportion of children with behavioral problems (25%) in which is higher than that of healthy children (32). Fan et al. (33) compared the cognitive function of patients with the right ($n = 25$) and left ($n = 15$) acoustic neuroma with healthy subjects, and their results revealed normality in the general cognitive function but declines in attention, information processing efficiency, executive function, and memory of the acoustic neuroma patients. Our study, not fully consistent with Fan's study, uncovered that in addition to the general cognitive function decline, significant impairments were induced in the attention, executive function, memory, visuospatial and visual perception abilities, motor speed, and information processing speed of patients with acoustic neuroma than healthy individuals. The acoustic neuroma patients included in this study showed worse neuropsychological test performance in more tasks, which is possibly attributed to our larger sample size and relatively high statistical power. Goebel et al. conducted their investigation on 27 patients with acoustic neuroma and 18 patients with meningioma, with the results demonstrating cognitive impairment in the majority of patients (69%), mainly manifested as decreased attention (such as alertness) and slowed visual motor speed (34), which is in agreement with our findings.

TABLE 3 Correlation analysis between mALFF and cognitive scale in patients with acoustic neuroma.

	mALFF of the right caudate nucleus in LAN patients ($n = 107$)	mALFF of the right rectus gyrus in RAN patients ($n = 91$)
MoCA scores	−0.373 ($p < 0.001$)***	−0.316 (0.002)**
Visuospatial executive	−0.338 ($p < 0.001$)***	−0.275 (0.008)**
Naming	−0.169 (0.081)	−0.215 (0.040)*
Attention	−0.127 (0.194)	−0.167 (0.113)
Language	−0.212 (0.028)*	−0.173 (0.100)
Language: sentence repetition	−0.192 (0.047)*	−0.157 (0.138)
Language: fluency task	−0.137 (0.159)	−0.080 (0.451)
Abstract thinking	−0.207 (0.032)*	−0.171 (0.105)
Delayed recall	−0.240 (0.013)*	−0.224 (0.032)*
Orientation	−0.088 (0.368)	−0.178 (0.090)
RAVLT immediate recall	−0.281 (0.003)**	−0.353 (0.001)***
RAVLT delay recall	−0.152 (0.119)	−0.244 (0.020)*
Stroop A (s)	0.342 ($p < 0.001$)***	0.295 (0.006)**
Stroop B (s)	0.179 (0.065)	0.273 (0.009)**
Stroop C (s)	0.217 (0.025)*	0.237 (0.024)*
SDMT	−0.291 (0.002)**	−0.234 (0.025)*
TMT A (s)	0.323 (0.001)***	0.236 (0.024)*
TMT B (s)	0.263 (0.006)**	0.249 (0.017)*

Data were expressed as spearman correlation coefficient (p-value). $^{*}p < 0.05$, $^{**}p \leq 0.01$, $^{***}p \leq 0.001$; ALFF, Amplitude of low-frequency fluctuations; LAN, left acoustic neuroma; RAN, right acoustic neuroma; MoCA, Montreal cognitive assessment.

Acoustic neuroma patients with tinnitus and cognition

Patients with acoustic neuroma are often associated with tinnitus. In our research, those patients accounted for 43.5% (30/69). To determine whether tinnitus interfered with the experiment, we tested the THI in patients with tinnitus symptoms and analyzed the correlation between neuropsychological tests and THI scores. The results showed that tinnitus did not affect cognitive function, anxiety, and depression, however, Chen et al. found that tinnitus affects cognitive function (35). We analyze the possible reasons as follows: first, the severity of tinnitus patients in the two experiments are different. Most of the tinnitus patients in their study are moderate and severe tinnitus of grade 3–4 (25/35, 71.43%), while most of our patients are mild tinnitus of grade 1–2 (29/30, 96.67%), and only 3.33% of moderate and severe tinnitus patients (1/30). Therefore, it may cause patient selection bias. The tinnitus symptoms of patients in our study are generally mild, which may be because patients are often not only complicated with symptoms such as tinnitus and hearing loss, but also headache, dizziness, and unstable walking, so it is more likely to attract the attention of patients and doctors, then examination found the existence of acoustic neuroma. Second, the heterogeneity of patients, our cases were acoustic neuroma with tinnitus symptoms, and their cases were patients with pure right tinnitus, so it may cause differences in experimental results. Third, the statistical power was limited due to the small number of tinnitus patients in the group, which also may have an impact on the experimental results. Meanwhile, Chen's study also found no correlation between tinnitus and anxiety or depression scale, which is consistent with our findings.

Correlations of ALFF and ReHo parameters with the cognitive function of acoustic neuroma patients

Excavating brain activity is important for understanding the brain and gaining insights into its function (36). ALFF and ReHo are two robust indicators with defined physiological significance and good reproducibility in rs-fMRI studies. ALFF was first proposed by Zang et al. (27) that could represent the intensity of local brain activity. The BOLD signal contains time domain and frequency domain information, and ALFF reflects the strength of voxel spontaneous activity in the resting state by focusing on the frequency domain of the brain signal. ReHo was first proposed by Zang et al. (28) and applied to fMRI based on the assumption that the adjacent voxels in

TABLE 4 Correlation analysis between mReHo and cognitive scale in patients with left acoustic neuroma.

	mReHo value of left superior frontal gyrus ($n = 107$)	mReHo value of left middle frontal gyrus ($n = 107$)	mReHo value of right superior frontal gyrus ($n = 107$)	mReHo value of right middle frontal gyrus ($n = 107$)
MoCA scores	0.133 (0.172)	0.201 (0.038)*	0.151 (0.120)	0.256 (0.008)**
Visuospatial executive	0.094 (0.336)	0.179 (0.065)	0.144 (0.138)	0.205 (0.034)*
Naming	0.084 (0.389)	0.024 (0.802)	0.044 (0.653)	0.112 (0.253)
Attention	0.210 (0.030)*	0.247 (0.010)**	0.211 (0.029)*	0.355 ($p < 0.001$)***
Language	0.202 (0.037)*	0.245 (0.011)*	0.269 (0.005)**	0.170 (0.081)
Language: sentence repetition	0.196 (0.043)*	0.268 (0.005)**	0.277 (0.004)**	0.132 (0.176)
Language: fluency task	0.090 (0.354)	0.060 (0.537)	0.137 (0.159)	0.177 (0.069)
Abstract thinking	0.081 (0.410)	0.159 (0.101)	0.155 (0.110)	0.106 (0.278)
Delayed recall	−0.036 (0.712)	0.020 (0.839)	−0.008 (0.932)	0.077 (0.433)
Orientation	0.169 (0.082)	0.131 (0.178)	0.063 (0.516)	0.320 (0.001)***
RAVLT immediate recall	0.152 (0.118)	0.186 (0.055)	0.140 (0.149)	0.185 (0.056)
RAVLT delay recall	0.123 (0.207)	0.127 (0.194)	0.108 (0.270)	0.174 (0.073)
Stroop A (s)	−0.125 (0.206)	−0.144 (0.146)	−0.032 (0.744)	−0.177 (0.072)
Stroop B (s)	−0.132 (0.175)	−0.172 (0.076)	−0.188 (0.053)	−0.216 (0.026)*
Stroop C (s)	−0.135 (0.164)	−0.186 (0.055)	−0.163 (0.093)	−0.198 (0.041)*
SDMT	0.088 (0.372)	0.157 (0.108)	0.013 (0.898)	0.129 (0.189)
TMT A (s)	−0.160 (0.099)	−0.200 (0.039)*	−0.084 (0.387)	−0.234 (0.015)*
TMT B (s)	−0.063 (0.520)	−0.122 (0.209)	−0.106 (0.279)	−0.236 (0.014)*

Data were expressed as spearman correlation coefficient (p-value). $^{*}p < 0.05$, $^{**}p \leq 0.01$, $^{***}p \leq 0.001$; ReHo, regional homogeneity.

the same functional region have similar time-varying BOLD signals. ReHo describes the synchronization of adjacent voxel time series. A higher ReHo value indicates better synchronicity between adjacent voxels but does not describes stronger local neuron activity.

This study adopted rs-fMRI data to assess the changes in brain function parameters in patients with acoustic neuroma and analyze their relevance to cognitive function. The results indicated alterations in the mALFF and mReHo values of patients with acoustic neuroma. As compared to the healthy individuals, increases were found in the mALFF values of the right caudate nucleus and the right thalamus of the patients with left-sided acoustic neuroma as well as in the right rectal gyrus of the patients with right-sided acoustic neuroma, suggesting the possible existence of functional compensation in the brains of patients with acoustic neuroma and laterality biased to the right; meanwhile, the mReHo values of bilateral superior frontal gyrus and middle frontal gyrus were decreased in patients with left-sided acoustic neuroma, but no obvious changes were found in the right-sided acoustic neuroma group. Since ReHo reflects the synchronization of adjacent voxel time series, it was elucidated that the synchronicity of BOLD signals between the bilateral superior frontal gyrus and the middle frontal gyrus was decreased and the connectivity was declined, affecting the functional differentiation and integration of the brain, particularly the integration. This consequence may be linked to cognitive decline. The study of Wang et al. in the patients with left ($n = 17$) and right ($n = 17$) acoustic neuroma and healthy subjects ($n = 22$) displayed no difference in neurocognitive MMSE scores, but an increased ReHo value was presented in the left parahippocampal gyrus (37). They regarded it as compensation for cognitive decline. The conclusion of our experiments was different from those of Wang et al., and this difference may be associated with several factors. For instance, Wang's study enrolled younger subjects than our experiment, wherein the patients with left-sided acoustic neuroma had a mean age of 45.7 years, and those with right-sided acoustic neuroma had a mean age of 43 years; whereas, the actual age of patients in this experiment had a mean age of about 50 years. In Wang's study, the enrolled patients had a higher level of education and more severe hearing loss. Additionally, the two studies possibly involved the different stages of the body. Our study focused on the functional decline while Wang et al. mainly focused on the functional compensation, thus resulting in different results. Besides, the sensitivity of the MMSE adopted by Wang et al. was inferior to that of the MOCA we used here, which may also elicit no detectable difference.

In the present study, cognitive function was regarded to be reversely correlated with the mALFF value. We

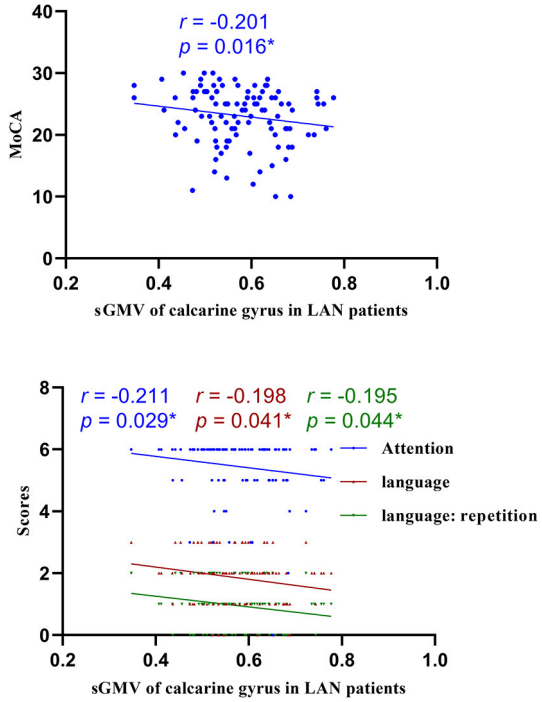

FIGURE 8
Correlations of sGMV of calcarine gyrus and MoCA in LAN patients. LAN, left acoustic neuroma; sGMV, smoothed gray matter volume. *$p < 0.05$.

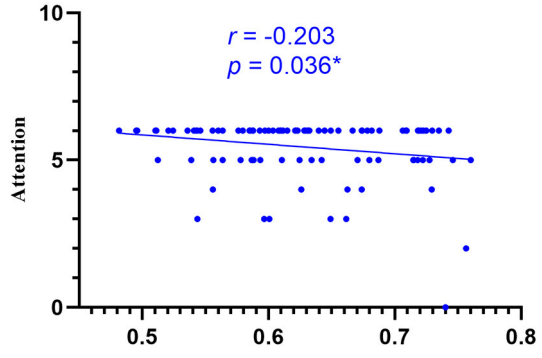

FIGURE 9
Correlations of sGMV of cuneus gyrus and attention of MoCA in LAN patients. LAN, left acoustic neuroma; sGMV, smoothed gray matter volume. *$p < 0.05$.

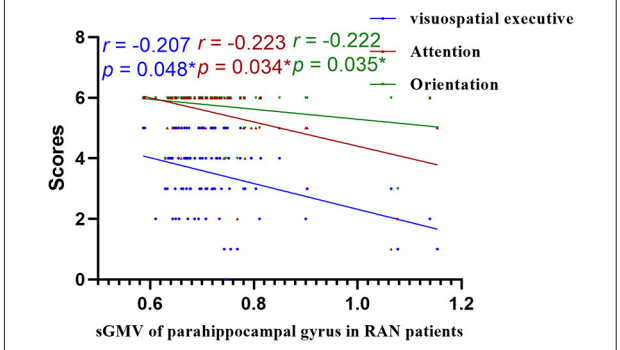

FIGURE 10
Correlations of sGMV of parahippocampal gyrus and MoCA in RAN patients. RAN, right acoustic neuroma; sGMV, smoothed gray matter volume. *$p < 0.05$.

analyzed whether the body requires more resources to compensate for the decline in cognitive function owing to the cognitive function impairment of patients. The caudate nucleus, which belongs to basal nuclei, and the rectal gyrus are the two brain regions presenting increased mALFF. Previous studies have linked the basal nuclei to motor regulation, but multiple studies have currently reported the close relationship between the basal nuclei and cognitive function, including memory disorders and visuospatial disorders (38). Also, the rectal gyrus shares an association with memory (39). Therefore, decreased memory and executive control ability in patients can trigger the strengthened activity of some brain regions to compensate for the decline in cognitive function.

Decreased ReHo values of the bilateral superior frontal gyrus and middle frontal gyrus in patients with left-sided acoustic neuroma affected the general cognitive function (MoCA score), especially attention and language (including language repetition) in MoCA scores; meanwhile, the ReHo value of bilateral middle frontal gyrus was inversely related to the TMT, Stroop B, and C. The Stroop can be applied to evaluate the executive function and attention of subjects, and the TMT is employed to evaluate attention, executive control ability, and visuospatial ability. The prefrontal cortex is highly relevant to executive control and attention (40), which reflects a neuropathological basis supporting the cognitive function decline in patients with left-sided acoustic neuroma. However, there was no significant relation between the ReHo value on the right and the cognitive scale, firstly suggesting different impacts of left-sided and right-sided acoustic neuromas on the brain, which was consistent with the findings obtained in the previous sections. Secondly, the UHL caused by acoustic neuroma leads to lateralization trends in brain reorganization. Most of the results revealed significant differences between the acoustic neuroma and healthy control groups, but no significant difference existed between the left-sided and right-sided acoustic neuroma groups. Although no statistically significant difference was found in the current study, the reorganization phenomenon was more pronounced in patients with left-sided acoustic neuroma than in those with right-sided acoustic neuroma, possibly attributable to the stronger

TABLE 5 Results of the analysis of the correlation between differential white matter volume and cognitive and clinical information.

	WMV of left putamen ($n = 131$)	WMV of right putamen ($n = 131$)	WMV of left rectus ($n = 131$)	WMV of left thalamus ($n = 131$)
MoCA scores	−0.191 (0.029)*	−0.169 (0.054)	−0.256 (0.003)**	−0.126 (0.151)
visuospatial executive	−0.147 (0.095)	−0.157 (0.074)	−0.200 (0.022)*	−0.129 (0.140)
Naming	−0.128 (0.145)	−0.042 (0.638)	−0.057 (0.519)	0.020 (0.817)
Attention	−0.259 (0.003)**	−0.247 (0.004)**	−0.134 (0.127)	−0.194 (0.027)*
Language	−0.076 (0.389)	−0.117 (0.184)	−0.140 (0.111)	−0.025 (0.775)
Language: Sentence repetition	−0.054 (0.542)	−0.095 (0.282)	−0.123 (0.163)	−0.023 (0.795)
Language: fluency task	−0.068 (0.437)	−0.131 (0.137)	−0.162 (0.064)	0.070 (0.425)
Abstract thinking	−0.091 (0.300)	−0.080 (0.363)	−0.203 (0.020)*	−0.012 (0.888)
Delayed recall	−0.073 (0.407)	−0.044 (0.615)	−0.154 (0.079)	−0.094 (0.286)
Orientation	−0.183 (0.036)*	−0.173 (0.048)*	−0.193 (0.027)*	−0.118 (0.181)
RAVLT immediate recall	−0.262 (0.002) **	−0.216 (0.013)*	−0.332 ($p < 0.001$)***	−0.176 (0.045)*
RAVLT delay recall	−0.261 (0.003)**	−0.25 (0.004)**	−0.265 (0.002)**	−0.156 (0.076)
Stroop A (s)	0.150 (0.095)	0.123 (0.171)	0.352 ($p < 0.001$)***	0.106 (0.240)
Stroop B (s)	0.113 (0.199)	0.155 (0.077)	0.252 (0.004)**	0.070 (0.425)
Stroop C (s)	0.148 (0.094)	0.137 (0.121)	0.323 ($p < 0.001$)***	0.041 (0.645)
SDMT	−0.083 (0.348)	−0.141 (0.110)	−0.331 ($p < 0.001$)***	0.017 (0.849)
TMT A (s)	0.132 (0.133)	0.234 (0.007)**	0.344 ($p < 0.001$)***	0.040 (0.647)
TMT B (s)	0.132 (0.132)	0.192 (0.028)*	0.323 ($p < 0.001$)***	0.069 (0.432)
Left PTA	0.204 (0.159)	−0.042 (0.777)	0.174 (0.232)	0.354 (0.013)*
Right PTA	0.077 (0.600)	0.284 (0.048)*	0.131 (0.370)	−0.112 (0.446)

Data were expressed as spearman correlation coefficient (p-value). *$p < 0.05$, **$p \leq 0.01$, ***$p \leq 0.001$; PTA, pure tone average; WMV, white matter volume.

resistance of the right ear to hearing damage and its more stable behaviors (37, 41).

Correlations of GMV and WMV parameters with the cognitive function of acoustic neuroma patients

Through VBM analysis of changes in the structures of gray and white matter in patients with acoustic neuroma, it was suggested that compared with healthy controls, patients with either left-sided or right-sided acoustic neuroma had increased GMV in several brain regions. Additionally, the WMV values in several brain regions were raised in the patients with left-sided acoustic neuroma, but none of the patients with right-sided acoustic neuroma showed brain regions with increased WMV. Also, none of the acoustic neuroma patients had reductions in the GMV and WMV values of the brain regions. Correlation analysis further revealed that the increases of GMV and WMV in acoustic neuroma patients were related to their attention, memory, executive function, etc.

Brain regions presenting an increased GMV contained the parahippocampal gyrus, fusiform gyrus, cuneus, and calcarine cortex, which are associated with functions such as computational ability, visuospatial ability, logical thinking, and memory (42). The parahippocampal gyrus is involved in memory formation (42). The fusiform gyrus, together with the middle and inferior temporal gyrus and the angular gyrus, participate in the formation of the temporoparietal language areas other than Wernicke's area, and together with the thalamus, represents the brain areas that are jointly activated by a sub-network (alertness) of the attention network and executive control network (40), which is involved in auditory semantic tasks, as well as meaning judgment of Chinese words, pictures, etc. (43). The cuneus and calcarine gyrus are related to functions such as visual function, calculation, and logical thinking (44). The increases in the volumes of the above-mentioned brain regions in patients with acoustic neuroma on the same side may be attributed to the reorganization of the brain structures to compensate for the decline in cognitive function. Different from our findings, Wang et al. (26) revealed atrophied cortical regions containing the bilateral anterior cingulate gyrus, the dorsolateral prefrontal cortex, the right superior frontal gyrus, and the bilateral middle frontal gyrus through comparisons among the patients with left-sided ($n = 24$) and right-sided ($n = 24$) acoustic neuroma and 24 normal subjects. They speculated that the aforementioned cognitive processing-related key structures may be related to cognitive dysfunction, but the

MMSE score showed no difference. There are several differences between our study and the study of Wang et al., such as the age of the included patients, educational level, and neuropsychological test scales. The patients in this study had an average age of about 50 years, and those in Wang's study showed an average age of about 45 years. The patients with left-sided and right-sided acoustic neuroma of enrolled in Wang's study received about 12.3 and 10.7 years of education, respectively, and patients in this experiment underwent about 9.0 years of education. Additionally, we used a variety of neuropsychological tests with higher sensitivity, including MoCA, RAVLT, Stroop, SDMT, and TMT. The neuropsychological test results illustrated different degrees of cognitive impairment in the enrolled patients. However, Wang et al. only used MMSE for evaluation and did not find any difference between acoustic neuroma patients and healthy individuals. Whether the subjects included in the two experiments are in two different stages of the disease is still unclear, thus large-scale longitudinal studies for further clarification are demanded. Given the aforesaid differences, the conclusions driven by the two sets of experiments may not be the same. Based on our experimental data, we surmised that the long-term cognitive decline in patients with acoustic neuroma might lead to cortical reorganization to compensate for the cognitive decline.

It is not yet reported that WMV is altered following UHL, our study the first time pointed out that the areas such as bilateral putamen, left thalamus, and left rectal gyrus showed an increased WMV in acoustic neuroma patients. White matter constitutes an essential structure in the whole brain, and O'Sullivan et al. have substantiated that the integrity of white matter affects overall cognitive function and executive function (45). The putamen, belonging to the basal nuclei, principally regulates movement. A great number of studies have confirmed that the basal nucleus is highly relevant to cognitive impairment, such as memory impairment and visuospatial impairment (38). In addition to a close relation to consciousness and physical functions, the functions of the thalamus are often involved in the impairment of high-level cognitive functions such as memory, calculation, and language (46). Impairment of the gyrus rectus leads to impaired memory in patients (39). Our correlation analysis indicated that the attention, memory, and executive functions of patients with acoustic neuroma were inversely correlated with the WMV values of the putamen, gyrus rectus, and thalamus. We considered that body could compensate for the decreased cognitive function in the patients with cognitive impairment, leading to an increase in WMV in the aforementioned regions. In the meantime, we identified a positive correlation between left PTA and WMV in the left thalamus region and also a positive correlation between right PTA and the WMV in the right putamen. Higher severity of the PTA correlated with worse hearing. Whether the increased volume of white matter in the left thalamus region and right putamen are jointly induced by hearing loss and cognitive decline remains still unclear, and is necessary to be validated through additional animal studies.

The changes in GMV and WMV in left-sided and right-sided acoustic neuromas were not completely consistent. Relatively smaller reorganization regions of brain structure can be induced by the right-sided acoustic neuroma, which is likely linked to the different effect mechanisms of the left-sided and right-sided acoustic neuromas on the body. This conclusion has been repeatedly substantiated by the experimental results in the previous sections. Some scholars believe that the right ear has enhanced resistance to hearing damage with higher stability (37). The left ear shows a stronger contralateral effect in the process of monaural reception of sound stimulation, while the right ear transmits the information evenly to both hemispheres. Once the acoustic neuroma interferes with normal patterns, the dysfunction of the left ear will induce a more pronounced disturbance to and affect the brain. GMV and WMV in patients with acoustic neuroma exhibited lateral changes, which were ipsilateral to the lesion. Thus, the compensatory mechanism of the body after the cognitive decline in patients often occurs on the same side of the lesion. Acoustic neuroma exhibits plasticity in the cognitive representation system, presenting anatomically distinguishable structural reorganizations to compensate for cognitive impairment resulting from impaired auditory input.

Conclusion

Cognitive dysfunction in patients with acoustic neuroma encompasses general cognitive function, executive function, attention, visuospatial executive ability, memory, visual perception ability, motor speed, information processing speed, etc. Changes can be found in the markers ALFF and ReHo in acoustic neuroma patients. Cognitive decline in the patients with acoustic neuroma activates functional activity in some brain regions, thereby compensating for the decline in cognitive function. In the meantime, the reductions in the ReHo values and connectivity of the bilateral superior frontal gyrus and middle frontal gyrus of the patients with lateral acoustic neuroma may affect the functional differentiation and integration of the brain, which is likely related to the cognitive function decline. Brain reorganization induced by UHL in patients with acoustic neuroma exhibits lateralization trends. Left-sided acoustic neuroma induces a more significant influence on the brain, and right-sided acoustic neuroma shows a more stable performance of the cerebral cortex. The cognitive function of patients with acoustic neuroma declines, the body undergoes structural reorganization, and the GMV and WMV values are increased compensatively in the cognitive-related brain regions to compensate for cognitive impairment.

Data availability statement

The raw data supporting the conclusions of this article will be made available by the authors, without undue reservation.

Ethics statement

The studies involving human participants were reviewed and approved by Ethics Committee of Nanchong Central Hospital. The patients/participants provided their written informed consent to participate in this study. Written informed consent was obtained from the individual(s) for the publication of any potentially identifiable images or data included in this article.

Author contributions

XD, LizL, and ZZ designed the study and collected the data. XD, QC, and LihL analyzed the data. XD wrote the paper. ZZ, LihL, and XH drafted the paper. All authors contributed to the article and approved the submitted version.

Funding

This work was supported by Bureau of Science and Technology Nanchong City (Grant Nos. 19SXHZ0273 and 20YFZJ0115), Nanchong Social Science Federation (Grant No. NC21B188), Sichuan Province Medical Youth Innovative Research Project Program (Grant No. Q21029), Primary Health Development Research Center of Sichuan Province (Grant No. SWFZ20-C-069), and Special Funding for Postdoctoral Research Projects of Chongqing (Grant No. 2021XM3012).

Conflict of interest

The authors declare that the research was conducted in the absence of any commercial or financial relationships that could be construed as a potential conflict of interest.

Publisher's note

All claims expressed in this article are solely those of the authors and do not necessarily represent those of their affiliated organizations, or those of the publisher, the editors and the reviewers. Any product that may be evaluated in this article, or claim that may be made by its manufacturer, is not guaranteed or endorsed by the publisher.

Supplementary material

The Supplementary Material for this article can be found online at: https://www.frontiersin.org/articles/10.3389/fpsyt.2022.968859/full#supplementary-material

References

1. Eggermont J. The role of sound in adult and developmental auditory cortical plasticity. *Ear Hear.* (2008) 29:819–29. doi: 10.1097/AUD.0b013e3181853030

2. King A, Moore D. Plasticity of auditory maps in the brain. *Trends Neurosci.* (1991) 14:31–7. doi: 10.1016/0166-2236(91)90181-S

3. Auer E, Bernstein L, Sungkarat W, Singh M. Vibrotactile activation of the auditory cortices in deaf versus hearing adults. *Neuroreport.* (2007) 18:645–8. doi: 10.1097/WNR.0b013e3280d943b9

4. Bavelier D, Neville H. Cross-modal plasticity: where and how? *Nat Rev Neurosci.* (2002) 3:443–52. doi: 10.1038/nrn848

5. Kotak V, Breithaupt A, Sanes D. Developmental hearing loss eliminates long-term potentiation in the auditory cortex. *Proc Natl Acad Sci USA.* (2007) 104:3550–55. doi: 10.1073/pnas.0607177104

6. Kral A, Hartmann R, Tillein J, Heid S, Klinke R. Hearing after congenital deafness: central auditory plasticity and sensory deprivation. *Cereb Cortex.* (2002) 12:797–807. doi: 10.1093/cercor/12.8.797

7. Lee J, Lee D, Oh S, Kim C, Kim J, Hwang C, et al. PET evidence of neuroplasticity in adult auditory cortex of postlingual deafness. *J Nucl Med.* (2003) 44:1435–9

8. Dye M, Baril D, Bavelier D. Which aspects of visual attention are changed by deafness? The case of the Attentional Network Test. *Neuropsychologia.* (2007) 45:1801–11. doi: 10.1016/j.neuropsychologia.2006.12.019

9. Proksch J, Bavelier D. Changes in the spatial distribution of visual attention after early deafness. *J Cogn Neurosci.* (2002) 14:687–701. doi: 10.1162/08989290260138591

10. Husain F, Pajor N, Smith J, Kim H, Rudy S, Zalewski C, et al. Discrimination task reveals differences in neural bases of tinnitus and hearing impairment. *PLoS ONE.* (2011) 6:e26639. doi: 10.1371/journal.pone.0026639

11. Oberg E, Lukomski J. Executive functioning and the impact of a hearing loss: performance-based measures and the Behavior Rating Inventory of Executive Function (BRIEF). *Child Neuropsychol* . (2011) 17:521–45. doi: 10.1080/09297049.2011.555760

12. Figueras B, Edwards L, Langdon D. Executive function and language in deaf children. *J Deaf Stud Deaf Educ.* (2008) 13:362–77. doi: 10.1093/deafed/enm067

13. Kronenberger W, Pisoni D, Henning S, Colson B. Executive functioning skills in long-term users of cochlear implants: a case control study. *J Pediatr Psychol.* (2013) 38:902–14. doi: 10.1093/jpepsy/jst034

14. Dye M, Bavelier D. Attentional enhancements and deficits in deaf populations: an integrative review. *Restor Neurol Neurosci.* (2010) 28:181–92. doi: 10.3233/RNN-2010-0501

15. Vasama J, Mäkelä J. Auditory pathway plasticity in adult humans after unilateral idiopathic sudden sensorineural hearing loss. *Hear Res.* (1995) 87:132–40. doi: 10.1016/0378-5955(95)00086-J

16. Schmithorst V, Holland S, Ret J, Duggins A, Arjmand E, Greinwald J. Cortical reorganization in children with unilateral sensorineural hearing loss. *Neuroreport.* (2005) 16:463–7. doi: 10.1097/00001756-200504040-00009

17. Wu C, Ng S, Wang J, Liu T. Diffusion tensor imaging of the subcortical auditory tract in subjects with congenital cochlear nerve deficiency. *AJNR Am J Neuroradiol.* (2009) 30:1773–7. doi: 10.3174/ajnr.A1681

18. Araújo P, Mondelli M, Lauris J, Richiéri-Costa A, Feniman M. Assessment of the auditory handicap in adults with unilateral hearing loss. *Braz J Otorhinolaryngol.* (2010) 76:378–83. doi: 10.1590/S1808-86942010000300018

19. Salvador K, Pereira T, Moraes T, Cruz M, Feniman M. Auditory processing in unilateral hearing loss: case report. *J Soc Bras Fonoaudiol.* (2011) 23:381–4. doi: 10.1590/S2179-64912011000400015

20. Seeley W, Menon V, Schatzberg A, Keller J, Glover G, Kenna H, et al. Dissociable intrinsic connectivity networks for salience processing and executive control. *J Neurosci.* (2007) 27:2349–56. doi: 10.1523/JNEUROSCI.5587-06.2007

21. Bengoetxea H, Ortuzar N, Bulnes S, Rico-Barrio I, Lafuente J, Argandoña E. Enriched and deprived sensory experience induces structural changes and rewires connectivity during the postnatal development of the brain. *Neural Plast.* (2012) 2012:305693. doi: 10.1155/2012/305693

22. Kral A, Eggermont J. What's to lose and what's to learn: development under auditory deprivation, cochlear implants and limits of cortical plasticity. *Brain Res Rev.* (2007) 56:259–69. doi: 10.1016/j.brainresrev.2007.07.021

23. Suzuki M, Kouzaki H, Nishida Y, Shiino A, Ito R, Kitano H. Cortical representation of hearing restoration in patients with sudden deafness. *Neuroreport.* (2002) 13:1829–32. doi: 10.1097/00001756-200210070-00029

24. Bilecen D, Seifritz E, Radü E, Schmid N, Wetzel S, Probst R, et al. Cortical reorganization after acute unilateral hearing loss traced by fMRI. *Neurology.* (2000) 54:765–7. doi: 10.1212/WNL.54.3.765

25. Zhang GY, Yang M, Liu B, Huang ZC, Chen H, Zhang PP, et al. Changes in the default mode networks of individuals with long-term unilateral sensorineural hearing loss. *Neuroscience.* (2015) 285:333–42. doi: 10.1016/j.neuroscience.2014.11.034

26. Wang X, Xu P, Li P, Wang Z, Zhao F, Gao Z, et al. Alterations in gray matter volume due to unilateral hearing loss. *Sci Rep.* (2016) 6:25811. doi: 10.1038/srep25811

27. Zang Y, He Y, Zhu C, Cao Q, Sui M, Liang M, et al. Altered baseline brain activity in children with ADHD revealed by resting-state functional MRI. *Brain Dev.* (2007) 29:83–91. doi: 10.1016/j.braindev.2006.07.002

28. Zang Y, Jiang T, Lu Y, He Y, Tian L. Regional homogeneity approach to fMRI data analysis. *Neuroimage.* (2004) 22:394–400. doi: 10.1016/j.neuroimage.2003.12.030

29. Newman C, Jacobson G, Spitzer J. Development of the Tinnitus Handicap Inventory. *Arch Otolaryngol Head Neck Surg.* (1996) 122:143–8. doi: 10.1001/archotol.1996.01890140029007

30. Ashburner J. SPM: a history. *Neuroimage.* (2012) 62:791–800. doi: 10.1016/j.neuroimage.2011.10.025

31. Carew P, Mensah F, Rance G, Flynn T, Poulakis Z, Wake M. Mild-moderate congenital hearing loss: secular trends in outcomes across four systems of detection. *Child Care Health Dev.* (2018) 44:71–82. doi: 10.1111/cch.12477

32. Lieu J, Tye-Murray N, Fu Q. Longitudinal study of children with unilateral hearing loss. *Laryngoscope.* (2012) 122:2088–95. doi: 10.1002/lary.23454

33. Fan ZY, Fan Z, Li SC, Shi YJ, Ding D, Zhu, W. The effects of acoustic neuroma on cognitive function. *Chin J Clin Neurosci.* (2020) 28:52–8.

34. Goebel S, Mehdorn H. A missing piece? Neuropsychiatric functioning in untreated patients with tumors within the cerebellopontine angle. *J Neuro Oncol.* (2018) 140:145–53. doi: 10.1007/s11060-018-2944-z

35. Chen, Y.-C., Zhang H, Kong Y, Lv H, Cai Y, et al. Alterations of the default mode network and cognitive impairment in patients with unilateral chronic tinnitus. *Quant Imaging Med Surg.* (2018) 8:1020–9. doi: 10.21037/qims.2018.11.04

36. Raichle M. Two views of brain function. *Trends Cogn Sci.* (2010) 14:180–90. doi: 10.1016/j.tics.2010.01.008

37. Wang X, Fan Y, Zhao F, Wang Z, Ge J, Zhang K, et al. Altered regional and circuit resting-state activity associated with unilateral hearing loss. *PLoS ONE.* (2014) 9:e96126. doi: 10.1371/journal.pone.0096126

38. Grahn J, Parkinson J, Owen A. The role of the basal ganglia in learning and memory: neuropsychological studies. *Behav Brain Res.* (2009) 199:53–60. doi: 10.1016/j.bbr.2008.11.020

39. Drumm DA, Spetzler RF. Neurobehavioral deficits following rupture of anterior communicating artery aneurysms: the AcoA anaurysm syndrome. *BNI.* (1993) 9:2–12.

40. Fan J, Mccandliss B, Fossella J, Flombaum J, Posner M. The activation of attentional networks. *Neuroimage.* (2005) 26:471–9. doi: 10.1016/j.neuroimage.2005.02.004

41. Burton H, Firszt J, Holden T, Agato A, Uchanski R. Activation lateralization in human core, belt, and parabelt auditory fields with unilateral deafness compared to normal hearing. *Brain Res.* (2012) 1454:33–47. doi: 10.1016/j.brainres.2012.02.066

42. Aminoff E, Kveraga K, Bar M. The role of the parahippocampal cortex in cognition. *Trends Cogn Sci.* (2013) 17:379–90. doi: 10.1016/j.tics.2013.06.009

43. Chee M, Weekes B, Lee K, Soon C, Schreiber A, Hoon J, et al. Overlap and dissociation of semantic processing of Chinese characters, English words, and pictures: evidence from fMRI. *Neuroimage.* (2000) 12:392–403. doi: 10.1006/nimg.2000.0631

44. Zhao QL, Xie S, Zhang ZX, Pan H, Li K, Zhang JY, et al. A whole-brain gray and white matter analysis in children with 45XO karyotype Turner syndrome: voxel-based morphometry. *China J Radiol.* (2013) 47:421–5. doi: 10.3760/cma.j.issn.1005-1201.2013.05.008

45. O'sullivan M, Summers P, Jones D, Jarosz J, Williams S, Markus H. Normal-appearing white matter in ischemic leukoaraiosis: a diffusion tensor MRI study. *Neurology.* (2001) 57:2307–10. doi: 10.1212/WNL.57.12.2307

46. Kalashnikova L, Gulevskaia T, Kashina E. [Disorders of higher mental functions in localization of separate infarctions in the optic thalamus and in the region of thalamo-frontal tracts]. *Zhurnal Nevrologii i Psikhiatrii Imeni S.S. Korsakova.* (1998) 98:8–13.

frontiers | Frontiers in Psychiatry

TYPE Original Research
PUBLISHED 03 August 2022
DOI 10.3389/fpsyt.2022.956895

OPEN ACCESS

EDITED BY
Qinji Su,
Guangxi Medical University, China

REVIEWED BY
Xueqin Song,
Zhengzhou University, China
Zhifen Liu,
First Hospital of Shanxi Medical University, China

*CORRESPONDENCE
Huiling Wang
hlwang@whu.edu.cn

SPECIALTY SECTION
This article was submitted to Neuroimaging and Stimulation, a section of the journal Frontiers in Psychiatry

RECEIVED 30 May 2022
ACCEPTED 08 July 2022
PUBLISHED 03 August 2022

CITATION
Chen C, Huang H, Qin X, Zhang L, Rong B, Wang G and Wang H (2022) Reduced inter-hemispheric auditory and memory-related network interactions in patients with schizophrenia experiencing auditory verbal hallucinations.
Front. Psychiatry 13:956895.
doi: 10.3389/fpsyt.2022.956895

Reduced inter-hemispheric auditory and memory-related network interactions in patients with schizophrenia experiencing auditory verbal hallucinations

Cheng Chen[1], Huan Huang[1], Xucong Qin[1], Liang Zhang[1], Bei Rong[1], Gaohua Wang[1,2] and Huiling Wang[1,3]*

[1]Department of Psychiatry, Renmin Hospital of Wuhan University, Wuhan, China, [2]Hubei Institute of Neurology and Psychiatry Research, Wuhan, China, [3]Hubei Provincial Key Laboratory of Developmentally Originated Disease, Wuhan, China

Background: Inter-hemispheric disconnection is a primary pathological finding in schizophrenia. However, given the inherent complexity of this disease and its development, it remains unclear as to whether associated inter-hemispheric changes play an important role in auditory verbal hallucination (AVH) development. As such, this study was developed to explore inter-hemispheric connectivity in the context of schizophrenia with AVH while excluding positive symptoms and other factors with the potential to confound these results.

Method: In total, resting-state functional magnetic resonance imaging (fMRI) was used to assess 42 patients with AVH (APG), 26 without AVH (NPG), and 82 normal control (NC) individuals. Inter-hemispheric connectivity in these subjects was then assessed through the use of voxel-mirrored homotopic connectivity (VMHC) and Pearson correlation analyses.

Result: Relative to HC and NPG subjects, APG individuals exhibited a decrease in VMHC in the superior temporal gyrus (STG) extending into Heschl's gyrus, the insula, and the Rolandic operculum as well as in the fusiform gyrus extending into the para-hippocampus (Corrected $p < 0.005$, cluster size $= 52$). Among APG individuals, these observed impairments of inter-hemispheric connectivity were negatively correlated with Hoffman auditory hallucination scores.

Conclusion: These results support the schizophrenia hemitropic disconnection hypothesis, and provide novel evidence suggesting that there may be a relationship between reductions in inter-hemispheric connectivity in auditory and memory-related networks and the pathogenesis of AVH in patients with schizophrenia following the exclusion of confounding factors from other positive symptoms.

KEYWORDS

schizophrenia, auditory verbal hallucinations, voxel-mirrored homotopic connectivity, auditory-related network, memory-related network

Introduction

Auditory verbal hallucinations (AVHs) are a common symptom in patients diagnosed with schizophrenia, affecting up to 60–70% of these individuals (1). The pathological basis for AVH development has been linked to the hemispheric specialization of functional connectivity within the brain (2–4). As noted previously, relative increases in the contributions of right hemisphere language areas may correspond to the more complex experiential characteristics of AVHs (5), with reductions in language lateralization potentially contributing to the perceived reality of these hallucinatory sounds. Other functional magnetic resonance imaging (fMRI) studies have reported schizophrenia to be associated with decreases in the typical lateralization of language processing in the brain (left > right), with AVH severity being associated with decreased functional lateralization (6, 7). Other studies have further linked the development of schizophrenia to interhemispheric disconnectivity, with the specific localization of such abnormalities in affected patients potentially playing a role in AVH development (8–10). At present, it remains unclear as to whether left-greater-than-right or right-greater-than-left lateralization is most closely associated with AVH development. Differences in interhemispheric connectivity that have previously been observed when comparing patients with and without AVHs may also be confounded by other positive symptoms such as excitement, delusions, or confusion. Given this possibility and inconsistencies among prior studies, there is a clear need to conduct further studies exploring the relationships between changes within and between hemispheres and AVH incidence in individuals with schizophrenia. We supposed that there might be a relationship between reductions in inter-hemispheric connectivity in auditory and memory-related networks and the pathogenesis of AVH in patients with schizophrenia.

The present study was developed to assess interhemispheric connectivity in schizophrenia patients with and without AVHs through the use of a voxel-mirrored homotopic connectivity (VMHC) approach in order to establish the relationship between interhemispheric changes and AVH development. The results of these analyses will serve as the first exploration of the mechanistic basis for AVH incidence in patients with schizophrenia as a function of inter-hemispheric connectivity when analyzed in a manner that minimized the confounding effects of other positive symptoms and related clinical symptoms on associated phenotypes.

Materials and methods

Study participants

In total, 68 individuals diagnosed with schizophrenia were recruited from the inpatients of the Psychiatry department of Renmin Hospital of Wuhan University (Wuhan, China). Diagnoses were confirmed by administering the Structured Clinical Interview for the Diagnostic and Statistical Manual of Mental Disorder (SCID), 4th edition (DSM-IV). These patients were further separated into two groups based on whether they do or do not experience AVHs (42 APG and 26 NPG, respectively). Classification standards were based upon PANSS scores and details pertaining to current and past symptoms obtained through a combination of face-to-face interviews and a review of prior medical records. Patients were included in the APG group if they exhibited a P3 (hallucination) score of > 4 and reported experiencing AVHs a minimum of once per month. APG status was additionally assessed by Professor HL Wang using the Hoffman Auditory Hallucination scale so as to establish the content, frequency, emotional impact, severity, and degree of attention associated with these hallucinations (11). Participants in the NPG group were patients that had not experienced AVH during the course of their illness. In addition, a normal control (NC) group consisting of 82 age-, sex-, and handedness (right-handed)-matched native Chinese speakers were recruited for this study, which received approval from the local research ethics committee. All subjects provided written informed consent to participate following the review of a complete study description. Patient clinical and demographical data are compiled in Table 1.

MRI acquisition

A GEHDXT 3.0T Scanner was used to conduct all MRI scanning at the Radiology Department of Renmin Hospital of Wuhan University. High-resolution 3D T1-weighted structural imaging and resting-state fMRI scanning was performed for all patients. The following parameters were used for high-resolution 3D brain volume sequencing: TR/TE = 2000/30 ms; FOV = 220 mm × 220 mm; matrix = 64 × 64; FA = 90°; slice thickness = 1 mm; no gap in 188 sagittal slices. Resting-state fMRI data were generated with gradient-echo single-shot echo-planar imaging sequence with the following settings: TR/TE = 2000/30 ms; FOV = 220 mm × 220 mm; matrix = 64 × 64; FA = 90°; slice thickness = 4 mm; gap = 0.6 mm; 32 interleaved axial slices; and 240 volumes.

Data preprocessing

MATLAB (MathWorks) was used for the preprocessing of generated data using the Data Processing Assistant for Resting-State fMRI (DPARSF) tool based upon Statistical Parametric Mapping (SPM8) and the Resting-State fMRI Data Analysis Toolkit(REST) (12). To eliminate any aberrant changes in the initial fMRI signal, the first five time points for each patient were omitted from analyses. Images were then corrected for head movement and slice trimming. Participants were only included

TABLE 1 Demographics and clinical characteristics of the participants.

	NC ($n = 82$)	APG ($n = 42$)	NPG ($n = 26$)	*P*
Age	24.67 ± 4.71	24.64 ± 5.24	25.31 ± 5.51	0.836[a]
Gender (M/F)	82 (41/41)	42 (19/23)	42 (16/10)	0.419[b]
Education (year)	14.01 ± 1.84	12.33 ± 2.66	12.23 ± 3.29	0.000[a]
Illness duration (month)		39.24 ± 42.09	51.50 ± 60.33	0.652
Medicine		408.33 ± 220.01	397.12 ± 190.57	0.284
PANSS total		86.05 ± 12.10	84.35 ± 9.98	0.603
PANSS positive score		23.24 ± 3.56	21.70 ± 5.14	0.100
P1 (delusion)		5.02 ± 0.95	5.35 ± 1.16	0.146
P2 (conception confusion)		1.50 ± 0.74	2.15 ± 0.97	0.098
P3 (hallucination)		5.10 ± 0.96	0.92 ± 0.56	0.000*
P4 (excitement)		2.05 ± 1.10	2.54 ± 0.86	0.569
P5 (exaggeration)		2.69 ± 1.24	3.31 ± 1.32	0.601
P6 (skepticism)		5.05 ± 1.06	5.42 ± 1.36	0.131
P7 (hostility)		1.74 ± 1.04	2.04 ± 1.15	0.377
PANSS Negative score		20.45 ± 5.15	20.23 ± 5.87	0.406
PANSS General psychopathology		42.35 ± 7.40	42.43 ± 7.10	0.956
Hoffman score		24.69 ± 2.38	-	-

The data are presented as the means ± standard deviation.
APG, Auditory hallucination patient group; NC, healthy controls; NPG, non-hallucinating patient group.
[a]P values were obtained by one-way analysis of variance tests.
[b]P value for gender distribution in the three groups was obtained by the chi-square test ($P < 0.05$).
*The P values were obtained using two sample t-test ($P < 0.05$).

in these analyses if they exhibited a maximum of 3 mm of displacement in the *x*, *y*, or *z* directions and no more than 3° of angular motion during scanning. The EPI template was then used to normalize functional images (voxel size: 3 × 3 × 3 mm^3)(13), with the resultant normalized images being smoothed using a 3D isotropic Gaussian kernel (FWHM: 6 mm). Low-frequency drifts and high-frequency physiological noise were mitigated with a temporal filter (0.01–0.10 Hz). As recent evidence suggests that the effects of head motion can be more effectively eliminated when using higher-order models (14), mean frame-wise displacement (FD), which measures voxel-wise differences in motion and associated derivations, was assessed as a means of measuring head micromovements for study participants (15, 16). Nuisance regression was conducted through the use of cerebrospinal fluid (CSF), white matter, and global signals as covariates.

Voxel-mirrored homotopic connectivity analyses

VMHC for each patient was measured based on the observed resting-state functional connectivity (rs-FC) among pairs of symmetric inter-hemispheric voxels. Briefly, VMHC maps were generated through Pearson correlation analyses of individual voxels and the mirror voxel in the opposite hemisphere of the brain (17). Measured correlation values were then subjected to Fisher z-transformation to improve associated normality, and group analyses were conducted with the resultant VMHC z-value data.

Statistical analysis

Group comparisons were made by entering VMHC z-value maps into SPM8. Differences among the three participant groups were compared using one-way ANOVAs with groups as the between-subjects factor. Mean FD parameters including age, sex, education, illness duration, age of onset, and Chlorpromazine equivalents were used as covariates for group-level analyses. $P < 0.001$ was the significance threshold for group comparisons, with AlphaSim correction for multiple comparisons. *Post hoc* S-N-K *t*-tests were then used to assess sources of differences among groups in these analyses, with Pearson correlation analyses then being used to examine associations between VMHC results and patient symptoms.

Results

Study subject characteristics

Participants included in this group were age- and sex-matched, although patients in the NC group exhibited higher levels of educational attainment as compared to

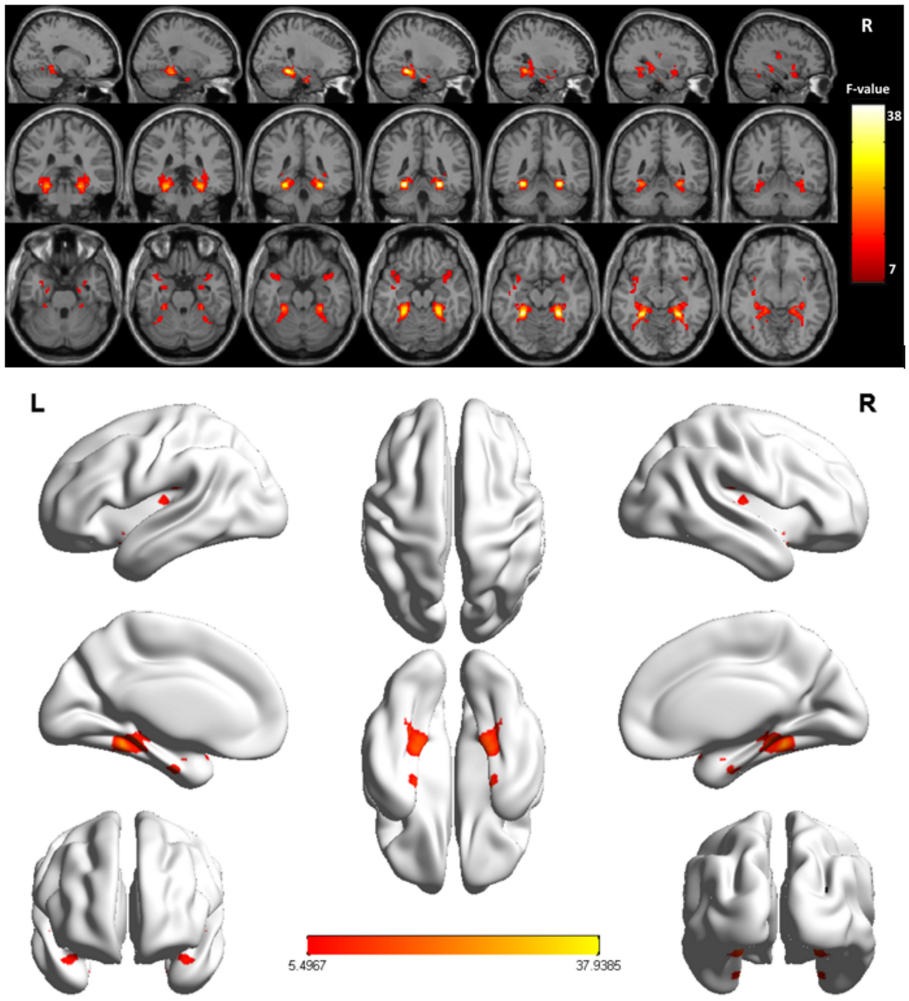

FIGURE 1
Significant differences of the VMHC values were fusiform gyrus extending into parahippocampus (fusiform cluster), STG extending into Heschl's gyrus, insula, and Rolandic operculum (STG cluster) across the three groups (NC, APG and NPG) (Corrected $p < 0.005$, cluster size = 52). Color bar indicates the F score.

TABLE 2 One-way ANOVA comparison on VMHC among three groups.

Cluster location	Peak-MNI (X Y Z)	Voxel number	F
Fusiform cluster	±24 −42 −15	80	37.94
STG cluster	±42 −24 21	68	5.50

patients in the other groups. There were no significant differences between the two schizophrenia patient groups with respect to age, sex, level of education, duration of illness, average antipsychotic drug doses, or PANSS scores, although P3 (hallucination) scores did differ significantly between these groups ($P < 0.01$). The characteristics of all participating study subjects are compiled in Table 1.

Differences in VMHC values among groups

Overall, VMHC values in the superior temporal gyrus (STG) extending into Heschl's gyrus, insula, and Rolandic operculum (collectively referred to as the STG cluster) and the fusiform gyrus extending into the parahippocampus (collectively referred to as the fusiform cluster) differed significantly among these three participant groups (Figure 1 and Table 2). *Post hoc t*-tests indicated that relative to individuals in the NC and NPG groups, patients in the APG group exhibited lower VMHC values in the fusiform cluster whereas no significant differences in this cluster were evident when comparing the NC and NPG groups. Additionally, reductions in STG cluster VMHC values were observed in both NPG and APG patients relative to NC individuals, although these changes were more pronounced for APG patients (Table 3).

TABLE 3 *Post hoc* pairwise comparisons of the mean VMHC z-score in three groups (*$p < 0.05$).

Cluster location	NC	APG	NPG	F	*Post-hoc t*-test
Fusiform cluster	0.80 ± 0.18	0.57 ± 0.16	0.83 ± 0.12	37.94	NC /NPG > APG
STG cluster	0.87 ± 0.17	0.63 ± 0.17	0.73 ± 0.18	5.50	NC>NPG>APG

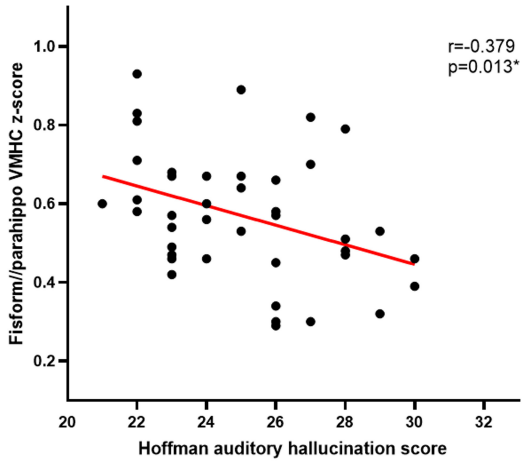

FIGURE 2
The Hoffman score was negatively correlated with the VMHC in the fusiform cluster in APG ($p < 0.05$).

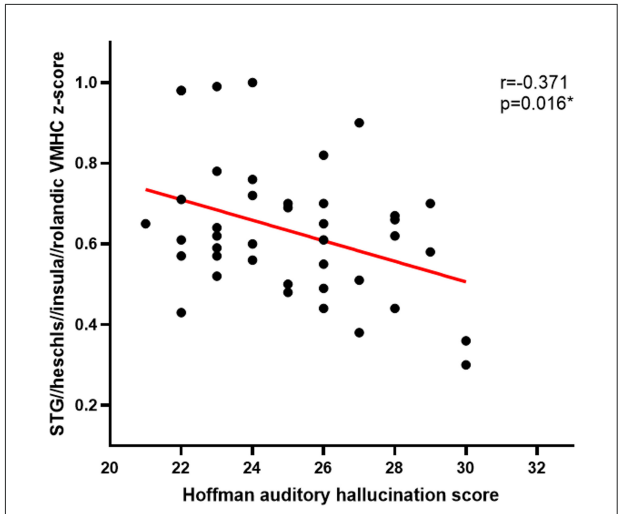

FIGURE 3
The Hoffman score was negatively correlated with the VMHC in the STG cluster in APG ($p < 0.05$).

Correlations between VMHC results and patient symptoms

Pearson correlation analyses revealed Hoffman scores and VMHC values were negatively correlated with one another in the fusiform cluster ($r = -0.379$, $P = 0.013$) (Figure 2) and the STG cluster ($r = -0.371$, $P = 0.016$) (Figure 3) among APG patients ($P < 0.05$).

Discussion

The results of this study, which suggest that schizophrenia patients that experience AVHs exhibit significant changes in interhemispheric connectivity, offer robust neuroimaging support for the relationship between homotopic dysconnectivity and the occurrence of such hallucinations in schizophrenia (18). In contrast to prior studies, the present analysis was conducted after fully taking participant characteristics into consideration based on the assumption that other PANSS positive score items other than AVHs, such as delusions and suspicion, may have confounded the true relationship between AVH incidence and abnormal. As such, the comparable PANSS total score, PANSS negative score, PANSS positive score (with the exception of P3), and PANSS general psychopathology results in the APG and NPG groups in the present analysis effectively mitigated the potential confounding effects of these variables. Even after controlling for these factors, greater abnormal homotopic connectivity was still observed in schizophrenia patients affected by AVHs relative to patients not affected by these hallucinations.

The fusiform gyrus plays important roles in visual and sensory processing. When individuals experience abnormal sensory processing and aberrant voice recognition, this may lead to the false identification of one's own voice as emanating from an external source, contributing to the perception of AVHs (19). The observed aberrant homotopic connectivity of the fusiform gyrus in patients with AVHs in the present study cohort supported this conclusion. Notably, this abnormal homotopic connectivity of the fusiform cluster extended to the para-hippocampal gyrus in those patients that experienced AVHs. In a study conducted by Xiao et al., all analyzed schizophrenia patients similarly exhibited para-hippocampus abnormalities (18), in contrast to the results of the present study in which abnormalities in the para-hippocampus were only evident in AVH patients. VMHC values for this region of the brain were significantly negatively correlated with Hoffman scores, although more research will be necessary to explain this finding. The parahippocampus is an important component of the limbic system, which regulates memory storage and retrieval (20). Schizophrenia patients primarily report AVHs as consisting of critical speech hallucinations, and often report similar comments in their previous memories. Abnormal activity and connectivity of the parahippocampal gyrus may result in incorrect perceptions pertaining to the storage and

extraction of information (8, 21). AVHs may thus develop as a consequence of the abnormal processing and retrieval of certain memories, as supported by a prior study in which patients experiencing hallucinations exhibited greater difficulty in determining the sources of memories (22).

With respect to the STG cluster, several studies have demonstrated that the role of the temporal lobe in voice recognition is inextricably linked to auditory hallucinations (23, 24). The more pronounced reduction in VMHC values in the STG and Heschl's gyrus in schizophrenia patients affected by AVHs further suggested that these regions are linked to the development of these hallucinations. Decreases in VMHC values in the STG and Heschl's gyrus would contribute to the dysfunctional cognition underlying AVHs through the incorrect identification of one's own voice as emanating from an external source. The Rolandic operculum is located in the frontal lobe and has repeatedly been shown to be closely linked to the mechanisms underlying psellism (7). One prior theoretical analysis of individuals with high schizotypy revealed alterations in both global properties and a reduction in the density of the gray matter in the Rolandic operculum in these patients (25). The Rolandic operculum also plays a role in the processing of auditory feedback, which may be linked to the processing of auditory feedback underlying AVH development (26). The insula is a multimodal convergence zone that plays a role in emotional regulation, contributing to the development of chronic positive symptoms together with the amygdala (27). One meta-analysis of functional data revealed a close relationship between AVHs in schizophrenia patients and the hippocampus, auditory cortex, and hippocampus (28). Consistently, structural and functional abnormalities may be suggestive of a central role for the insula in the production of AVHs (29).

Conclusion

In conclusion, these results offer evidence in support of the homotopic disconnection hypothesis of schizophrenia, and are the first to suggest a potential role for reduced interhemispheric connectivity of the auditory and memory-related brain networks in the pathogenesis of AVHs following the exclusion of the effects of other confounding clinical symptoms on these results. In future analyses, additional participants will be recruited to conduct longitudinal analyses in which additional confounding factors will be excluded to minimize any potential bias.

Data availability statement

The raw data supporting the conclusions of this article will be made available by the authors, without undue reservation.

Ethics statement

The studies involving human participants were reviewed and approved by Renmin Hospital of Wuhan University. The patients/participants provided their written informed consent to participate in this study.

Author contributions

CC, HW, and HH developed the initial idea for the manuscript. CC wrote the main body of the paper and including citations. HW and GW contributed to revision and editing of the manuscript. BR, LZ, and XQ analyzed the data. All authors contributed to approved the final manuscript.

Funding

This research was supported by supported by the Fundamental Research Funds for the Central Universities (2042022kf1108) and the Medical Science Advancement Program of Wuhan University (TFLC2018001).

Acknowledgments

The authors would like to thank all the participants and staff involved in this study.

Conflict of interest

The authors declare that the research was conducted in the absence of any commercial or financial relationships that could be construed as a potential conflict of interest.

Publisher's note

Supplementary material

The Supplementary Material for this article can be found online at: https://www.frontiersin.org/articles/10.3389/fpsyt.2022.956895/full#supplementary-material

References

1. Bauer SM, Schanda H, Karakula H, Olajossy-Hilkesberger L, Rudaleviciene P, Okribelashvili N, et al. Culture and the prevalence of hallucinations in schizophrenia. *Compr.Psychiatry.* (2011) 52:319–25. doi: 10.1016/j.comppsych.2010.06.008

2. Kantrowitz JT, Sehatpour P, Avissar M, Horga G, Gwak A, Hoptman MJ, et al. Significant improvement in treatment resistant auditory verbal hallucinations after 5 days of double-blind, randomized, sham controlled, fronto-temporal, transcranial direct current stimulation (tDCS): a replication/extension study. *Brain Stimul.* (2019) 12:981–91. doi: 10.1016/j.brs.2019.03.003

3. Bohlken MM, Hugdahl K, Sommer IE. Auditory verbal hallucinations: neuroimaging and treatment. *Psychol Med.* (2017) 47:199–208. doi: 10.1017/S003329171600115X

4. Kubera KM, Rashidi M, Schmitgen MM, Barth A, Hirjak D, Sambataro F. et al. Structure/function interrelationships in patients with schizophrenia who have persistent auditory verbal hallucinations:a multimodal MRI study using parallel ICA. *Prog Neuropsychopharmacol Biol Psychiatry.* (2019) 93:114–21. doi: 10.1016/j.pnpbp.2019.03.007

5. Ercammen A, Knegtering H, Bruggeman R, Aleman A. Subjective loudness and reality of auditory verbal hallucinations and activation of the inner speech processing network. *Schizophrenia Bulletin.* (2011) 37:1009–16. doi: 10.1093/schbul/sbq007

6. Razafimandimby A, Maiza O, Herve PY, Lecardeur L, Delamillieure P, Brazo P, et al. Stability of functional language lateralization overtime in schizophrenia patients. *Schizophr Res.* (2007) 94:197–206. doi: 10.1016/j.schres.2007.04.011

7. Steinmann S, Leicht G, Mulert C. The interhemispheric miscommunication theory of auditory verbal hallucinations in schizophrenia. *Int J Psychophysiol.* (2019) 145:83–90. doi: 10.1016/j.ijpsycho.2019.02.002

8. Curčić-Blake B, Ford JM, Hubl D, Orlov ND, Sommer IE, Waters F, et al. Interaction of language, auditory and memory brain networks in auditory verbal hallucinations. *Prog Neurobiol.* (2017) 148:1–20. doi: 10.1016/j.pneurobio.2016.11.002

9. Huang J, Zhuo C, Xu Y, Lin X. Auditory verbal hallucination and the auditory network: from molecules to connectivity. *Neuroscience.* (2019) 410:59–67. doi: 10.1016/j.neuroscience.2019.04.051

10. Tang P, Guo F, Xi YB, Peng L, Cui LB, Wang H, et al. Distinct hemispheric specialization of functional connectivity in schizophrenia with and without auditory verbal hallucinations. *Neuroreport.* (2019) 30:1294–8.

11. Chang CC, Tzeng NS, Chao CY, Yeh CB, Chang HA. The effects of add-on fronto-temporal transcranial direct current stimulation (tDCS) on auditory verbal hallucinations, other psychopathological symptoms, and insight in schizophrenia: a randomized, double-blind,sham-controlled trial. *Int J Neuropsychopharmacol.* (2018) 21:979–87. doi: 10.1093/ijnp/pyy074

12. Dong ZY, Long XY. Li SF, Zuo XN, Zhu CZ, et al. REST: a toolkit for resting-state functional magnetic resonance imaging data processing. *Plos ONE.* (2011) 6:e25031. doi: 10.1371/journal.pone.0025031

13. John Ashburner. A fast diffeomorphic image registration algorithm. *Neuroimage.* (2007) 38:95–113. doi: 10.1016/j.neuroimage.2007.07.007

14. Yan CG, Craddock RC, Zuo XN, Zang YF, Milham MP. Standardizing the intrinsic brain: towards robust measurement of inter-individual variation in1000 functional connectomes. *Neuroimage.* (2013) 80:246–62. doi: 10.1016/j.neuroimage.2013.04.081

15. Yan CG, Cheung B, Kelly C, Colcombe S, Craddock RC, Di Martino A, et al. A comprehensive assessment of regional variation in the impact of head micromovements on functional connectomics. *Neuroimage.* (2013) 1:183–201. doi: 10.1016/j.neuroimage.2013.03.004

16. Siegel JS, Mitra A, Laumann TO, Seitzman BA, Raichle M, Corbetta M, et al. Data Quality Influences Observed Links Between Functional Connectivity and Behavior. *Cereb Cortex.* (2017) 27:4492–502. doi: 10.1093/cercor/bhw253

17. Zuo XN, Kelly C, Di Martino A, Mennes M, Margulies DS, Bangaru S, et al. Growing together and growing apart: regional and sex differences in the lifespan developmental trajectories of functional homotopy. *J Neurosci.* (2010) 30:15034–43. doi: 10.1523/JNEUROSCI.2612-10.2010

18. Chang X, Xi YB, Cui LB, Wang HN, Sun JB, Zhu YQ, et al. Distinct inter-hemispheric dysconnectivity in schizophrenia patients with and without auditory verbal hallucinations. *Sci Rep.* (2015) 5:11218. doi: 10.1038/srep11218

19. Jing RX Li S, Zhang XJ, Long J, Zhou TH, Zhuo CJ. Aberrant functional connectivity patterns of default mode network may play a key role in the interaction between auditory verbal hallucinations and insight. *Chin Med J.* (2018) 131:736–8. doi: 10.4103/0366-6999.226905

20. Christopher L, Duff-Canning S, Koshimori Y, Segura B, Boileau I, Chen R, et al. Salience network and parahippocampal dopamine dysfunction in memory-impaired Parkinson disease. *Ann Neurol.* (2015) 77:269–80. doi: 10.1002/ana.24323

21. Mallikarjun PK, Lalousis PA, Dunne TF, Heinze K, Reniers RL, Broome MR, et al. Aberrant salience network functional connectivity in auditory verbal hallucinations: a first episode psychosis sample. *Transl Psychiatry.* (2018) 8:69. doi: 10.1038/s41398-018-0118-6

22. Zhuo C, Jiang D, Liu C, Lin X, Li J, Chen G, et al. Understanding auditory verbal hallucinations in healthy individuals and individuals with psychiatric disorders. *Psychiatry Res.* (2019) 274:213–9. doi: 10.1016/j.psychres.2019.02.040

23. Ben AD, Kelly D, Charles F. Judith M F, Guillermo H, Daniel S, et al. Auditory hallucinations and the brain's resting-state networks: findings and methodological observations. *Schizophr Bull.* (2016) 42:1110–23. doi: 10.1093/schbul/sbw078

24. Chen C, Wang GH, Wu SH, Zou JL, Zhou Y, Wang HL. Abnormal local activity and functional dysconnectivity in patients with schizophrenia having auditory verbal hallucinations. *Curr Med Sci.* (2020) 40:979–84. doi: 10.1007/s11596-020-2271-4

25. Wang Y, Yan C, Yin DZ, Fan MX, Cheung EF, Pantelis C, et al. Neurobiological changes of schizotypy: evidence from both volume-based morphometric analysis and resting-state functional connectivity. *Schizophr Bull.* (2015) 41:S444–54. doi: 10.1093/schbul/sbu178

26. Behroozmand R, Shebek R, Hansen DR, Oya H, Robin DA, Howard MA. 3rd, et al. Sensory–motor networks involved in speech production and motor control: An fMRI study. *NeuroImage.* (2015) 109:418–28. doi: 10.1016/j.neuroimage.2015.01.040

27. Nagai M, Kishi K, Kato S. Insular cortex and neuropsychiatric disorders: a review of recent literature. *Eur Psychiatry.* (2007) 22:387–94. doi: 10.1016/j.eurpsy.2007.02.006

28. Jardri R, Pouchet A, Pins D, Thomas P. Cortical activations during auditory verbal hallucinations in schizophrenia: a coordinate-based meta-analysis. *Am J Psychiatry.* (2011) 168:73–81. doi: 10.1176/appi.ajp.2010.09101522

29. Zweerings J, Hummel B, Keller M, Zvyagintsev M, Schneider F, Klasen M, et al. Neurofeedback of core language network nodes modulates connectivity with the default-mode network: a doubleblind fMRI neurofeedback study on auditory verbal hallucinations. *Neuroimage.* (2019) 189:533–42. doi: 10.1016/j.neuroimage.2019.01.058

frontiers | Frontiers in Psychiatry

TYPE Original Research
PUBLISHED 10 August 2022
DOI 10.3389/fpsyt.2022.972939

OPEN ACCESS

EDITED BY
Liang Liang,
Xinjiang Medical University, China

REVIEWED BY
Xiaobing Jiang,
Huazhong University of Science and Technology, China
Yunhua Zhang,
Hubei Provincial Hospital of Traditional Chinese Medicine, China

*CORRESPONDENCE
Jun Li
lj690222@sina.com
Sheng Zhang
42701213@qq.com
Hongwei Ren
14214949@qq.com

†These authors share first authorship

SPECIALTY SECTION
This article was submitted to Neuroimaging and Stimulation, a section of the journal Frontiers in Psychiatry

RECEIVED 19 June 2022
ACCEPTED 08 July 2022
PUBLISHED 10 August 2022

CITATION
Wu J, Wu J, Guo R, Chu L, Li J, Zhang S and Ren H (2022) The decreased connectivity in middle temporal gyrus can be used as a potential neuroimaging biomarker for left temporal lobe epilepsy. *Front. Psychiatry* 13:972939. doi: 10.3389/fpsyt.2022.972939

The decreased connectivity in middle temporal gyrus can be used as a potential neuroimaging biomarker for left temporal lobe epilepsy

Jinlong Wu[1,2†], Jun Wu[3†], Ruimin Guo[1], Linkang Chu[1], Jun Li[3*], Sheng Zhang[4*] and Hongwei Ren[1*]

[1]Department of Imaging Center, Tianyou Hospital Affiliated to Wuhan University of Science and Technology, Wuhan, China, [2]Key Laboratory of Occupational Hazards and Identification, Wuhan University of Science and Technology, Wuhan, China, [3]Department of Neurosurgery, The Central Hospital of Wuhan, Tongji Medical College, Huazhong University of Science and Technology, Wuhan, China, [4]Liyuan Hospital of Tongji Medical College, Huazhong University of Science and Technology, Wuhan, China

Objective: We aimed to explore voxel-mirrored homotopic connectivity (VMHC) abnormalities between the two brain hemispheres in left temporal lobe epilepsy (lTLE) patients and to determine whether these alterations could be leveraged to guide lTLE diagnosis.

Materials and methods: Fifty-eight lTLE patients and sixty healthy controls (HCs) matched in age, sex, and education level were recruited to receive resting state functional magnetic resonance imaging (rs-fMRI) scan. Then VHMC analyses of bilateral brain regions were conducted based on the results of these rs-fMRI scans. The resultant imaging data were further analyzed using support vector machine (SVM) methods.

Results: Compared to HCs, patients with lTLE exhibited decreased VMHC values in the bilateral middle temporal gyrus (MTG) and middle cingulum gyrus (MCG), while no brain regions in these patients exhibited increased VMHC values. SVM analyses revealed the diagnostic accuracy of reduced bilateral MTG VMHC values to be 75.42% (89/118) when differentiating between lTLE patients and HCs, with respective sensitivity and specificity values of 74.14% (43/58) and 76.67% (46/60).

Conclusion: Patients with lTLE exhibit abnormal VMHC values corresponding to the impairment of functional coordination between homotopic regions of the brain. These altered MTG VMHC values may also offer value as a robust neuroimaging biomarker that can guide lTLE patient diagnosis.

KEYWORDS

left temporal lobe epilepsy, voxel-mirrored homotopic connectivity, rs-fMRI, support vector machine, neuroimaging biomarker

Introduction

Epilepsy is a common neurological disorder that causes affected patients to experience altered brain activity and recurrent seizures (1). An estimated 50 million individuals worldwide are thought to suffer from epilepsy, experiencing a range of psychiatric and psychosocial comorbidities in addition to the physical challenges and seizures that are inherent to this disease state (2, 3). TLE is among the most prevalent subtypes of partial epilepsy. While some left temporal lobe epilepsy (lTLE) patients can attain significant from antiepileptic drug (AED) treatment, others fail to achieve remission (4, 5). Findings in lTLE patients often include impaired speech activity that may coincide with damage to the left hippocampus, lateral white matter, and lateral temporal cortex regions of the brain (6, 7). Recent work suggests that rather than merely arising as a consequence of localized neurological abnormalities, epilepsy may represent a form of network disorder (8). Accordingly, the majority of patients with lTLE experience varying types of cognitive dysfunction including altered attention, consciousness, memory, or behavior after experiencing recurrent seizures (8, 9). Efforts to diagnose lTLE and other forms of epilepsy are currently based on a combination of medical history and electroencephalogram (EEG) analyses (10). While EEG can be highly effective in this setting, only roughly half of epileptic discharges can be successfully recorded in affected patients, and healthy individuals may also exhibit false-positive results in this setting (11). As epileptic seizures can occur suddenly and are transient in nature, this can further complicate diagnostic efforts. As such, there is a clear need for the establishment of reliable, accurate, and specific approaches to diagnosing lTLE in order to guide patient care efforts.

The development of novel neuroimaging platforms holds great promise as a means of diagnosing lTLE and other neurological diseases. For example, resting state functional magnetic resonance imaging (rs-fMRI) is a non-invasive blood oxygen level-dependent neuroimaging strategy that can be used to directly visualize and assess functional connections among regions of the brain in a quantitative manner, allowing for the interrogation of neural network connections between the hemispheres of the brain (12). Several rs-fMRI studies to date have shown that TLE patients exhibit specific changes in brain network functionality, particularly in the default mode network (DMN), suggesting that these individuals may be at an elevated risk of experiencing cognitive decline (13, 14). Abnormal functional connectivity is thus likely to underlie declines in cognitive function and performance in individuals diagnosed with TLE, with several studies having explored this topic. Recently, voxel-mirrored homotopic connectivity (VMHC) was proposed as a conceptual approach to characterizing the synchronicity of spontaneous functional activity between geometrically consistent mirrored regions in the two cerebral hemispheres (15). VMHC values can be used to gain quantitative insight regarding functional connections based on time series correlations between mirrored voxels on either side of the brain. Abnormal VMHC values have been observed in the context of diseases including depression (16), schizophrenia (17), congenital amusia (18), diabetes mellitus (19), hyperthyroidism (20), and Parkinson's disease (21). As such, measuring VMHC represents a sensitive strategy that can be leveraged to evaluate altered interhemispheric coordination in physiological and pathological contexts. To date, however, VMHC-based studies of lTLE patients have been limited. In one report, Yang et al. (22) determined that individuals diagnosed with idiopathic generalized epilepsy and generalized tonic-clonic seizures exhibited significant increases in VMHC values in the bilateral medial anterior curvature and anterior cingulate gyrus, while negative correlations were observed between illness duration and VMHC values in the bilateral cerebellum, thalamus, and orbital frontal cortex in these patients. In light of these prior observations, the present study was developed based on the hypothesis that lTLE patients may exhibit abnormal VMHC in the DMN, and that these altered VMHC values may be correlated with the course of TLE symptoms such that studying VMHC in these patients may offer insight into the pathophysiology of cognitive dysfunction in this patient population.

Artificial intelligence-based strategies have been used with increasing frequency in the context of diagnostic neuroimaging, with computer-aided SVM approaches being a subject of growing interest in this field that can aid in automating the diagnostic processing and identifying lesions. Owing to their high-resolution, rapidity, and non-invasive nature, neuroimaging techniques are commonly used to guide the diagnosis and evaluation of epilepsy patients. For example, abnormal degree centrality as a potential imaging biomarker for right temporal lobe epilepsy (10); decreased network homogeneity values in the right posterior cingulate cortex (PCC)/precuneus may be a potential neuroimaging marker for obsessive–compulsive disorder (23), and abnormal fractional amplitude of low-frequency fluctuation as a potential imaging biomarker for first-episode major depressive disorder (24).

Support vector machine (SVM) techniques enable the automated recognition of patterns within particular datasets (24), making them ideally suited to analyses of high-dimensional data types in which the number of potential features is greater than the number of samples available is common in the context of fMRI imaging. SVM approaches can identify an optimal separating hyperplane in high-dimensional space, with the closest instance of this hyperplane being referred to as a support vector. For fMRI analyses, SVM scales are overlaid onto the original functional space, with important scales then being plotted in different brain regions (25). Prior work has demonstrated the benefits of leveraging SVM techniques to transform high-dimensional neuroimaging data into information that can guide clinical decision-making (26), with SVM approaches having successfully used to

differentiate between control individuals and persons diagnosed with major depressive disorder (27), schizophrenia (28), and bipolar disorder (29). No studies to date, however, have employed an SVM analytical approach to assess whether altered VMHC values can be used to differentiate between lTLE patients and controls.

Here, a combination of VMHC values and an SVM approach was utilized to assess resting-state functional connectivity between the two hemispheres of the brain and to examine how this relationship is linked to lTLE patient clinical characteristics. The overall goal of this approach was to establish the ability of altered VMHC values to facilitate the neuroimaging-based diagnosis of lTLE patients.

Experimental procedures

Participants

In total, 58 lTLE patients that had been diagnosed as per the criteria established by the International League Against Epilepsy (2017) were recruited for the present study from Tianyou Hospital affiliated with Wuhan University of Science and Technology. In parallel, 60 age-, sex-, and education level-matched healthy control (HC) participants were recruited. All lTLE patients met a minimum of two of the following criteria (30): a history of seizure-related symptoms consistent with the location of epileptic foci within the left temporal lobe; MRI or CT showed hippocampal sclerosis, atrophy, or temporal lobe lesions in the left temporal lobe, and interictal electroencephalographic traces revealing the presence of epileptic foci within the left temporal lobe. The exclusion criteria were as follows: age <14 years or age >60 years; patients who had a history of drug abuse or take drugs that could impair cognition, such as cannabis users and others; history of mental illness or systemic disease. exhibited a Mini-Mental State Examination (MMSE) score <24, presented with MRI findings consistent with the presence of other structural lesions in the brain such as tumors or vascular malformations, had suffered a traumatic brain injury, and exhibited contraindications that precluded MRI scanning. All participants provided written informed consent to participate. The Medical Ethics Committee of Tianyou Hospital affiliated with Wuhan University of Science and Technology approved this study, which was consistent with the Helsinki Declaration.

Receive resting state functional magnetic resonance imaging

An Ingenia 3.0 T scanner (Philips, Amsterdam, Netherlands) equipped with a standard head coil was used to perform rs-fMRI scanning for all study participants. Scanning was conducted while participants remained still while lying down with their heads fixed in place with a belt. Foam padding and earplugs were used to mitigate scanner-related noise and head movements. Participants were directed to remain awake and not think about anything specific. rs-fMRI scans were performed with the following settings: repetition time = 2,000 ms, echo time = 25 ms, 36 axial slices, slice thickness = 3 mm, gap = 1 mm, 90° flip angle, field of view = 220 mm × 220 mm. The duration of rs-fMRI scanning for each participant was 8 min, with 240 volumes being obtained per participant.

Data pre-processing

The MATLAB Data Processing Assistant for rs-fMRI (DPARSF) application was used to pre-process rs-fMRI data (31). The initial five time points for each participant were excluded from the analysis to mitigate the effects of initial signal instability and ambient scanner noise on the resultant data. Slice trimming was then conducted, after which the images were realigned to correct for any head movement. Participants were excluded from analysis if they exhibited >2 mm maximal displacement along the x, y, or z axes or $>2°$ of maximal rotation. Data were then subjected to spatial registration in the standard Montreal Neurological Institute (MNI) space followed by resampling at 3 mm × 3 mm × 3 mm. The resultant images were then smoothed using a Gaussian kernel, linearly detrended, and subjected to bandpass filtering (0.01–0.08 Hz). Covariates such as head movement parameters, average whole-brain signals, white-matter signal, and signal derived from a defined ventricular region of interest were removed. Global signal was retained throughout rs-fMRI connectivity data processing.

Voxel-mirrored homotopic connectivity analyses

The RSET toolkit[1] was used to conduct VMHC analyses. Prior to these analyses, images were standardized to a symmetrical spatial template as follows: an average image for all participants was generated by averaging all normalized gray matter images; the established mean image was averaged with its bilateral mirror version to produce a symmetrical template mask to facilitate VMHC statistical analyses; and individual gray matter images were registered to this template, followed by non-linear transformation to yield functional images. Images were then smoothed using a 6 mm full-width at half-maximum isotropic Gaussian kernel. The time-series data

1 http://www.restfmri.net/forum/

for each voxel in the cerebral hemisphere were then extracted for each participant group following pretreatment and registration to the standard Montreal (MNI) space, after which Pearson correlation coefficients were calculated between individual voxels in symmetrical positions on either side of the brain to generate VMHC values. The resultant data were then converted *via* Fisher Z-transformation into a *Z*-value graph to facilitate subsequent statistical comparisons between groups. VMHC statistical analyses were performed using cerebral hemispheres in the symmetric template generated above. A previous study has described the details of VMHC acquisition (32).

Statistical analyses

SPSS 22.0 was used to analyze all data. Results were reported as x ± s. Demographic and clinical data were compared between lTLE patients and HCs using independent sample *t*-tests, whereas gender ratios were compared between groups using chi-square tests. Whole-brain VMHC profiles for these two groups were subjected to voxel-based analyses of covariance to examine between-group differences, with results being Gaussian Random Field corrected at a threshold of $P < 0.01$.(voxel significance: $P < 0.001$; cluster significance: $P < 0.01$).

Correlation analyses

Mean VMHC values from identified abnormal brain regions were extracted, and Pearson's correlation analyses were employed to assess the relationship between these values and clinical parameters of interest.

Classification analyses

The MATLAB LIBSVM package was used to implement an SVM analysis. The LIBSVM classifier was trained using providing examples of the form, where x represents the VMHC values of these abnormal clusters, and c is the class label (c = + 1 represent patients with lTLE while $c = -1$ for HCs). In order to evaluate the classification performance of unobserved data, the sample set of SVM was divided into training set and test set. We perform classification and feature selection by constructing random SVM cluster based on subjects' brain fMRI data. The grid search method and default functional kernels of Gaussian radial basis were applied to optimize the parameters with the "leave-one-subject-out" method to acquire the optimal sensitivity and specificity. VMHC values extracted from the bilateral middle cingulum gyrus (MCG) and middle temporal gyrus (MTG) were assessed for their ability to differentiate between lTLE patients and HC individuals using this approach based the method.

Results

In total, 58 patients with lTLE and 60 HCs were recruited for the present study. The clinical and demographic characteristics of these study participants are reported in Table 1. No significant differences in age, sex, disease course, or years of education were observed when comparing these groups.

Voxel-mirrored homotopic connectivity differences between groups

Significant reductions in VMHC values were observed in the bilateral MCG and MTG when comparing patients with lTLE to HC individuals (Figure 1 and Table 2). No analyzed brain regions exhibited increased VMHC values in individuals diagnosed with lTLE.

Support vector machine results

An SVM approach was next separately used to analyze the observed VMHC reductions in the bilateral MCG and MTG in lTLE patients, revealing that the lower VMHC values in the MTG were associated with higher diagnostic accuracy (75.42%, 89/118) when differentiating between lTLE patients and HC individuals, with respective sensitivity and specificity values of 74.14% (43/58) and 76.67% (46/60) (Figure 2).

Correlations between voxel-mirrored homotopic connectivity values and clinical parameters

Lastly, mean VMHC values were obtained for the bilateral MCG and MTG regions, with Pearson's correlation analyses then being used to examine the relationship between these values and clinical parameters including age at seizure onset and disease duration. However, no significant correlations

TABLE 1 The *p*-value for gender distribution was obtained by the chi-square test.

Characteristics	Patients ($n = 58$)	HCs ($n = 60$)	*P*-value
Gender (male/female)	58 (37/21)	60 (31/29)	0.183
Age, years	28.97 ± 8.19	26.54 ± 4.96	0.052
Years of education, years	11.76 ± 1.90	12.67 ± 2.33	0.023
illness duration, years	5.76 ± 5.01		

The *p*-values were obtained by two sample *t*-tests.
HCs, healthy controls.
Compared with HCs, $P < 0.01$.

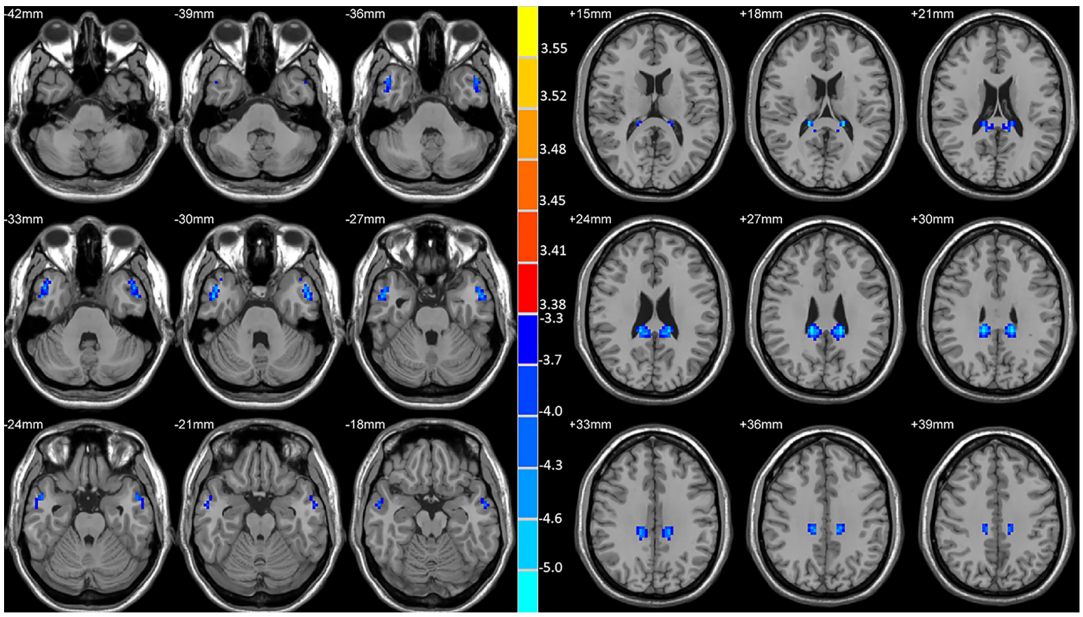

FIGURE 1
Statistical maps showing VMHC differences between the subject groups. Blue denotes lower VMHC, red denotes higher VMHC, and the color bar indicates the *T*-values from two-sample *t*-tests.

TABLE 2 Regions showing significant differences in VMHC between lTLE patients and HCs.

Cluster location	Peak (MNI)			Number of voxels	T-value
	X	Y	Z		
MTG	±51	0	−30	82	−4.9412
MCG	±15	−36	37	112	−5.3268

MNI, Montreal neurological institute; X, Y, Z, coordinate of primary peak locations in the MNI space. MTG, middle cingulum gyrus; MCG, middle cingulum gyrus.

between VMHC values and these variables were detected in this patient cohort.

Discussion

Here, rs-fMRI data were used to compare differences in interhemispheric VMHC values between lTLE patients and HC individuals. Relative to these controls, lTLE patients exhibited reduced VMHC values in the bilateral MTG and bilateral MCG. This is the first report to our knowledge to have employed an SVM approach to gauge the diagnostic utility of VMHC abnormalities in the bilateral MTG and MCG as an lTLE-related neuroimaging biomarker. This strategy ultimately revealed that reduced bilateral MTG VMHC values may offer significant value as a sensitive and specific biomarker capable of distinguishing between lTLE patients and HCs.

Prior work has shown that lTLE patients exhibit reduced VMHC values in the MTG, bilateral medial superior frontal gyrus, bilateral inferior parietal lobule, and supplementary motor area (33). Zhao et al. (34) observed significant reductions in the bilateral MTG connectivity in lTLE patients, in line with the VMHC results from the present study. The inferior temporal gyrus (ITG) and superior temporal gyrus (STG) are, respectively, located on the dorsal and ventral sides of the MTG. While once considered a structurally homogenous brain region (35), recent work has shown the MTG to play diverse roles in the context of social cognition, logical reasoning, memory, auditory processing, language, and emotion (9). One meta-analysis reported the MTG to be associated with the DMN and the semantic memory network (36). MTG impairment has been found to be associated with many different psychiatric and neurological disorders including autism spectrum disorder (37), major depressive disorder (38), bipolar disorder (39), TLE (40), and obsessive compulsive disorder (41). The MTG has also been identified as a promising target for surgical intervention in TLE patients *via* the *trans*-MTG approach (42). The MTG can be subdivided based on patterns of anatomical connectivity into the aMTG, mMTG, pMTG, and sMTG subregions. Of these, the aMTG is primarily connected to DMN-associated regions of the brain, indicating that it may be a critical component of the DMN (43). In contrast, the mMTG plays an essential role in the context of semantic memory (44), while the pMTG facilitates language processing, particularly in the context of repetition and reading (45), and the sMTG is linked to speech comprehension (46). Reductions in VMHC between the bilateral MTG has

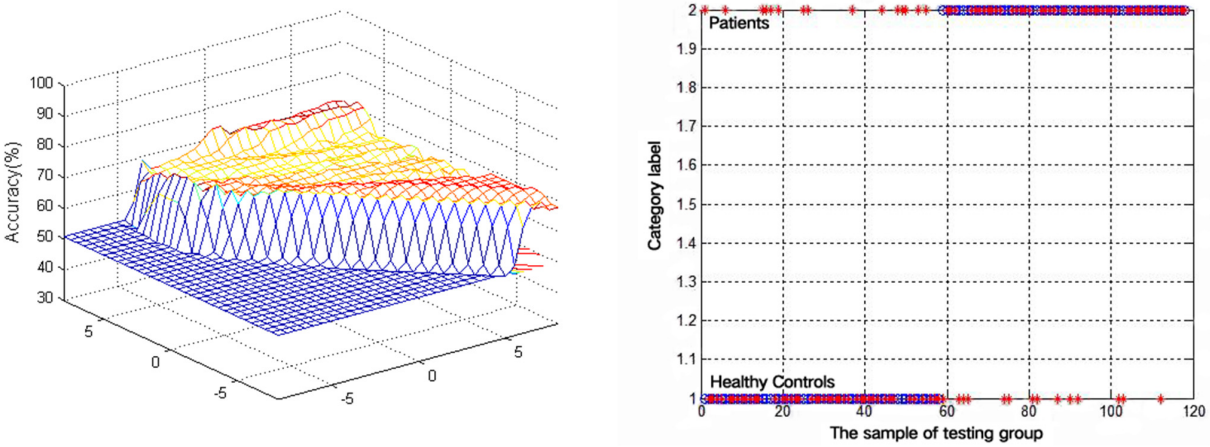

FIGURE 2
Visualization of classifications through support vector machine (SVM) using the decreased VMHC values in the MTG to discriminate lTLE patients from HCs. Left: SVM parameters result of 3D view. Right: Classified map of the VMHC values in the MTG.

the potential to contribute to complex visual abnormalities, language disorders, memory impairment, and other cognitive deficits. In a study of patients with diabetes, researchers reported a positive correlation between MTG VMHC values and scores on the Montreal Cognitive Assessment Scale (19), with reductions in MTG VMHC values potentially explaining the cognitive impairment that these patients develop. As such, reduced MTG homotopy may similarly be linked to cognitive impairment in TLE patients.

The cingulate gyrus functions as an important mediator of learning and retention in addition to connecting the medial temporal lobe and the PCC (47, 48). The cingulum is a key marginal lobe component that connects different cerebral lobes together (48). The cingulate gyrus is broadly separated into four subregions based on structural characteristics and receptor distributions, including the anterior/PCC, the posterior splenic cortex, and the middle lingual cortex (49). Of these regions, the middle cingulate cortex has been linked to negative affect and cognitive control (50), primarily facilitating response selection based on the relevance of those potential responses to associated motivations (48). Several memory task-based analyses have shown the MCG in particular to be critically important in the context of working memory (51). Decreased PCC flexibility has been reported in individuals diagnosed with lTLE who experience memory impairment, particularly in the right hemisphere with a ∼22% reduction in connectional flexibility (52). These researchers were successfully able to utilize contralateral resting PCC flexibility as a biomarker to differentiate between individuals with and without memory impairment based on memory status, with an overall accuracy of 94% consistent with a link between PCC flexibility and memory function in lTLE patients. Other reports have identified significant shifts in normal resting-state activity in the cingulate gyrus in TLE patients, potentially accounting for the psychiatric symptoms, memory/learning deficits, and loss of consciousness that these patients experience. These results further highlight the potential for the impairment of the MCG to act as a critical node linked with lTLE-related cognitive dysfunction.

Here, reduced bilateral MTG and MCG VMHC values were evident in lTLE patients. The key regions of the DMN include the MTG and the PCC/precuneus (53), which coordinate processes associated with visuospatial functionality, self-reflection, and consciousness (54). Prior work has similarly confirmed that TLE patients exhibit reductions in functional connectivity in the DMN (40), and that repeated or prolonged epileptic discharges can impact this network. In one study, significant resting-state weakening was observed in several DMN-associated brain regions in individuals diagnosed with TLE (55). Consistently, medial TLE patients affected by hippocampal sclerosis were found to exhibit significant reductions in functional connection strength and structural connections between most regions of the brain in the DMN and other non-DMN regions of the brain (56). In line with these prior reports, the present study explored the link between the DMN and cognitive dysfunction in lTLE patients, with this relationship potentially linked to altered cognition and memory. In other reports, resting-state DMN activity has been shown to be significantly altered in individuals with TLE, potentially contributing to certain symptoms that these patients experience including psychiatric symptoms, memory or learning disorders, and loss of consciousness (57). The consistency between these previous reports and the present study further support a link between altered DMN activity and the pathophysiological development of TLE, with the reduced VMHC observed in lTLE patients in this study suggesting that reductions in DMN interhemispheric integration or coordination may contribute

to the cognitive impairment experienced by patients with this disease. Roughly 40% of individuals diagnosed with epilepsy exhibit multiple forms of cognitive impairment (58), and prior work has revealed damage in several functional brain networks in patients with TLE including the alert network (59) and the executive network (40). These networks exhibit homotopy with respect to their structure and function, with the joint activity of both cerebral hemispheres being important for the maintenance of normal cognitive and emotional functionality. Altered information exchange or integration between these hemispheres can result in functional alterations such that the impaired homotopy observed in certain regions of the brain in individuals diagnosed with TLE may partially account for the functional deficits in these patients. Decreased VMHC values in the DMN thus offer neuroimaging-based support for prior evidence supporting a link between the pathogenesis of TLE and neurodegeneration.

The advent of increasingly advanced artificial intelligence strategies has been leveraged to guide neuroimaging-based computer-guided diagnostic efforts for patients with a range of neurological and pathological diseases. Novel MRI scanning and reconstructive strategies have been successfully leveraged to aid in diagnosing various diseases. Gao et al. (10), for example, found that a combination of elevated DC values in the left SFGdor and right SFGmed could be used as a neuroimaging biomarker for rTLE, with respective accuracy, sensitivity, and specificity values of 99.34, 100.00, and 98.55%. SVM strategies have been employed to aid in diagnosing psychiatric conditions such as schizophrenia (28) and major depression (24). Here, an SVM approach was used to assess abnormally altered VMHC values in the bilateral MTG and MCG, revealing that altered MTG VMHC values offered value as a biomarker capable of distinguishing between lTLE patients and HCs, with respective accuracy, sensitivity, and specificity values of 75.42, 74.14, and 76.67%. This study is the first to our knowledge to have explored the ability of altered MTG VMHC values to serve as an lTLE-related neuroimaging biomarker.

There are certain limitations to this analysis. For one, patients were treated for an extended period with AEDs, potentially altering rs-fMRI signals and associated study results. Indeed, as some AEDs have been shown to alter nervous system activation, it is not possible to exclude that AED treatment may have impacted the inter-group differences observed herein, underscoring the need for further research regarding the link between AED use and VMHC changes. Second, this was a cross-sectional study. Future longitudinal analyses are warranted to explore dynamic VMHC changes in particular regions of the brain. Lastly, this study was based on resting-state analyses, and further experiments combining both resting- and task-state fMRI have the potential to provide further insight regarding the magnitude of VMHC alterations in different regions of the brain under task conditions.

In summary, altered VHMC values in the bilateral MCG and MTG may correspond to altered resting-state activity in these areas in lTLE patients. Changes in VMHC values in the MTG may also offer great potential as a neuroimaging biomarker that can guide lTLE diagnosis.

Data availability statement

The original contributions presented in this study are included in the article/supplementary material, further inquiries can be directed to the corresponding authors.

Ethics statement

The studies involving human participants were reviewed and approved by the Ethics Committee of the Tianyou Hospital Affiliated to Wuhan University of Science and Technology. Written informed consent to participate in this study was provided by the participants' legal guardian/next of kin.

Author contributions

JW, RG, LC, and HR: conceptualization, project planning and methodology, and manuscript review and editing. JLW, SZ, and JL: data analysis and manuscript first draft. All authors contributed to the article and approved the submitted version.

Funding

The investigation was supported by the grant from the Natural Science Joint Foundation of Hubei province (Grant Nos. WJ2019H232 and WJ2019H233), the Health Commission of Hubei Province Scientific research project (Grant Nos. 2020CFB512 and WJ2021M007), and the Education Department of Hubei Province research project (Grant No. B2021022).

Acknowledgments

We express sincere thanks to all participants. We are grateful for access to the MATLAB and SPSS software. We also express their gratitude to REST (http://www.restfmri.net/) for the services provided.

Conflict of interest

The authors declare that the research was conducted in the absence of any commercial or financial relationships that could be construed as a potential conflict of interest.

The reviewer XJ declared a shared affiliation with the author(s) JW, JL, and SZ at the time of review.

Publisher's note

References

1. Li DB, Liu RS, Wang X, Xiong PA, Ren HW, Wei YF, et al. Abnormal ventral attention network homogeneity in patients with right temporal lobe epilepsy. *Eur Rev Med Pharmacol Sci.* (2021) 25:2031–8. doi: 10.26355/eurrev_202102_25107

2. Beghi E, Giussani G, Nichols E, Abd-Allah F, Abdela J, Abdelalim A, et al. Global, regional, and national burden of epilepsy, 1990–2016: a systematic analysis for the global burden of disease study 2016. *Lancet Neurol.* (2019) 18:357–75. doi: 10.1016/S1474-4422(18)30454-X

3. Gao Y, Zheng J, Li Y, Guo D, Wang M, Cui X, et al. Abnormal default-mode network homogeneity in patients with temporal lobe epilepsy. *Medicine (Baltimore).* (2018) 97:e11239. doi: 10.1097/MD.0000000000011239

4. Chen Z, Brodie MJ, Liew D, Kwan P. Treatment outcomes in patients with newly diagnosed epilepsy treated with established and new antiepileptic drugs: a 30-year longitudinal cohort study. *JAMA Neurol.* (2018) 75:279–86. doi: 10.1001/jamaneurol.2017.3949

5. Alqahtani F, Imran I, Pervaiz H, Ashraf W, Perveen N, Rasool MF, et al. Non-pharmacological interventions for intractable epilepsy. *Saudi Pharm J.* (2020) 28:951–62. doi: 10.1016/j.jsps.2020.06.016

6. Chang YA, Kemmotsu N, Leyden KM, Kucukboyaci NE, Iragui VJ, Tecoma ES, et al. Multimodal imaging of language reorganization in patients with left temporal lobe epilepsy. *Brain Lang.* (2017) 170:82–92. doi: 10.1016/j.bandl.2017.03.012

7. Bruder JC, Wagner K, Lachner-Piza D, Klotz KA, Schulze-Bonhage A, Jacobs J. Mesial-temporal epileptic ripples correlate with verbal memory impairment. *Front Neurol.* (2022) 13:876024. doi: 10.3389/fneur.2022.876024

8. Zhang Z, Zhou X, Liu J, Qin L, Ye W, Zheng J. Aberrant executive control networks and default mode network in patients with right-sided temporal lobe epilepsy: a functional and effective connectivity study. *Int J Neurosci.* (2020) 130:683–93. doi: 10.1080/00207454.2019.1702545

9. Chang W, Lv Z, Pang X, Nie L, Zheng J. The local neural markers of MRI in patients with temporal lobe epilepsy presenting ictal panic: a resting resting-state postictal fMRI study. *Epilepsy Behav.* (2022) 129:108490. doi: 10.1016/j.yebeh.2021.108490

10. Gao Y, Xiong Z, Wang X, Ren H, Liu R, Bai B, et al. Abnormal degree centrality as a potential imaging biomarker for right temporal lobe epilepsy: a resting-state functional magnetic resonance imaging study and support vector machine analysis. *Neuroscience.* (2022) 487:198–206. doi: 10.1016/j.neuroscience.2022.02.004

11. Liu G, Xiao R, Xu L, Cai J. Minireview of epilepsy detection techniques based on electroencephalogram signals. *Front Syst Neurosci.* (2021) 15:685387. doi: 10.3389/fnsys.2021.685387

12. Wu L, Wang C, Liu J, Guo J, Wei Y, Wang K, et al. Voxel-mirrored homotopic connectivity associated with change of cognitive function in chronic pontine stroke. *Front Aging Neurosci.* (2021) 13:621767. doi: 10.3389/fnagi.2021.621767

13. Gao Y, Wang M, Yu R, Li Y, Yang Y, Cui X, et al. Abnormal default mode network homogeneity in treatment-naive patients with first-episode depression. *Front Psychiatry.* (2018) 9:697. doi: 10.3389/fpsyt.2018.00697

14. Zhang Y, Huang G, Liu M, Li M, Wang Z, Wang R, et al. Functional and structural connective disturbance of the primary and default network in patients with generalized tonic-clonic seizures. *Epilepsy Res.* (2021) 174:106595. doi: 10.1016/j.eplepsyres.2021.106595

15. Hu G, Ge H, Yang K, Liu D, Liu Y, Jiang Z, et al. Altered static and dynamic voxel-mirrored homotopic connectivity in patients with frontal glioma. *Neuroscience.* (2022) 490:79–88. doi: 10.1016/j.neuroscience.2022.03.006

16. Zhang Y, Mu Y, Li X, Sun C, Ma X, Li S, et al. Improved interhemispheric functional connectivity in postpartum depression disorder: associations with individual target-transcranial magnetic stimulation treatment effects. *Front Psychiatry.* (2022) 13:859453. doi: 10.3389/fpsyt.2022.859453

17. Yang G, Zhang S, Zhou Y, Song Y, Hu W, Peng Y, et al. Increased resting-state interhemispheric functional connectivity of striatum in first-episode drug-naive adolescent-onset schizophrenia. *Asian J Psychiatr.* (2022):103134. doi: 10.1016/j.ajp.2022.103134

18. Jin Z, Huyang S, Jiang L, Yan Y, Xu M, Wang J, et al. Increased resting-state interhemispheric functional connectivity of posterior superior temporal gyrus and posterior cingulate cortex in congenital amusia. *Front Neurosci.* (2021) 15:653325. doi: 10.3389/fnins.2021.653325

19. Zhang Y, Wang J, Wei P, Zhang J, Zhang G, Pan C, et al. Interhemispheric resting-state functional connectivity abnormalities in type 2 diabetes patients. *Ann Palliat Med.* (2021) 10:8123–33. doi: 10.21037/apm-21-1655

20. Zhi M, Hou Z, Zhang Y, Yue Y, Li L, Yuan Y. Cognitive Deficit-Related interhemispheric asynchrony within the medial hub of the default mode network aids in classifying the hyperthyroid patients. *Neural Plast.* (2018) 2018:9023604. doi: 10.1155/2018/9023604

21. Gan C, Wang L, Ji M, Ma K, Sun H, Zhang K, et al. Abnormal interhemispheric resting state functional connectivity in Parkinson's disease patients with impulse control disorders. *NPJ Parkinsons Dis.* (2021) 7:60. doi: 10.1038/s41531-021-00205-7

22. Yang T, Ren J, Li Q, Li L, Lei D, Gong Q, et al. Increased interhemispheric resting-state in idiopathic generalized epilepsy with generalized tonic-clonic seizures: a resting-state fMRI study. *Epilepsy Res.* (2014) 108:1299–305. doi: 10.1016/j.eplepsyres.2014.06.010

23. Chen Y, Ou Y, Lv D, Yang R, Li S, Jia C, et al. Altered network homogeneity of the default-mode network in drug-naive obsessive-compulsive disorder. *Prog Neuropsychopharmacol Biol Psychiatry.* (2019) 93:77–83. doi: 10.1016/j.pnpbp.2019.03.008

24. Gao Y, Wang X, Xiong Z, Ren H, Liu R, Wei Y, et al. Abnormal fractional amplitude of low-frequency fluctuation as a potential imaging biomarker for first-episode major depressive disorder: a resting-state fMRI study and support vector machine analysis. *Front Neurol.* (2021) 12:751400. doi: 10.3389/fneur.2021.751400

25. Qiu Y, Yang M, Li S, Teng Z, Jin K, Wu C, et al. Altered fractional amplitude of low-frequency fluctuation in major depressive disorder and bipolar disorder. *Front Psychiatry.* (2021) 12:739210. doi: 10.3389/fpsyt.2021.739210

26. Zhang H, Li X, Pang J, Zhao X, Cao S, Wang X, et al. Predicting SSRI-resistance: clinical features and tagSNPs prediction models based on support vector machine. *Front Psychiatry.* (2020) 11:493. doi: 10.3389/fpsyt.2020.00493

27. Yan M, He Y, Cui X, Liu F, Li H, Huang R, et al. Disrupted regional homogeneity in melancholic and non-melancholic major depressive disorder at rest. *Front Psychiatry.* (2021) 12:618805. doi: 10.3389/fpsyt.2021.618805

28. Jin K, Xu D, Shen Z, Feng G, Zhao Z, Lu J, et al. Distinguishing hypochondriasis and schizophrenia using regional homogeneity: a resting-state fMRI study and support vector machine analysis. *Acta Neuropsychiatr.* (2021) 33:182–90. doi: 10.1017/neu.2021.9

29. Jan Z, Ai-Ansari N, Mousa O, Abd-Alrazaq A, Ahmed A, Alam T, et al. The role of machine learning in diagnosing bipolar disorder: scoping review. *J Med Internet Res.* (2021) 23:e29749. doi: 10.2196/29749

30. Manford M, Fish DR, Shorvon SD. An analysis of clinical seizure patterns and their localizing value in frontal and temporal lobe epilepsies. *Brain.* (1996) 119:17–40. doi: 10.1093/brain/119.1.17

31. Chao-Gan Y, Yu-Feng Z. DPARSF: a MATLAB toolbox for "pipeline" data analysis of resting-state fMRI. *Front Syst Neurosci.* (2010) 4:13. doi: 10.3389/fnsys.2010.00013

32. Zuo XN, Kelly C, Di Martino A, Mennes M, Margulies DS, Bangaru S, et al. Growing together and growing apart: regional and sex differences in the lifespan developmental trajectories of functional homotopy. *J Neurosci.* (2010) 30:15034–43. doi: 10.1523/JNEUROSCI.2612-10.2010

33. Liu HH, Wang J, Chen XM, Li JP, Ye W, Zheng J. Interhemispheric functional and structural alterations and their relationships with alertness in unilateral temporal lobe epilepsy. *Eur Rev Med Pharmacol Sci.* (2016) 20:1526–36.

34. Zhao X, Kang H, Zhou Z, Hu Y, Li J, Li S, et al. Interhemispheric functional connectivity asymmetry is distinctly affected in left and right mesial temporal lobe epilepsy. *Brain Behav.* (2022) 12:e2484. doi: 10.1002/brb3.2484

35. Briggs RG, Tanglay O, Dadario NB, Young IM, Fonseka RD, Hormovas J, et al. The unique fiber anatomy of middle temporal gyrus default mode connectivity. *Oper Neurosurg (Hagerstown).* (2021) 21:E8–14. doi: 10.1093/ons/opab109

36. Jeffrey R, Binder RHDW, Conant LL. Where is the semantic system? A critical review and meta-analysis of 120 functional neuroimaging studies. *Cereb Cortex.* (2009) 19:2767–96.

37. Ro A, Ksab C, Jma B, Jt C, Rh A, Ty B, et al. Abnormal cortical activation during silent reading in adolescents with autism spectrum disorder. *Brain Dev.* (2019) 41:234–44. doi: 10.1016/j.braindev.2018.10.013

38. Cheng C, Dong D, Jiang Y, Ming Q, Zhong X, Sun X, et al. State-related alterations of spontaneous neural activity in current and remitted depression revealed by resting-state fMRI. *Front Psychol.* (2019) 10:245. doi: 10.3389/fpsyg.2019.00245

39. Hwang M, Roh YS, Talero J, Cohen BM, Baker JT, Brady RO, et al. Auditory hallucinations across the psychosis spectrum: evidence of dysconnectivity involving cerebellar and temporal lobe regions. *Neuroimage Clin.* (2021) 32:102893. doi: 10.1016/j.nicl.2021.102893

40. Gao YJ, Wang X, Xiong PG, Ren HW, Zhou SY, Yan YG, et al. Abnormalities of the default-mode network homogeneity and executive dysfunction in people with first-episode, treatment-naive left temporal lobe epilepsy. *Eur Rev Med Pharmacol Sci.* (2021) 25:2039–49. doi: 10.26355/eurrev_202102_25108

41. Fan S, Cath DC, van den Heuvel OA, van der Werf YD, Schols C, Veltman DJ, et al. Abnormalities in metabolite concentrations in tourette's disorder and obsessive-compulsive disorder-A proton magnetic resonance spectroscopy study. *Psychoneuroendocrinology.* (2017) 77:211–7. doi: 10.1016/j.psyneuen.2016.12.007

42. Bozkurt B, Da SCR, Chaddad-Neto F, Da CM, Goiri MA, Karadag A, et al. Transcortical selective amygdalohippocampectomy technique through the middle temporal gyrus revisited: an anatomical study laboratory investigation. *J Clin Neurosci.* (2016) 34:237–45. doi: 10.1016/j.jocn.2016.05.035

43. Fan L, Wang J, Zhang Y, Han W, Yu C, Jiang T. Connectivity-based parcellation of the human temporal pole using diffusion tensor imaging. *Cereb Cortex.* (2014) 24:3365–78. doi: 10.1093/cercor/bht196

44. Cho S, Metcalfe AW, Young CB, Ryali S, Geary DC, Menon V. Hippocampal-prefrontal engagement and dynamic causal interactions in the maturation of children's fact retrieval. *J Cogn Neurosci.* (2012) 24:1849–66. doi: 10.1162/jocn_a_00246

45. Saur D, Kreher BW, Schnell S, Kummerer D, Kellmeyer P, Vry MS, et al. Ventral and dorsal pathways for language. *Proc Natl Acad Sci USA.* (2008) 105:18035–40. doi: 10.1073/pnas.0805234105

46. Xu J, Wang J, Fan L, Li H, Zhang W, Hu Q, et al. Tractography-based parcellation of the human middle temporal gyrus. *Sci Rep.* (2015) 5:18883. doi: 10.1038/srep18883

47. Bubb EJ, Metzler-Baddeley C, Aggleton JP. The cingulum bundle: anatomy, function, and dysfunction. *Neurosci Biobehav Rev.* (2018) 92:104–27. doi: 10.1016/j.neubiorev.2018.05.008

48. Maldonado IL, Parente DMV, Castro CT, Herbet G, Destrieux C. The human cingulum: from the limbic tract to the connectionist paradigm. *Neuropsychologia.* (2020) 144:107487. doi: 10.1016/j.neuropsychologia.2020.107487

49. Vogt BA. Pain and emotion interactions in subregions of the cingulate gyrus. *Nat Rev Neurosci.* (2005) 6:533–44. doi: 10.1038/nrn1704

50. Tolomeo S, Christmas D, Jentzsch I, Johnston B, Sprengelmeyer R, Matthews K, et al. A causal role for the anterior mid-cingulate cortex in negative affect and cognitive control. *Brain.* (2016) 139:1844–54. doi: 10.1093/brain/aww069

51. Heany SJ, Phillips N, Brooks S, Fouche JP, Myer L, Zar H, et al. Neural correlates of maintenance working memory, as well as relevant structural qualities, are associated with earlier antiretroviral treatment initiation in vertically transmitted HIV. *J Neurovirol.* (2020) 26:60–9. doi: 10.1007/s13365-019-00792-5

52. Douw L, Leveroni CL, Tanaka N, Emerton BC, Cole AJ, Reinsberger C, et al. Loss of resting-state posterior cingulate flexibility is associated with memory disturbance in left temporal lobe epilepsy. *PLoS One.* (2015) 10:e131209. doi: 10.1371/journal.pone.0131209

53. Yeshurun Y, Nguyen M, Hasson U. The default mode network: where the idiosyncratic self meets the shared social world. *Nat Rev Neurosci.* (2021) 22:181–92. doi: 10.1038/s41583-020-00420-w

54. Qin P, Wu X, Wu C, Wu H, Zhang J, Huang Z, et al. Higher-order sensorimotor circuit of the brain's global network supports human consciousness. *Neuroimage.* (2021) 231:117850. doi: 10.1016/j.neuroimage.2021.117850

55. Laufs H, Hamandi K, Salek-Haddadi A, Kleinschmidt AK, Duncan JS, Lemieux L. Temporal lobe interictal epileptic discharges affect cerebral activity in "default mode" brain regions. *Hum Brain Mapp.* (2007) 28:1023–32. doi: 10.1002/hbm.20323

56. Zhang Z, Lu G, Zhong Y, Tan Q, Chen H, Liao W, et al. FMRI study of mesial temporal lobe epilepsy using amplitude of low-frequency fluctuation analysis. *Hum Brain Mapp.* (2010) 31:1851–61. doi: 10.1002/hbm.20982

57. Stretton J, Pope RA, Winston GP, Sidhu MK, Symms M, Duncan JS, et al. Temporal lobe epilepsy and affective disorders: the role of the subgenual anterior cingulate cortex. *J Neurol Neurosurg Psychiatry.* (2015) 86:144–51.

58. Coimbra ER, Rezek K, Escorsi-Rosset S, Landemberger MC, Castro RM, Valadao MN, et al. Cognitive performance of patients with mesial temporal lobe epilepsy is not associated with human prion protein gene variant allele at codons 129 and 171. *Epilepsy Behav.* (2006) 8:635–42. doi: 10.1016/j.yebeh.2006.02.007

59. Nie L, Jiang Y, Lv Z, Pang X, Liang X, Chang W, et al. A study of brain functional network and alertness changes in temporal lobe epilepsy with and without focal to bilateral tonic-clonic seizures. *BMC Neurol.* (2022) 22:14. doi: 10.1186/s12883-021-02525-w

frontiers | Frontiers in Psychiatry

TYPE Original Research
PUBLISHED 22 August 2022
DOI 10.3389/fpsyt.2022.966362

OPEN ACCESS

EDITED BY
Yujun Gao,
Wuhan University, China

REVIEWED BY
Kaihua Jiang,
Changzhou Children's Hospital, China
Mengting Li,
Zhejiang Normal University, China

*CORRESPONDENCE
Xiaoxia Du
duxiaoxia@sus.edu.cn
Jun Ma
majun@shsmu.edu.cn

†These authors have contributed equally to this work

SPECIALTY SECTION
This article was submitted to Neuroimaging and Stimulation, a section of the journal Frontiers in Psychiatry

RECEIVED 10 June 2022
ACCEPTED 12 July 2022
PUBLISHED 22 August 2022

CITATION
Zhong S, Zhang L, Wang M, Shen J, Mao Y, Du X and Ma J (2022) Abnormal resting-state functional connectivity of hippocampal subregions in children with primary nocturnal enuresis. *Front. Psychiatry* 13:966362. doi: 10.3389/fpsyt.2022.966362

Abnormal resting-state functional connectivity of hippocampal subregions in children with primary nocturnal enuresis

Shaogen Zhong[1†], Lichi Zhang[2†], Mengxing Wang[3], Jiayao Shen[4], Yi Mao[1], Xiaoxia Du[5*] and Jun Ma[1*]

[1]Department of Developmental and Behavioral Pediatrics, Shanghai Children's Medical Center, School of Medicine, Shanghai Jiao Tong University, Shanghai, China, [2]School of Biomedical Engineering, Shanghai Jiao Tong University, Shanghai, China, [3]College of Medical Imaging, Shanghai University of Medicine and Health Sciences, Shanghai, China, [4]Department of Nephrology, Shanghai Children's Medical Center, School of Medicine, Shanghai Jiao Tong University, Shanghai, China, [5]School of Psychology, Shanghai University of Sport, Shanghai, China

Objective: Previous neuroimaging studies have shown abnormal brain-bladder control network in children with primary nocturnal enuresis (PNE). The hippocampus, which has long been considered to be an important nerve center for memory and emotion, has also been confirmed to be activating during micturition in several human imaging studies. However, few studies have explored hippocampus-related functional networks of PNE in children. In this study, the whole resting-state functional connectivity (RSFC) of hippocampus was investigated in children with PNE.

Methods: Functional magnetic resonance imaging data of 30 children with PNE and 29 matched healthy controls (HCs) were analyzed in our study. We used the seed-based RSFC method to evaluate the functional connectivity of hippocampal subregions defined according to the Human Brainnetome Atlas. Correlation analyses were also processed to investigate their relationship with disease duration time, bed-wetting frequency, and bladder volume.

Results: Compared with HCs, children with PNE showed abnormal RSFC of the left rostral hippocampus (rHipp) with right fusiform gyrus, right Rolandic operculum, left inferior parietal lobule, and right precentral gyrus, respectively. Moreover, decreased RSFC of the left caudal hippocampus (cHipp) with right fusiform gyrus and right supplementary motor area was discovered in the PNE group. There were no significant results in the right rHipp and cHipp seeds after multiple comparison corrections. In addition, disease duration time was negatively correlated with RSFC of the left rHipp with right Rolandic operculum ($r = -0.386$, $p = 0.035$, uncorrected) and the left cHipp with right fusiform gyrus ($r = -0.483$, $p = 0.007$, uncorrected) in the PNE group, respectively. In the Receiver Operating Characteristic (ROC) analysis, all the above results of RSFC achieved significant performance.

Conclusions: To our knowledge, this is the first attempt to examine the RSFC patterns of hippocampal subregions in children with PNE. These findings indicated that children with PNE have potential dysfunctions in the limbic network, sensorimotor network, default mode network, and frontoparietal network. These networks may become less efficient with disease duration time, inducing impairments in brain-bladder control, cognition, memory, and emotion. Further prospective research with dynamic observation of brain imaging, bladder function, cognition, memory, and emotion is warranted.

KEYWORDS

primary nocturnal enuresis, resting-state functional connectivity, children, hippocampus, subregion

Introduction

Primary nocturnal enuresis (PNE) is the most common form of elimination disorder in childhood characterized by symptoms of intermittent incontinence during sleep without a previous dry period of more than 6 months (1, 2). Approximately 5–10% of 7-year-old children wet at night and 0.5–1% of adults still suffer from this condition, although the spontaneous remission rate is about 15% per year (3). The persistence of bed-wetting increases children's risk for physical and mental problems, such as chronically disturbed sleep, chronic lower self-esteem, and various psychiatric conditions (3, 4). Nevertheless, some children with PNE remain resistant to all clinically available treatments, largely because the pathogenesis of PNE is still unclear.

It is generally believed that nocturnal polyuria, arousal dysfunction, and abnormal nocturnal bladder function are three main factors implicated in the pathogenesis of PNE (4–6), and maturational delays of the central nervous system have been considered to be related to the pathogenesis of PNE (7). Over the past few decades, magnetic resonance imaging (MRI) technology, especially functional MRI (fMRI), has been validated as an efficient, non-invasive, and promising approach to investigating the neural mechanisms of bladder control in healthy and pathological participants (8). In recent years, brain MRI studies have shown that PNE is strongly linked to alterations in brain structure and function (7). Our previous resting-state fMRI study has found that spontaneous activity abnormalities of the prefrontal cortex (PFC) and midbrain are likely linked to micturition control impairment in children with PNE (9). Additionally, we have also found that structural changes in PFC and precuneus may be linked to micturition and sleep problems of PNE in children (10). The above brain regions are mainly involved in the neural circuits within a micturition control model presented by Griffiths (11). Apart from dysfunction in the bladder control during sleep, an inability to wake up from the sense of full bladder is another common complaint among parents of children suffering from bed-wetting. The insular activity is strongly associated with bladder sensation. One fMRI study on the control of low urinary tract in healthy subjects suggested that the activity of right anterior insular enhanced during "attempted micturition" in the full-bladder condition (12). Notably, hippocampus has been revealed as an integrated component implicated in interoception (13), such as visceral sensations. As a main part of the human limbic system, hippocampus, an elongated structure (14), has long been regarded as a major center for memory, cognition, and emotion (15). Yet, there could be more function in hippocampus. For example, hippocampal activation during micturition has been confirmed in human and animal imaging studies (16–18). A previous study on the neural network controlling rat's bladder, hippocampus has been labeled (19). Moreover, children with PNE have shown potential impairments in working memory (20, 21), response inhibition (22), attention (23), and emotional response (24) during various fMRI studies, which might be related to hippocampal activities. Taken together, PNE-related symptoms and behaviors may be influenced by interactions between hippocampus and other cortical regions. Along its longitudinal axis, hippocampus varies in structure, function, and connectivity. The anterior hippocampus is primarily responsible for emotion, whereas the posterior hippocampus is implicated in memory and cognition (25). Previous studies have shown abnormal RSFC patterns of the hippocampus in a great number of psychiatric diseases, such as depression (26, 27), schizophrenia (28, 29), and posttraumatic stress disorder (30). Nevertheless, the RSFC patterns of the hippocampus functionally linked to other brain areas in children with PNE have not been investigated so far.

Given the potential roles of hippocampus in bladder sensation, micturition, bladder control, PNE-related cognitive and emotional deficits, we aimed to explore the RSFC patterns of the hippocampus in children with PNE using a seed-based RSFC method in this work. We mainly hypothesized that there are anomaly RSFC patterns of hippocampal subregions with other cortical regions compared with healthy controls (HCs). The second analysis was to investigate the association

TABLE 1 Demographic and clinical data for PNE and HC children.

Baseline characteristic	PNE group ($n = 30$)	HC group ($n = 29$)	*P*-value
Age, years, median (IQR)	8.5 (7–10)	8 (7–10)	0.969[a]
Gender, *n* (%)			0.358[b]
Male	14 (46.7)	17 (58.6)	
Female	16 (53.3)	12 (41.4)	
Handedness, *n* (%)			NA
Right	30 (100.0)	29 (100.0)	
Left	0 (0.0)	0 (0.0)	
Mean FD, mean ± SD	0.15 ± 0.05	0.19 ± 0.10	0.063[c]
Duration time, years, median (IQR)	3.5 (2–5)	NA	NA
Bed-wetting frequency, per week, median (IQR)	4 (1.75–6.25)	NA	NA
Bladder volume, ml, mean ± SD	177.03 ± 75.47	NA	NA

PNE, primary nocturnal enuresis; HC, healthy control; IQR, interquartile range; FD, framewise displacement; SD, standard deviation; NA, not applicable; [a]Mann-Whitney test; [b]Chi-squared test; [c]Two-sample *t*-test.

between altered RSFC patterns of hippocampal subregions and clinical characteristics in children with PNE, and the predictive value of RSFC patterns of hippocampal subregions with other cortical regions, gaining access to key information that may have clinical implications.

Materials and methods

Participants

Thirty-three children with PNE were enrolled in the outpatient clinic of Shanghai Children's Medical Center, and 33 HCs matched for age and gender were recruited by advertisement. All patients had bed-wetting, with one or more episodes per month for at least 3 months, and were diagnosed by senior pediatricians following the International Children's Continence Society (ICCS) criteria (1). Their urine tests were normal without glucosuria and leukocytes. Ultrasound examination of their urinary systems uncovered no organic problems in the kidney, urinary tract, and bladder. Moreover, the bladder volume was acquired by the ultrasound when patients had a strong desire to void. We also collected information on the age, gender, disease duration time, and bed-wetting frequency by a questionnaire in which a detailed clinical history was recorded. HCs were no enuresis and could wake up in response to the sensation of full bladder during sleep since they were 5 years old. The clinical features of participants were presented in Table 1.

The inclusion criteria of all participants were: 5–18 years; right-handedness; with an IQ above 75 (Wechsler Intelligence Scale for Children-Revised); a clinical assessment and diagnosis by senior developmental and behavioral pediatricians; without an organic history causing bed-wetting (e.g., diabetes mellitus, epilepsy, urinary infection); without any history of other psychiatric or neurological diseases (e.g., intellectual disability, attention-deficit/hyperactive disorder, autism spectrum disorder, cerebral palsy); without receiving any treatments or drugs about anti-enuresis before MRI scanning. And the exclusion criteria of all participants were: with any daytime lower urinary tract symptoms; left-handedness; with an IQ below 75; contraindications for MRI; with obvious head movement (translation > 2 mm, rotation $> 2^{\circ}$) on these brain images; receiving any other antipsychotics.

Ethical approval was obtained from the IRB of Shanghai Children's Medical Center, School of Medicine, Shanghai Jiao Tong University (No: SCMC-201014). This study was conducted under the Declaration of Helsinki. All guardians and their children provided written informed consent before study enrollment.

MRI data acquisition

The structural and functional MRI data were acquired on the 3.0 T MR imaging system (Prisma, Siemens, Germany) at Shanghai Key Laboratory of Magnetic Resonance (East China Normal University, Shanghai, China). fMRI sequence parameters were as follows: volume number = 240, acquisition matrix = 64 × 64, repetition time (TR)/echo time (TE) = 2,000/30 ms, voxel size = 3.5 × 3.5 × 3.5 mm^3, acquisition time = 486 s, flip angle = 90°, field of view (FOV) = 224 × 224 mm^2, slice number = 33. All children were told to stay awake and still, keeping their eyes closed during scanning. We also collected high-resolution T1-weighted images from all children, sequence parameters were set as follows: acquisition matrix = 256 × 256, inversion time = 1,100 ms, TR/TE = 2,530/2.98 ms, flip angle = 7°, FOV = 256 × 256 mm^2, voxel size = 1 × 1 × 1 mm^3, 192 slices (scan time of 361 s).

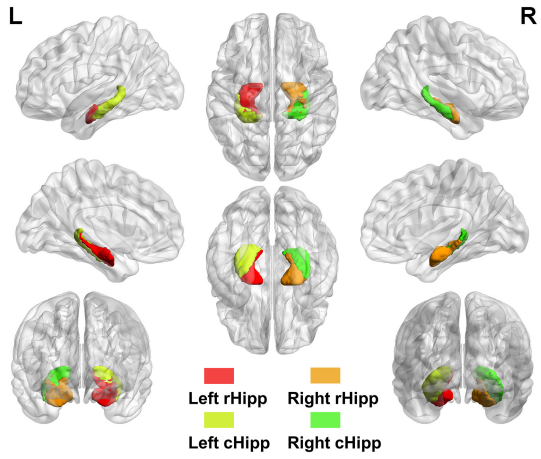

FIGURE 1
The anatomical location of hippocampal subregions. Hippocampal subregions based on the Human Brainnetome Atlas, including left rostral hippocampus (rHipp), right rostral hippocampus (rHipp), left caudal hippocampus (cHipp), and right caudal hippocampus (cHipp).

Data preprocessing

All MRI data were preprocessed in the MATLAB 2014a (The MathWorks, Inc., Natick, Massachusetts, USA) using RESTplus version 1.24 (31), a toolkit based on SPM12 (http://www.fil.ion.ucl.ac.uk/spm/; Wellcome Trust Centre for Neuroimaging, University College London, UK). Preprocessing included these following steps: (1) removing the first 10 time points of each rs-fMRI data for participants' acclimatization and signal's stability; (2) slice-timing to correct the remaining time points; (3) realignment; (4) normalizing to Montreal Neurological Institute (MNI) template as well as resampling into a new $3 \times 3 \times 3$ mm^3 voxel size by using T1 image unified segmentation; (5) smoothing with a Gaussian kernel (full-width-half-maximum, FWHM of 6 mm); (6) detrending; (7) regressing common covariates out, including Friston's 24 head motion parameters (32), white matter (WM), and cerebrospinal fluid (CSF) signals; (8) filtering (0.01–0.08 Hz). There were 3 children with PNE and 4 HCs excluded for excessive head motion (translation $>$ 2 mm, rotation $>$ 2°). Thus, 30 children with PNE and 29 HCs were included in our final analyses.

Resting-state functional connectivity analysis

Analyses of the seed-based RSFC were conducted using the RESTplus version 1.24 toolkit. The bilateral hippocampi were divided into four subregions based on the Human Brainnetome Atlas (33), including left rostral hippocampus (rHipp), right rostral hippocampus (rHipp), left caudal hippocampus (cHipp), and right caudal hippocampus (cHipp) (Figure 1). First, we selected the left rHipp, right rHipp, left cHipp, and right cHipp as regions of interest (ROIs) for analyses. Then, the average time series of each hippocampal subregion seed was calculated in each subject to generate correlation maps by voxel-wise correlation coefficients, respectively. Finally, by using Fisher's r-to-z transformation, we converted these correlation coefficients into z-values to improve normality.

Receiver operating characteristic analysis

The significantly altered RSFC z-values of hippocampal subregion seeds were extracted and used for the Receiver Operating Characteristic (ROC) analysis using MedCalc for Windows, version 18.2.1 (MedCalc Software, Ostend, Belgium). As a frequently used summary measure of the ROC curve, the maximum Youden index (sensitivity + specificity − 1) (34) and the corresponding sensitivity, specificity, 95% confidence intervals (CIs) for each altered brain region were computed.

Statistical analysis

We conducted statistical analyses of RSFC using the RESTplus version 1.24 toolkit. First, group comparisons on the RSFC z-values derived from each hippocampal subregion seed between PNE and HCs groups were carried out *via* the two-sample *t*-test. The age and gender of each participant were set as covariates during the between-group comparisons in the RESTplus software to reduce their potential confounding effects on the results. Second, we utilized multiple comparison corrections, namely Gaussian Random Field (GRF) corrections, for RSFC results of all hippocampal subregion seeds (GRF correction, single-voxel $P < 0.001$ as well as cluster-level $P < 0.05$). Third, the abnormal RSFC z-values based on each hippocampal subregion seed after GRF correction were extracted. Then, we performed Person's correlation analysis between clinical characteristics (e.g., disease duration time, bed-wetting frequency, and bladder volume) and the above aberrant RSFC z-values in the PNE group.

Results

Demographic and clinical characteristics

Overall, 59 right-handed participants, 30 children with PNE [8.5 (7–10) years] and 29 HCs without enuresis [8 (7–10) years], were included in our final analyses. There were no differences in age, gender, and mean FD (35) between the groups (Table 1).

TABLE 2 Brain regions presenting significant differences in functional connectivity with left hippocampus between PNE and HC children (GRF corrected for single-voxel $P < 0.001$ and cluster-level $P < 0.05$).

Brain regions	BA	Cluster size	MNI coordinates			Peak Z-value
			X	Y	Z	
Left rHipp seed	NA	165	−22	−14	−19	NA
Right fusiform gyrus	NA	147	39	−45	−15	−4.2595
Right Rolandic operculum	NA	163	48	−9	9	−3.9642
Left inferior parietal lobule	NA	199	−45	−27	42	−4.2606
Right precentral gyrus	6	297	21	−18	69	−4.1855
Left cHipp seed	NA	172	−28	−30	−10	NA
Right fusiform gyrus	19	170	24	−60	−12	−4.4981
Right supplementary motor area	24	168	9	−6	48	−4.1969

BA, Brodmann's area; PNE, primary nocturnal enuresis; HC, healthy control; MNI, Montreal Neurological Institute; NA, not applicable; rHipp, rostral hippocampus; cHipp, caudal hippocampus; hippocampal subregions seeds were transformed into MNI coordinates according to the Human Brainnetome Atlas.

Group comparisons in the RSFC of hippocampal subregions

rHipp

Compared with HCs, children with PNE showed decreased RSFC of the left rHipp with right fusiform gyrus, right Rolandic operculum, left inferior parietal lobule (IPL), and right precentral gyrus, respectively (Table 2; Figure 2). However, there were no significant RSFC results based on the right rHipp seed.

cHipp

Reduced RSFC of the left cHipp with right fusiform gyrus and right supplementary motor area was also discovered in the PNE group relative to the HCs group (Table 2; Figure 3). Nevertheless, we found no differences in the RSFC of the right cHipp seed between the groups.

ROC curves results

When taking into account the area under the curve (AUC) and 95% CIs, it was determined that the RSFC z-value between the left rHipp and right fusiform gyrus exhibited the most accurate classification. For AUC, the altered brain regions all reached significant levels of $p < 0.0001$ (Table 3; Figure 4).

Relationship between clinical characteristics and RSFC

Disease duration time was negatively correlated with RSFC of the left rHipp with right Rolandic operculum ($r = -0.386$, $p = 0.035$, uncorrected) and the left cHipp with right fusiform gyrus ($r = -0.483$, $p = 0.007$, uncorrected) in the PNE group, respectively (Figure 5), yet there were no significant relationships between bet-wetting frequency or bladder volume and RSFC z-values of significantly altered brain clusters.

Discussion

Compared with HCs, we primarily found that children with PNE showed abnormal RSFC of the left rHipp with right fusiform gyrus, right Rolandic operculum, left IPL, and right precentral gyrus, respectively. The reduced RSFC of the left cHipp with right fusiform gyrus and right supplementary motor area was also discovered in children with PNE. However, there were no statistically significant clusters based on the right rHipp and cHipp seeds. Furthermore, disease duration time was negatively correlated with RSFC for the left rHipp with right Rolandic operculum in the PNE group. RSFC for the left cHipp with right fusiform gyrus was also negatively associated with disease duration time in the PNE group. In the ROC analysis, all the above results of RSFC were significant. Based on these findings, children with PNE may have potential dysfunctions in the limbic network, sensorimotor network, default mode network (DMN), and frontoparietal network, which may become less efficient with disease duration. The above networks are involved in bladder sensation, low urinary tract control, cognition, memory, and emotion. Therefore, further prospective research that ongoing observation of brain imaging, bladder function, cognition, memory, and emotion is warranted.

One of our main results was that decreased RSFC of the left rHipp with right fusiform gyrus was uncovered in children with PNE relative to HCs. The rHipp, namely the anterior hippocampus, contributes to episodic memory, imagination, and visual scene perception, with widespread connectivity (15). The fusiform gyrus is considered to be implicated in the processing of high-order visual functions, such as face

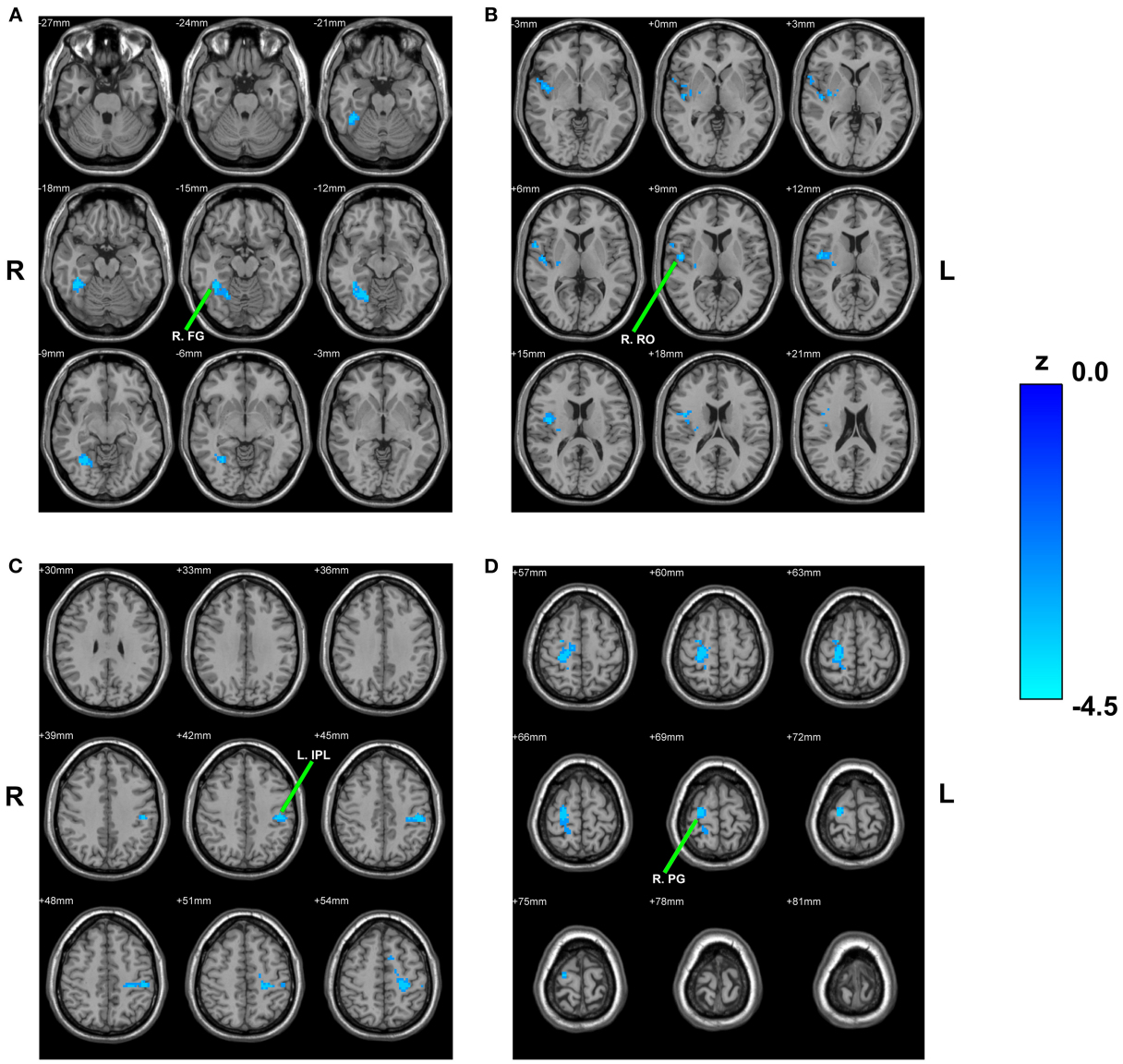

FIGURE 2
Between-group comparison based on the left rHipp. The reduced RSFC of the left rHipp with right fusiform gyrus **(A)**, right Rolandic operculum **(B)**, left inferior parietal lobule **(C)**, and right precentral gyrus **(D)** in children with PNE, respectively. rHipp, rostral hippocampus; PNE, primary nocturnal enuresis; R. FG, right fusiform gyrus; R. RO, right Rolandic operculum; L. IPL, left inferior parietal lobule; R. PG, right precentral gyrus; color bar, z value.

perception, object recognition, and reading (36). A categorical n-back task fMRI study indicated that there was a lower percentage of correct responses and longer mean reaction time to correct response in children with PNE, possibly associated with dysfunction in the left cerebella (21). Although there was no significant difference in the hippocampus and fusiform gyrus between-group comparison, the fusiform gyrus was activated in both PNE children and controls in this study (21). In another fMRI research, the hippocampus and fusiform gyrus have been proven to be engaged in different kinds of categorization learning (37). Therefore, the interaction of the hippocampus and fusiform gyrus might play a vital role in the cognitive impairments of PNE children.

Our results also exhibited reduced RSFC between the left rHipp and some sensorimotor areas, including the right Rolandic operculum and right precentral gyrus. Integrated exteroceptive-interoceptive signals are processed by the Rolandic operculum for bodily self-awareness and interoceptive awareness (38, 39). The hippocampus also plays an important role in interoception (13). It is well known that children

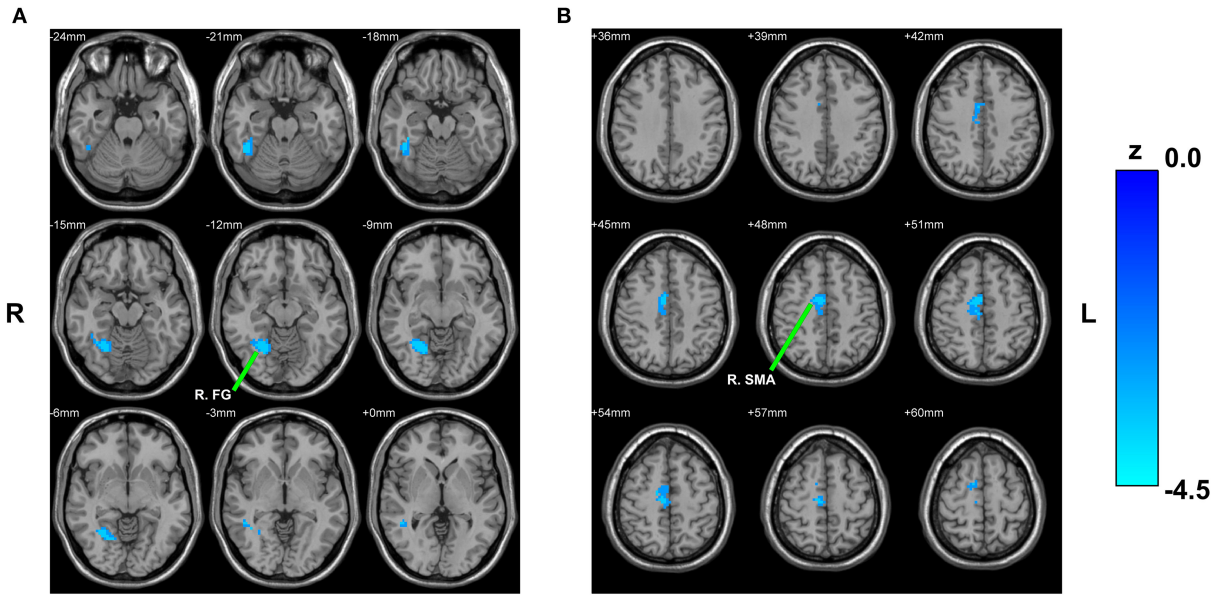

FIGURE 3
Between-group comparison based on the left cHipp. The decreased RSFC of the left cHipp with right fusiform gyrus **(A)** and right supplementary motor area **(B)** in children with PNE, respectively. cHipp, caudal hippocampus; PNE, primary nocturnal enuresis; R. FG, right fusiform gyrus; R. SMA, right supplementary motor area; color bar, z value.

TABLE 3 The ROC analysis for altered brain regions that distinguish PNE children from HC children.

Brain regions	SEN	SPE	AUC	95% CI
Left rostral hippocampus				
zFC_right fusiform gyrus	60.00%	96.55%	0.832	0.712–0.917
zFC_right Rolandic operculum	86.67%	62.07%	0.790	0.664–0.885
zFC_left inferior parietal lobe	83.33%	68.97%	0.805	0.681–0.896
zFC_right precentral gyrus	80.00%	79.31%	0.808	0.685–0.899
Left caudal hippocampus				
zFC_right fusiform gyrus	73.33%	86.21%	0.825	0.704–0.912
zFC_right supplementary motor area	83.33%	75.86%	0.821	0.699–0.908

SEN, sensitivity; SPE, specificity; AUC, area under the ROC curve; CI, confidence interval; PNE, primary nocturnal enuresis; HC, healthy control; zFC, functional connectivity z values.

with PNE have difficulty waking up to bladder signals during sleep. Therefore, the abnormal RSFC between the left rHipp and Rolandic operculum might be implicated in micturition desire-awakening in children with PNE. Post-stroke patients can experience intense psychological symptoms following stroke (e.g., apathy, depression, anxiety, and stress) if the right Rolandic operculum is damaged (40). As mentioned before, the rHipp relates to stress, emotion, and affect (25). Bed-wetting tends to be rated as one of the most stressful life events for children (4). Hence stress coupled with rHipp change might present in children with PNE. Moreover, we found that bed-wetting duration time was negatively correlated with RSFC of the left rHipp with right Rolandic operculum in the PNE group. In clinical practice, children with persistent bed-wetting often have secondary psychological problems, such as low self-esteem, anxiety and depression, though the problems may be mild.

On the other hand, the precentral gyrus is where the primary motor cortex is located (41). Our previous fMRI study (42) found that the reduced RSFC between the precentral gyrus and thalamus in children with PNE might be related to arousal dysfunction. The primary motor cortex is not only a structure for controlling motor movements but also a dynamic substrate that may also contribute to motor learning and cognitive processes (43). Children with PNE displayed a slower motor performance than controls, especially repetitive hand and finger movements, suggesting a possible maturation deficit in the motor cortex circuitry (44). Furthermore, pathologic performance on visuomotor integration abilities was more

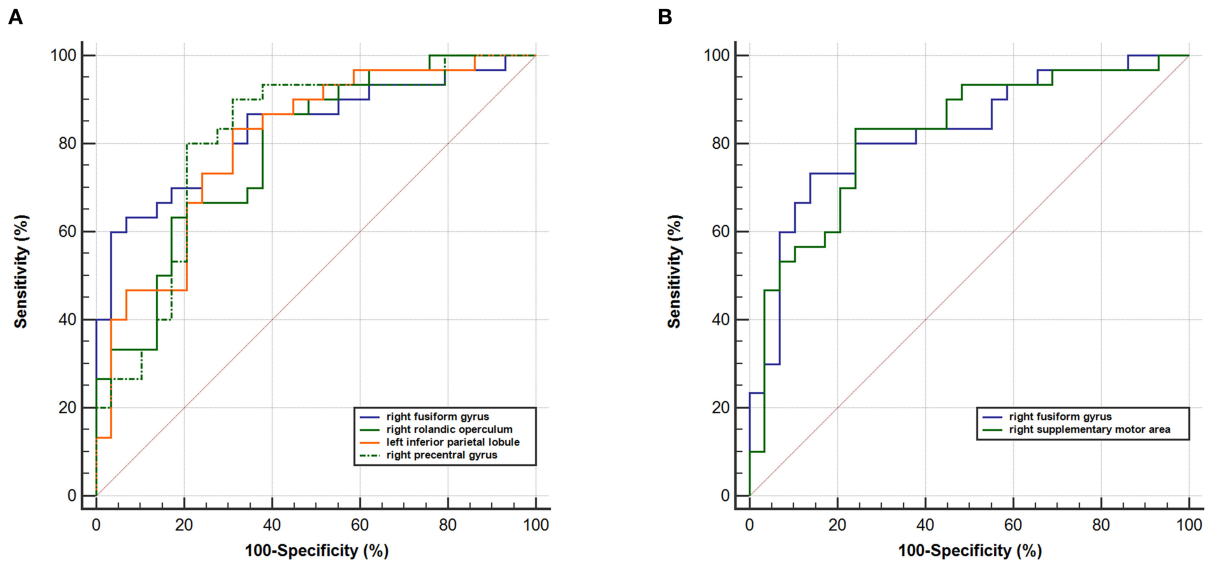

FIGURE 4
ROC curve analysis. ROC curve for altered RSFC patterns based on the left **(A)** rHipp and **(B)** cHipp to distinguish children with PNE from HCs. rHipp, rostral hippocampus; cHipp, caudal hippocampus; PNE, primary nocturnal enuresis; HCs, healthy controls.

prevalent in PNE children, despite not experiencing impairment in visual or motor tasks (45). In a word, these findings demonstrated that the abnormal RSFC between the left rHipp and some sensorimotor areas may be associated with mild neuromotor development delay in children with PNE.

As an integral part of the DMN, the left IPL plays an essential role in a variety of higher cognitive functions (46). The well-known DMN, which is active at rest condition and deactivated when external attention is required, plays an important role in maintaining continence together with the salience network (11). In our results, the decreased RSFC between the left rHipp and left IPL was also discovered in children with PNE. As mentioned before, the hippocampal activation is observed during micturition in human and animal (16–18). Taken together, we assumed that the interplay of DMN and limbic network through left IPL might be involved in micturition problem in children with PNE.

Another important finding in the present work showed that children with PNE had reduced RSFC of the left cHipp with the right fusiform gyrus and right supplementary motor area. The cHipp, namely the posterior hippocampus, performs primarily cognitive functions (25). As mentioned before, the fusiform gyrus is implicated in the processing of high-level visual functions (36). Evidence from some fMRI studies supported the hypothesis that episodic memory performance is linked to the anterior hippocampus, while spatial memory performance is associated with the posterior hippocampus (47, 48). In addition, we found that bed-wetting duration time was negatively correlated with RSFC for the left cHipp with right fusiform gyrus in the PNE group. Thus, we inferred that the left cHipp might play a different role in the cognitive deficit of PNE children. In a prospective study, short-term memory improved after desmopressin treatment in children with PNE (49), indicating the action of desmopressin treatment on the central nervous system, not simply on the kidney. The central vasopressin receptors are abundantly expressed in the hippocampus (50). These findings may provide additional evidence to confirm that the hippocampus is involved in cognitive deficit in children with PNE. For another thing, the supplementary motor area is mainly related to motor-related functions as well as speech and language processing (51). Interestingly, bed-wetting is associated with neuromotor and language development (45, 52).

In this study, there were no significant results based on the right rHipp and cHipp seeds after multiple comparison corrections. This might result from left-right hemispheric differences of the hippocampus. A meta-analysis study found intra- and interhemispheric differences in anterior and posterior functional and structural connectivity, between the right and left hippocampi (53). However, further study is needed to explore the varying functions of the right and left hippocampi. Based on our results, the abnormal brain areas are not simply related to micturition control in children with PNE but are also associated with cognition, emotion, neuromotor, and language development. Thus, we inferred that PNE might be related to brain cognitive and emotional change which has also been proved by many other studies. Sleep is strongly associated with vigilant attention (54), memory (55), emotion regulation (56), and academic performance (57). It is well established that sleep

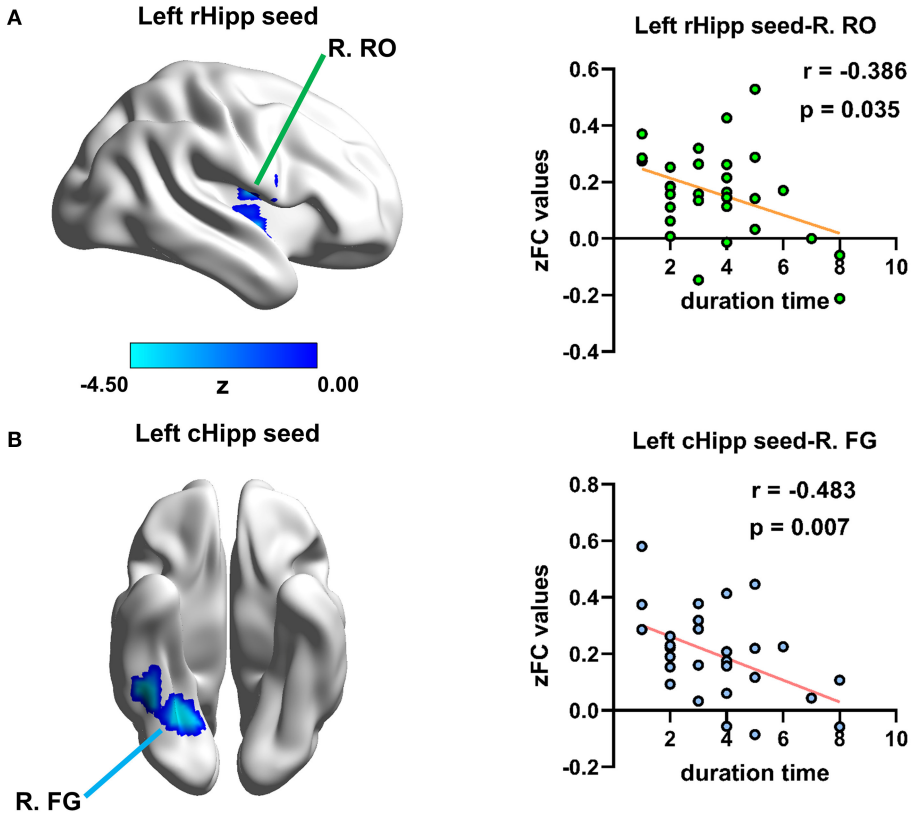

FIGURE 5
Relationship between disease duration time and altered RSFC values in children with PNE. Disease duration time was negatively correlated with RSFC of **(A)** the left rHipp with right Rolandic operculum and **(B)** the left cHipp with right fusiform gyrus in the PNE group, respectively. rHipp, rostral hippocampus; cHipp, caudal hippocampus; PNE, primary nocturnal enuresis; R. RO, right Rolandic operculum; R. FG, right fusiform gyrus; color bar, z value.

problems, such as sleep fragmentation and daytime sleepiness, are more common in children with PNE (58). Children with PNE often suffer from poor sleep quality (59). In many cases, sleep on the one hand, and developmental delay on the other, have led to mild cognitive, memory, and emotion disturbance in children with PNE. In this study, we indicated that bed-wetting duration time was negatively correlated with RSFC for the left rHipp with right Rolandic operculum and the left cHipp with right fusiform gyrus in the PNE group, respectively. Based on previous literature, persistent bed-wetting might harm children's brain function and corresponding behavior. The present study offered more evidence for the link between PNE and brain function, the brain function might get worse with PNE duration time increased. In the ROC analysis, results of RSFC based on hippocampal subregions obtained significant performance, suggesting that these RSFC values might be used as potential neuroimaging marks to distinguish children with PNE from HCs, or potential predictive factors of therapeutic effectiveness. Further studies are warranted to combine these crucial indices to achieve a higher prediction precision.

The strengths of our study include two sides. First, it is novel to explore the RSFC patterns of hippocampus in children with PNE. Second, merely focusing on some proven brain regions may limit our knowledge of the brain basis of PNE, our study provided a new insight into PNE-related deficits. The growing knowledge may continue to expand the pathological model of PNE. Nevertheless, there are some limitations in this study which need to be addressed in the future. First, the relatively small sample size might reduce the statistical power of our results and therefore more participants need to be included for validating our findings in later research. Second, the collected clinical data were relatively few, especially in detailed behavior assessment, that may limit our comprehensive analysis on relationship between brain and behavior in children with PNE. Third, we only selected four parts of hippocampus as seeds, but this is not a very delicate anatomical segmentation, and as such it could have been missed out some important information. The more refined parceling methods should be considered in future studies. Fourth, confounders such as age, gender, emotion status, and bladder volume were not taken into account for the

correlation analysis. Fifth, we only explored a simple correlation between brain and clinical information in children with PNE, but the causality could not be determined.

Conclusion

In this study, we examined the RSFC patterns of hippocampal subregions in children with PNE, which is the first attempt to our knowledge. The findings indicated that children with PNE may have potential dysfunctions in the limbic network, sensorimotor network, DMN, and frontoparietal network, which may become less efficient when bed-wetting persists without timely treatment, inducing impairments in brain-bladder control, cognition, memory, and emotion. Further prospective research with ongoing observation of brain imaging, bladder function, cognition, memory, and emotion is warranted.

Data availability statement

The raw data supporting the conclusions of this article will be made available by the authors, without undue reservation.

Ethics statement

The studies involving human participants were reviewed and approved by the IRB of Shanghai Children's Medical Center, School of Medicine, Shanghai Jiao Tong University. Written informed consent to participate in this study was provided by the participants' legal guardian/next of kin.

Author contributions

JM, SZ, LZ, and XD co-designed this study. SZ and LZ completed all data analysis relevant to this work and drafted the initial manuscript. MW, JS, and YM acquired the data. XD and JM revised the manuscript. All authors reviewed and approved the final manuscript. All authors contributed to the article and approved the submitted version.

Funding

This work was supported by grants from the Science and Technology Commission of Shanghai Municipality (20ZR1434700) and the National Natural Science Foundation of China (81901720 and 62001292).

Conflict of interest

The authors declare that the research was conducted in the absence of any commercial or financial relationships that could be construed as a potential conflict of interest.

Publisher's note

References

1. Austin PF, Bauer SB, Bower W, Chase J, Franco I, Hoebeke P, et al. The standardization of terminology of lower urinary tract function in children and adolescents: update report from the standardization committee of the International Children's Continence Society. *Neurourol Urodyn.* (2016) 35:471–81. doi: 10.1002/nau.22751

2. Gontard AV, Kuwertz-Bröking E. The diagnosis and treatment of enuresis and functional daytime urinary incontinence. *Dtsch Arztebl Int.* (2019) 116:279–85. doi: 10.3238/arztebl.2019.0279

3. Nevéus T, Fonseca E, Franco I, Kawauchi A, Kovacevic L, Nieuwhof-Leppink A, et al. Management and treatment of nocturnal enuresis-an updated standardization document from the International Children's Continence Society. *J Pediatr Urol.* (2020) 16:10–9. doi: 10.1016/j.jpurol.2019.12.020

4. Caldwell PH, Deshpande AV, Von Gontard A. Management of nocturnal enuresis. *BMJ.* (2013) 347:f6259. doi: 10.1136/bmj.f6259

5. Robson WL. Clinical practice. Evaluation and management of enuresis. *N Engl J Med.* (2009) 360:1429–36. doi: 10.1056/NEJMcp0808009

6. Pedersen MJ, Rittig S, Jennum PJ, Kamperis K. The role of sleep in the pathophysiology of nocturnal enuresis. *Sleep Med Rev.* (2020) 49:101228. doi: 10.1016/j.smrv.2019.101228

7. Dang J, Tang Z. Pathogenesis and brain functional imaging in nocturnal enuresis: a review. *Exp Biol Med.* (2021) 246:1483–90. doi: 10.1177/1535370221997363

8. Kitta T, Mitsui T, Kanno Y, Chiba H, Moriya K, Shinohara N. Brain-bladder control network: the unsolved 21st century urological mystery. *Int J Urol.* (2015) 22:342–8. doi: 10.1111/iju.12721

9. Lei D, Ma J, Du X, Shen G, Tian M, Li G. Spontaneous brain activity changes in children with primary monosymptomatic nocturnal enuresis: a resting-state fMRI study. *Neurourol Urodyn.* (2012) 31:99–104. doi: 10.1002/nau.21205

10. Wang M, Zhang A, Zhang J, Lu H, Xu S, Qin Z, et al. Morphometric magnetic resonance imaging study in children with primary monosymptomatic nocturnal enuresis. *Front Pediatr.* (2018) 6:103. doi: 10.3389/fped.2018.00103

11. Griffiths D. Neural control of micturition in humans: a working model. *Nat Rev Urol.* (2015) 12:695–705. doi: 10.1038/nrurol.2015.266

12. Kuhtz-Buschbeck JP, Gilster R, van der Horst C, Hamann M, Wolff S, Jansen O. Control of bladder sensations: an fMRI study of brain activity and effective connectivity. *Neuroimage.* (2009) 47:18–27. doi: 10.1016/j.neuroimage.2009.04.020

13. Harshaw C. Interoceptive dysfunction: toward an integrated framework for understanding somatic and affective disturbance in depression. *Psychol Bull.* (2015) 141:311–63. doi: 10.1037/a0038101

14. Knierim JJ. The hippocampus. *Curr Biol.* (2015) 25:R1116–21. doi: 10.1016/j.cub.2015.10.049

15. Zeidman P, Maguire EA. Anterior hippocampus: the anatomy of perception, imagination and episodic memory. *Nat Rev Neurosci.* (2016) 17:173–82. doi: 10.1038/nrn.2015.24

16. Griffiths D, Tadic SD. Bladder control, urgency, and urge incontinence: evidence from functional brain imaging. *Neurourol Urodyn.* (2008) 27:466–74. doi: 10.1002/nau.20549

17. Matsuura S, Kakizaki H, Mitsui T, Shiga T, Tamaki N, Koyanagi T. Human brain region response to distention or cold stimulation of the bladder: a positron emission tomography study. *J Urol.* (2002) 168:2035–9. doi: 10.1016/S0022-5347(05)64290-5

18. Tai C, Wang J, Jin T, Wang P, Kim SG, Roppolo JR, et al. Brain switch for reflex micturition control detected by FMRI in rats. *J Neurophysiol.* (2009) 102:2719–30. doi: 10.1152/jn.00700.2009

19. Grill WM, Erokwu BO, Hadziefendic S, Haxhiu MA. Extended survival time following pseudorabies virus injection labels the suprapontine neural network controlling the bladder and urethra in the rat. *Neurosci Lett.* (1999) 270:63–6. doi: 10.1016/S0304-3940(99)00462-0

20. Zhang K, Ma J, Lei D, Wang M, Zhang J, Du X. Task positive and default mode networks during a working memory in children with primary monosymptomatic nocturnal enuresis and healthy controls. *Pediatr Res.* (2015) 78:422–9. doi: 10.1038/pr.2015.120

21. Yu B, Guo Q, Fan G, Ma H, Wang L, Liu N. Evaluation of working memory impairment in children with primary nocturnal enuresis: evidence from event-related functional magnetic resonance imaging. *J Paediatr Child Health.* (2011) 47:429–35. doi: 10.1111/j.1440-1754.2010.02000.x

22. Lei D, Ma J, Du X, Shen G, Tian M, Li G. Altered brain activation during response inhibition in children with primary nocturnal enuresis: an fMRI study. *Hum Brain Mapp.* (2012) 33:2913–9. doi: 10.1002/hbm.21411

23. Yu B, Sun H, Ma H, Peng M, Kong F, Meng F, et al. Aberrant whole-brain functional connectivity and intelligence structure in children with primary nocturnal enuresis. *PLoS ONE.* (2013) 8:e51924. doi: 10.1371/journal.pone.0051924

24. Wang M, Zhang A, Qin Z, Xu S, Ban S, Zhang J, et al. Abnormal neural responses to emotional stimuli in children with primary monosymptomatic nocturnal enuresis. *Eur Child Adolesc Psychiatry.* (2019) 28:949–56. doi: 10.1007/s00787-018-1255-4

25. Fanselow MS, Dong HW. Are the dorsal and ventral hippocampus functionally distinct structures? *Neuron.* (2010) 65:7–19. doi: 10.1016/j.neuron.2009.11.031

26. Xiao H, Yuan M, Li H, Li S, Du Y, Wang M, et al. Functional connectivity of the hippocampus in predicting early antidepressant efficacy in patients with major depressive disorder. *J Affect Disord.* (2021) 291:315–21. doi: 10.1016/j.jad.2021.05.013

27. Cao X, Liu Z, Xu C, Li J, Gao Q, Sun N, et al. Disrupted resting-state functional connectivity of the hippocampus in medication-naïve patients with major depressive disorder. *J Affect Disord.* (2012) 141:194–203. doi: 10.1016/j.jad.2012.03.002

28. Gangadin SS, Cahn W, Scheewe TW, Hulshoff Pol HE, Bossong MG. Reduced resting state functional connectivity in the hippocampus-midbrain-striatum network of schizophrenia patients. *J Psychiatr Res.* (2021) 138:83–8. doi: 10.1016/j.jpsychires.2021.03.041

29. Zhou Y, Shu N, Liu Y, Song M, Hao Y, Liu H, et al. Altered resting-state functional connectivity and anatomical connectivity of hippocampus in schizophrenia. *Schizophr Res.* (2008) 100:120–32. doi: 10.1016/j.schres.2007.11.039

30. Lazarov A, Zhu X, Suarez-Jimenez B, Rutherford BR, Neria Y. Resting-state functional connectivity of anterior and posterior hippocampus in posttraumatic stress disorder. *J Psychiatr Res.* (2017) 94:15–22. doi: 10.1016/j.jpsychires.2017.06.003

31. Jia X-Z, Wang J, Sun H-Y, Zhang H, Liao W, Wang Z, et al. RESTplus: an improved toolkit for resting-state functional magnetic resonance imaging data processing. *Sci Bull.* (2019) 64:953–4. doi: 10.1016/j.scib.2019.05.008

32. Friston KJ, Williams S, Howard R, Frackowiak RS, Turner R. Movement-related effects in fMRI time-series. *Magn Reson Med.* (1996) 35:346–55. doi: 10.1002/mrm.1910350312

33. Fan L, Li H, Zhuo J, Zhang Y, Wang J, Chen L, et al. The human brainnetome atlas: a new brain atlas based on connectional architecture. *Cereb Cortex.* (2016) 26:3508–26. doi: 10.1093/cercor/bhw157

34. Fluss R, Faraggi D, Reiser B. Estimation of the Youden Index and its associated cutoff point. *Biom J.* (2005) 47:458–72. doi: 10.1002/bimj.200410135

35. Power JD, Mitra A, Laumann TO, Snyder AZ, Schlaggar BL, Petersen SE. Methods to detect, characterize, and remove motion artifact in resting state fMRI. *Neuroimage.* (2014) 84:320–41. doi: 10.1016/j.neuroimage.2013.08.048

36. Weiner KS, Zilles K. The anatomical and functional specialization of the fusiform gyrus. *Neuropsychologia.* (2016) 83:48–62. doi: 10.1016/j.neuropsychologia.2015.06.033

37. Lech RK, Güntürkün O, Suchan B. An interplay of fusiform gyrus and hippocampus enables prototype- and exemplar-based category learning. *Behav Brain Res.* (2016) 311:239–46. doi: 10.1016/j.bbr.2016.05.049

38. Triarhou LC. Cytoarchitectonics of the Rolandic operculum: morphofunctional ponderings. *Brain Struct Funct.* (2021) 226:941–50. doi: 10.1007/s00429-021-02258-z

39. Li D, Liu R, Meng L, Xiong P, Ren H, Zhang L, et al. Abnormal ventral somatomotor network homogeneity in patients with temporal lobe epilepsy. *Front Psychiatry.* (2022) 13:877956. doi: 10.3389/fpsyt.2022.877956

40. Sutoko S, Atsumori H, Obata A, Funane T, Kandori A, Shimonaga K, et al. Lesions in the right Rolandic operculum are associated with self-rating affective and apathetic depressive symptoms for post-stroke patients. *Sci Rep.* (2020) 10:20264. doi: 10.1038/s41598-020-77136-5

41. Ugur HC, Kahilogullari G, Coscarella E, Unlu A, Tekdemir I, Morcos JJ, et al. Arterial vascularization of primary motor cortex (precentral gyrus). *Surg Neurol.* (2005) 64 (Suppl. 2):S48–52. doi: 10.1016/j.surneu.2005.07.049

42. Zhang A, Zhang L, Wang M, Zhang Y, Jiang F, Jin X, et al. Functional connectivity of thalamus in children with primary nocturnal enuresis: results from a resting-state fMRI study. *Brain Imaging Behav.* (2021) 15:355–63. doi: 10.1007/s11682-020-00262-1

43. Sanes JN, Donoghue JP. Plasticity and primary motor cortex. *Annu Rev Neurosci.* (2000) 23:393–415. doi: 10.1146/annurev.neuro.23.1.393

44. von Gontard A, Freitag CM, Seifen S, Pukrop R, Röhling D. Neuromotor development in nocturnal enuresis. *Dev Med Child Neurol.* (2006) 48:744–50. doi: 10.1017/S0012162206001599

45. Esposito M, Gallai B, Parisi L, Roccella M, Marotta R, Lavano SM, et al. Visuomotor competencies and primary monosymptomatic nocturnal enuresis in prepubertal aged children. *Neuropsychiatr Dis Treat.* (2013) 9:921–6. doi: 10.2147/NDT.S46772

46. Wang J, Xie S, Guo X, Becker B, Fox PT, Eickhoff SB, et al. Correspondent functional topography of the human left inferior parietal lobule at rest and under task revealed using resting-state fMRI and coactivation based parcellation. *Hum Brain Mapp.* (2017) 38:1659–75. doi: 10.1002/hbm.23488

47. Persson J, Stening E, Nordin K, Söderlund H. Predicting episodic and spatial memory performance from hippocampal resting-state functional connectivity: evidence for an anterior-posterior division of function. *Hippocampus.* (2018) 28:53–66. doi: 10.1002/hipo.22807

48. Kühn S, Gallinat J. Segregating cognitive functions within hippocampal formation: a quantitative meta-analysis on spatial navigation and episodic memory. *Hum Brain Mapp.* (2014) 35:1129–42. doi: 10.1002/hbm.22239

49. Müller D, Florkowski H, Chavez-Kattau K, Carlsson G, Eggert P. The effect of desmopressin on short-term memory in children with primary nocturnal enuresis. *J Urol.* (2001) 166:2432–4. doi: 10.1016/S0022-5347(05)65609-1

50. Zagrean AM, Georgescu IA, Iesanu MI, Ionescu RB, Haret RM, Panaitescu AM, et al. Oxytocin and vasopressin in the hippocampus. *Vitam Horm.* (2022) 118:83–127. doi: 10.1016/bs.vh.2021.11.002

51. Hertrich I, Dietrich S, Ackermann H. The role of the supplementary motor area for speech and language processing. *Neurosci Biobehav Rev.* (2016) 68:602–10. doi: 10.1016/j.neubiorev.2016.06.030

52. Touchette E, Petit D, Paquet J, Tremblay RE, Boivin M, Montplaisir JY. Bed-wetting and its association with developmental milestones in early childhood. *Arch Pediatr Adolesc Med.* (2005) 159:1129–34. doi: 10.1001/archpedi.159.12.1129

53. Robinson JL, Salibi N, Deshpande G. Functional connectivity of the left and right hippocampi: evidence for functional lateralization along the long-axis using meta-analytic approaches and ultra-high field functional neuroimaging. *Neuroimage.* (2016) 135:64–78. doi: 10.1016/j.neuroimage.2016.04.022

54. Hudson AN, Van Dongen HPA, Honn KA. Sleep deprivation, vigilant attention, and brain function: a review. *Neuropsychopharmacology.* (2020) 45:21–30. doi: 10.1038/s41386-019-0432-6

55. Klinzing JG, Niethard N, Born J. Mechanisms of systems memory consolidation during sleep. *Nat Neurosci.* (2019) 22:1598–610. doi: 10.1038/s41593-019-0467-3

56. Palmer CA, Alfano CA. Sleep and emotion regulation: an organizing, integrative review. *Sleep Med Rev.* (2017) 31:6–16. doi: 10.1016/j.smrv.2015.12.006

57. Seoane HA, Moschetto L, Orliacq F, Orliacq J, Serrano E, Cazenave MI, et al. Sleep disruption in medicine students and its relationship with impaired academic performance: a systematic review and meta-analysis. *Sleep Med Rev.* (2020) 53:101333. doi: 10.1016/j.smrv.2020.101333

58. Cohen-Zrubavel V, Kushnir B, Kushnir J, Sadeh A. Sleep and sleepiness in children with nocturnal enuresis. *Sleep.* (2011) 34:191–4. doi: 10.1093/sleep/34.2.191

59. Üçer O, Gümüş B. Quantifying subjective assessment of sleep quality, quality of life and depressed mood in children with enuresis. *World J Urol.* (2014) 32:239–43. doi: 10.1007/s00345-013-1193-1

frontiers | Frontiers in Psychiatry

TYPE Original Research
PUBLISHED 06 September 2022
DOI 10.3389/fpsyt.2022.960294

OPEN ACCESS

EDITED BY
Chien-Han Lai,
National Yang-Ming University, Taiwan

REVIEWED BY
Weizhao Lu,
Shandong First Medical University, China
Deepak Gupta,
National Institute of Technology, Arunachal Pradesh, India

*CORRESPONDENCE
Shihong Xiong
215961973@qq.com
Hongwei Ren
14214949@qq.com
Yujun Gao
gaoyujun19820214@163.com

†These authors have contributed equally to this work and share first authorship

SPECIALTY SECTION
This article was submitted to Neuroimaging and Stimulation, a section of the journal Frontiers in Psychiatry

RECEIVED 02 June 2022
ACCEPTED 08 August 2022
PUBLISHED 06 September 2022

CITATION
Lin H, Xiang X, Huang J, Xiong S, Ren H and Gao Y (2022) Abnormal degree centrality values as a potential imaging biomarker for major depressive disorder: A resting-state functional magnetic resonance imaging study and support vector machine analysis. *Front. Psychiatry* 13:960294. doi: 10.3389/fpsyt.2022.960294

Abnormal degree centrality values as a potential imaging biomarker for major depressive disorder: A resting-state functional magnetic resonance imaging study and support vector machine analysis

Hang Lin[1,2†], Xi Xiang[3†], Junli Huang[4†], Shihong Xiong[5*], Hongwei Ren[4*] and Yujun Gao[1,6*]

[1]Department of Psychiatry, Tianyou Hospital Affiliated to Wuhan University of Science and Technology, Wuhan, China, [2]Key Laboratory of Occupational Hazards and Identification, Wuhan University of Science and Technology, Wuhan, China, [3]Department of Spine and Orthopedics, Tianyou Hospital Affiliated to Wuhan University of Science and Technology, Wuhan, China, [4]Department of Medical Imaging, Tianyou Hospital Affiliated to Wuhan University of Science and Technology, Wuhan, China, [5]Department of Nephrology, Tianyou Hospital Affiliated to Wuhan University of Science and Technology, Wuhan, China, [6]Department of Psychiatry, Renmin Hospital of Wuhan University, Wuhan, China

Objective: Previous studies have revealed abnormal degree centrality (DC) in the structural and functional networks in the brains of patients with major depressive disorder (MDD). There are no existing reports on the DC analysis method combined with the support vector machine (SVM) to distinguish patients with MDD from healthy controls (HCs). Here, the researchers elucidated the variations in DC values in brain regions of MDD patients and provided imaging bases for clinical diagnosis.

Methods: Patients with MDD (N = 198) and HCs (n = 234) were scanned using resting-state functional magnetic resonance imaging (rs-fMRI). DC and SVM were applied to analyze imaging data.

Results: Compared with HCs, MDD patients displayed elevated DC values in the vermis, left anterior cerebellar lobe, hippocampus, and caudate, and depreciated DC values in the left posterior cerebellar lobe, left insula, and right caudate. As per the results of the SVM analysis, DC values in the left anterior cerebellar lobe and right caudate could distinguish MDD from HCs with accuracy, sensitivity, and specificity of 87.71% (353/432), 84.85% (168/198), and 79.06% (185/234), respectively. Our analysis did not reveal

any significant correlation among the DC value and the disease duration or symptom severity in patients with MDD.

Conclusion: Our study demonstrated abnormal DC patterns in patients with MDD. Aberrant DC values in the left anterior cerebellar lobe and right caudate could be presented as potential imaging biomarkers for the diagnosis of MDD.

KEYWORDS

major depressive disorder, rest state fMRI, degree centrality, support vector machine, biomarker

Highlights

- The support vector machine (SVM) was used to differentiate between major depressive disorder (MDD) and healthy controls.
- Patients with MDD reported abnormalities in brain scans.
- The left cerebellum anterior and right caudate were the potential specific biological imaging markers for patients with MDD.

Introduction

Major depressive disorder (MDD), a well-researched psychiatric disorder, occurs with a high rate of disability, which presents a primary cause of the economic burden throughout the world (1). As per the World Health Organization report in 2017, about 322 million people suffer from depression, ranking second in the world's disease burden and growing to the largest in 2030 (2). Despite the tremendous burden brought by MDD, the existing studies have not found useful diagnostic markers.

Previous neurological imaging studies have implicated functional and structural aberrations in patients with MDD. However, different neuroimaging features between various investigations have been identified. Structural brain imaging studies show the lesser gray-matter volume in the insula and various subcortical and medial temporal regions, including the left sides of the caudate, hippocampus, parahippocampal gyrus, and cerebellar areas of patients with MDD (3). Also, hippocampal structural reductions have been tied explicitly to MDD illness progression (4). The common analysis methods of functional brain imaging include regional homogeneity (ReHo), low-frequency fluctuation (ALFF), and functional connectivity (FC). Previous research found elevated FC values in the bilateral parietal and left occipital regions (5) and depreciated resting-state functional connectivity (rsFC) between the left superior frontal gyrus and hippocampus (6). Besides, MDD patients showed elevated ALFF in the right superior frontal gyrus (SFG) and depreciated ALFF in the bilateral precuneus, bilateral cerebellum, and left occipital cortex (7). Geng et al. found elevated ReHo in the bilateral parahippocampal gyrus and left lingual gyrus but depreciated in the right middle frontal gyrus in patients with depressive disorders who showed somatic symptoms (8). These studies revealed abnormalities in brain function in patients with MDD. However, ALLF and ReHo reflect local brain activity and do not show the functional connection between different brain regions. When abnormal FC exists between two brain regions, the FC analysis method is challenging to determine the anomalous brain region. Our study aimed to use the technique of degree centrality (DC) to detect resting state functional connections in patients with MDD.

DC takes into account the relationship of a given region with that of the entire functional connectome and not just its relation to individual areas or separate more significant components (9). The DC analysis method completes functional connectivity across the brain and shows brain regions with abnormal signals. Previous studies have demonstrated the applicability of the DC analysis method to elucidate abnormalities in brain networks in different psychiatric and neurologic disorders. For instance, elevated levels of DC were identified in the schizophrenia group in the right inferior parietal lobule/angular gyrus relative to the HCs (10). However, the tinnitus patients showed elevated DC in the left inferior parietal gyrus and depreciated DC in the left precuneus within the dorsal attention network (11). This lack of consistency could be attributed to variations in disease characteristics or symptoms. It could also suggest aberrant brain activity that could be reflected in modifications in DC values. In addition, the abnormality of the DC value was also found in the research on MDD (12, 13). However, few researchers have combined DC and support vector machine (SVM) methods in studies of MDD.

SVM can be used as a rigorous machine learning methodology working by constructing a hyperplane that separates the samples based on the maximum margin approach (14). It could be used to predict psychosis based on neuroanatomical biomarkers. Compared with other machine learning methods such as artificial neural networks, SVM can successfully solve high dimensional and local minimum problems with better generalization. Therefore, SVM is widely

used to distinguish patients with epilepsy (15), Tourette syndrome (16), schizophrenia (17), and MDD (18) from HCs. This study investigated DC values in patients with MDD, studied brain areas with modified DC values, and described the regions as probable neurological imaging markers *via* the SVM method. We hypothesized that DC in patients with MDD might be abnormal, and SVM might screen out the most valuable brain regions for diagnosing MDD.

Materials and methods

Subjects

In this study, one hundred ninety-eight patients with MDD were selected from the Department of Psychiatry at the Tianyou Hospital, affiliated with the Wuhan University of Science and Technology. We applied a 17-item Hamilton Rating Scale for Depression (HRSD-17) to understand the severity of the depressive state of a patient, as per the Diagnostic and Statistical Manual of Mental Disorders, fourth edition (DSM-IV). Two psychiatrists completed the diagnosis. Two hundred thirty-four healthy controls (HCs) matched with the experimental group, including age, gender, and years of education, were recruited. HCs were repeatedly screened to exclude any background of mental illness.

The exclusion criteria for subjects were as follows: (1) subjects showing symptoms complying with the symptoms of other psychiatric disorders meeting DSM-IV diagnostic criteria, such as schizophrenia, anxiety disorders, and bipolar disorder; (2) past or present significant physical diseases, such as cardiovascular disease or diabetes; (3) a history of head injury or other neurologic diseases; (4) pregnancy; (5) contraindications for MRI scan. (6) Left-handedness.

The ethics committee of Tianyou Hospital, affiliated with the Wuhan University of science and technology, sanctioned the study protocol. Written informed consent was obtained from all study subjects.

Image acquisition

MRI scans were obtained using the Ingenia 3.0 T (Philips, Amsterdam, The Netherlands). The scanner noise was minimized using earplugs; the head motion was reduced using foam padding. Patients were required to stay conscious and relax. High-resolution 3D T1-weighted structural images were acquired with following parameters: echo time (TE) = 3.2 ms; repetition time (TR) = 7.2 ms; field of view (FOV) = 256 mm × 256 mm; flip angle (FA) = 7°. RS blood-oxygen-level-dependent (BOLD) fMRI data were obtained with the following parameters: FOV = 220 mm × 220 mm; TE = 30 ms; TR = 2021 ms; FA = 90°; slice thickness = 3.5 mm.

Imaging preprocessing

Resting state data were preprocessed using DPABI[1] on MATLAB 2013b. The first five time points were discarded until the subjects became accustomed to the scanner's noise. The remaining images were slice-time-corrected and spatially realigned for head motion. We estimated the translation volume in each direction and individual axial rotation to elucidate head motion parameters. The BOLD data for each subject were within the defined motion threshold (The translation threshold was set to ± 2 mm, while the rotation threshold was limited to ± 2°). Spatial normalization of the functional images was done using echo-planar imaging sequence templates. We performed linear detrending and filtering (0.01–0.08 Hz) of all images to reduce the high-pitch respiratory and cardiac noises. We performed regression analysis to remove the white matter signal, the head motion parameters, and the cerebrospinal fluid signal, followed by removing the linear trends.

Degree centrality analysis

DC is a theory-based graph method to elucidate the connection degree between each node and other nodes in the network. The REST[2] software calculated the voxel-based DC value of the whole brain gray matter. We calculated the Pearson correlation coefficient between the bold time processes of all voxel pairs. For a given voxel, DC is calculated as the sum of positive functional connections between this voxel and all other voxels in the gray matter above the threshold of 0.25 (19), and then the individual voxelwise DC was converted into a Z-score map. Finally, the resulting DC maps were spatially smoothed with a 6-mm full width at half-maximum (FWHM) Gaussian kernel (detailed information can be found in **Supplementary Material**).

Statistical analysis

SPSS v22.0 software was used to compare clinical data and demographic data. The age, HRSD score, and years of education of the two groups were compared by two-sample *t*-test, and the gender distribution was analyzed by chi-square test. To explore the difference of DC between MDD patients and HCs, a voxel-by-voxel two-sample *t*-test was performed. The significance threshold was set at $p < 0.01$ and Gaussian random field theory (GRF) was employed to correct multiple comparisons through using REST at $p < 0.05$ (voxel

1 http://rfmri.org/dpabi

2 http://www.restfmri.net/

significance: $p < 0.001$, cluster significance: $p < 0.05$). The abovementioned *t*-tests were performed with gender, age, and years of education as covariates as these factors may confound the results (2, 12).

Classification analyses

The SVM method has been diffusely applied in disease diagnosis for neuropsychosis (15, 18, 20). Running the LIBSVM[3] software package in MATLAB, the SVM methodology was used to test the sensitivity, accuracy, and effectiveness of using DC values identified in abnormal brain regions to distinguish MDD from HCs (detailed information can be found in **Supplementary Material**).

Results

Clinical characteristics of major depressive disorder and healthy controls

The clinical data of MDD and HCs are shown in **Table 1**. No significant intergroup differences were observed in age, gender, and education ($p > 0.01$). The HRSD scores of MDD groups were substantially higher than those of the HCs group ($p < 0.01$).

Degree centrality analysis

As shown in **Table 2** and **Figure 1**, the main results reported were based on the DC analysis. According to a two-sample *t*-test, compared with HCs, MDD displayed elevated DC in the left anterior cerebellar lobe, vermis, left hippocampus, left caudate, and depreciated DC in the left posterior cerebellar lobe, left insula, and right caudate.

Discriminating patients with major depressive disorder from healthy controls

We use SVM to distinguish MDD and HCs. As per the results, DC values in the left cerebellar anterior lobe and right caudate can distinguish MDD from healthy subjects with high accuracy, specificity, and sensitivity of 87.71% (353/432), 84.85% (168/198), and 79.06% (185/234), respectively (**Figure 2**).

3 https://www.csie.ntu.edu.tw/~cjlin/

TABLE 1 Demographic and clinical characteristics.

Characteristics	Patients ($n = 198$)	HCs ($n = 234$)	*P-values*
Gender (men/women)	198 (102/96)	234 (130/104)	0.401
Age, years	28.01 ± 7.442	27.87 ± 6.492	0.832
Years of education, years	12.05 ± 3.325	12.55 ± 2.931	0.100
HRSD-17	23.63 ± 2.547		

The *p-value* for the gender distribution was obtained by the Chi-square test. The other p-values were obtained by two sample t-tests.
HCs, healthy controls; HRSD-17, 17-item Hamilton Rating Scale for Depression.

TABLE 2 Significant DC differences across groups.

Cluster location	Peak (MNI)			Number of voxels	*t*-value
	X	Y	Z		
Left cerebellum posterior	−21	−39	−57	40	−8.6051
Left cerebellum anterior	−6	−54	−15	515	9.6958
Vermis	3	−84	−15	78	8.5139
Left hippocampus	−33	−33	3	179	8.8014
Left insula	−24	9	24	246	−8.9089
Left caudate	−6	−3	24	206	10.841
Right caudate	24	0	27	118	−7.8289

DC, degree centrality; MNI, Montreal Neurological Institute.

Discussion

The current diagnosis of MDD relies on the depression scale and the clinicians' subjective analysis, thus, lacking objective imaging methods. We investigated brain network node neutrality changes between MDD and HCs at rest. We found that compared with HCs, the DC values of patients with MDD in the left cerebellum posterior, left insula, and right caudate nucleus depreciated. In contrast, the DC values of the left cerebellum anterior, vermis, left hippocampus, and left caudate were elevated. In addition, the combination of DC values of the left cerebellum anterior and right caudate nucleus, as per the SVM analysis, might be used as potential imaging markers for the diagnosis of MDD.

More attention has been paid to cerebellar function in motor control, ignoring unexplained cognitive or neuropsychiatric phenomena. But studies in recent years have confirmed that the cerebellum participates in cognitive and emotional regulation through polysynaptic connections with different brain functional regions (21–24). For example, reduced lobular VIIA-vmPFC connectivity was significantly associated with impaired verbal working memory performance in depressed patients (25). In emotion regulation, MDD patients needed more vital expression to identify relaxing/positive emotions and sad emotions through slight expression, which implied that patients with MDD exhibited a bias in mood-congruence in facial expression procession. The posterior cerebellar lobe was confirmed to be involved in this dependent process. In

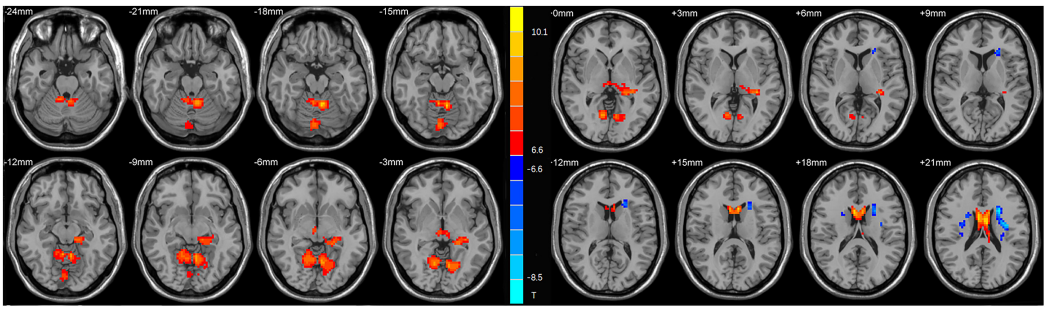

FIGURE 1
Statistical map depicts higher and lower degree centrality (DC) of major depressive disorder (MDD) patients compared with healthy controls (HCs). The threshold was set at $p < 0.01$. Blue denotes lower DC, and red denotes higher DC. The color bar indicates t-values from the two-sample t-test.

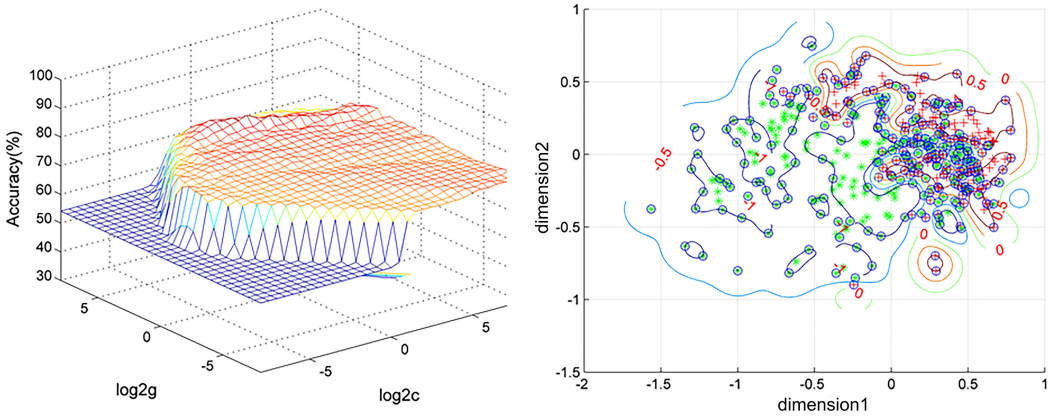

FIGURE 2
Visualization of classifications through support vector machine (SVM) using the combination of the degree centrality (DC) values in the left cerebellum anterior and right caudate. Left: SVM parameter result of 3D view. Right: Dimension 1 and dimension 2 represent the DC values in the left cerebellum anterior and right caudate, respectively. Red crosses represent healthy controls (HCs), and green crosses represent patients with major depressive disorder (MDD).

addition to emotional processing, some studies have shown that the posterior part of crus I and II of lobule VIIA and lobule IX are associated with DMN (26–28). There appears to be a strong correlation between MDD and DMN, a crucial aspect of the neurobiology of MDD, specifically for episodic memory retrieval, self-referential activity, intrinsic attention allocation, and emotional behavior modulation-induced symptoms (29). This further indicates that the cerebellum is critical for the pathophysiological process of MDD. It is noteworthy that most of these experimental results were in the posterior cerebellum. Still, we found abnormal DC values in the anterior cerebellar lobe of patients with MDD by combining them with SVM. This might have been related to the current course of treatment of the patients (30).

In addition, we also found the abnormal DC value in vermis in patients with MDD. Vermis has been found to play a regulatory role on the subcortical nodes of the salience networks (SN) (28). SN plays a crucial role in the bottom-up identification of relevant events to allow for the application of appropriate resources when relevant events are identified (31) and also alters the central executive networks and the default mode. This ability to switch has been confirmed to be impaired in patients with MDD. Therefore, we can infer that vermis regulates the cognitive and emotional function in patients with MDD.

The hippocampus is an important region involved in memory and cognitive function (32), composed of different subregions interacting with varying areas of the brain, resulting in a neuro-anatomical network of emotion regulation and cognitive processing (33). For instance, the hippocampal volume of patients with MDD depreciated substantially (34, 35) and elevated after electroconvulsive therapy (ECT) relative to HCs (36). Moreover, the less posterior-DMN-hippocampal connectivity was correlated to elevated cognitive activity and rumination in MDD (37). Hao et al. also found that different subareas of the hippocampus (including the subiculum and dentate gyrus) were substantially related to MDD (32). As per

our results, an elevated DC value was identified in the left hippocampus in patients with MDD, which confirmed that the hippocampus was involved in the pathogenesis of MDD.

In addition, a decrease in the DC value of the left insula was observed in MDD. The insula is a critical node for integrating external emotional stimuli (38). In previous studies of MDD, the functional activity and connectivity of the insula have been confirmed to be disturbed (39, 40), and gray matter volume also changed (41–43). The left insula is associated with empathy in affective perceptual and cognitive assessment forms (44). These studies reveal the vital role of the left anterior insula in social emotions, such as empathy, which also explains why patients with depression show higher personal pain and lower empathic attention to others when facing emotional situations.

The caudate was coactive with higher-level cognitive areas, such as the rostral anterior cingulate, dorsolateral prefrontal cortex, and inferior frontal gyri (45). The stimulation of the dorsolateral prefrontal cortex elevated neural activity and dopamine release in the caudate nucleus confirming it (46, 47). All these structures are well-known for their role in emotional and cognitive modulation and aberrations in the caudate nucleus in patients with MDD. For example, earlier studies found an abnormal increase in cerebral blood flow (GBF) in the right caudate of depression (48), and FC has a metabolic basis coupled with CBF and the rate of metabolism (49, 50). This indicates that FC in the right caudate is elevated in patients with MDD. In addition, Amiri found that the degree values of ventral caudate were substantially bilaterally higher in treatment-resistant depression (TRD) than in HCs (51). Those were the same as some of our results, indicating abnormalities in the caudate in patients with MDD. We found elevated DC in the left caudate and a decrease in the right caudate of MDD, which was reported for the first time in known studies. The possible explanation is that there are differences in bilateral cerebral hemispheres of MDD. Although this study is a cross-sectional design, we could not provide a reasonable explanation for this result; it presents a new idea for exploring the neural mechanism of MDD.

Limitations

This study had several limitations. First, we did not determine the disease course of patients with MDD (current patients with MDD and remitted patients with MDD). In future studies, we would set stricter exclusion criteria to exclude remission-induced depression. Since this was a cross-sectional study, the structural changes caused by MDD could not be reflected based on the changes in the DC value, so it was necessary to use other calculation methods for further research. Finally, noise could not be eliminated. The patients were requested to keep quiet as much as possible to reduce the error caused by physiological noise.

Conclusion

SVM combined with neuroimaging technology has been widely used in the study of various diseases. For example, Chen et al. found that combining the average ALFF and fall values of the right caudate nucleus and corpus callosum can diagnose MDD [accuracy (79.79%), sensitivity (65.12%), and specificity (92.16%)] (52). Gao et al. found that the combination of increased fALFF in the right precuneus and left superior frontal gyrus (SFG) with a diagnostic accuracy of 76.39% (18). When the sensitivity or specificity is less than 60%, this index may not meet the criteria of "diagnostic markers" (53). Our study found that DC values in the left antenna cerebellar lobe and right caudate could distinguish MDD from HCS with accuracy, sensitivity, and specificity of 87.71% (353/432), 84.85% (168/198), and 79.06% (185/234), respectively. To our knowledge, this study is the first to evaluate the utility of combining abnormal DC values in the left anterior cerebellar lobe and the right caudate nucleus as neuroimaging markers of MDD and provides a new idea for the diagnosis of MDD.

Data availability statement

The raw data supporting the conclusions of this article will be made available by the authors, without undue reservation.

Ethics statement

The studies involving human participants were reviewed and approved by the Ethics Committee of Tianyou Hospital Affiliated to Wuhan University of Science and Technology. The patients/participants provided their written informed consent to participate in this study. Written informed consent was obtained from the individual(s) for the publication of any potentially identifiable images or data included in this article.

Author contributions

HL and XX conceived the project idea. YG implemented the method and performed the experiments. HR and SX supervised the project. JH provided critical suggestions for the design of the experiment. All authors contributed to the article and approved the submitted version.

Funding

This study was supported by the Natural Science Joint Foundation of Hubei Province (grant nos. WJ2019H232

and WJ2019H233), the Health Commission of Hubei Province Scientific Research Project (grant no. 2020CFB512), and the Education Department of Hubei Province Research Project (grant no. B2021022).

Acknowledgments

We appreciate all subjects who served as research participants.

Conflict of interest

The authors declare that the research was conducted in the absence of any commercial or financial relationships that could be construed as a potential conflict of interest.

Publisher's note

Supplementary material

The Supplementary Material for this article can be found online at: https://www.frontiersin.org/articles/10.3389/fpsyt.2022.960294/full#supplementary-material

References

1. Smith K. Mental health: a world of depression. *Nature.* (2014) 515:181. doi: 10.1038/515180a

2. Zhang Q, Shu Y, Li X, Xiong C, Li P, Pang Y, et al. Resting-State functional magnetic resonance study of primary open-angle glaucoma based on voxelwise brain network degree centrality. *Neurosci Lett.* (2019) 712:134500. doi: 10.1016/j.neulet.2019.134500

3. Wise T, Radua J, Via E, Cardoner N, Abe O, Adams TM, et al. Common and distinct patterns of grey-matter volume alteration in major depression and bipolar disorder: evidence from voxel-based meta-analysis. *Mol Psychiatry.* (2017) 22:1455–63. doi: 10.1038/mp.2016.72

4. Belleau EL, Treadway MT, Pizzagalli DA. The impact of stress and major depressive disorder on hippocampal and medial prefrontal cortex morphology. *Biol Psychiatry.* (2019) 85:443–53. doi: 10.1016/j.biopsych.2018.09.031

5. Jiang X, Wang X, Jia L, Sun T, Kang J, Zhou Y, et al. Structural and functional alterations in untreated patients with major depressive disorder and bipolar disorder experiencing first depressive episode: a magnetic resonance imaging study combined with follow-up. *J Affect Disord.* (2021) 279:324–33. doi: 10.1016/j.jad.2020.09.133

6. Chen L, Wang Y, Niu C, Zhong S, Hu H, Chen P, et al. Common and distinct abnormal frontal-limbic system structural and functional patterns in patients with major depression and bipolar disorder. *Neuroimage Clin.* (2018) 20:42–50. doi: 10.1016/j.nicl.2018.07.002

7. Gong J, Wang J, Qiu S, Chen P, Luo Z, Wang J, et al. Common and distinct patterns of intrinsic brain activity alterations in major depression and bipolar disorder: voxel-based meta-analysis. *Transl Psychiatry.* (2020) 10:353. doi: 10.1038/s41398-020-01036-5

8. Geng J, Yan R, Shi J, Chen Y, Mo Z, Shao J, et al. Altered regional homogeneity in patients with somatic depression: a resting-state fmri study. *J Affect Disord.* (2019) 246:498–505. doi: 10.1016/j.jad.2018.12.066

9. Zuo XN, Ehmke R, Mennes M, Imperati D, Castellanos FX, Sporns O, et al. Network centrality in the human functional connectome. *Cereb Cortex.* (2012) 22:1862–75. doi: 10.1093/cercor/bhr269

10. Yu XM, Qiu LL, Huang HX, Zuo X, Zhou ZH, Wang S, et al. Comparison of resting-state spontaneous brain activity between treatment-naive schizophrenia and obsessive-compulsive disorder. *BMC Psychiatry.* (2021) 21:544. doi: 10.1186/s12888-021-03554-y

11. Hu H, Lyu Y, Li S, Yuan Z, Ye C, Han Z, et al. Aberrant resting-state functional connectivity of the dorsal attention network in tinnitus. *Neural Plast.* (2021) 2021:2804533. doi: 10.1155/2021/2804533

12. Zhou W, Yuan Z, Yingliang D, Chaoyong X, Ning Z, Chun W. Differential patterns of dynamic functional connectivity variability in major depressive disorder treated with cognitive behavioral therapy. *J Affect Disord.* (2021) 291:322–8. doi: 10.1016/j.jad.2021.05.017

13. Zeng M, Yu M, Qi G, Zhang S, Ma J, Hu Q, et al. Concurrent alterations of white matter microstructure and functional activities in medication-free major depressive disorder. *Brain Imaging Behav.* (2021) 15:2159–67. doi: 10.1007/s11682-020-00411-6

14. Kumar B, Gupta D. Universum based lagrangian twin bounded support vector machine to classify eeg signals. *Comput Methods Programs Biomed.* (2021) 208:106244. doi: 10.1016/j.cmpb.2021.106244

15. Gao Y, Xiong Z, Wang X, Ren H, Liu R, Bai B, et al. Abnormal degree centrality as a potential imaging biomarker for right temporal lobe epilepsy: a resting-state functional magnetic resonance imaging study and support vector machine analysis. *Neuroscience.* (2022) 487:198–206. doi: 10.1016/j.neuroscience.2022.02.004

16. Zito GA, Hartmann A, Beranger B, Weber S, Aybek S, Faouzi J, et al. Multivariate classification provides a neural signature of tourette disorder. *Psychol Med.* (2021):1–9. doi: 10.1017/S0033291721004232

17. Wang S, Zhang Y, Lv L, Wu R, Fan X, Zhao J, et al. Abnormal regional homogeneity as a potential imaging biomarker for adolescent-onset schizophrenia: a resting-state fmri study and support vector machine analysis. *Schizophr Res.* (2018) 192:179–84. doi: 10.1016/j.schres.2017.05.038

18. Gao Y, Wang X, Xiong Z, Ren H, Liu R, Wei Y, et al. Abnormal fractional amplitude of low-frequency fluctuation as a potential imaging biomarker for first-episode major depressive disorder: a resting-state fmri study and support vector machine analysis. *Front Neurol.* (2021) 12:751400. doi: 10.3389/fneur.2021.751400

19. Li S, Ma X, Huang R, Li M, Tian J, Wen H, et al. Abnormal degree centrality in neurologically asymptomatic patients with end-stage renal disease: a resting-state fmri study. *Clin Neurophysiol.* (2016) 127:602–9. doi: 10.1016/j.clinph.2015.06.022

20. Song Y, Huang C, Zhong Y, Wang X, Tao G. Abnormal reginal homogeneity in left anterior cingulum cortex and precentral gyrus as a potential neuroimaging biomarker for first-episode major depressive disorder. *Front Psychiatry.* (2022) 13:924431. doi: 10.3389/fpsyt.2022.924431

21. Huang M, de Koning TJ, Tijssen MAJ, Verbeek DS. Cross-Disease analysis of depression, ataxia and dystonia highlights a role for synaptic plasticity and the cerebellum in the pathophysiology of these comorbid diseases. *Biochim Biophys Acta Mol Basis Dis.* (2021) 1867:165976. doi: 10.1016/j.bbadis.2020.165976

22. Schmahmann JD. The cerebellum and cognition. *Neurosci Lett.* (2019) 688:62–75. doi: 10.1016/j.neulet.2018.07.005

23. Strick PL, Dum RP, Fiez JA. Cerebellum and nonmotor function. *Annu Rev Neurosci.* (2009) 32:413–34. doi: 10.1146/annurev.neuro.31.060407.125606

24. Tobyne SM, Ochoa WB, Bireley JD, Smith VM, Geurts JJ, Schmahmann JD, et al. Cognitive impairment and the regional distribution of cerebellar lesions in multiple sclerosis. *Mult Scler.* (2018) 24:1687–95. doi: 10.1177/1352458517730132

25. Alalade E, Denny K, Potter G, Steffens D, Wang L. Altered Cerebellar-Cerebral Functional Connectivity in Geriatric Depression. *PLoS One* (2011) 6:e20035. doi: 10.1371/journal.pone.0020035

26. Krienen FM, Buckner RL. Segregated fronto-cerebellar circuits revealed by intrinsic functional connectivity. *Cereb Cortex.* (2009) 19:2485–97. doi: 10.1093/cercor/bhp135

27. Buckner RL, Krienen FM, Castellanos A, Diaz JC, Yeo BT. The organization of the human cerebellum estimated by intrinsic functional connectivity. *J Neurophysiol.* (2011) 106:2322–45. doi: 10.1152/jn.00339.2011

28. Habas C, Kamdar N, Nguyen D, Prater K, Beckmann CF, Menon V, et al. Distinct cerebellar contributions to intrinsic connectivity networks. *J Neurosci.* (2009) 29:8586–94. doi: 10.1523/JNEUROSCI.1868-09.2009

29. Graham J, Salimi-Khorshidi G, Hagan C, Walsh N, Goodyer I, Lennox B, et al. Meta-analytic evidence for neuroimaging models of depression: state or trait? *J Affect Disord.* (2013) 151:423–31. doi: 10.1016/j.jad.2013.07.002

30. Cheng C, Dong D, Jiang Y, Ming Q, Zhong X, Sun X, et al. State-Related alterations of spontaneous neural activity in current and remitted depression revealed by resting-state fmri. *Front Psychol.* (2019) 10:245. doi: 10.3389/fpsyg.2019.00245

31. Wang X, Ongur D, Auerbach RP, Yao S. Cognitive vulnerability to major depression: view from the intrinsic network and cross-network interactions. *Harv Rev Psychiatry.* (2016) 24:188–201. doi: 10.1097/HRP.0000000000000081

32. Hao ZY, Zhong Y, Ma ZJ, Xu HZ, Kong JY, Wu Z, et al. Abnormal resting-state functional connectivity of hippocampal subfields in patients with major depressive disorder. *BMC Psychiatry.* (2020) 20:71. doi: 10.1186/s12888-020-02490-7

33. Shunkai L, Su T, Zhong S, Chen G, Zhang Y, Zhao H, et al. Abnormal dynamic functional connectivity of hippocampal subregions associated with working memory impairment in melancholic depression. *Psychol Med.* (2021):1–13. doi: 10.1017/S0033291721004906

34. Cao B, Luo Q, Fu Y, Du L, Qiu T, Yang X, et al. Predicting individual responses to the electroconvulsive therapy with hippocampal subfield volumes in major depression disorder. *Sci Rep.* (2018) 8:5434. doi: 10.1038/s41598-018-23685-9

35. Cao B, Passos IC, Mwangi B, Amaral-Silva H, Tannous J, Wu MJ, et al. Hippocampal subfield volumes in mood disorders. *Mol Psychiatry.* (2017) 22:1352–8. doi: 10.1038/mp.2016.262

36. Joshi SH, Espinoza RT, Pirnia T, Shi J, Wang Y, Ayers B, et al. Structural plasticity of the hippocampus and amygdala induced by electroconvulsive therapy in major depression. *Biol Psychiatry.* (2016) 79:282–92. doi: 10.1016/j.biopsych.2015.02.029

37. Figueroa CA, Mocking RJT, van Wingen G, Martens S, Ruhe HG, Schene AH. Aberrant default-mode network-hippocampus connectivity after sad memory-recall in remitted-depression. *Soc Cogn Affect Neurosci.* (2017) 12:1803–13. doi: 10.1093/scan/nsx108

38. Sridharan D, Levitin DJ, Menon VA. Critical role for the right fronto-insular cortex in switching between central-executive and default-mode networks. *Proc Natl Acad Sci USA.* (2008) 105:12569–74. doi: 10.1073/pnas.0800005105

39. Sliz D, Hayley S. Major depressive disorder and alterations in insular cortical activity: a review of current functional magnetic imaging research. *Front Hum Neurosci.* (2012) 6:323. doi: 10.3389/fnhum.2012.00323

40. Sprengelmeyer R, Steele JD, Mwangi B, Kumar P, Christmas D, Milders M, et al. The insular cortex and the neuroanatomy of major depression. *J Affect Disord.* (2011) 133:120–7. doi: 10.1016/j.jad.2011.04.004

41. Foland-Ross LC, Sacchet MD, Prasad G, Gilbert B, Thompson PM, Gotlib IH. Cortical thickness predicts the first onset of major depression in adolescence. *Int J Dev Neurosci.* (2015) 46:125–31. doi: 10.1016/j.ijdevneu.2015.07.007

42. Jones EC, Liebel SW, Hallowell ES, Sweet LH. Insula thickness asymmetry relates to risk of major depressive disorder in middle-aged to older adults. *Psychiatry Res Neuroimaging.* (2019) 283:113–7. doi: 10.1016/j.pscychresns.2018.12.011

43. Lai CH, Wu YT. Frontal-Insula gray matter deficits in first-episode medication-naive patients with major depressive disorder. *J Affect Disord.* (2014) 160:74–9. doi: 10.1016/j.jad.2013.12.036

44. Fan Y, Duncan NW, de Greck M, Northoff G. Is there a core neural network in empathy? An Fmri Based Quantitative Meta-Analysis. *Neurosci Biobehav Rev.* (2011) 35:903–11. doi: 10.1016/j.neubiorev.2010.10.009

45. Grahn JA, Parkinson JA, Owen AM. The cognitive functions of the caudate nucleus. *Prog Neurobiol.* (2008) 86:141–55. doi: 10.1016/j.pneurobio.2008.09.004

46. Knoch D, Treyer V, Regard M, Muri RM, Buck A, Weber B. Lateralized and frequency-dependent effects of prefrontal rtms on regional cerebral blood flow. *Neuroimage.* (2006) 31:641–8. doi: 10.1016/j.neuroimage.2005.12.025

47. Strafella AP, Paus T, Barrett J, Dagher A. Repetitive transcranial magnetic stimulation of the human prefrontal cortex induces dopamine release in the caudate nucleus. *J Neurosci.* (2001) 21:RC157.

48. He Z, Sheng W, Lu F, Long Z, Han S, Pang Y, et al. Altered Resting-state cerebral blood flow and functional connectivity of striatum in bipolar disorder and major depressive disorder. *Prog Neuropsychopharmacol Biol Psychiatry.* (2019) 90:177–85. doi: 10.1016/j.pnpbp.2018.11.009

49. Li Z, Zhu Y, Childress AR, Detre JA, Wang Z. Relations between bold fmri-derived resting brain activity and cerebral blood flow. *PLoS One.* (2012) 7:e44556. doi: 10.1371/journal.pone.0044556

50. Riedl V, Bienkowska K, Strobel C, Tahmasian M, Grimmer T, Forster S, et al. Local activity determines functional connectivity in the resting human brain: a simultaneous fdg-pet/fmri study. *J Neurosci.* (2014) 34:6260–6. doi: 10.1523/JNEUROSCI.0492-14.2014

51. Amiri S, Arbabi M, Kazemi K, Parvaresh-Rizi M, Mirbagheri MM. Characterization of brain functional connectivity in treatment-resistant depression. *Prog Neuropsychopharmacol Biol Psychiatry.* (2021) 111:110346. doi: 10.1016/j.pnpbp.2021.110346

52. Chen Q, Bi Y, Zhao X, Lai Y, Yan W, Xie L, et al. Regional amplitude abnormities in the major depressive disorder: a resting-state fmri study and support vector machine analysis. *J Affect Disord.* (2022) 308:1–9. doi: 10.1016/j.jad.2022.03.079

53. Gong Q, Wu Q, Scarpazza C, Lui S, Jia Z, Marquand A, et al. Prognostic prediction of therapeutic response in depression using high-field mr imaging. *Neuroimage.* (2011) 55:1497–503. doi: 10.1016/j.neuroimage.2010.11.079

frontiers | Frontiers in Psychiatry

TYPE Original Research
PUBLISHED 07 September 2022
DOI 10.3389/fpsyt.2022.963634

OPEN ACCESS

EDITED BY
Liang Liang,
Xinjiang Medical University, China

REVIEWED BY
Luke Norman,
King's College London,
United Kingdom
Yingying Tang,
Shanghai Jiao Tong University, China

*CORRESPONDENCE
Kangkang Xue
xuekang08yx@163.com

SPECIALTY SECTION
This article was submitted to Neuroimaging and Stimulation, a section of the journal Frontiers in Psychiatry

RECEIVED 07 June 2022
ACCEPTED 18 August 2022
PUBLISHED 07 September 2022

CITATION
Xue K, Chen J, Wei Y, Chen Y, Han S, Wang C, Zhang Y, Song X and Cheng J (2022) Altered dynamic functional connectivity of auditory cortex and medial geniculate nucleus in first-episode, drug-naïve schizophrenia patients with and without auditory verbal hallucinations. *Front. Psychiatry* 13:963634. doi: 10.3389/fpsyt.2022.963634

Altered dynamic functional connectivity of auditory cortex and medial geniculate nucleus in first-episode, drug-naïve schizophrenia patients with and without auditory verbal hallucinations

Kangkang Xue[1]*, Jingli Chen[1], Yarui Wei[1], Yuan Chen[1], Shaoqiang Han[1], Caihong Wang[1], Yong Zhang[1], Xueqin Song[2] and Jingliang Cheng[1]

[1]Department of Magnetic Resonance Imaging, The First Affiliated Hospital of Zhengzhou University, Zhengzhou, China, [2]Department of Psychiatry, The First Affiliated Hospital of Zhengzhou University, Zhengzhou, China

Background and objective: As a key feature of schizophrenia, auditory verbal hallucination (AVH) is causing concern. Altered dynamic functional connectivity (dFC) patterns involving in auditory related regions were rarely reported in schizophrenia patients with AVH. The goal of this research was to find out the dFC abnormalities of auditory related regions in first-episode, drug-naïve schizophrenia patients with and without AVH using resting state functional magnetic resonance imaging (rs-fMRI).

Methods: A total of 107 schizophrenia patients with AVH, 85 schizophrenia patients without AVH (NAVH) underwent rs-fMRI examinations, and 104 healthy controls (HC) were matched. Seed-based dFC of the primary auditory cortex (Heschl's gyrus, HES), auditory association cortex (AAC, including Brodmann's areas 22 and 42), and medial geniculate nucleus (MGN) was conducted to build a whole-brain dFC diagram, then inter group comparison and correlation analysis were performed.

Results: In comparison to the NAVH and HC groups, the AVH group showed increased dFC from left ACC to the right middle temporal gyrus and right middle occipital gyrus, decreased dFC from left HES to the left superior occipital gyrus, left cuneus gyrus, left precuneus gyrus, decreased dFC from right HES to the posterior cingulate gyrus, and decreased dFC from left MGN to the bilateral calcarine gyrus, bilateral cuneus gyrus, bilateral lingual gyrus. The Auditory Hallucination Rating Scale (AHRS) was significantly positively correlated with the dFC values of cluster 1 (bilateral calcarine gyrus, cuneus gyrus, lingual gyrus, superior occipital gyrus, precuneus gyrus, and posterior cingulate gyrus) using left AAC seed, cluster 2 (right middle temporal gyrus and right middle occipital gyrus) using left AAC seed, cluster 1 (bilateral calcarine gyrus, cuneus gyrus, lingual gyrus, superior occipital gyrus, precuneus gyrus

and posterior cingulate gyrus) using right AAC seed and cluster 2 (posterior cingulate gyrus) using right HES seed in the AVH group. In both AVH and NAVH groups, a significantly negative correlation is also found between the dFC values of cluster 2 (posterior cingulate gyrus) using the right HES seed and the PANSS negative sub-scores.

Conclusions: The present findings demonstrate that schizophrenia patients with AVH showed multiple abnormal dFC regions using auditory related cortex and nucleus as seeds, particularly involving the occipital lobe, default mode network (DMN), and middle temporal lobe, implying that the different dFC patterns of auditory related areas could provide a neurological mechanism of AVH in schizophrenia.

KEYWORDS

schizophrenia, auditory verbal hallucination, auditory cortex, medial geniculate nucleus, dynamic functional connectivity

Introduction

Schizophrenia is a kind of serious mental illness marked by hallucinations, delusions, and behavioral problems (1, 2), which is also described as a "disconnection syndrome" (3). With a prevalence of 60–90%, AVH is a major pathological feature of schizophrenia (4). Schizophrenia patients with AVH can vividly perceive sound without external real acoustic stimulation. The symptoms of AVH can lead to increased stress and dysfunction, and they are even linked to an increased risk of suicide (5). AVH persists after antipsychotic medication treatment in approximately 1/3 of schizophrenia patients with AVH (6, 7). Despite much research focusing on the mechanism of AVH, the results remained inconsistent. Therefore, the underlying neural mechanism of AVH is essential, which can improve our understanding of schizophrenia and guide more specific treatments (8–11).

Various neuropathological mechanism models of AVH have been proposed, among them, the verbal self-monitoring (VSM) model (12, 13) and auditory-related regions activations model (14) are the most concerned. Self-monitoring deficits in schizophrenia, according to the VSM model, are caused by abnormal brain integration impairing the communication of the associative discharge (15, 16). AVH is thought to be caused by aberrant functional connections between auditory and language-related brain areas, and these connectivity are strongly linked to the degree of AVH (17–22). There's also proof of aberrant static functional connectivity (sFC) in the auditory cortex, which is linked to default mode network (DMN) (21, 22). Alderson et al. (4) summarize that sFC in the left superior temporal gyrus is disrupted in schizophrenia patients with AVH and DMN appears atypical connectivity with other resting state networks (RSNs). According to the model of auditory-related regions activations, the abnormal self-activation of the auditory cortex generates auditory signals and transmits them to other areas even without external auditory stimulus, so as to appear auditory hallucinations in patients. Elevated activity in auditory-related areas is linked to AVH, Dierks et al. (23) found that the Broca area and primary auditory cortex were activated when auditory hallucination occurred by comparing the brain activities of the same patient with and without auditory hallucination at rest. Hunter et al. (24) also reported that the auditory cortex was abnormally activated when auditory hallucinations occurred through the study of patients with AVH without mental diseases. Taken together, whether abnormal spontaneous neural activity or connectivity with other regions, the auditory-related regions is of great significance to the AVH.

Auditory-related brain regions include several temporal gyri and nuclei. Combined with the electrophysiological research on primate auditory system and the functional imaging study of human auditory perception, the researchers propose that the sound is first received and preliminarily processed by the primary auditory cortex (Heschl's gyrus, HES), then transmitted to auditory association cortex (AAC, located in Brodmann's areas 22 and 42) for processing, and then transmitted to the higher information processing brain areas through the thalamus (mainly located in the medial geniculate nucleus, MGN) (25–28). Up to now, multiple studies have revealed abnormal activation or functional connectivity of auditory-related brain regions in schizophrenia patients with auditory hallucinations. Previous work has revealed that MGN, AAC and HES have been associated with AVH in schizophrenia (29, 30). Therefore, the study taking HES, AAC, and MGN as seeds will reveal the abnormal connections of auditory-related brain regions in schizophrenic patients with AVH, so as to verify the above hypothesis.

So far, the majority of fMRI studies investigate the mechanism of AVH in schizophrenia by using the method

of sFC, with the assumption that FC between brain regions is constant across the scanning time. However, a growing number of evidence shows the considerable fluctuations in rs-fMRI FC over time. Consequently, as an emerging approach, dynamic FC has been increasingly focused on by recent fMRI research to detect dynamic connectivity patterns throughout the scanning period, and reflect the dynamic characteristics of interregional communication (31–35). Dynamic functional connectivity has been successfully used to distinguish schizophrenia from other mental diseases (36) and classify schizophrenia (37, 38). So far, only a few researchers study the auditory hallucination mechanism of schizophrenia using the dFC method. Some studies underly the whole brain dynamic patterns with ICA, Zhang et al. (39) have manifested that schizophrenia patients with AVH switched among several states using the dFC method, with the aberrant connectivity of language-related areas. However, there is no study on the dFC of the auditory-related regions in schizophrenia with AVH.

In our study, first-episode and drug- naïve schizophrenia patients with and without AVH as well as HCs were recruited. We first investigated voxel-wise dFC between the auditory-related regions (AAC, HES, and MGN) and the whole brain in three groups; Furthermore, in schizophrenia patients with AVH, we analyze the correlation between changed dFC values and symptom indicators. We assumed that schizophrenia patients with AVH may present more or less dynamic FC fluctuation of auditory-related regions throughout scanning duration compared to NAVH and HC groups, which could allow us to understand more about the pathophysiological processes of AVH in schizophrenia.

Materials and methods

Participants

The present study collected 107 schizophrenia patients with AVH, 85 without AVH(NAVH), and 104 healthy controls (HC) matched by age and sex were recruited for this study. According to the Diagnostic and Statistical Manual of Mental Disorders, Fourth Edition (DSM-IV), two well-trained clinical psychiatrists confirmed the patients' diagnosis of schizophrenia. The patients had never got drug, physical therapy, or counseling, and the disorder had lasted no more than 3 years. The symptoms were assessed by the Positive and Negative Symptom Scale (PANSS), and the degree of AVH was evaluated by the Auditory Hallucination Rating Scale (AHRS). The questionnaire assessment of patients was completed by two investigators after training. Patients in the AVH group encountered AVH in the last 4 weeks, with the majority occurring in the previous week, whereas patients in the NAVH group had no AVH during their entire lifespan or in the previous 4 months.

The present study was approved by the Ethics Committee of the First Affiliated Hospital of Zhengzhou University. Participants in this study need to meet the following inclusion criteria: (1) All patients were diagnosed according to Diagnostic and Statistical Manual of Mental Disorders, Fourth Edition (DSM-IV), (2) First onset, without any treatment such as medication, psychotherapy, and electric shock, (3) Han nationality, right-handed, (4) The illness duration of all patients was < 3 years, and the diapause was < 6 months. Participants with the following conditions will be excluded from this study: (1) a history of head trauma or serious physical impairment, (2) drug abuse or alcohol addiction, (3) psychiatric illness produced by physical diseases, (4) pregnancy or any contraindications for MRI. Any neurological or psychiatric condition, as well as related family history, are exclusion factors for the HC group. Following a thorough explanation of the study, all participants completed informed consent.

Data acquisition

The magnetic resonance imaging (MRI) was carried out on a 3.0 T MRI scanner, and an 8-channel receiver array head coil (GE, USA) was used during scanning. All subjects were asked to lie still with their eyes closed and remain aware while using the foam cushioning. During scanning, earplugs were utilized to reduce strepitus impact.

The magnetic resonance imaging (MRI) was performed on a 3.0 T MRI scanner (Discovery MR750, GE, USA) with an 8-channel receiver array head coil. Participants were required to lie still using the foam padding and remain alert with their eyes closed without thinking anything. Earplugs were used to reduce the interference of noise during scanning. Structural images were acquired with a 3D T1 BRAVO sequence, the following sequence parameters were applied: repetition time (TR)/echo time (TE) = 8.2/3.2 ms, slices = 188, slice thickness = 1 mm, slice gap = 0 mm, flip angle (FA) = 12°, field of view (FOV) = 25.6 × 25.6 cm^2, number of Averages = 1, data matrix = 256 × 256, voxel size = 1 × 1 × 1 mm^3, scan time = 4.33 min. The following settings were used to acquire functional images transversely with a gradient spin echo planar imaging sequence: TR/TE = 2000/30 ms, slices = 32, slice thickness = 4 mm, slice gap = 0.5 mm, FA = 90°, field of view (FOV) = 22 × 22 cm^2, number of averages = 1, data matrix = 64 × 64, voxel size = 3.4375 × 3.4375× 4 mm^3, and 180 volumes lasting for 360 sec.

Data preprocessing

The resting state functional images preprocessing was preprocessed using DPABI toolbox (http://rfmri.org/dpabi) based on MATLAB (MathWorks). The first five volumes, which allowed participants to become adjusted to scanning

surroundings, were eliminated. Then, further preprocessing was performed: (1) slice timing, (2) realignment in order to correct head motion, participants with a head motion > 3 mm or a 3° rotation will be excluded from the study, (3) normalization, the DARTEL method was applied to conduct normalization. Individual structural images were initially co-registered to the mean functional image, after which the modified structural images were segmented and normalized to MNI space (the resampled voxel size of $3 \times 3 \times 3$ mm^3), (4) detrending, (5) temporal band-pass filtering (0.01–0.08 Hz); (6) head motion parameters, the averaged white matter signal, and the cerebrospinal fluid signal were all regressed out of the confounding signals (Friston-24).

Definition of region of interest

We selected 6 regions of interest (ROIs) to analyze whole-brain dFC, including bilateral HES, ACC, and MGN. The HES gyrus and medial geniculate (MGN) were selected as the ROIs for dFC analysis on the basis of the automated anatomical labeling atlas 3 (40). The Brodmann atlas was selected in the software WFU_PickAtlas (41) to produce the ROI of AAC, involving the combination of the Brodmann's areas 22 and 42.

Dynamic FC analyses

Sliding time-window analysis can explain the variance of dFC, which can be defined as the temporal features of FC during the scan. This method was adopted to generate dFC maps for each participant using DPABI toolbox (42). Previous studies have shown that the suitable length for capturing dynamic FC mode ranges from 30 sec to 1 min when using Hamming window for time window method (32). The sliding window's length was chosen to walk a fine line among detecting fast changing dynamic linkages with a shorter window and accurately estimating related activities over wider window sections. Finally, 30 TR width (60s) and 1 TR step was applied to this study, in which the time series of each participant were divided into 30 TR windows. In each window, we applied seed-based functional connectivity analysis, and within the entire brain, by computing the correlation of average time course between the seeds and all other voxels, the FC maps of all ROIs were acquired. Then, zFC maps were generated *via* Fisher's z-transformation. Finally, we calculated all voxels' dFC values through computing the standard deviation of zFC values over windows.

Statistical analysis

Statistical Package for the Social Sciences (SPSS) version 26.0 was used to analyze the demographic and clinical data. One-way analyses of variance (ANOVA) were used for age and years of education to estimate the differences among the AVH, NAVH, and HC groups. A chi-square test was used for gender comparisons among groups. Between AVH group and NAVH group, two sample *t*-tests were applied to estimate the difference in PANSS and AHRS scores. Statistical significance was all determined by $p < 0.05$.

ANOVA was performed to examine the differences in dFC of each ROI to all voxels in the entire brain among three groups (AVH, NAVH, and HC), with age, gender, years of education, and head motion included as covariates. Using DPABI toolbox, we applied the Gaussian random field (GRF) method for multiple comparison correction (voxel-wise $p < 0.005$, cluster-wise $p < 0.05$). The dFC values of clusters which is statistically significant were extracted separately to conduct *post hoc* pairwise comparisons ($p < 0.05$, Bonferroni correction).

We analyzed the correlation between the extracted dFC values of significant clusters (among AVH, NAVH and HC groups) and PANSS scores. In addition, we also analyzed the correlation between the extracted dFC values of significant clusters (between AVH and NAVH group) and the AHRS scores of AVH group. Spearman's correlation analyses were performed using SPSS with Bonferroni correction ($p < 0.05$).

Validation analysis

In the dynamic FC analysis by sliding window approach, the window width is an important characteristic. To confirm the dFC variability results in this study, aside from 30 TR, we also ran validation tests on other sliding window lengths. We reconstructed the dFC maps for each ROI by a window length of 50 and 60 TRs. Besides, between the AVH and NAVH groups, the dFC results were reanalyzed.

Results

Clinical and demographic characteristics

There were no significant differences in age, gender, and educational level between the AVH, NAVH, and HC groups. Between the AVH and the NAVH groups, there was no significant difference in PANSS total score, positive, negative, and general scores (Table 1).

Differences in dynamic functional connectivity

Auditory association cortex (AAC)

Among AVH, NAVH and HC groups, two clusters exhibiting statistical differences of dFC were showed using left AAC as seed. In *post hoc* statistical test, the AVH group showed no significant

TABLE 1 Demographic and clinical data of AVH, NAVH, and HC groups [Mean (SD)].

	AVH ($n = 107$)	NAVH($n = 85$)	HC ($n = 104$)	$F/\chi^2/t$	P
Age (yeas)	21.50 ± 8.33	23.60 ± 8.67	22.40 ± 5.53	1.814	0.165
Sex (male/female)	42/65	46/39	50/54	4.343	0.114
Education (years)	10.80 ± 2.84	11.19 ± 3.26	11.39 ± 3.33	0.957	0.385
AHRS	22.59 ± 1.15	-	-	-	-
PNASS					
Positive	20.79 ± 5.60	20.25 ± 5.99	-	0.652	0.515
Negative	21.21 ± 6.26	22.53 ± 6.67	-	1.404	0.162
General	41.83 ± 9.08	42.64 ± 8.78	-	0.618	0.537
Total scores	83.83 ± 17.40	85.41 ± 17.54	-	0.623	0.534
Mean FD (mm)	0.060 ± 0.041	0.063 ± 0.056	0.071 ± 0.048	1.611	0.201

Sex differences among AVH, NAVH and HC groups were examined by Chi-square tests. Differences of continuous variables among AVH, NAVH and HC groups were examined by one-way analyses of variance (ANOVA). The difference of PANSS scores between AVH and NAVH groups was examined by two sample T-tests. AVH, schizophrenia patients with auditory verbal hallucination; NAVH, schizophrenia patients without auditory verbal hallucination; HC, healthy control; FD, framewise displacement; PNASS, Positive and Negative Syndrome Scale; AHRS, Auditory Hallucination Rating Scale; SD, standard deviation.

difference between the left ACC and cluster1, and increased dFC between the left ACC and cluster2 was observed in the AVH group (see Figure 1, Table 2).

Among AVH, NAVH and HC groups, one cluster exhibiting statistical differences of dFC were showed using the right AAC as seed. In *post hoc* statistical test, no difference was found between right ACC and cluster1 in the AVH group (see Figure 1, Table 2).

Heschl's gyrus (HES)

Among AVH, NAVH and HC groups, two clusters exhibiting statistical differences of dFC were showed using left HES as seed. In *post hoc* statistical test, decreased dFC between the left HES and cluster1was observed in the AVH group, and no difference was found between left HES and cluster2 in the AVH group (see Figure 2, Table 2).

Among AVH, NAVH and HC groups, two clusters exhibiting statistical differences of dFC were showed using right HES as seed. In *post hoc* statistical test, no difference was found between right HES and cluster1 in the AVH group, and decreased dFC between the right HES and cluster2 was observed in the AVH group (see Figure 2, Table 2).

Medial geniculate nucleus (MGN)

Among AVH, NAVH and HC groups, one cluster exhibiting statistical differences of dFC was showed using left MGN as seed. In *post hoc* statistical test, decreased dFC between the left MGN and cluster1 was observed in the AVH group (see Figure 3, Table 2).

Among AVH, NAVH and HC groups, two clusters exhibiting statistical differences of dFC was showed using right HES as seed. In *post hoc* statistical test, no difference was found between right MGN and cluster1/cluster2 in the AVH group (see Figure 3, Table 2).

Spearman correlational analysis

The AHRS scores were significantly positively correlated with the dFC values of cluster 1 using left AAC seed ($r = 0.334$, $p = 0.000$), cluster 2 using left AAC seed ($r = 0.292$, $p = 0.002$), cluster 1using right AAC seed ($r = 0.222$, $p = 0.021$) and cluster 2 using right HES seed ($r = 0.202$, $p = 0.037$) in the AVH group (see Figure 4).

PANSS negative sub-scores were negatively correlated with the dFC values of cluster 2 using the right HES seed in both AVH and NAVH groups ($r = 0.157$, $p = 0.029$) (see Figure 4).

There is no significance between dFC values of all above regions and PANSS total scores, PANSS positive, and general sub-scores.

Validation results

To validate our core dFC conclusions, we tested two alternative sliding window widths. The sliding window lengths of 50 and 60 TRs produced alike outcomes to the 30 TR in our study. All validation analysis results were presented as Supplementary material.

Discussion

Our study investigated the whole-brain dFC using auditory-related regions as seeds in first-episode, drug- naïve schizophrenia patients with and without AVH compared to healthy controls. In our study, the AVH group showed

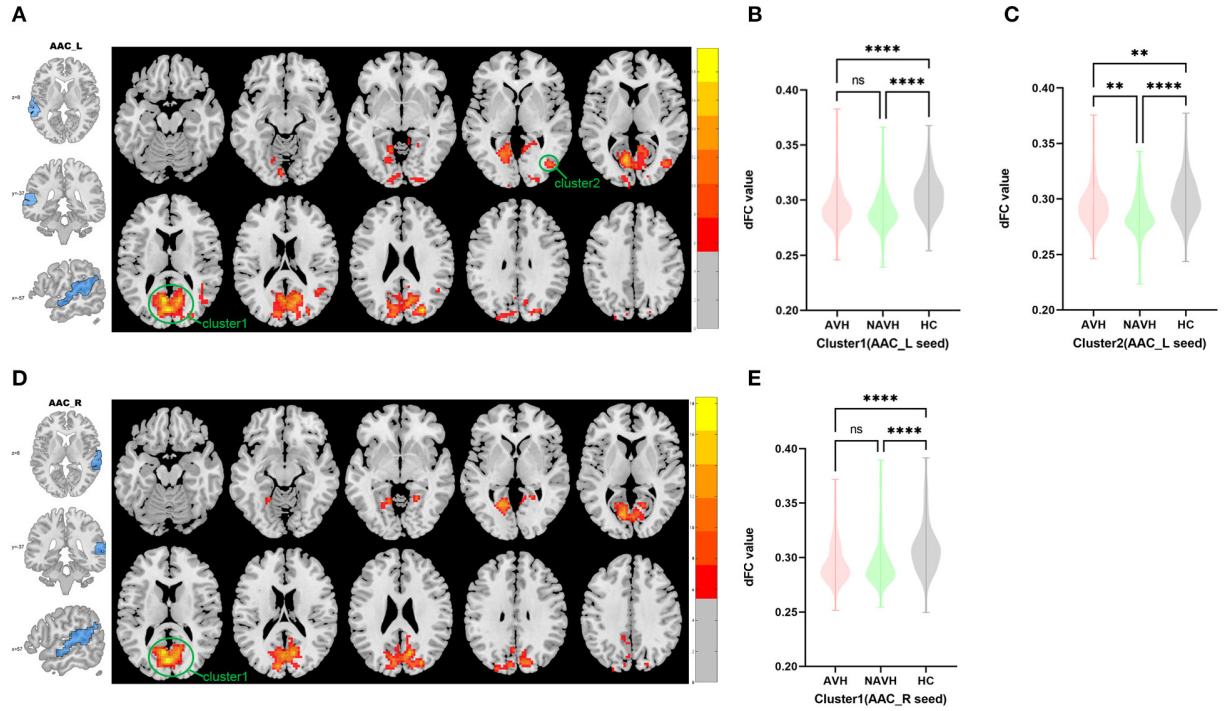

FIGURE 1
Brain regions showing abnormal dFC values among AVH, NAVH and HC groups in MNI space using left and right AAC as seeds. **(A)** Significant dFC value differences were observed in cluster1 (bilateral calcarine gyrus, bilateral cuneus gyrus, bilateral lingual gyrus, bilateral superior occipital gyrus, bilateral precuneus gyrus, posterior cingulate gyrus) and cluster2 (right middle temporal gyrus and right middle occipital gyrus) using left AAC as seed. **(B,C)** Altered dFC values in cluster1 and cluster2 among AVH, NAVH and HC groups using left AAC as seed. **(D)** Significant dFC value differences were observed in cluster1 (bilateral calcarine gyrus, posterior cingulate gyrus, bilateral cuneus gyrus, bilateral lingual gyrus, bilateral superior occipital gyrus, bilateral precuneus gyrus) using right AAC as seed. **(E)** Altered dFC values in cluster1 among AVH, NAVH and HC groups using right AAC as seed. ****Significant at 0.0001 level, ***significant at 0.001 level, **significant at 0.01 level and *significant at 0.05 level (2-tailed).

significantly increased dFC between left ACC and right middle temporal gyrus and right middle occipital gyrus, decreased dFC between left HES and left superior occipital gyrus, left cuneus gyrus, left precuneus gyrus, decreased dFC between right HES and posterior cingulate gyrus, and decreased dFC between left MGN and bilateral calcarine gyrus, bilateral cuneus gyrus, and bilateral lingual gyrus. Moreover, we found positive correlations between the AHRS and the dFC of significantly brain areas using left ACC, right ACC, and right HES as seeds respectively. Together, these results suggest that auditory related areas in schizophrenia patients present abnormal dynamic connectivity with multiple brain areas including the middle temporal gyrus, middle occipital gyrus, superior occipital gyrus, cuneus gyrus, precuneus gyrus, calcarine gyrus, cuneus gyrus, lingual gyrus, and posterior cingulate gyrus, which act a crucial part in the mechanism of AVH.

Taking the brain area related to auditory perception as the node and the relationship between the two nodes as the edge, the sum of these nodes and edges is called the auditory network, also known as the auditory pathway. Beginning with the primary auditory cortex, there are two auditory pathways—ventral and dorsal pathway (25, 26), which correspond to different specific functions in auditory information processing. Sound is first received and initially processed though the primary auditory cortex, afterwards transmitted to the secondary auditory cortex (located in BA22 and BA42) for processing, and then transferred to the higher information processing brain areas through the thalamus. Several research results speculate that the multiple auditory functions of the AVH group are abnormal, whether it is primary auditory processing or advanced language processing.

MGN is left-right symmetrical and located in the posterior medial part of the thalamus, which is an important relay station in the auditory pathway. The medial geniculate body can be segmented into ventral, dorsal, and central part. The ventral region and dorsal region can project to the auditory cortex through the thalamic cortical bundle, while the central region can also project to the non-auditory cortex (43). The central and dorsal regions involve the interaction of multiple senses and the interaction of auditory signals with other signals (44). In a word, MGN is one of the regions to complete the interaction between auditory and somatosensory signals. According to previous studies, auditory and somatosensory

TABLE 2 Whole-brain seed-based dynamic functional connectivity analysis results.

ROI	ANOVA results	AVHvsNAVH	Brain areas(L/R)	Cluster size (voxels)	Peak coordinates (MNI) x y z	*T*-value
AAC_L	Cluster1	/	calcarine gyrus (L/R), cuneus gyrus (L/R), lingual gyrus (L/R), superior occipital gyrus (L/R), precuneus gyrus (L/R), posterior cingulate gyrus	1244	27–78 24	19.67
	Cluster2	+	middle temporal gyrus (R) and middle occipital gyrus (R)	118	42–72 3	12.15
AAC_R	Cluster1	/	calcarine gyrus(L/R), posterior cingulate gyrus, cuneus gyrus (L/R), lingual gyrus (L/R), superior occipital gyrus (L/R), precuneus gyrus (L/R)	1077	−9–66 12	18.42
HES_L	Cluster1	–	superior occipital gyrus (L), cuneus gyrus (L), precuneus gyrus (L)	130	−21 42–21	10.81
	Cluster2	/	anterior orbitofrontal gyrus (L)	155	−15–84 30	10.22
HES_R	Cluster1	/	calcarine gyrus (L)	36	−18–66 12	8.87
	Cluster2	–	posterior cingulate gyrus	58	−3–30 30	10.43
MGN_L	Cluster1	–	calcarine gyrus (L/R), cuneus gyrus (L/R), lingual gyrus (L/R)	434	15–78 27	12.49
MGN_R	Cluster1	/	calcarine gyrus (L/R), cuneus gyrus(L/R), lingual gyrus (L/R)	191	−12–60 3	11.63
	Cluster2	/	precentral gyrus (L) and postcentral gyrus (L)	50	−36–15 63	8.70

MNI, Montreal Neurological Institute; ROI, region of interest; AAC, auditory association cortex; HES, Heschl's gyrus; MGN, medial geniculate nucleus; R, right; L, left; +, positive; –, negative; /, no significant difference.

signals will be transmitted to MGN and then transmitted to other cortex after processing (45), so we believe that the symptoms of verbal auditory hallucination may be related to the abnormal connection between the medial geniculate body and other brain regions. Our study found that the abnormal connections between the medial geniculate body and calcarine gyrus, cuneus gyrus, lingual gyrus, central anterior gyrus, and central posterior gyrus were related to auditory hallucination, although no significant correlation was found between these abnormal connections and AHRS.

The majority of fMRI studies on the mechanism of AVH in schizophrenia have concentrated on inherent connectivity of areas relating to auditory, and language processing, involving the frontal and temporal lobe. It is known to all that Broca's and Wernicke's areas act a crucial part in speech processing, Hoffman and many other researchers have observed increased connectivity between the left inferior frontal gyrus (IFG) and STG, which is a unique pattern of auditory hallucination in schizophrenia patients (46). According to the study reported by Shinn et al., compared with patients without AVH, schizophrenic patients with AVH presented increased FC between left HES and left frontal-parietal region, which is relevant to the severity of AVH (47). Moreover, the pre-frontal cortex is also one of 25 nodes in the AVH network revealed by Scheinost et al. (48). Our study found the abnormal functional connectivity between left HES and left anterior orbito-frontal gyrus among AVH, NAVH, and HC groups, with the mean dFC value in the AVH group higher than NAVH group, although the difference was not statistically significant. Combined with the results of this study, we found abnormal fronto-temporal dFC in both the AVH group and NAVH group compared with the HC group, which may reveal that the abnormal fronto-temporal functional connectivity is not only related to the mechanism of AVH in schizophrenia, but also the pathogenesis of schizophrenia. While the dFC value of AVH group is higher than that of NAVH group, which may indicate that the abnormal fronto-temporal functional connectivity plays a greater role in schizophrenia patients with AVH than NAVH. Thus, to some extent, our results reflect the role of abnormal fronto-temporal FC in the occurrence of AVH.

The middle temporal gyrus is located between the superior temporal sulcus and the inferior temporal sulcus. There are numerous studies showing that the middle temporal gyrus is related to language-related activities and processes (49, 50), such as semantic processing, semantic cognition (51), word generation (52), vocabulary integration (53), sentence

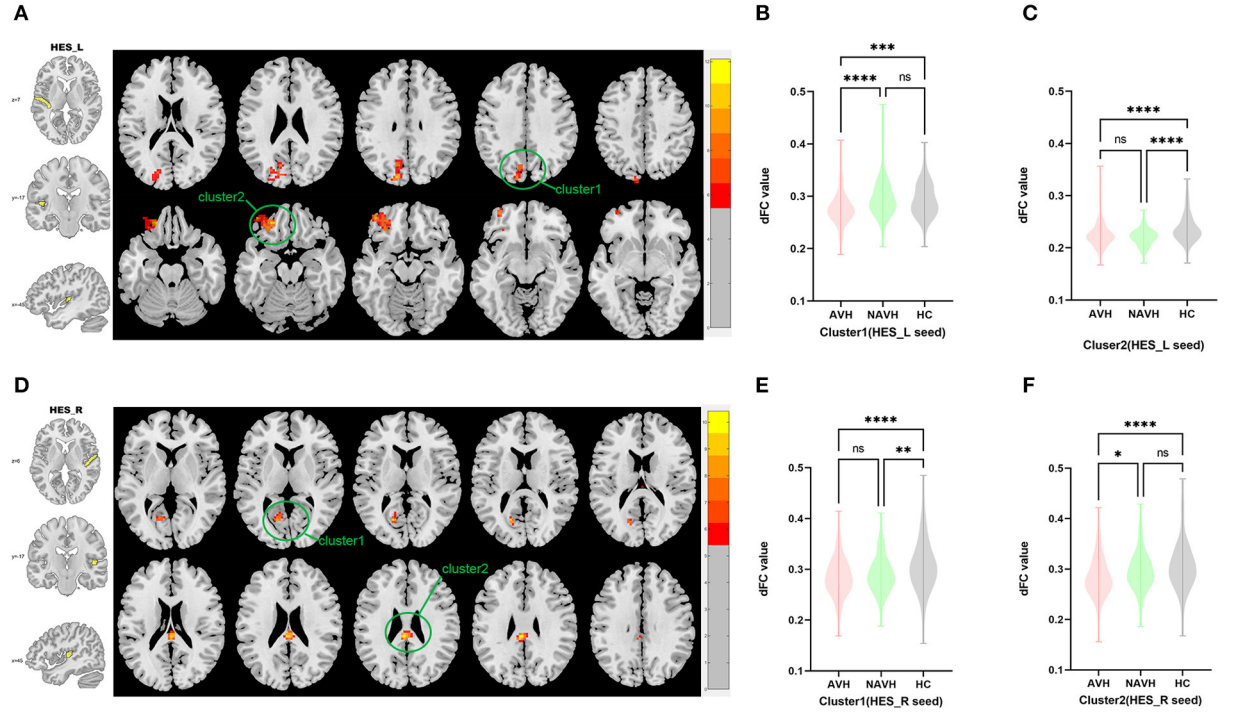

FIGURE 2
Brain regions showing abnormal dFC values among AVH, NAVH and HC groups in MNI space using left and right HES as seeds. **(A)** Significant dFC value differences were observed in cluster1 (left superior occipital gyrus, left cuneus gyrus, left precuneus gyrus) and cluster2 (left anterior orbitofrontal gyrus) using left HES as seed. **(B,C)** Altered dFC values in cluster1 and cluster2 among AVH, NAVH and HC groups using left HES as seed. **(D)** Significant dFC value differences were observed in cluster1 (left calcarine gyrus) and cluster2 (posterior cingulate gyrus.) using right HES as seed. **(E,F)** Altered dFC values in cluster1 among AVH, NAVH and HC groups using right HES as seed. ****Significant at 0.0001 level, ***significant at 0.001 level, **significant at 0.01 level and *significant at 0.05 level (2-tailed).

understanding, and complex sound processing. More and more studies observed structural and functional changes of the middle temporal gyrus which are significantly related to schizophrenia (54–57). Further, some researchers have found that AVH in patients with schizophrenia are related to the middle temporal gyrus (58, 59). Therefore, it is reasonable to believe that the abnormal FC between the middle temporal gyrus and auditory-related brain areas may be one of the mechanisms of auditory hallucination, which is also supported by the results of our study.

Less studies focus on the association between the occipital lobe and schizophrenia. Tohid et al. reviewed several studies (60) and discovered that schizophrenia is related to the abnormal structural and functional changes of the occipital lobe. The occipital lobe abnormalities were reported to act a crucial part in the mechanism of visual hallucination in schizophrenia. Up to now, few studies have found that the occipital lobe is related to auditory hallucination. Our data revealed that aberrant occipital-temporal and occipital-MGN dynamic FC may be associated with the mechanism of AVH in schizophrenia patients. More and more studies observed that the occipital lobe is associated with phonological and semantic modulation (61, 62), thus we speculate that abnormal conduction between the occipital lobe and auditory pathway may lead to aberrant phonological or semantic processing, which may lead to AVH in schizophrenia patients. Moreover, a "multisensory interplay" theory (63, 64) may be another corroboration of our results, Lewis et al. also reported that audio visual synchronization combines dynamic visual and aural inputs to create a more powerful and dependable multiple sensory system (65). Doehrmann et al. (66) revealed the sensory integrative effects of non-primary auditory and extra striate visual cortices by fMRI method. Eckert et al. (67) suggests that there is an obvious functional relevance between the primary auditory cortex and the anterior visual cortex. Thoma et al. (68) discovered that the occipital-temporal network showed significant AVH-related profiles, especially during AVH-off periods. Combined with the importance of connectivity between the auditory and visual cortex and the performance of audio-visual functional integration in the above studies, our results may suggest that abnormal occipitotemporal FC act a crucial part in the mechanism of AVH in schizophrenia patients.

Our study also observed abnormal dFC between the temporal lobe and posterior cingulate gyrus/precuneus, part of the DMN. Several articles have reported particular links between

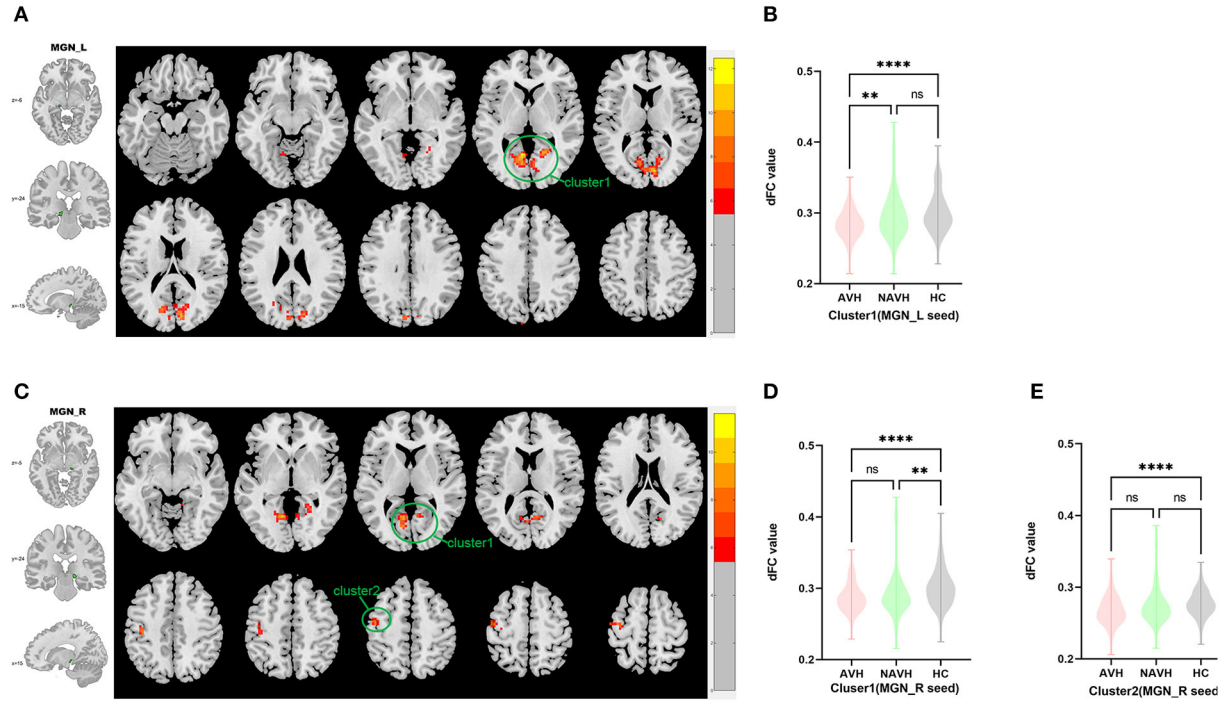

FIGURE 3
Brain regions showing abnormal dFC values among AVH, NAVH and HC groups in MNI space using left and right MGN as seeds. **(A)** Significant dFC value differences were observed in cluster1 (bilateral calcarine gyrus, bilateral cuneus gyrus, bilateral lingual gyrus) using left MGN as seed. **(B,C)** Altered dFC values in cluster1 among AVH, NAVH and HC groups using left MGN as seed. **(D)** Significant dFC value differences were observed in cluster1 (bilateral calcarine gyrus, bilateral cuneus gyrus, bilateral lingual gyrus) and cluster2 (left precentral gyrus and left postcentral gyrus) using right MGN as seed. **(E,F)** Altered dFC values in cluster1 among AVH, NAVH and HC groups using right MGN as seed. ****Significant at 0.0001 level.

DMN and auditory hallucinations. Northoff et al. (14) and Jardri et al. (69) observed a chaotic situation concerning resting-state activity and external stimulation produced by coactions between the auditory cortex and parts of the DMN, which lead to auditory hallucinations eventually. Scheinost et al. (48) discovered a prospective AVH network by data-driven analysis of functional connectivity consisting of 25 nodes, including the medial prefrontal cortex and posterior cingulate cortex, and revealing generous overlap with the DMN and language network.

Conventional sFC represents average connectivity strength between brain regions, while dFC reflects functional connectivity variability over temporal scales as a complementary method (31). Yet, there is increasing evidence that communication between different regions is not static but dynamic during the whole resting state scanning process, which is due to the conditional dependence of neural activity. Temporal variations in connectivity strength can't be captured by sFC. Consequently, the observation that the connections between brain regions increase or decrease over time is helpful to further understand the neural mechanism of AVH in schizophrenia from the perspective of temporal stability. In our study, dFC method was used to discover the variability of the functional connectivity over time between auditory related regions and other regions of the whole brain, which explain the role of auditory-related regions' connectivity stability in the mechanism of auditory hallucination.

Few potential limitations ought to be noticed in present study. First, the sample capacity of this study is not sufficient, so in the future, larger sample size is required to enhance the generalizability of the present findings. Second, patients in AVH group may suffer hallucinations or doze off in the process of scanning, which may disturb resting state design. Third, our study just obtained resting-state fMRI scans, and follow-up study ought to be regarded in the future. Fourth, we didn't evaluate further details on the severity of AVH, such as the incidence rate, content, and pain degree of auditory hallucinations. Future research needs to quantify the symptoms of auditory hallucinations in more detail. Consequently, our results ought to be regarded as initial, and further longitudinal studies with larger sample sizes should be investigated to formulate final conclusions.

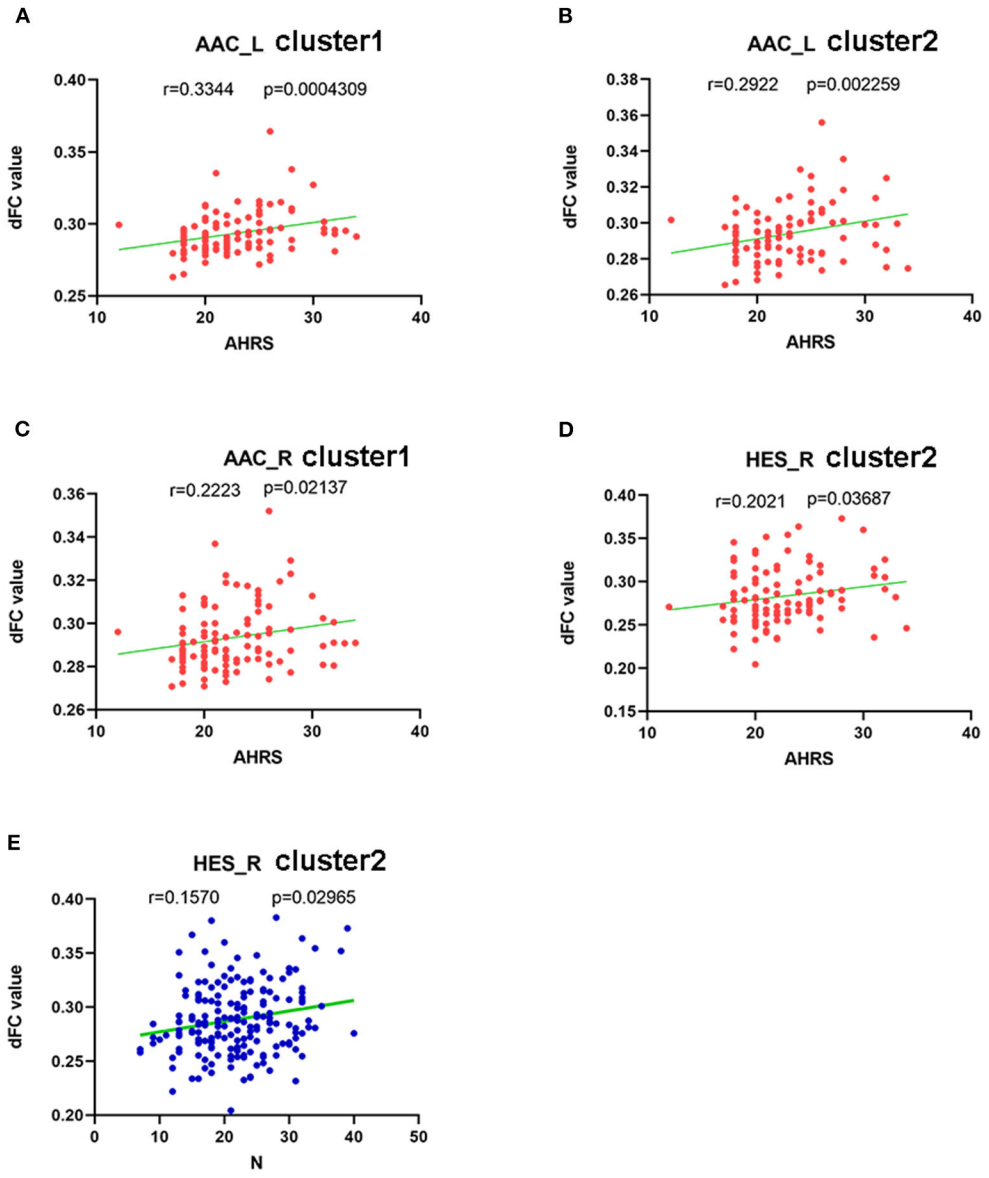

FIGURE 4
Correlations between abnormal dFC values and clinical variables. In schizophrenia patients with AVH. **(A)** a positive correlation was observed between the dFC values in the cluster1 using left AAC as seed and AHRS. **(B)** a positive correlation was observed between the dFC values in the cluster2 using left AAC as seed and AHRS. **(C)** a positive correlation was observed between the dFC values in the cluster1 using rihgt AAC as seed and AHRS, and **(D)** a positive correlation was observed between the dFC values in the cluster2 using right HES as seed and AHRS. In schizophrenia patients with AVH and NAVH. **(E)** a positive correlation was observed between the dFC values in the cluster2 using right HES as seed and PANSS negative sub-scores.

Conclusion

Our study used the dFC analysis to explore the abnormal dynamic functional connectivity of auditory-related regions in whole-brain areas in schizophrenia patients with AVH. We also correlated dFC values with PANSS and AHRS scores. The current results showed abnormal dynamic functional connectivity between the occipital lobe, middle temporal gyrus, posterior cingulate gyrus, precuneus gyrus, and cuneus gyrus with auditory-related regions, which is related to AVH. Taken together, the present findings demonstrate that schizophrenia patients with AVH showed multiple abnormal dFC brain regions using auditory related cortex and nucleus as seeds, suggesting that the distinct dFC patterns of auditory related regions may provide a potential neural mechanism of AVH in schizophrenia.

Data availability statement

The original contributions presented in the study are included in the article/Supplementary material, further inquiries can be directed to the corresponding author.

Ethics statement

The studies involving human participants were reviewed and approved by the Ethics Committee of the First Affiliated Hospital of Zhengzhou University. Written informed consent to participate in this study was provided by the participants' legal guardian/next of kin.

Author contributions

KX contributed to the conception and design of this study. JC and YW recruited the participants and performed the MRI examination. KX, SH, and CW performed data processing. YC performed the statistical analysis. KX wrote the first draft of the manuscript. YZ, XS, and JC provided critical revision of the manuscript. All authors contributed to the article and approved the submitted manuscript.

Funding

This work was supported by the Medical science and technology research project of Henan province (SBGJ202101013) and Medical Science and Technology Research Project of Henan Province (201701011).

Acknowledgments

We wish to express our thanks to all subjects who served as research participants.

Conflict of interest

The authors declare that the research was conducted in the absence of any commercial or financial relationships that could be construed as a potential conflict of interest.

Publisher's note

Supplementary material

The Supplementary Material for this article can be found online at: https://www.frontiersin.org/articles/10.3389/fpsyt.2022.963634/full#supplementary-material

References

1. Kahn RS, Sommer IE, Murray RM, Meyer-Lindenberg A, Weinberger DR, Cannon TD, et al. Schizophrenia. *Nat Rev Dis Primers.* (2015) 1:15067. doi: 10.1038/nrdp.2015.67

2. Buckholtz JW, Meyer-Lindenberg A. Psychopathology and the human connectome: toward a transdiagnostic model of risk for mental illness. *Neuron.* (2012) 74:990–1004. doi: 10.1016/j.neuron.2012.06.002

3. Friston KJ, Frith CD. Schizophrenia: a disconnection syndrome? *Clin Neurosci.* (1995) 3:89–97.

4. Alderson-Day B, McCarthy-Jones S, Fernyhough C. Hearing voices in the resting brain: A review of intrinsic functional connectivity research on auditory verbal hallucinations. *Neurosci Biobehav Rev.* (2015) 55:78–87. doi: 10.1016/j.neubiorev.2015.04.016

5. Battle DE. Diagnostic and Statistical Manual of Mental Disorders (DSM). *Codas.* (2013) 25:191–2.

6. Shergill SS, Murray RM, McGuire PK. Auditory hallucinations: a review of psychological treatments. *Schizophr Res.* (1998) 32:137–50. doi: 10.1016/S0920-9964(98)00052-8

7. Shinn AK, Pfaff D, Young S, Lewandowski KE, Cohen BM, Öngür D. Auditory hallucinations in a cross-diagnostic sample of psychotic disorder patients: a descriptive, cross-sectional study. *Compr Psychiatry.* (2012) 53:718–26. doi: 10.1016/j.comppsych.2011.11.003

8. Bauer SM, Schanda H, Karakula H, Olajossy-Hilkesberger L, Rudaleviciene P, Okribelashvili N, et al. Culture and the prevalence of hallucinations in schizophrenia. *Compr Psychiatry.* (2011) 52:319–25. doi: 10.1016/j.comppsych.2010.06.008

9. Gavrilescu M, Rossell S, Stuart GW, Shea TL, Innes-Brown H, Henshall K, et al. Reduced connectivity of the auditory cortex in patients with auditory hallucinations: a resting state functional magnetic resonance imaging study. *Psychol Med.* (2010) 40:1149–58. doi: 10.1017/S0033291709991632

10. Wolf ND, Sambataro F, Vasic N, Frasch K, Schmid M, Schönfeldt-Lecuona C, et al. Dysconnectivity of multiple resting-state networks in patients with schizophrenia who have persistent auditory verbal hallucinations. *J Psychiatry Neurosci.* (2011) 36:366–74. doi: 10.1503/jpn.110008

11. Hugdahl K, Sommer IE. Auditory verbal hallucinations in schizophrenia from a levels of explanation perspective. *Schizophr Bull.* (2018) 44:234–41. doi: 10.1093/schbul/sbx142

12. Frith CD, Done DJ. Towards a neuropsychology of schizophrenia. *Br J Psychiatry.* (1988) 153:437–43. doi: 10.1192/bjp.153.4.437

13. Allen P, Aleman A, McGuire PK. Inner speech models of auditory verbal hallucinations: evidence from behavioural and neuroimaging studies. *Int Rev Psychiatry.* (2007) 19:407–15. doi: 10.1080/09540260701486498

14. Northoff G, Qin P. How can the brain's resting state activity generate hallucinations? a "resting state hypothesis" of auditory verbal hallucinations. *Schizophr Res.* (2011) 127:202–14. doi: 10.1016/j.schres.2010.11.009

15. Stephan KE, Friston KJ, Frith CD. Dysconnection in schizophrenia: from abnormal synaptic plasticity to failures of self-monitoring. *Schizophr Bull.* (2009) 35:509–27. doi: 10.1093/schbul/sbn176

16. Nazimek JM, Hunter MD, Woodruff PWR. Auditory hallucinations: expectation-perception model. *Med Hypotheses.* (2012) 78:802–10. doi: 10.1016/j.mehy.2012.03.014

17. Fu CHY, Brammer MJ, Yágüez L, Allen P, Matsumoto K, Johns L, et al. Increased superior temporal activation associated with external misattributions of self-generated speech in schizophrenia. *Schizophr Res.* (2008) 100:361–3. doi: 10.1016/j.schres.2007.10.023

18. Lawrie SM, Buechel C, Whalley HC, Frith CD, Friston KJ, Johnstone EC. Reduced frontotemporal functional connectivity in schizophrenia associated with auditory hallucinations. *Biol Psychiatry.* (2002) 51:1008–11. doi: 10.1016/S0006-3223(02)01316-1

19. McGuire PK, Silbersweig DA, Wright I, Murray RM, David AS, Frackowiak RS, et al. Abnormal monitoring of inner speech: a physiological basis for auditory hallucinations. *Lancet.* (1995) 346:596–600. doi: 10.1016/S0140-6736(95)91435-8

20. Shergill SS, Bullmore E, Simmons A, Murray R, McGuire P. Functional anatomy of auditory verbal imagery in schizophrenic patients with auditory hallucinations. *Am J Psychiatry.* (2000) 157:1691–3. doi: 10.1176/appi.ajp.157.10.1691

21. Northoff G. Are auditory hallucinations related to the brain's resting state activity? a "neurophenomenal resting state hypothesis". *Clin Psychopharmacol Neurosci.* (2014) 12:189–95. doi: 10.9758/cpn.2014.12.3.189

22. Sadaghiani S, Hesselmann G, Kleinschmidt A. Distributed and antagonistic contributions of ongoing activity fluctuations to auditory stimulus detection. *J Neurosci.* (2009) 29:13410–7. doi: 10.1523/JNEUROSCI.2592-09.2009

23. Dierks T, Linden DEJ, Jandl M, Formisano E, Goebel R, Lanfermann H, et al. Activation of heschl's gyrus during auditory hallucinations. *Neuron.* (1999) 22:615–21. doi: 10.1016/S0896-6273(00)80715-1

24. Hunter MD, Eickhoff SB, Miller TWR, Farrow TFD, Wilkinson ID, Woodruff PWR. Neural activity in speech-sensitive auditory cortex during silence. *Proc Natl Acad Sci U S A.* (2006) 103:189–94. doi: 10.1073/pnas.0506268103

25. Romanski LM, Tian B, Fritz J, Mishkin M, Goldman-Rakic PS, Rauschecker JP. Dual streams of auditory afferents target multiple domains in the primate prefrontal cortex. *Nat Neurosci.* (1999) 2:1131–6. doi: 10.1038/16056

26. Kaas JH, Hackett TA. "What" and "where" processing in auditory cortex. *Nat Neurosci.* (1999) 2:1045–7. doi: 10.1038/15967

27. Hickok null, Poeppel null. Towards a functional neuroanatomy of speech perception. *Trends Cogn Sci.* (2000) 4:131–8. doi: 10.1016/S1364-6613(00)01463-7

28. Rauschecker JP. Cortical processing of complex sounds. *Curr Opin Neurobiol.* (1998) 8:516–21. doi: 10.1016/S0959-4388(98)80040-8

29. Huang J, Zhuo C, Xu Y, Lin X. Auditory verbal hallucination and the auditory network: From molecules to connectivity. *Neuroscience.* (2019) 410:59–67. doi: 10.1016/j.neuroscience.2019.04.051

30. Chun S, Westmoreland JJ, Bayazitov IT, Eddins D, Pani AK, Smeyne RJ Yu J, et al. Specific disruption of thalamic inputs to the auditory cortex in schizophrenia models. *Science.* (2014) 344:1178–82. doi: 10.1126/science.1253895

31. Preti MG, Bolton TA, Van De Ville D. The dynamic functional connectome: state-of-the-art and perspectives. *Neuroimage.* (2017) 160:41–54. doi: 10.1016/j.neuroimage.2016.12.061

32. Hutchison RM, Womelsdorf T, Allen EA, Bandettini PA, Calhoun VD, Corbetta M, et al. Dynamic functional connectivity: promise, issues, and interpretations. *Neuroimage.* (2013) 80:360–78. doi: 10.1016/j.neuroimage.2013.05.079

33. Chang C, Glover GH. Time-frequency dynamics of resting-state brain connectivity measured with fMRI. *Neuroimage.* (2010) 50:81–98. doi: 10.1016/j.neuroimage.2009.12.011

34. Hutchison RM, Womelsdorf T, Gati JS, Everling S, Menon RS. Resting-state networks show dynamic functional connectivity in awake humans and anesthetized macaques. *Hum Brain Mapp.* (2013) 34:2154–77. doi: 10.1002/hbm.22058

35. Calhoun VD, Miller R, Pearlson G, Adali T. The chronnectome: time-varying connectivity networks as the next frontier in fMRI data discovery. *Neuron.* (2014) 84:262–74. doi: 10.1016/j.neuron.2014.10.015

36. Rabany L, Brocke S, Calhoun VD, Pittman B, Corbera S, Wexler BE, et al. Dynamic functional connectivity in schizophrenia and autism spectrum disorder: Convergence, divergence and classification. *Neuroimage Clin.* (2019) 24:101966. doi: 10.1016/j.nicl.2019.101966

37. Rashid B, Arbabshirani MR, Damaraju E, Cetin MS, Miller R, Pearlson GD, et al. Classification of schizophrenia and bipolar patients using static and dynamic resting-state fMRI brain connectivity. *Neuroimage.* (2016) 134:645–57. doi: 10.1016/j.neuroimage.2016.04.051

38. Cetin MS, Houck JM, Rashid B, Agacoglu O, Stephen JM, Sui J, et al. Multimodal classification of schizophrenia patients with MEG and fMRI data using static and dynamic connectivity measures. *Front Neurosci.* (2016) 10:466. doi: 10.3389/fnins.2016.00466

39. Zhang Y, Wang J, Lin X, Yang M, Qi S, Wang Y, et al. Distinct brain dynamic functional connectivity patterns in schizophrenia patients with and without auditory verbal hallucinations. *Front Hum Neurosci.* (2022) 16:838181. doi: 10.3389/fnhum.2022.838181

40. Rolls ET, Huang C-C, Lin C-P, Feng J, Joliot M. Automated anatomical labelling atlas 3. *Neuroimage.* (2020) 206:116189. doi: 10.1016/j.neuroimage.2019.116189

41. Maldjian JA, Laurienti PJ, Kraft RA, Burdette JH. An automated method for neuroanatomic and cytoarchitectonic atlas-based interrogation of fMRI data sets. *Neuroimage.* (2003) 19:1233–9. doi: 10.1016/S1053-8119(03)00169-1

42. Chao-Gan Y, Yu-Feng Z, DPARSF. A MATLAB Toolbox for "Pipeline" Data Analysis of Resting-State fMRI. *Front Syst Neurosci.* (2010) 4:13. doi: 10.3389/fnsys.2010.00013

43. Donishi T, Kimura A, Okamoto K, Tamai Y. "Ventral" area in the rat auditory cortex: a major auditory field connected with the dorsal division of the medial geniculate body. *Neuroscience.* (2006) 141:1553–67. doi: 10.1016/j.neuroscience.2006.04.037

44. Campi KL, Bales KL, Grunewald R, Krubitzer L. Connections of auditory and visual cortex in the prairie vole (Microtus ochrogaster): evidence for multisensory processing in primary sensory areas. *Cereb Cortex.* (2010) 20:89–108. doi: 10.1093/cercor/bhp082

45. Viaene AN, Petrof I, Sherman SM. Synaptic properties of thalamic input to layers 2/3 and 4 of primary somatosensory and auditory cortices. *J Neurophysiol.* (2011) 105:279–92. doi: 10.1152/jn.00747.2010

46. Hoffman RE, Fernandez T, Pittman B, Hampson M. Elevated functional connectivity along a corticostriatal loop and the mechanism of auditory/verbal hallucinations in patients with schizophrenia. *Biol Psychiatry.* (2011) 69:407–14. doi: 10.1016/j.biopsych.2010.09.050

47. Shinn AK, Baker JT, Cohen BM, Öngür D. Functional connectivity of left Heschl's gyrus in vulnerability to auditory hallucinations in schizophrenia. *Schizophr Res.* (2013) 143:260–8. doi: 10.1016/j.schres.2012.11.037

48. Scheinost D, Tokoglu F, Hampson M, Hoffman R, Constable RT. Data-Driven analysis of functional connectivity reveals a potential auditory verbal hallucination network. *Schizophr Bull.* (2019) 45:415–24. doi: 10.1093/schbul/sby039

49. Hickok G. The cortical organization of speech processing: feedback control and predictive coding the context of a dual-stream model. *J Commun Disord.* (2012) 45:393–402. doi: 10.1016/j.jcomdis.2012.06.004

50. Whitney C, Jefferies E, Kircher T. Heterogeneity of the left temporal lobe in semantic representation and control: priming multiple versus single meanings of ambiguous words. *Cereb Cortex.* (2011) 21:831–44. doi: 10.1093/cercor/bhq148

51. Davey J, Thompson HE, Hallam G, Karapanagiotidis T, Murphy C, De Caso I, et al. Exploring the role of the posterior middle temporal gyrus in semantic cognition: Integration of anterior temporal lobe with executive processes. *Neuroimage.* (2016) 137:165–77. doi: 10.1016/j.neuroimage.2016.05.051

52. Python G, Glize B, Laganaro M. The involvement of left inferior frontal and middle temporal cortices in word production unveiled by greater facilitation effects following brain damage. *Neuropsychologia.* (2018) 121:122–34. doi: 10.1016/j.neuropsychologia.2018.10.026

53. Bakker-Marshall I, Takashima A, Schoffelen J-M, van Hell JG, Janzen G, McQueen JM. Theta-band oscillations in the middle temporal gyrus reflect novel word consolidation. *J Cogn Neurosci.* (2018) 30:621–33. doi: 10.1162/jocn_a_01240

54. Joo SW, Chon M-W, Rathi Y, Shenton ME, Kubicki M, Lee J. Abnormal asymmetry of white matter tracts between ventral posterior cingulate cortex and middle temporal gyrus in recent-onset schizophrenia. *Schizophr Res.* (2018) 192:159–66. doi: 10.1016/j.schres.2017.05.008

55. Winkelbeiner S, Cavelti M, Federspiel A, Kunzelmann K, Dierks T, Strik W, et al. Decreased blood flow in the right insula and middle temporal gyrus predicts negative formal thought disorder in schizophrenia. *Schizophr Res.* (2018) 201:432–4. doi: 10.1016/j.schres.2018.06.009

56. Hu M, Li J, Eyler L, Guo X, Wei Q, Tang J, et al. Decreased left middle temporal gyrus volume in antipsychotic drug-naive, first-episode schizophrenia

patients and their healthy unaffected siblings. *Schizophr Res.* (2013) 144:37–42. doi: 10.1016/j.schres.2012.12.018

57. Guo W, Hu M, Fan X, Liu F, Wu R, Chen J, et al. Decreased gray matter volume in the left middle temporal gyrus as a candidate biomarker for schizophrenia: a study of drug naive, first-episode schizophrenia patients and unaffected siblings. *Schizophr Res.* (2014) 159:43–50. doi: 10.1016/j.schres.2014.07.051

58. Cui Y, Liu B, Song M, Lipnicki DM Li J, Xie S, Chen Y, et al. Auditory verbal hallucinations are related to cortical thinning in the left middle temporal gyrus of patients with schizophrenia. *Psychol Med.* (2018) 48:115–22. doi: 10.1017/S0033291717001520

59. Zhang L, Li B, Wang H, Li L, Liao Q, Liu Y, et al. Decreased middle temporal gyrus connectivity in the language network in schizophrenia patients with auditory verbal hallucinations. *Neurosci Lett.* (2017) 653:177–82. doi: 10.1016/j.neulet.2017.05.042

60. Tohid H, Faizan M, Faizan U. Alterations of the occipital lobe in schizophrenia. *Neurosciences (Riyadh).* (2015) 20:213–24. doi: 10.17712/nsj.2015.3.20140757

61. Am P, A Z. Time course of brain activation during graphemic/phonologic processing in reading: an ERP study. *Brain Language.* (2003) 87:139. doi: 10.1016/S0093-934X(03)00139-1

62. Drakesmith M, El-Deredy W, Welbourne S. Differential phonological and semantic modulation of neurophysiological responses to visual word recognition. *Neuropsychobiology.* (2015) 72:46–56. doi: 10.1159/000379752

63. Driver J, Noesselt T. Multisensory interplay reveals crossmodal influences on "sensory-specific" brain regions, neural responses, and judgments. *Neuron.* (2008) 57:11–23. doi: 10.1016/j.neuron.2007.12.013

64. Ghazanfar AA, Schroeder CE. Is neocortex essentially multisensory? *Trends Cogn Sci.* (2006) 10:278–85. doi: 10.1016/j.tics.2006.04.008

65. Lewis R, Noppeney U. Audiovisual synchrony improves motion discrimination via enhanced connectivity between early visual and auditory areas. *J Neurosci.* (2010) 30:12329–39. doi: 10.1523/JNEUROSCI.5745-09.2010

66. Doehrmann O, Weigelt S, Altmann CF, Kaiser J, Naumer MJ. Audiovisual functional magnetic resonance imaging adaptation reveals multisensory integration effects in object-related sensory cortices. *J Neurosci.* (2010) 30:3370–9. doi: 10.1523/JNEUROSCI.5074-09.2010

67. Eckert MA, Kamdar NV, Chang CE, Beckmann CF, Greicius MD, Menon V. A cross-modal system linking primary auditory and visual cortices: evidence from intrinsic fMRI connectivity analysis. *Human Brain mapping.* (2008) 29:20560. doi: 10.1002/hbm.20560

68. Thoma RJ, Chaze C, Lewine JD, Calhoun VD, Clark VP, Bustillo J, et al. Functional MRI evaluation of multiple neural networks underlying auditory verbal hallucinations in schizophrenia spectrum disorders. *Front Psychiatry.* (2016) 7:39. doi: 10.3389/fpsyt.2016.00039

69. Jardri R, Thomas P, Delmaire C, Delion P, Pins D. The neurodynamic organization of modality-dependent hallucinations. *Cereb Cortex.* (2013) 23:1108–17. doi: 10.1093/cercor/bhs082

frontiers | Frontiers in Psychiatry

TYPE Original Research
PUBLISHED 24 October 2022
DOI 10.3389/fpsyt.2022.942905

OPEN ACCESS

EDITED BY
Yujun Gao,
Wuhan University, China

REVIEWED BY
Zhenhao Zhang,
Nanjing Medical University, China
Qinxiang Zheng,
Wenzhou Medical University, China

*CORRESPONDENCE
Yi Shao
freebee99@163.com

SPECIALTY SECTION
This article was submitted to Neuroimaging and Stimulation, a section of the journal Frontiers in Psychiatry

RECEIVED 13 May 2022
ACCEPTED 08 August 2022
PUBLISHED 24 October 2022

CITATION
Hu Q, Chen J, Kang M, Ying P, Liao X, Zou J, Su T, Wang Y, Wei H and Shao Y (2022) Abnormal percent amplitude of fluctuation changes in patients with monocular blindness: A resting-state functional magnetic resonance imaging study.
Front. Psychiatry 13:942905.
doi: 10.3389/fpsyt.2022.942905

Abnormal percent amplitude of fluctuation changes in patients with monocular blindness: A resting-state functional magnetic resonance imaging study

Qiaohao Hu[1], Jun Chen[1], Min Kang[1], Ping Ying[1], Xulin Liao[2], Jie Zou[1], Ting Su[3], Yixin Wang[1], Hong Wei[4] and Yi Shao[1]*

[1]Department of Ophthalmology, The First Affiliated Hospital of Nanchang University, Jiangxi Branch of National Clinical Research Center for Ocular Disease, Nanchang, China, [2]Department of Ophthalmology and Visual Sciences, The Chinese University of Hong Kong, Shatin, Hong Kong SAR, China, [3]Department of Ophthalmology, Massachusetts Eye and Ear, Harvard Medical School, Boston, MA, United States, [4]School of Optometry and Vision Sciences, College of Biomedical and Life Sciences, Cardiff University, Cardiff, United Kingdom

Purpose: Previous studies on monocular blindness (MB) have mainly focused on concept and impact. The present study measured spontaneous brain activity in MB patients using the percentage of amplitude fluctuation (PerAF) method.

Methods: Twenty-nine patients with MB (21 male and 8 female) and 29 age-, gender-, and weight-matched healthy controls (HCs) were recruited. All participants underwent resting state functional magnetic resonance imaging (rs-fMRI). The PerAF method was used to analyze the data and evaluate the spontaneous regional brain activity. The ability of PerAF values to distinguish patients with MB from HCs was analyzed using receiver operating characteristic (ROC) curves, and correlation analysis was used to assess the relationship between PerAF values of brain regions and the Hospital Anxiety and Depression Scale (HADS) scores.

Results: PerAF values in Occipital_Mid_L/Occipital_Mid_R/Cingulum_Mid_L were significantly lower in patients with MB than in controls. Conversely, values in the Frontal_Sup_Orb_L/Frontal_Inf_Orb_L/Temporal_Inf_L/Frontal_Inf_Oper_L were significantly higher in MB patients than in HCs. And the AUC of ROC curves were follows: 0.904, ($p < 0.0001$; 95%CI: 0.830–0.978) for Frontal_Sup_Orb_L/Frontal_Inf_Orb_L; Temporal_Inf_L 0.883, ($p < 0.0001$; 95% CI: 0.794–0.972); Frontal_Inf_Oper_L 0.964, ($p < 0.0001$; 95% CI: 0.924–1.000), and 0.893 ($p < 0.0001$; 95% CI: 0.812–0.973) for Occipital_Mid_L; Occipital_Mid_R 0.887, ($p < 0.0001$; 95% CI: 0.802–0.971); Cingulum_Mid_L 0.855, ($p < 0.0001$; 95% CI: 0.750–0.960).

Conclusion: The results of our study show abnormal activity in some brain regions in patients with MB, indicating that these patients may be at risk of disorder related to these brain regions. These results may reflect the neuropathological mechanisms of MB and facilitate early MB diagnoses.

KEYWORDS

MB, PerAF, resting state, fluctuation changes, functional magnetic resonance imaging

Introduction

Vision loss, including blindness, is a major public health problem, affecting individual lives, society, and the economy. Visual impairment has negative impacts on standard of living and self-care, is a heavy social burden, and may cause significant economic damage. Traditionally, the definition of blindness has been based on functional disability and quantized visual acuity (VA) value. However, the diagnostic criteria for blindness vary between countries (1). Many factors can cause blindness, including diseases, such as age-related macular degeneration (AMD) (2), cataract (3), trachoma (4), and glaucoma (5). Among them, AMD is the most important cause of blindness (2). Although there are treatments for these diseases, if they are not addressed promptly or effectively, they can cause irreversible damage to visual function and can eventually lead to blindness. The World Health Organization (WHO) estimated that about 1.3 billion people may suffer from visual impairment (VI) globally, with a range of causes (6). According to one study, it is estimated that worldwide in 2015 about 36 million people were blind, 216.6 million people suffered from moderate to severe VI, while 185.5 million people had mild VI (7). These data show that VI affects many people and this should arouse public attention. Blindness may be unilateral (monocular) or bilateral, and its incidence is related to factors such as heredity and environment. This paper focuses on monocular blindness (MB).

Monocular blindness is defined as the reduction or loss of visual input caused by the damage or destruction of retina or optic nerve. The naked visual acuity of blind eye is <0.05, and the naked visual acuity of contralateral eye is ≥ 0.05.Studies have shown that MB may occur at any age and affect either gender (8), and includes the loss of stereo vision, perception of shape and color and other visual functions (9). It should be noted that progression may continue beyond monocular blindness, and that if the other eye is not treated properly both eyes may become affected (10). Therefore, once MB is diagnosed the cause should be treated without delay to prevent the adverse consequences of binocular blindness.

The etiology of MB is varied, eye trauma being a major cause in children (11). In developing countries, adult cataracts and glaucoma are important causes (12–14), while in developed countries AMD and diabetic retinopathy are major causes (15).

As a non-invasive method, functional magnetic resonance imaging (fMRI) can evaluate brain structure and function, and researchers have found associations between fMRI measurement and clinical manifestations of diseases (16). Compared with other neuroscience technologies, the advantage of fMRI lies in its flexibility (17). Multi-level brain imaging analysis is an effective means to find brain structural and functional changes in early postoperative chronic disease. Yang used fMRI technology to explore the immediate brain effect of Moxibustion in patients with primary dysmenorrhea and found that positive activation was the main manifestation of local consistency and coordination in the brain area of patients, and the prefrontal lobe was likely to play an analgesic and sedative role. The change of prefrontal lobe-default network (DMN) functional connection may be an important central mechanism of analgesia (18).

Resting state functional magnetic resonance imaging (rs-fMRI) depends on the spontaneous low-frequency fluctuations in the blood oxygen level-dependent (BOLD) signal with non-invasive, zero radiation and high spatial resolution has become an effective new means of contemporary acupuncture research (19), which can objectively and visually observe the central functional regulation of the brain. Regional Homo geneity(Re HO),functional connection(FC), and fractional amplitude of low frequency fluctuation(fALFF) are the two most commonly used data analysis methods in rs-fMRI (20). The former represents the consistency of local functional activities in brain regions and reflects the synchronization of time series in local brain regions (21). The latter represents the strength of functional connection between brain regions (22), and can reflect the temporal correlation between region of interest (ROI) and whole brain networked function, fALFF has high sensitivity and specificity, and can accurately reflect the spontaneous neuronal activity in low-frequency local brain areas (23).

The peraf value is less affected by the error of signal intensity, and can be used for group level statistical analysis (24). It is not affected by the mixing of voxel specific fluctuation amplitude in the amplitude of low-frequency fluctuation method. It can measure the brain activity change of voxel level more accurately and efficiently (25). It is more accurate than other MRI analysis methods such as low-frequency fluctuation amplitude (26), regional homogeneity and degree centrality (27). It is of great

TABLE 1 Characteristics of participants included in the study.

Condition	MB	HCs	t	*P*-value*
Male/female	21/8	21/8	N/A	>0.99
Age (years)	47.76 ± 6.76	46.23 ± 6.61	0.168	0.792
Weight (kg)	71.87 ± 5.98	72.71 ± 6.87	0.286	0.881
Handedness	29R	29R	N/A	>0.99
Duration of MB (h)	58.54 ± 25.54	N/A	N/A	N/A
Best-corrected VA-left eye	0.25 ± 0.10	1.05 ± 0.15	−5.965	0.002
Best-corrected VA-right eye	0.20 ± 0.05	1.15 ± 015	−5.653	0.003

$p < 0.05$ independent *t*-tests comparing two groups, data shown as mean ± standard deviation. MB, monocular blindness; HCs, healthy controls; VA, visual acuity; N/A, not applicable.

significance for the diagnosis and treatment of monocular blindness (28).

After monocular blindness, one side of the visual function is normal, and the other side is damaged. At this time, the brain's visual reflex mechanism may increase in the normal side, and thus peraf changes. Another is the disorder of visual transmission mechanism in patients with monocular blindness. At this time, the brain may not be stimulated by visual activity, and the function of the corresponding parts will be reduced, resulting in changes in peraf (29). The peraf value is less affected by the error of signal intensity, and can be used for group level statistical analysis. It is not affected by the mixing of voxel specific fluctuation amplitude in the amplitude of low-frequency fluctuation method. It can measure the brain activity change of voxel level more accurately and efficiently. It is more accurate than other MRI analysis methods such as low-frequency fluctuation amplitude, regional homogeneity and degree centrality. It is of great significance for the diagnosis and treatment of monocular blindness (30).

The present study will apply percentage of amplitude fluctuation (PerAF) technology to study the spontaneous brain regional activity and clinical manifestations of MB patients, and to investigate whether this method can be used for early diagnosis of MB.

Materials and methods

Patients

Twenty-nine patients with MB (21 male and 8 female) were recruited at the Ophthalmology Department of the First Affiliated Hospital of Nanchang University. These subjects satisfied the following criteria: (1) blind in one eye; (2) contralateral eye is normal without cataract, optic neuritis, or other eye diseases; (3) exclude strabismus.

In addition, 29 healthy controls (21 male and 8 female) were recruited and the two groups were similar in gender balance ($p > 0.99$), age ($p = 0.792$), and weight ($p = 0.881$). Control subjects were included if they satisfied the following criteria: (1) normal naked eye or normal corrected vision; (2) no neurological diseases; (3) no mental disorder; (4) able to have an MRI scan (for example, they did not have pacemaker or implanted metal device) (Table 1).

The research was authorized by the Human Research Ethics Committee of the First Affiliated Hospital of Nanchang University. Each participant understood the aim, methods and possible risks of the research, and signed a declaration of informed consent.

Magnetic resonance imaging data collection

The Trio 3-Tesla MR scanner (Siemens, Munich, Germany) was used. Before scanning, each participant was asked to relax, close their eyes, and minimize movement (29). To obtain functional data, a 3D metamorphic gradient echo pulse sequence was used. The following parameters were used for a 176-image scan: acquisition matrix 256 × 256; field of view 250 mm × 250 mm; echo time 2.26 ms; repetition time 1,900 ms; thickness 1.0 mm; gap 0.5 mm; flip angle 9°. For a 240-image scan, parameters were as follows: acquisition matrix 64 × 64; field of view 220 mm × 220 mm; thickness 4.0 mm; gap 1.2 mm; repetition time 2,000 ms; echo time 30 ms; flip angle. 90°, 29 axial.

Functional magnetic resonance imaging processing

MRIcro software (Nottingham University, Nottingham, UK) was used to sort the data, and to identify and exclude incomplete or flawed data. Remaining data were processed, including space standardization, head movement correction, slice time, and digital image format conversion using DPARSFA.[1] Linear regression was used to

1 http://rfmri.org/DPARSF

TABLE 2 Brain areas with significantly different PerAF values between MB and HCs.

Brain areas	MNI coordinates			Number of voxels	T value	ROI
	X	Y	Z			
HCs < MB						
Frontal_Sup_Orb_L/Frontal_Inf_Orb_L	0	18	−27	169	−5.0299	1
Temporal_Inf_L	−42	−18	−27	98	−4.917	2
Frontal_Inf_Oper_L)	−39	15	9	111	−4.4132	5
HCs > MB						
Occipital_Mid_L	−36	−81	3	112	5.2095	3
Occipital_Mid_R	36	−81	6	112	4.5945	4
Cingulum_Mid_L	−3	9	33	50	4.5309	6

The statistical threshold was set at the voxel level with $p < 0.001$ for multiple comparisons using Gaussian random field theory ($p < 0.01$, cluster >49 voxels, AlphaSim corrected). PerAF, percent amplitude of fluctuation; ROI, regions of interest; HCs, healthy controls; MNI, Montreal Neurological Institute; MB: monocular blindness.

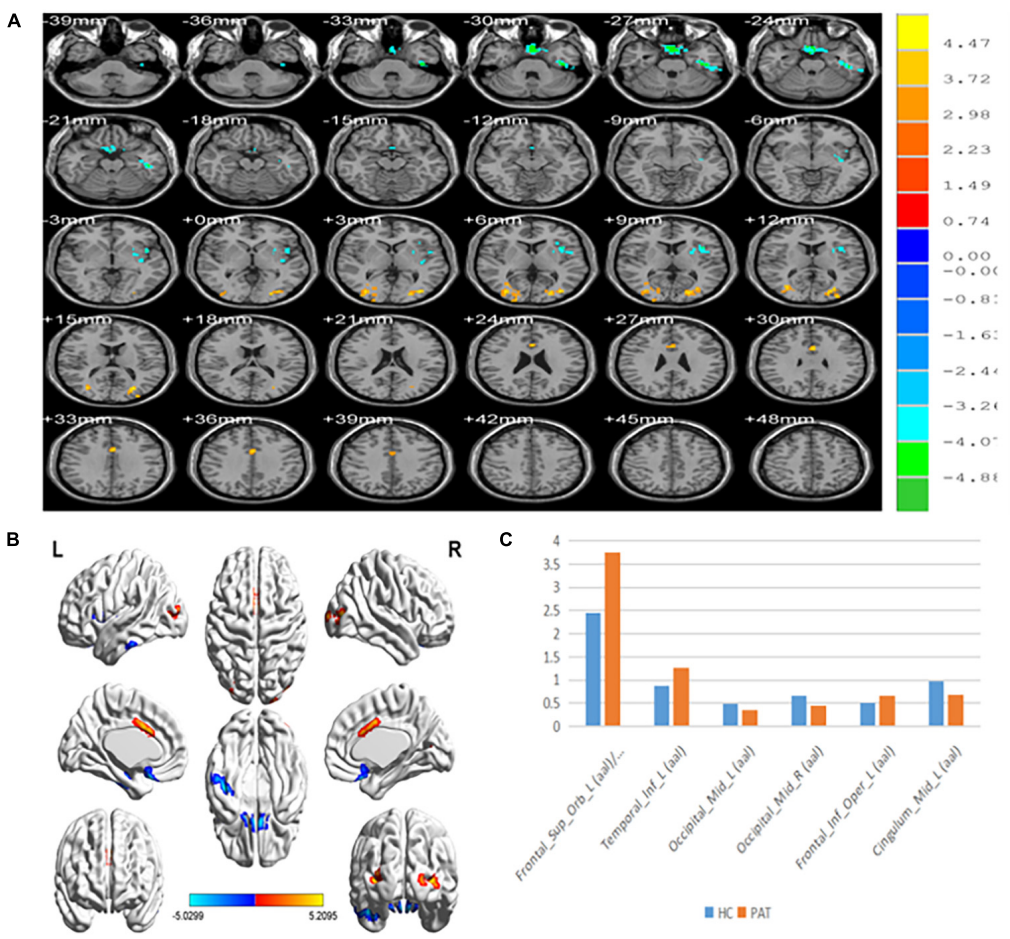

FIGURE 1
(A,B) Spontaneous brain activity in the MB patients and the HC group. **(C)** The mean PerAF signal value between the MB and HC groups. Warmer shades (yellow and red) represent moderate and high signal strength, respectively and blue represents lower signal strength. The signal values of Frontal_Sup_Orb_L/Frontal_Inf_Orb_L/Temporal_inf_L/Frontal_Inf_Oper_L regions in MB patients are higher than in controls, and on the contrary, the signal valuse of Occipital_Mid_L/Occipital_Mid_R/Cingulum_Mid_L are lower than controls. PerAF, percent amplitude of fluctuation; MB, monocular blindness; HCs, healthy controls.

eliminate the influence of factors such as signals originating from white matter.

Because excessive head movement may have a significant impact on the fMRI sequence, participants with head movements >3 mm and the data were excluded. Due to inter-individual variations in brain size and structure, each brain image was standardized (30). We used regions of interests (ROI) of the central white matter region to deal with irrelevant variables (31).

Functional magnetic resonance imagingdata were processed using the PerAF method, a relatively reliable and direct measurement of brain activity. First, the average BOLD signal value was calculated, then the signal strength at a range of time points was normalized to this value. This process resulted in an amplitude at each time point as a percentage of the average across the time series, and a signal change percentage similarity index, referred to as PerAF. The formula used to calculate the PerAF value of a single voxel is as follows:

$$\mathrm{PerAF} = 1n\Sigma i = 1n|Xi - \mu\mu| \times 100\% \quad (1)$$

$$\mu = 1n\Sigma i = 1nXi \quad (2)$$

Where Xi represents the signal strength, n is the total number of time points, and μ is the mean value of the time series (21).

Correlation analysis

We obtained the anxiety scores (AS) and depression scores (DS) of MB patients by doing the Hospital Anxiety and Depression Score (HADS). We looked for correlations between each score and the PerAF values of the following brain regions: Frontal_Sup_Orb_L/Frontal_Inf_Orb_L, and Frontal_Inf_Oper_L using Pearson's correlation analysis ($p < 0.05$ was considered significant). GraphPad Prism 8.0 software was used to plot linear correlations.

Statistical analysis

For between-group comparisons, SPSS software, version 20.0 (IBM Corp., Armonk, NY, USA) was used to conduct independent sample t tests, and $p < 0.05$ was considered significant. The REST software was used to conduct independent sample t tests comparing PerAF values between the two groups. Gaussian random field theory was used for multiple comparison correction, and the voxel level threshold was $p < 0.001$. AlphaSim, part of the REST toolbox, was used for correction, the cluster size was set at >49 voxels, and the level was $p < 0.05$. Receiver operating characteristic (ROC) curves were used to compare the average PerAF values of the relevant brain areas between MB and HC groups and to obtain estimates of diagnostic accuracy based on the area under the curve (AUC). As explained above, Pearson's correlation was used to evaluate the relationship between PerAF and anxiety/depression scores. All averaged data are presented in the form of mean ± standard deviation. The regions were defined using automatic anatomic labeling based on the Montreal Neurological Institute data set.

Results

Sample statistic and visual data

Gender ($p > 0.99$), age ($p = 0.792$), and weight ($p = 0.881$) were all similar in the two groups. However, significant differences were found between groups in monocular best-corrected visual acuity (VA) (left $P = 0.002$; right $p = 0.003$). The duration since MB diagnosis was 58.54 ± 25.54 h.

Percentage of amplitude fluctuation differences

Compared with HCs, PerAF values were significantly reduced in MB patients at the Occipital_Mid_L/Occipital_Mid_R/Cingulum_Mid_L. Conversely, values were significantly higher in MB than HC at the Frontal_Sup_Orb_L/Frontal_Inf_Orb_L/Temporal_Inf_L/Frontal_Inf_Oper_L. (**Table 2** and **Figure 1**).

Analysis of receiver operating characteristic curves

Area under the curve provides an indication of diagnostic accuracy. AUC ranges from 0 to 1, higher values indicating higher accuracy. The AUC for brain regions defined here were between 0.86 and 0.96 and all were statistically significant (<0.0001) (**Figure 2**).

Correlation analysis

Figure 3 shows that correlation between PerAF values and HADS scores were significant at Frontal_Sup_Orb_L/Frontal_Inf_Orb_L for AS ($r = 0.9338$, $p < 0.0001$) and DS ($r = 0.8361$, $p < 0.0001$). Similarly, PerAF values at the Frontal_Inf_Oper_L were significantly positively correlated with AS ($r = 0.5134$, $p < 0.05$) and DS ($r = 0.4313$, $p < 0.05$) (**Figure 3**).

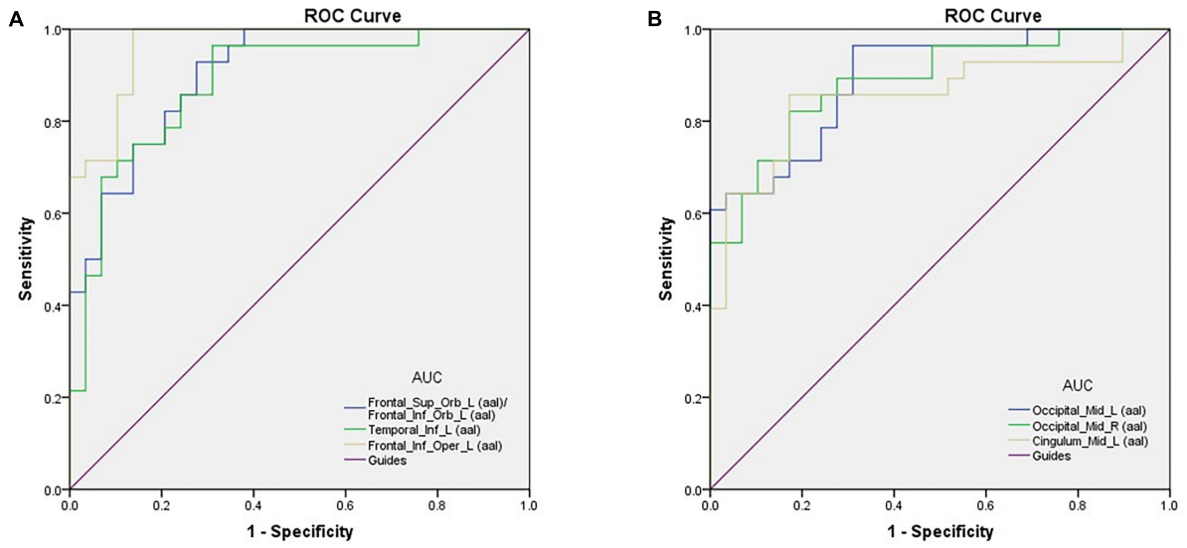

FIGURE 2
ROC curve analysis of the mean perAF values for altered brain regions. **(A)** The area under the ROC curve was 0.904, ($p < 0.0001$; 95% CI: 0.830–0.978) for Frontal_Sup_Orb_L (aal)/Frontal_Inf_Orb_L (aal); Temporal_Inf_L (aal) 0.883, ($p < 0.0001$; 95% CI: 0.794–0.972); Frontal_Inf_Oper_L (aal) 0.964, ($p < 0.0001$; 95% CI: 0.924–1.000). **(B)** The area under the ROC curve was 0.893 ($p < 0.0001$; 95% CI: 0.812–0.973) for Occipital_Mid_L (aal); Occipital_Mid_R (aal) 0.887, ($p < 0.0001$; 95% CI: 0.802–0.971); Cingulum_Mid_L (aal) 0.855, ($p < 0.0001$; 95% CI: 0.750–0.960). AUC, area under the curve; ROC, receiver operating characteristic.

Discussion

In this study, the PerAF method was used to increase understanding of MB, and to our knowledge this is the first study in which MB has been investigated using this approach. The method is widely used and has also been applied to study other diseases (32–34) (**Table 3**). Our results showed that the signal values of Frontal_Sup_Orb_L/Frontal_Inf_Orb_L/Temporal_Inf_L/Frontal_Inf_Oper_L regions are higher in MB patients than controls, while conversely signals are lower than controls at Occipital_Mid_L/Occipital_Mid_R/Cingulum_Mid_L (**Figure 4** and **Table 3**).

The results of correlation analyses showed that in Frontal_Sup_Orb_L/Frontal_Inf_Orb_L/Frontal_Inf_Oper_L, AS and DS were positively correlated with PerAF values. Higher HADS scores indicate more severe levels of anxiety or depression, so this result indicates deeper anxiety and depression with higher PerAF values.

The orbitofrontal cortex (OFC) is an area of the brain in front of the eyes, consisting of a large cortical region on the ventral side of the frontal lobe (35). The OFC includes the orbital superior frontal gyrus and orbital inferior frontal gyrus, and it receives input from the visual, somatosensory, olfactory and taste regions, the limbic region, and the dorsal raphe region (36, 37). Rolls et al. reported that the OFC is related to emotion and depression (38), and that OFC plays an important role in day-to-day transactions (5). Izquierdo et al. conducted an animal study and found that OFC is associated with reward for learning and decision making (39). Other research has shown that the OFC is associated with alcohol abuse and dependence (40). In the present study, PerAF values were increased in the Frontal_Sup_Orb_L/Frontal_Inf_Orb_L regions in MB patients, indicating hyperactivity of this brain region. We infer that MB may be associated with difficulties related to emotion and social ability.

PerAF was also increased in the Temporal_Inf_L of MB patients. This region is situated on the lateral and inferior surfaces of the temporal lobe, ventral to the middle temporal gyrus (41). Previous research has shown that it participates in multiple cognitive processes, such as visual perception and multi-mode sensory integration (42–44). Onitsuka et al. reported the inferior temporal gyrus is fundamental to the pathophysiology of cognitive impairments in Alzheimer's disease (41). In the present study, increased activity in this brain region suggests that a range of cognitive anomalies may occur in MB patients.

A study reported that the left inferior frontal cortex has an influence on reflect-Self contrast (45), and has a role in the guidance of intonation processing (46), Other research findings have shown that this region may be viewed as a neural intersection for different types of information, and is important for distinguishing between concrete and abstract concepts (47). Study (48) has shown that suppressing this region may allow activation of neural networks that lead to greater creativity. The left operculum of left inferior frontal cortex is

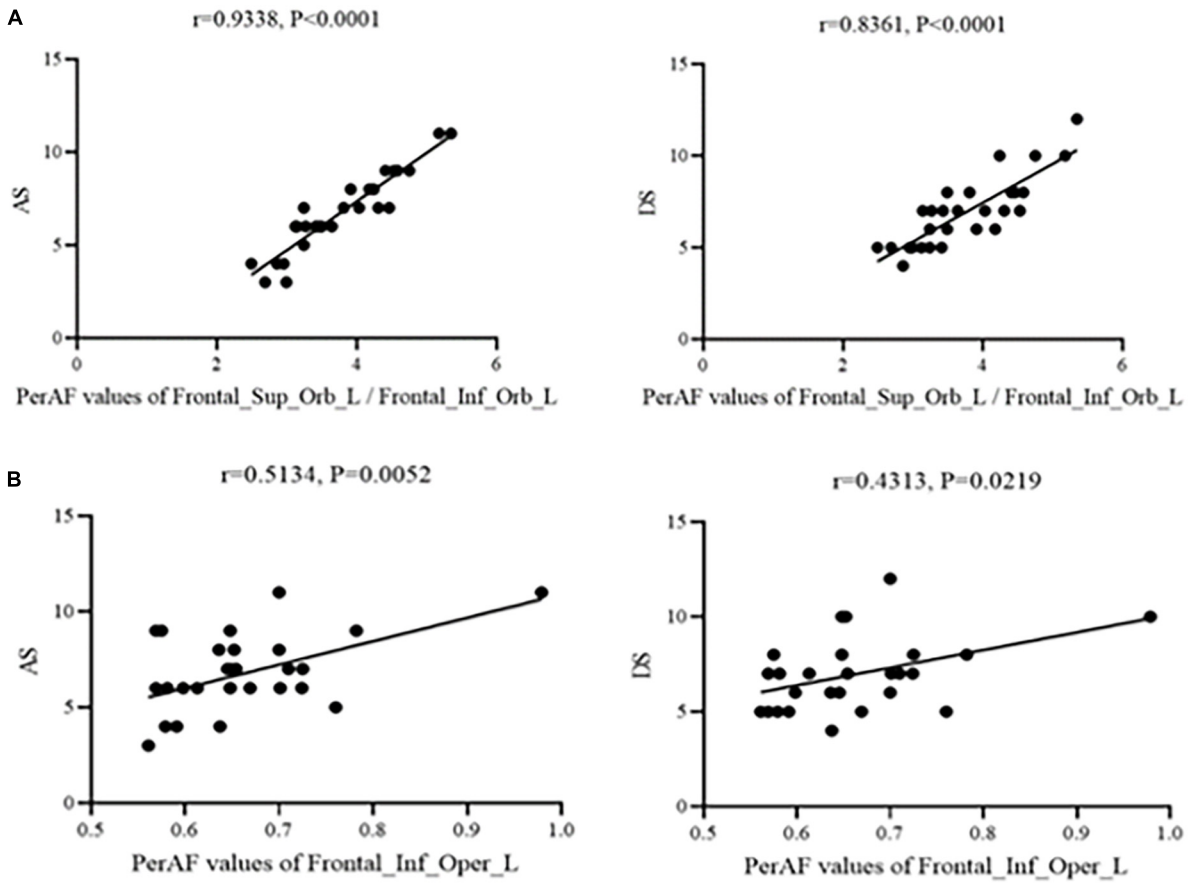

FIGURE 3
Correlation between PerAF and HADS scores. **(A)** Stands for monocular blindness group and **(B)** stands for healthy control group. In the MB group, the PerAF value of Frontal_Sup_Orb_L/Frontal_Inf_Orb_L showed a positive correlation with AS (r = 0.9338, $p < 0.0001$) and DS (r = 0.8361, $p < 0.0001$), and the value of Frontal_Inf_Oper_L also showed a positive correlation with AS (r = 0.5134, $p < 0.05$) and DS (r = 0.4313, $p < 0.05$). PerAF, percent amplitude of fluctuation; AS, anxiety scores; DS, depressed scores; MB, monocular blindness.

TABLE 3 PerAF method applied in ophthalmologic and neurogenic disease.

Brain areas	Experimental results	Brain functions	Anticipated results
Frontal_Sup_Orb_L/Frontal_Inf_Orb_L	HC < MB	Emotion and depression, economic decisions, rewarding learning, decision making, alcohol abuse and dependence	Emotion problems, disability in dealing with daily tasks, social problems
Temporal_Inf_L	HC < MB	visual perception, multi-mode sensory integration	Cognitive impairment, mental disorder
Frontal_Inf_Oper_L	HC < MB	Reflect-Self contrast, the guidance of intonation processing, distinguishing concrete concepts from abstract concepts,creativity	Semantic comprehension disorder, conceptual comprehension disorder
Occipital_Mid_L	HC > MB	Visual information processing, attention, emotional processing, verbal episodic memory,	Depression, affective dysfunction, mental problems, memory problems
Occipital_Mid_R	HC > MB	visual spatial information processing, attention, working memory	Spatial vision problems, attention problems, memory disorder,
Cingulum_Mid_L	HC > MB	Social cognition, emotion processing, motor control, maturity	Emotion problems, cognition dysfunction, motor control disorder, maturational delay

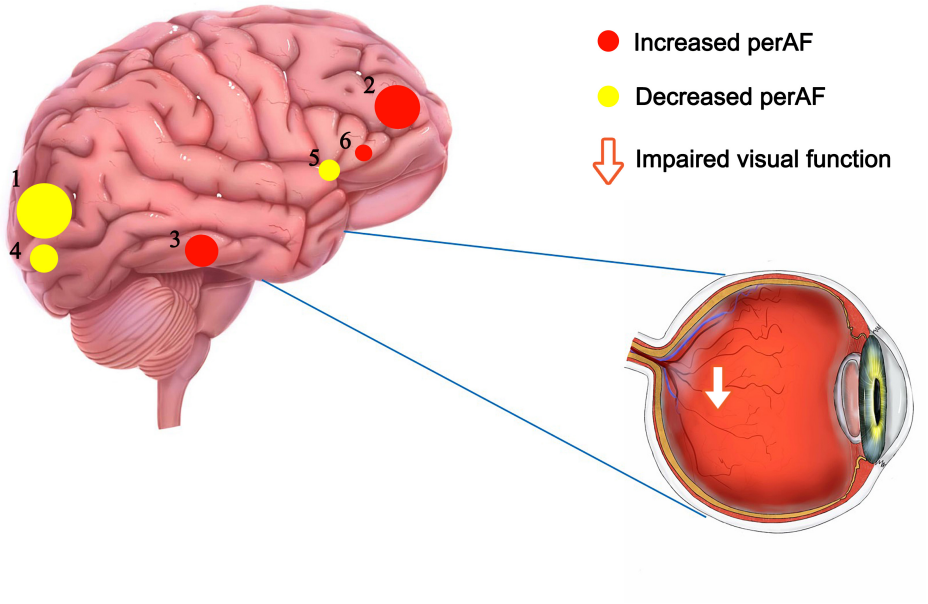

FIGURE 4
The mean perAF values of altered brain regions. Notes: Compared with the HCs, the perAF values of the following regions were increased to various extents: 2- Frontal_Sup_Orb_L/Frontal_Inf_Orb_L (t = -5.03), 3- Temporal_Inf_L (t = -4.92), 6- Frontal_Inf_Oper_L (t = -4.41). Compared with the HCs, the perAF values of the following regions were decreased to various extents: 1- Occipital_Mid_L (t = 5.21), 4- Occipital_Mid_R (t = 4.595), 6- Cingulum_Mid_L (t = 4.531). HCs, healthy controls; BA, Brodmann's area.

TABLE 4 Brain areas alternation and its potential functions. HC, healthy controls; MB, monocular blindness.

		Brain areas		
Author, year	**Disease**	**UDs > HCs**	**UDs < HCs**	**(Refs.)**
Yang et al. (32)	Retinal detachment	Right fusiform gyrus, left inferior temporal gyrus,		(32)
Wang et al. (33)	Epilepsy	Vermis, left cellebellar lobule, left percentral gyrus	Pecentral gyrus	(33A
Zeng et al. (34)	Sleep deprivation	Bilateral visual cortex, bilateral sensorimotor cortex	Bilateral dorsolateral prefrontal cortex, bilateral cerebellum posterior lobe	(34)

associated with sensorimotor function, such as the experience of pain (49). Since the PerAF value in this region is higher in MB patients than in HCs, we hypothesize that the risk of disease associated with dysfunction in this region may be increased in this group.

The occipital lobe, which takes up most of the visual cortex, helps with the processing of visual information and plays a role in exclamatory facial expressions, and in this study, it turned out that left middle occipital may be associated with depression in women (50), moreover, the region is also involved in attention (51), verbal episodic memory (52), and affective dysfunction (53), and Stern et al. (53) found that in adults with obsessive-compulsive disorder, spontaneous activity in this region is increased. In contrast to the brain regions discussed above, the decreased PerAF signal values in the left middle occipital in MB patients compared with HCs indicates that this brain region is functionally impaired in MB patients.

Similar to the left middle occipital, the right middle occipital lobe is associated with visual spatial information (54) and attention (55). Zeng et al. (56) found that function of the right middle occipital was positively correlated with object working memory. On the right side of the middle occipital gyrus, we observed decreased brain activity in MB patients, indicating that the function of this area was reduced.

Finally, we found a decrease in brain activity in the left middle cingulum in MB patients. The cingulate gyrus belongs to the medial cortex and medial temporal lobe (57), and plays an important role in social cognition (58), emotional processing (59) and motor control (60). A study on attention disorder/hyperactivity disorder found dysfunction of the left middle cingulum in MB patients, which was attributed

to delayed maturation (61). We infer that the abnormal spontaneous activity of this brain region in MB patients may reflect abnormality of functions related to this region (Table 4).

Limitations

This study included a small sample, which may not be representative of the wider population of patients with MB. In addition, the included MB patients had a range of durations since diagnosis of MB, which may have increased variance in the experimental results. Next, we will increase the sample size, conduct multi sequence analysis, follow-up patients, explore ways to treat brain function and try to make up for deficiencies.

Conclusion

In this study, we used the PerAF method to analyze regional brain activity in MB patients. Compared with healthy controls, hyperactivity in some brain regions and hypoactivity in other regions may be related to anomalous function and behavior associated with these brain regions. To the best of our knowledge, this is the first study on MB using the PerAF method. Future studies of this kind may further enhance understanding of neural changes in MB and may lead to the use of this method as an early diagnostic index.

Data availability statement

The original contributions presented in this study are included in the article/supplementary material, further inquiries can be directed to the corresponding author.

Ethics statement

The studies involving human participants were reviewed and approved by Medical Ethics Committee of The First Affiliated Hospital of Nanchang University (Nanchang, China). The patients/participants provided their written informed consent to participate in this study.

Author contributions

QH, JC, and MK analyzed the data and draft the manuscript. PY, XL, and JZ assisted with data interpretation and figure composing. TS, YW, and HW collected the data. YS conceived, designed, and directed the study, final revised, and approved the manuscript. All authors contributed to the article and approved the submitted version.

Funding

This work was supported by National Natural Science Foundation (No: 82160195); Central Government Guides Local Science and Technology Development Foundation (No: 20211ZDG02003); and Key Research Foundation of Jiangxi Province (Nos: 20181BBG70004 and 20203BBG73059).

Conflict of interest

The authors declare that the research was conducted in the absence of any commercial or financial relationships that could be construed as a potential conflict of interest.

Publisher's note

References

1. Vashist P, Senjam SS, Gupta V, Gupta N, Kumar A. Definition of blindness under National Programme for Control of Blindness: do we need to revise it? *Indian J Ophthalmol.* (2017) 65:92–6. doi: 10.4103/ijo.IJO_869_16

2. Fisher CR, Ferrington DA. Perspective on AMD pathobiology: a bioenergetic crisis in the RPE. *Invest Ophthalmol Vis Sci.* (2018) 59:AMD41–7. doi: 10.1167/iovs.18-24289

3. Lee CM, Afshari NA. The global state of cataract blindness. *Curr Opin Ophthalmol.* (2017) 28:98–103. doi: 10.1097/ICU.0000000000000340

4. Silva EJD, Pereira DP, Ambrózio JOAM, Barboza LM, Fonseca VL, Caldeira AP. Prevalence of trachoma and associated factors in students from the Jequitinhonha Valley, Minas Gerais, Brazil. *Rev Soc Bras Med Trop.* (2020) 53:e20200056. doi: 10.1590/0037-8682-0056-2020

5. Hu YX, Xu XX, Shao Y, Yuan GL, Mei F, Zhou Q, et al. The prognostic value of lymphocyte-to-monocyte ratio in retinopathy of prematurity. *Int J Ophthalmol.* (2017) 10:1716–21. doi: 10.18240/ijo.2017.11.13

6. Sahel JA, Bennett J, Roska B. Depicting brighter possibilities for treating blindness. *Sci Transl Med.* (2019) 11:eaax2324. doi: 10.1126/scitranslmed.aax2324

7. Bourne RRA, Flaxman SR, Braithwaite T, Cicinelli MV, Das A, Jonas JB, et al. Magnitude, temporal trends, and projections of the global prevalence of blindness and distance and near vision impairment: a systematic review and meta-analysis. *Lancet Glob Health.* (2017) 5:e888–97. doi: 10.1016/S2214-109X(17)30293-0

8. Richard AI. Monocular blindness in Bayelsa state of Nigeria. *Pan Afr Med J.* (2010) 4:6. doi: 10.4314/pamj.v4i1.53607

9. Jones RK, Lee DN. Why two eyes are better than one: the two views of binocular vision. *J Exp Psychol Hum Percept Perform.* (1981) 7:30–40. doi: 10.1037//0096-1523.7.1.30

10. Bansal RK, Khandekar R, Nagendra P, Kurup P. Magnitude and causes of unilateral absolute blindness in a region of Oman: a hospital-based study. *Eur J Ophthalmol.* (2007) 17:418–23. doi: 10.1177/112067210701700325

11. Eballe AO, Epée E, Koki G, Bella L, Mvogo CE. Unilateral childhood blindness: a hospital-based study in Yaoundé, Cameroon. *Clin Ophthalmol.* (2009) 3:461–4. doi: 10.2147/opth.s5289

12. Nwosu SN. Blindness and visual impairment in Anambra State, Nigeria. *Trop Geogr Med.* (1994) 46:346–9.

13. Huang X, Li D, Li HJ, Zhong YL, Freeberg S, Bao J, et al. Abnormal regional spontaneous neural activity in visual pathway in retinal detachment patients: a resting-state functional MRI study. *Neuropsychiatr Dis Treat.* (2017) 13:2849–54. doi: 10.2147/NDT.S147645

14. Harrell J, Larson ND, Menza E, Mboti AA. Clinic-based survey of blindness in Kenya. *Community Eye Health.* (2001) 14:68–9.

15. Buch H, Vinding T, La Cour M, Nielsen NV. The prevalence and causes of bilateral and unilateral blindness in an elderly urban Danish population. The copenhagen city eye study. *Acta Ophthalmol Scand.* (2001) 79:441–9. doi: 10.1034/j.1600-0420.2001.790503.x

16. Brown HD, Woodall RL, Kitching RE, Baseler HA, Morland AB. Using magnetic resonance imaging to assess visual deficits: a review. *Ophthalmic Physiol Opt.* (2016) 36:240–65. doi: 10.1111/opo.12293

17. Evans SL, Dowell NG, Prowse F, Tabet N, King SL, Rusted JM. Mid age APOE ε4 carriers show memory-related functional differences and disrupted structure-function relationships in hippocampal regions. *Sci Rep.* (2020) 10:3110. doi: 10.1038/s41598-020-59272-0

18. Yang J, Xiong J, Yuan T, Wang X, Jiang Y, Zhou X, et al. Effectiveness and safety of acupuncture and moxibustion for primary dysmenorrhea: an overview of systematic reviews and meta-analyses. *Evid Based Complement Alternat Med.* (2020) 2020:8306165. doi: 10.1155/2020/8306165

19. Ogawa S, Menon RS, Kim SG, Ugurbil K. On the characteristics of functional magnetic resonance imaging of the brain. *Annu Rev Biophys Biomol Struct.* (1998) 27:447–74. doi: 10.1146/annurev.biophys.27.1.447

20. Huang X, Li HJ, Ye L, Zhang Y, Wei R, Zhong YL, et al. Altered regional homogeneity in patients with unilateral acute open-globe injury: a resting-state functional MRI study. *Neuropsychiatr Dis Treat.* (2016) 12:1901–6. doi: 10.2147/NDT.S110541

21. Jia XZ, Sun JW, Ji GJ, Liao W, Lv YT, Wang J, et al. Percent amplitude of fluctuation: a simple measure for resting-state fMRI signal at single voxel level. *PLoS One.* (2020) 15:e0227021. doi: 10.1371/journal.pone.0227021

22. Li T, Liu Z, Li J, Liu Z, Tang Z, Xie X, et al. Altered amplitude of low-frequency fluctuation in primary open-angle glaucoma: a resting-state FMRI study. *Invest Ophthalmol Vis Sci.* (2014) 56:322–9. doi: 10.1167/iovs.14-14974

23. Pan ZM, Li HJ, Bao J, Jiang N, Yuan Q, Freeberg S, et al. Altered intrinsic brain activities in patients with acute eye pain using amplitude of low-frequency fluctuation: a resting-state fMRI study. *Neuropsychiatr Dis Treat.* (2018) 14:251–7. doi: 10.2147/NDT.S150051

24. Shao Y, Cai FQ, Zhong YL, Huang X, Zhang Y, Hu PH, et al. Altered intrinsic regional spontaneous brain activity in patients with optic neuritis: a resting-state functional magnetic resonance imaging study. *Neuropsychiatr Dis Treat.* (2015) 11:3065–73. doi: 10.2147/NDT.S92968

25. Wang ZL, Zou L, Lu ZW, Xie XQ, Jia ZZ, Pan CJ. Abnormal spontaneous brain activity in type 2 diabetic retinopathy revealed by amplitude of low-frequency fluctuations: a resting-state fMRI study. *Clin Radiol.* (2017) 72:340.e1–7. doi: 10.1016/j.crad.2016.11.012

26. Wu YY, Yuan Q, Li B, Lin Q, Zhu PW, Min YL, et al. Altered spontaneous brain activity patterns in patients with retinal vein occlusion indicated by the amplitude of low-frequency fluctuation: a functional magnetic resonance imaging study. *Exp Ther Med.* (2019) 18:2063–71. doi: 10.3892/etm.2019.7770

27. Zuo XN, Di Martino A, Kelly C, Shehzad ZE, Gee DG, Klein DF, et al. The oscillating brain: complex and reliable. *Neuroimage.* (2010) 49:1432–45. doi: 10.1016/j.neuroimage.2009.09.037

28. Zhao N, Yuan LX, Jia XZ, Zhou XF, Deng XP, He HJ, et al. Intra- and inter-scanner reliability of voxel-wise whole-brain analytic metrics for resting state fMRI. *Front Neuroinform.* (2018) 12:54. doi: 10.3389/fninf.2018.00054

29. Yang L, Yan Y, Wang Y, Hu X, Lu J, Chan P, et al. Gradual disturbances of the Amplitude of low-frequency fluctuations (ALFF) and fractional ALFF in Alzheimer spectrum. *Front Neurosci.* (2018) 12:975. doi: 10.3389/fnins.2018.00975

30. Chao-Gan Y, Yu-Feng Z. DPARSF: a MATLAB toolbox for "pipeline" data analysis of resting-state fMRI. *Front SystNeurosci.* (2010) 4:13. doi: 10.3389/fnsys.2010.00013

31. Fox MD, Snyder AZ, Vincent JL, Corbetta M, Van Essen DC, Raichle ME. The human brain is intrinsically organized into dynamic, anticorrelated functional networks. *Proc Natl Acad Sci U.S.A.* (2005) 102:9673–8. doi: 10.1073/pnas.0504136102

32. Yang YC, Li QY, Chen MJ, Zhang LJ, Zhang MY, Pan YC, et al. Investigation of changes in retinal detachment-related brain region activities and functions using the percent amplitude of fluctuation method: a resting-state functional magnetic resonance imaging study. *Neuropsychiatr Dis Treat.* (2021) 17:251–60. doi: 10.2147/NDT.S292132

33. Wang B, Wang J, Cen Z, Wei W, Xie F, Chen Y, et al. Altered cerebello-motor network in familial cortical myoclonic tremor with epilepsy type 1. *Mov Disord.* (2020) 35:1012–20. doi: 10.1002/mds.28014

34. Zeng B, Zhou J, Li Z, Zhang H, Li Z, Yu P. Altered percent amplitude of fluctuation in healthy subjects after 36 h sleep deprivation. *Front Neurol.* (2021) 11:565025. doi: 10.3389/fneur.2020.565025

35. Rudebeck PH, Rich EL. Orbitofrontal cortex. *Curr Biol.* (2018) 28:R1083–8. doi: 10.1016/j.cub.2018.07.018

36. Ongür D, Price JL. The organization of networks within the orbital and medial prefrontal cortex of rats, monkeys and humans. *Cereb Cortex.* (2000) 10:206–19. doi: 10.1093/cercor/10.3.206

37. Lv J, Chen Q, Shao Y, Chen Y, Shi J. Cross-talk between angiotensin-II and toll-like receptor 4 triggers a synergetic inflammatory response in rat mesangial cells under high glucose conditions. *Biochem Biophys Res Commun.* (2015) 459:264–9. doi: 10.1016/j.bbrc.2015.02.096

38. Rolls ET. The orbitofrontal cortex and emotion in health and disease,including depression. *Neuropsychologia.* (2019) 128:14–43. doi: 10.1016/j.neuropsychologia.2017.09.021

39. Izquierdo A. Functional heterogeneity within rat orbitofrontal cortex in reward learning and decision making. *J Neurosci.* (2017) 37:10529–40. doi: 10.1523/JNEUROSCI.1678-17.2017

40. Moorman DE. The role of the orbitofrontal cortex in alcohol use, abuse, and dependence. *Prog Neuropsychopharmacol Biol Psychiatry.* (2018) 87(Pt. A):85–107. doi: 10.1016/j.pnpbp.2018.01.010

41. Onitsuka T, Shenton ME, Salisbury DF, Dickey CC, Kasai K, Toner SK, et al. Middle and inferior temporal gyrus gray matter volume abnormalities in chronic schizophrenia: an MRI study. *Am J Psychiatry.* (2004) 161:1603–11. doi: 10.1176/appi.ajp.161.9.1603

42. Ishai A, Ungerleider LG, Martin A, Schouten JL, Haxby JV. Distributed representation of objects in the human ventral visual pathway. *Proc Natl Acad Sci U.S.A.* (1999) 96:9379–84. doi: 10.1073/pnas.96.16.9379

43. Herath P, Kinomura S, Roland PE. Visual recognition: evidence for two distinctive mechanisms from a PET study. *Hum Brain Mapp.* (2001) 12:110–9. doi: 10.1002/1097-0193(200102)12:23.0.co;2-0

44. Mesulam MM. From sensation to cognition. *Brain.* (1998) 121 (Pt. 6):1013–52. doi: 10.1093/brain/121.6.1013

45. McAdams CJ, Harper JA, Van Enkevort E. Mentalization and the left inferior frontal gyrus and insula. *Eur Eat Disord Rev.* (2018) 26:265–71. doi: 10.1002/erv.2580

46. van der Burght CL, Goucha T, Friederici AD, Kreitewolf J, Hartwigsen G. Intonation guides sentence processing in the left inferior frontal gyrus. *Cortex.* (2019) 117:122–34. doi: 10.1016/j.cortex.2019.02.011

47. Della Rosa PA, Catricalà E, Canini M, Vigliocco G, Cappa SF. The left inferior frontal gyrus: a neural crossroads between abstract and concrete knowledge. *Neuroimage.* (2018) 175:449–59. doi: 10.1016/j.neuroimage.2018.04.021

48. Kleinmintz OM, Abecasis D, Tauber A, Geva A, Chistyakov AV, Kreinin I, et al. Participation of the left inferior frontal gyrus in human originality. *Brain Struct Funct.* (2018) 223:329–41. doi: 10.1007/s00429-017-1500-5

49. Garcia-Larrea L. The posterior insular-opercular region and the search of a primary cortex for pain. *Neurophysiol Clin.* (2012) 42:299–313. doi: 10.1016/j.neucli.2012.06.001

50. Ouyang J, Yang L, Huang X, Zhong YL, Hu PH, Zhang Y, et al. The atrophy of white and gray matter volume in patients with comitant strabismus: evidence from a voxel-based morphometry study. *Mol Med Rep.* (2017) 16:3276–82. doi: 10.3892/mmr.2017.7006

51. Roxo MR, Franceschini PR, Zubaran C, Kleber FD, Sander JW. The limbic system conception and its historical evolution. *Sci World J.* (2011) 11:2428–41. doi: 10.1100/2011/157150

52. Li G, Ma X, Bian H, Sun X, Zhai N, Yao M, et al. A pilot fMRI study of the effect of stressful factors on the onset of depression in female patients. *Brain Imaging Behav.* (2016) 10:195–202. doi: 10.1007/s11682-015-9382-8

53. Shao Y, Yu Y, Pei CG, Tan YH, Zhou Q, Yi JL, et al. Therapeutic efficacy of intracameral amphotericin B injection for 60 patients with keratomycosis. *Int J Ophthalmol.* (2010) 3:257–60. doi: 10.3980/j.issn.2222-3959.2010.03.18

54. Bristow D, Frith C, Rees G. Two distinct neural effects of blinking on human visual processing. *Neuroimage.* (2005) 27:136–45. doi: 10.1016/j.neuroimage.2005.03.037

55. Thakral PP, Slotnick SD. The role of parietal cortex during sustained visual spatial attention. *Brain Res.* (2009) 1302:157–66. doi: 10.1016/j.brainres.2009.09.031

56. Ren Z, Zhang Y, He H, Feng Q, Bi T, Qiu J. The different brain mechanisms of object and spatial working memory: voxel-based morphometry and resting-state functional connectivity. *Front Hum Neurosci.* (2019) 13:248. doi: 10.3389/fnhum.2019.00248

57. Hau J, Aljawad S, Baggett N, Fishman I, Carper RA, Müller RA. The cingulum and cingulate U-fibers in children and adolescents with autism spectrum disorders. *Hum Brain Mapp.* (2019) 40:3153–64. doi: 10.1002/hbm.24586

58. Amodio DM, Frith CD. Meeting of minds: the medial frontal cortex and social cognition. *Nat Rev Neurosci.* (2006) 7:268–77. doi: 10.1038/nrn1884

59. Bush G, Luu P, Posner MI. Cognitive and emotional influences in anterior cingulate cortex. *Trends Cogn Sci.* (2000) 4:215–22. doi: 10.1016/s1364-6613(00)01483-2

60. Shao Y, Bao J, Huang X, Zhou FQ, Ye L, Min YL, et al. Comparative study of interhemispheric functional connectivity in left eye monocular blindness versus right eye monocular blindness: a resting-state functional MRI study. *Oncotarget.* (2018) 9:14285–95. doi: 10.18632/oncotarget.24487

61. Zhao Y, Cui D, Lu W, Li H, Zhang H, Qiu J. Aberrant gray matter volumes and functional connectivity in adolescent patients with ADHD. *J Magn Reson Imaging.* (2020) 51:719–26. doi: 10.1002/jmri.26854

Advantages of publishing in Frontiers

OPEN ACCESS
Articles are free to read for greatest visibility and readership

FAST PUBLICATION
Around 90 days from submission to decision

HIGH QUALITY PEER-REVIEW
Rigorous, collaborative, and constructive peer-review

TRANSPARENT PEER-REVIEW
Editors and reviewers acknowledged by name on published articles

Frontiers
Avenue du Tribunal-Fédéral 34
1005 Lausanne | Switzerland

Visit us: www.frontiersin.org
Contact us: frontiersin.org/about/contact

REPRODUCIBILITY OF RESEARCH
Support open data and methods to enhance research reproducibility

DIGITAL PUBLISHING
Articles designed for optimal readership across devices

FOLLOW US
@frontiersin

IMPACT METRICS
Advanced article metrics track visibility across digital media

EXTENSIVE PROMOTION
Marketing and promotion of impactful research

LOOP RESEARCH NETWORK
Our network increases your article's readership